PROCEEDINGS

7th International Symposium on Advances in Civil and Environmental Engineering Practices for Sustainable Development

ACEPS-2019

Department of Civil and Environmental Engineering
Faculty of Engineering
University of Ruhuna
Hapugala, Galle
Sri Lanka

Publication Committee

ACEPS - 2019

Symposium Proceedings of ACEPS

ISSN 2279-1329

© 2019 Department of Civil and Environmental Engineering, University of Ruhuna, Sri Lanka.

All rights reserved. No part of this publication may be reproduced, stored or transmitted in any form, or by any means, without prior written permission from the Editors.

The views expressed in the papers are of the individual authors. The editors are not liable to anyone for any loss or damage caused by any error or omission in the papers, whether such error or omission is the result of negligence or any other cause. All such liability is disclaimed.

Copies can be obtained from:
Dr. Neetha Dayanthi
Head of the Department,
Department of Civil and Environmental Engineering,
Faculty of Engineering,
University of Ruhuna,
Galle, Sri Lanka.
80000
Email : hod@cee.ruh.ac.lk
Telephone : +94-91-2245765~67
Fax : +94-91-2245762
Website : http://www.dcee.ruh.ac.lk/

Cover Page

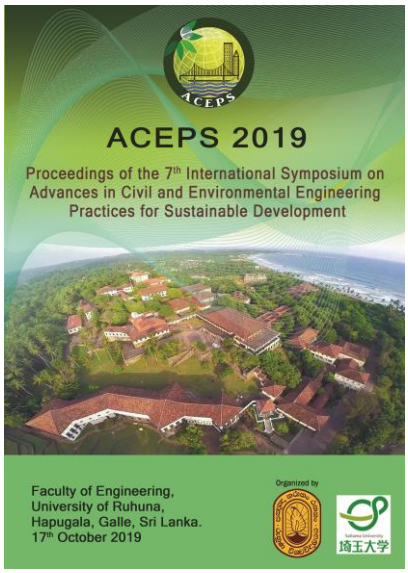

University of Ruhuna, Sri Lanka

With a vision of being the prime intellectual thrust of the nation, the University of Ruhuna has made tremendous progress over the years as an ambassador for excellence in the higher education. The University celebrated its 40th anniversary recently. The main campus of the University of Ruhuna located at Wellamadama, Matara is a spectacular sight. Designed by the world-renowned architect Geoffrey Bawa, the main campus is a functional intellectual hub, yet an enchanting facility, which embraces the natural character of the landscape – the terrain and the vegetation. It has been built amongst the calm and greenery in such a way that it can maintain the balance between infrastructure development and preservation of natural beauty. The facility itself, presents a case-study to an inquisitive mind as modern construction should focus on creating sustainable built-environments. Since its establishment in 1978, the university has been nourishing the young minds of the future promoting social responsibility and sustainability.

Cover designed by Gihan Pathirana and M.M.D. Chinthaka

Preface

The seventeen sustainable development goals adopted by the United Nations include goals such as 'clean water and sanitation', 'industry, innovation and infrastructure', 'sustainable cities and communities' and 'climate action', which are directly related to the field of civil engineering, highlighting the importance of sustainable civil engineering systems.

There is an obvious trade-off between the economic development and the environmental sustainability. Simply, the sustainable development means an economic development conducted without depletion of natural resources. In order to achieve this, the development strategies should encompass environmental protection strategies. Unsustainable economic development has presently caused ecological collapses. On the other hand, collapses are evident in civil engineering systems due to the aftermath of ecological collapses such as extreme summer temperatures, droughts, flash floods, and rising numbers of freeze-thaw cycles. This highlights that unsustainable civil engineering systems cause adverse impacts on the environment, and they are even unable to withstand the disasters caused by the environment destructed by them. Civil engineering systems are greatly responsible for the man kinds' well-being and day-to-day lives because the infrastructure being built at present will shape their lives in the future. Thus, the civil engineering systems should comply with the environmental protection policies.

Sustainable civil engineering systems are a result of better material performance, lower production costs, improved construction and monitoring techniques, reduced health and environmental impacts and etc. Research oriented toward above directions are imperative in terms of sustainable systems. Much research in this area has been conducted in the region to come up with sustainable innovations in civil engineering. Bringing all such region-wide innovations on to one platform would inevitably be a convincing approach for sustainable civil engineering related developments.

ACEPS-2019 symposium is such a platform, on which sustainability-oriented research in civil engineering carried out in the region, is presented. The Department of Civil and Environmental Engineering, Faculty of Engineering, University of Ruhuna, Galle, Sri Lanka is honoured to organize the 7th international symposium on Advances in Civil and Environmental Engineering Practices for Sustainable Development (ACEPS) on 17th October 2019, in collaboration with Saitama University, Japan. The objective of this symposium is to provide an international forum for sustainability oriented civil engineering research. The symposium aimed at presenting and publishing the most recent research and development in the field, consists of a unique set of topics of sustainable civil engineering practices under the following sub-divisions:

Structures and Building Materials
Infrastructure for Changing Climate and Sustainable Built Environment
Coastal and Lagoon Environment
River Engineering and Hydroinformatics

Challenges and Solutions in Geotechnical Engineering
Environmental Engineering and Management

The symposium is held in Galle, a historic city, which houses the largest existing colonial fortress in Asia. This colonial fortress has been withstanding every obstacle over centuries, thus can be cited as a symbol of sustainable development. The construction materials for this development have been picked up from the surrounding environment. Hence, it showcases the great interdependency between the man-made and the natural environment. The existence of the fortress as well as the development of many large-scale infrastructure facilities have made the city an ideal venue for the symposium.

ACEPS-2019 symposium consists of forty-four research papers presented in nine technical sessions, three keynote papers presented in plenary sessions and six abstracts of industry research and case studies. The symposium is graced by three keynote speeches delivered by internationally recognized experts, namely, Dr. Taweep Chaisomphob, Dr. Takeshi Saito and Mr. Upul Goonasekera. Dr. Taweep Chaisomphob from the School of Civil Engineering and Technology, Sirindhorn International Institute of Technology, Thammasat University, Thailand, shares his long experience in structural engineering, by delivering a keynote address entitled "Experimental and numerical study on mechanical behaviour of cold-formed steel built-up box beams composed of two C-sections". Dr. Takeshi Saito from the Graduate School of Science and Engineering, Saitama University, Japan, based on his vast research experience, delivers a keynote address entitled "Overview of chemical contaminant behaviours in groundwater and subsurface thermal pollution as a new contamination issue". Mr. Upul Goonasekera working at Uma Oya Project, Central Engineering Consultancy Bureau, Sri Lanka, based on his long-time experience in the construction field, delivers a keynote speech entitled "Uma Oya Multipurpose Development Project – Socio-Environmental impacts of tunnelling works and Engineering challenges of remedial and mitigation works".

All accepted articles in the ACEPS-2019 proceedings have been peer-reviewed by two referees, and selected based on originality, significance and clarity. These articles include studies focused on solving real engineering problems, case studies on sustainable practices as well as original studies of academic interest. Research published by ACEPS-2019 is expected to be helpful in working out a strategic framework to advance the region with sustainable infrastructure development.

Publication Committee (ACEPS-2019)
17th October 2019

Message from the Vice Chancellor

The global programme initiated by United Nations on sustainable development is getting established in Sri Lanka. Engineering plays a major role in achieving Sustainable development goals.

Technology is changing rapidly. Advances in engineering practices should be adopted to every developing country to face the challenges of sustainable development.

Scientific symposia and conferences are important events to disseminate knowledge for discussion and adoption of these practices to any developing country.

Intersectoral cooperation and team work play a major role in achieving sustainable development. Sectors that should be incorporated include education, health, engineering, economic and infrastructure development departments.

Hence ACEPS-2019 is an important event organized by the Department of Civil and Environmental Engineering, Faculty of Engineering, University of Ruhuna in an attempt to disseminate advanced knowledge and engineering practices.

In this regard organizing a conference in collaboration with Saitama University, Japan is an important activity to foster Future Corporation for sustainable development.

I congratulate the entire organizing committee headed by Dr. Neetha Dayanthi, Head of the Department of Civil and Environmental Engineering, Faculty of Engineering, and wish every success.

Prof. Sujeewa Amarasena
Vice Chancellor, University of Ruhuna

Message from the Deputy Vice Chancellor

In this occasion, as the Deputy Vice Chancellor of University of Ruhuna, it is a great privilege for me to write a message to International Symposium on Advances in Civil and Environmental Engineering Practices for Sustainable Development (ACEPS-2019) to motivate organisers of the symposium and to encourage researchers and students.

An organization's research output obviously helps to fill the gaps in knowledge and develop new products and services. In that, Department of Civil and Environmental Engineering of Faculty of Engineering, University of Ruhuna extends a huge contribution by setting out a platform to share the important new knowledge in specific fields of engineering in their annual symposium, ACEPS. The core themes selected in this symposium covers a broad array of Civil Engineering disciplines, the novel knowledge of which can contribute to the development of Sri Lanka in many ways.

ACEPS will offer a platform to academics, students and practitioners to showcase their most recent findings in the field of civil engineering. This will ultimately open up new avenues for research and practical applications in civil engineering.

ACEPS-2019 would continue in enhancing research and development in the field of civil engineering, and hence encourage innovative and sustainable solutions for the burning problems in the society. ACEPS-2019 will be a very good opportunity for young students to learn new things and to develop their soft skills in different areas such as team work, leadership and communication.

I thank the organising committee of the ACEPS-2019, Dean of Faculty of Engineering and the faculty staff for their great efforts in organising this symposium, which symbolises the intellectual pride of Faculty of Engineering, University of Ruhuna. I wish ACEPS-2019 would be a very successful forum paving a way for the Faculty of Engineering to broaden their scope of knowledge and practices.

Prof. E.P.S. Chandana
Deputy Vice Chancellor, University of Ruhuna

Message from the Dean

It is indeed with great pleasure that I write this message for the symposium "Advances in Civil and Environmental Engineering Practices for Sustainable development" (ACEPS). ACEPS is the longest running international symposium of the Faculty of Engineering, University of Ruhuna and this is its 7th edition. A research symposium of this nature, particularly under a very important theme of sustainable built environment, is a fulfilment of the part of our social obligation as a higher education institute to disseminate new knowledge for the benefit of the society. Department of Civil and Environment Engineering has been at the forefront of our effort to inculcate research culture at the Faculty of Engineering and the success of this research symposium is testimony to those sustained endeavors.

It is a pleasure to learn that the ACEPS have grown from strength to strength over the years maintaining its original values of being a free symposium for contributors since its inception. This has been possible thanks to the generous contributors of this symposium and their steadfast support for ACEPS's original values and principles. It is a great pleasure to note that Saitama University of Japan, Sri Lanka Steel Corporation (commonly known as LANWA brand) and Sanstha Cement (now owned by Siam City Cement Lanka Pvt Ltd also known as INCEE cement) have become the principal force behind ACEPS symposium from its inception.

Over the years, ACEPS have provided a platform for the academics, engineers, scientists, administrators and other professionals of local and international universities and organisations including Saitama University of Japan who have partnered with us, to gather at our faculty on a single day to share their knowledge on advances in sustainable civil engineering practices. We have seen the novel ideas and concepts presented at ACEPS having evolved into major research collaboration, attracting funding from both private and public organizations and national and international funding agencies. I am glad to note that this year's edition has attracted more than forty research papers, which will be presented in four parallel sessions covering many specialties of civil and environmental engineering decorated by a number of keynote presentations by experts from different fields of specializations.

Organizing an event like this is no trivial task. I take this opportunity to appreciate the hard work by the various organizing committees of this event. My appreciation also goes to the reviewers of the research papers for their volunteer service and the industrial sponsors who made this event possible with their generous contributions. Finally, I take this opportunity to wish ACEPS-2019 a great success.

Dr. H.P. Sooriyaarachchi
Dean, Faculty of Engineering, University of Ruhuna

Message from the Head, Department of Civil and Environmental Engineering, University of Ruhuna and Symposium Co-chair

I am extremely delighted to send this complimentary message to the 7th international symposium on Advances in Civil and Environmental Engineering Practices for Sustainable Development (ACEPS-2019) on 17th October 2019, organized by the Department of Civil and Environmental Engineering, in collaboration with Saitama University, Japan.

Sustainable development blends environmental policies with development strategies. The present failures in civil engineering systems due to extreme natural disasters have proved that there should be a balance between the environmental sustainability and economic development. Since the sustainable development goals are directly related to the field of civil engineering, sustainable civil engineering systems are greatly responsible for achieving the world's sustainable goals. The detrimental impacts caused by undefendable civil engineering systems can endanger the public safety. Hence, these systems should be embedded with sustainable development principles.

In this respect, I hold the opinion that ACEPS-2019 symposium being a platform to publish research based on sustainability oriented civil engineering systems, is a timely necessity. The symposium features three keynote speeches by two renowned academics and a professional in the field of civil engineering. The full-day event explores ways to foster productive exchange of research among various interested parties. It is a great platform for the attendees to exchange their research interests.

Organizing this kind of event needs tireless contribution from a number of individuals. On the symposium organizing committee's behalf, I hereby extend my sincere gratitude to all those who contributed to this event.

I wish that ACEPS-2019 would be a successful event.

Dr. W.K.C. Neetha Dayanthi
Head, Department of Civil and Environmental Engineering,
University of Ruhuna
Co-chair, ACEPS – 2019

Message from the Symposium Co-chair

Around 15 years, I and collaborative partners in Sri Lanka have conducted many studies through the constructed wetland project with the researchers in University of Peradeniya (UoP) which had fruitful output including a textbook 'Wetlands for tropical applications: Wastewater treatment by constructed wetlands' published by Imperial College Press, the JSPS AACORE Program with UoP, University of Ruhuna (UoR) and University of Moratuwa (UoM) (2010-2012), the JST-JICA SATREPS (Science and Technology Research Partnership for Sustainable Development) project (2011- 2016), and SL-JP bilateral project under the Program by JSPS with UoR and UoP (2018-2019). The AACORE was designed to create high potential research hubs in selected fields within the Asian and African regions while fostering the next generation of leading researchers by Saitama University collaborating with three Sri Lankan universities. In the JST-JICA SATREPS project, UoP, UoR, Institute of Fundamental Studies (IFS), National Solid Waste Management Support Center (NSWMSC), and Central Environmental Authority (CEA) participated from Sri Lanka, and Saitama University and collaborative research institutes and universities participated from Japan. We are now conducting joint research by SL-JP bilateral project under the JSPS Program (2018-2019) about the topic on Ecosystem-based Disaster Risk Reduction (Eco-DRR) for tsunami. The collaborative research projects have strengthened the knowledge in that field.

I am very happy to jointly chair the 7th International Symposium on Advances in Civil and Environmental Engineering Practices for Sustainable Development (ACEPS-2019) in Galle, Sri Lanka, which will jointly be organized by the Department of Civil and Environmental Engineering, Faculty of Engineering, University of Ruhuna and the Department of Civil and Environmental Engineering, Saitama University, Japan. I hope the symposium will provide an excellent opportunity to establish fruitful international collaboration between the above-mentioned universities.

I would like to thank Dr. Neetha Dayanthi, Symposium Co-chair, all the Scientific Committee and the Local Organizing Committee members of ACEPS-2019 for their efforts in organizing this symposium.

Prof. Norio Tanaka
International Institute for Resilient Society, Saitama University, Japan
Graduate School of Science and Engineering, Saitama University, Japan
Co-chair, ACEPS - 2019

Organizational Structure of the Symposium

Co-organizers

Department of Civil and Environmental Engineering, University of Ruhuna, Sri Lanka

Department of Civil and Environmental Engineering, Saitama University, Saitama, Japan

Organizing Committee

Symposium Co-chairs

Dr. Neetha Dayanthi - University of Ruhuna, Sri Lanka

Prof. Norio Tanaka – Saitama University, Japan

Symposium Secretary

Dr. Samanthi Seneviratne, University of Ruhuna, Sri Lanka

International Scientific Committee

Prof. Ananda Jayawardana, University of Moratuwa, Sri Lanka

Prof. Anura Nanayakkara, University of Moratuwa, Sri Lanka

Prof. Gamini Senanayake, University of Ruhuna, Sri Lanka

Prof. Heekwan Lee, Incheon University, Korea

Prof. Hiroshi Mutsuyoshi, Saitama University, Japan

Prof. Kypros Pilakoutas, University of Sheffield, UK

Prof. Priyan Dias, University of Moratuwa, Sri Lanka

Prof. Ranjith Dissanayake, University of Peradeniya, Sri Lanka

Prof. Sarath Abeykoon, University of Peradeniya, Sri Lanka

Prof. Tomonori Kawakami, Toyama Prefectural University, Japan

Dr. Joe Odencrantz, Tri-S Environmental (Tri-S), California, USA

Dr. Nayana Alagiyawanna, University of Ruhuna, Sri Lanka

Dr. Antony Peter Darby, Bath University, UK

Logistic Committee

Dr. W.M.K.R.T.W. Bandara (Chairperson)

Dr. Sujeewa Wimalasena

Dr. T. N. Wickramaarachchi

Dr. G.G. Tushara Chaminda

Dr. N.H. Priyankara

Mr. M.N.M. Shayan

Mr. Achinthaka Maduranga

Mr. M.F.M. Ishqy

Ms. Nishanthini Jegatheesan

Ms. R.G.F. Harshini

Publication Committee

Dr. Samanthi Seneviratne (Chairperson)

Dr. Terrance M. Rengarasu

Dr. Champika Ellawala

Dr. T. N. Wickramaarachchi

Dr. Anuruddhika Jayasinghe

Dr. Vidura Vithana

Dr. G.S.Y. De Silva

Ms. Nishanthini Jegatheesan

Ms. R.G.F. Harshini

Ms. T.H.F. Aagani

Ms. Chamari Udeshika

Ms. Sureshi Priyamali

Mr. M.M.D. Chinthaka

Technical Committee

Dr. Anuruddhika Jayasinghe, University of Ruhuna, Sri Lanka

Dr. Champika Ellawala, University of Ruhuna, Sri Lanka

Dr. Chandana Siriwardena, University of Moratuwa, Sri Lanka

Dr. Chinthaka Mallikarachchi, University of Moratuwa, Sri Lanka

Dr. G.G. Tushara Chaminda, University of Ruhuna, Sri Lanka

Dr. G.H.M.J. Subhashi, University of Ruhuna, Sri Lanka

Dr. G.S.Y. De Silva, University of Ruhuna, Sri Lanka

Dr. Ganga Samarasekara, University of Sri Jayewardenepura, Sri Lanka

Dr. J.M.R.S. Appuhamy, University of Ruhuna, Sri Lanka

Dr. Kasun De Silva, University of Moratuwa, Sri Lanka

Dr. Neetha Dayanthi, University of Ruhuna, Sri Lanka

Dr. Nimal Wijayarathna, University of Moratuwa, Sri Lanka

Dr. Niranga Amarasingha, Sri Lanka Institute of Information Technology

Dr. Ravindra Thilakaratne, Transit Specialist, City of Grande Prairie, Canada

Dr. Samanthi Seneviratne, University of Ruhuna, Sri Lanka

Dr. Sujeewa Wimalasena, University of Ruhuna, Sri Lanka

Dr. T. M. Rengarasu, University of Ruhuna, Sri Lanka

Dr. T.N. Wickramaarachchi, University of Ruhuna, Sri Lanka

Dr. U.P. Nawagamuwa, University of Moratuwa, Sri Lanka

Dr. Vidura Vithana, University of Ruhuna, Sri Lanka

Dr. W.M.K.R.T.W Bandara., University of Ruhuna, Sri Lanka

Ms. S.N. Malkanthi, University of Ruhuna, Sri Lanka

Sponsors

Siam City Cement (Lanka) Pvt Limited

Ceylon Steel Corporation Pvt Limited

Saitama University, Japan

Acknowledgement

Organization of a symposium is always a challenging endeavour; the success of the event being the culmination of all untiring efforts. As ACEPS-2019 is unrolling at the moment, we would like to take a moment to express our heartiest thanks to all who helped to make ACEPS-2019 a success.

First and foremost, we are much grateful to Senior Professor Sujeewa Amarasena, Vice Chancellor, University of Ruhuna for his support for the symposium and gracing the event as the Chief Guest.

We also wish to acknowledge Professor E.P.S. Chandana, Deputy Vice Chancellor, University of Ruhuna for his valuable presence at ACEPS -2019.

Our thanks especially go to Dr. Harsha Sooriyaarachchi, Dean, Faculty of Engineering, University of Ruhuna for his enormous support and guidance for organizing ACEPS -2019.

If not for the leadership of the Symposium Co-chairs, ACEPS- 2019 would not have been a reality. Dr. Neetha Dayanthi, being the Symposium Co-chair and the Head of the Department of Civil and Environmental Engineering guided the team towards achieving many goals that constitute the organisation of the event as a whole. The enormous support of Professor Norio Tanaka, representing the Saitama University, Japan helped resolving many issues smoothly and essentially drove the symposium towards the excellence.

We express our special thanks to the keynote speakers of the symposium. We are privileged to have Dr. Taweep Chaisomphob, Thammasat University, Thailand, for sharing his experience as a keynote speaker. We take this opportunity to thank Dr. Takeshi Saito, Saitama University of Japan, for sharing his knowledge and wisdom with us. Our sincere gratitude is extended to Eng. Upul S. Goonasekera, Chief Residential Engineer-Head Works, Uma Oya Multipurpose Development Project, Sri Lanka for sharing his expertise with us as a keynote speaker.

We also appreciate the assistance of the International Scientific Committee, whose guidance helped the ACEPS-2019 organizing committee to comply with the international standards.

We are particularly grateful to the multi-disciplinary Technical Committee of ACEPS- 2019 for their contribution to the reviewing process. Their dedication and timely support were indispensable to maintain the high standard of the symposium and we greatly appreciate their continuous service to this task since the inception of the ACEPS.

We take this opportunity to thank all the session co-chairs and the members of the committee appointed for evaluating the oral presentations for their enormous contribution.

Furthermore, our special thanks go to the authors who submitted papers for ACEPS-2019. Without their support and trust in us, this symposium would not have been possible.

We would like to offer our sincere gratitude to the sponsors, Siam City Cement (Lanka) Limited *(INSEE)*, Ceylon Steel Corporation Limited *(LANWA)* and Saitama University for providing us with the financial support for the successful organization of the symposium.

We gladly acknowledge the academic and non-academic staff of the Department of Civil and Environmental Engineering for lending their untiring efforts to organize the symposium. We also extend our thanks to the students of the Department of Civil and Environmental Engineering who contributed greatly in numerous ways to the organization and success of the symposium.

Last, but not least, we would like to thank all members of the Organizing Committee for their hard work and dedication. The success of the symposium is defined by the diligent efforts of each member who gave his/her best to ensure the realization of the potential of this symposium.

Publication Committee (ACEPS-2019)
17th October 2019

Table of Contents

Keynote Addresses

Experimental and numerical study on mechanical behaviour of cold-formed steel built-up box beams composed of two C-sections 1
T. Chaisomphob and V. T. Trung

Overview of chemical contaminant behaviours in groundwater and subsurface thermal pollution as a new contamination issue 10
Takeshi Saito

Uma Oya Multipurpose Development Project – Socio-environmental impacts of tunneling works and engineering challenges of remedial and mitigation works. 16
U.S. Goonasekera

Challenges and Solutions in Geotechnical Engineering

Enhancement of engineering characteristics of peaty clay using wet cement mixing method 23
D.S.R.C.V.Perera and N.H.Priyankara

Influence of grouting pressure on pullout resistance of soil nail 28
R.G.F.Harshini and N.H.Priyankara

Study the behavior of load transfer platform of geosynthetic reinforced piled embankments using a numerical model 34
S.K.E.Sanjaya and N.H. Priyankara

Advancements in rail track technology: application of rubber elements in rail track for sustainable transport infrastructure 39
S.K. Navaratnarajah

Variation of geotechnical properties of municipal solid waste due to biodegradation. 48
W.T.R.A.Pradeep, N.H.Priyankara and A.M.N.Alagiyawanna

Modelling soil-gas diffusivity in aggregated porous media. 57
J.R.R.N. Jayarathne, T.K.K. Chamindu Deepagoda, M.C.M. Nasvi, K. Smits, T.J. Clough, S. Thomas and B. Elberling

Effects of soil moisture on simulated methane flow in a differently-compacted soil. 65
M. Shanujah, T.K.K. Chamindu Deepagoda, M.C.M. Nasvi, A. K. Karunarathna, V. Shreedharan and G.L.S. Babu

Characterization of the properties of manufactured sand and natural river sand 73
U. Wijepala, S. Jayakody, A.M.Z. Zimar, J.M.N.D. Jayasinghe and W.K.W.S. Jayasena

Coastal and Lagoon Environment

Application of satellite altimeter data for extreme wave modelling in north eastern coastal sea of Sri Lanka. 79
R.W.W.M.C.J.B. Wijekoon and H.P.V. Vithana

Review of existing coastal defence system in Sri Lanka against tsunami. 84
T.L.C.Vinodh and N.Tanaka

Tsunami intrusion in rivers: a review and new perspectives on Sri Lankan rivers 92
Romitha Wickramasinghe and Norio Tanka

Environmental Engineering and Management

Field scale combined stabilization pond system and constructed wetland for leachate treatment controlling loading conditions 99
R.M.L.D.Rathnayake, E.I.K.Gamakaranage, W.M.D.C.Walisundara and G.B.B. Herath

Sorption experiments on heavy metal removal in contaminated groundwater by landfill-leachate using Permeable Reactive Barriers (PRBs) packed with waste materials. 105
I.U.Nagasinghe and W.K.C.N.Dayanthi

Evaluation of the water quality of community managed water supply schemes in Matara district 113
A.M.Asarudeen, Tushara Chaminda, K.C.Ellawala, M.N.M.Shayan and W.B. Gunawardena

Composite adsorbent using waste materials to treat dissolved organic matter and nutrients in landfill-leachate. 118
W.T.C.Udeshika and W.K.C.N.Dayanthi

Water use patterns and sensitivity to tariff: A study in a community with access to alternative water sources other than pipe borne water. 125
K.C.Ellawala and V.Vinojkanth

Column experiment on recycling waste materials to treat dissolved organic matter and nutrients in landfill-leachate. 130
G.L.P.M.Punyawardhana and W.K.C.N.Dayanthi

Assessment of domestic greywater quality to determine the potential reuse in urban residentials. 136
H.U.E. Imasha, G.G.T. Chaminda, M. Otaki, Y. Otaki and C.P. Rupasinghe

Laboratory wastewater treatment using clay bio char composites in horizontal flow bio-geo filters 144
S.Niruparan, K.Karthika , W.G.D.K.S.Madushika and B.C.L.Athapattu

Treating heavy metals in the groundwater contaminated by landfill-leachate using Permeable Reactive Barriers (PRBs) packed with building wastes and dewatered alum sludge. 151
W.R.A.U. Dilrukshi and W.K.C.N.Dayanthi

An analysis of household perception on solid waste separation – special reference to Kesbewa municipal council area. 158
G.G.R.Wijesingha, W.H.A.Shantha and G.M.W.L.Gunawardena

Comparison of cyclone performance with theoretical predictions based on inlet velocity and particle loading rate. 165
G.B.Sakura and Andrew Y.T.Leung

Infrastructure for Changing Climate and Sustainable Built Environment

Simulation of pedestrian evacuation in the underground train station: a case study of MRT Huai Khwang station 173
P. Boonsomparn and M. Piantanakulchai

Speed variation of vehicles correspondent to road, driver, and environmental characteristics 181
N. Amarasingha and N.N. Samarasinghe

Carbonized rice husk particles as bitumen modifier in hot mix asphalt 189
Mohamed Juzaafi, T.M.Rengarasu, Wasala.M.K.R.T.W.Bandara and Nishanthini Jegatheesan

Suitability of recycled concrete aggregates in hot mix asphalt concrete. 196
T.Pradheep, M.K.K.D.Wimalasena and Terrance M. Rengarasu

A comparative study of HMA with modified asphalt by polyethylene terephthalate and polypropylene fibers. 203
Mehalathan .S, Jegatheesan .N , Juzaafi .M , Rengarasu . T.M and Bandara W.M.K.R.T.W

An analysis of frequently observed roadside green boundary wall facades in Western province, Sri Lanka: visual configurations, cost and operational challenges 211
W.C.M.S.Madushanka, M.F.M.Althaf , M.S.M. Sajjad, Tushara Chaminda G.G and G.N. Samarasekara

Factors affecting safety at construction sites of Sri Lanka 219
R. M. N. D. Rathnayaka, P. I. A. Gomes and A. A. A. Afthal

Geocoding for post-disaster compensation projects in Sri Lanka (Special reference to selected disaster-prone areas) 225
R.M.P.S Rathnayake, W.H.A. Shantha and G.M.W.L. Gunawardena

River Engineering and Hydroinformatics

Assessment of open technologies-based measurements as a potential dataset for hydrological modelling in Deduru Oya river basin of Sri Lanka 232
E.J. Warusavitharana, B.H. Sudantha, R. Ratnayake, P.K.S. Mahanama, R.J. Warusavitharana, M. Cannata and D. Strigaro

Climate change in Sri Lanka - What does the data actually reflect? 240
P. Hettiarachchi and M.K.J. Madhavie

Structures and Building Materials

Behaviour of cold-formed stainless steel beams with elliptical web opening under web crippling 251
Ishqy Fareed, K.S. Wanniarachchi, P. Keerthan, S. Gunalan, P. Gatheeshgar, R. Heshachanaa

Condition assessment and rating of building structures in Sri Lanka against Tsunami 257
B.H.J. Pushpakumara, H.D.K.A. Wijerathne and W.S.W. Mendis

Investigation on flexural performance of heavily cracked concrete beams strengthened with cfrp 265
H.A. Dissanayake, P.D. Dharmaratne, M.A.L. Silva, J.C.P.H. Gamage

Lime stabilization for compressed stabilized earth blocks with reduced clay and silt 272
S.N. Malkanthi, N. Balthazaar and A.A.D.A.J.Perera

Investigating the behavior of Clay Roof Tile (CRT) Physical properties by introducing lime as an additive. 279
B. D. K. K. Thilakarathna, K.M.A.K. Kulatunga, C. P. Jayalath

Finite element modelling of reinforced concrete horizontally curved beams strengthened for shear using carbon fiber reinforced polymer 288
M.W.C. Himasha and J.C.P.H Gamage

Use of superabsorbent polymers to improve the properties of fresh concrete. 296
G.H.P.N. Pushpakumara and J.M.R.S. Appuhamy

Possibility of production of bricks using waste materials and natural binding materials in Sri Lanka 301
D.M. Shanuka Jayathunge, Rohantha Rukshan Jayasinghe and Madujith Sagara

Study on suitable wall thermal insulation methods for dwellings under tropical climatic conditions: A review. 306
E.M.J.C.Silva, Madujith Sagara Chandra

Investigation of properties of reusable interlocking cement blocks 314
R. Heshachanaa, S.V.T.J. Perera

Effect of waste rice hush ash and ceramic sludge on structural properties of fried clay roof titles 322
T.H.F.Aagani and G.H.M.J. Subashi De Silva

Effects of cassava peel powder as an admixture on properties of concrete 329
H.M.I.D. Dissanayake and S.V.T.J. Perera

Industry Research and Case Studies

Structural performance of novel technique to repair corroded reinforced concrete elements 335
H.P Sooriyaarahchi

Failure of gravel compaction pile supported embankment: Case study 339
N. H. Priyankara

Case study on efficiency of domestic wastewater treatment plants in western province of Sri Lanka 340
T. Prasanthan, D.K. Pathirana and W.K.C.N. Dayanthi

Durability of mass concretes in hot weather 341
Kalinda Dasanayaka

Cost-effective structural system for retrofitting existing houses in flood prone areas 342
T. *R. S. T Wijewardana, Dhanushka Jayathilaka, Gihan Ranasinghe, C. Jayasinghe, M. T. R Jayasinghe, Shawn L. Platt and Pete Walker*

Design a transitional shelter for post disaster recovery 343
S.M.M.Infas,T. R. S. T Wijewardana, Dhanushka Jayathilake, Udeni P Nawagamuwa

Keynote Addresses

Keynote Address

Experimental and Numerical Study on Mechanical Behaviour of Cold-Formed Steel Built-Up Box Beams Composed of Two C-Sections

by

Dr. Taweep Chaisomphob

(School of Civil Engineering and Technology, Sirindhorn International Institute of Technology (SIIT), Thammasat University, Thailand)

Dr. Taweep Chaisomphob is an Associate Professor at Sirindhorn International Institute of Technology (SIIT), Thammasat University, Thailand. Presently, he leads the Efficient Urban Research Center at SIIT and carries out cutting-edge research on a wide range of topics. These include advanced design methods of steel and composite structures, shear lag behavior of thin-walled structures, development of run-of-river hydropower projects, public participation in infrastructure project development, and development of efficient composting systems. His work had been published in numerous national and international conferences and journals. Engaging the next generation of scholars in building his legacy, Dr. Chaisomphob had supervised many masters and doctoral thesis. In recognition of his work, the Thammasat University named him the 'Outstanding Researcher' in the year of 1998.

Apart from research, he has extended his service to academia in many ways undertaking varied responsibilities over the last 25 years. These include his service to Thammasat University as the Vice Rector for Academic Affairs (2011-2013 and 2004-2007), Vice Rector for Research and Educational Services (2010-2011), Head of School of Civil Engineering and Technology of SIIT (2009-2010), Assistant Director for Student Affairs (1999-2003), Chairperson of Civil Engineering Department of SIIT (1996-1999), and as the Academic Secretary of SIIT (1994-1996).

Proceedings of the 7th International Symposium on

Advances in Civil and Environmental Engineering Practices for Sustainable Development

ACEPS - 2019

Experimental and numerical study on mechanical behaviour of cold-formed steel built-up box beams composed of two C-sections

T. Chaisomphob[1], V. T. Trung[1]

[1]School of Civil Engineering and Technology, Sirindhorn International Institute of Technology, Thammasat University, THAILAND.

K e y w o r d s

Cold-formed steel
Built-up box beam
Face-to-face C-sections
Moment capacity
Connection spacing

A B S T R A C T

The mechanical behaviour of the cold-formed steel built-up C-section box beam was investigated both experimentally and numerically in this paper. Four connection spacings are considered for each of the five C-sections, and thus 20 built-up beams are tested under four-point bending. The built-up sections were assembled by batten plate and self-drilling screws from two face-to-face C-section. It is shown from the test results that the connection spacing influenced on the mechanical behavior of the built-up box beam considerably. The finite element model using ABAQUS is conducted to verify experimental results. It is shown that the FEM models are capable for predicting the behavior of the cold-formed steel built-up C-section box beams with difference connection spacings.

1. INTRODUCTION

The box beam composed of two face-to-face C-section beams is getting popular in the cold-formed steel construction due to its advantage in strength such as: high strength-to-weight ratio, easy prefabrication, economy in transportation and speedy. CFS is an integral part of the construction industry. For example, CFS beams are used as floor joists, wall studs, roof purlins and rafters in industrial/commercial buildings and residential houses (Yu 2016, Zhou *et al.* 2005).

The structural behaviour of cold-formed steel beams has been studied for a long time. Yu and Schafer (2003, 2006) did a series of bending tests on CFS C- and Z-section beams to deal with distortional buckling and local buckling phenomena. Wang and Zhang (2009) carried out a numerical and experimental study on the behaviour of various C-section beams with different edge stiffeners subjected to bending. The results revealed that the beam strength is greatly affected by the edge stiffener. Laím *et al* (2013) conducted a series of bending test and numerical analysis of CFS beams, including box beams. Their study has revealed that the ultimate load-carrying capacities of R beam (a box section consisting of C- and U-channels) and 2R beam (a box section consisting of the two R beams) were 1.45 times and 2.9 times larger than that of the I-beam, respectively.

The increasing use of the CFS beam is a direct result of continuing research. L. Wang and B. Young (2017) studied the flexural behaviour of cold-formed steel built-up box beam composed of two face-to-face plain sections with circular web holes about failure modes and the moment capacities. The test and numerical results were compared with the strength calculated by the direct strength method given in North American Specification (AISI Standard 2016). L. Wang and B. Young (2015) investigated the local buckling and/or distortional buckling behavior of the built-up closed sections with intermediate stiffeners using self-tapping

screws located at web or flange. L. Wang and B. Young (2018) presented the influence of different screw arrangements on the behaviour of cold-formed steel built-up box beams. The study indicated that the screw spacing affected significantly on the moment capacities of those beams. Anbarasu M. (2019) studied the structural behaviour of cold-formed steel (CFS) built-up sigma sections box beams. Modelling issues such as geometric nonlinearity, contact nonlinearity, fastener modelling, initial geometric imperfections, and convergence issues were addressed in this study.

Currently, no clear design rules are available for this type of built-up box beam (Australian/New Zealand Standard 2018, AISI Standard 2016). There have been a lot of researches about the built-up box. However, the research about the connection method, such as the connection spacing, is somewhat limited. Therefore, the objective of this research is to propose a design method for a box beam composed of two face-to-face CFS C-section beams. The impact of connection spacing on the beam's strength is primarily investigated. All the experiments are conducted in the Structures Laboratory of the Chulachomklao Royal Military Academy in Thailand.

2. EXPERIMENTAL INVESTIGATION

2.1. Test specimens

Five different C-sections shown in Table 1 are employed in this study. Variables in the table are defined in Figure 1.a. Two identical C-sections form a box section, as illustrated in Figure 1.b. A thin batten plate with the length of 80 mm, the width of 80 mm and the thickness of 1.9 mm is screwed to the top and bottom flanges of the box beam, respectively, to fasten the C-section beams intermittently. Four 4.8 mm self-drilling screws are used for each batten plate (Figure 1.b & Figure 2).

The overall length of the beam specimen is 4000 mm and the distance between the centers of two bearings is 3800mm. Four different spacings between the adjacent screwed connections are considered. The center-to-center spacings in the four cases are L/2 (1750 mm), L/3 (1167 mm), L/4 (875 mm) and L/6 (583 mm), respectively. The center of the rightmost batten plate of the specimen is always 250 mm away from the right end while the center of the leftmost batten plate always 250 mm away from the left end. The distance between the centers of the two end batten plates L is therefore 3500 mm. The schematic of the box-beam specimen with the connection spacing of L/6 is presented in Figure 3.

Table 1 Dimension of C-section

C-section	t (mm)	D (mm)	B (mm)	ℓ (mm)
C10012	1.2	102	51	12.5
C10015	1.5	102	51	13.5
C15019	1.9	152	64	16.5
C15024	2.4	152	64	18.5
C20019	1.9	203	76	19.0

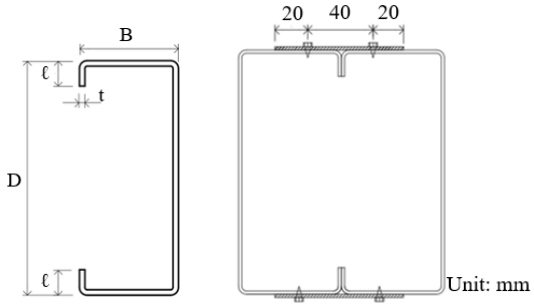

a. Definition of variables b. Built-up box section

Figure 1 Cross-section

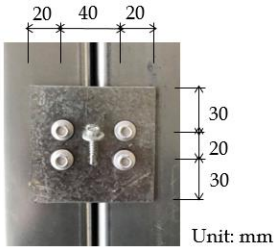

Figure 2 Batten plate and self-drilling screws

With the five C-sections and the four connection spacings, 20 box beam specimens are experimentally conducted for this study. The specimens are listed in Table 2. The specimen name shows its features. For example, C15019-L6 indicates that it is composed of two face-to-face C-sections of C15019 with the connection spacing equal to L/6.

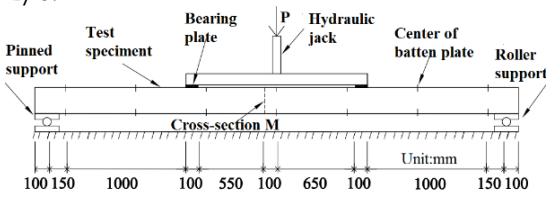

Figure 3 The schematic of the box-beam specimen with connection spacing of L/6

2.2. Test setup

The experimental arrangement is shown in Figure 4. The box-beam test specimen (No. 1) is supported. A load is applied by the hydraulic jack (No. 2) that hangs down from the loading frame. The load is transferred to an I-steel beam (No. 3) and then to the two bearing plates (No. 4) on the beam specimen. Thus, it is a four-point bending test. The two bearing plates are placed symmetrically concerning the center of the beam specimen, which gives uniform bending moment between the two bearing plates. A load cell (No. 5) is used, which is positioned beneath the hydraulic jack to control the magnitude of the load. The load cell is connected to a data logger.

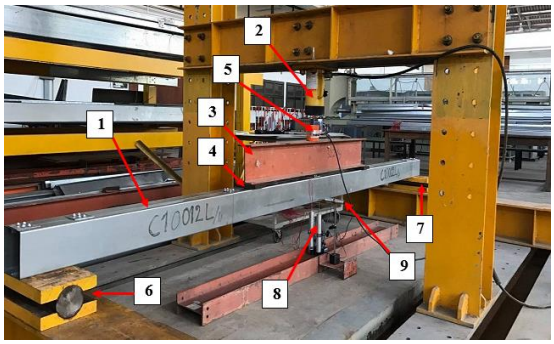

Figure 4 Test setup

To achieve a simple support condition, a bearing is used in each bearing, allowing bending rotation. At one bearing (No. 6), the roller bearing, the beam displaces horizontally while at the other bearing (No. 7), the pinned bearing, the horizontal displacement is constrained by clamps as Figure 5.

a. Pinned support b. Roller support

Figure 5 Support setup

2.3. Test procedure

At the beginning, a small load is applied for the beam specimen to settle in the position. The load is then increased gradually. The vertical and horizontal displacements are measured at Cross-section M shown in Figure 3 and recorded together with the load. Linear variable displacement transducers (LVDTs; Nos. 8 and 9) are used for measuring the displacements at Cross-section M. As shown in Figure 3, Cross-section M is located 100 mm away from the mid-span.

2.4. Material properties

Tensile coupon tests are carried out, following the procedure specified in the Australian Standard (Australia Standard, 2007). The following values of the yield strength F_y have been obtained: 536 MPa for the thickness of 1.2mm, 504 MPa for 1.5mm, 510 MPa for 1.9mm, and 484 MPa for 2.4mm. The yield strengths obtained are all larger than the respective minimum yield strengths given in Material Specification from NS BlueScope Lysaght (Thailand) Limited (2014).

2.5. Experiment results and discussions

Table 2 reveals that the connection spacing influences on the mechanical behaviour of the built-up box beam considerably. As the spacing becomes smaller, the strength P_{EXP} increases. The exception is observed in the result of the C15024 series of box beams: the strength of C15024-L4 is 48.70 kN while that of C15024-L3 is 50.61 kN, of the C10012 series: the strength of C10012-L4 is 8.55 kN while that of C10012-L3 is 8.69 kN. In all the other tests, the shorter spacing has resulted in a larger strength.

Failure modes are also influenced by connection spacing. The basic failure modes associated with the CFS C-section beam are lateral–torsional buckling (LTB), local buckling (LB) and distortional buckling (DB). The three modes are illustrated schematically in Figure 6. Indeed, the test beams have failed in those modes. But pure DB didn't occur. It tended to go with LB, resulting in the mixed mode of DB and LB. DB+LB in Table 2 indicates this mixed-mode failure. Figure 7 presents the typical failures observed in the experiments.

Table 2 shows that the beam fails in LB when the connection spacing is equal to or less than L/4. For a larger spacing, the beam undergoes DB+LB or LTB except for C15024-L3 that fails in LB. The connection spacing influences the failure mode then changes in strength. The connection spacing becomes smaller, the two C-section beams tend to

Table 2 Test result

Specimen	P_{tu} (kN)	Failure mode	
		C-section 1	C-section 2
C10012-L6	9.29	LB	LB
C10012-L4	8.55	LB	LB
C10012-L3	8.69	DB + LB	DB + LB
C10012-L2	8.25	DB + LB	LTB
C10015-L6	15.50	LB	LB
C10015-L4	15.03	LB	LB
C10015-L3	14.25	DB + LB	DB + LB
C10015-L2	11.69	DB + LB	LTB
C15019-L6	36.82	LB	LB
C15019-L4	36.50	LB	LB
C15019-L3	34.24	DB + LB	DB + LB
C15019-L2	30.58	DB + LB	LTB
C15024-L6	51.50	LB	LB
C15024-L4	48.70	LB	LB
C15024-L3	50.61	LB	LB
C15024-L2	45.22	DB + LB	LTB
C20019-L6	48.00	LB	LB
C20019-L4	47.50	LB	LB
C20019-L3	40.48	DB + LB	DB + LB
C20019-L2	36.70	DB + LB	LTB

*LTB: lateral–torsional buckling; LB: local buckling; DB: distortional buckling.

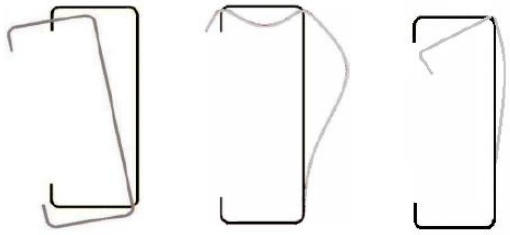

(a) (b) (c)

(a) Lateral–torsional buckling (LTB)
(b) Local buckling (LB)
(c) Distortional buckling (DB)

Figure 6 Failure mode of C-section beam

(a) LTB

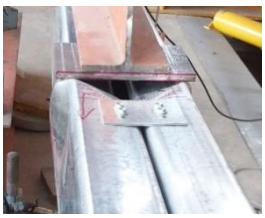

(b) LB

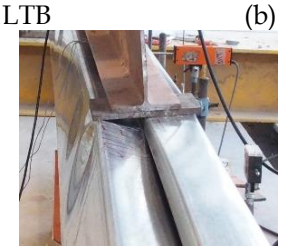

(c) DB+LB

Figure 7 Typical failure in experiment

behave together, increasing the member stiffness and thus failing not in the member buckling but rather locally.

The change in the failure mode is also recognized in the load-displacement curve. For example, Figure 8 shows the experimental results of the C20019 series of box beams. When the connection spacing is large, horizontal displacement starts increasing nonlinearly at a very early stage of loading. At the failure, Cross-section M has displaced over 30 mm horizontally. The vertical displacement also starts deviating from the linear response at an early stage in case of the beams with large connection spacing. On the other hand, for the box beams with the smaller spacings (L/4 and L/6), the horizontal displacement was very small until failure (less than 3 mm); the load-displacement relationship is almost linear up to the failure. The load-displacement curve is thus another evidence for the influence of the connection spacing on the failure mode.

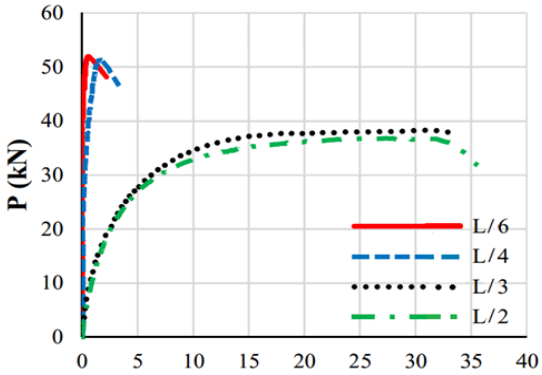

(a)Horizontal Displacement (mm)

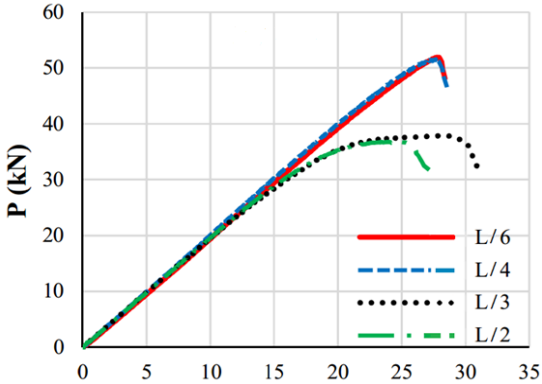

(b)Vertical Displacement (mm)

Figure 8 The experimental load-displacement curve for built-up box-beam (C20019)

All the experimental results prove that the connection spacing of L/4 would have two face-to-face C-section beams fastened sufficiently. The moment capacity has increased by further reducing the connection

spacing to L/6, while the failure mode remains the same. The connection spacing of L/6 would make the region of the C-section beam covered by the batten plates larger. The cross-section with the batten plate increases the cross-sectional area. Therefore, the increase in the moment capacity of the box beam with the connection spacing of L/6 may be attributable to the stiffening effect of the batten plate.

Last but not least, no failure or damage has been found in the batten plates and the screws in all the tests. The present screwed connection has thus proved satisfactory.

3. NUMERICAL ANALYSIS

The finite element program ABAQUS is a computational software for modelling structures with material and geometric nonlinear behaviour (Schafer *et al*. 2010). In this study, 20 numerical tests were conducted to compare with the experimental results in terms of maximum loads and failure modes.

3.1. Element type

C-sections and stiffening plates were modelled with shell elements (S4R). Based on Kirchhoff theory, when one dimension was very small compared with the other two dimensions, the shell element is recommended for the calculation process. Load bearing plates and support bearing plates were modelled by using solid elements (C3D8R).

3.2. Material properties

Material nonlinearity (plasticity) was considered for the CFS C-sections profile. A yield strength and a Young's Modulus were obtained from the coupon test. Elastic stress-strain was considered for the stiffening plate because there was no failure at the stiffening plate during the testing process. Besides, the material properties for load bearing plates and support bearing plates were assumed as rigid steel with the value of Young's Modulus equal to one thousand times greater than that of normal steel. The elastic modulus of steel was equal to 208 GPa and the Poisson's ratio to 0.3.

3.3. Fastener and contact conditions

Since there was no failure at the screw connection during the test, so the function fastener in ABAQUS (Faridmehr *et al*. 2015) was used to represent the screws to be simple in the calculation process. In addition, fastener properties were created that all rotational and translational degrees of freedom of the nodes were constrained at the screw location. The radius of the screw was equal to 1.95 mm and used as the radius dimension in ABAQUS program.

The contact between two lips of both C-sections, load-bearing plate with the beam, and C-sections with the support bearing plate were also defined in the modelling analysis.

3.4. Boundary and loading

For the test set-up, at both ends of the beam specimen, the steel supports were installed. The box beam section was above the steel plate of the support, as shown in Fig. 9. Moreover, the steel bearing plate was used in the test to distribute the load from the I load-transferring beam to the beam section at two points, as shown in Figure 9.

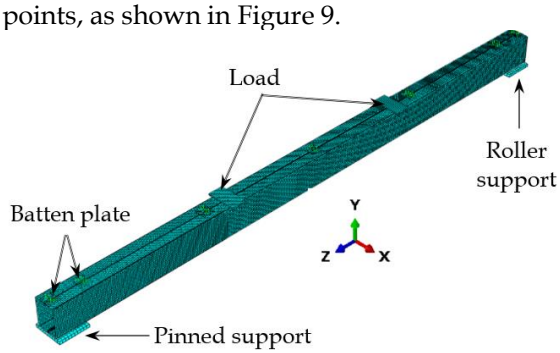

Figure 9 The numerical model used in the finite element analysis

3.5. Finite element mesh

The finite mesh sizes of cold-formed steel sections were approximately 10mm×10mm. The support plates were provided with approximate mesh size of 20mmx20mmx20mm, and the load bearing plate of 10mmx10mmx10mm. For the curve at the corner of the C section and the lip, three divisions were applied to get more accurate results.

3.6. Analysis procedure

Each of the models was analysed in two steps. Firstly, linear buckling analysis was performed to get the buckling shape (eigenvectors). The buckling shape has been used to represent initial imperfection shape with scale factors. Mode 1 in the analysis was

taken to be the mode shape. Then, general material and geometrical nonlinear static analysis with imperfections were conducted to simulate the structural behaviour of CFS built-up box beam.

Table 3 Comparison between experiment and FEM results

Specimen	Experimental results			FEM results			Ratio P_{FEM}/P_{EXP}
	P_{tu} (kN)	Failure mode C-section 1	Failure mode C-section 2	P_{FEM} (kN)	Failure mode C-section 1	Failure mode C-section 2	
C10012-L6	9.29	LB	LB	9.70	LB	LB	1.04
C10012-L4	8.55	LB	LB	9.33	LB	LB	1.09
C10012-L3	8.69	DB + LB	DB + LB	9.68	DB + LB	DB + LB	1.11
C10012-L2	8.25	DB + LB	LTB	8.22	DB + LB	LTB	1.00
C10015-L6	15.50	LB	LB	14.14	LB	LB	0.91
C10015-L4	15.03	LB	LB	13.69	LB	LB	0.91
C10015-L3	14.25	DB + LB	DB + LB	13.66	DB + LB	DB + LB	0.96
C10015-L2	11.69	DB + LB	LTB	12.32	DB + LB	LTB	1.05
C15019-L6	36.82	LB	LB	34.51	LB	LB	0.94
C15019-L4	36.50	LB	LB	34.03	LB	LB	0.93
C15019-L3	34.24	DB + LB	DB + LB	34.32	DB + LB	DB + LB	1.00
C15019-L2	30.58	DB + LB	LTB	30.59	DB + LB	LTB	1.00
C15024-L6	51.50	LB	LB	46.23	LB	LB	0.90
C15024-L4	48.70	LB	LB	44.78	LB	LB	0.92
C15024-L3	50.61	LB	LB	45.84	LB	DB + LB	0.91
C15024-L2	45.22	DB + LB	LTB	41.48	DB + LB	LTB	0.92
C20019-L6	48.00	LB	LB	45.72	LB	LB	0.95
C20019-L4	47.50	LB	LB	43.95	LB	LB	0.93
C20019-L3	40.48	DB + LB	DB + LB	44.33	DB + LB	DB + LB	1.10
C20019-L2	36.70	DB + LB	LTB	39.52	DB + LB	LTB	1.08

1

3.7. Comparison between numerical and experimental results

The ultimate load and main failure mode of cold-formed steel beam obtained from numerical analysis are compared with test results, as summarized in Table 3. It is seen that the ultimate load obtained numerical analysis is consistent with the test results. Table 3 shows that the differences in the FEM-to-test ultimate loading capacity ratio are from 0.90 to 1.11. Table 3 indicates that most of the failure modes of numerical analysis are the same with the test results, except C15024 beam with connector spacing L/3. The load–vertical displacement curves at midspan of C20019 beam are plotted and compared with test results, as seen in Figure 10. The FEM failure modes of C20019 beam are also presented and compared with test results, as seen in Figure 11. It can be concluded that the finite element model predicted with acceptable accuracy about the behavior of cold-formed steel beams. Load capacity increases when the thickness of the steel C-section increases and connection spacing decreases. The FEM curves agree well with the test curves from beginning to maximum loading stage.

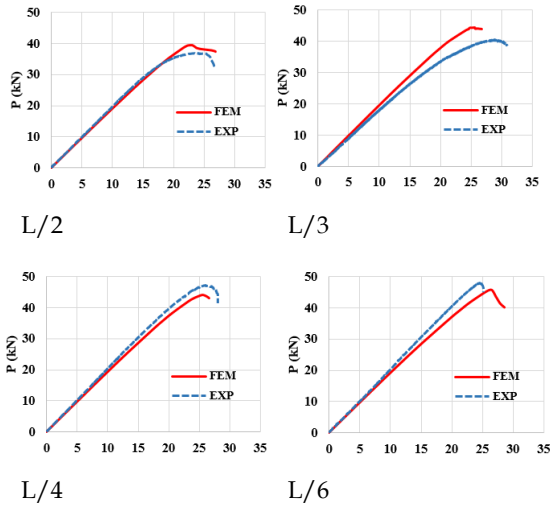

Figure 10 Load–vertical displacement comparison between experimental and numerical results (C20019)

a. L/2

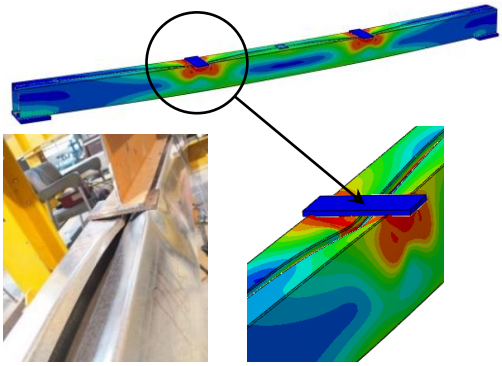

b. L/3

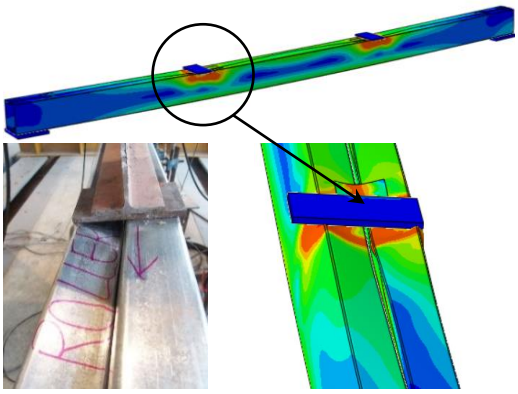

c. L/4

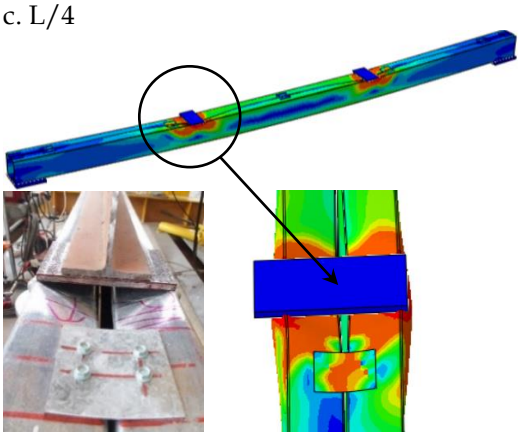

d. L/6

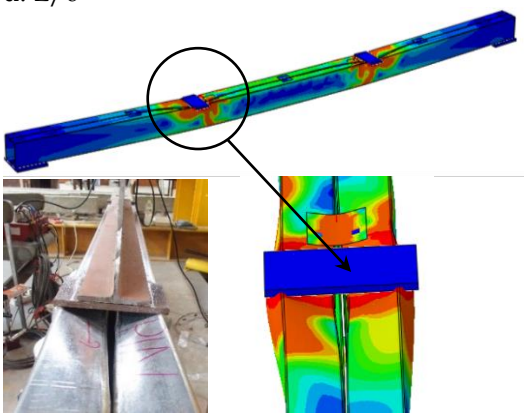

Figure 11 The failure modes comparison between experimental and numerical results (C20019)

4. CONCLUSIONS

The mechanical behaviour of the box beams composed of two face-to-face CFS C-sections under bending conditions consisting of four connection spacing L/2, L/3, L/4 and L/6 with five types of section C10012, C10015, C15019, C15024, and C20019 have been investigated experimentally and numerically. Through the results of the study, the following conclusions are drawn:

- The connection spacing influences on the mechanical behaviour of the built-up box beam considerably. The spacing becomes smaller, the strength of the built-up C-section box beam increases.
- The connection spacing of L/4 provides sufficient connection between the two C-section beams. When the connection spacing is equal or smaller than L/4, the local buckling occurs for all the built-up box beams. Otherwise, the two C-section beams of the built-up box beam may fail in the member buckling mode, such as the lateral-torsional buckling mode, the mixed mode of distortional buckling and local buckling.
- When the connection spacing is equal or smaller than L/4, the horizontal displacement is quite small even at the failure. Otherwise, the load-displacement response deviates from linearity at the early stage of the loading, and large displacement results at the failure.
- The batten plates and the screws did not fail in all experiments tests. Therefore, the screwed connection employed in the present experiment has proved satisfactory.

Based on the results of the study, the recommended design for the box beam composed of two face-to-face CFS C-sections includes the center-to-center connection spacing is L/4 or smaller, and a batten plate (80x80x1.9) is screwed to the top and bottom flanges of the box beam by four 4.8-mm self-drilling screws at the connections.

Finally, the good agreement between the experimental and numerical results proves that the finite element analysis is a useful tool to produce reasonably accurate results. For future research, parametric studies are recommended using the proposed finite

element model to investigate the influence of the thickness, height, beam's length and connection spacings of the beams on its buckling behavior. Based on this parametric studies results, a simple equation could be developed to calculate the ultimate moment capacities of CFS face-to-face C-section beam without conducting all full-scale tests that is inevitably very time-consuming and expensive.

5. ACKNOWLEDGMENTS

The authors are grateful to NS BlueScope Lysaght (Thailand) Limited for providing the CFS beam specimens. The authors would also like to especially thank Mr. Wasan Patwichaichote and the Structures Laboratory of the Chulachomklao Royal Military Academy, Thailand for their supports.

6. REFERENCES

American Iron and Steel Institute, Washington DC, 2016, *AISI Standard: North American Specification for the Design of Cold-Formed Steel Structural Members, AISI S100.*

American Iron and Steel Institute, Washington DC, 2016, *AISI Standard: Cold-Formed Steel Framing Design Guide, AISI D110-16.*

Australia New Zealand Standard, Sai Global Limited, Sydney, 2018, *Cold-formed steel structures, AS/NZS 4600:2018.*

Australia Standards, Sydney, 2007, *Metallic Materials – Tensile Testing at Ambient Temperature, AS 1391:2007.*

Anbarasu, M., 2019, 'Simulation of flexural behaviour and design of cold-formed steel closed built-up beams composed of two sigma sections for local buckling', *Engineering Structures*, 191, 549-562.

Faridmehr, I., Tahir, M. M., Osman, M. H., Nejad, A. F. & Hodjati, R., 2015, 'An experimental investigation of stiffened cold-formed C-channels in pure bending and primarily shear conditions', *Thin-Walled Structures*, 96, 39-48.

Laím, L., Rodrigues, J. P. C. & Da Silva, L. S., 2013, 'Experimental and numerical analysis on the structural behaviour of cold-formed steel beams', *Thin-Walled Structures*, 72, 1-13.

Schafer, B. W., Li, Z. & Moen, C. D., 2010, 'Computational modelling of cold-formed steel', *Thin-Walled Structures*, 48, 752-762.

Wang, H. & Zhang, Y., 2009, 'Experimental and numerical investigation on cold-formed steel C-section flexural members', *Journal of Constructional Steel Research*, 65, 1225-1235.

Wang, L. & Young, B., 2015, 'Behaviour of cold-formed steel built-up sections with intermediate stiffeners under bending. I: tests and numerical validation', *Journal of Structural Engineering*, 142, 04015150.

Wang, L. & Young, B., 2017, 'Design of cold-formed steel built-up sections with web perforations subjected to bending', *Thin-Walled Structures*, 120, 458-469.

Wang, L. & Young, B., 2018, 'Behaviour and design of cold-formed steel built-up section beams with different screw arrangements', *Thin-Walled Structures*, 131, 16-32.

Yu, C., 2016, *Recent Trends in Cold-formed Steel Construction*, Woodhead Publishing.

Yu, C. & Schafer, B. W., 2003, 'Local buckling tests on cold-formed steel beams', *Journal of Structural Engineering*, 129, 1596-1606.

Yu, C. & Schafer, B. W., 2006, 'Distortional buckling tests on cold-formed steel beams', *Journal of structural engineering*, 132, 515-528.

Zhou, X.-H., Shi, Y. & Zhou, T.-H., 2005, 'Cold-formed steel framing system of low-rise residential building', *Journal of Architecture and Civil Engineering*, 22, 1-14.

Patwichaichotea, W., Chaisomphob, T., Yamaguchi, E., Tran, H. T., 2019, 'Bending behaviour of box beam composed of two face-to-face cold-formed steel C-sections', *Proceedings of 9th International Conference on Steel and Aluminium Structures (ICSAS19)*, Bradford, UK, 3-5, 617-627.

NS Bluescope Lysaght Limited, 2014 (http://professionals.lysaght.com/sites/default/files/LysaghtZedCeesPart1July2014.pdf).

Keynote Address

Overview of Chemical Contaminant Behaviors in Groundwater and Subsurface Thermal Pollution as a New Contamination Issue

by

Dr. Takeshi Saito

(Graduate School of Science and Engineering, Saitama University, Japan)

Saito is an Assistant Professor at the Graduate School of Science and Engineering, Saitama University, Japan. He received his PhD from University of Tsukuba in 2011. His main research area is Hydro-geochemistry and Environmental Engineering. He is working on understanding mass and heat transport in soil and groundwater as well as development of environment-friendly remediation technique for soil and groundwater contamination. His current research interests are to understand effect of thermal pollution on behaviors of chemical contaminants in soil and groundwater.

Proceedings of the 7th International Symposium on

Advances in Civil and Environmental Engineering Practices for Sustainable Development

ACEPS - 2019

Overview of chemical contaminant behaviours in groundwater and subsurface thermal pollution as a new contamination issue

Takeshi Saito

Graduate School of Science and Engineering, Saitama University, 255 Shimo-Okubo, Sakura-ku, Saitama, 338-8570, JAPAN.

K e y w o r d s

Groundwater resource
Chemical contaminants
Contaminant behaviours
Subsurface thermal pollution
Groundwater quality
Heavy metals

A B S T R A C T

At least half of the global population depends on groundwater as a source of drinking water and thus, it is highly important to preserve groundwater resource from chemical contaminants. For proper management of groundwater resource, basic knowledge about chemical contaminants and their behaviours in groundwater was presented with overview of current status for the groundwater contamination in Japan. For making its suitable remediation strategy, the importance for understanding behaviours of targeted chemical contaminants in subsurface environment was reaffirmed. Subsurface thermal pollution as a newly possible negative phenomenon and its effect on groundwater quality were also discussed. Recently, subsurface thermal pollution (i.e. temperature increase) has been recognized in many parts of the world. The thermal pollution may trigger changes in physical, chemical, and biological processes in subsurface environment and changes in concentration of several chemical components including heavy metals in groundwater were suggested to occur in a previous study. Because the effect of thermal pollution on groundwater quality has not been sufficiently studied, further research will be strongly needed for making clear the details.

1. INTRODUCTION

Freshwater including groundwater and river water exists with approximately 2.5% out of total water on the earth. Among freshwater resources, the abundance ratio of river water is pretty small and is estimated to be only around 0.006%, while the abundance ratio of groundwater is considerably larger and reaches to almost 30% (Shiklomanov 1998). Especially in developing countries, groundwater is often used for drinking due to the cleanness and less treatment needed (Appelo & Postma 2005).

Actually, at least half of the global population depends on groundwater as the source of drinking water. The usage of groundwater is highly multiple such as agricultural, industrial, and life water purposes. Approximately 2.5 billion people depend only on groundwater for their daily water usage (WWAP 2015). Thus, groundwater is markedly essential for the biosphere on the earth from both qualitative and quantitative aspects as the most promising freshwater resource.

Groundwater is commonly characterized by significantly lower flow rate and longer residence time which is approximately 1500 years as a mean value. On the other hand, river water as one of freshwater resources has an averaged residence time of around 16 days (Shiklomanov 1998). Therefore, it is highly important to preserve groundwater resource from chemical contaminants due to anthropogenic and natural processes.

In this paper, to protect and manage groundwater resource properly, basic knowledge about chemical contaminants and their behaviours in groundwater is presented with an overview of current status for the groundwater contamination in Japan as a case study. Also, subsurface thermal pollution as a newly possible negative phenomenon and its effect on groundwater quality are discussed based on previous studies.

2. CHEMICAL CONTAMINANTS AND THEIR BEHAVIOURS IN GROUNDWATER

There are several types of chemical contaminants in subsurface environment, for example, heavy metals, volatile organic compounds (VOCs), mineral oils and the associated petroleum hydrocarbon, pesticides, nitrate and nitrite, and other compounds including persistent organic pollutants (POPs) and radioactive materials.

Once these chemical contaminants are exposed to soil and groundwater systems, they are gradually transported along with the groundwater flow and the contamination widely spread out. During the transport process, behaviours of chemical contaminants are significantly different from each other and highly depend on their chemical and physical properties.

For example, behaviours of heavy metals including lead (Pb), cadmium (Cd), arsenic (As), chromium (Cr), fluorine (F), and boron (B) are highly complex and depend mainly on pH and Eh (redox potential) of groundwater. Heavy metals existing as cationic forms can be predominantly adsorbed onto soil, sediment, and rock in subsurface environment. On the other hand, heavy metals with anionic forms relatively show less adsorptive property and are sometimes transported to the downstream of groundwater flow. Figure 1 illustrates Eh and pH diagram for As. The chemical form of As (III) is predominant under reductive condition in groundwater and it shows higher toxicity and less adsorptive property compared to the chemical form of As (V). According to Figure 1, the chemical form of As (V) usually exists as anionic form in groundwater.

As described above, behaviours of heavy metals change mainly by pH and Eh of groundwater, however, they are never degraded to non-toxic compounds. Some of chemical contaminants such as tetrachloroethene (PCE) and trichloroethene (TCE) that are categorized as VOCs, and nitrate and nitrite can be biodegraded finally to non-toxic compounds. For example, the principal biodegradation process of PCE is reductive di-chlorination and ethene is finally produced under strong reductive condition in groundwater. The biodegradation process, however, is often incomplete, resulting in the formation of intermediate compounds including vinyl chloride which is more toxic than PCE.

For making appropriate remediation strategy for groundwater contamination, it is highly important to understand behaviours of targeted chemical contaminants in subsurface environment.

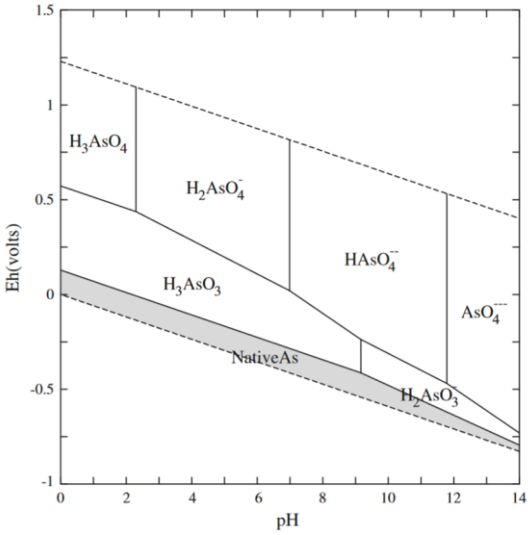

Figure 1 Eh and pH diagram for the system As-O-H at 25°C and 1 bar. Total As concentration is set as 10^{-6} M. Area coloured with grey shows the solid phase (Lu & Zhu 2011).

3. CURRENT STATUS OF THE GROUNDWATER CONTAMINATION IN JAPAN

Figure 2 presents temporal variations of exceeded percentages for several chemical contaminants which exceed environmental criteria in groundwater of Japan. Chemical contaminants which are frequently detected in groundwater are shown in Figure 2 and the monitoring has been carried out in different groundwater wells every year by Ministry of the Environment (Government of Japan). The environmental criteria for nitrate and nitrite, As, F, PCE, TCE, and Pb is 10 mg/L, 10 μg/L, 0.8 mg/L, 10 μg/L, 30 μg/L, and 10 μg/L, respectively.

Nitrate and nitrite are still one of predominant contaminants in groundwater and these contaminants are mainly derived from anthropogenic processes such as excess fertilization and leakages of livestock excreta and sewage. Also, PCE and TCE originate

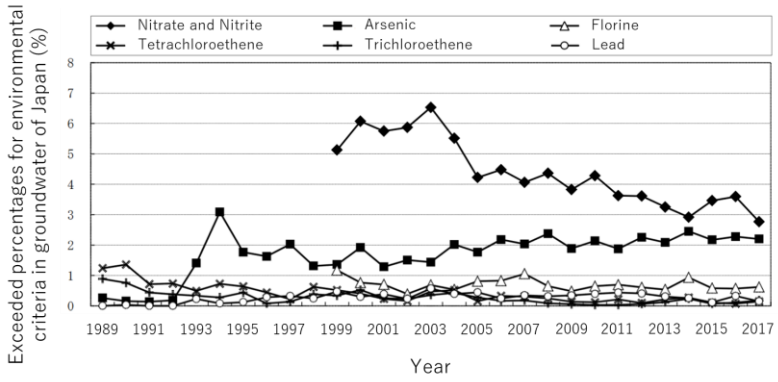

Figure 2 Temporal variations of exceeded percentages for several chemical contaminants which exceed environmental criteria in groundwater of Japan (after Ministry of the Environment (Government of Japan) 2018)

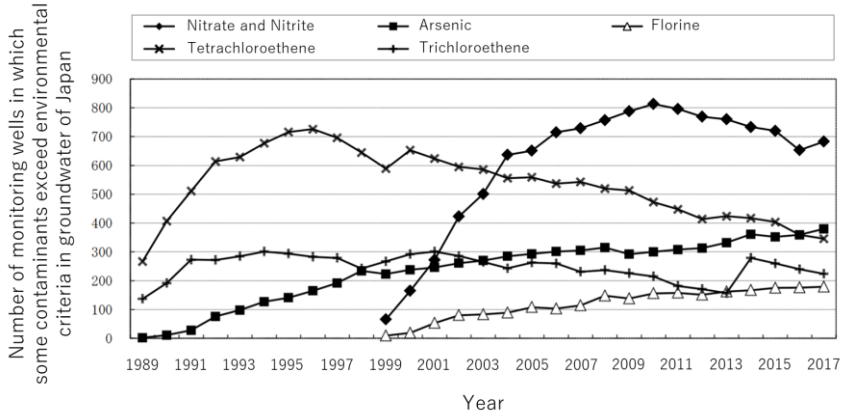

Figure 3 Temporal variations for number of monitoring wells in which some contaminants exceed environmental criteria in groundwater of Japan (after Ministry of the Environment (Government of Japan) 2018)

from industrial activity. Heavy metals including As and F are sometimes released naturally from soil, sediment, and rock in subsurface environment.

In Japan, the continuous groundwater monitoring is carried out, when chemical contaminants are detected in certain wells. This annual groundwater monitoring is continued until the contamination will disappear. The result of this monitoring, that is, temporal variations for number of monitoring wells in which some contaminants exceed environmental criteria in groundwater of Japan are shown in Figure 3. This figure may reflect current status of groundwater contamination in Japan, showing that almost the same chemical contaminants in Figure 2 are detected with high frequency.

Especially in developing countries, the groundwater contamination may not be sometimes recognized as one of serious environmental issues. Therefore, current status of the groundwater contamination in Japan will probably give peoples specially in developing countries important information to effectively deal with groundwater contamination in the near future.

4. SUBSURFACE THERMAL POLLUTION AND ITS EFFECT ON GROUNDWATE QUALITY

Temperature increase in subsurface environment, i.e. thermal pollution, has been observed in many parts of the world (Harris & Chapman 1997; Pollack et al. 1998; Perrier et al. 2005; Taniguchi et al. 2007; Kooi 2008). This phenomenon is suggested to be derived

from surface warming effects such as global warming and urbanization (Huang et al. 2000; Taniguchi et al. 2003). Additionally, large scale underground infrastructure including subways and shopping complexes especially in urban areas can discharge excess heat directly into subsurface environment, resulting in possibility of locally serious temperature increase. This subsurface thermal pollution may trigger changes in physical, chemical, and biological processes in subsurface environment and several possible negative effects such as groundwater quality change are assumed to occur.

Therefore, the author is trying to reveal the effect of subsurface temperature increase on groundwater quality. In-situ, long-term thermal loading experiment has been conducted at the established site of Saitama University in Japan since 2011. In this experiment, thermal loading is given by circulating approximately 40˚C and 60˚C water inside closed loop U-tube heat exchanger installed up to 50 m depth. Based on results by three runs of thermal loading experiment, changes in concentration of several chemical components in groundwater are obtained (Saito et al. 2016). Especially, concentrations of B and As show an increasing trend with increase in subsurface temperature, illustrated in Figure 4 as the example of As.

Because the effect of subsurface thermal pollution on groundwater quality has not been sufficiently studied, further research specially based on in-situ experiment is essentially needed for clarifying the details.

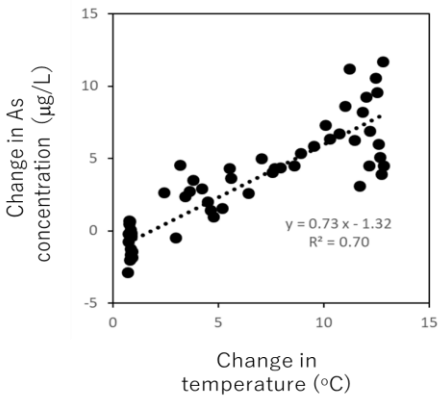

Figure 4 Relationship between changes in As concentration (µg/L) and temperature (˚C) (after Saito et al. 2019)

5. ACKNOWLEDGMENTS

This work was supported from Core Research for Evolutionary Science and Technology (CREST) by Japan Science and Technology Agency (JST), a Grant-in Aid for Scientific Research (no. 26889015 and 16K20954) and Bilateral Joint Research Projects with the National Center for Scientific Research (CNRS) in France by the Japan Society for the Promotion of Science (JSPS), and Research Grants by LIXIL JS Foundation (no. 15-63) and The Iwatani Naoji Foundation, Japan.

6. REFERENCES

Appelo, C.A.J. & Postma, D., 2005, *Geochemistry, Groundwater and Pollution, 2nd Edition*. A.A. Balkema Publishers, Leiden, the Netherlands.

Harris, R.N., & Chapman, D.S., 1997, 'Borehole temperatures and a baseline for 20th-century global warming estimates', *Science* 275, 1618-1621.

Huang, S., Pollack, H.N., & Shen, P.-Y., 2000, 'Temperature trends over the past five centuries reconstructed from borehole temperatures', *Nature* 403, 756-758.

Kooi, H., 2008, 'Spatial variability in subsurface warming over the last three decades; Insight from repeated borehole temperature measurements in The Netherlands', *Earth and Planetary Science Letters* 270 (1-2), 86-94.

Lu, P. & Zhu, C., 2011, 'Arsenic Eh-pH diagrams at 25°C and 1 bar', *Environmental Earth Sciences* 62 (8), 1673-1683.

Ministry of the Environment (Government of Japan), 2018, Monitoring Results of Groundwater Quality in FY 2017 (in Japanese).

Perrier, F., Le Mouel, J.-L., Poirier, J.-P., & Shnirman, M.G., 2005, 'Long-term climate change and surface versus underground temperature measurement in Paris', *International Journal of Climatology* 25 (12), 1619-1631.

Pollack, H.N., Huang, S., & Shen, P.-Y., 1998, 'Climate change record in subsurface temperatures: A global perspective', *Science* 282, 279-281.

Saito, T., Hamamoto, S., Takemura, T., & Komatsu, T., 2019, 'In-situ, long-term thermal loading experiment for evaluating the effect of subsurface thermal disturbance on groundwater quality', *Proceedings of the 13th JGS (Japanese Geotechnical Society) Symposium on Environmental Geotechnics*, Sapporo, Japan, September 10-11, 2019, 29-32 (in Japanese).

Saito, T., Hamamoto, S., Ueki, T., Ohkubo, S., Moldrup, P., Kawamoto, K., & Komatsu, T., 2016, 'Temperature change affected groundwater quality in a confined marine aquifer during long-term heating and cooling', *Water Research* 94, 120-127.

Shiklomanov, I.A., 1998, World Water Resources: A New Appraisal and Assessment for the 21st Century, UNESCO International Hydrological Programme (IHP), Paris, France.

Taniguchi, M., Shimada, J., & Uemura, T., 2003, 'Transient effects of surface temperature and groundwater flow on subsurface temperature in Kumamoto Plain, Japan', *Physics and Chemistry of the Earth A/B/C* 28 (9-11), 477-486.

Taniguchi, M., Uemura, T., & Jago-on, K., 2007, 'Combined effects of urbanization and global warming on subsurface temperature in four Asian cities', *Vadose Zone Journal* 6 (3), 591-596.

WWAP (United Nations World Water Assessment Programme), 2015, The United Nations World Water Development Report 2015: Water for a Sustainable World, UNESCO, Paris, France.

Keynote Address

Uma Oya Multipurpose Development Project – Socio-Environmental Impacts of Tunneling Works and Engineering Challenges of Remedial and Mitigation Works.

by

Mr. Upul Goonasekera

(Uma Oya Multipurpose Development Project, Central Engineering Consultancy Bureau, Uva Province, Sri Lanka)

Mr. Upul Goonasekera graduated from the St Petersburg Mining Institute of the USSR in July 1978 and obtained a MSc degree in Geotechnical Engineering . He obtained a post graduate diploma in Engineering Geology from ITC, Delft, Netherlands in 1989.

He has obtained corporate membership of the Institution of Mining and Metallurgy UK in 1982 and registered as a chartered engineer in Engineering Council of UK. He is a corporate member of IESL since 1992. He has obtained corporate membership of the Institute of Geology in 2017. He started his career as a Geotechnical Engineer/Engineering Geologist in CECB in October 1978 and he was holding an Additional general Manager post by the time he left CECB. During his 40 year professional career in hydropower engineering, he has performed Feasibility Studies of many Hydro Power Projects. He has conducted Geotechnical Investigation in the course of planning study, construction supervision of tunnels and dams, quality control of engineering materials in many hydropower projects that were explored and developed by CECB in collaboration with international consultancy firms. During his career, He has worked as an Engineering Geologist, Geotechnical Engineer, Tunnel Engineer, Dam Engineer, Materials Engineer, and Road Engineer. He worked in the capacity of the Deputy Team Leader of Japanese's engineering consultants to Upper Kotmale Hydro Power Project for a period of 9 years. Since March 2015, he has been working in the capacity of the Chief Resident Engineer/Team Leader –Uma Oya Project.

Proceedings of the 7th International Symposium on

Advances in Civil and Environmental Engineering Practices for Sustainable Development

ACEPS - 2019

Uma Oya Multipurpose Development Project – Socio-environmental impacts of tunneling works and engineering challenges of remedial and mitigation works.

U.S. Goonasekera

Uma Oya Multipurpose Development Project, Central Engineering Consultancy Bureau, Uva Province, SRI LANKA.

K e y w o r d s

Uma Oya Project
Tunneling works
Tunnel Boring Machine
Engineering challenges
Mitigation works

A B S T R A C T

Uma Oya project, the largest multipurpose project in Sri Lanka is being implemented with a huge investment. The primary objective of Uma Oya project is the diversion of part of excess water from the Uma Oya basin to Kirindi Oya basin in order to alleviate water scarcity in the Southern dry zone. Ongoing Uma Oya is subject to many environmental concerns and especially a serious water ingress problem of geological nature was encountered during the Headrace Tunnel excavation which is the first ever tunnel to be excavated with a Tunnel Boring Machine. Excavation was proceeding in fresh gneissic rock, and at Chainage 11160 m, a sudden inrush of water into tunnel caused flooding of face area and tunnel, which caused large cracks on walls and foundations of some houses making them unsuitable for living and dewatering of domestic wells and several springs located over a limited area close to the area of water ingress. To overcome these issues, following remedial actions were considered in these projects, namely; post–grouting of water ingress areas to form a continuous grouted ring around the tunnel, improvement to intensity of pre-grouting, introduction of new chemical grouting materials and additives for cement grouting and improvement to method of prediction of problematic zones for pre-treatment. Probing in combination with pre-grouting and post-grouting, however, permitted continuation of tunnel excavation work minimizing the socio-environmental impact.

1. INTRODUCTION

Uma Oya project, the largest multipurpose project in Sri Lanka is being implemented with a huge investment. This project is expected to deliver many outcomes that included enhancement of hydropower generation of Sri Lanka, provision of drinking water for dwellers in dry areas of southern Sri Lanka and enhancement of agricultural lands. Primary objective of Uma Oya project is diversion of part of excess water from the Uma Oya basin to Kirindi Oya basin to alleviate the water scarcity in the Southern dry zone without affecting the water users and the environment in Uma Oya basin and generate electrical energy using the potential difference between the two basins.

However, the ongoing Uma Oya multi-purpose project is subject to many environmental concerns. Especially a serious water ingress problem of geological nature was encountered during the Headrace Tunnel excavation which is the first ever tunnel to be excavated with a Tunnel Boring Machine (TBM) in Sri Lanka. Also, Uma Oya tunnel happens to be the longest tunnel in Sri Lanka. Social and Environmental impacts caused by water ingress events during tunnel construction at Uma Oya received wide publicity in the print and electronic media as never before.

This paper briefly presents the nature of the problem, technical issues of excavation and the socio-environmental impact of Uma Oya multi-purpose project.

1.1. Purpose of the project and the components of the project

The Uma Oya project involves construction of two new reservoirs namely Dam across Uma Oya at Puhulpola and Dam across Mahathotilla Oya at Dyraaba. A total of 145 MCM of water is diverted to Kirindi Oya and 251 GWh of electricity will be generated by the power house with 120 MW installed capacity. 23 km long tunnel system is to be used to divert water to the southern area of Sri Lanka. This tunnel system consists of 'Main tunnel', 'Link tunnel', 'Tailrace tunnel' and Main components of this project are presented in Table 1.

Table 1 Main components of this project

Components	Description
Two Storage reservoirs	At Puhulpola and Dyraaba in Welimada area
Link tunnel	3.8 Km long running between Puhulpola and Dyraaba reservoirs
Headrace tunnel	15.2 Km long and convey water to power house
Tailrace Tunnel	3.49 Km long and convey water from the power house to downstream irrigation works
Caverns	Underground Power Station with 120 MW installed capacity. [Cavern size 35 m X 18 m X 67 m] Transformer Chamber[Cavern size [18.5 m X 14 m X 37 m]
Shafts	Pressure Shaft (3.2 m diameter, 618 m high) Surge shaft (3.6 diameter, 141 m high) Cable shaft (3.2 m diameter, 58 m high)
Transmission line	27.2 km long

Except the two dams, almost all the other structures are located underground. Total length of tunnels excavated for water conveyance and providing services is about 26 km (Headrace Tunnel-HRT, Link Tunnel, Tailrace Tunnel-TRT, Main Access Tunnel-MAT and other tunnels around powerhouse). Six hundred and eighteen meter deep underground pressure shaft at Uma Oya project is the deepest shaft ever excavated in Sri Lanka. Other two shafts at Uma Oya are 'Surge Shaft' and 'Cable' Shaft. All shaft excavations were executed using Raise boring method. Total estimated cost of Uma Oya Head woks is US$ 514Mn (LKR 76,316,000,000) and funded by Export Development Bank of Iran (EDB) and the Government of Sri Lanka (GOSL).

All the head-works elements of the Uma Oya project are located in the hill country above Wllawaya and the water discharged from the Uma Oya Power station is used to irrigate a large area in Kirindi Oya basin. Development of new lands for agriculture and improvement of water supply to existing large and small irrigation schemes is the main objective of downstream works. Main components of downstream works are listed below.

a) Storage Reservoirs - construction new reservoirs and restoration

- Alikota Ara reservoir (6.5 MCM)
- Kuda Oya reservoir (29.0MCM)
- Modification to existing Handapanagala tank to increase capacity from 6.5 MCM to 14 MCM.
- Restoration of selected existing tanks.

b) Canals

- 36km long Main canal from Alikota Ara to Kuda Oya reservoir .This includes 0.4km and 2.5 km long tunnels.
- 30 km long Main canal From Kuda Oya reservoir to Sinhalayagama Tank.
- 11km long new section of Handapanagala LB canal.

After the completion of this project, apart from the benefits from power generation and irrigation, the public will get several benefits, including drinking water supply from Puhulpola reservoir to Atampitiya area, drinking water supply from Dyraaba reservoir to Bandarawela area, drinking water supply from Kuda Oya reservoir to Hambegamuwa area, livestock and inland fisheries development and employment opportunities

Among many underground excavations of Uma Oya, Headrace tunnel construction has

caused significant environmental issues. 3.5 km long Tailrace tunnel excavated using the TBM did not cause socio-environmental issues. Similarly, 4km long Link tunnel that was excavated using conventional drill and blast method also did not cause environmental issues. Headrace tunnel of Uma Oya project is 15.2 km long and it is the longest tunnel in Sri Lanka (Table 2). Boring method in tunnel construction is used for the first time in Sri Lanka at Uma Oya. Two-track railway system is used for removal of tunnel muck and for other services.

In all the hydropower tunnels in previous projects undertaken in Sri Lanka, excavation was done using Drill and Blast method employing rubber tired vehicles or a railway system for removal of tunnel muck.

Table 2 Parameters of Headrace Tunnel

Parameter	Measurement
Elevation Intake (Invert)	960 masl
Length	15.2 km
Slope	1.0 % and 0.2%
Excavation method	TBM
Excavation diameter	4.3 m
Design Discharge	19.5 m3 /s
Flow condition	Pressure flow
Ground Cover	150-635 m
Note: Tunnel excavation was completed on October 02, 2019	

Owing to its long span, along its route, Uma Oya Headrace tunnel covers major anticlinal and synclinal structures and a large number of steep lineaments. Only, some of those lineaments crisscrossing the tunnel route are represented by steep, open fracture zones. They form a drainage network within the less conductive rock mass.

As the tunnel excavation revealed, major rock types encountered along the tunnel route are as follows.

Rock types

- Charnockitic gneiss
- Quartzo-feldspathic gneiss
- Biotite Gneiss
- Garnetiferous quartz rich gneiss
- Khondalite
- Quartzite
- Impure crystalline Limestone (Marble)

All these rock types belong to the high grade metamorphic rocks. These rocks were in fresh condition throughout the tunnel except for 9 sheared zoned where effects of weathering could be seen. Total thickness of weathered seams is about 200m. The weathered seams mostly showed only moderate water seepage. Such zones were fully lined with concrete segments and subjected to additional consolidation grouting.

2. PROBLEM IDENTIFIED

2.1. Description of First event of water ingress

There are two tunnel boring machines engaged in excavation of Uma Oya Headrace tunnel. Two headings are called US drive and DS drive.

In February 2014, HRT excavation commenced with opening of US drive from the Karandagolla end of tunnel. By the mid December about 3750 m of tunnel had been excavated. Lowest ground cover of 150 m and the highest ground cover of 635 m happens to be within the first 3750m tunnel section. Throughout that length, excavation revealed fresh gneissic rock and thick layers of fresh crystalline limestone. Joint intensity was moderate to low and that again was mostly associated with gneissic rock types. Joints were tight and only occasional minor seepages or dripping water were observed there.

During the night of 24th of December 2014, excavation was proceeding in fresh gneissic rock , and at Chainage 11160 m , a sudden inrush of water into tunnel caused flooding of face area and tunnel. Subsequent inspection revealed that the inflow comes through a system of fresh, steep, open joints. Estimated initial peak inflow from this point is around 400 l/s.

Excavation was stopped to attend to contain the inflow and its effects on excavation. The next day, lowering of water levels were reported from Makulella area located above that area of tunnel. Area of lowering of groundwater levels started as a narrow strip spreading outward from the tunnel. Within two to three weeks areas of water lowering spread through Heel Oya towards Medaperuwa valley occupied by paddy fields and vegetable plots. Several surface springs in paddy fields of Makulella valley also dried up. Adding to that, within the

first few days of this ingress incident large cracks appeared on walls and foundations of some houses making them unsuitable for living.

2.2. Grievance Redress Mechanism for affected people

A survey was conducted over this valley and surrounding area to assess the conditions of buildings and extent of spread of the impact. This survey of condition of buildings was done by a team of engineers, valuers and Gramanildharis. Occupants of houses that suffered major damages were relocated to other safe buildings rented out by the main contractor-Farab Company.

As shown by the survey, effects on majority of the houses were limited to minor hairline cracks. When an affected building showed that the damages could be repaired and further occupation of building poses no danger , compensation were paid to carry out the repairs and no relocation was done. Thus, relocation of families to other area or continuation of occupation of the buildings, and houses were based on the findings of the ground survey.

For families whose domestic wells were affected, a water supply service was established using water tankers. Houses were provided with individual PVC water tanks.

Concurrent with the surveys and remedial works initiated by the client and the contractor, NBRO was requested to initiate an independent study of the situation and report the findings. Sri Lanka Army personnel were mobilized to accelerate the water distribution work. Simultaneously, Disaster Management Centre also initiated a programme of migratory work.

Due to lack of pre-construction base-line data on the condition of buildings of the affected area, the project had to entertain claims on damages caused not only by the lowering of water table but also by other effects not related to the project activities. Thus, a fresh ground survey was launched to collect and monitor existing conditions of buildings, streams and domestic wells located along the remaining part of the tunnel.

In many other projects of Sri Lanka, tunneling works have seen events of dewatering over limited surface areas or some minor caving-in of shallow tunnels. For example, in 1988, excavation of 5.4 km long headrace tunnel of Samanalawewa project encountered a water inrush of 500 l/s coming through open joints in fresh rock. It caused dewatering of domestic wells and several springs located over a limited area close to the area of water ingress. As a remedial measure water delivery service was arranged with tankers to supply water for drinking and other domestic uses. After sealing the ingress from inside the tunnel and filling the tunnel for operation, it took about 12 months for the water wells to recover. Natural springs that went dry also became activated within that period.

2.3. Sealing of the water ingress

The Government of Sri Lanka was extremely concerned about the Environmental issues such as the damages to houses and loss of water in domestic wells at Uma Oya and appointed a Sri Lankan Panel of Experts and also directed the contractor to appoint an international Panel of Experts to study the causes of the water ingress and make recommendations to remedy to the situation.

3. RECOMMENDATION OF EXPERTS

In order to eliminate the negative environmental impact from the encountered ingress, Panel of Experts (POE) recommended post-grouting of that area immediately.

Method of post-grouting treatment recommended by the grouting experts and the details of execution of post-grouting work are described below.

Aim of the recommendations are to minimize occurrence of impact from fresh ingress event in the future and sealing the previously encountered water ingresses.

POE recommendations cover mainly 4 aspects of work.

a) Post –grouting of water ingress areas to form a continuous grouted ring around the tunnel.

b) Improvement to intensity of pre-grouting
c) Introduction of new chemical grouting materials and additives for cement grouting.
d) Improvement to method of prediction of problematic zones for pre-treatment.

3.1. Post-grouting of water ingress areas to form a continuous grouted ring around the tunnel

After pre-grouting work, for long term stabilization of groundwater, it is necessary to seal the permeable areas around the tunnel. For this purpose, a special post grouting programme was conducted in the area behind the excavation heading as the excavation proceeded.

In addition to the sealing achieved by grouting the pea-gravel filling around the segment lining, post-grouting creates an impermeable ring in the rock mass around the tunnel. Thickness of the grouted ring is 4 m and that would isolate the groundwater from the tunnel.

Prost-grouting procedure include drilling of drain holes to relieve pressure to facilitate grouting process. Grouting of rock mass is done using several rounds of grouting through holes arranged in a pattern.

For post grouting Ordinary Portland Cement with additives was used.

3.2. Improvement to method of prediction of problematic zones for pre-treatment

For Prediction of condition of rock mass ahead of the tunnel heading, seismic testing method [TSP] was in place and frequency of testing was increased with more overlap.

- **TSP test**

  With TSP test, about 150 m length of section of rock mass ahead of the tunnel face can be investigated. The test can measure 6 physical property parameters.

  Investigated area is divided into zones based on following properties derived from the test results

  a. P-Wave Velocity(Pressure wave or Primary wave)
  b. S-Wave velocity(Secondary wave or transverse wave) [Vp >> Vs]
  c. Deformation modulus (Dynamic Young's modulus, Shear modulus, Bulk modulus, Poisson's ratio)

  Behavior of such parameters and their combinations are used to make judgments about the ground ahead.

  For generation of seismic waves, in this test, small blasts are done in two shallow bore holes drilled on the tunnel wall behind the TBM shield. To receive the generated seismic waves, 24 seismic receivers are placed in 24 shallow drill holes drilled on the tunnel wall. In order to conduct each TSP test, tunnel excavation has to be stopped for several hours.

- **Probe drilling**

  For improvement of prediction of condition of rock mass, intensity of **probe drilling** was also increased. Though the depth of coverage of this method is less, being a direct test, it has the advantage of easy interpretation.

3.3. Improvement to intensity of pre-grouting

In order to enhance the coverage and density of pre-grouting umbrella ahead of the excavation, a significant improvement to TBM was required. On experts' recommendations, TBM was modified to accommodate more pre-grout-hole positions. With the modification the number of grout-hole positions could be increased from 9 to 27 positions. Excavation was stopped for about 30 days to carry out this modification to the TBM. Inclinations of grout holes from the tunnel axis are 7, 11 and 15 degrees. Target thickness of grouted ring around the tunnel is 6m.

3.4. Introduction of new chemical grouting materials and additives for cement grouting

From the beginning of excavation, pre-grouting of ground was done using water-cement grout mixes using high speed mixers. Depending on the ingress situation chemical additives were used in the grout mixes to accelerate the setting time or enhance the flow properties.

Initially, Ordinary Portland cement (OPC) was used in all grouting works with the additive- RheoBuild1000.

Micro-fine Cement (MFC) that has a rapid, yet controllable setting characteristics was brought in. MFC showed good performance in sealing when used with accelerating additives, Tamcrete 28[from Master Builders] and SA-160[from BASF].

Level of ingress control achievable from the use of OPC became inadequate to control the serious environmental consequences. Thus, Polyurethane foams and quick reacting Polyurethane resins were introduced for grouting work. These chemical grouts in combination with the newly modified array of pre-grout holes were to prevent potentially disastrous concentrated flows. Such chemicals had been successfully used in arresting water ingress in other similar underground works.

Such chemical system are very suitable for sealing of open fissures as they quickly react to generate expanding foam–and the foam does not dissolve in water.

At Uma Oya HRT, following two component polyurethane foam mixes were used for water sealing.

a. Products of TPH Co. of Germany

PUR-O-STOP FS [Resin] with PUR-O-STOP –C [Additive] or PUR-O-STOP –FS-TX [Additive]

b. Products od DIS Co. of Germany

DYWI INJECT PURE 8032 with DYWI INJECT PURE X 8032 FAST [Additive]

When resin component reacts with water they generate expanding foam. The second component acts as a catalyst and helps to increase the thickness of the produced foam.

In pre-grouting, when water flow under pressure, setting up of packers for grouting was a challenge. So, more robust type of packer was introduced.

4. CONCLUSIONS

- Probing in combination with pre-grouting and post-grouting permitted continuation of tunnel excavation work minimizing the socio-environmental impact. Investigation to be conducted from within the tunnel is an essential element for a successful excavation of a tunnel.
- After grouting work and filling the tunnel, ground water would replenish. Though it may take some time (say 1.5-2 years).
- Execution of remedial works arising from the environmental impact required considerable financial resources when compared to the cost of the project.
- Loss of income from power generation and agricultural production nearly over 3 years of delay period in completion of project added to the environmental impact damage.
- Management of the Uma Oya project contract showed contractual complexities involved in underground works with inherent uncertainties arising from geological conditions.

Challenges and Solutions in Geotechnical Engineering

Proceedings of the 7th International Symposium on

Advances in Civil and Environmental Engineering Practices for Sustainable Development

ACEPS - 2019

Enhancement of engineering characteristics of peaty clay using wet cement mixing method

D.S.R.C.V.Perera[1] and N.H.Priyankara[2]

[1] Civil and Environmental Engineer, Geotechnical Engineering Division, National Building Research Organization, Colombo 5, SRI LANKA.
[2] Senior Lecturer, Department of Civil and Environmental Engineering, Faculty of Engineering, University of Ruhuna, Hapugala, Galle, SRI LANKA.

K e y w o r d s

Wet and deep mixing
unconfined compressive strength
consolidation
Rice husk ash

A B S T R A C T

Developments compel the engineers to erect structures on a variety of subsoil conditions varying from the desired to the worst founding soil i.e. peaty clay in Sri Lankan context. Some prominent projects in Sri Lanka are facing the issue of peat being the thick founding soil on which to build new structures. Construction on peat leads to substantial problems during the construction and long-term settlements during the service due to its lower shear strength and higher compressibility. Disposal of peat and refilling with fair soil, despite the fact that inadmissible environmental impacts occur, is also being practiced. Preloading efforts have also been practiced which have yielded long-term strength gain pattern owing to lengthier less intense loading, for soil having low shear strength avoiding sustaining a higher load once inhibiting accelerated workflow. The cement mixing strategy is one of the most environmentally friendly and economically feasible ground improvement techniques, acknowledged around the world. The sui generis purpose of the strategy is to enhance sub-soil characteristics by in-situ mixing the soil with cement and other binders replacing cement to optimize the cost. In this research, the effect of wet cement mixing on improvement of strength and compressibility of peaty clay were assessed.

1. INTRODUCTION

Nowadays, infrastructures have been dramatically increased in the developing countries. In Sri Lanka, most of the infrastructure development projects, such as expressway constructions are on-going at locations where there are soft soils with substantial thickness. For example, Southern Expressway Extension Project and Outer Circular Expressway Project are going through an area underlain with very soft peaty clays. Peaty clay gives rise to enormous geotechnical engineering problems due to its high water content, very low shear strength and very high compressibility. As such, peaty clay does not provide favourable conditions for construction on them. Therefore, Geotechnical Engineers face challenges in the construction of expressways through sites underlain with thick layers of peaty clay.

Improvement of existing soft soil to an adequate level and use of deep foundations to transfer the loads to an underlying competent soil layer are the two options available. With the developments of roads that occupy a large plan area, improvement of the in-situ ground condition be-comes the more viable option.

The deep mixing method is a world-wide accepted ground improvement technology at present (Souliman 2011). The unique purpose of this method is to improve strength parameters of soft soil by in-situ mixing with cement and other additives.

Although deep mixing technique has been successfully utilized to improve soft soil in other countries such as Japan and Sweden for more than 2 decades, it has been adopted in Sri Lanka to improve soft peaty clay in very recently (Saputhantiri & Kulathilaka 2011). Even though, in Sri Lanka, many researchers

have done laboratory scale studies on cement mixing technique, nowhere in the country has adopted this technique in the field for stabilizing soft organic clay or soft inorganic clay. In some of the recent infra-structure development projects in Sri Lanka, cement mixing technique has been proposed to improve the soft soil at the initial stage, however it has not been implemented due to many reasons, such as; not sufficient shear strength gain after mixing soft soil with cement at the laboratory scale tests and technical issues related to soil-cement mixing in the field. As such, remove and replacement method has been adopted instead of deep mixing technique without considering the environmental effect.

Cement mixing is considered as one of the most efficient and economical methods to improve soft soil, even though it is not yet successfully implemented in Sri Lanka. Hence, in this research study, attempts have been made to improve the engineering characteristics of soft peaty clay mixing with cement and other industrial by-products such as Rice Husk Ash (RHA).

2. METHODOLOGY

2.1. Material

Table 1 Basic properties of peaty clay

Property	Value
Natural moisture content	177 %
Bulk unit weight	11.38 kN/m^3
Specific gravity (Gs)	2.03
Organic content	23 %
Liquid Limit (LL)	155 %
Plastic Limit (PL)	61 %
Plastic Index (PI)	94 %
Linear shrinkage	8 %
pH value	5.3
Void ratio(e_0)	4.56
Compression Index (C_c)	1.57
Modified Compression Index (C_c')	0.28
Swelling Index (C_s)	0.06
Undrained shear strength (C_u)	12.0 kN/m^2

Soft peaty clay samples were collected from Nilwala flood plain where Southern Expressway Ex-tension Project is going on. Since deep mixing technique was rejected in this project without conducting any comprehensive study, applicability of the deep mixing technique for above ground condition was studied under this research. Basic properties of the peaty clay are illustrated in Table 1.

Commercially available Ordinary Portland Cement (OPC) was used as the main binding material and Rice Husk Ash (RHA) was used as the pozzolanic additive. RHA was collected from Brick kiln at Tissamaharama area.

2.2. Sample Preparation

Remoulded peaty clay samples were used for the laboratory test. Prior to each test, large debris, un-decayed pieces of wood, gravel particles and un-wanted particles were removed. After remoulding, peaty clay was kept in a water bath for few days to make sure that soil is fully saturated. With the objective of improving the engineering characteristics soft soil, soft peaty clay was mixed with cement slurry and RHA at different mix proportions as shown in Table 2. Sample prepared by mixing nine parts of peaty clay (90 %) with one part of cement (10%) on weight is designated as PC10. In similar lines, in samples PC20 and PC30, cement content was 20% and 30% respectively. Unimproved peaty clay is represented as PC0. Sample prepared by mixing eight parts of peaty clay (80 %) with one part of cement (10 %) and one part of RHA (10%) on weight is designated as PC10RHA10.

Peat was obtained from Nilwala flood plain where expressway projects are underway. RHA was collected from domestic brick kilns in Thissamaharama area. Initial basic properties Wet cement slurry was prepared by keeping a water to cement ratio of 0.3. Mix proportions were selected on weight basis and in order to ensure uniform level of mixing, all samples were mixed in the concrete mixer at same rotation speed of 60 revolutions per minute for a period of 10 minutes. For each mix proportion, 5 test cubes, which are 150 mm x 150 mm x 150 mm dimensions, were cast-ed. After 24 hours, steel moulds were removed and soil-cement blocks were submerged in a water bath for curing to simulate the field condition. One test cube from each mix proportion was tested for

compressive strength after 14 days where as 3 test cubes were tested after 28 days to evaluate the short term stabilization. The remaining test cube was tested after 100 days to evaluate the long term stabilization.

Oedometer samples with diameter of 50 mm and thickness of 20 mm were prepared for each mix proportion and these specimens were kept under submerged conditions for 28 days. Then oedometer tests were conducted for each specimen to find the improvements in the compressibility characteristics.

3. RESULTS AND DISCUSSION

3.1. Effect of Cement on Strength Improvement

The unconfined compressive strength of improved peaty clay is illustrated in Table 2. Figure 1 clearly illustrated that unconfined compressive strength of soft peaty clay is significantly increased with the increase of cement content. Effect of curing period on strength gain is also illustrated in the same figure. Similar to the concrete, it can be clearly seen that strength gain of soil-cement mixtures after 14 days is about 70% of that of 28 days strength. Further, it can be noted that unlike the strength gain trend of concrete, cement slurry treated peaty clay exhibit the effect of long term curing, where there is a considerable strength gain after 100 days. In longer duration, much time is available for Ca2+ irons in the cement to get attached with soil particles and to occur flocculation and thereafter the pozzolanic reaction. This implies, cement hydration and pozzolanic reaction occur for a long period of time after mixing, as such strength of cement treated peaty clay is in-creased with time. Note that by mixing 10% of cement with peaty clay, 28 days unconfined compressive strength could be increased to about 1 MPa.

3.2. Effect of RHA on Strength Improvement

The variation of unconfined compressive strength of peaty clay improved with 10% cement over Rice Husk Ash (RHS) is shown in Figure 2. Based on the results, it can be seen that unconfined compressive strength gradually increases with the addition of RHA. Due to presence of about 88% of SiO2 within the RHA enhance the development of secondary cementitious product. However, when the RHA content is more than 20%, unconfined compressive strength is drastically decreased irrespective of the curing period. Addition of RHA by replacing cement may cause to reduce the Ca2+ iron content within the peat-cement mixture. As such, even though SiO2 increases with the addition of RHA, the secondary cementitious product will not develop, resulting low strength. Similar behaviour can be observed with higher cement percentages on peat-cement mixtures. Hence, it can be concluded that addition of 10% cement together with 20% RHA is effective in increasing the 28 days unconfined compressive strength of peaty clay to more than 2 MPa.

Table 2 Strength of improved peaty clay

Mix Proportion	Unconfined compressive strength q_u(MPa)		
	After 14 days	After 28 days	After 100 days
PC0	C_u=12 kPa		
PC10	0.71	0.97	1.14
PC20	2.42	3.43	4.40
PC30	5.45	6.76	7.11
PC10-RHA10	2.04	2.73	3.25
PC10-RHA20	2.23	3.37	4.64
PC10-RHA30	0.73	1.47	1.57
PC20-RHA10	5.60	7.13	7.89
PC20-RHA20	3.15	5.76	7.77
PC20-RHA30	1.31	1.37	1.47
PC30-RHA10	13.80	15.57	22.9
PC30-RHA20	17.18	21.59	25.37
PC30-RHA30	5.31	6.40	7.16

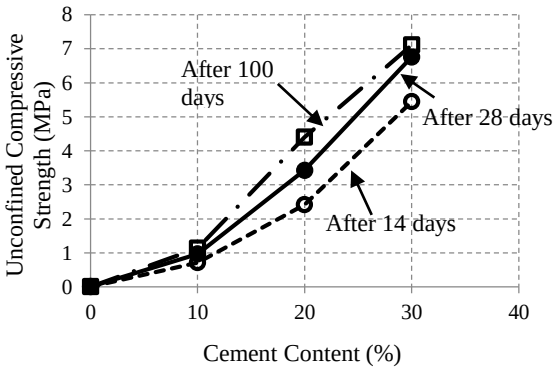

Figure 1 Effect of cement on unconfined compressive strength

3.3. Variation of e Vs Log (σ_v') relationship

Variations of primary consolidation characteristics were illustrated through *e* vs log (σ_v') plot and results are summarized in Table 3. The typical plots for 10% cement treated peaty clay together with RHA are presented in Figure 3. It can be clearly seen that initial void ratio significant reduced with the addition of cement. The combine use of cement and RHA can further reduce the initial void ratio. Similar to the strength behaviour, when the RHA content is more than 20%, initial void ratio has been increased.

It can be observed that modified compression index {$C_c/ (1+e_0)$} significantly decreased with the cement content. Just adding 10% of cement, modified compression index could be reduced by an order. A noticeable reduction in modified compression index could be achieved by combining RHA with cement.

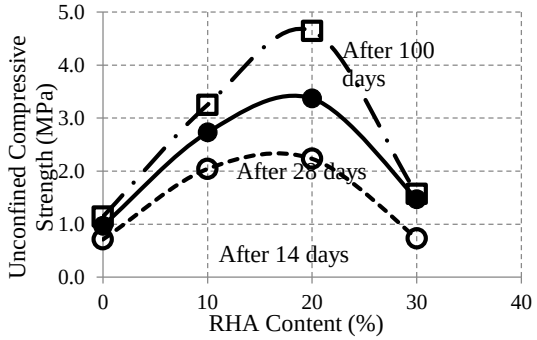

Figure 2 Effect of RHA on unconfined compressive strength

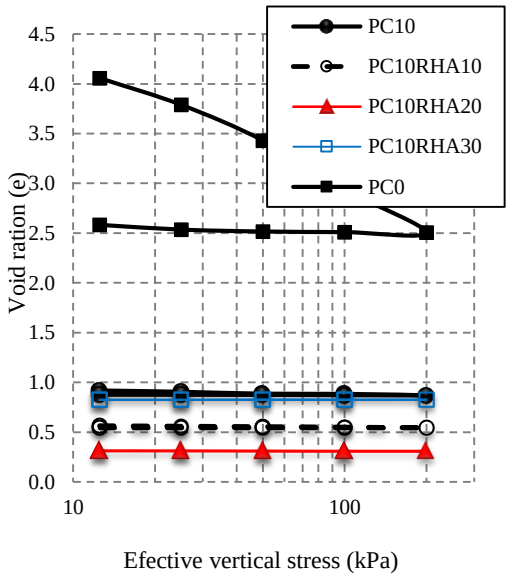

Figure 3 *e* vs log (σ_v') relationship for 10% cement treated peaty clay

3.4. Variation of coefficient of volume compressibility

Coefficient of volume compressibility (mv) can be considered as an alternative parameter for estimating settlement. It was evaluated at each and every stress level. The influence of cement and RHA on mv is illustrated in Figure 4. The figure clearly illustrated that mv values were drastically reduced when the peaty clay mixed with cement. mv value has been further reduced with the addition of RHA.

Table 3 Consolidation characteristics

Mix Proportion	e_0	C_c	$C_c/(1+e_0)$
PC0	4.560	1.5700	0.2820
PC10	0.922	0.0532	0.0277
PC20	0.756	0.0199	0.0113
PC30	0.411	0.0099	0.0070
PC10-RHA10	0.565	0.0149	0.0095
PC10-RHA20	0.322	0.0066	0.0050
PC10-RHA30	0.836	0	0
PC20-RHA10	0.431	0.0099	0.0069
PC20-RHA20	0.320	0.0150	0.0114
PC20-RHA30	0.442	0	0
PC30-RHA10	0.121	0.0033	0.0029
PC30-RHA20	0.236	0.0121	0.0098
PC30-RHA30	0.353	0.0033	0.0024

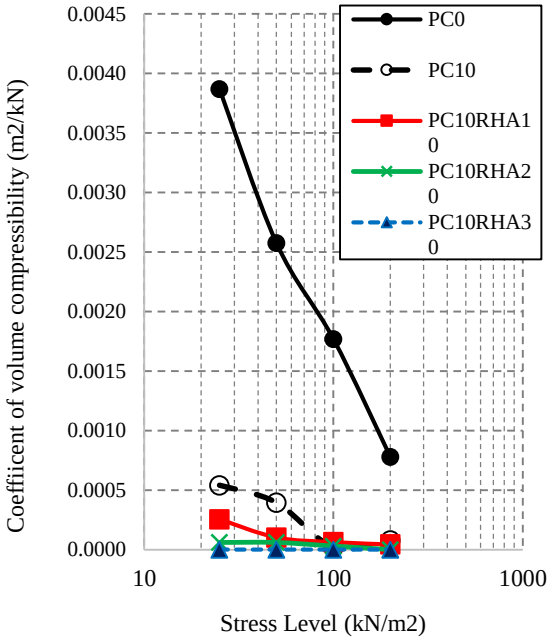

Figure 4 Variation of m_v with stress level

3.5. Scanning Electron Microscope (SEM) Analysis

The behaviour of unconfined compressive strength and compressibility characteristics over varying cement and RHA contents could be justified by the Scanning Electron Microscope (SEM) observations where material interlock and bond structure were the key parameters. Figure 5 shows the SEM images of untreated and treated peaty clay. The irregular shapes of the peaty clay particles together with voids are shown in Figure 5(a). Particles have been changed to more flocculated structure after mixing 10% of cement with peaty clay as depicted in Figure 5(b). Irregular shapes of the peaty clay have been changed to slightly bar shapes due to formation of secondary cementitious material. This behaviour has been further improved after mixing with RHA as shown in Figure 5(c).

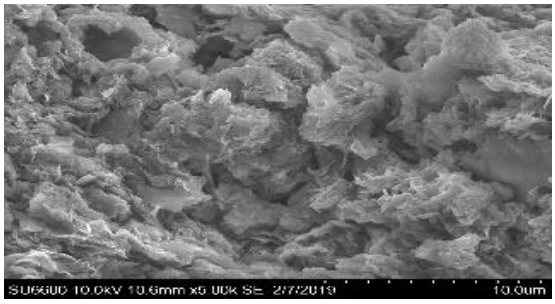

(a) PC0

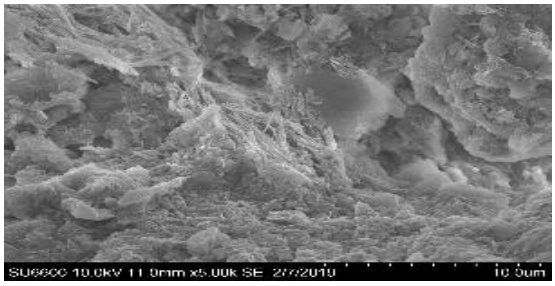

(b) PC10

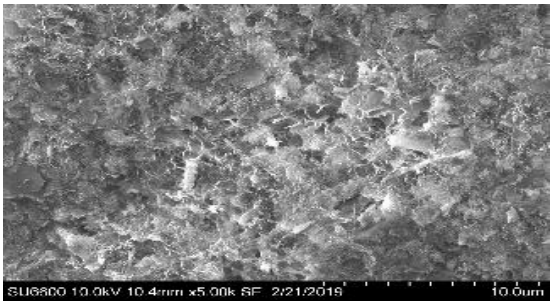

(c) PC10RHA10

Figure 5 Change of microstructure

4. CONCLUSIONS

Wet deep mixing provides higher improvements in terms of both unconfined compressive strength and compressibility. 28 days unconfined compressive strength of cement treated peaty clay was more than 3 MPa when the cement content is more than 20%. However, the usage of high amounts of cement as the sole stabilizing agent for wet deep mixing is not cost effective. Considerable improvements could be extracted from 10% of cement with added 10% RHA despite the fact it was less than that of the 20 % cement mixes. 100 days unconfined compressive strength illustrated that cement hydration and pozzolanic reaction can last for long period of time after mixing. Compressibility characteristics of peaty clay were significantly improved by mixing with cement. By adding RHA to peat-cement mixes, compressibility characteristics could be further reduced. Thus it could be concluded that 10% of wet cement slurry together with 10% of RHA would be the ideal combination to improve soft peaty clay with respect to both economy and structural fit.

5. REFERENCES

Saputhantiri D.R & Kulathilaka S.A.S, 2011, 'Enhancement of Engineering Characteristics of Peaty Clay due to Mixing with Cement', *Annual Transactions of Institute of Engineers Sri Lanka*, 118-126.

Souliman, M.,2011, 'International Case Studies of Peat Stabilization by Deep Mixing Method', *Jordan Journal of Civil Engineering*, Irbid: Jordan University of Science and Technology.5(3), 424-430.

Proceedings of the 7th International Symposium on

Advances in Civil and Environmental Engineering Practices for Sustainable Development

ACEPS - 2019

Influence of grouting pressure on pullout resistance of soil nail

R.G.F.Harshini[1] and N.H.Priyankara[2]

[1]Department of Civil and Environmental Engineering, Faculty of Engineering, University of Ruhuna, Hapugala, Galle, SRI LANKA.
[2] Senior Lecturer,Department of Civil and Environmental Engineering, Faculty of Engineering, University of Ruhuna, Hapugala, Galle, SRI LANKA.

K e y w o r d s

Soil nailing
Pullout resistance
Grouting pressure

A B S T R A C T

Soil nailing is an in-situ reinforcement technique that is being increasingly used in slopes, especially cut slopes, to improve the stability of slopes. Advantages such as short construction period and low cost are the main reasons for its increasing popularity. Furthermore, it is very suitable for stabilizing slopes in congested areas where access of heavy equipment is a problem. The pullout resistance of soil-nail is an important factor in design. The pullout resistance of soil-nail is mainly influenced by the soil–nail inter-face shear strength. Experience and previous research have shown that grouting pressure increases the soil–nail interface shear strength. It is common practice with soil-nail construction to adopt gravity or low pressure grouting. The use of grouting pressure is an effective way of increasing the soil nail pullout resistance. However, the mechanism of how the grouting pressure influence the pullout resistance of soil-nails is not well understood. As such, in this research study, laboratory scale model setup was used to study the effect of grouting pressure on pullout resistance.

1. INTRODUCTION

Soil nailing technique is a quite flexible construction method to stabilize, preserve and rehabilitate both existing and new manmade earth structures (Hong 2013 & Tokhi *et al* 2016). This versatile construction method has implemented in many countries due to its benefits; such as low construction cost, easy procedure, minimum construction period and utilization of machinery in the congested area (Chan *et al* 2005 & Su *et al* 2008). A soil nail, basically a passive reinforcing slender structure without pretension, typically in the form of steel bar, is installed in a pre-drilled hole and encased with cement slurry (Tokhi *et al* 2017). When a soil nailed slope is sliding down, the soil nailing system in the stabilizing zone, which already installed beyond the critical failure surface and it subjects to pull-out force by the moving of soil mass (Zhou *et al* 2009). In a design perspective, the pullout resistance of the soil nail is a crucial factor. It depends on mainly the interface shear strength between soil-nail and surrounding soil (Yin *et al* 2006). However, the pullout resistance of a soil-nail system is arduous to estimate because of the uncertainties in the field, such as soil dilation, grouting pressure, drilling method, soil properties, overburden pressure etc. (Zhang *et al* 2009).

Although most of the soil nails have been installing commonly without grouting pressure, the pressure grouted nail can be enhanced the interface shear strength of soil nails (Yin *et al* 2009). Pressure grouted soil nail has many advantages compared to conventional gravity flow or low pressure grouting methods. However, the mechanism of how grouting pressure influences the interface shear strength of soil nail is still not well understood. As such, this research study focuses on the effect of grouting pressure on the pullout resistance of soil nail by laboratory-scale model setup. Furthermore, experimental studies were simulated by numerical software (PLAXIS 2D) inoder to comare the laboratory results.

2. METHODOLOGY

2.1. Materials

Commonly available lateritic soil was used as the test material. The basic properties of soil are depicted in Table 1. It was classified as well-graded sand (SW) according to the Unified Soil Classification System (USCS).

Table 1 Basic properties of Lateritic soil

Property	Value
Optimum Moisture Content (%)	17.53
Maximum Dry Unit Weight (kN/m^3)	17.0
Specific Gravity (G_s)	2.39
Coefficient of Uniformity (C_u)	6.39
Coefficient of Curvature (C_c)	1.09

2.2. Laboratory model setup

Figure 1 depicts the fundamental arrangement of the laboratory setup, which encompasses pullout box, portal frame and grouting cylinder. The internal dimensions of the box are 600 mm in length, 460 mm in height and 600 mm in height. A lubrication oil was applied on the internal surfaces of the box to reduce the friction between soil and the steel surfaces. After which, the well-graded sand was compacted into the steel box.

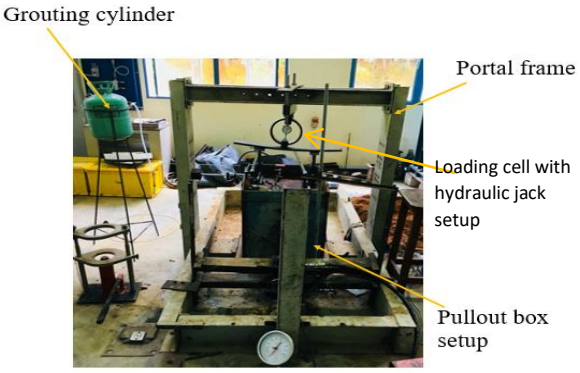

Figure 1 Laboratory setup

An additional chamber was connected to the end of the box with the dimension of 280 mm (length) X 130 mm (width) X 130 mm (height). This chamber was filled with the same compacted soil, which was compacted in the box. A horizontal hole was drilled from the front end of the steel box to 200 mm into the additional chamber by hand auger. Afterwards, a nail was inserted into the pre-drilled hole with centralizers and grouted with cement slurry. After curing, soil in the additional chamber was removed and it could be seen that 200 mm of the length of the part of the grouted nail was at the outside of the steel box. Therefore, during the pullout test, the nail can be fully contacted with soil within the steel box up to 200 mm of horizontal displacement.

Soil nail was grouted by grouting cylinder, which consists of three valves, namely grout inlet, grout outlet and inlet for compressed air (Figure 1). Grouting pressure was controlled through values which were fixed at grout outlet and air pressure inlet.

2.3. Laboratory test procedure

The soil was compacted into the steel box with 90% of the maximum dry unit weight (15.3 kN/m^3) and moisture content was 17.00%. The soil was filled with compacted layers having 50mm of thickness. A total of five Earth Pressure Sensors (EPS) were embedded into the soil at three different depths. 3 number of EPS were installed at 40 mm above the soil nail interface at near to the nail head, middle and tail. Other two EPS were placed 100 mm away from both the top and the bottom of the steel box surface, as shown in Figure 2. The cross-section of the laboratory model together with instruments is shown in Figure 2.

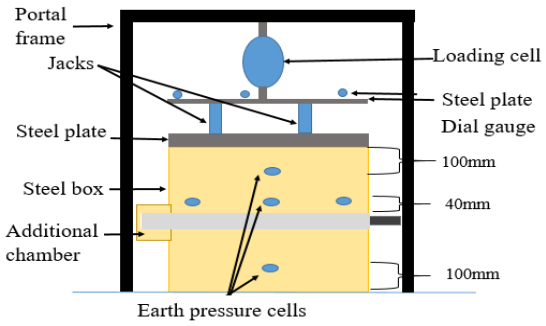

Figure 2 Cross section of laboratory model setup

After the soil compaction, the top cover of the steel box was fixed. Then, constant vertical pressure was applied to the top of the box by jacking two hydraulic jacks (simultaneously) fixed to the rigid portal frame and monitored by a load cell (see Figure 2). The vertical pressure should be applied before the drilling to investigate the stress-release of soil during the drilling. At this stage, EPS were begun to recorded by a computer-controlled data acquisition system. From the data, it can be

observed that all five EPS were experienced an equal amount of applied vertical pressure plus self-weight of the soil that was above them. Once the readings were reached at a constant value (the compacted soil in the equilibrium stage), after about 24 hours from the application of vertical pressure, 50 mm diameter of a horizontal hole was drilled manually from the front of the steel box to 200 mm into the additional chamber by a hand auger. A ribbed steel bar (diameter – 10 mm) was installed at the center of the pre-drilled hole with centralizers.

The hole was grouted with specified grouting pressure for each test. Four numbers of model tests were conducted with varying grouting pressure from 40 kPa to 100 kPa at intervals of 20 kPa. Water-cement ratio of cement grout was kept as 0.5 by weight (Pradhan *et al* 2006). The nonshrinkage admixture was mixed with cement slurry to increase flowability and harden period.

The compressed air was applied at the grouting cylinder which pushed down the cement slurry through the plastic tube into the pre-drilled hole.

According to Yin *et al* (2009), cement slurry could gain sufficient strength after 5 days of curing. Then pullout test was conducted using a hydraulic jack and pullout force readings were noted together with horizontal displacement manually. Throughout the test, EPS readings were recorded using a computer control data acquisition system.

2.4. Numerical Analysis

Numerical modelling was done using PLAXIS-2D software in order to simulate the conditions of the laboratory model setup for a soil-nail interface to obtain the pullout resistance numerically. The input geometry of the model is shown in Figure 3 and input parameters were obtained through numerical equations, laboratory tests and Rawat & Gupta (2016) guidelines. A prescribed overburden pressure was assigned to the input geometry. Grouting pressure was simulated by applying a surcharge load, which is equivalent to the grouting pressure, surrounding the soil nail system. Pullout forces were obtained by applying prescribed displacements to the nail head. Horizontal sdisplacements were varied up to 60 mm at 5 mm interval and the frictional stresses developed at the soil nail interface were resulted from the model analysis. The analysis was done in staged construction mode and the stresses at each phase were resulted from the analysis.

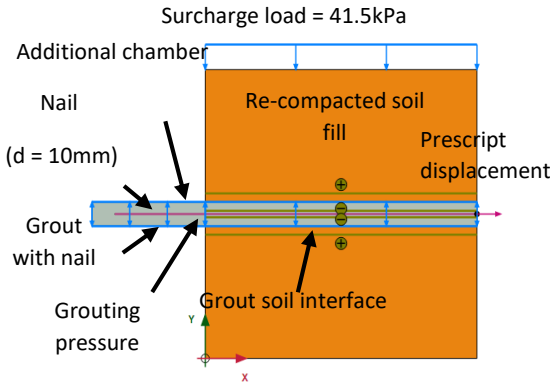

Figure 4 Input geometry of PLAXIS 2D model

3. RESULTS AND DISCUSSION

3.1. Variation of earth pressure during the soil compaction and EPSs installation

Change of earth pressure during the application of overburden pressure of 40 kPa is depicted in Figure 4. Soon after the application of the surcharge, earth pressures indicate slightly higher overburden pressure than the actual due to movement of the soil particles in contact with EPS.

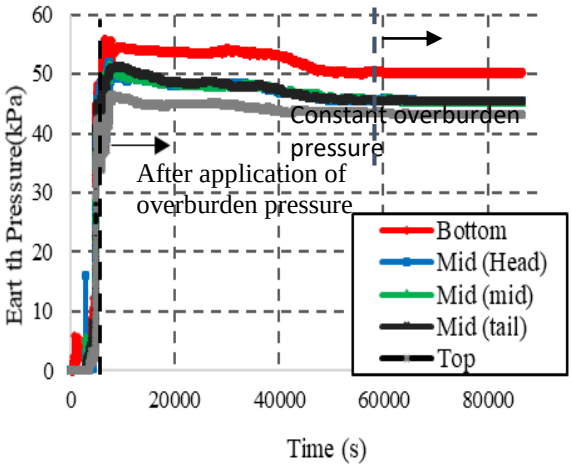

Figure 4 Variation of earth pressure due to application of overburden pressure

After about 16 hours, there is no any changes in the measured earth pressures indicating that the vertical stress of the soil has reached to constant and reflected the applied overburden pressure.

3.2. Variation of earth pressure during drilling, nail installation and grouting

During the drilling for nail installation, vertical pressure is reduced due to stress release in surrounding soil. As such, normal stress on the nail may vary during the installation indicating the importance of simulation of stress release and examination of earth pressure variations. This behaviour is clearly illustrated in the Figure 5. From the figure, it can be observed that earth pressure has slightly increased due to outward movement of the soil particles during the drilling operation. Once the drilling tool had passed the location of the EPS, earth pressure has reduced due to release of stress. Further, it can be noted that earth pressure has reached to slightly equilibrium condition before apply the grouting pressure. A rapid increase of earth pressure could be observed at middle EPS at about 1100 second owing to the action of pressure grouting. The pressure increase was lasted for about 8 minutes and then pressure has reduced and reached to equilibrium; this value is approximately equal to the pressure before grouting.

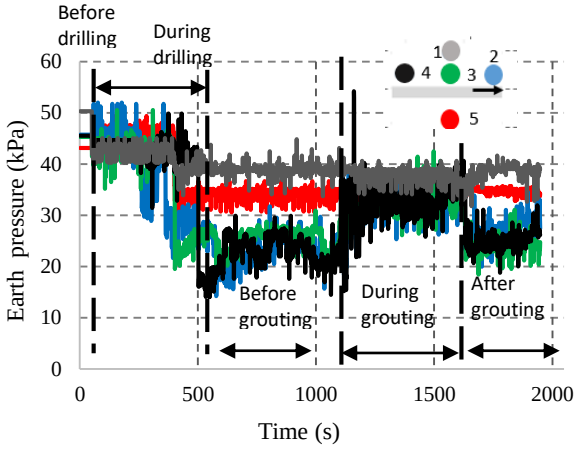

Figure 5 Variation of earth pressure during drilling, nail installation and grouting

This pressure reduction was due to hardening effect of cement grout and reasons are described below,

- The cement slurry had a sufficient amount of water as the water-cement ratio was 0.5. During the grouting, water, which was consist of cement slurry, was absorbed by the surrounding soil. As a result, the pressure was declined due to dissipation of water pressure in the grout.
- Once the pre-drilled hole was compacted with cement slurry, there was no further grout transition into the hole. Therefore, grouting pressure could not be increased or maintained.
- Harding of cement slurry increased with time, as a result, no further grout transition into the pre-drilled hole.

3.3. Pullout resistance

Figure 6 illustrates the measured pullout force plotted against nail head displacement under an overburden pressure of 40 kPa and grouting pressure of 40 kPa, 60 kPa, 80 kPa and 100k Pa. It can be seen that pullout force increases with the grouting pressure. During the drilling of a hole to install nail, surrounding soil of the hole is loosened and soil-arching effect developed to retain the soil above the hole. During the pressurized grouting, the hole is compacted with cement slurry. Further, cement grout has penetrated into the voids of loosened soil particles around the drill hole and solidify the soil particles, resulting increase the bond strength. The higher the grouting pressure, greater the increase in bond strength. This could be further verified by inspecting the grouted nail diameter after the test as presented in Table 2. Even though predrilled hole diameter is 50 mm, with the grouting pressure, grouted nail diameter is more than 50mm. Greater the grouting pressure, larger the grouted nail diameter. As such, pullout resistance increases with grouting pressure.

Table 2 Grouted nail diameter over grouting pressure

Grout pressure (kPa)	Grouted nail diameter (mm)
40	54.94
60	57.06
80	59.60
100	62.90

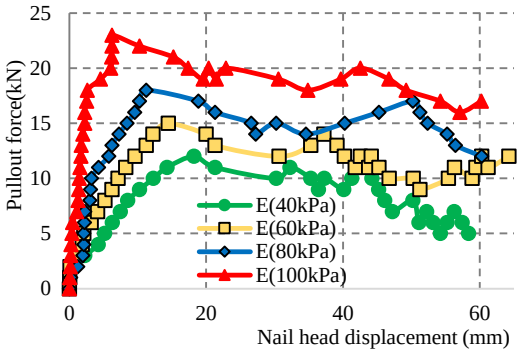

Figure 6 Variation of pullout force over nail head displacement (E – Experimental results)

3.4. Variation of earth pressure during pullout test

The earth pressure variation during pullout test is shown in Figure 7. There is no any variation of earth pressure away from the nail (nails at top and bottom) indicating that effect of pulling of nail to the surrounding soil is localized. It can be seen that earth pressure close to nail head had increased to highest value at peak pullout force. The pressure response of EPS at middle and tail of the nail were delayed when com-pared with that of EPS at nail head. This is a clear indication that gradual transfer of stresses from soil to the nail.

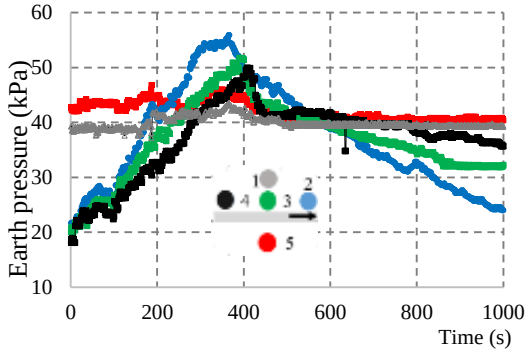

Figure 7 Variation of earth pressure during pullout test

3.5. Comparison of experimental results with numerical results

The comparison of the experimental results and numerical results over grouting pressure is shown in Figure 8. It can be noted that numerical results are well agreed with the experimental results. The comparison of peak pullout forces on experimental and numerical analysis is illustrated in Figure 9. It is very clear that peak pullout forces determined based on both methods are almost same indicating the accuracy of the parameters adopted for the numerical modelling.

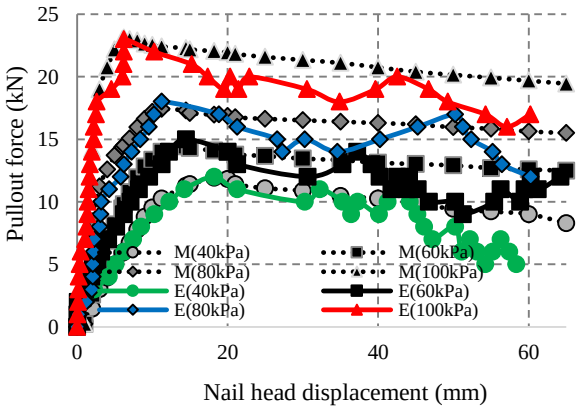

Figure 8 Comparison of experimental and numerical results (M-Model results and E-Experimental results)

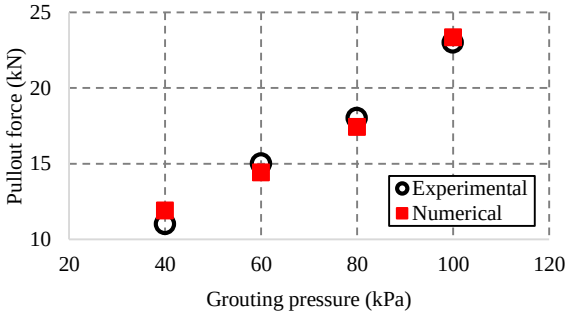

Figure 9 Comparison of peak pullout results

The development of higher earth pressure close to the nail head during pullout test is associated with the greater shear displacement. This behaviour could be clearly illustrated numerically as shown in Figure 10, where greater shear stress has developed near the nail head. As such, greater shear displacement has occurred close to the nail head resulting higher earth pressure. Further, it can be clarified through relative displacement of soil particles within the steel box as shown in Figure 11.

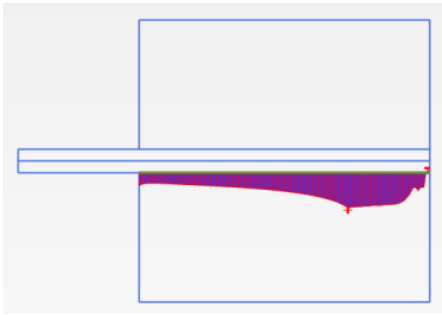

Figure 10 Variation of interface shear stress along the nail during pullout test

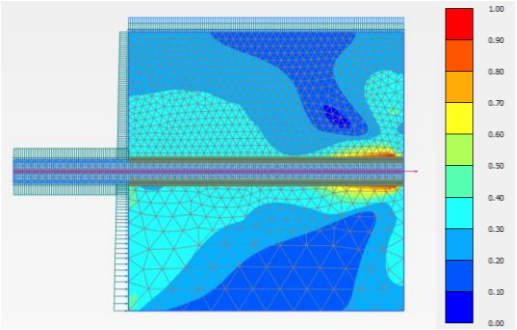

Figure 11 Relative displacement of soil during the pullout of soil-nail

4. ACKNOWLEDGMENTS

Authors wish to thanks to Department of Civil and Environmental Engineering, University of Ruhuna who support to carry out this research work with success.

5. CONCLUSIONS

- The earth pressure surrounding hole has dropped during the drilling to place nail due to release of stress.
- By increasing the grouting pressure, pullout resistance could be significantly increased.
- Greater earth pressure was developed close to the nail head than that of tail during pullout of nail due to development of higher shear displacement close to the nail head.
- The stresses of soil were gradually transferred to nail starting from nail head to the nail tail during the pullout of nail.

6. REFERENCES

Hong, C.Y., Yin, J.H., Pei, H.F. & Zhou, W.H., 2013, 'Experimental study on the pullout resistance of pressure-grouted soil nails in the field', *Canadian geotechnical journal*, 50(7), 693-704.

Pradhan, B., Tham, L.G., Yue, Z.Q., Junaideen, S.M. & Lee, C.F., 2006, 'Soil–nail pullout interaction in loose fill materials', *International Journal of Geomechanics*, 6(4), 238-247.

Rawat, S. & Gupta, A.K., 2016, 'Analysis of a nailed soil slope using limit equilibrium and finite element methods', *International Journal of Geosynthetics and Ground Engineering*, 2(4), 34.

Su, L.J., Yin, J.H. & Zhou, W.H., 2010, 'Influences of overburden pressure and soil dilation on soil nail pull-out resistance', *Computers and Geotechnics*, 37(4), 555-564.

Tokhi, H., Ren, G. & Li, J., 2016, 'Laboratory study of a new screw nail and its interaction in sand', *Computers and Geotechnics*, 78, 144-154.

Tokhi, H., Ren, G. & Li, J., 2017, 'Laboratory pullout resistance of a new screw soil nail in residual soil', *Canadian Geotechnical Journal*, 55(5), 609-619.

Yin, J.H. & Su, L.J., 2006, 'An innovative laboratory box for testing nail pull-out resistance in soil', *Geotechnical Testing Journal*, 29(6), 451-461.

Yin, J.H., Su, L.J., Cheung, R.W.M., Shiu, Y.K. & Tang, C., 2009, 'The influence of grouting pressure on the pullout resistance of soil nails in compacted completely decomposed granite fill', *Geotechnique*, 59(2), 103-113.

Zhou, W.H., Yin, J.H. & Hong, C.Y., 2011, 'Finite element modelling of pullout testing on a soil nail in a pullout box under different overburden and grouting pressures', *Canadian Geotechnical Journal*, 48(4), 557-567.

Proceedings of the 7th International Symposium on

Advances in Civil and Environmental Engineering Practices for Sustainable Development

ACEPS - 2019

Study the behavior of load transfer platform of geosynthetic reinforced piled embankments using a numerical model

S.K.E.Sanjaya[1] and N.H. Priyankara[1]

[1]Department of Civil and Environmental Engineering, Faculty of Engineering, University of Ruhuna, Hapugala, Galle, SRI LANKA.

K e y w o r d s

Piled Embankment
Geosynthetic Reinforcement
Finite Element Analyze
Load Transfer Platform
Soil Arching
Collin Method

A B S T R A C T

The construction of infrastructure on soft soils such as peat incurs many challenges for Geotechnical Engineers due to huge consolidation settlement. Geosynthetic Reinforced Piled Embankments can be considered as a groundbreaking solution, which could use to reduce surface settlements, cost and construction period. Even though, this method has been successfully utilized in the construction industry, still load transfer mechanism of piled embankment is unclear due to complexity of the behavior of the load transfer platform. As such, in this research study, 2 different load transfer mechanisms such as BS8006 and Collin's method were analyzed using Plaxis 2D software. BS 8006 method assumes that vertical stress distribution across the base of the embankment is non-uniform whereas Collin's method assumes that reinforcement creates a stiffened beam of reinforced soil to distribute the load enacted by the embankment to the columns. Plaxis 2D analysis was carried out by observing the settlement, lateral displacement of the embankments and pile, vertical stress on the ground surface, forces and bending moments in piles by varying parameters of pile cap size, thickness of load transfer platform, pile spacing and number of geosynthetic layers. Finally, most suitable cost effective and technical feasible load transfer mechanism is presented in the research study.

1. INTRODUCTION

Ground improvement techniques are widely using all around the world to enhance the stability and to reduce the settlements in construction on soft soil. Preloading, preloading with wick drains, deep mixing, and dynamic compaction could be conveyed as most popular ground improvement techniques. Selection of the ground improvement technique may depend on the soft soil layer thickness, Parameters of the soft soil layers, accessibility, available time and the cost. While preloading considers as a reliable option when the soft soil layer is between 4m-10m, piles could be acquired when the week layer thickness is more than 10 m and also when the construction time is limited.

Pile embankment technique is an improvement of pile foundation technique. Initially pile embankments were designed with closer corner piles or inclined piles as shown in Figure 01 and with a concrete slab acting as a pile cap to transfer the embankment loads to the piles.

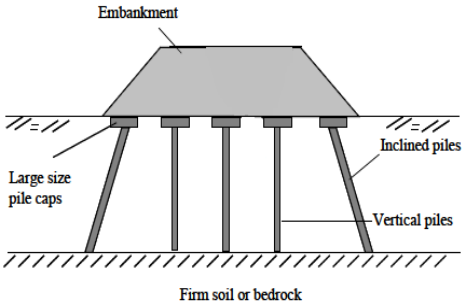

Figure 1 Conventional Pile Embankment System

The construction of said pile cap type slab has incurred high construction cost and difficulties in workmanship. Anyhow with the development of Geosynthetic materials and techniques, designers realized that the use of

geotextile layers as load transfer platform (LTP) in pile embankment construction could support to overcome the weaknesses of the slab component. Recently, Geosynthetic Reinforced Pile Supported Embankments (GRPE) have become popular among Geo technical engineers due to the cost and time affectivity.

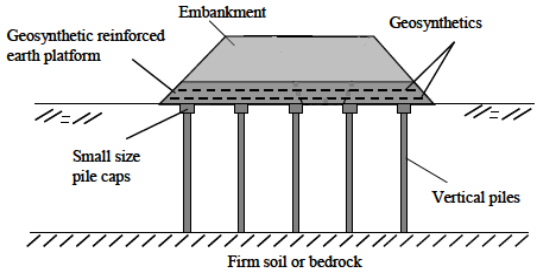

Figure 2 Geosynthetic Reinforced Pile Supported Embankment (GRPE) system

The construction sequence of the GRPE could be explained as follows. As shown in Figure 02, after installation of piles in equal spacing a comparably small pile cap would place on the top of the pile. Consequently, geosynthetics and compacted earth platform would be laid in-order to transfer the embankment loads to the piles. Since the load transfer mechanism is complex inside the platform, several researchers have developed several methods to explain the composite behaviour of this system. These design procedures were developed considering the arcing ability of soil, tension capacity of the Geosynthetic membrane and composite behaviour.

In this study, a comparison was done among several developed methods assisting numerical models to the evaluate the best suitable method to fulfil the serviceability conditions.

2. SOIL ARCHING

Soil arching ability contribute to a significant portion of the function of the load transfer platform. Soil arching normally consider as "the ability of material to transfer loads from one location to another in response to a relative displacement between locations.
A majority of the currently available design methods assumes that the embankment load is transferred to the piles by the soil arching mechanism introduced by Terzaghi (1943). Guido *et al.* (1987) proposed a design approach based on model tests performed on sand in a rigid box with multiple layers of geogrid reinforcement. Hewlett and Randolph (1988) presented a semi-spherical arching model to describe the load transfer mechanism based on their three-dimensional model tests. However, the effect of geosynthetic reinforcement on the load transfer mechanism was not considered in this method (Ariyarathne & Liyanapathirana.2014).

3. GEOSYNTHETIC TENSION

In GRPE, addition to soil arching, the load transfer platform design relies on the geosynthetic developing resistance to tension. The vertical load from the soil within the arch and any surcharge load, if the thickness of the embankment is not great enough to develop the full arch, is carried by the reinforcement.
Composite behaviour of both Soil arching effect and the tensile capacity of the geosynthetic layers need to be understood while studying the mechanism of the load transferring platform.

4. PILED EMBANKMENT DESIGN METHODS

Load transform platform can essentially be designed using two methods. In the first method, reinforcement functions as a catenary and is the one that is employed by the British Standard, the Swedish and the German approaches. Through the reinforcement, the load is shifted from the embankment fill to the piles by passing through catenary tension in the strengthening. The reinforcement essentially functions as a structural component and any advantages obtained by the development of compound strengthened soil mass are disregarded.

The other methodology to develop the LTP, called the Collin Method, is occasionally called the Guido Method. The Collin Method of reinforcement employs multiple reinforcement layers to develop a stiff reinforced soil mass. The reinforced soil mass functions as a beam that shifts the LTP over the platform to the piles beneath. (Ramesh 2014)

5. FINITE ELEMENT ANALYSING METHODS (FFM)

Finite element analysing methods (FFM) are widely using to solve complex structural and geotechnical designs.

Plaxis software is considered as one of the most reliable effective software to analyse complex geotechnical problems. In this study Plaxis 2D v 8.3 was utilized to model the GRPE problem using an FEM approach. The effects of certain factors like pile modulus, stiffness of the geosynthetic reinforcement, height of the embankment, effect of the soil layer directly below the Geogrids which are not considered by other available methods are studied using a finite element program – Plaxis 2D.(Rutugandha Gangakhedkar).

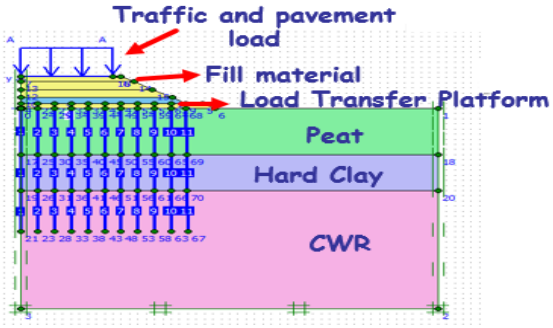

Figure 2 Geosynthetic Reinforced Pile Supported Embankment (GRPE) system

In this study Plaxis models were developed for LTP with only a ABC layer, with only Pile Caps, using single geosynthetic layer to represent the BS method and using three geosynthetic layers to represent Collins method. For each arrangement the ABC layer Thickness, Pile Spacing and Pile Cap Size was varied and observed the maximum settlement at the top of the embankment, maximum settlement at the top of the Geosynthetic Reinforcement, Axial Force of each pile, Bending Moment of each pile. As shown in Figure 2, soil profile consists of a 9mthick Peat layer with a 7m hard clay soil layer below that. Underlying the hard clay layer, there is a Completely Weathered Rock (CWR) layer, 23m thickness. The height of the embankment is 5.2 m he cress width of the embankment is 24m and the side slopes are 1:1.5. The processes of the construction considered in the analysis as follow.

- Stage 01 2.0 m height embankment construction (Period is 28 days)
- Stage 02 2.0 m height embankment construction (Period is 28 days)
- Stage 03 2.0 m height embankment construction (Period is 28 days)
- Stage 04 1.5 m height embankment construction (Period is 28 days)
- Stage 05 Defect liability Period with 20kN Traffic load (Period is 300 days)
- Stage 06 20kN Traffic load (Period is 1080 days)

6. RESULTS

A shown in Figure 3, it was observed that the settlement of embankment is decreasing with the incensement of the pile cap size. There is also a significant reduction of settlement with the addition of Geosynthetic Reinforcement with the same total stiffness to the LTP.

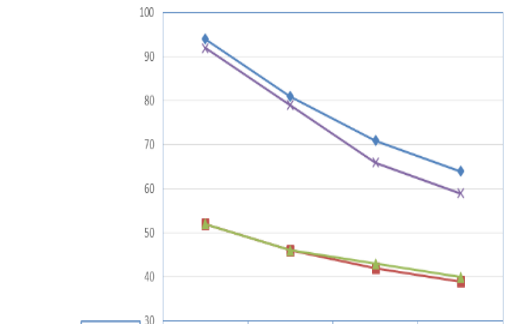

PILE CAP SIZE	1	1.2	1.4	1.6
With 1200mm ABC Layer	94	81	71	64
With 2400mm ABC Layer	92	79	66	59
1 layer -600/50	52	46	42	39
3 layers -200/50	52	46	43	40

Figure 3 Settlement(mm) of the Embankment Considering Different Pile Cap Sizes (m)

The pile spacing also had a pronounced effect on the maximum settlements recorded during the numerical analysis as shown in Figure 4. Maximum settlements decreased for the decrease in pile spacing, for both reinforced and unreinforced cases at both settlements monitored locations.

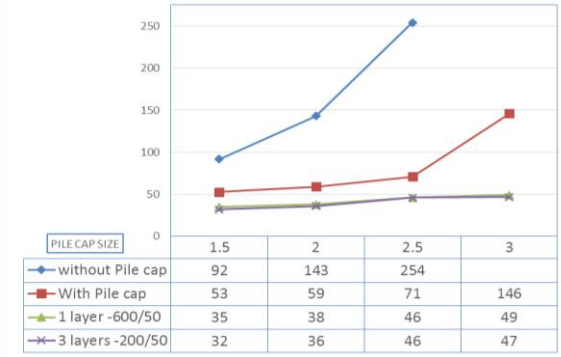

PILE CAP SIZE	1.5	2	2.5	3
without Pile cap	92	143	254	
With Pile cap	53	59	71	146
1 layer -600/50	35	38	46	49
3 layers -200/50	32	36	46	47

Figure 4 Settlement(mm) of the Embankment Considering Different Pile Spacing(m)

As shown in Figure 5, the inclusion of geosynthetic reinforcement had a significant influence on the vertical stress distribution between the piles, on the LTP and on the geosynthetic reinforcement layers.

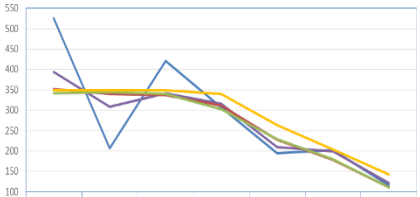

Pile From Center	2→	3→	4→	5→	6→	7→	Edge Pile
With 1200mm ABC Layer	525	207	421	306	195	201	116
With 1.2m Pile cap	395	308	342	316	210	199	121
BS8006 Method	352	339	337	311	228	178	111
Plaxis-Collin Method	341	345	339	303	229	179	111
Manual Calculation	349	349	349	339	264	203	143

Figure 5 Axial Load(kN) on Piles for Different LTF Arrangements

The bending moment variation graph shown in Figure 6 also follows the same arrangement. With the increment the number of geotextiles, the LTP getting more stiff and the top end of the pile is acting as a fixed support.

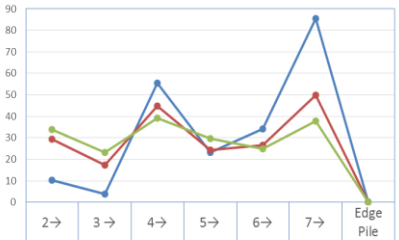

	2→	3→	4→	5→	6→	7→	Edge Pile
With 1.2m Pile cap	10.36	3.86	55.62	23.23	34.1	85.5	0.193
BS8006 Method	29.28	17.33	44.9	24.23	26.51	50	0.228
Collins Method 33.9	33.9	23.18	39.15	29.56	24.89	37.9	0.228

Figure 6 Bending Moment(kN/m/m) on Piles for Different LTP Arrangements

7. CONCLUSIONS

Even though increasing the ABC layer thickness have reduced the settlement in the embankment, the reduction is not sufficient to design a feasible embankment. Hence it could be concluded to fulfil the serviceability requirements, that the Geosynthetic Reinforcement is mandatory in Piled embankment construction.

Increasing pile spacing and decreasing the pile cap size vidently reduce the load transfer to piles from the embankment and surcharge. This leads to the decrease of efficiency due the increase of geosynthetic tension and soil arching. Ultimately, this will also upsurge the maximum and differential settlements of the embankment.

Another concern regarding the geosynthetics is that the sufficiency and possible advantages of using several layer of geosynthetics in construction. According to this study, there is no significant effect to the embankment settlement or total settlement from the increasing the no of geotextiles with the same total tensile capacity in the load transfer platform. However, this should be confirmed from future research works in order to optimize the design.

BS 8006 method and Collin method assumed a uniformly distributed load on the geosynthetic layer but the numerical analysis results do not conform this assumption. Anyhow, it could be concluded that the increasing the number of geosynthetic layers have a significantly effect to the variation of axial load and bending moment among the piles used in the embankment. Hence, the conclusion could be made that the inclusion of geotextiles has enhance the stiffness of the LTF and makes transfer of the embankment load to piles much more efficiently.

Even though the BS 8006 and Collin method are not providing piercing guidelines to consider the bending moment on pile, according to the numerical analysis the valves are significant. Since, inclusion of geotextiles have enhanced the stiffness of the LTF and could reduce the variation of the bending moment the inclusion will positively affect to the long term stability of the piles.

8. REFERENCE

Rutugandha Gangakhedkar, 2004, 'Geosynthetic reinforced pile supported embankments', *Graduate school of the University of Florida.*

Priyanath Ariyarathne & D.S. Liyanapathirana, 2014, 'Review of existing design methods for geosynthetic-reinforced pile-supported embankments'.

Ramesh Gangatharan, 2014, 'Comparison between piled embankment and load transfer platform – rigid inclusion for soft soil',*University of Sydney.*

Proceedings of the 7th International Symposium on

Advances in Civil and Environmental Engineering Practices for Sustainable Development

ACEPS - 2019

Advancements in rail track technology: application of rubber elements in rail track for sustainable transport infrastructure

S.K. Navaratnarajah[1]

[1]Department of Civil and Engineering, Faculty of Engineering, University of Peradeniya, Peradeniya, Sri Lanka

K e y w o r d s

Ballast
Degradation
Under Sleeper Pads
Under Ballast Mats
Cyclic Load
Shear Load

A B S T R A C T

Railway industries are placing greater emphasis on implementing fast and heavy haul corridors for bulk freight and commuter transport to deliver more efficient and cost-effective services. It is imperative that rail networks be enhanced to meet the increasing demand for transport from a growing, ageing and urbanizing population. Improving railroad stability to operate fast passenger trains and heavy haul freight services has become one of the key challenges in many countries including Sri Lanka. The deterioration of a rail track due to large dynamic wheel loads is inevitable and that leads to more frequent high-cost maintenance. This problem is more critical in isolated rail track locations where the ballast is in direct contact with much stiffer interfaces such as bridges and tunnels and in locations where heavier concrete sleepers are used. One measure used to minimize track deterioration in these isolated places is the use of rubber elements at the hard interfaces. In recent years, the use of soft synthetic rubber elements in track foundations to alleviate track damage has become increasingly popular. This study focuses on a comprehensive assessment of the geotechnical characteristics and the associated response of ballast under cyclic and shear loading. This study proves that by using rubber elements in the track, the deformation and the degradation can be significantly curtailed, and the durability of the track can be enhanced. A substantial reduction in ballast breakage and extended track longevity would embrace blatant 'green' implications (i.e. less quarrying and environmental degradation) while accruing substantial annual savings to the rail asset owners. Some of the rubber elements used in this study were manufactured from the recycled shredded tire. In terms of national benefits, manufacturing these rubber mats from recycled rubber tires would reduce their volume at spoil tips and contribute to more effective land use, especially in expensive urban suburbs.

1. INTRODUCTION

The rail networks in many countries play a prominent role in the conveyance of bulk freight and commuter transport. The railway industries are emphasizing the implementation of high train speed corridors and heavier freight operations to achieve efficient and cost-effective services. However, increased train speeds and higher freight loads accelerate the deterioration of the track foundation, which in turn increases the maintenance costs. A major proportion of track maintenance funds is spent on the geotechnical related problems of the substructure, including the frequent removing and cleaning and replacing the ballast layer (Indraratna *et al* 2002; Ionescu *et al* 1998; Navaratnarajah & Indraratna 2017). The engineering behaviour of ballast is one of the most important aspects governing the stability and performance of a railway track because its progressive degradation under heavy cyclic loads from freight and passenger trains contributes largely to overall track deformation (Indraratna *et al* 2011). This, therefore, necessitates a thorough understanding of the geotechnical behaviour of the ballast layer, if the costs of track maintenance are to be reduced.

Rail tracks are subjected to faster deterioration in sections where (i) a reduced ballast thickness is used; (ii) in locations where heavier concrete sleepers are used; and (iii)

track on stiff subgrades (e.g. track on bridges). From a structural viewpoint, the damping capacity of the track at these locations is inadequate. In this respect, using resilient pads underneath the concrete sleepers (i.e. Under Sleeper Pads - USPs) and resilient mats on top of a stiff subgrade (i.e. Under Ballast Mats - UBMs) are popular ways of restoring the resiliency of stiffer track substructure. Resilient elements are also a better alternative to reduce the thickness of the ballast and/or subballast layers, which makes reducing the amount of quarrying raw materials (aggregates) and eliminating the difficulties of compacting thicker substructure layers. Apart from reducing track stiffness, USPs increase the contact area between sleeper and ballast which leads to a reduction in stress transmitted from the sleepers to the substructure layer (Navaratnarajah *et al* 2018; Sol-Sanchez *et al* 2014). This ultimately helps to distribute the wheel load to more adjacent sleepers. These rubber elements also even out the differences in stiffness along transition zones and turnouts (Loy, 2009). While USPs are more suitable to increase the elasticity of track, UBMs are more efficient in reducing the excessive rate of ballast deterioration if it is placed on top of stiffer substructures such as bridges and tunnels (Navaratnarajah & Indraratna 2017; Navaratnarajah *et al* 2016; Nimbalkar *et al* 2012). In terms of performance, UBMs installed in stiffer foundations are much more effective than mats installed in a track built over soft soil subgrade (Indraratna *et al* 2014). However, studies conducted to analyse the effectiveness of UBMs in minimising ballast deformation and degradation under cyclic loading are limited.

The primary objectives of this research study are to assess the stress-strain and degradation behaviour of ballasted rail track and verify its performance when resilient rubber elements (USPs and UBMs) are used in track foundation to stabilise the ballast materials. Large-scale process simulation triaxial testing was conducted to evaluate the stress-strain and degradation characteristics of ballast with and without USP and UBM. As the track foundation is consists of a layered system, the interface of different elements plays a significant role in influencing the overall shear behaviour of the track. Therefore, the interface behaviour of ballast with sleeper materials (concrete and timber sleepers) and rubber elements also evaluated in this study.

2. LARGE-SCALE TESTINGS

To assess the role of USPs and UBMs in more detail, a series of cyclic loading tests were conducted using the state-of-the-art large-scale Process Simulation Prismoidal Triaxial Apparatus (PSPTA) at the University of Wollongong, Australia. The PSPTA simulates a unit cell of Australian rail tracks as shown in Figure 1. The triaxial chamber of the PSPTA which simulates the track unit cell is shown in Figure 2.

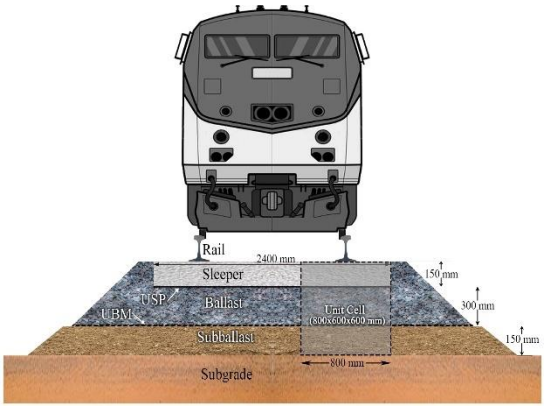

Figure 1 Rail track and Track Unit Cell

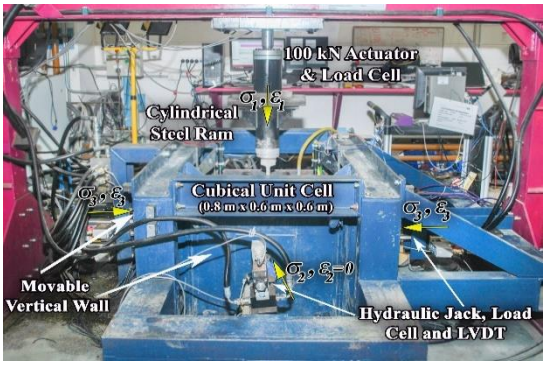

Figure 2 PSPTA Cubical Triaxial Chamber

The size of the cubical triaxial chamber is 0.8 m × 0.6 m × 0.6 m. This apparatus can realistically simulate the stress and boundary conditions found in ballasted track. In a real rail track, lateral movement of the ballast is not fully restrained, particularly parallel to the sleepers (Indraratna *et al* 2001). Therefore, the four vertical walls of the PSPTA chamber were built to allow free movement under applied cyclic loading. In this study, only two walls parallel to the sleeper were allowed to move

under low confinement, the other two walls were locked in a position to simulate a typical straight track (longitudinal deformation parallel to the rail is negligible).

To evaluate the interface behaviour of the ballast materials with rubber and other sleeper elements, direct shear tests were conducted at the University of Peradeniya using the large-scale shear apparatus shown in Figure 3. The shear chamber of this apparatus is 0.3 m high and 0.4 m diameter. Details of the test materials and their specifications and the cyclic and shear load test procedures are discussed in the following section.

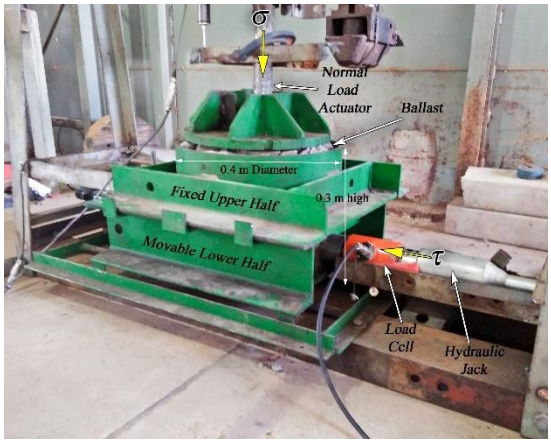

Figure 3 Large-Scale Shear Apparatus

2.1. Test Materials

The test materials used in this study were fresh ballast, subballast, synthetic UPSs, UBMs made from recycled tyre waste, concrete base, concrete sleeper and interface materials made from concrete and timber sleepers. The fresh ballast and subballast tested for cyclic load tests were obtained from the Bombo quarry, near Wollongong, New South Wales (NSW), Australia which commonly used in NSW rail tracks. The ballast for the shear test was obtained from a stock pile of Railway Department near Gampola Station, Sri Lanka which stored for use in Central Sri Lanka rail tracks. The ballast and subballast samples were prepared in accordance with current Australian and Sri Lankan practices for Cyclic and Shear tests, respectively. The laboratory ballast samples were cleaned by water to remove any dust and clay adhering to the surface of the aggregates and dried before screening through selected sieves and then mixed in desired proportions to obtain the required particle size distribution (PSD). The PSD of the ballast and subballast materials are shown in Figure 4. Subballast was used as the base materials when conducting cyclic load tests with and without USP placed under the concrete sleeper. To simulate a hard subgrade condition such as a rail track over a concrete bridge, a reinforced concrete base was placed underneath the ballast layer and cyclic load tests were conducted with and without UBMs palced on top of the concrete base. The USPs and UBMs used in this study are 10 mm in thickness and the bedding modulus are 0.22 N/mm^2 and 0.20 N/mm^2 and the unit weights are 4.2 kg/m^2 and 9.2 kg/m^2, respectively.

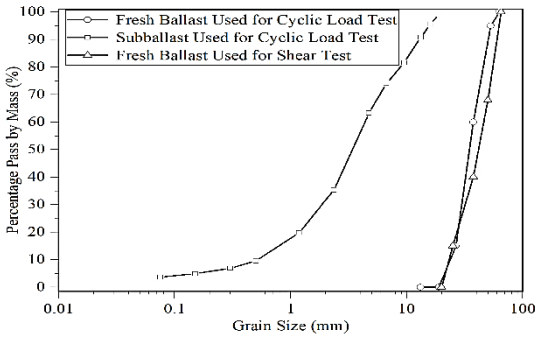

Figure 4 Particle Size Distribution of Ballast and Subballast

2.2. Test Procedure: Cyclic Load Test

The cyclic loading from moving trains along a rail track was simulated by the PSPTA showed in Figure 2. The test specimen consisted of a 150 mm thick subballast or concrete base overlain by a 300 mm thick layer of ballast. When testing with UBM, a rubber mat was placed on top of the concrete base and when testing with USP, the base layer was replaced with subballast material and a USP layer was placed under the concrete sleeper. Tests were conducted with and without USPs and UBMs. Ballast aggregates were placed on top of the subballast base/concrete base/rubber mat in three equal 100 mm thick layers, compacted by a rubber-padded vibratory hammer to a typical field density of approximately 1560 kg/m^3. The rail-sleeper assembly was placed on top of the compacted ballast, and the space around the concrete sleeper was filled with a 150 mm thick compacted crib ballast. Figure 5 shows the photographs of the Cyclic load test procedure.

The cyclic loading was the equivalent of a 25t axle load to simulate a passenger train, and a 35t axle load for a freight train with a loading

frequency of 15 and 20 Hz; this simulated a train traveling at about 110 and 145 km/h, respectively (Indraratna *et al* 2015). The amplitude of cyclic loads was determined using the American Railway Engineering Association (AREA) method (Li & Selig 1998). Lateral confinement was applied by hydraulic jack connected to movable lateral vertical walls that simulated low confining stress of 10-15 kPa. The longitudinal walls were locked for movements in that direction to ensure plane strain conditions, while the pressure exerted on the longitudinal walls was measured. Electronic potentiometers, settlement plates, and pressure cells were used to measure the deformation and stress variation in the ballast layer. The vertical and lateral loads and associated stress and deformation were recorded by data loggers connected to computers. A total of 500,000 load cycles were applied for each cyclic load test. Ballast degradation was evaluated using the Ballast Breakage Index (BBI) method proposed by Indraratna *et al*. (2005).

Figure 5 Photographs of Cyclic Load Test

2.3. Test Procedure: Interface Shear Test

The interface behaviour of ballast with other rail track elements such and sleepers and rubber inclusions were tested using the large-scale direct shear apparatus shown in Figure 3. The upper half of the apparatus is fixed to a frame and the lower half is free to move horizontally with the application of lateral load until shear failure occurs at the interface. Hydraulic jack connected with load cell was used to apply the lateral shear load with a shearing rate of 4 mm/min. The normal load was applied through the actuator connected to the top-loading plate as shown in Figure 3. Shear and vertical displacements were measured using two displacement gauges fixed to top-loading plate and lover half of the apparatus. Applied shear force was measured using load cell fixed between hydraulic jack and lower half of the apparatus. Both the displacement gauges and the load cell were connected to a data logger to record load and deformation data. Normal loads were applied using the lever arm technique. Tests were performed under three normal stresses of 30 kPa, 60 kPa and 90 kPa. Specimens were sheared until a 60 mm maximum displacement corresponding to 15% shear strain is reached. The photographs of test procedures are shown in Figure 6. The shear behaviour of three different interfaces of ballast (concrete sleeper, rubber on top of concrete sleeper and timber sleeper) were tested and compared with the interface shear of the fresh ballast. At the end of each test, ballast materials were screened through the standard sieves to calculate the BBI.

Figure 6 Photographs of Shear Load Test

3. RESULTS AND DISCUSSION

A total of sixteen cyclic load tests were carried out with and without USP and UBM at varying frequencies (15 Hz and 20 Hz) and axle loads (25 t and 35 t). Twelve direct shear tests with normal loads of 30 kPa, 60 kPa and 90 kPa by varying 4 different interfaces were carried out to understand the ballast interface behaviours. The stress-strain response and degradation of ballast observed in these tests

and a comparison with and without the use of rubber elements and various interface shear resistance are explained in the following sections.

3.1. Cyclic Stress-Strain Response

The vertical (ε_{vp}) and lateral (ε_{hp}) plastic deformations of ballast under cyclic loading with and without USP and UBM were measured at selected number of load cycles (N=1, 100, 500, 1000, 5000, 10000, 50000, 100000,…..500000) and are shown in Figures 7 (a),(b) and 8 (a),(b), respectively. For all the different load, frequency and substructure layers' cases, the results indicated that the ballast deformed rapidly up to around 10,000 cycles due to its initial densification and further packing after the corners of the sharp angular aggregates began to break, but once the ballast stabilised after around 100,000 cycles, the rate of ballast strain decreased as the load cycles increased. As expected, the plastic deformation of ballast increasing with the increase of axle loads and train speeds.

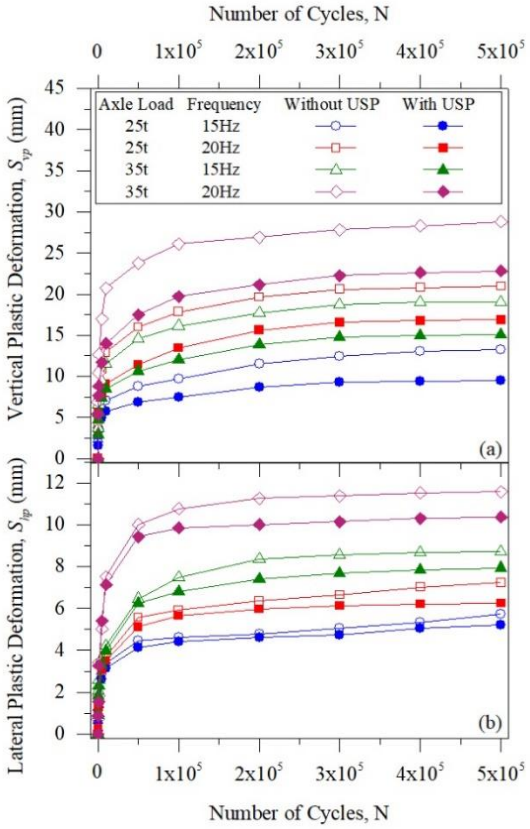

Figure 7 Plastic Deformation of Ballast with and Without USP: (a) Vertical Plastic Deformation; and (b) Lateral Plastic Deformation (Data sourced from Navaratnarajah *et* al (2018))

The vertical and lateral plastic deformation with and without USP for 25t and 35t axle loads shown in Figures 7 (a) & (b) confirmed that the ballast deformation has decreased significantly by using USP. The increased contact area of ballast by the USP at the sleeper-ballast interface reduced the induced stresses at the interface and at the particle-particle contact, allowing for a more uniform distribution of stress which in turn decreased the overall deformation. Based on the loading frequencies of 15 and 20 Hz tested in this study, the vertical deformation decreased up to about 29% for a 25t axle load and up to about 21% for a 35t axle load when USP was used with the concrete sleeper. Lateral deformation decreased up to about 14% for a 25t axle load and up to about 11% for a 35t axle load. This shows attaching USPs at the bottom face of the concrete sleepers is an ideal technique to reduce the long-term plastic settlement of a track subjected to repetitive cyclic loading.

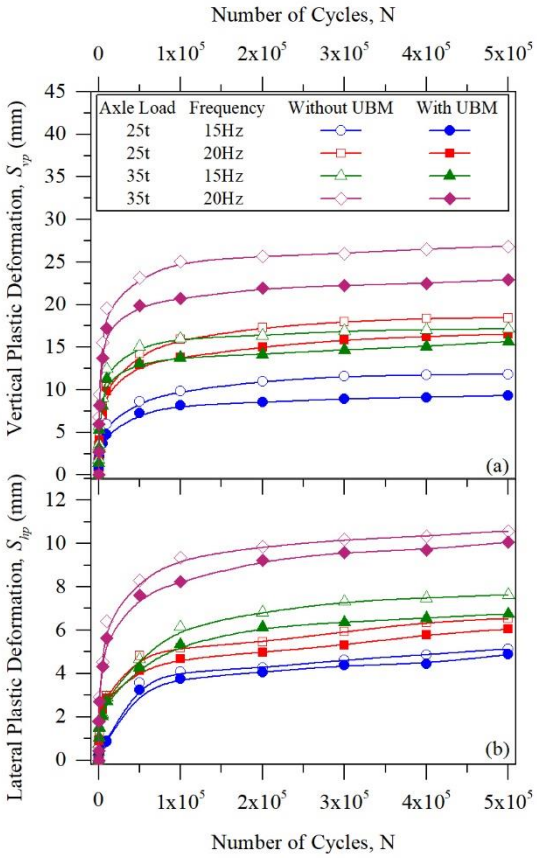

Figure 8 Plastic Deformation of Ballast with and Without UBM: (a) Vertical Plastic Deformation; and (b) Lateral Plastic Deformation (Data sourced from Navaratnarajah & Indraratna (2017))

As expected, the vertical and lateral plastic deformation of ballast shown in Figures 8 (a) & (b) are high due to the stiffer concrete base at the bottom of the ballast. However, the plastic deformation of the ballast significantly reduced by the use of UBM on top of the concrete base. Vertical plastic deformation was reduced by 10-20% and the lateral plastic deformation was reduced by 5-10% for the loading frequencies and axle loads tested in this study.

3.2. Cyclic Stress Variation in the Ballast

Pressure cells were placed at three different levels of the ballast layer (i) top: sleeper-ballast interface; (ii) middle: ballast-ballast interface; and (iii) bottom: ballast-subballast/concrete base interface to measure the dynamically induced pressure variation along with the depth of the ballast mass. Figures 9 and 10 show the variations in pressure with the loading frequencies and axle loads for the two different layer cases with and without USP and UBM tested in this study, respectively.

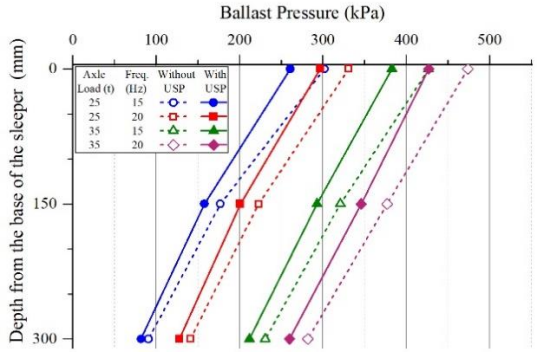

Figure 9 Ballast Pressure Variation with and Without USP (Data sourced from Navaratnarajah et al (2018))

It is evident that the dynamically induced stresses in the ballast increased with the axle load and train speed (loading frequency). When USP was placed under the concrete sleeper, there was a definite reduction in stress within the ballast mass because the dynamically induced stress is now reduced by the softer interface between ballast and concrete sleeper by the USP. Based on Figure 9, the average percentage reduction of stress is varying from about 12 and 10% at the sleeper-ballast interface, 10 and 8.5% in the middle of the ballast layer and about 9.5 and 8% at the ballast-subballast interface for 25 and 35t axle loads, respectively. The reduction in stress is higher in the zone near the USP-ballast interface. When a USP is used with the concrete sleeper, the ballast aggregates made a more uniform and increased area of contact at the sleeper-ballast interface that leads to a reduction in ballast stresses.

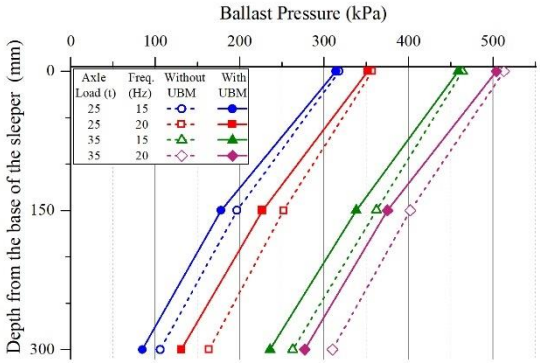

Figure 10 Ballast Pressure Variation with and Without UBM (Data sourced from Navaratnarajah & Indraratna (2017))

Results in Figure 10 clearly showed that the dynamically induced stresses in the ballast increase with the axle load and train speed as in the previous case. When a UBM is placed on top of a concrete base, there is a notable reduction in stress in the ballast mass, especially at the bottom (ballast-concrete base interface) and middle layers. Stress amplification due to a stiff base is now curtailed about 1-1.5% at the top, 5-10% at the middle and 10-20% at the bottom by the softer interface introduced by the UBM between the ballast and the concrete base.

3.3. Ballast Degradation due to Cyclic Load

In the application of a repetitive cyclic load, ballast particles undergo different types of particle degradation such as grinding (abrasion), angular corner breakage (attrition) and distinct splitting across the body of particles (fracture). Since the ballast breakage potential varies with depth due to changes in stress along with the depth of the ballast layer, the ballast mass was divided (and colour coded) into the top (red), middle (green), and bottom (blue) layers as shown in Figure 11 and analyzed separately. These layers correspond to ballast breakage governed by variations in stress and the type of interfaces. The top is the sleeper-ballast zone, the middle is the ballast-

ballast-zone, and the bottom is the ballast-subballast/concrete base zone. The Ballast Breakage Index (BBI) method proposed by Indraratna *et al*. (2005) was used to evaluate ballast degradation. The PSD was carried out and plotted to evaluate their BBI as per the method proposed in Indraratna *et al.* (2005).

Figure 11 Photographs of Fresh and Degraded Ballast in Different layers

Figures 12 and 13 show the BBI with and without USP and UBM for different axle loads and loading frequency, respectively. As expected, ballast breakage was greater at the top layer due to having a higher interface and inter-particle contact stress at the top, followed by the middle, and then the bottom layers. It is also evident from this study, the ballast degradation increased with the axle load and train speed (loading frequency).

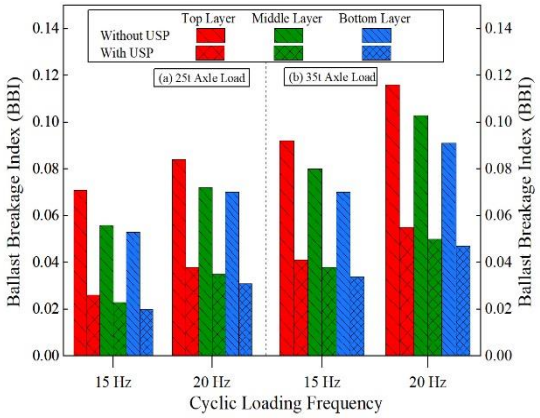

Figure 12 Ballast Breakage Index (BBI) with and Without USP (Data sourced from Navaratnarajah et al (2018))

The results in Figure 12 indicate that ballast degradation was significantly reduced by the USP used under the concrete sleeper. The increased contact area due to USP and the subsequent reduction in the interface and inter-particle ballast stress is probably the main reason behind this substantial reduction of ballast breakage. Considering each ballast layer separately, the reduction for the 25 and 35t axle loads tested with 15 and 20 Hz frequency was in the order of 53-63% for the top layer, 51-59% for the middle layer, and 48-62% for the bottom layer. When all three layers are considered, on average, the USP reduced degradation by more than 50%.

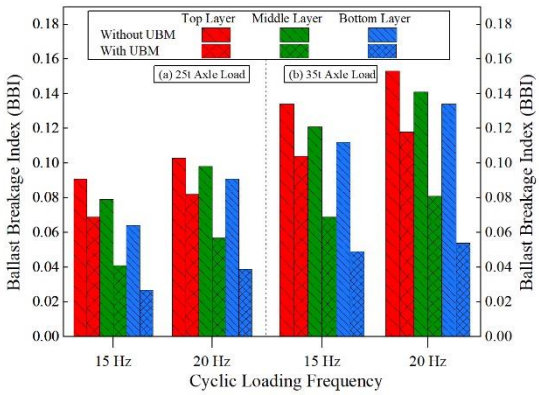

Figure 13 Ballast Breakage Index (BBI) with and Without UBM (Data sourced from Navaratnarajah & Indraratna (2017))

The results in Figure 13 show that ballast degradation is reduced significantly by the use of UBM on top of the concrete base. On average, when all three layers are considered, UBM reduced degradation by more than 40%. When individual layers are considered, the reduction percentages are 20-25% at the top, 30-50% at the middle and 50-60% at the bottom layers

3.4. Interface Stress-Strain Response

Figure 14 illustrates the shear stress-strain behaviour of fresh ballast and the other three types of interfaces under different normal loads. The shear resistance of the ballast and different interfaces are increasing with the applied normal stress. The highest shear resistance occurred in fresh ballast due to the particle interlocking of highly angular fresh ballast which immensely contributed to these peak values. In all the other three interfaces, the surface friction between ballast and interface material is the contributing factor that affects the stress-strain behaviour. Out of the three interfaces, the concrete interface showed the highest shear resistance due to the

relatively rough and hard surface compared to the other two interfaces. The timber sleeper interface exhibited the lowest shear resistance. When rubber elements inserted on the concrete face, the shear resistance becomes lower than that of the concrete interface, but it is higher than what was observed for the timber interface. As the rail industries are moving towards replacing timber sleepers with concrete sleepers, attaching rubber elements works better in terms of increasing shear resistance compared to ballast-timber interface resistance and which also significantly reduces the stress-strain and degradation of ballast layer as discussed earlier.

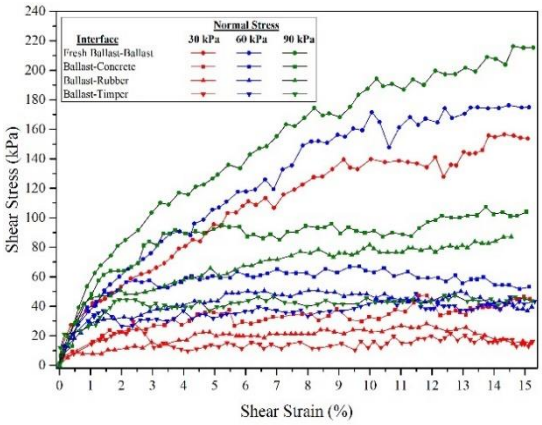

Figure 14 Stress-Strain Variation of Ballast with Different Interfaces

4. CONCLUSIONS

A series of large-scale cyclic loading tests using the Process Simulation Prismoidal Triaxial Apparatus (PSPTA) were carried out with axle loads of 25 and 35t and at varying loading frequencies of 10 and 15 Hz to investigate the performance of USP and UBM stabilized at the harder interface (concrete sleeper-ballast interface and ballast-concrete base interface). A regular open track simulated by placing subballast underneath the ballast layer and a USP attached on the bottom face of a concrete sleeper and a track on harder subgrade such as track on bridges and tunnels simulated by placing concrete base layer underneath the ballast and the UBM placed on top of the concrete base showed promising outcomes in the reduction of vertical and lateral deformations, stress and degradation of ballast. Generally, concrete sleepers transmit stress to the ballast through a finite number of small discrete contacts at the sleeper-ballast interface. However, it is evident from the study that the USP attached with a concrete sleeper enhances the interface contacts and markedly reduces the stresses in the ballast especially at the top zone which leads to a reduction in ballast deformation (vertical and lateral) and degradation. Based on this study, using USPs on concrete sleepers is a favorable solution to reduce the stress-strain and degradation of ballast, and in a practical sense to minimize the maintenance costs of ballasted rail tracks.

The UBMs used in this study were manufactured from recycled tyre waste. The test results confirmed that UBM reduced the ballast deformation, stress and degradation quite considerably. The interparticle stress and the interface stress at the ballast-concrete base interface were significantly reduced by the use of UBM. The reduction of degradation at the interface near the UBM was observed is significant from this study.

This study also confirms when the timber sleepers are replaced by harder concrete sleepers, having rubber elements at the interface of concrete and ballast give significant improvement on shear resistance compared to timber sleeper and reduction in ballast degradation when used along with concrete sleepers. It is evident from this study that by placing rubber elements, loads on the ballast bed can be distributed more homogeneously than by a hard base and thereby improves track stability. The benefits of reducing degradation with rubber elements potentially minimize the number of maintenance operations and reduce the life cycle costs of track foundations. Especially, when these rubber elements made of recycled materials such as tyre waste gives more value to the waste materials and makes rail track infrastructures more sustainable.

5. ACKNOWLEDGMENTS

The author wishes to acknowledge the Australian Research Council (ARC) for its financial support. The author expresses sincere gratitude to Distinguished Professor Buddhima Indraratna and Asst. Prof. Cholachat Rujikiatkamjorn at the University Wollongong, Australia for the guidance provided to complete the research study. The work carried out at the University of Peradeniya, Sri Lanka was supported by the Accelerating Higher Education Expansion and

Development (AHEAD) Operation of the Ministry of Higher Education funded by the World Bank (Grant No: AHEAD/DOR/No. 63) and University of Peradeniya, Sri Lanka Research Grant (Grant No. URG-2017-29-E) are also acknowledged with the appreciation by the Author.

6. REFERENCES

Indraratna, B., Biabani, M. & Nimbalkar, S., 2015, 'Behavior of Geocell-Reinforced Subballast Subjected to Cyclic Loading in Plane-Strain Condition', *Journal of Geotechnical and Geoenvironmental Engineering*, 141(1), 1-16.

Indraratna, B., Lackenby, J. & Christie, D., 2005, 'Effect of confining pressure on the degradation of ballast under cyclic loading', *Géotechnique*, 55(4), 325-328.

Indraratna, B., Nimbalkar, S., Navaratnarajah, S. K., Rujikiatkamjorn, C. & Neville, T., 2014, 'Use of shock mats for mitigating degradation of railroad ballast', *Sri Lankan geotechnical journal - Special issue on ground improvement*, 6(1), 32-41.

Indraratna, B., Salim, W. & Christie, D., 2002, 'Improvement of recycled ballast using geosynthetics', *Proc. 7th International Conference on Geosynthetics*. Nice, France.

Indraratna, B., Salim, W., Ionescu, D. & Christie, D., 2001, 'Stress-strain and degradation behaviour of railway ballast under static and dynamic loading, based on large-scale triaxial testing', *Proc. 15th Int. Conference on Soil Mechanics and Geotechnical Engineering*. Istanbul.

Indraratna, B., Salim, W. & Rujikiatkamjorn, C., 2011, *Advanced Rail Geotechnology: Ballasted Track*. Rotterdam, Netherlands: CRC Press/Balkema.

Ionescu, D., Indraratna, B. & Christie, H. D., 1998, 'Behaviour of railway ballast under dynamic loads', *Proc. 13th South East Asian Geotechnical Conference*. Taipei, November, 9-12, 1998.

Li, D. & Selig, E., 1998, 'Method for Railroad Track Foundation Design. I: Development', *Journal of Geotechnical and Geoenvironmental Engineering*, 124(4), 316-322.

Loy, H., 2009, 'Under Sleeper Pads in Turnouts', *Railway Technical Review 2*, 35-38.

Navaratnarajah, S. K. & Indraratna, B., 2017, 'Use of Rubber Mats to Improve the Deformation and Degradation Behavior of Rail Ballast under Cyclic Loading', *ASCE Journal of Geotechnical and Geoenvironmental Engineering*, 143(6), 04017015.

Navaratnarajah, S. K., Indraratna, B. & Ngo, N. T., 2018, 'Influence of Under Sleeper Pads on Ballast Behavior Under Cyclic Loading: Experimental and Numerical Studies', *ASCE Journal of Geotechnical and Geoenvironmental Engineering*, 144(9), 04018068.

Navaratnarajah, S. K., Indraratna, B. & Nimbalkar, S., 2016, 'Application of Shock Mats in Rail Track Foundation Subjected to Dynamic Loads', *Procedia Engineering*, 143, 1108-1119.

Nimbalkar, S., Indraratna, B., Dash, S. & Christie, D., 2012, 'Improved Performance of Railway Ballast under Impact Loads Using Shock Mats', *Journal of Geotechnical and Geoenvironmental Engineering*, 138(3), 281-294.

Sol-Sanchez, M., Moreno-Navarro, F. & Rubio-Gámez, M. C., 2014, 'Viability of using end-of-life tire pads as under sleeper pads in railway', *Construction and Building Materials*, 64, 150-156.

Proceedings of the 7th International Symposium on

Advances in Civil and Environmental Engineering **Practices** for Sustainable Development

ACEPS - 2019

Variation of geotechnical properties of municipal solid waste due to biodegradation.

W.T.R.A.Pradeep[1], N.H.Priyankara[2] and A.M.N.Alagiyawanna[2]

[1]Division of Major Dams and Reservoir Operations, Mahaweli Authority of Sri Lanka, Maduruoya, SRI LANKA.
[2]Department of Civil and Environmental Engineering, Faculty of Engineering, University of Ruhuna, Galle, SRI LANKA.

K e y w o r d s

Synthetic Municipal Solid Waste
Biodegradation
Geotechnical properties
Hydraulic conductivity
Compressibility
Shear strength
Slope stability

A B S T R A C T

Landfill disposal is the most commonly used waste management technique throughout the world. Slope stability is the most important aspect of Municipal Solid Waste (MSW) landfill; it depends on the geotechnical properties of MSW. The geotechnical properties vary with time as a result of biodegradation which in turn affects slope stability issues. Hence, the aim of this research study is to determine the variation of geotechnical properties of Synthetic Municipal Solid Waste (SMSW) at different phases of degradation. SMSW samples were prepared based on the composition of MSW generated in the Galle Municipal Council. To accelerate the degradation, leachate was recirculated in bioreactors. Degradation phases were quantified based on the leachate characteristics and the samples exhumed from the bioreactors at different phases of degradation were tested for the Geotechnical properties. Shear strength, compressibility and hydraulic conductivity of the SMSW at different phases of degradation were investigated in the laboratory. Hydraulic conductivity of SMSW was reduced from 5.231×10^{-5} for initial fresh waste to 2.932×10^{-5} due to degradation. Compression ratio was reduced from 0.61 for initial fresh waste to 0.26 for the degraded waste. Direct shear tests showed that cohesion increased from 8kPa for fresh SMSW to 22kPa for degraded SMSW and that the friction angle decreased from 35° for fresh SMSW to 30° for degraded SMSW. Slope stability analysis was done using SLOPE/W software and to evaluate the slope stability, a typical landfill section was used. Finally variation of slope stability with different slope types related to MSW landfill was investigated in the presence of seepage effect.

1. INTRODUCTION

Municipal solid waste (MSW) is the waste generated in a community with the exception of industrial and agricultural wastes. Hence MSW includes residential waste (e.g., households), commercial (e.g., from stores, markets, shops, hotels etc), and institutional waste (e.g., schools, hospitals etc). Paper, paperboard, garden and food waste can be classified in a broad category known as organic or biodegradable waste (Tchobanoglous *et al*. 1993).

The generation of solid waste has become an important global environmental issue as a consequence of increases in waste production parallel to the drastic growth in world population during past few decades. This had led to unregulated disposal of solid waste levels are approximately 1.3 billion tons per year, and are expected to increase to approximately 2.2 billion tons per year by 2025 (Hoornweg *et al*. 2012). In addition to that in South Asia, approximately 70 million tons of waste is generated per year, with per capita values ranging from 0.12 to 5.1 kg per person per day and an average of 0.45 kg/capita/day (Hoornweg *et al*. 2013). According to World Bank statistics in 2012, Sri Lanka is among the largest MSW producing countries in terms of daily per capita generation. Although proper waste disposal is vitally important in the management of MSW, developing countries including Sri Lanka have not paid due attention on the proper disposal of MSW over primarily in urban and sub-urban areas. Lack of attention given to solid waste disposal has led to the poor practice of disposal of solid

waste in open dumps (The Sunday Times (Sri Lanka), March 22, 2009).

Available land in urban and suburban areas have become more and more scarce over the years; this has forced the municipal councils to strain the existing open dumps to a level where the landfills are reaching critical volumes. The lack of sufficient land has resulted in dumping waste in high mounds and in steep slopes resulting in catastrophic failures in MSW slopes (Vilar *et al*. 2004).

One example that can be taken in this regard is the Payatas Landfill in Manila, Philippines which was subjected to a shear failure on July 10, 2000 where 1.2 Million m^3 of waste of the top layer slip down the slope; this resulted in 230 reported deaths and over 800 people are reported to have gone missing (Jafari *et al*. 2013).

An example for one such failure in Sri Lanka is the shear failure of the 80feet high Bloemendhal open dump in Maligawatta Sri Lanka this took place in mid-2009. Although, no harm for human life was recorded, the shear failure of the dump caused considerable property damage pertinent to nearby dwellings in the adjoin area. (The Island (Sri Lanka), March 09, 2009).

The recent disaster of shear failure in Sri Lanka is the 20 meters high Meethotamulla open dump in Potuwilkumbura Sri Lanka which occurred on 14th April, 2017. More than 30 people died on that day when the garbage dump collapsed on them, whilst most were celebrating the Sinhala and Hindu New Year. More than 100 houses were completely destroyed (The Sunday Times (Sri Lanka), March 11, 2018).

However, MSW landfills are commonly adopted for disposal of MSW in urban development at present (Vilar *et al*. 2004). The behavior of MSW landfill slopes is unique in comparison, when compared to the conventional natural slope. The stability of the landfill slope depends on the geotechnical properties of the MSW (Pandey & Tiwari 2015). The geotechnical properties of MSW are of paramount importance in designing and assessing the performance of landfill and in ensuring safe long-term containment of MSW; due attention in this regard is ultimately important to ensure the environmental and human wellbeing. Geotechnical properties of MSW are difficult to determine because of the heterogeneity, wide variation in particle size distribution and time dependent degradation. (Pandey & Tiwari 2015). Characterization of geotechnical properties of MSW, such as unit weight and shear strength parameters (cohesion and angle of internal friction), is one of the most important aspect of MSW landfill slope design. But the geotechnical properties of MSW keep changing with time as well as degree of decomposition. Hence, estimating the geotechnical properties of MSW at different phases of degradation plays an important role in the stability analysis of landfill slope (Reddy *et al*. 2009).

Geotechnical properties of the MSW play an important role in designing of the landfill and in considering the slope stability issues. Slope stability of MSW landfill mainly depends on the geotechnical properties of solid waste. Because of waste degradation, the geotechnical properties vary with time as well as degree of decomposition, which is of vital concern from the point of view of slope stability issues. Therefore, aim of this research study is to determine the variation of geotechnical properties of MSW at different phases of degradation.

The key objectives of the present research are,

(i) Determination of geotechnical properties of municipal solid waste at different phases of biodegradation.
(ii) Evaluate the Variation of slope stability of MSW landfill at different phases of decomposition.

2. METHODOLOGY

2.1 Fresh Synthetic Municipal Solid Waste (SWSW) Preparation

In this study, synthetic municipal solid waste (SMSW) is used to investigate the geotechnical engineering properties of MSW. Fresh SMSW was prepared in the laboratory to be represented of the typical composition of MSW generated in the Galle Municipal Council. According to the Galle municipal council disposal data, selected composition of typical MSW sample consists of 79% kitchen waste, 15% garden waste, 5% paper and 1% soft plastic.

The preparation of SMSW involved weighing required amounts of fresh individual components and then placing them all together. Leachate from a landfill (Wekunugoda landfill) was added. To expedite the degradation of SMSW, anaerobic

digester sludge could be obtained from a wastewater treatment plant (Elephant house company water treatment plant at Ranala) also was added.

SMSW components, sludge and leachate were mixed by manual method until the sludge and leachate distributed uniformly and the material appeared homogeneous. The SMSW was placed in the specially designed bioreactor landfill reactors.

2.2 Bioreactor assembly and operation

The bioreactor consisted of a cylindrical cell fitted with Perspex plates at the top and the bottom. The tubing was made of acrylic and had an outer diameter of 150 mm and a length of 500 mm. Top plate have two ports: one for leachate recirculation and another to measure gas pressure. Leachate will be collected through the port provided at the bottom. All connections to the reactors were properly sealed with anaerobic sealant to prevent any leak or air intrusion. The reactor was accompanied by a recirculation cell. Six identical reactors R1, R2, R3, R4, R5 and R6 were prepared by placing 3kg of SMSW in each reactors and compacted up to 20cm height. Then the bulk weight of SMSW sample was 8.38 kN/m^3.

To ensure efficient leachate recirculation, a filter paper and geotextile were placed at the bottom prior to the loading of SMSW into the reactor. All connection ports were properly sealed using anaerobic sealant. After ensuring the complete anaerobic condition, all reactors were placed in a laboratory at a room temperature for providing a favourable environment for the growth of microbes. The figure 1 shows the model experimental setup installed in the geotechnical laboratory.

Figure 1 Laboratory experimental setup

2.3 Acceleration of biodegradation process

Leachate recirculation was carried out to accelerate the biodegradation process. Leachate volume of 10% total weight of SMSW was recirculated through the waste samples. On the first day, leachate collected from a landfill (Wekunugoda landfill) was used for recirculation, since the amount of leachate generated from the reactors were less than required. After second day leachate could be collected from the reactors was mixed with leachate obtained from the landfill to recirculate the desired volume. Then Leachate was recycled thrice a week and this procedure was continued throughout the research.

2.4 Identification of biodegradation phases

Different phases of biodegradation were demarcated based on the "Khalil and Sharma's analysis", which has shown in figure 2.

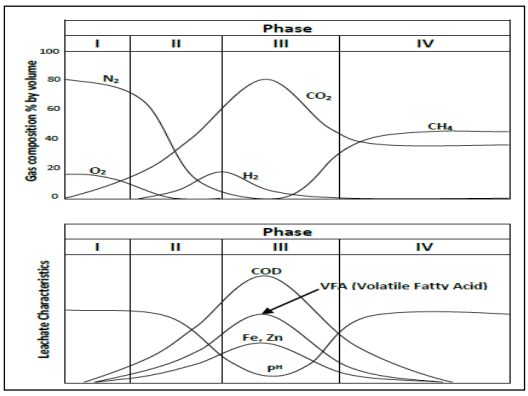

Figure 2 Variation of gas composition and leachate characteristics with biodegradation process (Khalil & Sharma Analysis)

Under this reference, Biodegradation process was monitored by measuring the characteristics of leachate generated by SMSW in each reactor. In this study, different phases of biodegradation were identified based on the composition of pH and COD (Chemical Oxygen Demand) of leachate generated.

(i) Phase I: Hydrolysis

This process is very fast and it is completed within one or two day. Therefore, by using simple laboratory experiments difficult to identify this phase (Khalil & Sharma Analysis).

(ii) Phase II: Acidogenesis

Acidogenesis will be characterized by measuring H_2 production according to the Figure 2. The appearance of H_2 and a reduction in pH due to the formation and dissolution of organic acid.

(iii) Phase III: Acetogenesis

Acetogenesis will be identified by measuring pH, COD and composition of gas. According to the Figure 2, COD maximum, pH minimum and CO_2 composition maximum in Acetogenesis phase.

(iv) Phase IV: Methanogenesis

Methanogenesis will be characterized by measuring gas composition. In Methanogenesis phase CO_2 and CH_4 will be stabilized according to the Figure 2.

According to the Khalil and Sharma's analysis, first SMSW sample was exhumed after three days assuming which was became Hydrolysis phase.

Acetogenesis phase was demarcated based on the variation of COD (Chemical Oxygen Demand) and pH of leachate generated. Second SMSW sample was exhumed when COD maximum and pH minimum.

Fresh sample and Samples from each phase of biodegradation was characterized by testing for moisture content, organic content, specific gravity, and gradation based on the standard testing procedures. Moisture content was determined in accordance with the standard procedure, but the samples were dried at a lower constant temperature of 60°C (to avoid possible burning of any organic constituents) until the mass remained constant. The organic content, which is a representation of volatile solids in the SMSW were measured.

2.5. Geotechnical Investigation

The SMSW samples retrieved from the reactors will be air-dried for number of days and then their moisture was adjusted to 50% on a wet weight basis (100% on dry weight basis). Then the SMSW was used to prepare specimens for hydraulic conductivity, compressibility, and shear strength testing in the laboratory as described below.

2.5.1 Drained Shear Strength

Drained shear strength properties of the SMSW were determined by direct shear tests. Specimens were compacted into a circular shear box with inside diameter 60 mm and thickness 20 mm in layers. Wet unit weight of the sample was 12kN/m^3, with moisture content of 50% on wet basis. Porous stones were placed on the top and the bottom of the specimen. Before applying shear, SMSW sample was consolidated (24 hours) for each load cases. When the consolidation process was finished, shear was applied. The specimen was subjected a constant normal stress and then sheared at a constant strain rate 0.15mm/min. The horizontal deformation and shear stress were recorded periodically. The testing was continued until the horizontal displacement reached 15% or more of the specimen diameter (none exhibited peak shear response).

The fresh and hydrolysis phase SMSW was tested under normal stresses of 15, 25 and 35kPa. The acetogenesis phase SMSW was tested under normal stresses of 35, 45 and 55kPa.For each normal load increment, shear stress vs. strain readings were recorded using an electronic data logger. Then peak value is obtained from shear stress versus shear strain graph. But in this case, samples showed no decreasing in shear stress. Hence the stress at 15 % shear strain was obtained Finally maximum shear stress vs. corresponding normal stress was graphed and shear strength parameters (cohesion and friction angle) were obtained using Mohr-Coulomb failure envelope. All direct shear tests were conducted under drained condition to obtain shear strength parameters.

2.5.2. Compressibility

Confined compressibility test was carried out in a locally produced compressibility apparatus to determine the compressibility characteristics of SMSW with varying normal stress. Figure 3 depicts the compressibility testing apparatus. Confined compressibility testing was carried out in a large scale compressibility apparatus to determine the compressibility characteristics of fresh SMSW with varying normal stress.

Figure 3 Consolidation test apparatus

In this testing, the SMSW sample was placed in the compressibility apparatus with one porous stone on the top and another on the bottom of the sample. The compressibility test was conducted in load increments in four steps and unloaded in three steps. The samples were placed into the ring (49.76 mm diameter and 20 mm thick) in two layers, and each layer was compacted. The compacted samples had initial wet unit weight of 12 kN/m^3 with target moisture content of 50% on a wet weight basis. The compacted sample was saturated by filling the water bath with water. Once a water level was visible on the surface of the sample it was assumed to be fully saturated. Upon saturation of the sample the loading piston was brought into contact with the sample and loaded. Settlement of the sample was monitored for a period of 48 hours for each loading stages. The testing procedure involved was subjecting the specimen to a constant vertical stress of 0-25 kPa and observing compression for 24 hours. Subsequently, the vertical stress was increased to 25-50, 50-100 and 100-200 kPa, and compression was monitored for 48 hours under each vertical stress. Unloading was also tested to 200-100, 100-50 and 50-0 kPa, for the same unit weight and moisture content conditions of SMSW.

For each loading stage, the coefficient of consolidation (C_v) was found considering both log time method and square root time method. The coefficient of consolidation (C_v) was defined for primary consolidation of solid waste.

Volume compressibility (m_v) of each loading stage was also calculated by the following Eq. (1).

$$mv = \Delta H / H.\Delta\sigma \qquad (1)$$

Where, ΔH – Settlement
H – Layer thickness
$\Delta\sigma$ – Stress change

The compression index (C_c) of MSW was calculated from the slope of the graph of Void ratio vs. Logσ.

Variation of void ratio with time was used to find the time for primary consolidation (t_p) and secondary compression index (C_α).

2.5.3. Hydraulic conductivity

Constant head method can be adapted as the standard test method in determination of saturated hydraulic conductivity (K_0). Darcy law was applied in order to calculate saturated hydraulic conductivity (K_0).

$$ln\left(\frac{hi}{h}\right) = \left(\frac{koA}{aL}\right) \qquad (2)$$

Where *hi* is the initial height of water column, "*h*" is the final height of water column, "*A*" is cross sectional area of the sample, "*a*" is the cross sectional area of the stand pipe, *L* is the length of the sample. Schematic Diagram of Saturated Hydraulic Conductivity test is illustrated in Figure 4.

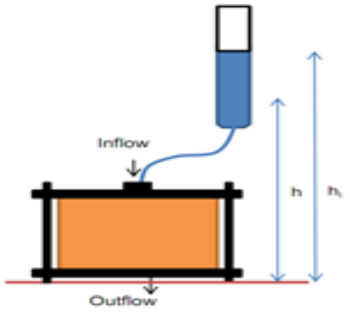

Figure 4 Schematic Diagram of Saturated Hydraulic Conductivity test

2.5.3. Evaluation of Slope Stability

The slope stability of MSW landfill is directly affected by rainfall. An identical relationship exists between the rainfall and seepage pressure. Same as the rainfall has Moreover rainfall infiltration will lead to unstable situations in MSW landfill. In this research, slope stability was analysed by using both seepage analysis and slope stability analysis. GeoStudio software was used to investigate these analyses. The SEEP/W was used to investigate how seepage will occur in a slope under rainfall conditions. Rainfall data from year 2005-2001 were obtained from Baddegama meteorological station which is in Galle district and which is the closest rainfall monitoring station to the Galle city. After analysing the obtained data, effect of seepage on the recorded maximum rain fall was checked.

If slope stability remains intact even under the maximum rainfall, slope stability would be less affected under the minimum rainfall as opposed to the maximum rainfall. The rainfall was applied on the slope as a unit flux. The results of the SEEP/W analysis were incorporated into SLOPE/W using parent analysis.

SLOPE/W was used to analyse the effect of seepage on the factor of safety of the MSW

landfill on slope. Different slope types were used to investigate the slope stability under a specified rainfall condition. The factors of safety (FOS) were evaluated with the Morgenstern-Price method in this study. Figure 5 represents the typical section of MSW landfill which was used to analyse slope stability.

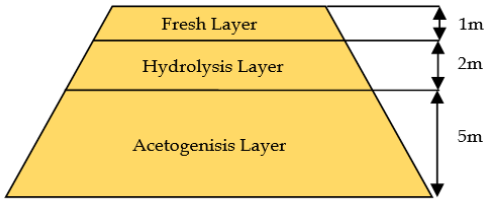

Figure 5 Typical section of MSW landfill

Finally, variation of slope stability (Factor of safety) with different slope type of MSW landfill was investigated.

3. RESULTS AND DISCUSSION

The SMSW samples retrieved from the reactors in each degradation phases were air-dried and then their moisture was adjusted to the same 50% on a wet weight basis (100% on dry weight basis) prior to testing for hydraulic conductivity, compressibility, and shear strength testing. And also the basic properties of the SMSW, such as moisture content, organic content, specific gravity, and grain size distribution were evaluated for the exhumed SMSW samples from the bioreactors at different phases of degradation.

3.1. Basic properties of SMSW

The basic properties moisture content, organic content, degree of decomposition and specific gravity of the exhumed SMSW samples from the bioreactors at different phases of degradation are summarized in Table 1.

Table 1 Characteristics of Fresh and Degraded SMSW

Bioreactor	Degradation Phase	Moisture content (%)	Organic content (Volatile solid) (%)	Degree of Decomposition (%)	Specific Gravity
-	Fresh	80	80.4	0	1.47
R_1	Hydrolysis	83	70.2	43	1.73
R_2	Acetogenisis	84	60.7	60	2.03

3.1.1. Particle size distribution

Figure 6 shows the particle size distribution of SMSW at different phase of biodegradation, which is represent the particle size distribution of fresh and hydrolysis (R_1) stage and Acetogenisis (R_2) stage MSW.

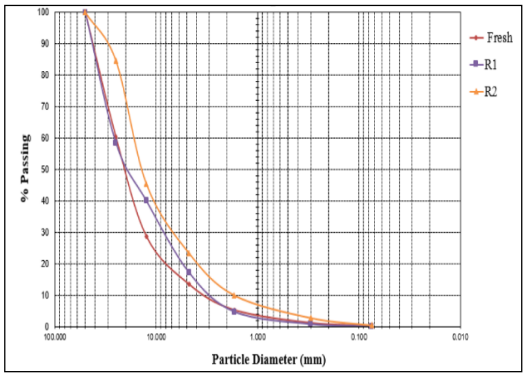

Figure 6 Particle size distribution of SMSW at different phases of biodegradation.

3.2. Geotechnical Parameters of SMSW

3.2.1. Hydraulic Conductivity

Constant head method was used as the standard test method in determination of saturated hydraulic conductivity (K_0). The bulk unit weight of fresh SMSW was 8.38 kN/m^3. The hydraulic conductivity of the degraded SMSW (Hydrolysis stage) was one and half orders of magnitude less than the fresh SMSW. This decrease in hydraulic conductivity can be attributed to the degradation and the increase in density of the samples. Moreover, SMSW, with the degradation yielded hydraulic conductivity was reduced due to their reduction in particle size. Table 2 represents the hydraulic conductivity (K_0) values for fresh and degraded SMSW from hydraulic conductivity test.

Table 2 Hydraulic conductivity (K_0) values for fresh and degraded SMSW

Bioreactor	Degradation Phase	Hydraulic conductivity (K_0) (m/s)
-	Fresh	5.231×10^{-5}
R_1	Hydrolysis	3.614×10^{-5}
R_2	Acetogenisis	2.932×10^{-5}

Figure 7 shows how hydraulic conductivity of SMSW varies with the degree of decomposition.

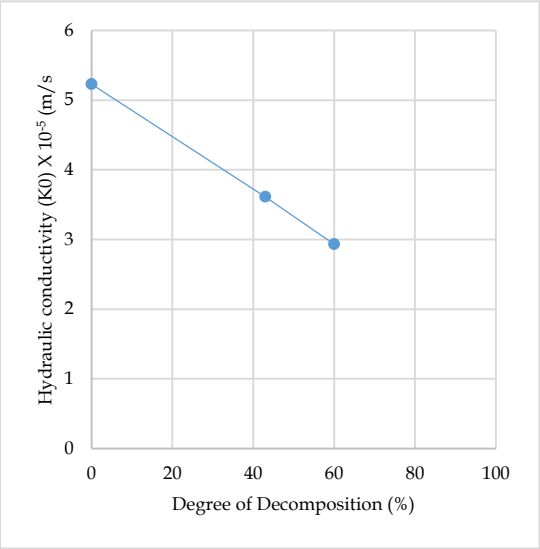

Figure 7 Variation of Hydraulic conductivity (K_0) with degree of decomposition

3.2.2. Compressibility Characteristics

Compressibility Characteristics were observed in fresh and each degradation stages of MSW. Settlement was observed in each load cases and then settlement versus time (log) graphs were plotted. Using both log time method and square root time method, Coefficient of consolidation (C_v) was calculated. In addition to that the volume compressibility (m_v) was also calculated in each load cases. Compression index (C_c) was observed using tangent of void ratio versus log stress graph and secondary compression index (C_α) was also calculated by using tangent of void ratio versus time (log) graph. At the end, variation of compression index (C_c) and secondary compression index (C_α) with degree of decomposition was analysed.

The compression ratio (C_c) of the SMSW varied in the range of 0.61 to 0.26. As the waste degraded, the compression ratio decreased. Figure 8 shows the variation of compression ratio with the degree of decomposition.

The calculated secondary compression ratio of the SMSW varied in the range of 0.16 to 0.1. A decrease in secondary compression ratio with increase in degradation of SMSW was observed. Figure 8 also shows the variation of secondary compression ratio with the degree of decomposition, showing similar behaviour to primary compression ratio.

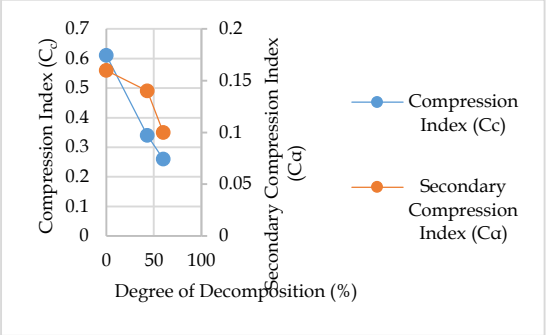

Figure 8 Variation of compression ratio and secondary compression ratio with the degree of decomposition

3.2.3. Shear strength parameters based on direct shear tests

Drained Shear strength parameters such as friction angle and cohesion were observed in fresh and each degradation stages of SMSW.

Drained cohesion of SMSW varied from 8-22 kPa and the drained friction angle ranged from 35°-30°. The decrease in the friction angle 35° to 30° may be attributed to the lack of materials such as metals, plastics and textiles in the samples. As the sample degrades, there is an increase in the cohesion and decrease in frictional angle.

Figure 9 shows the variation of shear strength parameters with the degree of decomposition.

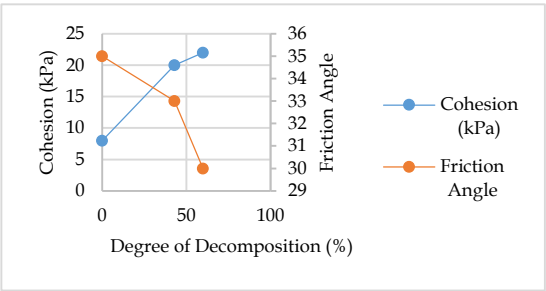

Figure 9 Variation of shear strength parameters with the degree of decomposition

3.2.4. Slope Stability Analysis

To analyse the slope stability of MSW landfill from Geo-slope software, seepage effect was observed firstly using SEEP/W. According to the hydraulic conductivity of each layers and rainfall condition, seepage effect was evaluated. Figure 10 shows the how seepage effect was computed by SEEP/W software.

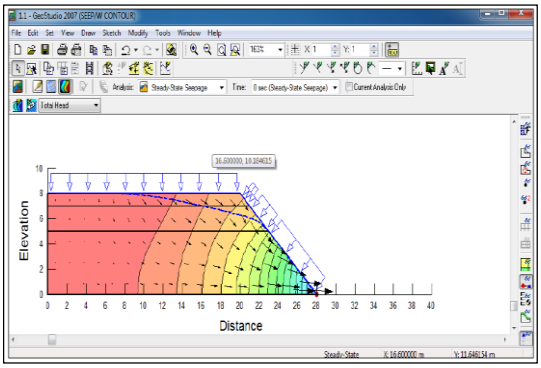

Figure 10 Analysis of seepage effect with SEEP/W

The results obtained from seepage modelling can be directly linked into SLOPE/W. A particular cohesion, friction angle and density values corresponding to each waste layers, were selected to analyse the slope stability using Slope/W 2007 software. Figure 11 shows the how slope stability was computed by SLOPE/W software.

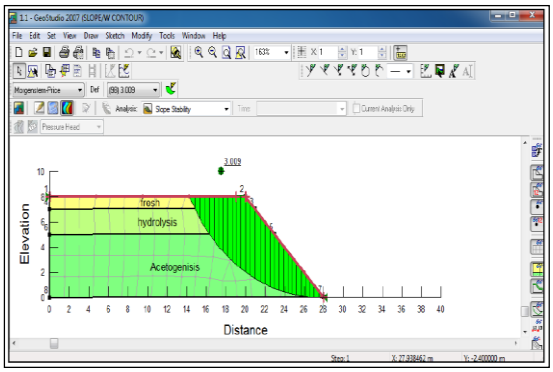

Figure 11 Analysis of slope stability with SLOPE/W

According to the slope stability analysis the factor of safety (FOS) was computed under different types of slope of MSW landfill. Table 4.9 shows how vary the factor of safety with variation of slope.

Table 3 Variation of FOS with different types of slopes

Slope (V:H)	FOS
1:0.5	2.5
1:0.6	2.8
1:1	3.0
1:1.5	3.7
1:2	4.3

4. CONCLUSIONS

Basic and geotechnical properties of SMSW at different stages of biodegradation were investigated in laboratory. Basic properties of SMSW are moisture content, organic content, degree of decomposition and specific gravity. Geotechnical properties of SMSW are hydraulic conductivity, compression characteristics, and shear strength parameters (friction angle and cohesion).

Hydraulic conductivity of SMSW was reduced from 5.231×10^{-5} for initial fresh waste to 2.932×10^{-5} due to degradation. Within the degradation, MSW particles become more fines and attains a higher unit weight, which resulted in lower hydraulic conductivity of the degraded MSW.

Compression ratio was reduced from 0.61 for initial fresh waste to 0.26 for the degraded waste. Secondary Compression ratio was also reduced from 0.16 for initial fresh waste to 0.1 for the degraded waste. Degraded MSW shows lower settlement compared to fresh MSW. With increased degradation, primary and secondary compression ratios were decreased.

Direct shear tests showed that the fresh and degraded SMSW exhibited continuous strength gain with the increase in horizontal deformation, with the cohesion increased from 3 kPa for fresh SMSW to 14 to 16 kPa for degraded SMSW and the friction angle decreased from 44° for fresh SMSW to 37° for degraded SMSW. As the sample degrades, there is an increase in the cohesion and a decrease in frictional angle.

Decreased friction angle and increased cohesion occurred due to the highly cohesive nature of the MSW with degradation. From this study we also emphasize that significant changes in geotechnical properties of MSW can occur due to enhanced degradation induced by leachate recirculation.

Slope stability analysis was done using SLOPE/W software and the seepage analysis was carried out by using SEEP/W software. A typical landfill section was used to evaluate the slope stability. Seepage effect was computed by using maximum rainfall data of Galle. After that the Slope stability was computed using SLOPE/W software in the presence of seepage effect. Finally, variation of slope stability with different slope types of MSW landfill were investigated.

Overall, this research emphasized the variation of geotechnical properties at different phases of degradation with bioreactor approach. The variation in properties can be significant and may be useful in analysis and design of landfills, spatially for bioreactor landfills.

5. ACKNOWLEDGMENTS

Authors would like to acknowledge Mr. W.M.I.Vipula Shantha who gave the assistance with laboratory experiments and also Mr. L.N.Kalansooriya giving us his support by arranging experiment setup of laboratory.

6. REFERENCES

Tchobanoglous, G., Theisen, H. & Vigil, S.A., 1993, 'Integrated Solid Waste Management: Engineering Principle and Management Issue', *McGraw Hill Inc.*, New York.

Hoornweg, D. & Bhada-Tata, P., 2012, 'What a waste: A Global Review of Solid Waste Management', *World Bank Review*, 9.

Hoornweg, D., Bhada-Tata, P., & Kennedy, C., 2013, 'Waste production must peak this century', *Nature,* 502, 615–617.

Berenger, L. & Fazlulhaq, N., 2009, 'Garbage crisis growing by the day', *The Sunday Times (Sri Lanka)*, March 22, 11.

Vilar, O., & Carvalho, M., 2004, 'Mechanical properties of municipal solid waste', *ASTM Journal of Testing and Evaluation*, 32 (6), 1–12.

Jafari, N.H., D. Stark, T., & Merry, S., 2013, 'The July 10 2000 Payatas Landfill Slope Failure', *International Journal of Geoengineering Case histories*, 2(3), 208-228.

De Silva, L., & Jayamanne, D., 2009, 'Bloemendhal garbage dump in danger of exploding – CMC', *The Island (Sri Lanka)*, March 09, 10.

Pandey, R.K., & Tiwari, R.P., *2015,* 'Physical Characterization and Geotechnical Properties of Municipal Solid Waste', 12(1), 15-21.

Reddy, K.R., Hettiarachchi, H., Parakalla, N., Gangathulasi, J. & Bogner, J.E., 2009, 'Geotechnical properties of landfilled municipal solid waste under short-term leachate recirculation operations', *Waste Management and Research*, 27(6), 578-587.

Khalil, M.J., Gupta, R., & Sharma, K., 'Microbiological Degradation of Municipal Solid Waste in Landfills for LFG Generation', 10–14.

Proceedings of the 7th International Symposium on

Advances in Civil and Environmental Engineering Practices for Sustainable Development

ACEPS - 2019

Modelling soil-gas diffusivity in aggregated porous media.

J.R.R.N. Jayarathne[1], T.K.K. Chamindu Deepagoda[1,3], M.C.M. Nasvi[1], K. Smits[2], T.J. Clough[3], S. Thomas[4] and B. Elberling[5]

[1]Dept. of Civil Engineering, Faculty of Engineering, University of Peradeniya, 20400 Peradeniya, SRI LANKA.
[2]Dept. of Civil Engineering, University of Texas, Arlington, TX 76019, USA.
[3]Dept. of Soil and Physical Sciences, Lincoln University, P.O. Box 85084, Lincoln, 7647, NEW ZEALAND.
[4]Plant & Food Research Lid, Gerald St, Lincoln 7608, NEW ZEALAND.
[5]Dept. of Geosicences and Natural Resources Management, Center for Permafrost (CENPERM), University of Copenhagen, Øster Volgade 10, DK-1350 Copenhagen, DENMARK

K e y w o r d s

Aggregated porous media
Pore size distribution
Inter aggregate pores
Intra aggregate pores
Gas diffusivity
Two-Region model

A B S T R A C T

Aggregated porous media are widely used as plant growth substrates due to its inherent structural properties and their distinctive mass transport characteristics. Soil-gas diffusivity (D_p/D_o; where D_p and D_o are gas diffusion coefficients for a given gas in porous medium and free air, respectively) characterizes the ability of the media to facilitate diffusion-controlled movement of gases, and is a function of air-filled porosity (ε) and gaseous phase tortuosity (τ) of the functional media gaseous phase. Due to the inherent two-region/bimodal characteristics (i.e., inter-aggregate and intraaggregate) in aggregated media, the classical gas diffusivity models developed originally for unimodal soils markedly mischaracterize the diffusive behavior in aggregated media. Specially developed bimodal models are therefore required in explaining gas diffusivity in well-aggregated and structured soils. This study investigated 7 naturally aggregated soils and 4 manufactured bimodal porous media in relation to their D_p/D_o behavior. Pore size distribution analysis well explained the two-pore domains in the selected media. We compared the measured D_p/D_o data against six diffusivity models including classical and recently developed bimodal diffusivity models and found that a recently developed Two-Region model outperformed other models by accurately parametrizing and characterizing D_p/D_o behaviors of aggregated porous media.

1. INTRODUCTION

Aggregated porous media have been widely used as promising plant growth substrates in current day agricultural and horticultural applications (Jones *et al*. 2003). Agricultural soils are a naturally occurring aggregated porous media due to the presence of high organic matter and frequent tilling operations facilitating soil structure development (Moldrup *et al*. 2000; Chamindu Deepagoda *et al*. 2011a). Manufactured media also have long received significant attention in horticultural applications due to the pronounced properties facilitating plant growth (Jones *et al*. 2003). Both natural and artificially formed porous media are of greater diversity depending on the raw material used, structural arrangement and size distribution of pores, density (or lightness/ heaviness), strength and temperature resistivity. An aggregated medium will essentially have two distinct porosity regions, i.e., the pore space between aggregates -interaggregate pores and the pore space within the media aggregates-intraaggregate pores. The availability of two distinct pore regions influences media's properties such as its ability in transporting gases typically described by soil-gas diffusion coefficient (D_p, $m^2\ s^{-1}$), which is also a governing criterion in selecting prospective growth media for cultivation (Jones and Or, 1998). D_p is expressed in terms of soil-gas diffusivity (D_p/D_o, where D_o ($m^2\ s^{-1}$) is the diffusion coefficient of same gas in free air)

which is a function of soil air-filled porosity (ε, $cm^3\ cm^{-3}$) and gaseous phase tortuosity (ζ) of the functional soil gas phase.

Accurate determination of D_p/D_o is largely restricted by the necessity of specific apparatus and controlled boundary conditions. Therefore, the use of predictive models to estimate D_p/D_o from easy-to-measure soil physical properties (soil air-filled porosity and total porosity) is the common practice over experimental determination.

Starting from the pioneering single-parameter Buckingham (1904) model, predictive D_p/D_o models have historically adopted two-parameter functions, and multi-parameter linear functions, power-law functions and combinations thereof for non-aggregated soils (Marshall, 1959; Millington and Quirk, 1961; Moldrup *et al*. 2013). The use of these models for aggregated soils may result in biased results due to their incapability in capturing the gas diffusivity through two distinct pore regions. Two-region diffusivity models specifically developed for aggregated media are available in the literature (e.g., Resurreccion *et al*. 2008; Resurreccion *et al*. 2010; Density-Corrected model (Chamindu Deepagoda *et al*. 2011a)), but are of limited applicability. The two-region soil-gas diffusivity model developed by Jayarathne *et al*. (2019) performed well in characterising the two-region diffusivity behaviour of aggregated agricultural soils as compared to other bimodal diffusivity models, but has not been tested against a wide range of aggregated media including the manufactured media.

In this study, we selected 11 aggregated porous media from literature representing 7 natural agricultural soils and 4 manufactured porous media (growth media) to analyse their soil gas diffusivity. Measured data were tested against selected widely used conventional diffusivity models, two- region models and the suggested two-region model for selecting a suitable model for bimodal porous media with a wider property variation.

2. MATERIALS AND METHODS

2.1. Porous Media and Data

Natural and manufactured porous media, 11 in total, were selected from literature to represent a wide range of soil total porosity. Natural porous media consist of agricultural soils from Peradeniya Pasture (PD-P) (≤ 2 mm) from Jayarathne *et al* (2019), Nishi-Tokyo Pasture (NT-P) and Nishi-Tokyo Cultivated (NT-C) from Chamindu Deepagoda *et al* (2011b), and four manufactured porous media: Turface (2.0-5.0 mm), Profile (0.25 - 0.85 mm), Zeophonic (0.25 - 1.0) and Pumice (3.2-9.5 mm) from Chamindu Deepagoda *et al* (2012).

Agricultural soils were sampled in bulk, air-dried and sieved (≤ 2 mm) to desired particle size fractions. Manufactured media have their own size-range and distribution. Further detail can be obtained from Chamindu Deepagoda *et al* (2012). Aggregated media are repacked into pre-determined dry densities as presented in Table 1 below.

Table 1:Porous media properties and data reference

Porous Media	Φ ($cm^3\ cm^{-3}$)	ρ_b ($g\ cm^{-3}$)	Reference
PD-P (1.0 g cm^{-3})	0.55	1.0	This study / Jayarathne *et al* (2019)
PD-P (1.3 g cm^{-3})	0.53	1.3	
NT-P	0.76	NA	Chamindu Deepagoda *et al* (2011b)
NT-C	0.74-0.76	NA	
Turface (2.0-5.0 mm)	0.75	0.62	Chamindu Deepagoda *et al* (2012)
Profile (0.25-0.85 mm)	0.74	0.65	
Zeophonic (0.25-1.0 mm)	0.61	0.97	
Pumice (3.2-9.5 mm)	0.83	0.36	
PD-P – Peradeniya Pasture soil NT-P – Nishi-Tokyo Pasture soil NT-C – Nishi-Tokyo Cultivated soil			Φ – Total porosity ρ_b – Bulk density NA – Not Available

2.2. Measurement methods

2.2.1. Soil-gas diffusivity

Soil-gas diffusivity of all repacked media was measured using samples repacked at desired bulk densities into 100 cm^3 stainless steel annular cores according to the one-chamber method introduced by Taylor (1949). D_p/D_o measurements were calculated following the Currie's (1960) method.

2.2.2. Pore size distribution

Pore size distribution of each porous media is determined using the first derivative of the bimodal van-Genuchten-type water retention function (Durner 1994) shown in Eq. (1) below.

$$S_e = \frac{\theta-\theta_r}{\theta_s-\theta_r} = \sum_{i=1}^{2} w_i \left[1 + a_i|\psi|^{n_i}\right]^{-m_i} \qquad (1)$$

Where θ_s is the soil-water content at saturation ($cm^3\ cm^{-3}$), θ_r is the residual water content ($cm^3\ cm^{-3}$), w_1 and w_2 are model weighting factors, α_1 and α_2 are model scaling factors (cm^{-1}), n_1, n_2, $m_1=(1-1/n_1)$ and $m_2=(1-1/n_2)$ are model shape factors and ψ is the matric potential. The first derivative of Eq. (1) yields.

$$\frac{d\theta(r)}{dlog_{10}r} = \frac{d\theta(pF)}{d(pF)} = \frac{d\theta(\psi)}{dlog_{10}|\psi|} = \frac{d\theta(\psi)}{d\psi} = [log_e 10]|\psi|\frac{\partial\theta}{\partial\psi} \qquad (2)$$

Where $pF=log$ (-ψ, cm H_2O) (Schofield 1935).

2.3. Soil-Gas Diffusivity modelling

For evaluating the applicability of existing predictive models, six models were selected representing the evolution of models up to bimodal multi-parameter fitting models as follows. Buckingham (1904) (Eq.3) is the pioneering soil-gas diffusivity model built with a single parametric input, soil air-filled porosity (ε).

$$\frac{D_p}{D_o} = \varepsilon^2 \qquad (3)$$

Marshall (1959) (Eq.4) is a combination of pore-size distribution based permeability equation and Darcy' law to yield single parameter power low function.

$$\frac{D_p}{D_o} = \varepsilon^{3/2} \qquad (4)$$

Millington & Quirk (1961) is a multi-parameter soil type dependent model universally accepted and frequently used by environmental authorities and modern risk assessment tools and also considered to be a competitor for new models.

$$\frac{D_p}{D_o} = \frac{\varepsilon^{10/3}}{\emptyset^2} \qquad (5)$$

Structure-Dependent Water-Induced Linear Reduction (SWLR) model by Moldrup *et al* (2013) is a highly recommended model for use in simulations of gas diffusion and fate in the soil vadose zone especially due to its special capability in well representing and distinguishing between intact and repacked soils using its complexity factor Cm

$$\frac{D_p}{D_o} = \varepsilon^{(1+C_m)}\left(\frac{\varepsilon}{\emptyset}\right) \qquad (6)$$

Where C_m is the media complexity factor =1 for repacked soils and =2.1 for intact soils.

Density Corrected (DC) model by Chamindu Deepagoda *et al* 2011a) is well known for its better performance in predicting D_p/D_o of different soil types and densities across all moisture saturation levels occurring under natural field conditions and especially its better performance in parameterizing aggregated soils.

- For Region 1:

$$\frac{D_p}{D_o} = 0.1\left[2\left(\frac{\varepsilon}{\emptyset_1}\right)^3 + 0.04\left(\frac{\varepsilon}{\emptyset_1}\right)\right] \quad (pF \le 3.0) \qquad (7)$$

- For Region 2:

$$\frac{D_p}{D_o} = \frac{D_p}{D_o}\Big|_{pF=3.0} + (\varepsilon - \emptyset_1)^2 \qquad (pF > 3.0) \qquad (8)$$

Where Φ_1 is the interaggregate porosity assumed equal to the air-filled porosity measured at pF 3.0 and $D_p/D_o|_{pF=3.0}$ is the predicted gas diffusivity at pF=3.0.

Two-Region model by Jayarathne *et al* (2019) outperformed all classical and newly developed one region and two-region models in better parametrising soil-gas diffusivity behaviour in aggregated agricultural soils. This is a multi-parameter fitting model capable of numerically indicating the fraction of inter and intra aggregate porosities using a best-fit weighting factor w.

- For Region 1:

$$\frac{D_p}{D_o} = \frac{\alpha_1}{w^{\beta_1}}\left(\frac{\varepsilon}{\emptyset}\right)^{\beta_1} \qquad \varepsilon \le w\emptyset \qquad (9)$$

- For Region 2:

$$\frac{D_p}{D_o} = \alpha_1 + \frac{\alpha_2}{(1-w)^{\beta_2}}\left(\frac{\varepsilon - w\emptyset}{\emptyset}\right)^{\beta_2} \qquad \varepsilon \le (1-w)\emptyset \quad (10)$$

Where α_1, α_2 are model scaling factors representing Region-1 and Region-2, respectively, while β_1, β_2 are corresponding shape factors and hereafter combined effect of Eq. (9) and (10) are referred to as Eq. (10).

2.4. Statistical analysis

The conformity of the proposed model with the measured soil-gas diffusivity data and the overall performance of the existing models were evaluated and compared using RMSE and bias. To evaluate the overall fit of a model to the measured data, the RMSE was used:

$$RMSE = \sqrt{\frac{1}{n}\sum_{i=1}^{n}(d_i)^2} \qquad (11)$$

And the bias was used to evaluate whether a model provided an overprediction (positive bias) or an underprediction (negative bias).

$$BIAS = \frac{1}{n}\sum_{i=1}^{n}(d_i) \qquad (12)$$

3. RESULTS AND DISCUSSION

3.1. Pore size distribution

Pore size distributions of selected porous media are presented under Figure 1 below as (a) exhibits the pore distribution in natural soils while (b) represents the pore distribution in manufactured porous media. As the figure shows, there are two distinct pore regions in each media represented with two peaks in each curve. Apparently, in PD-P soils, the variation of pore sizes is limited to a narrow region as the peaks are located closer while the density of intraaggregate pores are comparatively high. For NT soils, the distribution of pore sizes has spaned considerably over a wide range and the density of inter and intra pores are not much differed as in PD-P soils. Though the density of inter aggregate pores is high, comparatively an equal density of intra aggregate pores is also available. A good correlation of pore sizes with aggregate sizes can be observed with the shift of peak in NT soils. As the aggregate size increases, the inter aggregate pore peak shifted rightwards implying an increase in inter aggregate pore size.

Concerning the manufactured growth media, the distribution of pores had occurred through a wider range having comparatively high pore radii for inter aggregate pores and smaller radii for intra aggregate pores. Further, it can be seen that the distribution of pores is clearly discontinuous in all four media. There is a region of zero pore density between the two peaks of each curve, suggesting that there are no pores of the particular size. The correlation of pore size

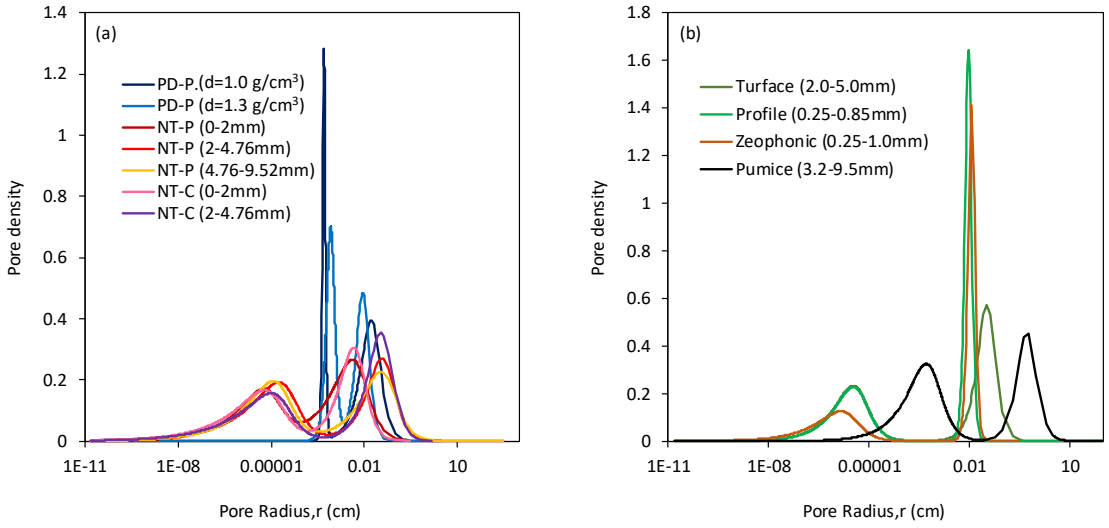

Figure 1: Pore size distribution of (a) natural agricultural soils and (b) manufactured growth media.

distribution and the aggregate size can be well explained with Turface (92.0-5.0 mm) and Profile (0.25-0.8 5mm) pore distribution curves. We note that the Profile (0.25-0.85m) is an invariant of Turface (2.0-5.0 mm). Turface has a higher inter aggregate pore radius with comparatively less pore density while Profile has a smaller inter aggregate pore radius with a higher pore density. However, both the media has the same intra aggregate porosity in radius and density as clearly shown by the coincided curves. Zeophonic and Pumice, made of different materials, showed a good correlation of pore sizes with their aggregate sizes as expected.

3.2. Modelling D_p/D_o: Two-region model

The suggested Two-Region model (Eq. 9) for characterising gas diffusivity in well aggregated porous media fitted to measured data are presented in Figure 2. The figure shows the measured diffusivity data for (a) natural agricultural soils (PD-P, NT-P and NT-C) (b) manufactured growth media with the parameterized two-region model. In each application, β_2 is set equal to unity to capture the apparent linearity in the intraaggregate region. The unique structural fingerprints of D_p/D_o measurements in a well aggregated porous media are demonstrated by the figure. In Figure 2(a), considered at a particular ε value, all agricultural media showed a higher diffusivity in smaller air-filled porosities or the wet end of the curves, when the density is high or the aggregate size is smaller. As the density increases or the aggregate size decreases, at the same air-filled porosity, size of the interaggregate pores get smaller and hence the amount of water retaining within the pores is less (Moldrup *et al*. 2005a). Conversely, under near-saturated conditions, the amount of water stored within pores is high as the pore size increases thus creating a water bridging effect. As a result, high-dense media with smaller aggregates show a higher diffusivity in interaggregate region compered to low dense or larger aggregate soils. As the pores drain sequentially, the pattern rearranges to have higher diffusivity values from low dense soils or soils with bigger aggregates due to the opening of less tortuous pathways (Currie 1984). Towards the dry end, it was 2-4.76 mm NT-P or NT-C or PD-P (1.0 g/cm^3) showed the highest diffusivity values.

Similar trend could be observed with manufactured growth media too as shown by the Figure 2(b). Turface and Profile are two aggregate sizes of the same material with equal intraaggregate pore distribution, Turface showed a higher tortuosity originated due to water bridging effect up to a considerable porosity range where draining of water suddenly started to diffuse gas through the medium. Profile, being smaller in size, gave D_p/D_o results within entire saturation range clearly distinguishing between intra and inter aggregate pore diffusivity. Zeophonic, having similar pore size distribution showed similar behaviour in

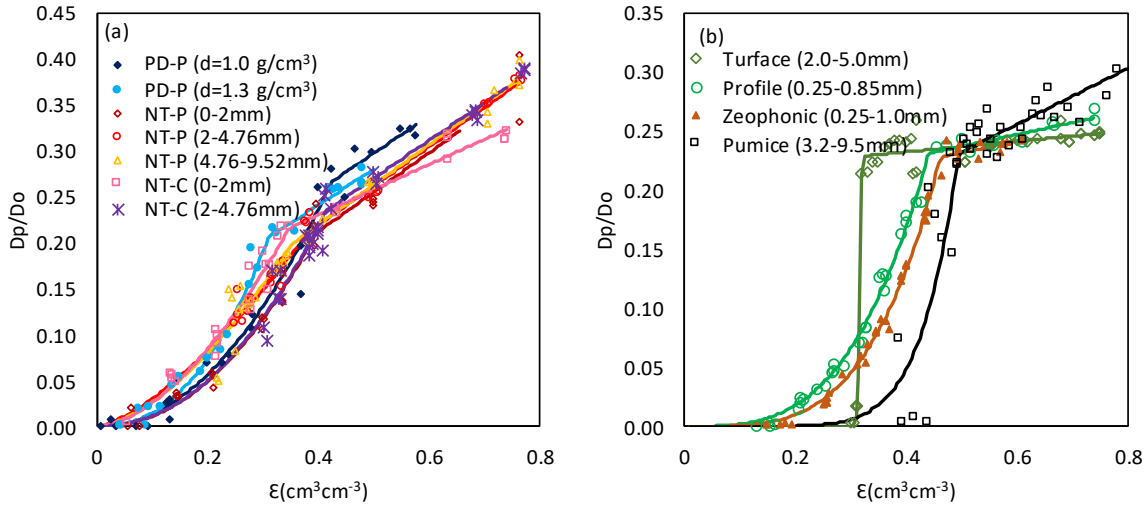

Figure 2: Scatterplot for measured diffusivity values of (a) natural agricultural soils and (b) Manufactured growth media along with the fitted Two-Region model (Solid lines)

diffusivity too. With a low pore density in intraaggregate pores, the span of the linear region of the curve is comparatively shorter although the gradient stayed parallel with Profile. Pumice, having considerably higher pore radii for both inter and intra aggregate pores, and a moderate density showed low diffusivity values taken at an air-filled porosity compared to other media. However, a sudden increase of gas diffusivity could be observed as the media get dried, when intra aggregate pores are open for gas migration. Therefore, it is evident that the suggested two-region model is well capable of adequately characterise and parameterise the gas diffusivity of aggregated porous media clearly distinguishing between inter and intra aggregate porosities.

3.3. Model comparison

The promising behaviour of two-region model is further confirmed by the compared results of measured diffusivity values against modelled diffusivity based on the classical and recently developed as well as the recently developed DC and the two-region models as demonstrated in Figure 3. Staggered scatter points in Figure 3(a), (b), (c), and (d) emphasize the inability of classical models to accurately characterize gas diffusivity in aggregated media. All Buckingham (1904), Millington & Quirk (1961) and SWLR (Moldrup *et al*. 2013) models underpredicted the diffusivity values during wet region (lower air-filled porosities) and highly overpredicted as the media drain toward the dry ends, hence leading to marked overall mischaracterization. Comparatively the two-region models, DC (Figure 3(e)) and the two-region models (Figure 3(f)) showed a minor disparity with measured data. Noticeably, DC was unable to accurately parameterise the diffusivity behaviour of some porous media, specially Turface (2 – 5 mm) and Pumice (3.2-9.5 mm) which are of larger aggregate sizes. The model overpredicted across the entire saturation range. As both the media having a considerable percolation threshold in their diffusivity towards the wet end due to the water-induced tortuosity, no diffusivity results were observed though DC model gives diffusivity results. Outperforming all the models, the two-Region model could

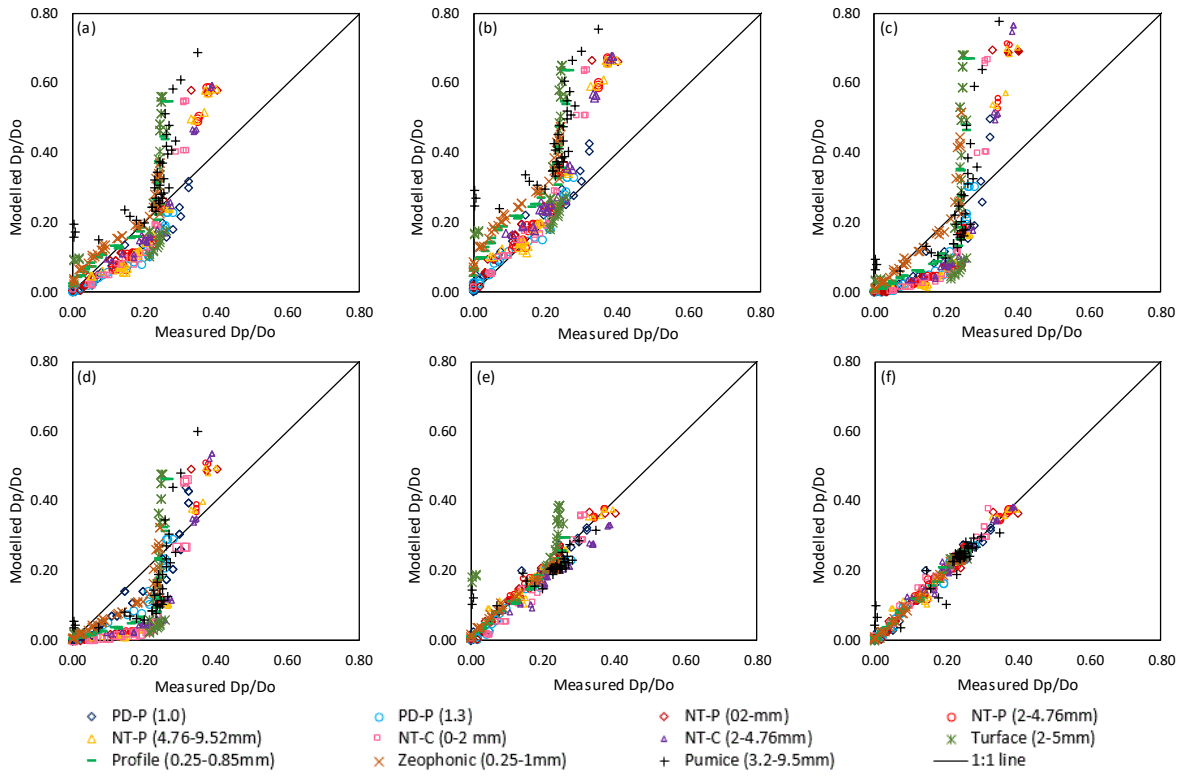

Figure 3: Scatter point comparison for measured D_p/D_o of selected porous media against modelled D_p/D_o results from (a) Buckingham (1904), (b) Marshall (1959) (c)Millington and Quirk (1961), (d) SWLR (Moldrup *et al*. 2013) (e) Density Corrected - DC (Chamindu Deepagoda *et al.* 2011a) and (f)Two-Region model (Jayarathne *et al.* 2019) models.

adequately capture the unique features of media and their diffusivity behaviours and gave a good correlation between measured and modelled values. The scatter points are laying along the 1:1 line except for few deviations by Pumice (3.2-9.5 mm) samples.

Numerical comparison results of the models using two statistical indices RMSE and BIAS are given under the Table 2 below. RMSE values are reported for each porous media and the corresponding BIAS values are given within parenthesis. As the results are shown by Table 2, Two-region model gave the least RMSE value for all the soils and satisfactory BIAS values.

The suggested two-region model provides a tool to the accurate parameterization of gas diffusivity through aggregated porous media under varying conditions of bulk density and moisture. this in turn, will facilitate in selection of suitable porous media in specific applications by conducting a quick analysis with basic physical parameters such as media total porosity and air-filled porosity under varying moisture statuses.

4. CONCLUSIONS

This study investigated the effect of porous media status such as aggregation, bulk density, porosity variation and aggregate size distribution on gas diffusivity (D_p/D_o) in natural agricultural soils, and manufactured growth media. The analysis revealed strongly aggregated behaviour and the presence of the inter and intra aggregate pores regions within all selected media. The suggested two-region model by Jayarathne *et al* (2019) accurately parameterised and characterised measured diffusivity (D_p/D_o) data from all aggregated porous media as compared to widely known conventional and recently-developed models.

Table 2: Statistical performance of classical models and two-region model against measured D_p/D_o data.

Porous Media	Buckingham (1904)	Marshall (1959)	MQ (1961)	SWLR	DC	Two-Region
PD-P (1.0 g cm^{-3})	0.0437 (-0.0290)	0.0454 (0.0324)	0.0755 (-0.0133)	0.0499 (-0.0122)	0.0544 (-0.0466)	0.0162 (-0.0003)
PD-P (1.3 g cm^{-3})	0.0594 (-0.0468)	0.0293 (0.0127)	0.0697 (-0.0468)	0.0545 (-0.0367)	0.0237 (-0.0176)	0.0106 (-0.0004)
NT-P (0-2 mm)	0.0804 (0.0083)	0.1160 (0.0751)	0.1379 (-0.0200)	0.1076 (-0.0618)	0.0201 (0.0084)	0.0157 (-0.0009)
NT-P (2-4.76 mm)	0.0998 (0.0013)	0.1343 (0.0833)	0.1636 (-0.0287)	0.1294 (-0.0891)	0.0495 (0.0084)	0.0105 (-0.0001)
NT-P (4.76-9.52 mm)	0.0959 (-0.0085)	0.1237 (0.0704)	0.1582 (-0.0395)	0.1294 (-0.0930)	0.3361 (-0.0235)	0.0182 (0.0001)
NT-C (0-2 mm)	0.0995 (-0.0102)	0.1251 (0.0606)	0.1546 (-0.0348)	0.1252 (-0.0819)	0.0345 (-0.0230)	0.0145 (-0.0002)
NT-C (2-4.76 mm)	0.0925 (0.0041)	0.1322 (0.0945)	0.1701 (-0.0256)	0.1400 (-0.0969)	0.0485 (-0.0448)	0.0150 (0.0002)
Turface (2.0-5.0 mm)	0.1770 (0.0902)	0.2384 (0.1822)	0.2319 (0.0758)	0.1543 (-0.0182)	0.0918 (0.0566)	0.0088 (-0.0002)
Profile (0.25-0.85 mm)	0.0865 (0.0449)	0.1487 (0.1241)	0.1170 (0.0059)	0.0870 (-0.0407)	0.0163 (-0.0053)	0.0070 (0.0006)
Zeophonic (0.25-1.0 mm)	0.0526 (0.0414)	0.1339 (0.1275)	0.0903 (0.0396)	0.0477 (-0.0231)	0.0168 (-0.0038)	0.0062 (0.0004)
Pumice (3.2-9.5 mm)	0.1428 (0.1101)	0.2261 (0.2097)	0.1324 (0.0277)	0.1119 (-0.0498)	0.0488 (-0.0143)	0.0331 (0.0004)

PD-P – Peradeniya Pasture soil
NT-P – Nishi-Tokyo Pasture soil
NT-C – Nishi-Tokyo Cultivated soil
MQ (1961) – Millington and Quirk (1961) model
SWLR – Structure-Dependent Water-Induced Linear Reduction model (Moldrup et al., 2013)
DC – Density corrected model (Chamindu Deepagoda et al.,2011DC)

RMSE values and BIAS values (given within parenthesis) of all diffusivity models in parametrizing measured diffusivity data are presented.

5. AKNOWLEDGEMENT

The authors gratefully acknowledge the financial support from National Research Council of Sri Lanka (NRC-17-019) and New Zealand Agricultural Greenhouse Gas Research Centre (NZAGRC).

6. SREFERENCES

Buckingham, E., 1904, 'Contributions to our knowledge of the aeration of soils', *Bur. Soil Bull. 25*, U.S. Gov. Print. Office, Washington, DC.

Chamindu Deepagoda, T.K.K., Moldrup, P., Jensen, M.P., Jones, S.B., de Jonge, L.W., Schjønning, P., Scow, K., Hopmans, J.W.,Rolston, D.E., Kawamoto, K., & Komatsu, T., 2012, 'Diffusion aspects of designing porous growth media for earth and space soils', *Soil Sci. Soc.* Am.J.76, 1564-1578.

Chamindu Deepagoda, T.K.K., P. Moldrup, P. Schjønning, K. Kawamoto, T. Komatsu, and L.W. de Jonge, 2011b, 'Generalized density corrected model for gas diffusivity in variably saturated soils', *Soil Sci. Soc.* Am.J.74, 1302-1317.

Chamindu Deepagoda, T.K.K., P. Moldrup, P. Schjonning, L.W. de Jonge, K. Kawamoto, and T. Komatsu, 2011a, 'Density-corrected models for gas diffusivity and air permeability in unsaturated soil', *Vadose Zone,* J.10, 2136.

Currie J.A., 1960, 'Gaseous diffusion in porous media', *Part 2. – Dry granular materials.* Br. J. Appl. Phys. 11,318–324.

Currie J.A. 1984. *Gas diffusion through soil crumbs: the effects of compaction and wetting.* J. Soil Sci., 35,1-10.

Durner, W., 1994, 'Hydraulic conductivity estimation for soils with heterogeneous pore structure', *Water Resour,* Res. 30, 211–223.

Jayarathne, J.R.R.N., Chamindu Deepagoda T.K.K., Clough T.J., Nasvi M.C.M., Thomas S., Elberling B., 2019, 'Gas-Diffusivity Based Characterization of Aggregated Agricultural Soil', *Soil Science Society of America Journal* (Under review).

Jones, S.B., and D. Or., 1998, '*Particulated growth media for optimal liquid and gaseous fluxes to plant roots in microgravity*', Adv. Space, Res. 22,1413–1418.

Jones, S.B., D. Or, and G.E. Bingham, 2003., 'Gas diffusion measurement and modeling in coarse- textured porous media', *Vadose Zone,* J. 2,602–610.

Marshall, T.J., 1959,'The diffusion of gases through porous media', J. *Soil Sci*.,10,79–82.

Millington, R.J., & J.M. Quirk., 1961, 'Permeability of porous solids', *Trans. Faraday Soc.*, 57,1200–1207.

Moldrup P, T. Olesen, J. Gamst, P. Schjonning, T. Yamaguchi, & D.E. Rolston., 2000,' Predicting the gas diffusion coefficient in undisturbed soil from soil water characteristics', *S. Sci. Soc*. Am. J. 64,94-100.

Moldrup P., T. Olesen, S. Yoshikawa, T. Komatsu, & D. E. Rolston, 2005, 'Predictive Descriptive models for gas and solute diffusion coefficients in variably saturated porous media coupled to pore-size distribution: I Gas diffusivity in repacked soil', *Soil Sci*., 170,843-853.

Moldrup P., T.K.K. Chamindu Deepagoda, S. Hamamoto, T. Komatsu, K. Kawamoto, D. E. Rolston & L.W. de Jonge, 2013, 'Structure-Dependent Water-Induced Linear Reduction Model for Predicting Gas Diffusivity and Tortuosity in Repacked and Intact Soil', *Vadoze Zone*, J. 10,2136.

Resurreccion, A.C., P. Moldrup, K. Kawamoto, S. Hamamoto, D.E. Rolston & T. Komatsu, 2010,' Hierarchical, bimodal model for gas diffusivity in aggregated, unsaturated soils',*Soil Sci. Soc.* Am. J. 74,481–491.

Resurreccion, A.C., P. Moldrup, K. Kawamoto, S. Yoshikawa, D.E. Rolston & T. Komatsu, 2008, 'Variable Pore Connectivity Factor Model for Gas Diffusivity in Unsaturated, Aggregated Soil', *Vadose Zone* J. 7,397-405.

Taylor, S.A., 1949, 'Oxygen diffusion in porous media as a measure of soil aeration'. *Soil Sci. Soc*. Am. Proc. 14,55-61.

Proceedings of the 7th International Symposium on

Advances in Civil and Environmental Engineering Practices for Sustainable Development

ACEPS - 2019

Effects of soil moisture on simulated methane flow in a differently-compacted soil.

M. Shanujah[1], T.K.K. Chamindu Deepagoda[1], M.C.M. Nasvi[1], A. K . Karunarathna[2], V. Shreedharan[3] and G.L.S. Babu [4]

[1]Department of Civil Engineering, Faculty of Engineering, University of Peradeniya, 20400 Peradeniya, Sri Lanka
[2]Department of Agricultural Extension, Faculty of Agriculture, University of Peradeniya, 20400 Peradeniya, Sri Lanka
[3]Goverentment College of engineering, Kannur, India
[4]Indian Institute of Technology, Bangalore, India

K e y w o r d s

Gas migration and emission
Soil-water characteristic (SWC)
Gas-diffusivity
Concentration profile
Air-fill porosity
Tortuosity

A B S T R A C T

Soil density plays a crucial role in controlling migration of greenhouse gases (GHG) from terrestrial soils to the atmosphere. Soil moisture is the fundamental soil physical control of gas migration and emission in subsurface soil. This study explored migration of methane gas developed from a simulated methane source buried in a differently – compacted pasture soil. Simulations of methane flow were carried out as a density-dependent, multiphase flow of multicomponent mixtures of pasture soil (methane, water vapour and air) underneath various soil moisture conditions. Measured soil-water characteristic (SWC) and gas diffusivity data at five density levels (1.1, 1.2, 1.3, 1.4, and 1.5 Mg m^{-3}) were used to parameterize a recent gas diffusivity model. Permeability was estimated utilizing measured SWC-data based on a saturated hydraulic conductivity function. Results revealed a pronounce effect of soil density and soil moisture on simulated methane concentration profile across the depth. Comparatively, smaller profile of methane concentration at dry condition was observed in low dense soil where permeability, gas diffusivity and air-filled porosity are high, and the concentrations increased with the increasing density. In partially saturated conditions, smaller air-filled porosity and higher moisture-controlled tortuosity resulted in smaller permeability and gas diffusivity as compared to dry soils, yielding high methane concentrations within the profile for all density levels.

1. INTRODUCTION

Elevated atmospheric presence of greenhouse gases (GHG) has caused significant changes in the global climate, including global warming and climate shifts during the recent decades (IPCC 2014). Methane is a highly potent GHG, with a global warming potential 86 times greater than CO_2 on a 20-year basis and 25 times greater over a 100-year time horizon (Jackson *et al.* 2013). Methane-mediated climate changes may prompt to extreme weather events such as prolong droughts, uncommon floods, depletion of polar ice sheets, sea level rises etc. Methane, in addition, is a poisonous, explosive, and highly flammable gas, and hence may provide serious concerns of occupational safety of individuals who live in the vicinity of large potential methane sources such as landfills and natural gas infrastructure. Additionally, methane-induced chemical reactions in the stratosphere produce water vapor, which enhances the destruction of stratospheric ozone layer. Therefore, understanding of controlling mechanisms of methane emissions from various ecological systems is an important prerequisite to find long-term solutions to GHG-related environmental consequences.

A considerable amount of methane can be generated from agricultural soils (Smith *et al*. 2007), for example from grazed pasture, where anaerobic soil conditions may prevail following irrigation or rainfall events. Fate

and transport of methane in subsurface soil are primarily controlled by soil heterogeneity, soil moisture, temperature, and pressure gradients (Poulsen *et al.* 2003). Subsurface methane concentrations may pose wide negative implications for the subsurface ecosystem's health, causing the death of deep-rooted plants in agricultural systems. Excessive use of agricultural implements and animal treading at high stocking rates cause a major change in soil density in agricultural fields. Density-induced changes in soil structure influence soil-water retention, gas diffusivity (D_p/D_o, where D_p and D_o are gas diffusion coefficients in soil and free air, respectively) (Croney & Coleman 1954; Gupta *et al.* 1989) and hydraulic conductivity/permeability (Gent *et al*. 1983), which, in turn, affect potential subsurface greenhouse gas emissions and transport.

The main objective of this study was to investigate the effect of soil density on methane migration in dry and partially saturated soil systems. Using a simulated methane source buried in differently-compacted soil, we obtained a useful numerical insight of methane migration under dry and a selected soil moisture condition.

2. METHODOLOGY

2.1 Materials and Methods

Soil from the selected pasture site at Duncan Block (43°38′0.7′′ S, 172°29′40′′ N) managed by Lincoln University, New Zealand was selected for this study. The soil was recognized as a Templeton silt loam, *Typic Immature Pallic* under the New Zealand Soil Classification system (Hewitt 1998). We utilized the measured soil water characteristic (SWC) and gas diffusivity information from Balanine *et al*. (2016) to parameterize the models. The soils, sampled at a depth of 15 cm, were air-dried and sieved (< 2 mm) before packing at five bulk density (ρ_b) levels: 1.1, 1.2, 1.3, 1.4, and 1.5 Mgm^{-3}. The samples were later systematically drained at 11 equal intervals of matric potential (ψ; –1.0 to –10 kPa). One chamber diffusion apparatus (Taylor 1949) was used to measure Soil-gas diffusivity (D_p/D_o) at each matric potential. All measurements were done in triplicates. We used the multiphase transport simulator TOUGH2 (Pruess *et al.* 1999) and the Equation of State module EOS7CA (Oldenburg 2015) for numerical simulations. TOUGH2/EOS7CA has the capability of simulating subsurface flow and transport of liquid and gas phases under isothermal or non-isothermal conditions.

A 2-D Cartesian numerical domain (width; 10m, height; 0.15m) as shown in Figure 1 was divided into 270 elements for simulating methane flow in the subsurface using TOUGH2/EOS7A modelling framework. The height of the domain represents the sampling depth. The left and right boundaries and the bottom boundary of the domain were set as no-gas flow condition (Neumann-type), whereas the top boundary is considered as an open boundary for gas flow. Methane was injected at a single point in the mid of the domain 10 cm above the bottom boundary (Figure 1) with the flux rate of 9 µmol m^2 h^{-1}, which is the average methane flux rate in pasture soil (Oertel *et al.* 2016). Simulations were carried out for both fully dry ($\theta = \theta_r$) and partially saturated (θ = 0.30-0.50 cm^3 cm^{-3}) condition at the temperature of 20°C.

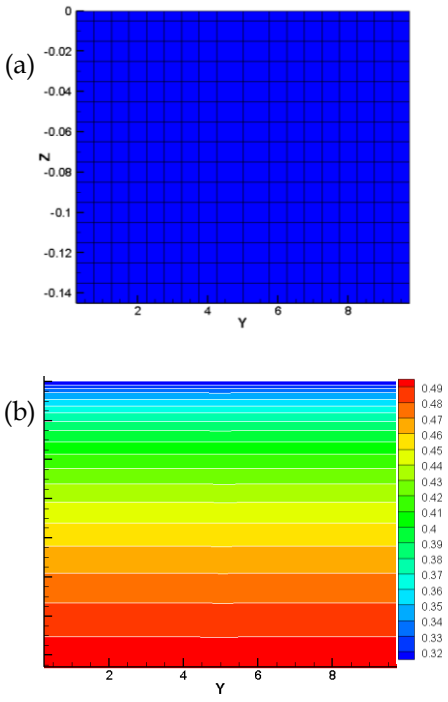

Figure 1 2-D computational domains for methane migration simulations in (a) completely dry soil, and (b) partially-saturated soil with soil moisture gradient.

3. NUMERICAL MODELING

3.1 Soil-water characteristics

We used the van Genuchten (1980) parametric water retention unimodal function to parameterize the capillary suction (ψ)-soil moisture content (θ) relation as follows:

$$\theta(\psi) = \theta_r + (\theta_s - \theta_r)\left(\frac{1}{1+|\alpha\psi|^n}\right)^m \quad (1)$$

Where θ_r (cm^3cm^{-3}) is the volumetric water content, ψ (cm) is the matric potential, θ_s (cm^3cm^{-3}) and θ_r (cm^3cm^{-3}) are the saturated and residual water contents, respectively, α is scaling factor(cm^{-1}) and n and m are model shape factors. The shape factor m can be directly linked to n (m=1-1/n). Aschonitis et al., (2012) developed a numerical function for maximum slope of θψ (Eq. 1) at the inflection point (i.e., at $d^2\theta/dh^2 = 0$) can be represented by S as below:

$$S_i = -m^{1+m} n\alpha(\theta_s - \theta_r)(1+m)^{-m-1} \quad (2)$$

3.2 Hydraulic conductivity and permeability

We used an empirical hydraulic conductivity function (Aschonitis & Antonopoulos, 2013) based on the parameterized van Genuchten model which can be presented as:

$$f = \alpha\Phi_e \quad (3)$$

Where Φ_e is the effective porosity at the suction of -33 kPa (Ahuja *et al*. 1984). Intrinsic permeability, *k*, (m^2) of a porous medium can be calculated from the hydraulic conductivity (K_s) as follows:

$$K_s = k\frac{\rho g}{\eta} \quad (4)$$

where,

$$K_s = 1632.5|S|(3.9f)^{(-3.9.f)}$$

3.3 Soil-gas diffusivity

We selected a recent empirically-based soil gas diffusivity model which account density effect on soil-gas diffusivity (Chamindu Deepagoda *et al.* 2010). The Model takes the form of:

$$\frac{D_p}{D_o} = 0.4\left(2\left(\frac{\varepsilon}{\Phi}\right)^{5.2} + 0.04\left(\frac{\varepsilon}{\Phi}\right)\right) \quad (5)$$

Where Ø is total porosity and ε is air-fill porosity. The best-fit van Genuchten model parameters, together with the basic soil properties, are given in Table 1.

Table 1 Basic soil physical properties and parameterization.

Bulk density Mg m^{-3}	Total porosity $m^3\,m^{-3}$	soil-gas diffusivity (dry soil)	Permeability¶ (x 10-12 m2)	Soil water characteristic			
				θ_r	α	n	m
1.1	0.58	0.069	19.54	0	0.07	3	0.15
1.2	0.55	0.06	11.68	0	0.05	2.5	0.16
1.3	0.51	0.036	6.84	0	0.038	1.9	0.21
1.4	0.47	0.023	2.81	0	0.012	1.65	0.3
1.5	0.43	0.016	1.3	0	0.005	0.94	0.48

¶ Estimated from K_{sat} assuming a fluidity of 9.81 x 10^6 m^{-1} s^{-1} at 20°C

Figure 2 illustrates measured soil water-characteristic (SWC) at five different density levels of the selected pasture soil together with parameterized van Genuchten model, Eq.1 (denoted by solid lines). Noticeably, a decrease in saturated moisture content (θ_s) with increasing density was observed because of the drop in total porosity due to the compaction. Compaction not only decreases the overall volume of the pores, but also causes a major shift in dominant pore regions, thereby creating a control on pore size distribution. Compaction causes an increase in micropore (pore dia. < 0.02 µm), and mesopore (0.02-30 µm) regions, which result a considerable increase in the air-entry pressure/bubbling pressure (P_b) with increasing density, as also demonstrated by the Fig. 2, however, compaction decreases macropore (> 30 µm) domains (Yahya *et al.* 2011). Note the slight between measured and simulated data for 1.1 and 1.2 (g cm^{-3}) density levels around 10 kPa matric suction, which is probably due to the aggregation of soil under low bulk density.

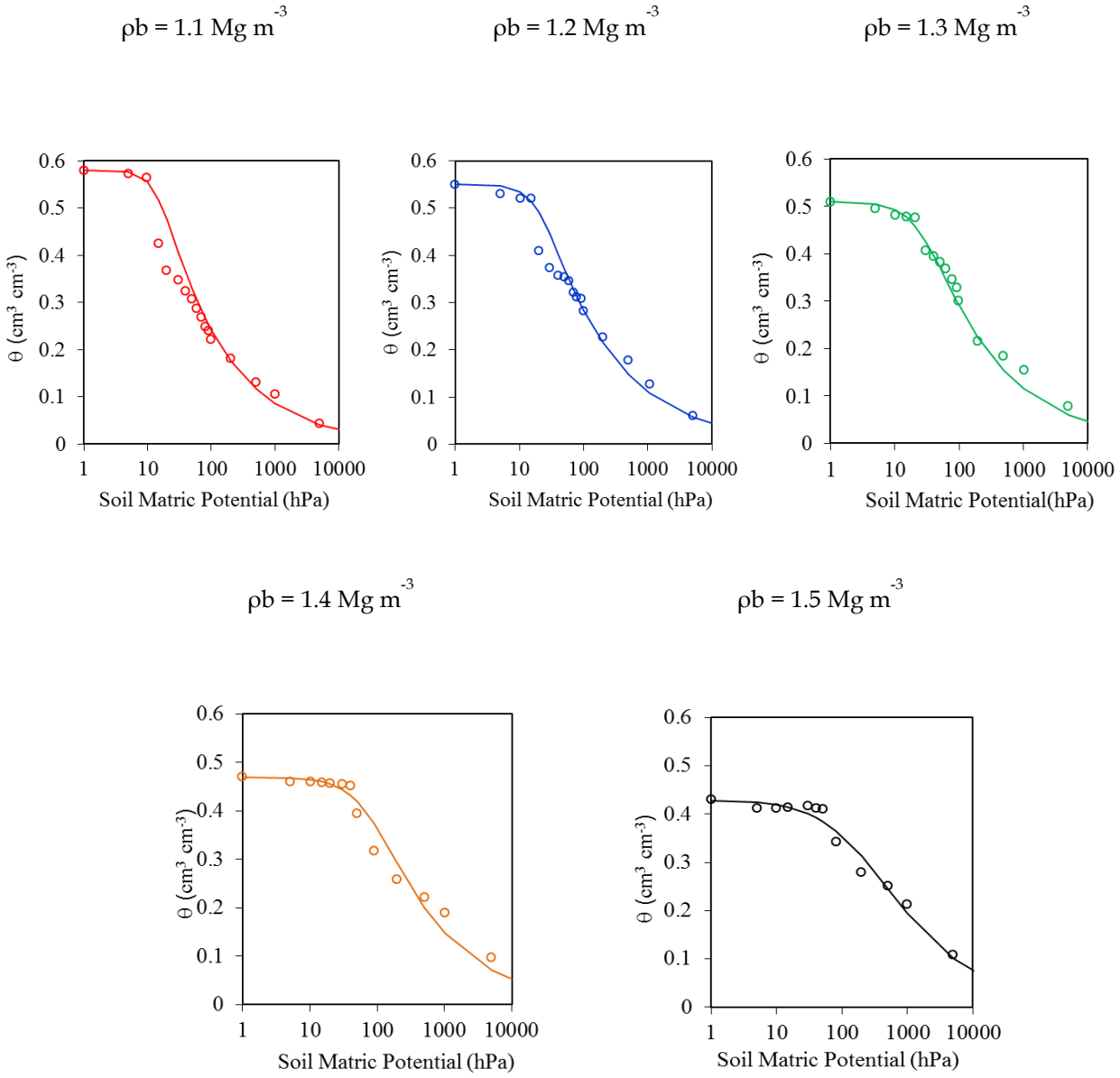

Figure 2 Measured soil-water characteristic data for five differently-compacted pasture soil together with parameterized van Genuchten model (Eq. 1) are also shown (in solid lines).

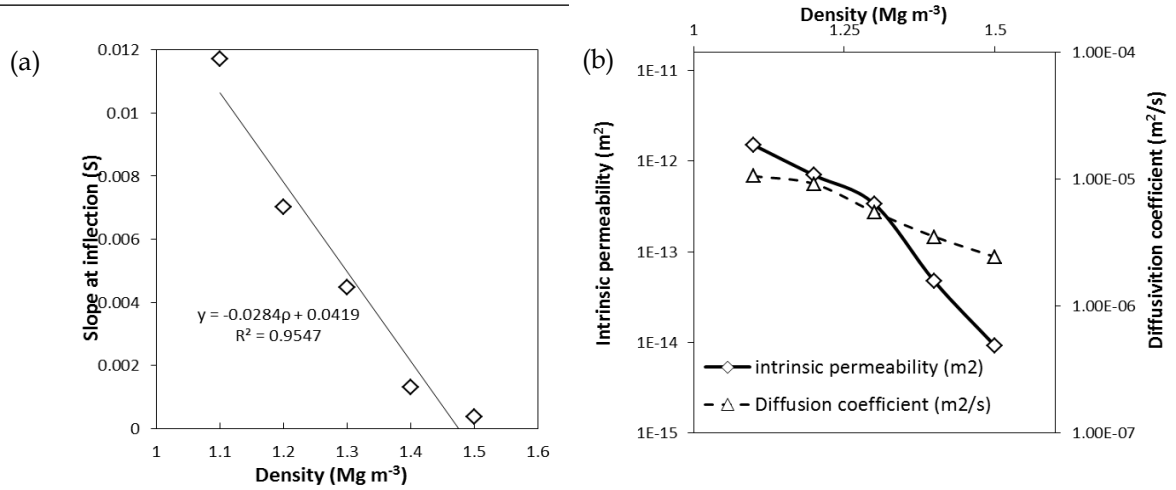

Figure 3 (a) Derived slope (Eq. 2) at the inflection point of the soil-water characteristic curve together with the best-fit linear regression line (shown in solid line). (b) Intrinsic permeability (*k*, Eq. 3 &4) and soil gas diffusion coefficient D_s, Eq. 5 against soil density.

Interestingly, a linear decrease of slope of the curve, *S* (Eq. 2) at the inflection point with the increase of density can be seen in Figure 3(a). This good linear relationship suggests the adaptability of S as a good indicator of the degree of soil densification/compaction, as demonstrated also by previous studies (e.g., Aschonitis *et al.* 2012 & Dexter 2004). Figure 3(b) represents the variation of intrinsic permeability, *k* (m^2) (Eq. 3 & 4), and soil-gas diffusion coefficient, D_s (m^2/s) (Eq. 5), with different compaction level of pasture soil. Although both parameters show the same behaviours over the density, within the range of measured density, *k* varies over a three orders-of-magnitude whereas D_s varies only less than an order-of-magnitude. Advective flow of gases in porous media mainly depends on air permeability and this advective gas flow occurs in macro-pore regions of the porous media. As depicted before, density of micro pore decreases with the increases of density which induces a significant drop in air permeability. On the other hand, diffusivity gas flow occurs in all available pore region, Soil-gas diffusion coefficient is controlled predominantly by the soil texture. However, since compaction decrease the total porosity and (solid-induced) tortuosity, a decrease in D_s can also be observed with increase of density.

Steady-state methane concentration profiles across the depth for the five density levels of dry soils at 20°C are shown in Fig. 4. An upward-protruding methane profile can be seen at all density levels due to the advective flow, which preferentially occurs upwards from the gas source whereas lateral and downward movements are only diffusion-dependent. Noticeably, the diffusive gas movement is nearly similar in all directions at a given density. However, as discussed earlier, compaction decrease in total porosity, diffusion coefficient and permeability (see Fig. 2b), which result the outward development of methane is compelled, causing an expansion in methane concentration within the profile.

Figure 5 illustrates simulated steady-state methane concentration profiles for partially-saturated conditions, white colour represent the saturation contours, after the simulations. Methane concentration contours in dry condition are completely different, that of in dry condition of the soil systems (Fig. 4), which shows a reasonable impact of soil moisture on subsurface methane movement. According to figure 4 soil moisture on methane concentration profiles is more influenced in low-dense soil (ρ_b = 1.1 g cm^{-3}) than the high-dense soil (ρ_b = 1.5 g cm^{-3}). In spite of the fact that the low-dense soil has larger air-filled pore space than the high-dense soils under the same moisture status, water held predominantly in micropores to a great extent compel the development of CH_4 through the vaporous stage, which yields a remarkable change in CH_4 concentration profiles in low-dense soil. Eminently, the saturation contours are somewhat distorted close to the gas source in high dense soil (ρ_b = 1.5 g cm^{-3}) because of the inlet speed to take into account a gaseous phase in generally fully-saturated soil layers.

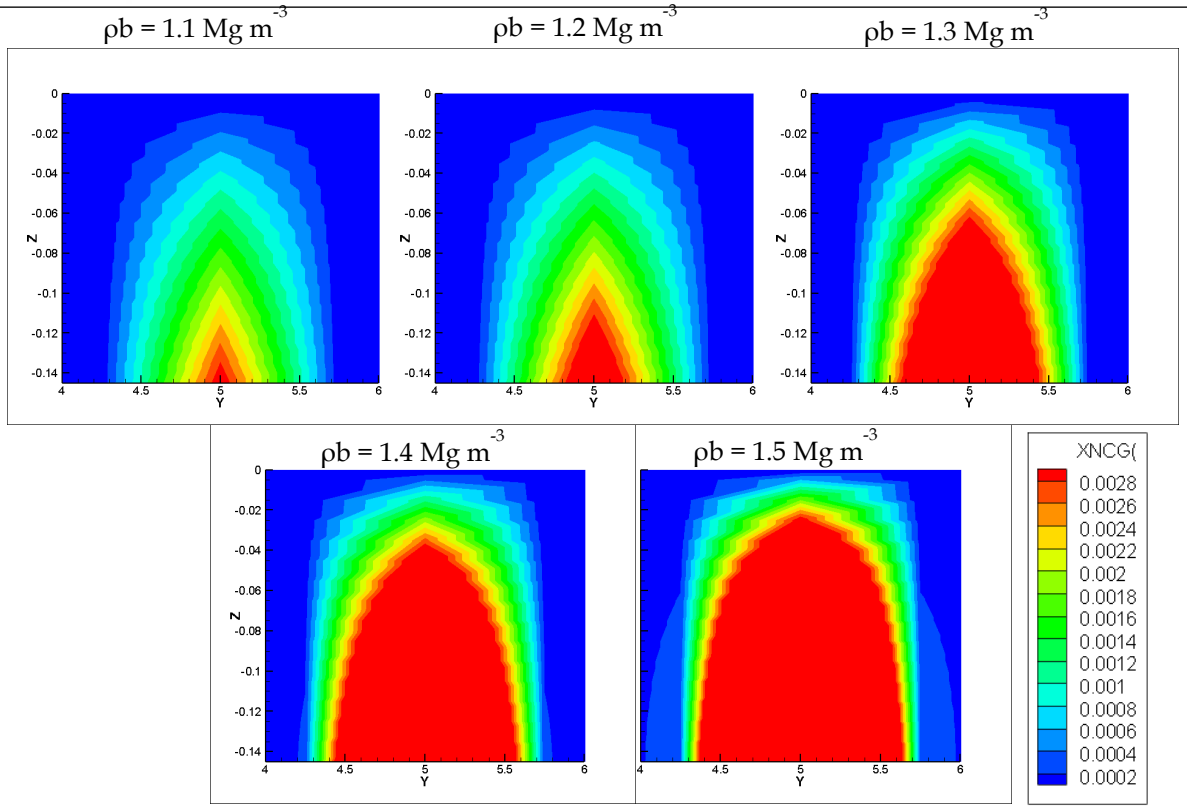

Figure 4 Simulated steady-state methane concentration profile for five density (ρ_b) levels for dry soils at 20°C. Colour contours indicate the mass fraction of methane.

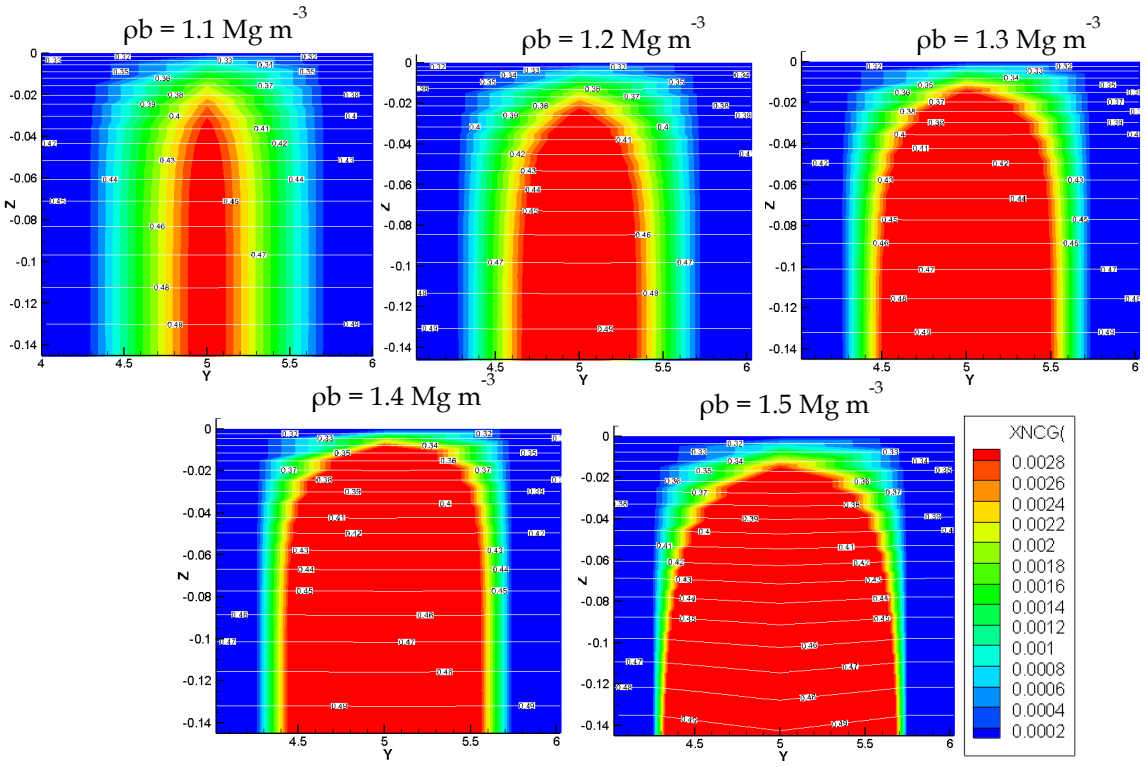

Figure 5 Simulated steady-state methane concentration profiles for five density (ρ_b) levels for partially saturated soils with a predefined soil moisture gradient at 20°C. Colour contours indicate the mass fraction of methane. White colour lines denoted the soil moisture contours after the methane flow.

4. CONCLUSIONS

We simulated subsurface methane concentration profiles in five differently-compacted soils, which provided an valuable computational insight to the density effects on methane flow under selected soil moisture conditions. We used the measured soil-water characteristic (SWC), soil gas diffusivity, and derived permeability characteristics for the simulation. Results pronounced a clear effect of soil moisture on subsurface methane concentration profiles with differently compacted soil. Furthermore, results show high methane concentration profile in high-dense soil both for dry and partially-saturated conditions. Effect of soil moisture was not evident in high-dense soils than low-dense soils. However, other environmental effects such as wind-induced atmospheric dynamics, porous media anisotropy, and methane oxidation could be needed for more accurate simulations.

5. AKNOWLEDGEMENT

The funding from Indian-Sri Lankan Inter Governmental Science and Technology Co-operation Programme (MTR/TRD/AGR /3/2/17) is gratefully acknowledged.

6. REFERENCE

Ahuja, L.R., Naney, J.W., Green, P.E. & Nielsen, D.R., 1984, 'Macro porosity to characterize spatial variability of hydraulic conductivity and effects of land management', 48: 699–702.

Aschonitis, V.G. & Antonopoulos, V.Z., 2013, 'New equations for the determination of soil saturated hydraulic conductivity using the van Genuchten model parameters and effective porosity', *Irrigation and Drainage*.

Aschonitis, V.G., Kostopoulou, S.K. & Antonopoulos, V.Z., 2012, 'Methodology to assess the effects of rice cultivation under flooded conditions on van Genuchten's model parameters and pore size distribution', *Transport in Porous Media*, 91,861-876.

Balaine, N., Clough, T.J., Beare, M.H., Thomas, S.M. & Meenken, E.D., 2016, 'Soil gas diffusivity controls N_2O and N_2 emissions and their ratio'. *Soil Sci. Soc. Am. J*, 80,529-540.

Chamindu Deepagoda, T.K.K., Smits, K.M. & Oldenburg, C.M., 2010, 'Effect of subsurface soil moisture variability and atmospheric conditions on methane gas migration in shallow subsurface', *Int J Greenh Gas Control*, 55,105–117.

Croney, D. & Coleman, J.D., 1954, 'Soil structure in relation to soil suction (pF)', *J. Soil Sci*, 5,75–84.

Dexter, A.R. 2004, 'Soil physical quality Part I. Theory, effects of soil texture, density, and organic matter, and effects on root growth', *Elsevier*, Geoderma, 120, 201-214.

Gent, J.A., Ballard, R. & Hassan, A.E., 1983, 'The impact of harvesting and site preparation on the physical properties of lower coastal plain forest soils', *Soil Sci. Soc. Am. J*, 47,595–598.

Gupta, S.C., Sharma, P.P & Defranchi, S.A., 1989, 'Compaction effects on soil structure', *Adv. Agron*, 42, 311–338.

IPCC. 2014, IPCC Special Report on *Renewable Energy Sources and Climate Change Mitigation*, prepared by Working Group III of the Intergovernmental Panel on Climate Change, Cambridge University Press, Cambridge, United Kingdom and New York, NY, USA, pp.1075 .

Jackson, R.B., Down, A., Phillips, N.G., Ackley, R.C., Cook, C.W., Plata, D.L. & Zhao, K., 2013, 'Natural gas pipeline leaks across Washington, DC', *Environ. Sci. Technol*, 48, 2051−2058.

Oertel, C., Matschullat, J., Zurba, K., Zimmermann, K. & Erasmi, S., 2016, 'Greenhouse gas emissions from soils - A review', *Soil Sci. Soc. Am. J*, 326-352.

Oldenburg, C.M., 2015, 'EOS7CA Version 1.0: TOUGH2 Module for Gas Migration in Shallow Subsurface Porous Media Systems', Lawrence Berkeley National Laboratory Report LBNL-175204.

Poulsen, T.G., Christophersen, M., Moldrup. & Kjeldsen, P., 2001, 'Modeling lateral gas transport in soil adjacent to old landfill', *J. Environ. Eng*, 127,145–153.

Pruess, K., Oldenburg, C.M. & Moridis, G.J., 1999, 'TOUGH2 User's Guide Version 2. E.O', Lawrence Berkeley National Laboratory Report, LBNL-43134.

Smith, P., Martino, D., Cai, Z., Gwary, D., Janzen, H., Kumar, P., McCarl, B., Ogle, S., O'Mara, F., Rice, C., Scholes, B. & Sirotenko, O., 2007, Agriculture in climate change: Mitigation, InContribution of Working Group III to the Fourth Assessment Report of the Intergovernmental Panel on Climate Change, edited by Metz, B., Davidson, O.R., Bosch, P.R., Dave, R. & Meyer L.A, Cambridge, UK: Cambridge University Press, 498–540.

Taylor, S.A., 1949, 'Oxygen diffusion in porous media as a measure of soil aeration', *Soil Sci. Soc. Am*, Proc. 14,55–6.

van Genuchten, M.T., 1980, 'A closed-form equation for predicting the hydraulic conductivity of unsaturated soils', *Soil Sci. Soc. Am. J*, 44,892–89.

Proceedings of the 7th International Symposium on

Advances in Civil and Environmental Engineering Practices for Sustainable Development

ACEPS - 2019

Characterization of the properties of manufactured sand and natural river sand

U. Wijepala[1], S. Jayakody[1], A.M.Z. Zimar[1], J.M.N.D. Jayasinghe[1] and W.K.W.S. Jayasena[1]

[1]Department of Civil Engineering, Faculty of Engineering, South Eastern University of Sri Lanka, SRI LANKA.

K e y w o r d s

River sand
Manufactured sand
California bearing ratio (CBR)

A B S T R A C T

River sand is the most preferred fine aggregate in construction industry. Mining the river sand causes environmental issues and therefore, requires alternatives to replace river sand to attempt towards the sustainable development. Manufactured sand is becoming popular as an alternative for fine aggregates which is produced by processing the by-products of rock quarries. However, no more engineering information is available on the properties of manufactured sand. Therefore, this study focused to investigate the properties of manufactured sand. A series of laboratory test on manufactured sand with & without mixing river sand was conducted to reveal the physical properties and to analyze the change of strength characteristics when manufactured sand presents in river sand. Results showed significant increase of the strength in terms of California bearing ratio (CBR) when the portion of manufactured sand increased in the river sand samples at their optimum moisture contents.

1. INTRODUCTION

Alternative materials for constructions are becoming popular with the issues encountered with conventional aggregates and, many research studies are being carried out all over the world (Jayakody *et al* 2017, Gobieanandh & Jayakody 2016, Jayakody *et al* 2019). River sand is the main fine aggregate used in constructions in Sri Lanka and demand in sand is high to satisfy the rapid infrastructural growth. However, Sri Lanka is facing shortage in good quality natural sand and mining of river sand causes serious threat to environment and society (Piyadasa 2009).

Researchers have begun to reveal the technical requisites of available alternative materials to replace natural sand and some of them are being used as a partial replacement of river sand (Sankh *et al* 2014). Manufactured sand (M-Sand) is one of the feasible alternatives to replace river sand in Sri Lanka since it is widely available and produced by processing the by-products of rock quarries. However, the suitability of manufactured sand for the purpose of the construction should be assessed by quality control checks before its use (Sunder & Asundi 2005).

Meghashree & Gowda (2016) introduced M-sand to replace the natural sand in concrete constructions; however, some issues of M-sand in concretes reported by researches when it fully replaced the natural sand. Zimar *et al.* (2017) reported less workability of concrete with M–sand due to the flaky shape and rough surface texture than river sand. Conversely, Shen *et al.* (2016) reported higher strength in concrete with M-sand than river sand. He further noticed significant effect of the stone powder, clay lump content and the gradation of M-sand on the strength on concrete.

Use of M-sand is relatively new for engineering applications in Sri Lanka and no more data on engineering properties of M-sand is available in Sri Lanka. Local investigations are required since the properties of the M-sand are governed by the properties of parent rock, other constituents and process of production. Therefore, M-sand

is not much popular in the industry and basic investigations are needed to reveal the engineering properties thereby, thoroughly assess the suitability. This research was focused on the characterization of manufactured sand and to compare them with river sand to evaluate the properties. Furthermore, experimental investigation was conducted to investigate the variation of properties when M-sand mixed with river sand in different portions. The outcomes of the results will increase the attention on M-sand to effectively use as fine aggregate in Sri Lankan construction industry.

2. MATERIALS AND METHODOLOGY

M-sand was obtained from a production plant in Gampaha District, Western Province in Sri Lanka and river sand was collected from Gal-Oya River, Eastern Province in Sri Lanka. Figure 1 shows the pictures of the sand samples.

(a)

(b)

Figure 1 (a) M-sand, (b) river sand

The Engineering properties of the M-sand were investigated together with the river sand for comparison. Further, it was required to determine the variation of properties of the river sand when M-sand blended in different ratios. The revealed properties of the mixed materials would be beneficial to partially replace the river sand by M-sand in particular applications. Table 1 shows the samples names with the mixed ratios of river sand and M-sand by percentage.

Table 1 Names of the test samples with mixed ratios of river sand and M-sand

Sample name	River sand – % by weight	Manufactured sand – % by weight
RS100/MS0	100	0
RS80/MS20	80	20
RS60/MS40	60	40
RS40/MS60	40	60
RS20/MS80	20	80
RS0/MS100	0	100

Six different samples were tested in the laboratories of the South Eastern University of Sri Lanka. Particle size distribution, constant head permeability test, proctor compaction test, direct shear test and California bearing ratio (CBR) test were conducted on the six samples. The gradation of the M-sand and river sand were determined by the dry sieve analysis according to the test method ASTM D422 standard (ASTM International 2007). Then other tests were conducted on the samples with particle size range 4.75 mm and 0.075 mm which is the particle size for sand as per ASTM. The constant head permeability test was carried out on six samples according to the ASTM D2434 standard (ASTM International 2006) to determine the hydraulic conductivity which reflect drainage properties of materials. Shear strength properties of the samples were obtained by conducting the direct shear test on the oven dried samples as per ASTM D3080 (ASTM International 2011). A square shape test sample with 60 mm length and 25 mm height shear box was used for the tests. Each sample was subjected to three tests at different vertical stresses of 30 kPa, 60 kPa and 120 kPa and the vertical loads were selected to represent heavy load as in the industry.

Strength of the sand samples was determined by CBR values as per standard CBR test ASTM D1883 (ASTM International 2016). CBR tests were carried out under two conditions; for the oven dried samples with zero moisture content and samples compacted to their respective optimum moisture contents (OMC). The OMC values

were determined by conducting standard proctor compaction method as per ASTM D698 (ASTM International 2012). River sand did not show compaction properties thus the OMC of the manufactured sand was applied to compact RS100/MS0 sample. The dry samples were compacted by a vibrator with surcharged load and tests were performed without curing time. The wet samples were compacted to corresponding maximum dry density values of the samples. The compacted water mixed samples then soaked for four days prior to the tests. The CBR tests were carried out on specimens with the diameter of 152 mm and the height of 177.8 mm. Load was applied through a plunger with 150 mm diameter at a constant rate of 1 mm/min.

3. RESULTS AND DISCUSSION

3.1. Particle size distribution

Particle size distribution (PSD) curves of the M-sand has drawn with the river sand for the comparison and shown in Figure 2.

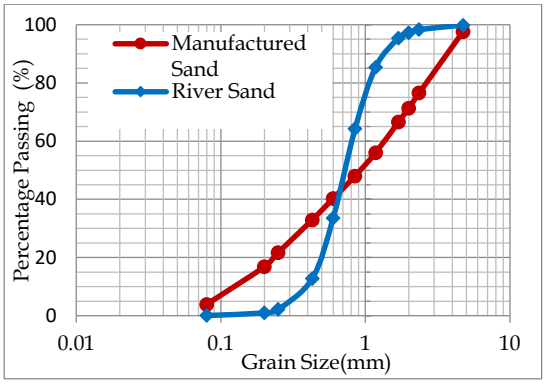

Figure 2 Particle size distribution curves of M-sand and river sand

The gradation of the river sand curve is more towards to the uniformly-graded distribution and particles are within the range of 0.3 mm to 2.00 mm. In contrast, M-sand shows well-graded distribution of their particle size and they are within the 0.08 mm to 5.00 mm. According to the ASTM standard, size of the sand should be within the range of 0.075 mm – 4.75 mm. The PSD curves illustrate lack of coarser particles in river sand than in M-sand. They show less than 3% of the coarser fraction of the sand with size range 2 mm to 4.75 mm in the river sand; while it is 30% in M-sand. Finer fraction of the river sand also very low which shows 1% of particles less than 0.1 mm sizes while it is 7.5% for M-sand. Well graded particle size distribution of the M-sand positively affects on the well compaction and high strength.

3.2. Permeability

Drainage properties of the sand samples were analyzed by their coefficient of permeability (k) values which were obtained by constant head permeability test. According to the Figure 3, the highest k value was recorded in river sand and gradually decreased with the increase of M-sand. High compaction with the well-graded particles distribution and presence of more flaky shapes of the M-sand particles (Shen *et al* 2016) restrict the water flow and decrease the permeability. Decrease the k values in M-sand reflect the water retaining ability than the river sand which is constructive to increase the workability when use as a filling material and for ground improvement applications.

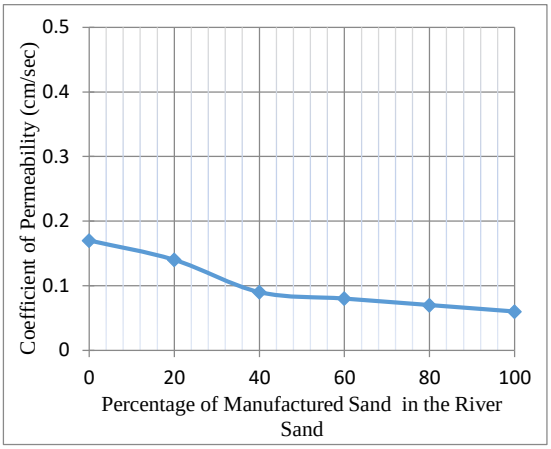

Figure 3 Variation of the hydraulic gradient of sand samples with the increase of M-sand

3.3. Shear strength properties

Shear strength properties of the sand samples were obtained for dry samples with zero moisture contents by direct shear test. The cohesion was determined as zero of the sand samples and friction angles were calculated by Mohr circles and failure envelopes. Figure 4 shows almost similar values of friction angles of M-sand and river sand as 36^0 and 33^0 respectively. The shape and surface roughness of the M-sand particles

have not significantly affected on the friction angle of the sand samples at the dry state. Compaction of the both river sand and M-sand was poor at the dry condition and arrangement of loose the particles caused similar behavior at the direct shear test consequently similar results were obtained. However, the blended sand samples; RS80/MS20 and RS40/MS60 revealed slightly higher friction angles as 40^0 and 46^0 respectively. The particle size distribution of the samples having the M-sand 20% and 40% with 80% and 20% of river sand respectively have been positively affected to increase the compaction and properly interlocked the fine aggregates thereby, increased the shear resistance.

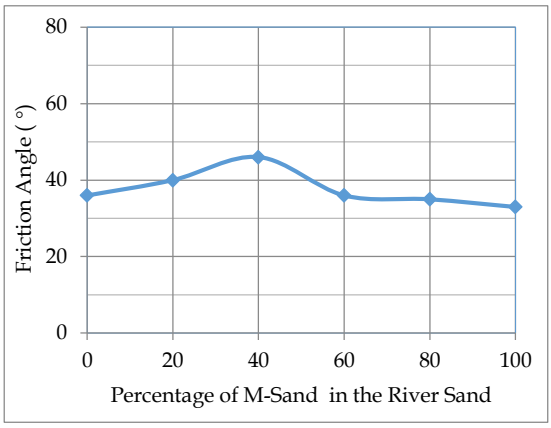

Figure 4 Variation of friction angle with the percentage of M-sand

3.4. California bearing ratio

CBR value is an indirect measure of the shear strength of the soil and aggregates (Jayakody *et al* 2014). The CBR values of the dry sand samples which are shown in Figure 5 further confirmed the shear strength properties in Figure 4. The dry Sand samples with 20% and 40% of M-sand revealed higher CBR strength as 20.5% and 23.5% respectively following the high friction angles which reflect the high resistance to fail. Therefore, blending the M-sand and river sand as per the RS80/MS20 and RS40/MS60 are the best proportions to be used under dry conditions.

The CBR values showed significant variation between dry and soaked conditions. The soaked samples had greater CBR at their OMC values than the unsoaked dry samples when M-sand presence. The M-sand gained high strength when they compacted with moisture and it was 40.5% of CBR in RS0/MS100. Moisture supports for high compaction and enhance the shear strength by increasing the particles' interlocking. The angular shape and surface roughness of the particles of the compacted wet samples contributes to increase the friction against sliding the particles under loading and consequently, increase the CBR values. According to the ICTAD specifications (ICTAD 2009), the minimum CBR value for road subbase which is 30% of CBR and the samples with 60%, 80% and 100% of manufactured sand achieved CBR values greater than 30%.

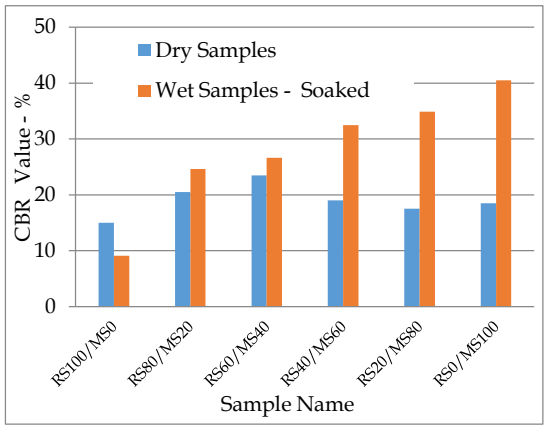

Figure 5 CBR values of the sand samples

4. CONCLUSIONS

A comprehensive laboratory evaluation of the geotechnical characteristics of M-sand was done along with river sand for comparison. The conclusions are summarized as follows:

- M-sand consists of well graded distribution of particle size and coarser fraction is greater than the river sand.
- The drainage property of the M-sand is lesser than the river sand and coefficient of permeability was gradually decreased with increasing the percentage of M-sand in river sand.
- The friction angles of the river sand and manufactured sand were not affected by the particle shape and surface roughness and observed similar values at the dry condition.

- However, blending the river sand and M-sand as per the samples RS80/MS20 and RS60/MS40 were recorded high friction angles.
- CBR values of the dry samples reflected higher strength in M-sand than river sand. Further, higher strength was recorded in blended sample, RS60/MS40 which shows the best ratios to be mixed to obtain for higher load bearing capacity at the dry state.
- The CBR strength of the wet sand samples gradually increased with the presence of M-sand and exceeded 40% of CBR in pure M-sand (RS0/MSM100). The physical properties of the M-sand positively affect on higher interlocking the particles of the compacted specimens at their corresponding optimum moisture contents.

5. ACKNOWLEDGMENTS

Authors thank South Eastern University of Sri Lanka for giving the opportunity for the research study. Further, authors thank CML (Pvt) Ltd for providing manufactured sand.

6. REFERENCES

ASTM International, 2006, *Standard Test Method for Permeability of Granular Soils (Constant Head) (Withdrawn 2015),* West Conshohocken, from www.astm.org.10.1520/D2434-68R06.

ASTM International, 2007, *Standard Test Method for Particle-Size Analysis of Soils (Withdrawn 2016),* ASTM West Conshohocken, from www.astm.org.10.1520/D0422-63R07E02.

ASTM International, 2011, *Standard Test Method for Direct Shear Test of Soils Under Consolidated Drained Conditions,* West Conshohocken, from www.astm.org.10.1520/D3080_D3080M-11.

ASTM International, 2012, *Standard Test Methods for Laboratory Compaction Characteristics of Soil Using Standard Effort (12 400 ft-lbf/ft³ (600 kN-m/m³)),*West Conshohocken, from www.astm.org.

ASTM International, 2016, *Standard Test Method for California Bearing Ratio (CBR) of Laboratory-Compacted Soils,* West Conshohocken, from www.astm.org.10.1520/D1883-16.

Gobieanandh, V. & Jayakody, S, 2016, 'Evaluate the strength of cement treated recycled construction and demolition aggregates as a pavement material', *The 7th International Conference on Sustainable Built Environment*, Kandy, Sri Lanka, Dec 16-18, 2016,62-67.

ICTAD, C. I. D. A., 2009, *Standard specifications for construction and maintenance of roads and bridges,* Colombo (Sri Lanka).

Jayakody, S., Gallage, C. & Kumar, A., 2014, 'Assessment of recycled concrete aggregates as a pavement material', *Geomechanics and Engineering, An International Journal,* 6**,** 235-248.

Jayakody, S., Gallage, C. & Ramanujam, J., 2017, 'Effects of reclaimed asphalt materials on geotechnical characteristics of recycled concrete aggregates as a pavement material', *Road Materials and Pavement Design,* 20**,** 754-772.

Jayakody, S., Hemal, G. K., Wijerathna, H. H. & Zimar, A. M. Z., 2019, 'Particle breakage potential of recycled construction and demolition waste (RCDW) as an unbound pavement material', *9th International Conference on Sustainable Built Environment*, Kandy (Sri Lanka).

Meghashree, M. & Gowda, A. K., 2016, 'Comparison of Physical Properties between Natural Sand and Manufactured Sand', *International Journal for Innovative Research in Science & Technology,* 3**,** 92-96.

Piyadasa, R. U. K., 2009 , 'River sand mining and associated environmental problems in Sri Lanka', *Sediment Problems and Sediment Management in Asian River Basins (Proceedings of the Workshop held at Hyderabad,* India, September , India.

Sankh, A. C., Biradar, P. M., Naghathan, S. J. & Ishwargol, M. B., 2014, 'Recent Trends in Replacement of Natural Sand With Different Alternatives', *IOSR Journal of Mechanical and Civil Engineering (IOSR-JMCE)***,** 59-66.

Shen, W., Zhenguo, Y., Cao, L., Cao, L., Liu, Y., Yang, H., Lu, Z. & Bai, J., 2016, 'Characterization of manufactured sand: Particle shape, surface texture and behavior

in concrete', *Construction and Building Materials,* 114**,** 595-601.

Sunder, P. S. & Asundi, J.,2005, 'Manufactured Sand Potential and Status in Karnataka',*Center for Study of Science Technology and Policy*, Bangalore, India.

Zimar, A., Samarawickrama, G., Karunarathna, W. & Jayakody, S, 2017,' Effect of manufactured sand as a replacement for fine aggregates in concrete', *8th International Conference on Structural Engineering and Construction Management*, Kandy (Sri Lanka).

Coastal and Lagoon Environment

Proceedings of the 7th International Symposium on

Advances in Civil and Environmental Engineering Practices for Sustainable Development

ACEPS - 2019

Application of satellite altimeter data for extreme wave modelling in north eastern coastal sea of Sri Lanka.

R.W.W.M.C.J.B. Wijekoon[1] and H.P.V. Vithana[1]

[1]Department of Civil and Environmental Engineering, Faculty of Engineering, University of Ruhuna, Hapugala, Galle, SRI LANKA.

K e y w o r d s

Extreme waves
Wave modelling
Satellite altimetry
Sri Lanka

A B S T R A C T

The effect of extreme oceanic events should be considered in the design of coastal structures to ensure their safety during the design life. Long term reliable data are required to calculate the probability of occurrence of extreme events. Lack of measured wave data is a serious draw back in the establishment of long term wave climate around the island. Wave height data derived from satellite altimetry is a potential data source provided they are used with adequate validation. Therefore, TOPEX altimeter sensor data obtained from NASA and wave height data measured using a wave rider buoy by the Coast Conservation Department of Sri Lanka for a location offshore of Galle for the 1989 – 1995 period, were used to establish a correlation between the two data sets. Offshore extreme waves for the north east were predicted using Weibull probability distribution and validated with measured data nearshore after transforming using DELFT3D wave model. Comparison with measured data at Oluvil showed that the satellite altimeter data can be used to predict extreme wave heights with reasonable accuracy in the absence of measured wave data.

1. INTRODUCTION

Sri Lanka is an island with 65,610 km^2 of land surrounded by the Indian Ocean (Figure 1). It is rich in coastal features such as bays, beaches, coral reefs, estuaries, lagoons, mangroves etc. The eastern coast is particularly famous as tourist destinations such as Arugambay, Pasikuda and Nilaweli beaches. Wave climate in the north east of the island is primarily governed by the north east monsoon that occur from December to February.

Extreme waves are necessary for the design of coastal structures minimising the probability of failure. However, the establishment of wave climate in the northern and eastern seas has been a challenge due to lack of long term measured wave data.

1.1 Objectives

Objective of this research is to establish offshore wave climate statistics in the north and east of the island using satellite altimeter data and predict extreme waves using the same data set. Thereafter, validation of the transformed waves is to be carried out using wave data measured at nearshore locations. The validated model is to be used to predict wave height for other nearshore locations along the north east coast.

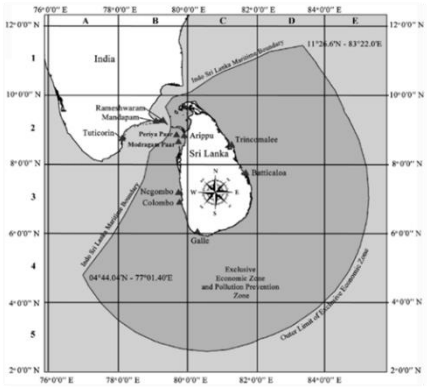

Figure 1 Location of Sri Lanka in the Indian Ocean (Source: Maritime boundaries data base, Flanders Marine Institute)

2. BACKGROUND

2.1 Extreme waves

The extreme waves have larger wave heights. The existence of extreme waves, as observed by seafarers, has been confirmed by data recording and modelling to be more common than previously assumed. Extreme waves mainly occur during major storms at sea by means of constructive interference of wave trains or by nonlinear wave interaction, but extreme waves may also be associated with tsunami or meteo-tsunami events (Hansom *et a*l 2015). Extreme waves result from excessive energy concentration over a small domain in space and time due to or reinforced by several factors, such as wind, opposing current, frequency/directional focusing, or bottom topography. The nonlinearity and instability in the evolution of the waves could also lead to or influence the self-focusing (Dao *et al* 2011).

In earlier stages of modelling extreme waves were considered as sinusoidal waves. However, variation of wave pattern and the lack of idealization has been a problem. Therefore, statistical methods are used to model the extreme waves. Some extreme events cannot be avoided.

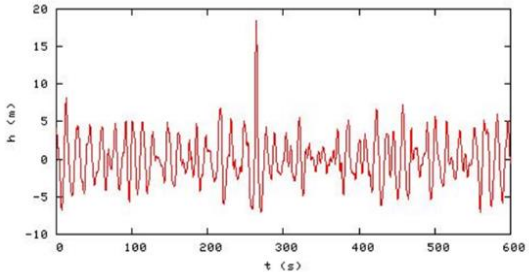

Figure 2 Extreme wave pattern (Kirstain *et al* 2005)

However, the impacts can be mitigated. In order to prepare for future coastal change including the hazard of extreme waves at the coast, stakeholders have been forced to rethink many aspects of hazard response and adaptation strategies including modelling the predicted impact of extreme wave events, engineering the environment through the construction of larger and more robust sea defences and adopting supplementary or alternative responses to such events (Hansom *et al* 2015).

2.2 Climate Conditions

In Sri Lanka wave climate is characterised by south west and north east monsoons. South west monsoon is active from May to September followed by inter-monsoon period occurring from October to November. Precipitation in Southern and Western regions is higher than other part of Sri Lanka during this period. During the North East monsoon that occurs from December to February, north and east of the island have significant rainfall. This period is followed by inter-monsoon weather spanning the time from March to April (Ranasinghe & Gunaratne 2011). The occurrence of extreme waves is more likely during storms generated by severe monsoonal winds.

2.3 Weibull Analysis - Equations

Extreme wave heights are determined by using Weibull probability distribution. It will function to extrapolate peak wave heights occurring in independent storm events exceeding a selected threshold wave height.

2.1.1. Weibull Probability Distribution:

The probability of exceedance, which is the probability that any wave height H' exceeding a specified wave height H is given by

$$Q = Q\,(H'>H) = 1\text{-}exp\,\{-\,[-\ \ [\![(H-\gamma)/\lambda\ ]\!]\ ^{\wedge}k\}\quad (1)$$

Probability of exceedance can be defined as

$$Q = \quad (i-c1)/(N+c2)\ \ldots\quad (2)$$

In this method, the significant wave heights are arranged in descending order of magnitude. N is the rank that was received for the lowest magnitude of wave height. In here,

$$c1 = 0.2+0.27/k \qquad (3)$$

$$c2 = 0.2+0.23/k \quad \text{--}(4)$$

The probability of exceedance Q is related to return period defined as

$$Q = 1/(\sigma\, T_R)\ \ldots.\quad (5)$$

Considering annual maximum significant wave height for the maximum wave height determination. So σ =1. Then, extreme wave heights can be predicted according to the different return periods using Weibull distribution.

$$Q = 1/T_R \qquad (6)$$

3. METHODOLOGY

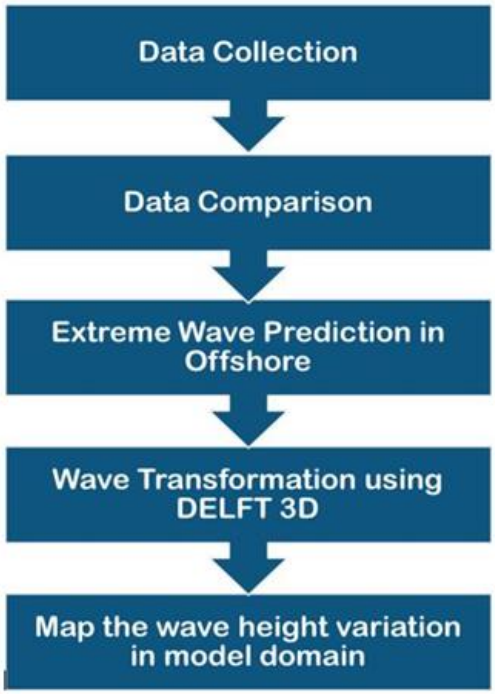

Figure 3 Methodology flow chart

3.1 Data Collection

All data used in this research are listed in Table 1.

Table 1 Data Type and Sources

Data Type	Data Source
Wave rider buoy measured directional wave height data (offshore of Galle)	Coast Conservation Department of Sri Lanka
Satellite altimeter wave height data	TOPEX Altimeter Sensor Data Record from POODAC of NASA.
Extreme wave heights and associated return period in Oluvil based on wave measurement	Lanka Hydraulic Institute (LHI)
Bathymetry Data	Marine Geoscience Data System (MGDS)

3.2 Data Comparison

A comparison of wave rider buoy measured data for Galle with satellite altimeter data for the same location for the same recording duration. Maximum monthly wave height was used in this comparison.

Objective of this comparison is to verify whether satellite data can be used instead of measured wave heights for the north east of the island where long term measured wave data are not available. Figures 4 and 5 show the comparison of data.

3.3 Extreme Wave Prediction

In extreme events, Weibull probability distribution is known to cause minimum error for the largest value. Therefore, extreme wave heights can be determined using Weibull probability distribution. It is used to extrapolate the peak wave heights (Makkonen, 2005). Offshore wave heights were extracted from the TOPEX Altimeter sensor data base (NASA). Using those wave heights annual maximum wave heights were calculated for 18 years. Then extreme wave prediction was carried out for different return periods.

3.4 Extreme Wave Transformation

DELFT3D spectral wave model was used to transform wave heights from offshore to nearshore. This model computes wave propagation, wave generation by wind, non-linear wave-wave interactions and dissipation, for a given bottom topography, wind field, water level and current field in waters of deep, intermediate and finite depth. Model calibration and validation was carried out using wave data measured by the Lanka Hydraulic Institute (LHI) during Oluvil harbour feasibility study (LHI, 2000).

4 RESULTS

4.1 Data Comparison Results

As shown in Figures 4 and 5, a comparison was made of monthly maximum significant wave heights derived from measured wave rider buoy data for offshore of Galle with satellite altimeter measured wave data for the same location and data recording period. As shown in Figure 5, R-squared value is 0.83 indicating a good correlation between the two data sets. Therefore, an assumption was made that the quality of the TOPEX data set can be applicable to north eastern coast.

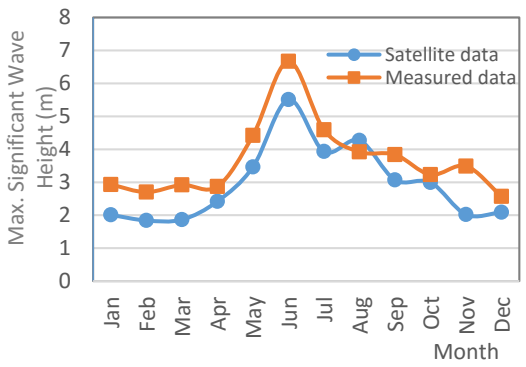

Figure 4 Maximmum significant wave height vs month

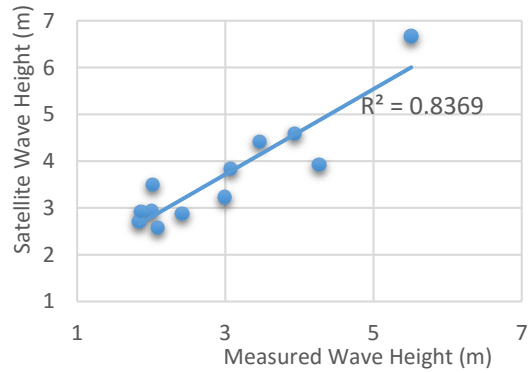

Figure 5 Wave rider buoy measured monthly maximum significant wave height vs satellite measured maximum significant wave height for offshore of Galle

4.2 Weibull Analysis

Significant wave heights obtained from satellite altimeter measurements were used to predict offshore extreme wave heights using Weibull probability distribution. Table 2 shows the predicted extreme wave heights in the offshore of north eastern coast against corresponding return period. Calculated extreme wave heights were then transferred into the nearshore using DELFT3D spectral wave model.

Table 2 Offshore extreme wave heights

Return Period (years)	Extreme Wave Heights (m)
1	5.4
5	5.6
10	6.0
25	6.2
50	6.4
100	6.6

4.2 Wave Modelling Results

Figures 6 (a) and (b) show the spatial distribution of extreme wave heights as calculated by DELFT3D model after wave transformation from offshore to nearshore during the North-East monsoon. The model was forced by the predicted offshore extreme wave heights at the northern and eastern boundaries.

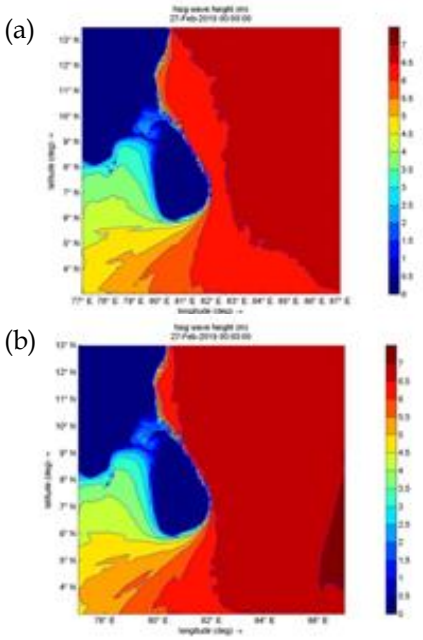

Figure 6 Contour maps of extreme wave heights for return periods of (a) 50 years (b) 100 years

Offshore extreme wave heights were transformed to a point near the Oluvil harbour at 9m water depth using DELFT3D wave model. Table 3 shows the comparison of modelled extreme wave heights with published extreme wave height data for Oluvil (LHI 2000).

Table 3 Extreme wave heights for Oluvil compared with modelled extreme wave heights from satellite data

Return Period (years)	Extreme Wave Heights (m)	
	Oluvil (LHI, 2000)	Present study
1	2.39	2.39
5	2.64	2.54
10	2.78	2.60
25	2.93	2.80
50	3.06	2.98
100	3.18	3.04

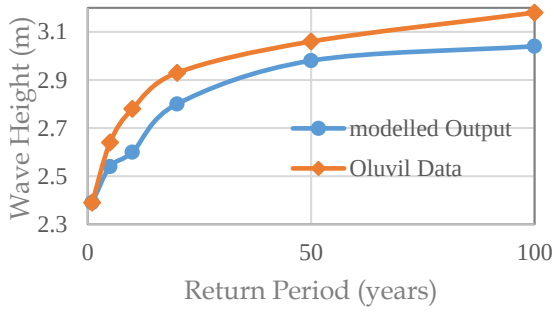

Figure 7 Comparison of modelled extreme wave heights with Oluvil data (LHI 2000)

As shown in Figure 7 and Table 3 the root mean square error between the two data sets was computed as 0.12m which lies between 3-5% relative to LHI estimate.

Using the validated model, wave heights for different return periods were calculated for main cities along the north eastern coastline as shown in Table 4.

Table 4 Extreme Wave heights for different locations in the north-eastern coast

City	H sig (m) for Return Period (years)					
	1	5	10	25	50	100
Point Pedro	1.24	1.36	1.46	1.61	1.72	1.81
Mulathivu	3.36	3.48	3.57	3.72	3.82	3.88
Polmoddai	2.35	2.51	2.65	2.89	3.13	3.22
Trincomalee	3.03	3.15	3.27	3.47	3.60	3.63
Pasikuda	2.53	2.67	2.76	2.96	3.15	3.19
Batticaloa	2.17	2.32	2.41	2.55	2.72	2.78
Kalmunai	2.54	2.71	2.78	3.03	3.21	3.27
Potuvil	2.29	2.57	2.68	3.04	3.29	3.36
Panama	2.78	3.00	3.09	3.33	3.53	3.59

5 CONCLUSION

Establishment of the wave climate and prediction of extreme waves are required to design coastal structures robust enough to withstand the uncertainties prevalent in the coastal sea. This study found that the satellite altimeter data can be used to predict extreme wave heights with reasonable accuracy in the absence of measured data. The rms deviation of the extreme wave heights predicted based on satellite data was about 3-5% of that predicted using wave rider buoy field measurements. Large differences in magnitude in the two data types narrowed when the waves propagate into the nearshore due to such processes as wave breaking.

6 AKNOWLEGEMENT

The authors would like to acknowledge the assistance of the Coast Conservation Department (CCD) and Lanka Hydraulic Institute (LHI) in securing relevant data.

7 NOTATIONS

H- Significant wave height

γ – Location parameter

λ – Scale parameter

k – Shape parameter

8 REFERENCES

Dao, M.H., Xu, H., Chan, E.S., & Tkalich, P., 2011, `Numerical modelling of extreme waves by smoothed particle hydrodynamics', *Nat. Hazards Earth Syst. Sci.* (11), 419–429.

Dysthe, K.B., Krogstad, H.E., Socquet-Juglard, H., Trulsen, K., 2005, Freak waves, rogue waves, extreme waves and ocean wave climate, *https://folk.uio.no/karstent/waves/index_en.html*

Hansom, J.D., Switzer, A.D., Pile, J., 2014, `Extreme waves: Causes, characteristics, and impact on coastal environments and society'. *Coastal and Marine Hazards, Risks, and Disasters*, 307-333.

Lanka Hydraulic Institute, 2000, `Oluvil Wave Measurements 1998/2000, Final Report'

Makkonen, L., 2005, Plotting position in extreme value analysis, *Journal of Applied Meteorology and Climatology*, 45, 334-340.

Ranasinghe, D.P.L. & Gunaratne, P.P., 2011, `Assessment of nearshore wave climate in southern coast of Sri Lanka', *Annual Research Journal of SLSAJ*, 11, 43-51.

Proceedings of the 7th International Symposium on

Advances in Civil and Environmental Engineering Practices for Sustainable Development

ACEPS - 2019

Review of existing coastal defence system in Sri Lanka against tsunami.

T.L.C.Vinodh[1] and N.Tanaka[1,2]

[1]Graduate School of Science and Engineering, Saitama University, 255 Shimo-okubo, Sakura-ku, Saitama 338-8570, JAPAN
[2]International Institute for Resilient Society, Saitama University, 255 Shimo-okubo, Sakura-ku, Saitama 338-8570, JAPAN

K e y w o r d s

Tsunami
Lagoon
Forest
Coral reef
Sand dune
Structural protection

A B S T R A C T

The 2004 Indian Ocean Tsunami (IOT) has brought the issue of coastal protection to the forefront in Sri Lanka. A review of recent research regarding the extent of coastal protection by nature as well as manmade structures was conducted that includes field surveys, laboratory experiments, numerical simulations and statistical analysis. However, results from several recent researches support the mitigating capabilities of nature-based defence in Sri Lanka where some places in need of further research and precautions in the aspect of tsunami mitigation. The recovery policies established by the Government of Sri Lanka after 2004 IOT is presented in this paper with special attention paid to the planned or existing structural/non-structural tsunami countermeasures and land use planning.

1. INTRODUCTION

The recent 2004 Indian Ocean Tsunami (IOT) has brought the issue of coastal protection to the forefront in Sri Lanka (Pomonis *et al* 2006). Before the 2011 Great East Japan tsunami (GEJT), Japan was considered worldwide a model country in the field of tsunami preparedness and resilience. However, the structures including breakwaters, sea walls, water gates, and tide water control forests were not designed for the huge tsunami like the 2011 GEJT (Suppasri *et al* 2013) resulting many were destroyed and could not mitigate the tsunami as expected. As Sri Lanka is recognized as a developing country hence the countermeasures against the tsunami are needed to be taken with utmost care by considering the lessons learnt from the past as well as from the worldwide model like Japan. The characteristics of the tsunami flow onshore were found to be extremely difficult to predict, being affected by the bathymetry, coastal topography, amount of entrained debris, vegetation, density of habitation and the location and resistance to tsunami loads of buildings and other structures in its path.

This review of recent research regarding the extent of coastal protection and mitigation by nature as well as manmade structures were conducted that includes field surveys, laboratory experiments, numerical simulations and statistical analysis with the objective of summarizing and discussing the improvements in tsunami related structural and non-structural countermeasures. The review study can be beneficial as a general reference for future tsunami research in various coastal engineering and related policies established by the Government of Sri Lanka after the 2004 IOT.

2. HISTORY OF TSUNAMIS AND EARTHQUAKES

Okal and Synolakis (2008) have identified four segments of subduction zones in the Indian Ocean that could generate destructive transoceanic tsunami. These seismic zones are located off Southern Sumatra, in the Arakan trench off Myanmar and in the Makran coast of Pakistan and Iran, besides the Northern Sumatra. Andaman fault which triggered the 2004 IOT and it is remembered as the most

devastating catastrophe in Sri Lanka, having caused 35,000 fatalities on two-thirds of the coastal belt, across 13 coastal districts (Pomonis *et al* 2006). Sri Lanka has no experience of tsunami events prior to the 2004 IOT, and after 1883 eruption of volcanic island of Krakatoa where hardly any damage occurred (Choi *et al* 2003). Wijetunge (2012) described a deterministic assessment of the tsunami hazard to Sri Lanka from all active subduction zones in the Indian Ocean Basin and found that an event similar to the 2004 IOT in the Northern Sumatra - Andaman subduction zone could be considered as the worst-case seismogenic tsunami scenario for any part of the coastline of Sri Lanka.

A great earthquake occurred northwest of Sumatra at 0:59 UTC, December 26, 2004 causing a moment magnitude (Mw) of 9.3 (Stein and Okal 2005). Following the earthquake, the ocean surface started to rise to a maximum of about 70 cm and showed a total trough-to-crest wave height of about 1 m (Gower 2005) using JASON 1 satellite image analysis. The wave travelled with a wave speed of about 750 km/h in water about 4500 m deep. The wave would have travelled about 1500 km in the 2 hours since the earthquake off the coast of Sumatra with a wavelength about 430 km and the wave period about 37 minutes as illustrated by Gower (2005). The results showed that the tsunami phenomenon is not limited to a single wave but a sequence of two or more main waves, including the maximum wave. After the 2004 IOT, four major tsunamis were triggered by earthquakes. The 2005 Nias earthquake (Mw 8.7), the 2007 Sumatra earthquake (Mw 8.5), the 2010 Mentawai earthquake (Mw 7.8) and the 2012 Indian Ocean earthquakes (Mw 8.0) as reported by Suppasri *et al*. (2015), but none of them caused any significant damages to Sri Lanka.

3. TSUNAMI HYDRODYNAMICS

The first signs of the 2004 IOT observed by the Sri Lankan public was a negative wave, although a smaller positive wave arrived first. The ocean receded by as much as 1 km in some areas. The recede was followed by a series of advancing tidal waves (Chapman 2005; Goff *et al* 2006; Pomonis *et al* 2006). Pomonis *et al.* (2006) reported that the inundation was greatest in the east coast near Batticoloa where inundation distances were close to 4km. The greatest inundation in the south was observed in Hambantota. In the south-west, the largest inundation was deduced to be just under 1km in Galle and just north of Hikkaduwa possibly at Peraliya where a 10 m high water level was recorded. The tsunami water levels measured at the shoreline were 4-6 m in the Jaffna Peninsula, 5-7 m in the east coast, 3-6 m in the south coast and 4-5 m in the west coast.

Wijetunge (2009a) and Pomonis *et al*. (2006) states that the higher in direct inundation in the district of Hambantota is primarily owing to the source directivity. Wijetunge (2009a) states that the influence of many water bodies such as lagoon and saltpans as well as other water ways present along that stretch of the coastal belt may increase the inundation further to the landward. Wijetunge (2006) mentioned that the north and the east coasts generally consist of low-lying, wide stretches of flat coastal lands compared to the rest of the country's coastal belt and hence tsunami penetrate more towards landside. The waves that arrived in the southwest and western coastal areas were the result of refraction around the southern continental shelf coupled with localized diffraction. The comparatively low tsunami heights in the west coast are recorded as this part of the coast is largely sheltered from direct tsunami impact and only diffracted waves with less energy could reach there (Wijetunge 2006). Inoue *et al.* (2007) reported that the inundation distances are lower in built-up areas because the momentum of tsunami would be weakened due to the collision with many buildings. It also indicates that inundation area would be wide in bare land, grassland or bushes because there are few obstacles to the propagation of the tsunami such as buildings or tall trees. Ioualalen *et al*. (2007) & Wijetunge (2009b) investigated that where underwater canyons are present at the coastline, the wave is diverging (concave-type iso-baths) and escapes from its sides (a defocusing). The effect of these canyons are to inhibit the wave amplification. For instance, the eastern areas such as Kalmunai and Batticaloa experienced greater inundation since the tsunami came head on and the water levels were generally high, and the terrain was low lying to a considerable distance inland.

4. ECOSYSTEM-BASED DISASTER RISK REDUCTION

Ecosystem-based Disaster Risk Reduction (Eco-DRR) is so vital and becoming a more popular trend as it is sustainable management, conservation and restoration of ecosystems to reduce disaster risk, with the aim to achieve sustainable and resilient development (Renaud *et al* 2013). The schematic figure of the concept of Eco-DRR is shown in Figure 1. In contrast to conventional engineering solutions such as floodwalls or dykes, Eco-DRR provides multiple benefits for human well-being regardless of a disaster event and involves relatively low-cost construction and maintenance where ecosystems are healthy and well managed. In this regard, Eco-DRR is a cost-effective and no regret of investment (Barbier 2016).

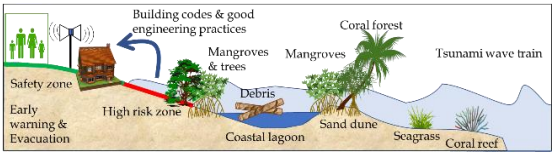

Figure 1 Schematic figure of Eco-DRR

It is important to recognize that ecosystems also have limits in providing protection against hazards (Tanaka *et al* 2009). Chatenoux and Peduzzi (2007) suggested that the protective potential role of vegetation was determined by its spatial arrangement and should be regarded as an important consideration. There were many projects around the world that were invested in an ecosystem without any systematic and scientific collection of evidence on the role of vegetation in protecting populations against the tsunami waves, ended with disappointing results (Cochard 2011). Thorough knowledge of wave phenomena occurred nearby coastal ecosystems is essential in effective coastal landscape planning by considering the scarcity of resources (Tanaka *et al* 2011).

4.1. Effect of sand dune

Sand dunes are locally well developed on the south eastern beaches of Sri Lanka, where sand supply is abundant, and the climate is relatively dry. Sand dunes are largely absent on beaches of the south and southwest coast as a result of frequent floods in the region. One prominent feature of the south coastal belt is the 7-10 m high sand dunes with thick cover of overgrowth. The presence of such sand dunes has certainly helped reduce tsunami penetration inland. However, wherever gaps existed in the dune system, or at locations where the dune height was low or had been cut open for various activities, it appears that the tsunami surge had rushed through with enormous power causing considerable destruction. For instance, the Yala Beach Resort once existed and was demolished to the ground, and substantially higher water and greater damage were found on the hotel grounds than in neighbouring areas located behind unaltered dunes (Liu *et al* 2005; Wijetunge 2006). Wijetunge (2006) found that dunes at north of Potuvil have protected some localities from severe flooding due to the recent tsunami. Tanaka *et al.* (2007) shown that the combination of the sand dune followed by vegetation toward landside retarded the tsunami.

4.2. Effect of coastal lagoon and salterns

It could be observed that nearby the lagoon the tsunami impact was very low during the post-tsunami field surveys of the 2004 IOT (Dahdouh-Guebas *et al* 2005; Wijetunge (2006); Inoue *et al* 2007).

Wijetunge (2006) reported around Batticaloa and Kalkudah, the lagoons and other water bodies have certainly helped convey the tsunami surge large distances inland. In Palatupana close to Yala National Park, the inundation height at the back of the lagoon (5.8 m) is around 60% less than the inundation height at the front of the lagoon (10.6 m), indicating that the tsunami would be reduced by the lagoon as illustrated by Inoue *et al*. (2007). Wijetunge (2009a) has shown that the comparatively vast extents of the salterns have also acted as sinks to absorb and spread water whilst the sand dunes, where present with sufficient elevation, have helped protect the settlements in their shadow from direct tsunami attack.

Wijetunge (2006) observed that the deepest tsunami wave penetration in the south coast is at Hambantota, up to three kilometres near the saltpans, and near Bundala albeit with the aid of the bay. Hungama-Tangalle beach to the west of Hambantota too has recorded notable inundation, especially where tsunami surge waves had been conveyed inland through water bodies opening to the sea such as lagoons and lakes. Wijetunge (2009b) found

that the surging tsunami front had moved across barrier spits and then into the lagoons in Batticaloa, which in some instances, unable to absorb all of the overland flow, had spilt over and flooded inland areas that would otherwise not have received direct inundation. In Hambantota, hundreds of buses, many allegedly carrying passengers, were reportedly swept into the Karagan Lewaya behind the town, necessitating a massive clearance effort (Synolakis *et al* 2005; Wijeyewickrema *et al* 2006). Wijeyewickrema *et al* (2006) reported that Karagan Lewaya was severely affected by seawater intrusion following the tsunami. The ecosystem following the tsunami attack was markedly changed due to the sudden change in salinity levels and bacterial decomposition. Another important aspect of tsunami damage was the decrease in flood control capacity of the lagoon due to the deposition of large quantities of sediments brought in by the seawater

4.3. Effect of coral reefs

There were many anecdotal reports suggesting that intact and healthy coral reefs reduced tsunami damage to communities on the coast prior reaching the shoreline. Some reports also suggested that human modification of the marine and coastal environment increased the damage on land (Liu *et al* 2005; Fernando *et al* 2008). In the case of Peraliya, illegal coral mining has been shown to have created low-resistance pathways that allowed focused flow and intensified destruction, leading to the large loss of life experienced by the derailment of the "Queen of the Seas" train (Fernando *et al* 2008). Although gaps in coral reefs may have provided relatively low-resistant paths for the tsunami surge to jet through (Fernando *et al* 2008) with some effects locally, Wijetunge (2014) suggested that, in general, the influence of onshore topography to have been more dominant in enhancing the tsunami impact in stretch Akurala compared to the neighbouring areas to the north and the south. Pomonis *et al*. (2006) reported that the damage in the southern part of town (between Thiranagama and Dodanduwa) certainly did not seem as serious as one might expect and this can probably be attributed to the natural breakwater protection offered by the coral reef. Further they observed that hotels along the coast suffered minor structural damage and were open to tourists at the time of the field mission.

Coral reefs were severely affected and damaged by the debris and sand transported during the inland and shoreward movement of tsunami (Rajasuriya *et al* 2006). Chatenoux and Peduzzi (2007) in a survey covering several Indian Ocean countries including the present site in Sri Lanka, found no significant influence of the presence of coral reefs in lessening the tsunami impact onshore.

4.4. Effect of coastal forests, mangroves and seagrass

The coastal forests, mangroves and seagrass were observed to help protect beaches from erosion, by dissipating some of the wave energy by drag force work and the slam. Depend on the tree species and their vegetation characteristics, the reduction effect of tsunami inundation depth varies and was mostly lost when the tsunami inundation depth exceeded 5 to 6 m (Tanaka *et al* 2007). A forest is effective as it stops driftwood and other drifts, reduces the water flow velocity and inundation height, provides a lifesaving means by catching persons carried off by the tsunamis and collects windblown sand and raises dunes, which act as a natural barrier against tsunamis (Tanaka *et al* 2007, Tanaka 2009). A negative opinion is that a forest may be ineffective against a giant tsunami, and at worst, trees themselves could become destructive forces to houses if cut down by the tsunami. Based on data analyses by Tanaka *et al.* (2009) and Samarakoon *et al*. (2013), a forest with two layers in the vertical direction of dense *Casuarina equisetifolia* and *Pandanus odoratissimus* grown in beach sand were found to be especially effective in providing protection from tsunami damage due to their density and complex aerial root structure. A pilot project in Matara City has already initiated (Tanaka 2009) and become successful in planting with the participation and support from local authorities and communities.

Chatenoux & Peduzzi (2007) statistically analysed the seagrass areas and found that results showed that lower impacts in area behind seagrass beds implying that either seagrass bed acting as a damping filter that help reducing the energy of the wave or because the seagrass beds are located in areas where configuration of bathymetry is not

favourable for wave amplification. Kerr & Baird (2007) pointed out that the significance of coastal vegetation in tsunami mitigation remains an open question due to the absence of proper studies, and more data and more powerful approaches may well find an association.

5. TSUNAMI RESISTANT BUILDING AND INFRASTRUCTURE

The main causes of damage to buildings and infrastructure can be identified as lateral water flow, wave loading, ground scour and debris impact. The main threats from a tsunami wave on a structure are overturning, sliding and scouring in addition to debris impact. Apart from the intensity of the tsunami flood flow, there are several other factors that could also influence the degree of damage suffered by a structure: these include the type of building material used (e.g., masonry or reinforced concrete), the orientation and the shape of the building, the presence of cross-walls and bracings, number of stories and the level of shielding and resistance provided by neighbouring buildings, trees and vegetation (Dias *et al* 2006; Goff *et al* 2006; Pomonis *et al* 2006). In Galle and Matara, most buildings are more than two storeys high, and it was observed that those immediately behind the first-row experienced limited damage, thus providing ample safety to their occupants (Pomonis *et al* 2006). In numerous locations in Sri Lanka, Buddhist temples, churches and mosques were left standing. In both locales, residents credited divine intervention; but places of worship are constructed to a higher standard than surrounding non-engineered buildings (Pomonis *et al* 2006).

Bridges of those observed along the Southwest coast of Sri Lanka, the major cause of their damage was the scouring of the retained-earth type abutments leading to failure of the decks. This had a dramatic impact on electricity and water supply because many of the cables and water mains were connected to the bridges so they could span the rivers. The damage to road bridges severely hampered the distribution of disaster relief and thus delayed the recovery (Pomonis *et al* 2006). The extension of wing walls along the roadside would reduce scouring. Some road sections although protected by a sea wall or an embankment with sufficient vegetation, suffered damage due to scouring, which undermined the founding subgrade (Pomonis *et al* 2006). Good engineering practice can reduce economic losses, but additional measures are like the creation of a buffer zone with appropriate vegetation is a land-use planning strategy required to reduce risk to the life.

6. COASTAL HARD STRUCTURES

The hard-structural defences are seriously challenged in many locations as their continual and costly maintenance, as well as their heightening and widening to keep up with the increasing disaster risk are becoming unsustainable (Temmerman *et al* 2013). Especially in developing countries like Sri Lanka, it is quite difficult to allocate enough budgets for constructing hard-type countermeasures against a tsunami. At present, Sri Lanka has no hard-structural tsunami defence system, else has structures which are designed for coastal erosion, port and harbour facilities that include revetment, seawalls, groynes, breakwaters and jetties.

Pomonis *et al*. (2006) reported that the Dutch fort in Galle sustained no visible structural damage, although flood damage to the museum within the fort walls has been reported. The main town is built along the coastline of the harbour bay between the Dutch Fort (to the west) and the main port (to the east). Heavy damage was observed in the first row of buildings facing the sea. These are located about 30 m from the shore at an elevation of about 1m above mean sea level. The depth of water within the harbour ranges from 10 m at the mouth of the harbour to 2m at the coastline. Many of the harbours require extensive dredging and removal of debris and sand from the basin. There were damages to the service facilities and harbour equipment including shore structures, dredgers, heavy mechanical equipment, ice plants, buildings, and boat repair yards (Pomonis *et al* 2006).

7. EARLY WARNING, EVACUATION SYSTEMS AND RECONSTRUCTION

Investing in ecosystems cannot be viewed as a single solution to risk reduction. Ecosystem-based measures could be part of a larger disaster risk management strategy and it would always be complementary to other essential risk management measures, such as

early warning systems and evacuation plans (Dengler & Preuss 2003).

Liu *et al.* (2005) reported that one of the village residents who has experience of a tsunami, recognized the sea withdrawal as a tsunami indicator and gave warning to run to higher ground, which nearly all his fellow residents followed. In this village of a few hundred, only one died. Similar incidents have been reported by Synolakis *et al*. (2005), a survival by tsunami warning between the two hotels in south and in Trincomalee. There is an interesting story about animals have been reported by Chapman (2005) that an Englishman living with a Sri Lankan family near Matara fled to high ground when an alarm was raised about the approaching wave and they were surprised to find cattle, which roam freely, already there. Despite the devastation, no dead animals have been found in Yala National Park. Similar findings were reported in Suppasri *et al*. (2015) as well. Some people were puzzled by the recession of the water and rushed forward to view this rare phenomenon only to then be caught by the ensuing waves. Pomonis *et al*. (2006) reported that people in Trincomalee were thought to have gathered "bag loads of colourful fish" before the tsunami crashed ashore. Casualties could have been avoided in many areas if people had not walked toward the shore when the sea had retreated before the arrival of the tsunami waves. The importance of educating the people and having an emergency evacuation procedure is essential.

Synolakis *et al*. (2005) stated the limitations of early warning were evident during the March 28, 2005. The earthquake was located, and the magnitude determined within 15 minutes using the worldwide seismic network, and a non-destructive tsunami was detected by tide gauges. Based on those readings, most nations issued evacuation warnings, and emergency managers everywhere waited for several hours to be sure there was no tsunami before they issued the all clear signal. Reliable prediction will require a network of real-time accurate tsunami sensors in the deep ocean. Combined with public education, these are still the best tools for averting the next Indian Ocean tsunami disaster.

Sri Lankan Government declared a coastal buffer zone where re-construction and new construction subject to certain conditions is prohibited with 100 m in the western and southern coastal areas and 200 m in eastern and north-eastern coastal areas soon after the 2004 IOT. The inundation measurements during post tsunami field surveys indicate that the extent of tsunami inundation was much greater than these imposed limits. The imposition of such a buffer zone was largely the enforcement of the *1981 Coastal Conservation Act*, which has not been strictly enforced as the post-tsunami surveys show about 54% of the damaged houses in the Pomonis *et al*. (2006)'s survey area is within 100m of the coast. Hence it was not be practical from a societal and economic viewpoint to move people too far inland as fishing communities who make up most of the coastal population want to remain close to the sea. The declaration limit was withdrawn and at present *Sri Lanka Coastal Zone and Coastal Resource Management Plan 2018* is used as the guideline for setback limits. The tsunami warning system and the evacuation plan is implemented by the Disaster Management Center (DMC) of Sri Lanka in collaboration with other relevant government institutions.

8. DISCUSSION

Since the tsunamis are low frequency, and devastating natural hazards, the interdisciplinary research on risk perception, awareness and lessons becomes critically important. From the overall review of research related to Sri Lanka, the following recommendations can be made.

Tsunami propagation characteristics in the Indian Ocean need to be reassessed and more research is required to better understand the effects of bathymetry on the magnitude of tsunami intensity and the effects of local topography including river and lagoon on the variation of damage from tsunami inundation. Tsunami hazard on Indian Ocean coastlines needs to be quantified and mapped based on more sophisticated vulnerability index. Policies related to coastal trees and mangrove reforestation in coastal lagoons, strengthening sand dunes and coral reef protection are among those that can have a tsunami mitigative effect where more vulnerable due to topographical features. The nature of damage from tsunami need to be understood and minimum specifications for building and infrastructure must be adopted in the larger context of other tsunami protection measures, such as evacuation strategies. As a result,

buildings whose structure has survived the tsunami can be reoccupied sooner, hence reducing the strain on the reconstruction effort. Good engineering practice can reduce economic losses, but additional measures such as early warning and evacuation strategies are required to incorporate together to reduce the risk to life.

9. ACKNOWLEDGMENTS

This study was partly funded by a JSPS bilateral project between Sri Lanka and Japan.

10. REFERENCES

Barbier, E.B., 2016, 'The Protective Value of Estuarine and Coastal Ecosystem Services in a Wealth Accounting Framework', *Environ. Resource Econ.* 64, 37-58.

Chapman, C., 2005, 'The Asian tsunami in Sri Lanka: A personal experience', *Eos (Washington. DC)*, 86(2), 13-14.

Chatenoux, B., Peduzzi, P., 2007,' Impacts from the 2004 Indian Ocean Tsunami: Analysing the potential protecting role of environmental features', *Nat. Hazards*, 40, 289–304.

Choi, B. H., Pelinovsky, E., Kim, K. O. & Lee, J. S., 2003, 'Simulation of the trans-oceanic tsunami propagation due to the 1883 Krakatau volcanic eruption', *Natural Hazards and Earth System Science*, 3(5), 321-332.

Cochard, R., 2011, 'The 2004 tsunami in Aceh and Southern Thailand: coastal ecosystem services, damages and resilience', *Tsunami Threat. Technol.*,179-216.

Dahdouh-Guebas, F., Jayatissa, L.P., Di Nitto, D., Bosire, J.O., Lo Seen, D. & Koedam, N., 2005, 'How effective were mangroves as a defence against the recent tsunami?', *Current Biology*, 15(12), R443–R447.

Dengler, L. & Preuss, J., 2003, 'Mitigation lessons from the July 17, 1998 Papua New Guinea tsunami', *Pure Appl. Geophys*. Birkhäuser-Verlag, 160, 2001-2031.

Dias, P., Dissanayake, R. & Chandratilake, R., 2006, 'Lessons learned from tsunami damage in Sri Lanka', *Proc. Inst. Civ. Eng. - Civ. Eng*. 159, 74-81.

Fernando, H.J.S., Samarawickrama, S.P., Balasubramanian, S., Hettiarachchi, S.S.L. & Voropayev, S., 2008, 'Effects of porous barriers such as coral reefs on coastal wave propagation', *J. Hydro-Environment Res*. 1, 187–194.

Goff, J., Liu, P.L.-F., Higman, B., Morton, R., Jaffe, B.E., Fernando, H., Lynett, P., Fritz, H., Synolakis, C. & Fernando, S., 2006,'Sri Lanka Field Survey after the December 2004 Indian Ocean Tsunami', *Earthq. Spectra* 22(S3), 155–172.

Gower, J., 2005, 'Jason 1 detects the 26 December 2004 tsunami. *Eos', Trans. Am. Geophys. Union*, 86(4), 37-38.

Inoue, S., Wijeyewickrema, A.C., Matsumoto, H., Miura, H., Gunaratna, P., Madurapperuma, M. & Sekiguchi, T., 2007, 'Field survey of tsunami effects in Sri Lanka due to the Sumatra-Andaman earthquake of December 26, 2004', *Pure Appl. Geophys*., 164, 395–411.

Ioualalen, M., Rentería, W., Ilayaraja, K., Chlieh, M. & Arreaga-Vargas, P., 2010, 'A synoptic picture of the impact of the 26th December 2004 Indian Ocean tsunami on the coast of Sri Lanka', *Environment Modelling Software*, 25, 1874–1880.

Kerr, A.M. & Baird, A.H., 2007, 'Natural Barriers to Natural Disasters', *Bioscience* 57(2), 102–103.

Liu, P.L.F., Lynett, P., Fernando, H., Jaffe, B.E., Fritz, H., Higman, B., Morton, R., Goff, J. & Synolakis, C., 2005, 'Observations by the International Tsunami Survey Team in Sri Lanka', *Science*. 308, 1595.

Okal, E.A. & Synolakis, C.E., 2008, 'Far-field tsunami hazard from mega-thrust earthquakes in the Indian Ocean', *Geophys. J. Int.*, 172, 995-1015.

Pomonis, A., Rossetto, T., Wilkinson, S., Del Re D., Peiris, N., Koo, R., Manlapig, R &, Gallocher, S., 2006, 'The Indian Ocean Tsunami of 26 December 2004: Mission Findings in Sri Lanka and Thailand', *London: Earthquake Engineering Field Investigation Team, Institution of Structural Engineers*, 180.

Wilkinson C. (ed.),2006, '*Status of Coral Reefs in Sri Lanka after the Tsunami*', Status of Coral Reefs in Tsunami Affected Countries.,2005, 99-110.

Renaud, F.G., Sudmeier-Rieux, K. & Estrella, M., 2013,'The role of ecosystems in disaster risk reduction', *United Nations University Press*, 476.

Samarakoon, M.B., Tanaka, N. & Iimura, K., 2013, 'Improvement of effectiveness of existing Casuarina equisetifolia forests in mitigating tsunami damage', *J. Environ. Manage*, 114, 105–114.

Stein, S. & Okal, E.A., 2005, 'Speed and size of the Sumatra earthquake', *Nature*, 434, 581-582.

Suppasri, A., Goto, K., Muhari, A., Ranasinghe, P., Riyaz, M., Affan, M., Mas, E., Yasuda, M. & Imamura, F., 2015, 'A Decade After the 2004 Indian Ocean Tsunami: The Progress in Disaster Preparedness and Future Challenges in Indonesia, Sri Lanka, Thailand and the Maldives', *Pure Appl. Geophys*., 172, 3313-3341.

Suppasri, A., Shuto, N., Imamura, F., Koshimura, S., Mas, E., Yalciner & A.C., 2013, 'Lessons Learned from the 2011 Great East Japan Tsunami: Performance of Tsunami Countermeasures, Coastal Buildings, and Tsunami Evacuation in Japan', *Pure Appl. Geophys*., 170, 993–1018.

Synolakis, C.E., Okal, E., Bernard, E., Synolakis C. & Okal, E.B.E., 2005, 'The Megatsunami of December 26, 2004', *Natl. Acad. Eng. Publ*. ,35, 26–35.

Tanaka, N., 2009, 'Vegetation bioshields for tsunami mitigation: Review of effectiveness, limitations, construction, and sustainable management', *Landsc. Ecol. Eng*., 5, 71-79.

Tanaka, N., Sasaki, Y., Mowjood, M.I.M., Jinadasa, K.B.S.N. & Homchuen, S., 2007, 'Coastal vegetation structures and their functions in tsunami protection: Experience of the recent Indian Ocean tsunami', *Landsc. Ecol. Eng*. 3, 33–45.

Tanaka, N., Nandasena, N.A.K., Jinadasa, K.B.S.N., Sasaki, Y., Tanimoto, K. & Mowjood, M.I.M., 2009, 'Developing effective vegetation bioshield for tsunami protection', *Civ. Eng. Environ. Syst*., 26(2), 163-180.

Tanaka, N., Jinadasa, K.B.S.N., Mowjood, M.I.M. & Fasly, M.S.M., 2011, 'Coastal vegetation planting projects for tsunami disaster mitigation: Effectiveness evaluation of new establishments', *Landsc. Ecol. Eng*. 7, 127–135.

Temmerman, S., Meire, P., Bouma, T.J., Herman, P.M.J., Ysebaert, T. & De Vriend, H.J., 2013, 'Ecosystem-based coastal defence in the face of global change', *Nature*, 504, 79-83.

Wijetunge, J.J., 2006,'Tsunami on 26 December 2004: Spatial Distribution of Tsunami Height and the Extent of Inundation in Sri Lanka', *Sci. Tsunami Hazards* 24, 225–239.

Wijetunge, J.J., 2009a, 'Field measurements and numerical simulations of the 2004 tsunami impact on the south coast of Sri Lanka',*Ocean Eng*. 36, 960–973.

Wijetunge, J.J., 2009b, 'Field Measurements and Numerical Simulations of the 2004 Tsunami Impact on the East Coast of Sri Lanka', *Pure Appl. Geophys*. 166, 593–622.

Wijetunge, J.J., 2012, 'Nearshore tsunami amplitudes off Sri Lanka due to probable worst-case seismic scenarios in the Indian Ocean',*Coast. Eng*. 64, 47–56.

Wijetunge, J.J., 2014, 'A deterministic analysis of tsunami hazard and risk for the southwest coast of Sri Lanka', *Cont. Shelf Res*. 79, 23–35.

Wijeyewickrema, A.C., Inoue, S., Gunaratna, P., Madurapperuma, M. & Matsumoto, H., 2006,' Field Survey of the Tsunami Caused by the Sumatra-Andaman Earthquake of December 26, 2004 and the Restoration of Impacted Inland Water Bodies in Sri Lanka', *J. Disaster Res*. 1, 123–130.

Proceedings of the 7th International Symposium on

Advances in Civil and Environmental Engineering Practices for Sustainable Development

ACEPS - 2019

Tsunami intrusion in rivers: a review and new perspectives on Sri Lankan rivers

Romitha Wickramasinghe[1] and Norio Tanka[2]

[1]Student, Graduate School of Science and Engineering, Saitama University, 255 Shimo-Okubo, Sakura-ku Saitama, 338-8570, JAPAN.
[2]Professor, International Institute for Resilient Society, Graduate School of Science and Engineering, Saitama University, 255 Shimo-Okubo, Sakura-ku Saitama, 338-8570, JAPAN.

K e y w o r d s

Tsunami propagation
River mouth
Bed slope
Sand mining
River morphology
Sri Lanka

A B S T R A C T

Tsunami intrusion in rivers can cause damages to near coast as well as upstream rivers. This paper reviews the role of different river parameters that dominate the phenomenon of tsunami propagation in rivers. River mouth morphology is the most influencing feature during a low magnitude tsunami, and bed slope acts major in an extreme event. Nevertheless, length and the impact of tsunami wave propagation in rivers depend on numerous features like tides, river discharge, meandering, river structures, flow branches and characteristics of embankments. During 2004 Indian Ocean tsunami in Sri Lanka, tsunami waves propagated significantly through a small river canal in Galle city causing local floods while the tsunami intruded in major rivers were dissipated due to existence of vast flood plains with trees around river mouths. This review also concentrates on human involvement to the evaluation of river morphology in Sri Lanka where unregulated sand mining has reduced the sediment supply to river mouth which can aggravate erosion during a tsunami event. Therefore, further investigations on small to mid-size rivers and quantitative analysis on the evolution of river morphology in Sri Lanka are vital for the management of potential tsunami related damage.

1. INTRODUCTION

Tsunamis are a series of ocean waves that send surges of water caused by earthquakes, underwater landslides, volcanic eruptions, or asteroids. Generally, it is called a wave train, where its destructive force may be able to travel 10-15 meters per second with having wave height of 03-30 meters causing catastrophic damage to both the coast and in the hinterlands.

There have been reported cases where tsunami intrusion in the river leads to damages the areas far upstream from the shoreline, in addition to its capability of damaging coastal facilities and structures. Then the possibilities for the tsunami disaster always exist near the coastal and upstream areas both. Tsunami waves propagate to river may not only a threat of damages to the infrastructure but also cause the environmental problems such as inundation and saline water intrusion to the rice field areas (H. Tanaka & Tinh 2012). Therefore, the study of tsunami impacts on river upstream becomes vital. Even though tsunami impacts on coastal areas have been subjected to countless studies, only a few studies have focused on tsunami impacts on rivers.

Hatori (1980) has reported some historical tsunamis originated in 1707 and 1854 in the Pacific Ocean of southwestern Japan, which caused inundations along the rivers. During the 1983 tsunami in Japan, Abe (1986) has recorded about development of a standing wave that propagated the tsunami wave up to 15km upstream of a river. Abe (1986) and Tolkova *et al.* (2015) have reported that the peak of intruded tsunami wave height lies approximately midway between the river mouth and the uppermost limit of tsunami inundation. Based on laboratory experiment

and theoretical approach Tsuji *et al.* (1991) found that the tsunami height in river might be amplified by a factor of 1.5 times the initial tsunami height in deep rivers or channels. This factor of increase can be used for the effective planning of river channel levees. According to N. Tanaka *et al.* (2012), the 2011 Great East Japan Tsunami (GEJT) had hit some hinterlands from both river and coastal directions during the Great East Japan Earthquake while making the evacuation process complex.

Tsunami observations in rivers also include records of several tsunamis on tide gauges in the Columbia River. It was disclosed that tsunami penetrated the Columbia River, and was influenced by a combination of convergent bathymetry and bed friction. Moreover, its high-frequency components were controlled by diffusion and scattering in the river estuary (Yeh *et al* 2012). Comparison of observed data of 2004 Indian Ocean Tsunami (IOT), 2010 Chilean Earthquake Tsunami (CET) and 2011 GEJT unveil the importance of river mouth morphology in terms of tsunami wave propagation along a river (Adityawan *et al* 2012; H. Tanaka & Tinh 2012; Roh *et al* 2011). Moreover, Mori *et al* (2011) have observed longest runups in the 2011 GEJT and the 2010 CET. Fritz *et al* (2011) have identified wave propagated 15 km up in Maule river in Chile during 2010 CET. H. Tanaka *et al* (2014) was mentioned that during the 2011 GEJT, waves propagated in Kitakami river reached to 49 km from river mouth even after overtopping from a weir. As stated by Liu *et al.* (2013), devastating tsunami inundation in the riverine plains of Kessen and Yahagi rivers have occurred where the propagated lengths are about four times the inundation distance in coastal area. A detailed study done in Sri Lanka after 2004 IOT reports that intruded tsunami waves to Sri Lankan rivers were mainly dissipated by vast flood plains around the river mouth (H. Tanaka *et al* 2008).

Along with observational and experimental studies, numerical simulations also have provided confident results in the area of tsunami intrusion in rivers. Yasuda (2010) has conducted a 1D numerical model on tsunami propagation up in river channels while computational results agree well with the observed data in 2003 Hokkaido tsunami in Japan. Viana-Baptista *et al.* (2006) had conducted a numerical simulation for Tagus estuary, Lisbon, based on historical events of tsunami propagation in river that caused severe flooding in the upstream area. After the Columbia River affected by the 2011 GEJT, Tolkova (2013) simulated the event that populated with realistic tide and riverine flow. It also confirmed the occurrence of a tide-tsunami interaction by reproducing the observed modulation of tsunami by tide. As claimed by Tolkova *et al.* (2015), observations of the 2011 GEJT and the 2010 CET in several rivers in Japan and the Columbia River in the USA described two tsunami effects in rivers. First, the river tide modulates the tsunami wave, and a strong near-field tsunami can cause significant prolonged water accumulation in lower river reaches. Using a simplified 1D nonlinear shallow-water model, the numerical experiments highlight the indispensable role of tsunami's interaction with tide and riverine flow (Tolkova *et al* 2015).

Moreover, to evaluate the wave heights of incident and reflected tsunami bores in Katakami River during 2011 GEJT, Tolkova & H. Tanaka (2016) have exercised the shock conditions with actual tsunami measurements in the river. These distinguishing features make this study relevant to enhance knowledge further on the phenomena of tsunami intrusion in rivers. This review focuses on parameters that dominate the tsunami intrusion in rivers and understand the research gaps in this sector in Sri Lanka.

2. EFFECT OF RIVER PARAMETERS

2.1. River Mouth Morphology

The tsunami wave propagating in rivers is related to various river parameters. In wave propagation process, river mouth morphology is one of the dominant factors because it is the entrance location of the wave (Adityawan *et al.* 2012; H. Tanaka & Tinh 2012; Roh *et al.* 2011).

Analyzing the data of the 2010 CET, Roh *et al* (2011) have mentioned the influence of the river characteristic on tsunami propagation including a numerical model. In the study, they have classified river mouth into two types (Figure 1) where Type 1 river mouth is located

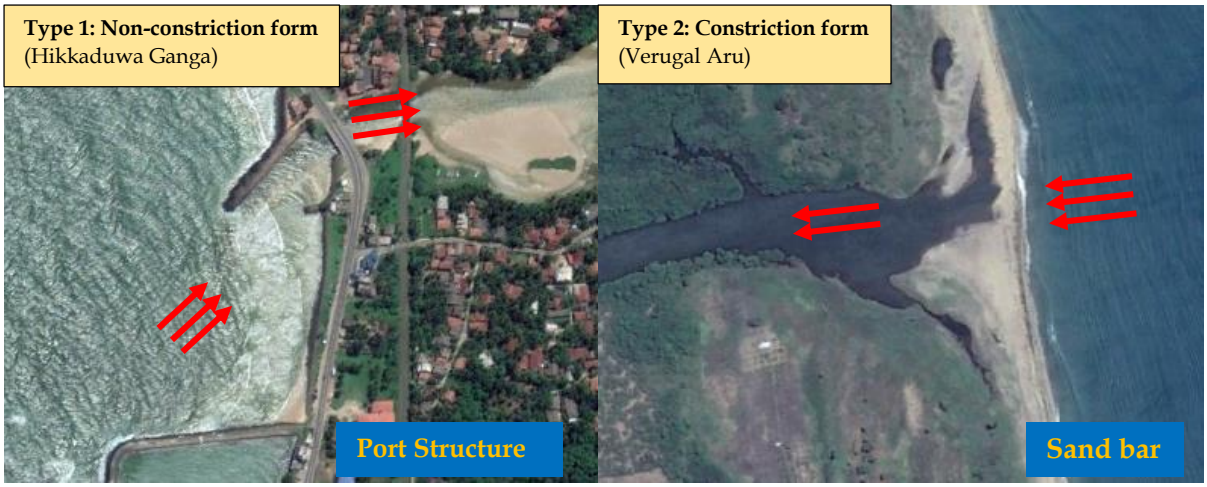

Figure 1 Examples for classification of river mouth types in Sri Lanka (Source: Google Maps). Modified from H. Tanaka & Tinh (2012).

inside of port or bay (non-constriction form), and Type 2 is that river mouth is composed by sand bar or sandy coast at river entrance (constriction form). The reasonable and consistent results of collected data and numerical analysis show that the defined Type 1 has a high vulnerability, where the most influential type of river mouth when the tsunami wave approaches the river area. Focusing on the impacts of the 2010 CET and the 2011 GEJT with respect to 25 rivers in Tohoku region of Japan, H. Tanaka & Tinh (2012) also has found Type 1 river mouths are vulnerable in terms of wave height and upstream propagation. Moreover, tsunami wave can be affected up to about 50km upstream of a large river and the measured tsunami travel time inside the river is almost similar to tsunami travel time calculated by using the long-wave theory (H. Tanaka & Tinh 2012).

Selecting rivers in Sendai coast-Japan and Aceh coast-Indonesia, Adityawan *et al* (2012) further elucidate the tsunami intrusion in rivers relating to three tsunamis caused by the 2004 IOT, the 2010 CET, and the 2011 GEJT. It delineates that river mouth morphological features play an essential role in the intrusion of low magnitude tsunami; nevertheless, the effect of these features is less significant in the case of an extreme tsunami.

Naturally formed river mouths with buffer have a greater capability on reducing tsunami wave energy compared to river mouths with no buffer (H. Tanaka *et al* 2014). It was recorded that there was an initial reduction in propagated tsunami wave height in Agano River due to existence of sandbars at the river mouth, which was exposed to the 1983 tsunami in Japan (Abe 1986). Moreover, N. Tanaka *et al.* (2012) also reports about the existence of sand-dune in the Mikawa River where most of the tsunami was stopped in the 2011 GEJT.

Based on Sri Lankan catastrophe in 2004, H. Tanaka *et al.* (2008) states that the distance of tsunami propagation in Sri Lankan rivers is dependent more on the scale of flood plains on both sides of the river, rather than on the size of the river mouth bar.

2.2. Bed Slope

River bed slope plays a major role in the wave propagation in extreme tsunami events. Since tsunami wave can propagate easily into river upstream area through steady and mild type river bed without losing large amount of wave energy, Adityawan *et al.* (2012) reports that tsunami intrusion in river due to massive tsunamis like the 2004 IOT and the 2011 GEJT is correlated to the bed slope with no significant effect from the river class or type of the river mouth. During the 2004 IOT, waves surged up along the small river canal with very mild bed slopes (Kapu Ela) in Galle city of Sri Lanka for approximately 2km upstream and caused localized flooding (H. Tanaka *et al* 2008).

The observational and numerical data of Tolkova *et al.* (2015) point to a correlation between the tsunami attenuation rate and the river bed slope in the tsunami path as well as a similar correlation between the tsunami intrusion distance and the river bed slope. H.

Tanaka *et al.* (2014) states that damping coefficient is closely related to the riverbed slope and river meandering may have different effect on this parameter.

2.3. Other Parameters

Apart from characteristics of river mouth and bed, there are other features that influence tsunami propagation through rivers. As per the previous studies, it is assumed that the outer bank side of a river meander is more vulnerable to overtopping during wave propagation in a river (Shi *et al* 1998; Yuhi *et al* 2000). In the studies of Abe (1986) and N. Tanaka *et al.* (2012) have found that the river embankments were overtopped at a meandering river section during tsunami wave propagation along the rivers. Furthermore, Abe (1986) concluded that various factors such as flow branching and artificial water intakes may complicate the propagation profiles during a tsunami event. According to Roh *et al.* (2011), tsunami waves are transmitted even in the low tidal level which will govern by river scale, river discharge and the bottom condition. Tolkova *et al.* (2015) report that tsunami penetration in rivers is largely determined by the interaction among the flow components such as tsunami wave strength, tide, and river discharge. According to H. Tanaka *et al.* (2008) strength of the abutment also plays an important role to withstand large return flow in rivers.

Based on available tsunami records in the Columbia River, USA Tolkova (2013) suggested that non-linear interaction between tsunami and river tide causes attenuation of tsunami signal during the receding tide in the river estuary, and facilitates tsunami propagation and confirmed this hypothesis in numerical simulations of tsunami intrusion into the Columbia River. Numerical simulation of Tolkova *et al.* (2015) has disclosed that high tide greatly facilitates the tsunami intrusion, whereas a receding tide efficiently dissipates the tsunami energy. Generated backwater effect during a tsunami propagation in a river can obstruct the river flow and lead to overtopping from embankments. Tolkova *et al.* (2015) have hypothesized and briefly illustrated this condition with numerical experiments. Having river structures like weirs can mitigate the tsunami propagation in a river, and it was observed during the Kitakami River and the Abukuma River in the 2011 GEJT (H. Tanaka *et al* 2014). However, H. Tanaka *et al.* (2014) stated that reflected tsunami wave due to structure can increase the inundation in downstream area.

In the 2011 GEJT, N. Tanaka *et al.* (2012) discovered that tsunami can hit from both directions from coast and river to hinterlands.

Situations like this have made the flow conditions and evacuation process of people complex during the propagation. According to H. Tanaka *et al.* (2008), similar kind of inundation type was observed in the Galle city during 2004 IOT (Figure 2). This elucidates the necessity of identifying vulnerable embankment locations and inundation types during an event to upgrade hazard maps as well as plan new cities.

3. TSUNAMI INTRUSION IN SRI LANKAN RIVERS

The IOT triggered on 26th December 2004 caused a massive loss of life and damage to property in the coastal belts of several Indian Ocean countries including Sri Lanka, Indonesia, and Thailand. Sri Lanka has been extremely hard-hit from this IOT in terms of loss of life, infrastructure, and economic assets where the 2004 IOT is widely acknowledged as the largest and most devastating natural catastrophe in the history of the country.

According to Wijetunge (2004), it left behind widespread destruction and killed nearly 40,000 people with 15,000 injured, destroyed over 89,000 homes entirely or partially, damaged natural ecosystems, and coastal infrastructure. The incurred overall damage is estimated to be around $1 billion, which is almost 4.5 percent of country`s GDP (ADB 2005).

Studies on tsunami intrusion to rivers in Sri Lanka is rare. However, a detailed study was conducted by H. Tanaka *et al* (2008) targeting Kalu Ganga, Gin Ganga, Galle city, Nilwala Ganga, Mahaweli River, and Yan Oya after the2004 IOT and observed field data are shown in Table 1

Table 1 Characteristic of rivers. Modified from H. Tanaka *et al* (2008).

Name of River	Size of Sand Bar	Status of River Banks	Distance of Propagation (Approx.)	Degree of Tsunami Energy Dissipation
Kalu	Large	Narrow flood plain	20km	Small
Gin	Small	Vast flood plain	5-6km	Large
Nilwala	Large	Vast flood plain with tress	8km	Medium
Yan	Medium	Dense tress	3-4km	Large
Mahaweli	Medium	Vast flood plain with tress	Unknown	Large

.Analyzing the data of Gin Ganga, Yan Oya and Mahaweli River, H. Tanaka *et al.* (2008) has revealed that the distance of tsunami propagation is dependent more on the scale of flood plains on both sides of the river, rather than on the size of the river mouth bar. In the same event, they have discovered that the tsunami intrusion along small river canals named Kapu Ela and Moragoda river inside in Galle city extending the impact of tsunami approximately 2km and 1km respectively in upstream area. It had caused flooding from both sea and river, where this inundation type (Figure 2) was similar to which was observed by N. Tanaka *et al.* (2012) during the 2011 GEJT in Abukumagawa and Kitakamigawa Rivers in Japan.

Figure 2 Inundation type of Galle city during the 2004 IOT (Source: Google Maps). Modified from N. Tanaka *et al* (2012).

Among the infrastructure damages, bridge damages were vital in the west and south coasts of Sri Lanka, where railway line and main road (A2) cross several rivers and streams. Here, H. Tanaka *et al.* (2008) had underlined the importance of detail analysis of tsunami effect on bridges with regard to future bridge designing while investigating and categorizing 34 bridges, culverts and their surrounding structures based on the damage. Since most of the Sri Lankan railway bridges are through bridges, and most of the road bridges are deck bridges, the clearance height between the girder and the water surface of railway bridges is higher than that of the road bridges. Therefore, the damage sustained by railway bridges is less compared to road bridges (H. Tanaka *et al* 2008). Additionally, in the study of Rossetto *et al.* (2007), it has identified three common bridge types based on the span in the surveyed areas which were affected by 2004 IOT. It has found that between Kaluthara and Matara, five road bridges and four railway bridges were severely damaged where most of the bridges consisted of damage to parapets or abutments. According to Rossetto *et al.* (2007), the primary mode of failure of the road bridges was the collapse of the concrete deck slab because of consequent failure of the masonry retaining wall abutments due to scouring. Even though the abutments of these bridges consisted of rock barrier on sea side, it lacked similar protection on upstream side which led to erosion, caused by backflow of propagated tsunami wave along the river.

Introducing a comparison concept of discharge and flow velocity of a flood induced by torrential rain and tsunami waves in small and large rivers, H. Tanaka *et al.* (2008) reported that, due to tsunami waves, the damage sustained by a bridge of a large river is relatively small compared to the damage sustained by a bridge of small rivers. Therefore, the lessons learned from the damage to the river bridges in Sri Lankan southwest can be used for planning and implementing necessary prior measures in bridge design in other countries. H. Tanaka *et*

al. (2008) indicates that the damage becomes more severe in terms of bridge collapse as the ratio of "tsunami wave height/bridge clearance height" exceeds 2.0. This can be used to estimate the severity of bridge damages in future tsunami events.

In addition, Richmond *et al.* (2006) claims that the removal of sand-dunes and extensive illegal dredging in rivers appear to have increased the inundation in the first place of tsunami in Sri Lanka. According to Samaranayake (2005), sand mining in Sri Lankan rivers not only resulted in a lower river bed and increased bank erosion, but also drastically reduced the sediment supply to the coast which increases the vulnerability of tsunami intrusion through river mouths.

4. SUMMARY & CONCLUSION

It was reported that damages due to tsunami intrusion in rivers can be more devastating due to its high potential to propagate in rivers compared to land. This phenomenon is mainly dominated by river morphology. In Sri Lanka, tsunami intrusion in rivers has obtained less attention, where integrated studies are required in future particularly considering the small and mid-sized rivers. Secondly, human impacts on river morphology also have greater influence on the evolution of river mouths and river bed. Indiscriminate and extensive sand mining in rivers, beaches, and dunes have triggered to loss of natural sand bars in river mouths. This loss increases the vulnerability of tsunami intrusion. Further it also reduces the amount of sand available to replenish what was lost during the tsunami events. Hence quantitative analysis should be attained to investigate the evolution of river mouth morphology.

5. REFERENCES

Abe, K., 1986, 'Tsunami propagation in rivers of the Japanese Islands', *Continental Shelf Research,* 5(6), 665–677.

Adityawan, M.B., Roh, M., Tanaka, H. & Farid, M., 2012, 'The Effect of River Mouth Morphological Features on Tsunami Intrusion', *Proceedings of the 8th International Conference on Disaster Management*, 75–83.

Asian Development Bank, 2005, '*Sri Lanka 2005 Post-Tsunami Recovery Program - Preliminary Damage and Needs Assessment*', Colombo, Sri Lanka: Asian Development Bank, Japan Bank for International Cooperation and, World Bank.

Fritz, H.M., Petroff, C.M., Catalán, P.A., Cienfuegos, R., Winckler, P., Kalligeris, N., Weiss, R., Barrientos, S.E., Meneses, G., Valderas-Bermejo, C., Ebeling, C., Papadopoulos, A., Contreras, M., Almar, R., Dominguez, J.C. & Synolakis, C.E., 2011, 'Field Survey of the 27 February 2010 Chile Tsunami', *Pure Appl. Geophys,* 168, 1989–2010.

Hatori, T., 1980, 'Field Investigation of the Nankaido Tsunamis in 1707 and 1854 along the Osaka and Wakayama Coasts, West Kii Peninsula'. *Bull. of the Earthq. Res. Inst.,* University of Tokyo, 55, 505–535.

Liu, H., Shimozono, T., Takagawa, T., Okayasu, A., Fritz, H.M., Sato, S. & Tajima, Y., 2013, 'The 11 March 2011 Tohoku Tsunami Survey in Rikuzentakata and Comparison with Historical Events', *Pure Appl. Geophys* ,170, 1033–1046.

Mori, N., Takahashi, T., Yasuda & T., Yanagisawa, H., 2011, 'Survey of 2011 Tohoku earthquake tsunami inundation and run-up', *Geophysical Research Letters* ,38, 6–11.

Richmond, B.M., Jaffe, B.E., Gelfenbaum & G., Morton, R.A., 2006, 'Geologic impacts of the 2004 Indian ocean tsunami on Indonesia, Sri Lanka, and the Maldives', *Z. Geomorphol.* 146, 235–251.

Roh, M., Nguyen, X.T. & Tanaka, H., 2011, 'Effect of river mouth morphology on tsunami propagation ascending rivers', *J. Japan Soc. Civ. Eng. Ser. A2 (Applied Mech.),* 67(2), 607-I_614.

Rossetto, T., Peiris, N., Pomonis, A., Wilkinson, S.M., Del Re, D., Koo, R., &Gallocher, S., 2007, 'The Indian Ocean tsunami of December 26, 2004: Observations in Sri Lanka and Thailand', *Nat. Hazards,* 42, 105–124.

Samaranayake, R. A. D. B., 2006, 'Pre-and post-tsunami coastal planning and land-use policies and issues in Sri Lanka', *In proceedings of the workshop on coastal area planning and management in Asian tsunami-affected countries,* Bangkok, Thailand, Food and Agriculture Organization of the United Nations, 27–29.

Shi, A., Teng, M.H. & Wu, T.Y., 1998, 'Propagation of solitary waves through

significantly curved shallow water channels'. *J. Fluid Mech*., 362, 157–176.

Tanaka, H., Ishono, K., Nawarathna, B., Nakagawa, H., Yasuda, H. & Watanabe, Y., Hasegawa, K., 2008, 'Field Investigation of Disasters in Sri Lankan Rivers Caused By the 2004 Indian Ocean Tsunami', *J. Hydrosci. Hydraul. Eng.* ,26(1), 91–112.

Tanaka, H., Kayane, K., Adityawan, M.B., Roh & M., Farid, M., 2014, 'Study on the relation of river morphology and tsunami propagation in rivers', *Ocean Dyn.* ,64, 1319–1322.

Tanaka, H. & Tinh, N.X., 2012, 'The 2010 Chilean and the 2011 Tohoku Tsunami Waves Impact to Rivers in the Tohoku Region, Japan', *In proceedings of 33rd International Conference on Coastal Engineering*.

Tanaka, N., Yagisawa, J. & Yasuda, S., 2012, 'Characteristics of damage due to tsunami propagation in river channels and overflow of their embankments in Great East Japan Earthquake', *Int. J. River Basin Manag.* ,10(3), 269–279.

Tolkova, E., 2013, 'Tide-Tsunami Interaction in Columbia River, as Implied by Historical Data and Numerical Simulations', P*ure Appl. Geophys.,* 170, 1115–1126.

Tolkova, E., Tanaka, H. & Roh, M., 2015, 'Tsunami Observations in Rivers from a Perspective of Tsunami Interaction with Tide and Riverine Flow', *Pure Appl. Geophys*., 172, 953–968.

Tolkova, E. & Tanaka, H., 2016, 'Tsunami Bores in Kitakami River', *Pure Appl. Geophys*., 173(12), 4039–4054.

Tsuji, Y., Yanuma, T., Murata, I. & Fujiwara, C., 1991, 'Tsunami ascending in rivers as an undular bore', *Nat. Hazards,* 4, 257–266.

Viana-Baptista, M.A., Soares, P.M. & Miranda, J.M., Luis, J.F., 2006, 'Tsunami Propagation Along Tagus Estuary (Lisbon, Portugal) Preliminary Results', *Sci. Tsunami Hazards,* 24(5), 329–338.

Wijetunge, J.J., 2004, 'Tsunami On 26 December 2004: Spatial Distribution Of Tsunami Height And The Extent Of Inundation In Sri Lanka', S*ci. Tsunami Hazards,* 24(3), 225–239.

Yasuda, H., 2010, 'One-dimensional study on propagation of tsunami wave in river channels', *J. Hydraul. Eng.* ,136(2), 93–105.

Yeh, H., Tolkova, E., Jay, D., Talke, S., Fritz, H., 2012, 'Tsunami hydrodynamics in the Columbia River', *J. Disaster Res.* ,7(5), 604–608.

Yuhi, M., Ishida, H., Mase, H., 2000, 'Numerical study of solitary wave propagation in curved channels', *Coast. Eng. 2000 - Proc. 27th Int. Conf. Coast. Eng*, Sydney, Australia, July 16-21, 2000, 519–532.

Environmental Engineering and Management

Proceedings of the 7th International Symposium on

Advances in Civil and Environmental Engineering Practices for Sustainable Development

ACEPS - 2019

Field scale combined stabilization pond system and constructed wetland for leachate treatment controlling loading conditions

R.M.L.D.Rathnayake[1], E.I.K.Gamakaranage[1], W.M.D.C.Walisundara[1] and G.B.B. Herath[1]

[1]Department of Civil Engineering, Faculty of Engineering, University of Peradeniya, Peradeniya, 20400, SRI LANKA

K e y w o r d s

Leachate
Stabilization ponds
Constructed wetlands
Controlled hydraulic loading

A B S T R A C T

Treatment of leachate in solid waste landfills is challenging due to strong mineral content of leachate and the high cost of treatment. Waste WSPs (WSPs) and constructed wetlands (CWs) are regarded as low cost treatment options which are widely used in developing countries. Previous studies found that treatment efficiencies of WSPs were significantly low mainly due to an uncontrolled loading condition. Therefore, in this study, performance of biological oxygen demand (BOD55), chemical oxygen demand (COD), nitrogen species, and phosphate removals in a field scale combined WSPs followed by CWs was investigated under controlled organic loading conditions by dilution with natural water. The overall BOD55, COD, and TN, and TP removals efficiencies were 97%, 89%, 86% and 61%, respectively. Moreover, CWs unit plays important role in removal of TN and TP from leachate. Even though the characteristics leachate affected by the environmental changes, its impact on performances of the treatment system was insignificant probably due to the controlling the loading condition. Therefore, results of this study revealed that operating the combined system by dilation of leachate with natural water would be a feasible alternative in operating combined WSPs and CWs during dry seasons of tropical regions.

1. INTRODUCTION

Treatment of leachate is a major issue in solid waste sanitary landfilling throughout the world. The strong mineral and organic content of leachate and the high cost of treatment are the two major problems in this regard(Youcai, 2018). When untreated leachate is leaked into the ground, ground water and surface water can be polluted.

At present, the most common and low costtreatment method for leachate treatment is on-site pre-treatment of activated sludge (Wiszniowski et al., 2006). Recently, novallab and pilot scale treatment systems for leachate treatment have been studied. For example, a modified sequencing batch reactors(Wang et al., 2013)or hybrid systems (Speer et al., 2012) for landfill leachate treatment. Stabilization ponds system is a low cost treatment options and attractively widely used in developing countries for wastewater treatment (Madera and Valencia-Zuluaga, 2009).WSPs are large, shallow basins in which raw sewage is treated entirely by natural processes involving both algae and bacteria. Many researchers investigated on the use of WSPs, a simple leachate treatment method for leachate treatment and have also observed promise as another form of landfill leachate treatment(Frascari et al., 2004;Mehmood et al., 2009; Renou et al., 2008;Thörneby et al., 2006).

In addition to stabilizations ponds, many studies reported constructed wetlands have been used for leachate treatments (Yalcuk and Ugurlu, 2009; Bulc et al., 1997;Akinbile et al., 2012;Wojciechowska et al., 2010).

Recently, Herath (2016) and Kothalawala et al. (unpublished data) reported the successful leachate treatment efficiencies of field scale and lab scale combined stabilization pond systems. However, they recommended

the coupling the pond system effluent with a polishing treatment stage is required to achieve the 30 mg/L BOD_5, 250 mg/L COD the standard requirements in Sri Lanka. In addition, performances of the system were significantly affected by mainly due to the non-availability of sufficient leachate loading during the dry season (Kothalawala et al,unpublished data).

In tropical regions the leachate treatment efficiency widely varies with natural environmental factors such as rainfall and temperature as characteristics and quantity of leachates depends upon the environmental conditions resulting different organic/hydraulic loading rates for treatment facilities (Kamaruddin et al., 2016).

Generally, constructed wetlands (CWs) can withstand high phosphate and nitrate values, and CWs uses as polishing treatment stage for wastewater(Mustapha et al., 2015;Weerakoon et al., 2018). Therefore, combined treatment system with WSPs and CWs may be feasible option for leachate treatment. However, performances of COD, BOD_5, and nitrogen and phosphate removal of a combined WSPs and CWs operated with controlling hydraulic loading system have not been investigated poorly investigated.

Therefore, maintaining the hydraulic loading condition to the leachate treatment system with dilution of leachate with natural water would enhance the performance of a stabilization pond and constructed wetland system.

Therefore, in this study, areal scale treating leachate treatment facility with stabilisation ponds and constructed wetland system was operated by controlling the hydraulic loading condition and performances of a field scale pond system and a constructed wetland.

2. MATERIALS AND METHOD

2.1. Operation of stabilization pond systems and constructed wetland system

A field scale stabilization pond system consists of anaerobic (3 m^3), facultative (3 m^3) and aerobic ponds (2 m^3) were constructed in Udapalatha, Gampola, Sri Lanka. The system was fed with real leachate produced in a lysimeter. Flow rate to the stabilization pond system was maintained at 160 L/day. This flow rate resulted HRT values of 19 days, 19 days, and 13 days for anaerobic, facultative, and aerobic ponds respectively. At a 75th day of starting operation of anaerobic pond, the effluent of the aerobic pond was fed to a free flow constructed wetland with 3m3 in volume which planted with Cattail plants

Figure 1 (A) The lysimeter in the Udapalatha landfill. (B) The field scale combined WSPs and CWs

Initially leachate was diluted by 50% with natural water, because we lysimeter didn't produce enough leachate due to dry period. After the 12th week we fed the system with 100% leachate as the area received significant. Because after the 12th week site received a good rainfall and as a result leachate production from lysimeter was in a good condition to maintain the same hydraulic loading rate without dilution of leachate.

2.2. Operation of stabilization pond systems and constructed wetland system

Influent and effluent samples were collected from each ponds and wetland at a frequency of one per each. The collected samples from WSPs and constructed wetland were tested for BOD_5, COD were measured using Winkler Titration Method and spectrophometer method, respectively. Total phosphorus (TP), ammonium (NH_4^+) and nitrate (NO_3-L) were measured using a

spectrophotometer (UNICO2100, UNICO Company, South Brunswick, NJ, USA).

3. RESULTSAND DISCUSSIONS

3.1. BOD_5 removal efficiency

BOD_5 in the influents and the effluents and their removal efficiencies shown in Figure 2(A) and Figure 2(B), respectively. Average BOD_5 (± standard deviation) in the influent and effluent of anaerobic pond with 50% dilution, were 1472±437 and 426±47 mg/L, respectively. This corresponded to an average total BOD_5 loading rates of 78.4±23 g-$BOD_5/m^3/d$. Moreover, the average BOD_5 (± standard deviation) in the influent and effluent of anaerobic pond without dilution were 1908±176 and 497±88 mg/L, respectively. This corresponded to an average total BOD_5 loading rate of 102±9 g-$BOD_5/m^3/d$. According to the student t-test, the BOD_5 concentrations amount two loading conditions were significantly different ($p=0.044 < 0.05$). Average BOD_5 (± standard deviation) in the effluent concentrations of facultative pond and aerobic pond were 291±69 and 77.2±10.7 mg/L. BOD_5 concentration of effluent of the CWs was 55.8 ± 4.3 mg/L, which was higher than the Sri Lankan wastewater discharge standards. The corresponding BOD_5 removal efficiencies were calculated and shown in Figure 2(B). Results revealed that the removal efficiencies of BOD_5 removal efficiencies of anaerobic pond, facultative pond, and aerobic pond were stable during the operation period. The BOD_5 in anaerobic pond, facultative pond and aerobic pond were 71.0±9.6%, 37.8± 11.6%, and 72.8±6.3%. Interestingly, these removal efficiencies showed that the overall BOD5 removal efficiency of the stabilization pond system was 95.5±1.2%. The BOD_5 removal efficiencies of ponds were not significantly different under loading with 50% dilution and non-diluted feeding conditions ($p>0.05$). The total BOD_5 removal loading rate was 87.2 g-$BOD_5/m^3/d$. After the constructed wetland treatment unit was added to the pond system, average effluent BOD_5 concretions was reduced to 55.8 ± 4.3 mg/L, increasing the overall BOD5 removal efficiency up to 97.0 ± 0.1%.The overall BOD_5 removal efficiency of our present study (95.5- 97.0%) is higher than the leachate treatment system using only stabilization pond system reported by Renou et. al. (2008), Orupold et. al. (2000), and Mæhlum et al. (1995). Moreover, the overall BOD_5 removal efficiency is comparable with the study reported by Herath (2016).

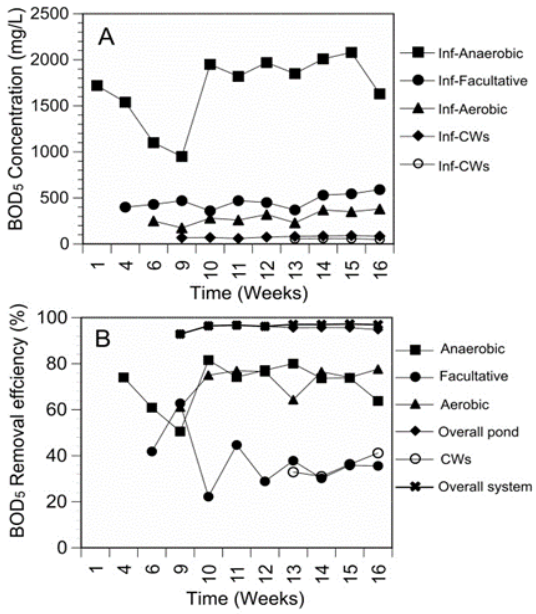

Figure 2 (A)BOD_5 concentrations in treatment units. (B)BOD_5 removal efficiencies of treatment system.

3.2. COD removal efficiency

COD in the influents and the effluents of ponds and their removal efficiencies shown in Figure 3(A) and Figure 3(B), respectively. Average COD (± standard deviation) in the influent and effluent of anaerobic pond with 50% dilution, were 5166 ± 1500 and 4660 ± 594 mg/L, respectively. This corresponded to average total BOD_5 loading rates of 275± 80.0 kg-$BOD_5/m^3/d$. Moreover, the average COD (± standard deviation) in the influent and effluent of anaerobic pond without dilution were 8080±394 and 5000±591 mg/L, respectively. This corresponded to an average total BOD_5 loading rate of 430±21 kg-$BOD_5/m^3/d$. According to the student t-test, the COD concentrations amount two loading conditions were significantly different ($p < 0.001$).

The corresponding COD removal efficiencies were calculated and shown in Figure 3(B). The COD removal efficiencies in anaerobic pond with 50% dilution and without dilution were 23.6±10.0% 38.3±4.3% respectively.The COD removal efficiencies of anaerobic ponds were significantly different under loading with 50% dilution and non-diluted feeding conditions ($p=0.004< 0.05$)

while those efficacies of other treatment systems were not significantly affected by the loading conditions. The facultative pond and aerobic pond were 30.9 ± 10.6%, 55.2 ± 5.0%, and 47.1±7.7% (Figure 3B).

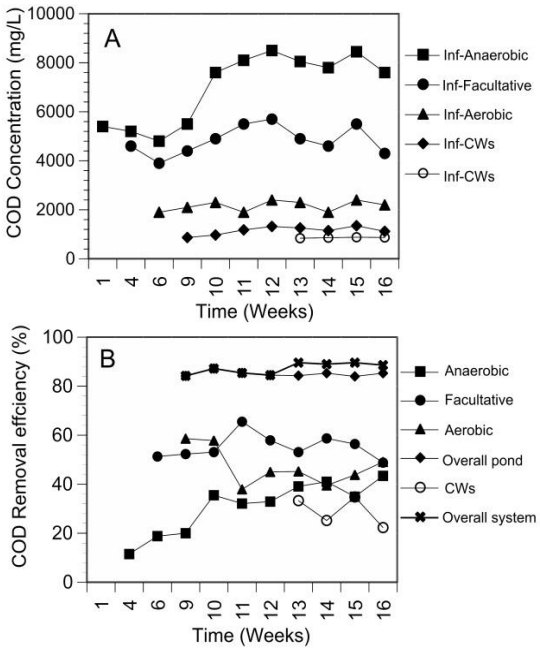

Figure 3 (A)COD concentrations in treatment units. (B)COD removal efficiencies of treatment system.

Interestingly, these removal efficacies showed that the overall COD removal efficacy of the stabilization pond system was 85.0±1.0%. The total COD removal loading rate was 327 g-COD/m^3/d. After the constructed wetland treatment unit was added to the pond system, average effluent COD concretions was reduced to 862.5±17.1 mg/L, increasing the overall COD removal efficiency up to 89.2 ± 0.5%. The overall COD removal efficiency of our present study (89.2%) is higher than the COD removal efficiency of stabilization pond system reported by Renou et. al. (2008), Orupold et. al. (2000), and Mzehlum et al. (1995). However, final COD concentration of effluents of the CWs was 862±17 mg/L is much above the Sri Lankan Wastewater disposal guidelines.

3.3. Nitrogen removal efficiency

NH_4^+concentration in the influents and the effluents of pond system and their NH_4^+removal efficiencies shown in Figure 3A. Average NH_4^+concentration (± standard deviation) in the influent and effluent of anaerobic pond were 304.1±57.2 and 176.0± 33.4 mg/L, respectively. Average NH_4^+concentration (± standard deviation) in the effluent of facultative pond and aerobic pond were 105.0±9.7 and 49.3±11.0 mg/L. After the constructed wetland treatment unit was added to the pond system, average effluent NH_4^+concentration were reduced to 37.8 ± 3.2 mg/L.

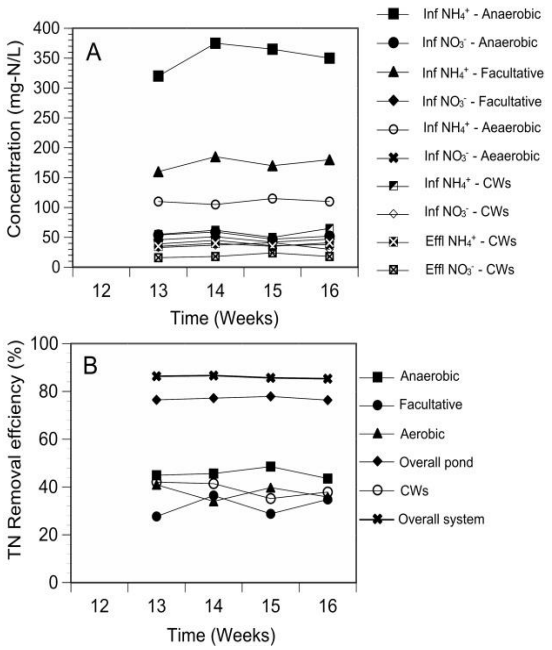

Figure 4 (A) Concentrations of NH_4^+ and NO_3^- in the treatment units. (B). TN removal efficiencies of treatment systems.

Average nitrate concentration (± standard deviation) in the influent and effluent of anaerobic pond were 53.0 ± 5.0 and 46.5 ± 3.7 mg/L, respectively. Average nitrate concentration (± standard deviation) in the effluent of facultative pond and aerobic pond were 39.5 ± 3.9 and 35.3 ± 4.8 mg/L. After the constructed wetland treatment unit was added to the pond system, average effluent nitrate concentration was reduced to 19.0 ± 3.5 mg/L. Total nitrogen removal efficiencies were calculated and shown in Figure 3(B). Results revealed that the total nitrogen removal efficiencies in anaerobic pond, facultative pond and aerobic pond were 37.2 ± 23.0%, 37.3 ± 9.5%, and 47.7 ± 11.9%. These removal efficacies showed that the overall nitrogen removal efficacy of the stabilization pond system was 39.1 ± 3.2%. After the constructed wetland treatment, total nitrogen removal efficiency has increased upto 86.0± 0.6%. The results suggest that the addition of CWs was highly appropriate in removal of total nitrogen.

3.4. Phosphate removal efficiency

Phosphate concentration in the influents and the effluents of pond system and their phosphate removal efficiencies shown in Figure 5A and Figure 5B, respectively. Average phosphate concentration (± standard deviation) in the influent and effluent of anaerobic pond were 51.0 ± 3.2 and 45.0 ± 2.3 mg/L, respectively. Average phosphate concentration (± standard deviation) in the effluent of facultative pond and aerobic pond were 40.5 ± 3.4 and 34.5 ± 2.6 mg/L. The corresponding phosphate removal efficiencies were calculated and shown in Figure 5B. The phosphate removal efficiencies in anaerobic pond, facultative pond and aerobic pond were 11.6 ± 5.5%, 10.1 ± 4.3%, and 14.7 ± 3.9% (Figure 5B). Overall phosphate removal efficiency of the WSPs was 32.0 ± 8.4%. After the constructed wetland treatment unit was added to the pond system, average effluent phosphate concentration was reduced to 20.0 ± 2.6 mg/L, increasing the overall phosphate removal efficiency up to 60.8 ± 3.9%. Therefore, CWs unit plays significant role in enhancing the total phosphate removal efficiency of the system.

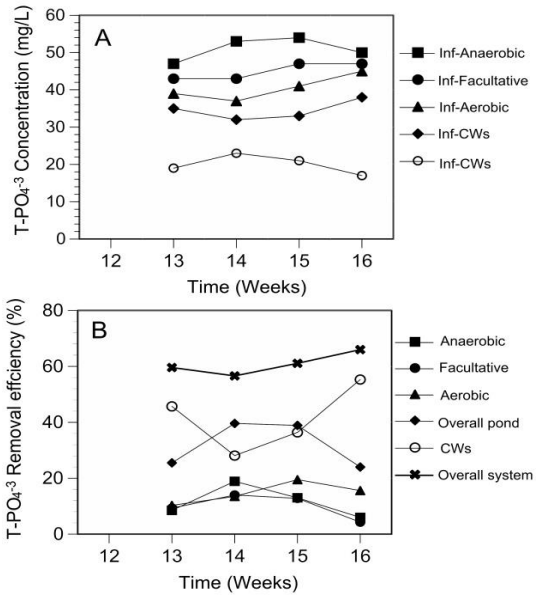

Figure 5 (A) TP concentrations in the treatment units (B). TP removal efficiencies of treatment units.

4. CONCLUSIONS

A field scale combined WSPs with a free flow CWs treating real leachate generated from domestic solid waste landfilling was investigated. Study showed that the overall BOD_5, COD, and TN, and TP removals were 97%, 89%, 86% and 61%, respectively. Moreover, CWs unit plays important role in removal of TN and TP from leachate. The operating the combined system during the dry season by dilation of leachate with natural water would be a feasible alternative in operating combined WSPs and CWs during dry seasons of tropical regions. However, operational conditions of this simple cost-effective combined system are required to achieve a 30 mg/L BOD_5, and 250 mg/L COD the standard requirements in Sri Lanka for safe discharge of leachate.

5. AKNOWLEDGMENT

Authors wish to acknowledge the financial support received though the Science and Technology Research Partnership for Sustainable Development at University of Peradeniya and Tokyo Cement Lanka PLC.

6. REFERANCES

Akinbile, C.O., Yusoff, M.S. and Ahmad Zuki, A.Z., 2012, 'Landfill leachate treatment using sub-surface flow constructed wetland by Cyperus haspan', *Waste Manag*. 32 (7), pp.1387-1393.

Bulc, T., Vrhovšek, D. and Kukanja, V., 1997, 'The use of constructed wetland for landfill leachate treatment', *Water Science and Technology*,35 (5): pp.301-306.

Frascari, D., Bronzini, F., Giordano, G., Tedioli, G. and Nocentini, M., 2004, 'Long-term characterization, lagoon treatment and migration potential of landfill leachate: A case study in an active Italian landfill', *Chemosphere*, 54(3), pp.335-343.

Madera, C. and Valencia-Zuluaga, V., 2009, 'Landfill leachate treatment: one of the bigger and underestimated problems of the urban water management in developing countries', *9th World Wide Workshop for Young Environmental Scientists WWW-YES-Brazil-2009*,Brazil. Available at:https://hal.archives-ouvertes.fr/hal-00593299/document (visited on 15th July 2019)

Mehmood, M.K., Adetutu, E., Nedwell, D.B. and Ball, A.S., 2009, 'In situ microbial treatment of landfill leachate using aerated

lagoons', Bioresour, Technol, 100(10), pp.2741-2744.

Mustapha, H.I., van Bruggen, J.J.A. and Lens, P.N.L., 2015, 'Vertical subsurface flow constructed wetlands for polishing secondary Kaduna refinery wastewater in Nigeria', *Ecol. Eng.*, 84, pp.588-595.

Renou, S., Givaudan, J.G., Poulain, S., Dirassouyan, F., Moulin, P., 2008, 'Landfill leachate treatment: Review and opportunity', *J. Hazard. Mater.*, 150(3), pp.468-493.

Speer, S., Champagne, P. and Anderson, B., 2012, 'Pilot-scale comparison of two hybrid-passive landfill leachate treatment systems operated in a cold climate', Bioresour, Technol, 104, pp.119-126.

Thörneby, L., Mathiasson, L., Mårtensson, L., and Hogland, W., 2006, 'The performance of a natural treatment system for landfill leachate with special emphasis on the fate of organic pollutants', *Waste Manag. Res.*, 24(2), pp.183-194.

Wang, K., Wang, S., Zhu, R., Miao, L. and Peng, Y., 2013, 'Advanced nitrogen removal from landfill leachate without addition of external carbon using a novel system coupling ASBR and modified SBR', Bioresour, Technol, 134, pp.212-218.

Weerakoon, G.M.P.R., Jinadasa, K.B.S.N., Herath, G.B.B., Mowjood, M.I.M. and Ng, W.J., 2018, 'Applicability of constructed wetlands for water quality improvement in a tea estate catchment: The Pussellawa case study Water', 10(3), pp.332, https://doi.org/10.3390/w10030332

Wiszniowski, J., Robert, D., Surmacz-Gorska, J., Miksch, K. and Weber, J. V., 2006, 'Landfill leachate treatment methods: A review', *Environ. Chem. Lett.* , 4(1), pp.51–61.

Wojciechowska, E., Gajewska, M. and Obarska-Pempkowiak, H., 2010, 'Treatment of landfill leachate by constructed wetlands: Three case studies', *Polish J. Environ. Stud.*, 19(3), pp.643–650.

Yalcuk, A. and Ugurlu, A., 2009, 'Comparison of horizontal and vertical constructed wetland systems for landfill leachate treatment', Bioresour, Technol, 100(9), pp.2521-2526.

Youcai, Z., 2018, 'Leachate treatment engineering processes, in: pollution control technology for leachate from municipal solid waste',1st Eddition, Butterworh-Heinemann, pp.361-522.

Proceedings of the 7th International Symposium on

Advances in Civil and Environmental Engineering Practices for Sustainable Development

ACEPS - 2019

Sorption experiments on heavy metal removal in contaminated groundwater by landfill-leachate using Permeable Reactive Barriers (PRBs) packed with waste materials.

I.U.Nagasinghe[1] and W.K.C.N.Dayanthi[2]

[1]Graduate School of Science and Engineering, Saitama University, Saitama, 338-8571, JAPAN.
[2]Department of Civil and Environmental Engineering, Faculty of Engineering, University of Ruhuna, Hapugala, Galle, SRI LANKA.

K e y w o r d s

Permeable Reactive Barrier (PRB)
Landfill-leachate
Adsorption
Isotherms
Heavy metals

A B S T R A C T

Permeable Reactive Barriers (PRBs) stand out as a promising technique for remediating contaminated groundwater. There is also a great potential in PRBs to treat groundwater contaminated by landfill-leachate by selecting appropriate reactive materials for the reactive zone. Hence, the reactive zone filled with reactive materials is the key component of a PRB. PRBs have already been identified as a low-cost in-situ treatment system. If low-cost/waste materials can effectively be utilized as reactive materials, PRBs can be made more cost effective, and it would be a solution for the disposal issues of those waste materials. Hence, the application of the selected low-cost/waste materials in PRBs as reactive materials to treat heavy metals was studied using batch sorption experiments. These experiments were used to optimize the contact time and the mass of reactive materials, and fit adsorption isotherms to characterize the adsorption properties. Dewatered Alum Sludge (DAS), Red Laterite Soil (RLS), Washed Quarry Dust (WQD), Washed Sea Sand (WSS), Bio Char (BC), and Saw Dust (SD) were the selected reactive materials. Fe was removed 100% by RLS, WSS, and BC. Langmuir isotherm was fitted to both RLS and SD for remediating Fe and Cd respectively. WQD was the best adsorbent for Zn.

1. INTRODUCTION

Permeable Reactive Barrier (PRB) has been evidenced as a rewarding in-situ method for remediating contaminated groundwater over the traditional pump and treat methods in terms of pollutant removal efficiency and cost-effectiveness (Carey *et al* 2002). PRBs are capable of either immobilizing or chemically transforming contaminants biologically or abiotically to a more desirable state whilst contaminated water passes through the reactive zone, which is placement of reactive materials of a PRB in the flow path of contaminated groundwater (Powell *et al.* 2002). Moreover, it implies that reactive materials play a noteworthy role for removing contaminants, hence, selection of proper reactive materials for correspondent contaminant enhances the performance of PRB (Snow 1999). Through that, PRBs can be further improved to treat groundwater contaminated by landfill-leachate, which has been recently recognized as one of the conspicuous factors of groundwater contamination (Dharmarathne & Gunatilake 2013, Wagh *et al* 2014). There are highly concentrated hazardous constituents, which enclose a range of dissolved organic matters, inorganic compounds, and heavy metals, particularly recorded in the landfill - leachate of municipal solid waste (Wagh *et al* 2014).

According to Bradl (2004), the ionic form of heavy metals are the most toxic inorganic pollutants, which can be found in soil compared to other contaminants. As per Sewwandi *et al* (2013), Fe (3000 µg/L; max. permissible limit by CEA, Sri Lanka) is exceeded in ten out of twelve dumpsites investigated in Sri Lanka. Moreover, the

maximum concentration of Cd recorded is 172 µg/L, which is approximately double the maximum permissible level of 100 µg/L. Zn is varied from 400 µg/L to 20, 000 µg/L, where the maximum permissible limit is 5000 µg/L. Therefore, it is very much essential to remove heavy metals in the landfill- leachate up to acceptable standards before discharge to the environment.

Use of low-cost/ waste materials as reactive materials would further enhance the effectiveness of PRBs, if they could alter the most commonly used reactive materials like zero-valent iron(ZVI), activated carbon(AC), oxygen releasing compounds(ORC) and zeolites, etc., which have limitations like considerable cost, good at removal of specific contaminants and less availability (Obiri-Nyarko *et al* 2002).

In this study, batch sorption experiments were carried out using low-cost/waste materials for scrutinizing the capability of heavy metals removal, particularly, Fe, Cd, and Zn in the groundwater contaminated by the landfill-leachate. Optimizing the contact time and the mass of the reactive materials, and fitting adsorption isotherms to characterize the adsorption properties were first and second objective respectively.

2. LITERATURE REVIEW ON ADSORPTION ISOTHERMS

2.1 Langmuir Isotherm

The linear form of Langmuir adsorption isotherm is shown in Eq. (1) where, q_e is contaminant adsorbed at equilibrium mg/mg); q_m is the maximum adsorption capacity (mg/mg), C_e is equilibrium concentration (mg/L), K_L is the adsorption coefficient which can be obtained from the graph of C_e/q_e against C_e, and C_o is the initial concentration of the adsorbate in solution (Farouq & Yousef 2015).

$$\frac{C_e}{q_e} = \frac{1}{q_m K_L} + \frac{C_e}{q_m} \qquad (1)$$

It is assumed that there is monolayer adsorption of solutes on to a surface of finite number of identical sites having homogenous adsorption energy. Moreover, adsorption is not further proceeded in a site where once molecule occupies it.

2.2 Freundlich Isotherm

Freundlich isotherm can be linearized as shown in Eq. (2) (Banerjee *et al* 2013).

$$log q_e = log K_F + \frac{1}{n} log C_e \qquad (2)$$

1/n and K_F indicate the adsorption intensity (L/mg) and adsorption capacity(mg/g) respectively, which can be determined from the slope and intercept the graph of log (q_e) vs. log (C_e) correspondingly. Favorable adsorption is indicated when $1<n<10$ (Ali *et al* 2016). Freundlich isotherm is applicable for multilayer adsorption on a heterogeneous surface with an exponential distribution of active sites.

2.3 Dubinin-Raduskevich (D-R) Isotherm

D-R isotherm is represented by Eq. (3) as follows (Ekpete *et al* 2011).

$$ln q_e = ln q_m - \beta\varepsilon^2 \qquad (3)$$

where, β is associated to the free energy of sorption and q_m is the D-R isotherm constants related with the degree of sorbate sorption by the reactive material surface. Eq. 4 expresses ε which is known as Polanyi potential.

$$\varepsilon = RTln\left[1 + \frac{1}{C_e}\right] \qquad (4)$$

R represents the gas constant ($Jmol^{-1}\ K^{-1}$) and T is the absolute temperature. E; mean free adsorption energy of D - R isotherm can be obtained using Eq. 5.

$$E = \frac{1}{\sqrt{-2\beta}} \qquad (5)$$

2.4 Temkin Isotherm

It is considered that adsorption energy linearly decreases with the coverage as per the Temkin isotherm, which is shown in Eq. (6) (Farouq & Yousef 2015).

$$Q_e = BlnE_T + BlnC_e \qquad (6)$$

Temkin constant related to the heat of adsorption and the equilibrium binding constant corresponding to the maximum binding energy (L/mg) are denoted by B and E_T respectively. E_T and B can be determined from the intercept and the slope of the linear plot of experimental data of q_e vs. ln (C_e).

2.5 Elovich Isotherms

Eq. (7) displays the isotherm of Elovich. K_E denotes Elovich constant. When the adsorption is followed the Elovich isotherm, q_m and K_E can be obtained from the slope and intercept respectively using the graph of $\ln(q_e/C_e)$ vs. q_e (Farouq & Yousef 2015).

$$ln\frac{q_e}{C_e} = lnK_E q_e - \frac{1}{q_m}.q_e \qquad (7)$$

3. METHODOLOGY

3.1 Overall Procedure

DAS, RLS, WQD, WSS, BC, and SD were selected low-cost/waste materials based on the literature. The following citations provide evidence for the treatment capacities of these materials. DAS (Bugbee & Frink 1985); RLS (Abhayawardana 2015); WQD (Mungathia 2009); WSS (Nebagha *et al* 2015); BC (Reddy & Lee 2014, Mandu *et al* 2015); and SD) (Yu *et al* 2000). These reactive materials were washed by tap water and sun-dried, then ground into particle sizes equal to or less than 0.75 µm. Afterward, the prepared materials were stored in air-tight bottles until usage.

The landfill-leachate collected from the Heenpandala dumpsite, Galle, Sri Lanka, was preserved using conc. HNO_3 with pH< 2 and diluted by 10 times using deionized water (DI) to make its characteristics approximately equal to groundwater contaminated by landfill-leachate. DI water was produced by Thermo Scientific: smart 2 pure 3 UV, ensured the temperature of 35.3℃ - 35.5℃ and electrical conductivity (EC) of 0.055 µS/cm throughout the study.

There were two batch sorption experimental series as kinematic experiments and adsorption isotherm experiments. The optimum contact time obtained from the kinematic experiments was kept constant in adsorption isotherm experiments, in which the mass of reactive materials was varied.

Atomic absorption spectrophotometer (TRACE AI1200) was used for analyzing Cd and Zn. Fe was determined by the most common method of complexation of Fe with 1, 10- phenanthroline (Pittsburgh 2005) on a UV visible spectrophotometer. The removal efficiencies of heavy metals were calculated using Eq. (8), where C_i is the initial concentration of adsorbate(mg/L) and C_e is the final equilibrium concentration of adsorbate after adsorption has occurred(mg/L) (Farouq & Yousef 2015).

$$Removal\ efficiency(\%) = \frac{C_i - C_e}{C_i} * 100\% \qquad (8)$$

3.2 Kinematic Experiments

The optimum contact time for heavy metal removal from each reactive material was found by kinematic experiments. 250 ml of 10 times-diluted landfill-leachate was added into 10 g of each reactive material, which was placed in a conical flask of 250 ml. At the room temperature, they were stirred at 600 rpm using magnetic stirrers for different time periods; 1 h, 2 h, 3 h, 4 h, 6 h, and 15 h. The supernatant of each samples was filtered using a vacuum pump separately by 0.45 µm filter papers after the sedimentation of materials in the stirred samples. The filtrate of each sample was characterized in terms of Fe, Cd, and Zn. The filtrate of the original sample, which was the 10 times-diluted landfill-leachate, was also analyzed. By plotting the graph of removal efficiencies of each heavy metal vs. contact time for each material, the optimum contact time for each reactive material with respect to each heavy metal was identified.

3.3 Adsorption Isotherm Experiments

100 ml of 10 times-diluted landfill-leachate was used for each sample. While ensuring the same solid to liquid ratio as in kinematic experiment, a set of reactive material masses; 0.6 g, 1.2 g, 2.4 g, 4.0 g, 4.8 g, and 6.0 g, which were lesser and greater than 10 g, were used to carry out adsorption isotherm experiments. At the speed of 600 rpm, samples were stirred in the room temperature within the optimized contact time. The removal efficiencies of each heavy metal vs. the mass of reactive material (adsorbent) were plotted in order to obtain the optimum mass for each reactive material.

3.4 Adsorption Isotherms

Langmuir, Freundlich, Dubinin-Raduskevich (D-R), Temkin and Elovich isotherms were considered to identify the best-fitted adsorption isotherm for removal of each heavy metal. The amount of heavy metals adsorbed per unit mass of adsorbent was calculated by Eq. (9) (Farouq & Yousef 2015).

$$q_e = \left(\frac{C_i - C_e}{m}\right) * V \qquad (9)$$

3.5 Chemical Parameter Analysis

For each sample of both in kinematic and adsorption isotherm experiments, pH, electric conductivity (EC) and oxidation-reduction potential (ORP) were measured in addition to the selected heavy metals. HQ40d multi was used to measure pH and EC. ORP was determined utilizing ORP meter, later each parameter vs. contact time and masses of reactive materials were plotted to investigate the variation of chemical parameters with the interaction of landfill-leachate in kinematic and adsorption isotherm experiments, respectively.

4. RESULTS AND DISCUSSION

4.1 Kinematic Experiment and Adsorption Isotherm Experiment

'Fe' removal efficiency against different contact time for different reactive materials is shown in Figure 1. The highest efficiencies of 'Fe' removal by RLS, BC and WSS were 98.7%, 98.1%, and 90.7% at 2 h, 1 h and 1 h respectively. Remarkably, RLS showed an efficiency above 90% throughout the kinematic experiment compared to BC and WSS. 57.5% of Fe removed by SD within 3h indicating its optimum performance. DAS also considerably removed 41.5% of Fe at 6 h whereas WQD was not good at treating Fe, therefore, WQD was not used for mass optimization experiments for Fe removal.

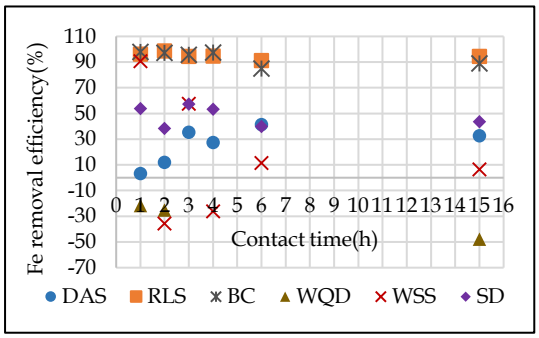

Figure 1 Fe removal efficiency vs. contact time for different reactive materials

Figure 2 illustrates Cd removal efficiency against different contact time values. The optimum removals of Cd from DAS and RLS were recorded at 6 h as 70.6% and 60.3%, respectively. At 4 h, WQD removed Cd in an efficiency of 55.3% whereas 45.8% by SD. WSS shows its optimum removal of 43.8% at 1 h. Furthermore, 58.6% of Cd is removed by BC at both 2 h and 15 h. All materials show a considerable removal for Cd with respect to others.

Zn removal efficiency during the optimizing contact time is displayed in Figure 3. As per Figure 3, BC showed 57% of the highest removal of Zn at the end of 24 h. WSS displayed 47.7% removal efficiency at 15 h. 44.5% of Zn was treated by DAS for 6 h. RLS did not perform well for the remediation of Zn during the whole period. Hence, RLS was not further considered for adsorption isotherms experiments on Zn.

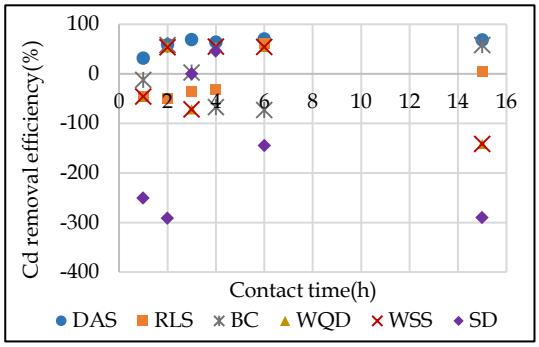

Figure 2 Cd removal efficiency vs. contact time for different waste materials

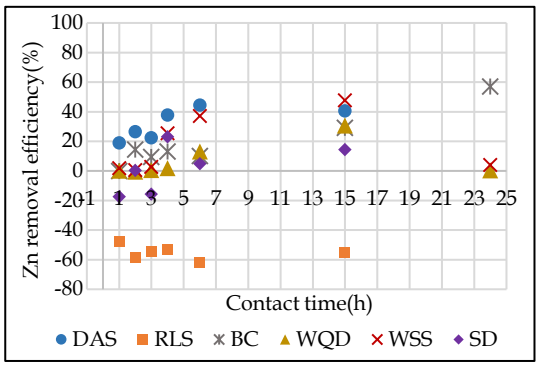

Figure 3 Zn removal efficiency vs. contact time for different reactive materials

The summary of the kinematic experiment is presented in Table 1.

Table 1 The summary of time optimization experiments

Heavy metal	Best reactive material	Optimum contact time (h)	Removal efficiency (%)
Fe	RLS	6	98.7
Cd	DAS	6	70.6
Zn	BC	24	57.0

Figure 4 displays the Fe removal against a range of masses for different reactive materials. Interestingly, RLS and WSS remediated Fe 100% at the optimum mass of 4.8g. For 6.0 g of BC also shows 98.1 % removal efficiency. DAS and SD display 67% and 45.1% treatment efficiencies, respectively.

Cd removal vs. masses of different reactive materials is illustrated in Figure 5. SD shows around 45% removal efficiency, and 31.4% of Cd was removed by BC at the same amount of mass; 0.6 g. Other reactive materials did not perform considerably for removing Cd.

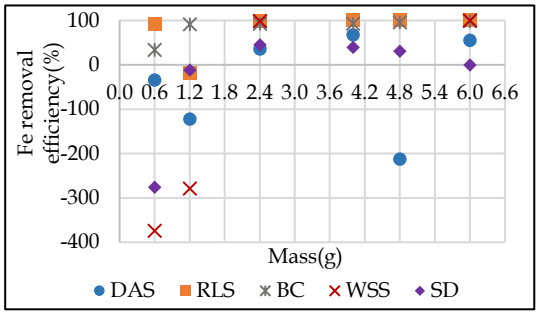

Figure 4 Fe removal efficiency vs. mass for different reactive materials

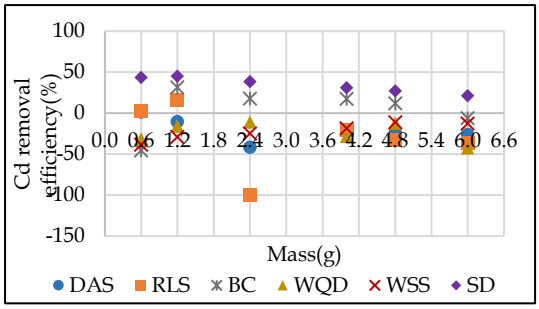

Figure 5 Cd removal efficiency vs. mass for different reactive materials

Figure 6 presents Zn removal efficiency in mass optimization experiments. WQD reveals highest removal efficiency of 95.8% at 4.0g over the other reactive materials.

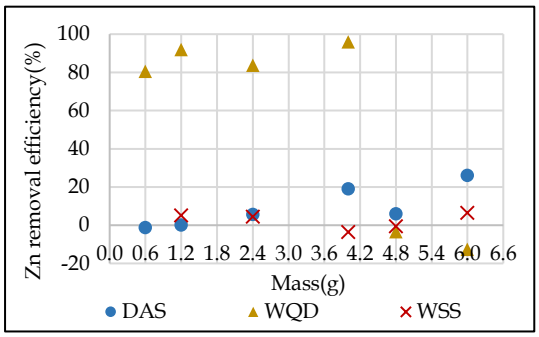

Figure 6 Zn removal efficiency vs. mass for different reactive materials

Table 2 summarizes the best reactive material for removing heavy metals at their optimum masses. According to time and mass optimization experiments, RLS is proved as the best reactive material for Fe removal, from contaminated groundwater by landfill-leachate, which has 100% efficiency. Nihapi *et al* (2011) showed that carbonized rice husks removed 56.7% of Zn and 8.24% of Cd while 77.2%of Zn and 43.4% of Cd removed by activated rice husk from industrial wastewater. It reveals that even without any pretreatment, waste materials used in this study show a significant removal potential for Cd and Zn compared to treated rice husk.

Table 2 The summary of mass optimization experiment

Heavy metal	Best reactive material	Optimum mass (g)	Removal efficiency (%)
Fe	RLS/WSS	4.8	100.0
Cd	SD	0.6	44.9
Zn	WQD	4.0	95.8

Moreover, with the iteration of reactive materials, chemical characteristics of groundwater contaminated landfill-leachate considerably changed. pH variation with respect to the contact time is shown in Figure 7. Initial pH of 2 increased gradually in all most all the reactive materials along with the time.

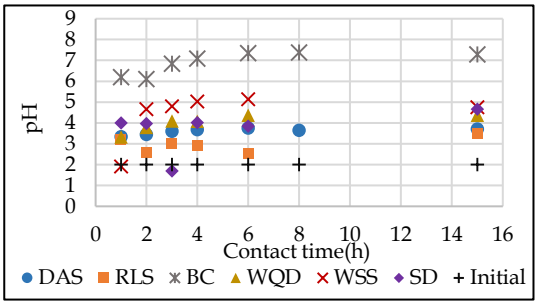

Figure 7 pH variation vs. contact time for different reactive materialss

BC shows the highest increment of pH and adsorbate became neutralized at around 7 at 4h of stirring. WSS caused pH to be about 5 after the same time as BC. Likewise, pH plateaued off at just below pH of 4 in DAS. During the mass optimization, the change of pH was quite similar to that of the time optimization. BC showed pH of about 8 in all three cases of heavy metal removal at its best removal. Similarly, WSS displayed pH 7-8 at

6.0g of mass. pH of DAS indicated just below 4 at 4.8g during the treating of Fe, Zn, and Cd, which is coincided with those of the time optimization. As a whole, pH fluctuation depicts the consistency between the time and mass optimization experiments.

Figure 8 displays the ORP variation against the contact time for different reactive materials. As per Bourg & Loch (1995), the potential release of stored pollutants to aqueous phase is dominantly affected by the pH and redox conditions, which are interdependent. Approximately 500 mV of ORP was indicated as initial in both time and mass optimization experiments. At the same time, the change of ORP during the reactions observed as similar in Figure 8 for Fe, Zn, and Cd removal in mass optimization experiments. The highest drop of ORP is seen with BC, which is the half of the initial value. WSS had the second-largest reduction of ORP during interaction of contaminated groundwater by landfill-leachate. ORP of SD showed a constant final value of 200 mV in all cases. The reduction of ORP indicates that the compounds in the solutions have undergone more reduction reactions than oxidation reactions.

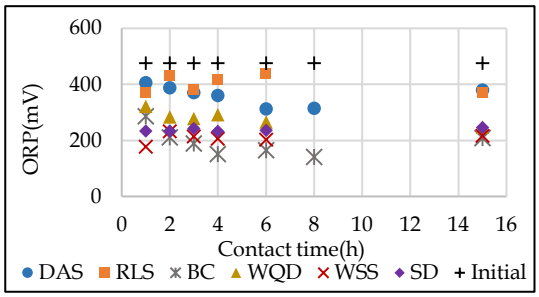

Figure 8 ORP variation vs. contact time for different reactive materials

EC variation of reactive materials against the contact time is presented in Figure 9.

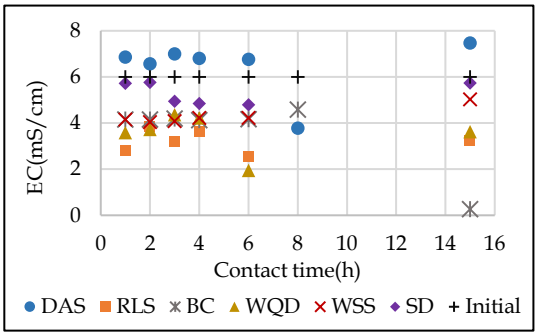

Figure 9 EC variation vs. contact time for different reactive materials

The ability to conduct an electrical current is referred as electrical conductivity (EC) of the solvent (Mlkadmi *et al*, 2018). In time optimization experiments, EC decreases with time due to reaction in all reactive materials except DAS with time. However, all materials including DAS displayed lower EC value compared to initial of around 5mS/cm in the case of mass optimization experiments.

4.2 Best Fitted Isotherms

Figure 10 displays the Langmuir isotherm for Fe removal by RLS, which indicates determination coefficient; R^2 of 0.99 showing a strong correlation. WSS also fitted to Langmuir isotherm with R^2 of 0.72 for removing Fe from contaminated groundwater contaminated by landfill-leachate, which is presented in Figure 11.

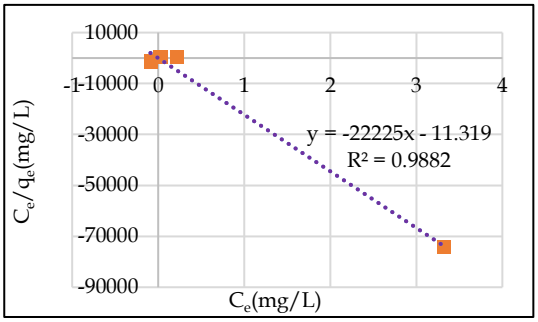

Figure 10 Langmuir isotherm for Fe removal by RLS

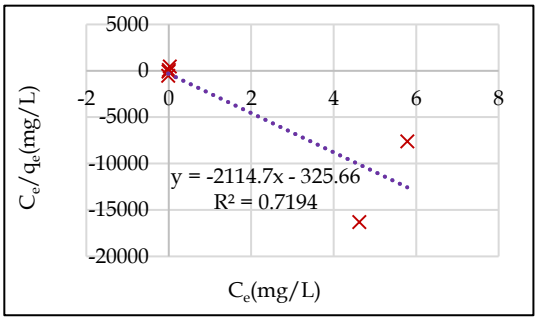

Figure 11 Langmuir isotherm for Fe removal by WSS

Figures 12 and 13 show Freundlich isotherm for BC and SD respectively. BC displays 0.94 correlation with Fe removal whereas SD also has the same correlation as BC even though removal efficiency is relatively low. Moreover, SD and BC are correlated to Freundlich isotherm with R^2 of 0.81 indicating n = 2.35, which reiterates that BC and SD are good adsorbents for removing Fe.

Remediation of Cd by SD presents R^2 of 0.94 with Langmuir isotherm as shown in Figure 14 while Figure 15 displays that Zn removal by WQD fits D-R isotherm signifying R^2 of 0.91.

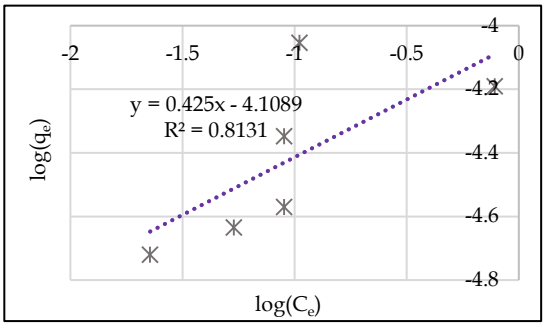

Figure 12 Freundlich isotherm for Fe removal by BC

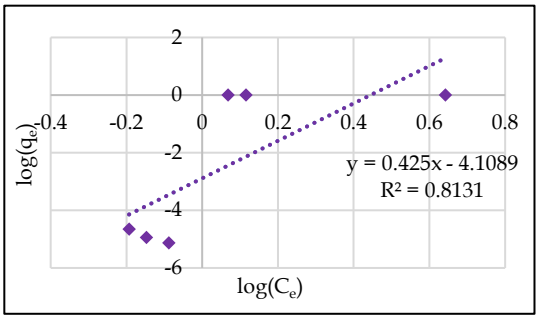

Figure 13 Freundlich isotherm for Fe removal by SD

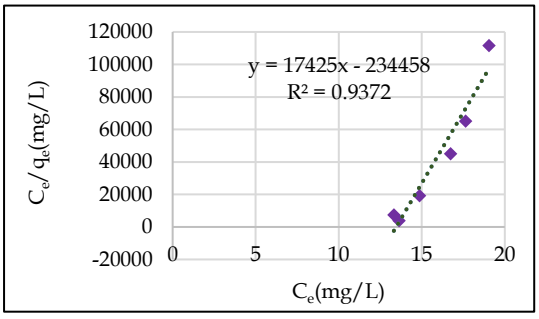

Figure 14 Langmuir isotherm for Cd removal by SD

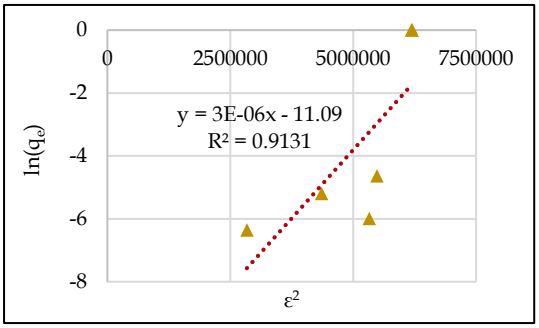

Figure 15 D-R isotherm for Zn removal by WQD

Table 3 summarizes the best-fitted isotherm for each contaminant with their adsorption capacity.

Table 3 Best fitted isotherm for each heavy metal and adsorption capacities

Heavy metal	Reactive material	Best-fitted isotherm model	R^2	Adsorption capacity [q_e=x/m] (mg/g)
Fe	RLS	Langmuir	0.99	0.06
Cd	SD	Langmuir	0.94	1.81
Zn	WQD	D-R	0.91	1.72

5. CONCLUSIONS

It is proved that RLS, WSS, and BC have a significant potential of removing Fe from groundwater contaminated by landfill-leachate. They show 100% of Fe removal. Even though removal efficiency was comparatively low, SD also has the ability in adsorbing Fe, which is proved by n > 1 of Freundlich isotherm. Furthermore, SD and WQD are the best reactive material for removing Cd and Zn, respectively.

The effects of pH, temperature and initial concentration on heavy metal removal have to be studied in order to develop treatment methods using these materials as filter/reactive media.

6. ACKNOWLEDGEMENTS

The authors wish to acknowledge the assistance given by Ms D. A. M. Nimal Shanthi, laboratory attendant; Mr Nilantha of Department of Civil and Environmental Engineering, University of Ruhuna.

7. REFERENCES

Abhayawardana, G. P. R., 2015, 'Removal of Lead in Landfill-leachate using Permeable Reactive Barriers with Natural Red Earth and Peat', *ENGINEER*, XLVIII, 04, pp.51-57.

Banerjee, S., Chattopadhyaya, M. C., Srivastava, V., and Chandra Y., 2013, 'Adsorption Studies of Methylene Blue onto Activated Saw Dust: Kinetics, *Equilibrium and Thermodynamic Studies', Environmental Progress & Sustainable Energy.*

Bourg A.C.M. and Loch J.P.G., 1995, 'Mobilization of heavy metals as affected by pH and redox conditions', *Bio-geo-dynamics of Pollutants in Soils and Sediments,Environmental Science,* Springer, Berlin, Heidelberg.

Bradl, B.H., 2004, 'Adsorption of heavy metal ions on soils and soils constituents', *Journal of Colloid and Interface Science*, pp.277, 1-18.

Carey, M. A., Fretwell, B. A., Mosley N. G., and Smith J. W. N., 2002, 'Guidance on the use of permeable reactive barriers for remediating contaminated groundwater', *National Groundwater & Contaminated Land Centre report NC/01/51*, Environment Agency NC/01/51, Bristol.

Dharmarathne, N., and Gunatilake, J., 2013,'Leachate characterization and surface groundwater pollution at Municipal Solid Waste landfill of Gohagoda, Sri Lanka', *International Journal of Scientific and Research Publications*, 3(11), pp.1-7.

Ekpete O. A., Horsfall, Jnr M., & Tarawou, T., 2011, 'Adsorption of chlorophenol from aqueous solution on fluted and commercial activated carbon', *J. Nepal Chem. Soc*., 27.

Farouq, R., and Yousef, N. S., 2015, 'equilibrium and kinetics studies of adsorption of Copper (ii) ions on natural biosorbent', *International Journal of Chemical Engineering and Applications*, 6(5),pp.319-324.

Mandu I. I., Gao B., Yao, Y., Xue, Y., Zimmerman, A., Mosa, Pullammanappallil, A., Ok, Y. S. and Cao, X., 2015, 'A review of biochar as a low-cost adsorbent for aqueous heavy metal removal', *Critical Reviews in Environmental Science and Technology*.

Mkadmi, Y, Benabbi, O., Fekhaoui, M., Benakkam, R., Bjijou, W., Elazzouzi, M., Kadourri, M. and Chetouani, A., 2018, 'Study of the impact of heavy metals and physico-chemical parameters on the quality of the wells and waters of the Holcim area (Oriental region of Morocco)', *J. Mater. Environ. Sci.,* 9 (2), pp.672-679.

Mungathia, J. K., 2009, 'Use of Washed Quarry Dust in the Treatment of Industrial Effluents: Case Study of Electroplating Industry', *MSc. Thesis, Jomo Kenyatta*, University of Agriculture and Technology.

Nhapi, I., Banadda, N., Murenzi, R., Sekomo, C.B. and Wali, U.G, 2011, 'removal of heavy metals from industrial wastewater using rice husks', *The Open Environmental Engineering Journal*,4, pp.170-180.

Obiri-Nyarko, F., Grajales-Mesa, and S. J., Malina, G., 2002, 'An overview of permeable reactive barriers for in situ sustainable groundwater remediation', *Chemosphere*, 111, pp.243–259.

Powell, R. M., Powell, P. D. and Puls, R.W., 2002, 'economic analysis of the implementation of permeable reactive barriers for remediation of contaminated groundwater', EPA/600/R-02/034.

Reddy, D.H.K. and Lee, S.M., 2014, 'Magnetic biochar composite: Facile synthesis, characterization and application for heavy metal removal', *Colloids and Surfaces A: Physicochemical and Engineering Aspects*.

Sewwandi, B. G. N., Takahiro, T., Kawamoto, K., Hamamoto, S., Asamoto S. and Sato, H., 2013, 'Evaluation of Leachate Contamination Potential of Municipal Solid Waste Dumpsites in Sri Lanka Using Leachate Pollution Index'. *14th International Waste Management and Landfill Symposium.*

Snow, D. H., 1999, 'Overview of Permeable Reactive Barriers, pp.204-213.

Wagh, M P, Bhandari, P K, Kurade S., 2014, 'Groundwater Contamination by Leachate', *International Journal of Innovative Research in Science, Engineering and Technology*, 3(4).

Yu, B., Zhang, Y., Shukla, A., Shukla, S. S. and Dorris, K. L., 2000, 'The removal of heavy metal from aqueous solutions by sawdust adsorption - removal of Copper', *Journal of Hazardous Materials*, 80, pp.33–42.

Proceedings of the 7th International Symposium on

Advances in Civil and Environmental Engineering Practices for Sustainable Development

ACEPS - 2019

Evaluation of the water quality of community managed water supply schemes in Matara district

A.M.Asarudeen[1], Tushara Chaminda[1], K.C.Ellawala[1], M.N.M.Shayan[1] and W.B. Gunawardena[2]

[1]Department of Civil and Environmental Engineering, Faculty of Engineering, University of Ruhuna, Hapugala, Galle, SRI LANKA
[2]Department of Civil Engineering, Faculty of Engineering, University of Moratuwa, Katubedda, Moratuwa, SRI LANKA

K e y w o r d s

Community management
Water supply scheme
Water quality index
Matara

A B S T R A C T

Evaluation of water quality of community managed water supply schemes in Matara district aid to evaluate the level of hygienic quality of community managed water supply system that provides drinking water to the Matara district and to develop the Water Quality Index for the community managed water supply system in Matara district to ensure the safe drinking of water. There are 333 Community Based Organisations are functioning in the Matara district and 26482 families consume water from the above schemes. Among them 172 Community Based Organizations were selected for the evaluation collected from the 15 divisional secretariats of Matara district from different water sources such as rivers, tube wells, conventional wells and streams. Totally 90 samples and 78 samples were evaluated for the well and stream water and among them significant amount of samples are failed for the parameters such as Turbidity, pH, conductivity, *E.coli* and total coliform according to the standard guidelines. Rating of water is defined as excellent, good, fair, marginal and poor according to the water quality range 95-100, 80-94, 60-79, 45-59 and 0-45 respectively From the evaluated results for the 97 samples its shows the 40 samples of the community schemes are in the fair rating of water qualit , 28 samples are in the marginal and 20 samples are in the poor rating of water quality. The recommendation should be classified for the water as disinfection, normal physical treatment and disinfection, Normal physical treatment, chemical treatment and disinfection, could be used with advance treatment, can't be used for drinking according to the above water quality range respectively.

1. INTRODUCTION

A community managed water supply can be defined as a public water supply system that serves minimum 25 residents throughout the whole year and it may consist of one or multiple reservoirs or wells. (Mimrose et al. 2011). According to NWSDB 77% of the population has safe access to drinking water, of which 32% is covered by pipe-borne water supply system by NWSDB and remaining is meet their requirements by alternative ways such as hand pumped tube wells, conventional wells etc. (National Water supply and Drainage Board 2007). Sufficient amount of hygienic drinking water is one of the major factors for a healthy life. Hence, rural population of the Matara district, water supply is monitored by community managed water supply scheme. There are 333 Community Based Organisations are functioning in the Matara district and 26482 families consume water from the above schemes. Among them 172 Community Based Organizations were selected for the evaluation. The major sources of the drinking water are from different sources such as hand pump tube wells, wells, springs, dug wells, river and water board. But people are consuming the water without a proper treatment and some people are doing a basic treatment at home such as filtering and

boiling. There was complaint made by the people regarding the taste, colour and depletion of white layers in cooking equipment due to the high amount of hardness. Although physically these parameters can be identified, but numerically the water quality parameters values are not defined in those areas. But in some case, whose health risk is significant because they might have been affected by bacteriological contamination, presence of heavy metals, rich in fluoride and hardness etc. Due to these reasons, the prevalence of water born disease by accessing to unsafe drinking water source may be increase in future. So, evaluating the hygienic quality of the drinking water is a main objective of this research as well as developing the water quality index for it to ensure the safe drinking of water. This research will be conducted as a collaborative research with ministry of irrigation and water supply, southern provincial council and department of community water supply. According to the gathered information from relevant literature reviews, there is no evidence of research that have been conducted in community managed water supply schemes in Matara district.

2. METHODOLOGY

2.1. Study area

172 samples were collected from the 15 divisional secretariats of Matara district from different water sources such as rivers, tube wells, conventional wells and streams. Figure 1 shows the Divisional secretariat of Matara and number of samples.

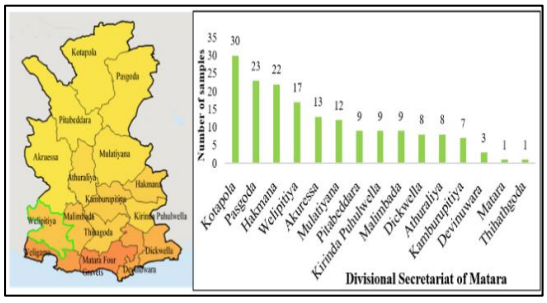

Figure 1 Divisional secretariat of Matara and number of samples

2.2. Selection of water quality parameters

There are 15 parameters are selected under physical, chemical and biological category for evaluation such as Temperature, pH, Turbidity, Conductivity, Iron (as Fe), Manganese (Mn), Nitrate (as NO_3), Fluoride (as F), Total Hardness (as $CaCO_3$), Arsenic, Cadmium, Lead, E.-coli bacteria, Other coliform and total Coliform bacteria.

2.3. Development of water quality index

Canadian water quality index was selected for calculating water quality index. There are three factors are used to form the water quality index based on the numbers of failed parameters and the tests that is deviate from the standard guide line. These three factors are Scope (F_1), Frequency (F_2), and Amplitude (F_3). The index yields a number between 0 and 100.

$$F_1 = \left(\frac{Number\ of\ failed\ parameters}{Total\ number\ of\ parameters}\right)x100$$

$$F_2 = \left(\frac{Number\ of\ failed\ tests}{Total\ number\ of\ tests}\right)x100$$

$$F_3 = \left(\frac{nse}{0.01\ nse+0.01}\right)$$

When the test value must not exceed or not fall below the standard guideline use the following excursions respectively.

$$Excursion = \left(\frac{Failed\ test\ value}{Guideline\ Value}\right) - 1 \quad or \quad Excursion = \left(\frac{Guideline\ Value}{Failed\ test\ value}\right) - 1$$

The normalised sum of the excursions (nse) is calculated by for failed parameters of the sample by Following equation,

$$nse = \left(\frac{\Sigma excursion}{Total\ number\ of\ tests}\right)$$

$$Water\ Quality\ Index = 100 - \frac{\left(\sqrt{F1^2+F2^2+F3^2}\right)}{1.732}$$

3. RESULTS AND DISCUSSION

Water quality parameters are analyzed according to the Divisional Secretariat and source wise. The SLS 614 2013 guideline was followed to analyze the parameters. For the maximum and minimum value of pH are obtained as 10.04 and 4.36 for the Kamburubitya and Welipitiya DS respectively. Minimum and maximum Turbidity value are obtained as 0.74 NTU and 305 NTU for the Mulatiyana and Hakmana area respectively. The reason for the high

turbidity value is the water seems to be cloudy. For the conductivity, minimum and maximum values are 17.5 and 2059 µs/cm for Kotapola and Welipitiya area respectively. Nitrate value of all the samples are not exceeded the standard guideline value. When considering the *E.coli* and total coliform It was highly present in the well water in few areas in between the range 600-850 no/100 ml. But 142 samples were failed in the *E.coli* and 128 samples were failed in total coliform among 172 samples. For the dissolved iron 4 samples were failed and the maximum value obtained is 0.41 mg/l for the stream in Kotapola DS area.

3.1. Evaluation of Parameters by the source

3.1.1. Well

Totally 90 schemes were evaluated for the well water and among them significant amount of samples are not compliant with SLS (614 2013) for the parameters such as Turbidity, pH, conductivity, *E.coli* and total coliform according to the standard guidelines. But almost all the samples satisfied the allowable limit for the parameters such as Total hardness, Nitrate, Iron (dissolved), and Fluoride. Figure 2 shows the evaluated parameters for well water.

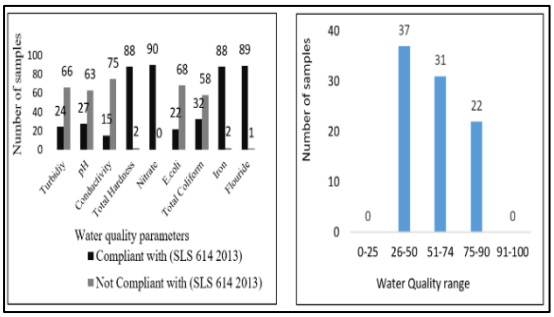

Figure 2 Evaluated parameters and water quality index for well

3.1.2. Stream

Totally 78 schemes were evaluated for the well water and among them most of the samples are not compliant with SLS (614 2013) guidelinesfor the parameters such as pH, *E.coli* and total coliform according to the standard guidelines. Figure 3 shows the evaluated parameters and water quality range for the stream water

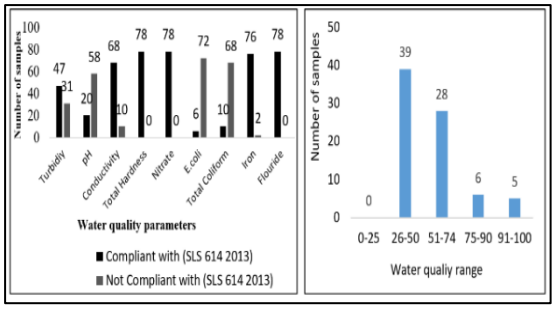

Figure 3 Evaluated parameters and water quality range of stream

3.1.3. Tube well

Totally 3 samples were evaluated for the well water and among them all 3 samples are failed for the conductivity. Figure 3 shows the evaluated parameters for the tube well.

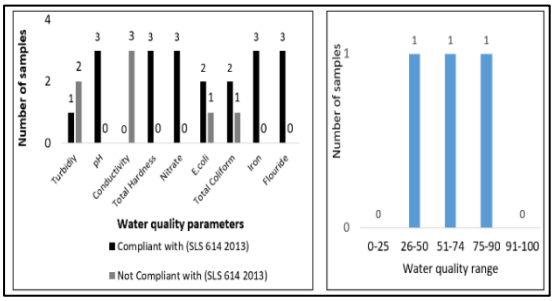

Figure 4 Evaluated parameters and water quality range of tube well

3.2. Overall analysis

Over all 172 samples were evaluated for the Matara community manged water supply scheme and among them significant amount of samples are failed for the parameters such as Turbidity, pH, *E.coli* and total coliform according to the standard guidelines. But approximately half of the samples failed for the conductivity. Almost all the samples satisfied the allowable limit for the parameters such as Total hardness, Nitrate, Iron (dissolved), and Fluoride. Figure 5 shows the overall analysis of the parameters.

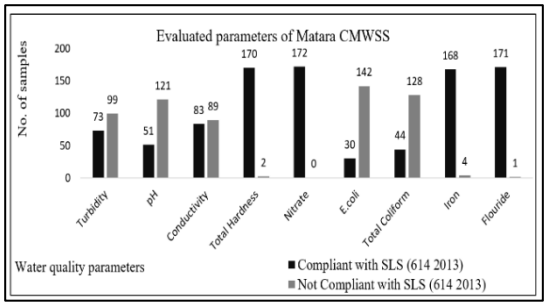

Figure 5 Overall analysis of the parameter

3.3. Water quality index

From the evaluated results for the 97 schemes its shows the most of the community schemes are in between the range 26-50 and 51-74. It shows the community managed water supply scheme need a further treatment before drinking. Figure 6 shows the number of samples evaluated in between the water quality range.

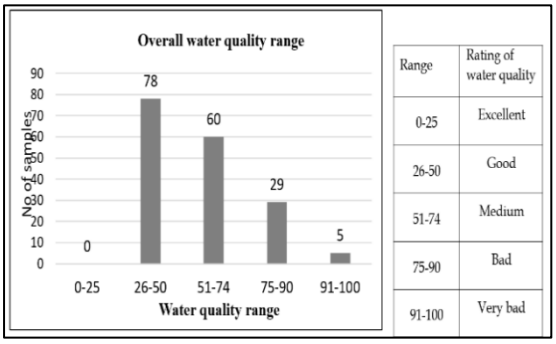

Figure 6 Number of samples evaluated between the water quality range

4. CONCLUSION & RECOMENTATIONS

According to the evaluated results the number *E.coli* are highly present in the well water in between the range 650 – 700 for few samples. Total coliform also highly present in the well water in some areas. But the two tube wells are free of both *E.coli* and total coliform. So, it is more preferable to drink tube well waters compare to the other sources such as well and stream in terms of biological parameters. According to the details obtained from CBO officers few communities managed water supply schemes use the chlorination as conventional disinfection method. Further pH value of most failed samples are fall below the 6.5. It clearly shows the most water sources are subject to the acidity.

All samples are at least failed in one parameter. So, the rating of water quality is defined from the water quality index. Among the 172 schemes 2.9% of the schemes are rated as under the category of excellent water and 16.9% schemes are rated as good quality, although it is favour for drinking, It should be treated with normal disinfection such as boiling or chlorination. 35.5% schemes are undergoing to the medium quality and it should be treated with primary treatment such as disinfection, sedimentation and coagulation and flocculation. But the rest of schemes are consuming a bad quality water. So, the community manged water supply officers should take serious attention to uplifting the quality of water according to the standards. The schemes should be treated with secondary treatment for the safe drinking of consumers.

5. ACKNOWLEDGEMENT

First of all, I gratefully acknowledged Dr. Champika Ellawala, and Dr (Ms). W.B. Gunawardana (University of Moratuwa), the Co-Supervisor, of my research for helping me and giving ideas to improve the research.and Miss. Nimalshanthi , the technical officer who helped for conducting experiment successfully.

6. REFERENCES

Boyacioglu, H., 2007. Development of a water quality index based on a European classification scheme. *Water Sa*, *33*(1).

Carter, R.C., Tyrrel, S.F. and Howsam, P., 1999. The impact and sustainability of community water supply and sanitation programmes in developing countries. *Water and Environment Journal*, *13*(4), pp.292-296.

Chandrajith, R., Nanayakkara, S., Itai, K., Aturaliya, T.N.C., Dissanayake, C.B., Abeysekera, T., Harada, K., Watanabe, T. and Koizumi, A., 2011. Chronic kidney diseases of uncertain etiology (CKDue) in Sri Lanka: geographic distribution and environmental implications. *Environmental geochemistry and health*, *33*(3), pp.267-278

De Silva C. S , Water quality assessment in Jaffna, Vavuniya, Anuradhapura, Kurunagala and Hambantota in Sri Lanka for domestic purposes.

de França Doria, M., 2010. Factors influencing public perception of drinking water quality. *Water policy*, *12*(1), pp.1-19.

Ellawala, K.C. and Priyankara, D.P.M.P., 2016. Consumer satisfaction on quantity and quality of water supply: a study in Matara, Southern Sri Lanka. *Water Practice and Technology*, *11*(3), pp.678-689.

Fawell, J. and Nieuwenhuijsen, M.J., 2003. Contaminants in drinking water Environmental pollution and health. British medical bulletin, *68(1),* pp.199-208.

Hickey, H., 2008. Water supply systems and evaluation methods, volume I: Water supply concepts. June 2014,Water sector of Sri Lanka Embassy of the Kingdom of the Netherlands.

Lye, D.J., 2002. Health Risks Associated with Consumption of Untreated Water from Household Roof Catchment Systems 1. *JAWRA Journal of the American Water Resources Association*, *38*(5), pp.1301-1306.

Mimrose, D.M.C.S., Gunawardena, E.R.N. and Nayakakorala, H.B., 2011. Assessment of sustainability of community water supply projects in Kandy District.

Fan, M., 2015. Sri Lanka's water supply and sanitation sector: achievements and a way forward.

Mandara, C.G., Butijn, C. and Niehof, A., 2013. Community management and sustainability of rural water facilities in Tanzania. *Water Policy*, *15*(S2), pp.79-100.

National Water Supply and Drainage Board , 2007, Annual Report.

Operations Evaluation Department, August 2007, Sri Lanka Country Assistance Program Evaluation: Water Supply and Sanitation Sector Assistance Evaluation.

Raut, K., 2014. *Sustainability of community water supply system managed by water user committee: a case study of rural water supply system in Nepal* (Master's thesis, Norwegian University of Life Sciences, Ås).

Summary Report, 2016, Impact Evaluation of the Rural Water Supply and Sanitation Program in Ethiopia 2006 -2004.

Proceedings of the 7th International Symposium on

Advances in Civil and Environmental Engineering Practices for Sustainable Development

ACEPS - 2019

Composite adsorbent using waste materials to treat dissolved organic matter and nutrients in landfill-leachate.

W.T.C.Udeshika[1] and W.K.C.N.Dayanthi[1].

[1]Department of Civil and Environmental Engineering, Faculty of Engineering, University of Ruhuna, Hapugala, Galle, SRI LANKA

K e y w o r d s

Landfill Leachate
Composite Adsorbent
sCOD
Nutrients
Batch sorption experiment

A B S T R A C T

In this study, the ability of a low-cost composite adsorbent to treat dissolved organic compounds in terms of soluble COD (sCOD), ammonium, total nitrogen, and total and ortho-phosphorus were investigated. The composite adsorbent was prepared using washed sea sand (WSS), dewatered alum sludge (DAS) and powdered activated carbon (PAC). The removal efficiency of sCOD in landfill-leachate by the composite adsorbent was 61.9%, which was followed by DAS (44.87%) and WSS (32.65%). Compared to PAC (91.1%), the sCOD removal efficiency by the composite media is somewhat low. This efficiency of the composite adsorbent occurred for a contact time of 60 minute at an initial pH of 7.17 and 30˚C for an adsorbent dosage of 36 g/L. The corresponding adsorption capacity was 14 mg/g. The maximum removal efficiencies of the composite adsorbent for NH_3-N, TN, and PO_4^{3-}-P were 58.7%, 30.5% and 81.4% respectively. A study on the behavior of equilibrium data revealed that Elovich isotherm provided the best fit for most of the adsorption processes above in comparison to other models.

1. INTRODUCTION

At present day, Municipal Solid Waste Management (MSW) has become a major problem due to industrialization, population growth and urbanization. In many regions, landfills or dumpsites are used to dispose of the MSW and resultant landfill-leachate causes major environmental problems when leachate contaminates ground and surface water (Dayanthi et al, 2004). Therefore, landfill-leachate management has become one of the main concerns in landfill management. Landfill-leachate is characterized by physical, chemical and biological parameters. Among them, parameters such as COD, BOD, pH, suspended solids, ammonia nitrogen (NH_3-N), total nitrogen (TN), orthophosphate (PO_4^{3-}-P), total phosphorus (TP) and heavy metals are significant (Renou, et al., 2008). Biological treatment methods are the most effective in treating these contaminants. However, it is only effective in the early phase of the landfill and with the period of time in the stabilized landfills this process gets slow down due to the presence of a high concentration of ammonia (Renou et al,2008). The common features of stabilized leachate are high strengths of ammoniacal nitrogen (3000–5000 mg/L) and moderately high strengths of COD (5000–20,000 mg/L), as well as a low ratio of BOD_5/COD (less than 0.1) (Li &Zhao cited in Halim, et al., 2010).

To overcome this problem, adsorption; a physiochemical process is used in many countries using different types of adsorbents. Activated carbon, zeolite, activated alumina are some of the most effective adsorbents, but are expensive. There are some low-cost adsorbents that can be used as substitutes for the conventional adsorbent media, namely, fly ash, lime, dewatered alum sludge (Yang , et al., 2006; Fernando, et al., 2016), sea sand (Fernando, et al., 2016), building wastes (Upasena, 2017), agricultural wastes such as rice husk ash, sugarcane bagasse derived carbon (Azmi, et al., 2015) and cockle shells (Daud, et al., 2017). However, they are not

much effective in removing both COD and nutrients.

Therefore, this study was aimed to investigate the treatment potential of a composite waste material adsorbent for the organic compounds and nutrients in the landfill-leachate using batch sorption experiments. Waste matter, namely DAS (Dewatered Alum Sludge) and the locally available SS (Sea Sand) were selected as the low-cost materials for the composite adsorbent preparation. PAC (Powdered Activated Carbon) was also selected to include in the composite adsorbent in a low percentage because it is well known as one of the most effective commercial adsorbents for the removal of organic pollutants from the aqueous or the gaseous phase. DAS is one of the wastes produced at the water treatment plants, and there is no proper way to dispose of those waste, and is a potential adsorbent for phosphorus removal.

The objectives were to optimize the contact time and adsorbent dosage; to obtain the adsorption capacities and plot isotherms; and to find out the variation of the removal efficiency with the change of the initial adsorbate concentration, pH and temperature. Reuse of waste materials is environmentally viable while providing benefits in commercial applications.

2. MATERIALS AND METHODS

2.1. Raw materials collection and influent characterization

Landfill-leachate samples were collected from the Rathgama Monroviawatta composting site located in Galle district. Leachate aged less than 3 years was collected from organic leachate storage tanks. Samples were filled into 3L plastic containers, transported to the laboratory and stored at 4˚C. Leachate samples were characterized (Table 1) according to the standard analysis method of water and wastewater (APHA, 2005). According to Table 2, the leachate showed a characteristic similar to a stabilized leachate because pH was more than 5 and the BOD_5/COD ratio (0.14) was very small.

Collected washed sludge was subjected to dry in direct sunlight. This dried sludge was then ground and sieved to prepare the composite adsorbent with the particle size between 75µm- 150µm. Collected sea sand also was washed and subjected for drying in direct sunlight as done previously. The dried WSS (Washed Sea Sand) was sieved to the particle size between 75µm-150µm.

Table 1 Landfill leachate characteristics

Parameter	Value
BOD_5	930 mg/l
COD	6770 mg/l
pH	7.47
Conductivity	24.5 µs/cm
Turbidity	65.6 NTU
ORP	-83 mv
TSS	4130 mg/l
NH_3 -N	17.36 mg/l
NO_3^--N	151 mg/l
PO_4^{3-} -P	0.012 mg/l
TP	0.014 mg/l

2.2. Composite adsorbent preparation

The composite adsorbent was prepared from DAS (45% w/w), WSS (45% w/w) and PAC (10% w/w) by mixing with water (50% w/w). The composite media was dried in an oven at 104˚C for 24 h and crushed and sieved to a particle size range of 75µm -150µm

2.3. Batch sorption experiment

This study was to determine the influences of adsorbent contact time and dosage for the adsorption and obtain the optimal adsorption capacity for different types of wastewater parameters. Figure 1 shows the overall procedure of the collection of materials and the experiments.

Batch experiment was conducted for each adsorbent separately prior to the experiments based on the composite adsorbent. First, kinematic experiments (to determine optimum contact time) were conducted in a series of seven 250 ml conical flasks containing each with 10 g of adsorbents and 250 ml of 25 times diluted leachate. These flasks were then placed on magnetic stirrers at 400 rpm for 180 min at 25˚C. The experiment was set at six different contact times as 15 min, 30 min, 60 min, 90 min, 120 min, 150 min, and 180 min. After the time period was over, the samples

were kept for settling and the supernatant of each was filtered with glass fiber filter papers with 1.2 µm pore size. The optimum contact time was determined using the removal efficiencies calculated using the initial and final COD values. In addition to that, pH, conductivity, and ORP were determined.

The adsorption isotherm experiment was conducted by preparing a series of 250 ml conical flasks, each filled with 3 g, 6 g, 9 g, 12 g, 15g and 18 g of adsorbent and 250 ml of 25 times diluted landfill leachate for the optimized time obtained from the kinematic experiment. The supernatant was then filtered and taken to analyze the effluent COD concentration. The optimum contact dosage of the adsorbent was determined using the analyzed data.

Then, the effect of the change of the initial concentration, pH and the temperature on the removal of COD by the composite adsorbent was determined using a series of batch experiments.

Batch experiments were conducted to optimize the contact time and adsorbent dosage off NH_3-N, TN and PO_4^{3-}-P.

The absorbed quantity per unit was evaluated using Eq (1).

$$q_e = \frac{(Ce-Co)V}{m} \qquad (1)$$

Where, Co is an initial concentration in leachate (mg/L), Cs is leachate concentration at equilibrium (mg/L), V is leachate volume (L) and m is adsorbent mass(g).

Then, the adsorption isotherms were determined using the isotherm equations. Adsorption isotherm has been conducted based on the adsorption isotherm experiments by varying the amount of adsorbent and plotting using the isotherm equations: Langmuir, Freundlich, Elovich, and Tempkin.

Langmuir Isotherm (Eq 2) - valid for monolayer adsorption onto a surface containing a finite number of identical sites. Assumptions of this model are as follows,

- Fixed number of accessible sites that have the same energy is available on the adsorbent surface.
- Adsorption is reversible (Metcalf & Eddy, 2015)

$$\frac{1}{qe} = \frac{1}{K_l \times q_m} + \frac{1}{C_e} + \frac{1}{q_m} \qquad (2)$$

Freundlich Isotherm (Eq 3) - assumes uptakes of adsorbate occur on a heterogeneous surface by multilayer adsorption. The amount of adsorbate adsorbed increases infinitely with an increase in concentration (Dada, et al., 2012)

$$q_e = K_f \times C_e^{\frac{1}{n}} \qquad (3)$$

Elovich Isotherm (Eq 4) - mainly applicable for chemisorption kinetics. The equation is often valid for a system in which the adsorbing surface is heterogeneous assuming the adsorption sites increase exponentially with adsorption, which implies multilayer adsorption.

$$log\ \frac{C_e}{q_m} = \log(\ K_E\ q_m\ ) - \frac{1}{q_m}\ (q_e) \qquad (4)$$

Tempkin Isotherm (Eq 5) - assumes that the heat of adsorption of all the molecules increases linearly with coverage.

$$q_e = B \ln A_r + B\ lnC_e \qquad (5)$$

Where, K_l, K_f, K_E, B, Ar are related constants.

3. RESULTS AND DISCUSSION

3.1. COD

3.1.1. Optimum contact time

It can be determined from Figure 1, that the COD removal efficiency of the PAC (93.9%) is the highest value followed by the COD removal efficiency of the composite adsorbent (72.8%), WSS (44.1%), and DAS (33.2%), respectively.

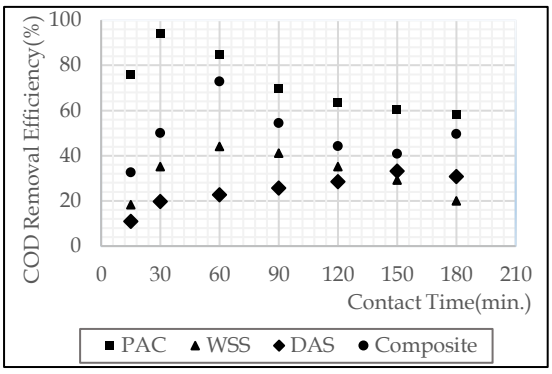

Figure 1 COD removal efficiencies vs. contact time

Also, it can be determined that 60 min (1hr) is the contact time for maximum removal of COD by the composite adsorbent.

3.1.2. Optimum contact dosage

According to Figure 2, maximum COD removal efficiency (91.1%) at contact dosage of 12g is followed by the PAC followed by composite (61.8%), DAS (44.9%) and WSS (32.6%), respectively.

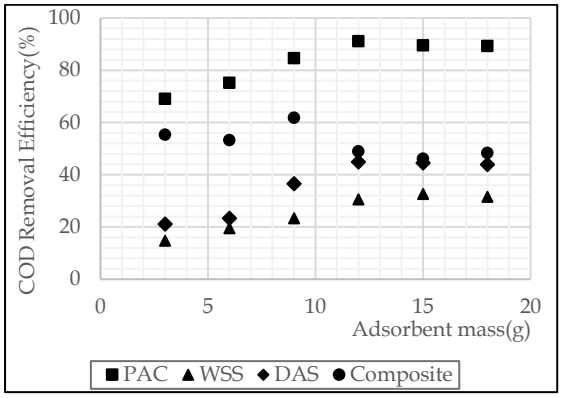

Figure 2 COD removal efficiencies vs. contact dosage

From the beginning of the curve of composite media, the percentage removal increases with the increment of adsorbent dosage and it reached its optimum contact mass of 9g (36 mg/L). Then in the further increment of mass, it can be seen decrement of removal efficiencies. The cause can be explained as that the amount of available sites increase s until the optimum mass is reached and further increment in mass may result in decreasing the probability of molecules contacting all available adsorption sites (Daud, et al., 2017).

3.1.3. Adsorption isotherm

The isotherm study expresses the process of adsorption and the interaction between the adsorbent surface and adsorbate.

Using the results gained from the dosage study, Table 3 was obtained with the best fitted with the isotherm models corresponded to each adsorbent. According to the isotherm studies for the composite adsorbent, the R^2 value is 0.82 that the sorption data fitted well to the Elovich isotherm model. Figure 3 illustrates the best fitted Elovich isotherm with WSS.

Table 3 Adsorption isotherm results on COD removal

Adsorbent	Isotherm Model	R^2	Ads. capacity (mg/g)
PAC	Freundlich	0.8254	1.5
WSS	Elovich	0.9531	7.1
DAS	Elovich	0.7985	12.5
Comp.	Elovich	0.8751	14.7

Freundlich isotherm model for PAC explains that heterogeneous surface adsorption in which the surface concentration of the adsorbate on the adsorbent increases with the increase in the initial concentration of the solution (Metcalf & Eddy, 2015). Meanwhile, for the composite media and the rest it describes that the adsorption sites increase exponentially with adsorption, which implies multilayer adsorption.

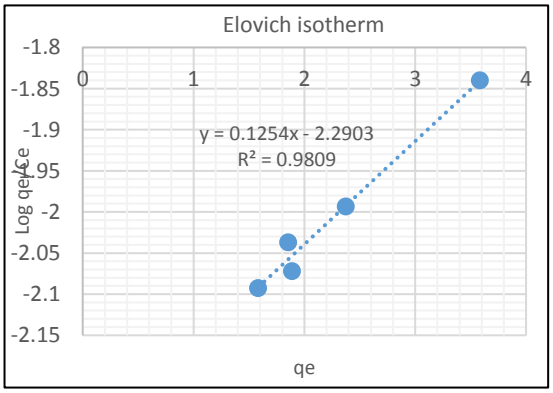

Figure 3 Elovich isotherm fitted for the adsorption of COD on WSS

3.1.4. Effect of pH

It is identified that increasing solution pH caused an increase in COD removal efficiency and a pH of 7.17 was identified as the optimal pH for COD removal (51.53 %; 152mg/L) according to Figure 4. When pH increases in the solution, the number of negatively charged sites increases and positively charge site decreases. Therefore, there may be an electrostatic attraction between the charged particles. The COD removal decrease form pH 7.17 may cause by the dissociation that occurs

at the solid to liquid boundary because of the acid and base interaction (Daud, et al., 2017).

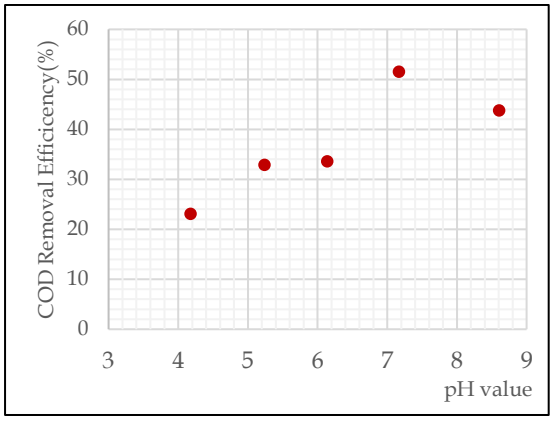

Figure 4 Effect of the pH on COD removal

3.1.5. Effect of concentration

An increase in initial concentration shows a negative effect on COD removal. Figure 5 shows that the maximum efficiency of 49.65% is shown at the concentration of 284 mg/L. It reveals that at higher COD concentration the number of active sites reduced due to the high competition between adsorbate molecules for occupying these vacant sites (Mahdavi, et al., 2018)

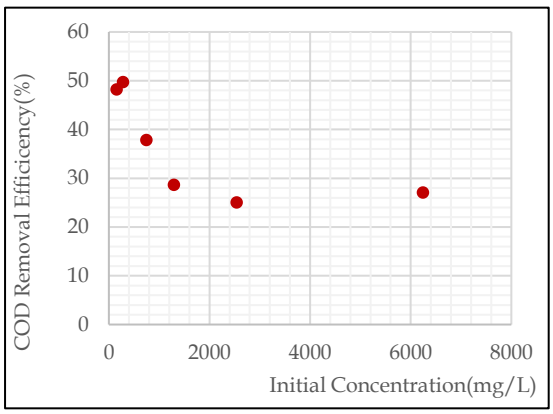

Figure 5 Effect of the concentration on COD Removal

3.1.6. Effect of temperature

According to Figure 6, the process is endothermic, because of the COD removal raised from 142mg/L at 25˚C to 157mg/L at 30˚C. Then the COD removal is decreased and gets approximately constant. Raising temperature decreases adsorption somewhat because the adsorbed molecules have gathered vibrational energies and are therefore more likely to desorb from the surface.

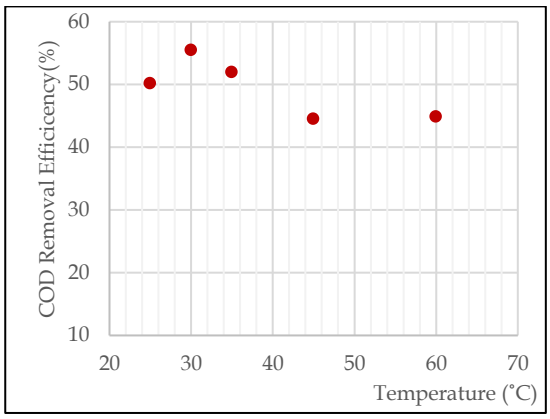

Figure 6. Effect of the temperature on COD removal

3.2. Nutrients removal

3.2.1. Optimum contact time.

Figure 7 illustrates the removal efficiencies in terms of NH_3-N, TN, and PO_4^{3-}-P. Vs. contact time. Optimum contact times obtained were 120min (53.27%), 90min (27.56%), and 15min (74.11%) for NH3-N, TN and PO43--P respectively

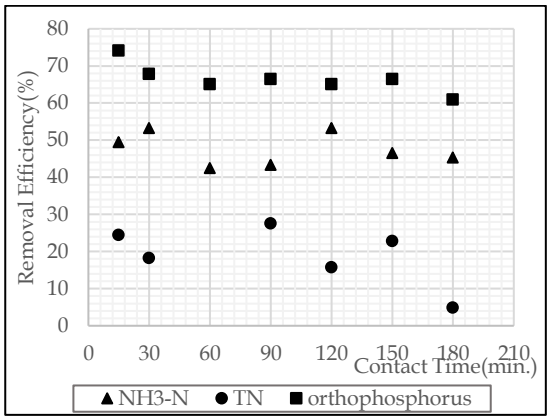

Figure 7 Removal efficiencies in terms NH_3-N, TN, PO_4^{3-}-P vs. contact time

3.2.2. Optimum contact dosage

From Figure 8, it can be obtained the removal efficiencies in terms of NH_3-N, TN, and PO_4^{3-}-P vs. contact dosage. Optimum contact dosage obtained was 12g (58.68%), 3g (30.48%), and 3g (81.36%) for NH_3-N, TN and PO_4^{3-}-P. Adsorption capacities were 0.15mg/g,7.04mg/g and 0.0077mg/g.

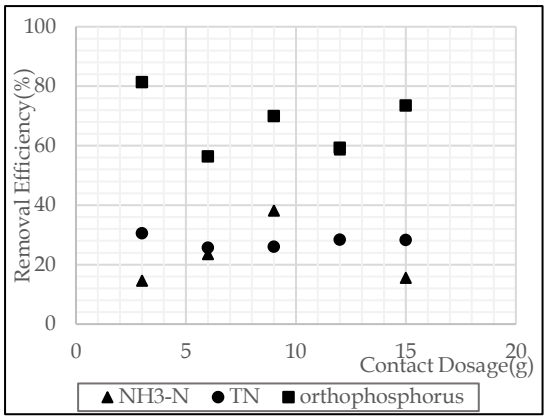

Figure 8 Removal efficiencies in terms NH_3-N, TN, PO_4^{3-}-P vs. contact dosage

4. CONCLUSIONS AND FUTURE DIRECTIONS

The results of this comparison study of composite adsorbent with DAS, WSS and PAC indicated that the removal efficiency of the sCOD in landfill leachate by composite adsorbent is 61.9% is followed by DAS (44.87%) and WSS (32.65%), respectively. PAC showed the highest COD removal efficiency (91.1%) which is used as the most popular commercial adsorbent. Adsorption capacities of PAC, WSS, DAS and composite were 1.5mg/g, 7.1mg/g,12.54mg/g and 14.66 mg/g. A study on the behaviour of equilibrium data revealed that Elovich isotherm provided the best fit for most of the adsorption process above in comparison to other models on sCOD removal. Maximum removal efficiencies of NH3-N, TN, and PO43--P were 58.7%, 30.5% and 81.4% respectively by the composite adsorbent and the adsorption capacities were 0.15mg/g, 7.04mg/g and 0.0077mg/g. Further batch studies on composite adsorbent media indicated that the optimum conditions of sCOD removal take place at the temperature 30°C, initial concentration 284mg/L and pH 7.17.

The importance of composite adsorbent lies with the fact that it can treat more than one contaminant simultaneously, whereas the activated carbon is good for only sCOD removal. Also, the application of DAS is sustainable because it would be a reuse application for them for which proper disposal sites are highly limited.

Research on field-scale experiments should be done to investigate further the potential of these composite adsorbent to be used. Also, varied proportions should be experimented in order to increase the removal capacity.

5. ACKNOWLEDGEMENT

The authors gratefully acknowledge Ms. Nimal Shanthi and the technical staff, Environmental laboratory, Faculty of Engineering, University of Ruhuna, for their technical assistance during this study.

6. REFERENCES

Andersson, M. & Saterskog, H., 2015, 'Treatment of landfill leachate;removal of organic contaminants, metals and sludge characterisation', *Master's Thesis.*

APHA, 2005, *Standard Methods for the Examination of Water and Wastewater.* 18 ed. Washington,United States: American Public Health Association.

Azmi, N., Singarayah, A., Bashir, M. & Sethupathi, S., 2015, Landfill leachate treatment by low-cost Activated Carbon prepared from agricultural waste', *Jounal of engineering research and technology,* 2(1).

Cooney, D., 1998, '*Adsorption Design for Wastewater Treatment*', Washington D.C.: Lewis Publishers.

Dada, A., Olalekan, A., Olatunya, A. & DADA, O., 2012, 'Langmuir, Freundlich, Temkin and Dubinin–Radushkevich isotherms studies of equilibrium sorption of Zn2+ unto Phosphoric Acid Modified Rice Husk', *IOSR Journal of Applied Chemistry (IOSR-JAC),* 3(1), pp. 38-45.

Daud, Z. et al., 2017, 'Adsoption studies of leachate on cockle shells', *GEOMET,* 12(29), pp. 46-52.

Dayanthi, W., Arthanayaka, A., Asiri, K. & Malkanthi, K., n.d. 'Applicability of waste matter as reactive media in Permeable Reactive Barriers (PRBs) to treat landfill-leachate contaminated groundwater', *Journal of IESL.*

Dayanthi, W., Jayalath, M. & Guawansha, T., 2014,'Applicability of low-cost organic

materials as reactive media in Permeable Reactive Barriers (PRBs) to treat landfill-leachate', *Journal of IESL.*

Halim, A. et al., 2011, 'Ammonia and COD removal from synthetic leachate using rise usk composite adsorbent', *Journal of Urban and Environmental,* Volume 5(1), pp. 24-31.

Halim, A. et al., 2012, 'Semi-Aerobic Landfill Leachate Treatment', *Environmental engineering science,* 29(5).

Halim, A., Hamidi, A., Johari, M. & Ariffin, K., 2010, 'Comparison study of ammonia and COD adsorption on zeolite, activated carbon and composite materials in landfill leachate treatment', *Desalination,* pp. 31-35.

Mahdavi, A. R. et al., 2018, 'COD removal from landfill leachate using a highperformance', *Chemical Engineering Communications,* 205(9), pp. 1193 - 1206.

Metcalf & Eddy, 2015, *Wastewater engineering,Treatment and reuse.* 4 ed. s.l.:McGraw Hill Education(India) Pvt..

Renou, S. et al., 2008, 'Landfill leachate treatment: review and opportunity', *Journal of Hazardous Material',* Volume 150, pp. 68-493.

Rong, L., 2009, 'Management of landfill leachate', *Final Thesis.*

Shreyas, B. & Istalingamurthy, D., 2016, 'The reuse of dewatered alum sludge collected from water treatment plant for phophorous removal in domestic wastwater', *Internatioanal research journal engineering and technology(irjet),* 3(7).

Upasena, K., 2017, 'Batch sorption experiment on recycling building waste and dewatered alum sludge as Reactive Packing Media in PRBs to treat the dissolved organic compounds and ammonium of the groundwater contaminated by landfill leachate, *Final Thesis.*

Yang , Y., Tomlinson , D., Kennedy, S. & Zhao, Y., 2006, 'Dewatered alum sludge:a potential adsorbent for phosphorus removal', *IWA Publishing.*

Proceedings of the 7th International Symposium on

Advances in Civil and Environmental Engineering Practices for Sustainable Development

ACEPS - 2019

Water use patterns and sensitivity to tariff: A study in a community with access to alternative water sources other than pipe borne water.

K.C.Ellawala[1] and V.Vinojkanth[1]

[1]Department of Civil and Environmental Engineering, Faculty of Engineering, University of Ruhuna, Hapugala, Galle, SRI LANKA

K e y w o r d s

Tariff
Water consumption
Pipe borne water
Alternative water sources

A B S T R A C T

Water tariff is a part of integrated water resource management to balance the supply and the demand. Batticaloa municipality has alternative water resources other than pipe borne water supplied by NWS&DB. Willingness to pay, number of family members and water use pattern have a significant influence in determining NWS&DB water consumption, while income is not a determinant. Both high consumption and low consumption group shows sensitivity to increase in tariff. In an 10% increase in tariff, low consumption group shows a dramatic increase in using pipe borne water for drinking only.

1 INTRODUCTION

National Water Supply and Drainage Board (NWS&DB) is the national institute, which takes the responsibility to provide potable water for municipal, public, stand posts, schools and religious institutions, commercial, government hospitals, industrial, shipping, community-based organizations and so on (Hettiarachi, 2012) in Sri Lanka. Currently, 43.4% population in Sri Lanka is supplied with potable water by the NWS&DB and further 25% is supplied by rural water supply schemes, altogether the safe drinking water supply in Sri Lanka being approximately 65% of the population. Sri Lankan government targets to provide safe drinking water supply for all by 2025 and 60% safe drinking water supply coverage by 2020. (Gamini, 2014). Thus, Sri Lanka spends more than Rs. 20,000 million per year for the provision of potable water (Ministry of water Supply and Drainage, National water Supply and Drainage Board, 2014).

Water tariff is a part of integrated water resource management to balance the supply and demand (Gamini, 2014). The cost of production of potable water is determined by the alternatives to the pipe borne water, the treatment costs and distribution costs. If the area is plentiful with pure water, the need to have the potable water is less. So, the production amount and the cost also be reduced. The alternatives to the pipe borne water in Sri Lanka are wells with or without the pumps, rain water harvesting systems, bottled water and bowser water supplies. In addition to that, the charges should not only be based on the cost for the production, distribution, maintenance and operation. It should be based on the amount of consumption, the category of various consumer parties, the possibility of water wastage for each party and also the ethical way in which the tariff should be designed.

The costs relevant to the provision of potable water are, capital investment for establishing water supply, operation and maintenance cost of water supply, replacement and rehabilitation cost, environmental cost related with the treatment of waste water, opportunity cost (cost of raw water) (Gamini, 2014).

The target of the government is to

provide potable water to all in Sri Lanka so that it is not easy to reach that task by not considering the current difficulties the NWS&DB face nowadays. Then only, the overcoming of the problem and the certain expansion tasks in the water sector can be achieved. The major constraints the NWS&DB face are; (Gamini, 2014) lack of capital due to poor cost recovery, need of high per capita investment for the water resource development and distribution networks even for a small density area requirement, need for the new water resource development as there may be scarcity at the current water resources, water sharing issues and pollution of water bodies indiscriminately (Gamini, 2014).

Expenses are recollected by the NWS&DB by charging from the consumers in order to maintain the system regularly and to expand the system in future. But in practical it is not possible to generate sufficient revenues to recover the financial cost of utility. Only some portion in the cost can be attained through the tariffs. The cost recovery by the NWS&DB could be improved by activities such as improvement in billing and collection efficiency, control on unaccounted for water, capacity building, adequate meter coverage suitable subsidy design, inclusion of consumer's willingness to pay in water pricing, improvement in unreliability etc. (Singh, 2005).

Therefore, this study aims to determine the relationship among, income, water use patterns and sensitivity to tariff in a community with alternative water sources other than pipe borne water supplied by NWS&DB. Understanding on such patterns may help in modifying existing tariff systems and/or implementing new tariff systems without the community opposing. In the meantime, this type of studies may help policy developers in identifying the sub groups in the community who desperately need subsidies, rather giving subsidy for everyone.

2 METHODOLOGY

2.1 Study Area

The study was limited to Batticaloa municipal council area. Batticaloa municipal water supply has approximately 43000 water supply connections. Among them 391 households were randomly selected for the study. 98% of households had an alternative water supply resource, except pipe borne water.

Table 1 Key questions in the questionnaire

Question	Question type and Answers given
The average no of units of pipe borne water consumed per month for last six months (in m^3)	
The water sources other than the pipe borne water, by which you can be benefited	Multiple response questions which includes answers: Tube wells Shallow Wells (Private) Rainwater harvesting Common wells Abstraction from river/ lakes etc.
Monthly income of the family	Single response questions which includes answers; Less than Rs. 10,000/= More than Rs. 10,000/= & less than Rs. 25,000/= More than Rs. 25,000/= & less than Rs. 40,000/= More than Rs. 40,000/= & less than Rs. 60,000/= More than Rs. 60,000/= & less than Rs. 90,000/= More than Rs. 90,000/=

Question	Question type and Answers given
What amount of payment that the consumers are willing to pay per month	Single response question which includes answers; Up to Rs. 150/= More than Rs. 150/= & less than Rs. 250/= More than Rs. 250/= & less than Rs. 400/= More than Rs.400/= & less than Rs.600/= More than Rs.600/= & less than Rs.900/= More than Rs. 900/=
No of members in the houses	
Availability of the storage tank fixed to the piped network of NWS&DB	'Yes 'or 'No' answers
For which activities pipe borne water is used?	Single response questions which includes answers; Only for drinking For drinking and cooking For drinking, cooking and bathing For drinking, cooking, bathing and washing clothes For drinking, cooking, bathing and washing clothes and toilet flushing For drinking, cooking, bathing, washing clothes, toilet flushing and gardening For drinking, cooking, bathing, washing clothes, toilet flushing, gardening and any other
If there is a 5% increase in tariff, for which activities pipe borne water will be used?	Single response questions which includes answers; Will be restricted to drinking only Will be restricted for drinking and cooking Will be restricted for drinking, cooking and bathing Will be restricted for drinking, cooking, bathing, washing clothes and toilet flushing Will be for drinking, cooking, bathing, washing clothes, toilet flushing and gardening
If there is a 10% increase in tariff, for which activities pipe borne water will be used?	Single response questions which includes answers; Will be restricted to drinking only Will be restricted for drinking and cooking Will be restricted for drinking, cooking and bathing Will be restricted for drinking, cooking, bathing, washing clothes and toilet flushing Will be for drinking, cooking, bathing, washing clothes, toilet flushing and gardening

2.2 Methodology

A door-to-door questionnaire survey was conducted in 391 houses located in the municipality area. The questionnaire was aimed to obtain information. Table 1 shows the questions used to evaluate water use patterns, income and sensitivity to tariff. The questionnaire was conducted in local languages (Sinhala/ Tamil).

2.3 Data Analysis

Oneway ANOVA was used to analyze the influence of income, number of family members, water consumption pattern and willingness to pay on average monthly water consumption.

The sample was subjected to a k means cluster analysis based on their socio-economic characteristics and water consumption

patterns. The analysis was carried out using R statistical analysis software package.

3 RESULTS AND DISCUSSION

People living in Batticaloa Municipal Council area most commonly have wells and tube wells for obtaining water (98%). This has been observed in households located in Gampaha, Kaluthara and Galle districts also, but in a lower percentage (Nauges and van den Berg, 2006).

Many people have two water supply lines to their homes, one from NWS&DB and the other from their own source. Income was not a significant factor in determining average monthly water consumption, while willingness to pay, number of family members and consumption pattern were significant.

Table 2 Results of oneway ANOVA

Variable	F value	P<
Income	1.48	0.22
Water use pattern	270.00	0.00
Number of Family members	209.52	0.00
Willingness to pay	54.5	0.00

This community can be clustered into two clusters based on their socio-economic characteristics and water consumption patterns. Cluster 1 is high consumption group (HC) with an average water use of 22.68 ± 5.68 m^3 and cluster 2 is low consumption group (LC) with an average water use of 9.22 ± 4.94 m^3. Two clusters had no difference in alternative water source availability and income. But two clusters had a difference in number of family members, willingness to pay, usage pattern of pipe borne water supplied by NWS&DB, response to increase of water tariff.

The high consumption cluster has families with more members and a higher percentage of families using water for uses other than drinking, cooking and bathing. Meanwhile, low consumption group has nearly 60% of population who use pipe borne water for drinking, cooking and bathing only. Additionally, high consumption group has a higher percentage of families with more members. Two clusters have a notable difference in the water use pattern. Nearly 70% of people in HC cluster use water for drinking, cooking, bathing and washing clothes and toilet flushing. In LC cluster less than 20% show that water use pattern. The highest portion of people in LC cluster use water for drinking, cooking and bathing. Further, more than 50% of people use pipe borne water only for drinking, drinking and cooking or drinking, cooking and bathing.

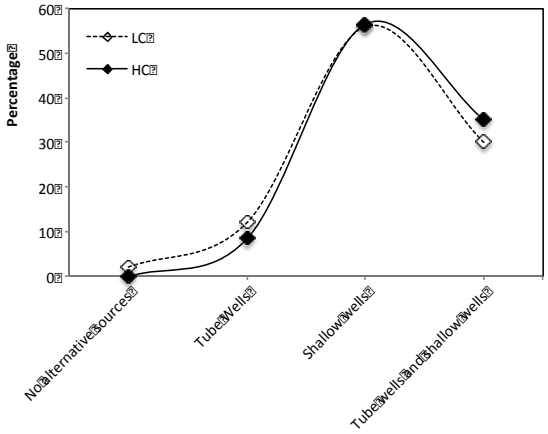

Figure 1 Alternative water source availability in Batticaloa municipality

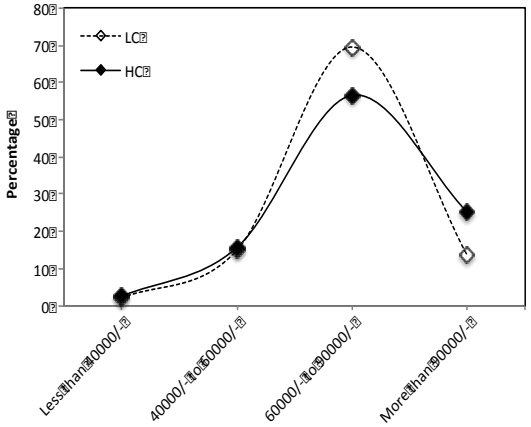

Figure 2 Income category variation in the sample, in two clusters

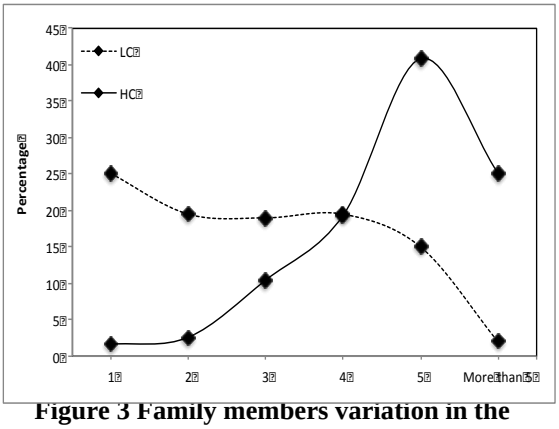

Figure 3 Family members variation in the sample, in two clusters

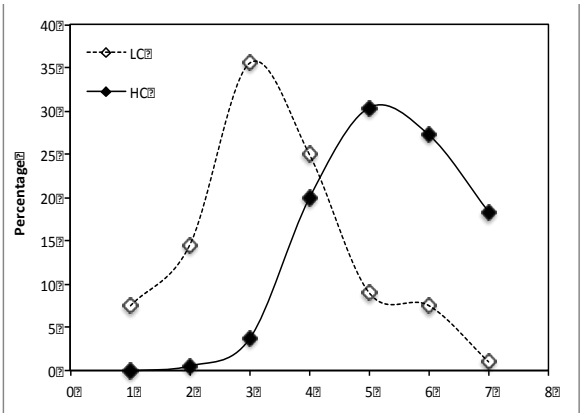

Figure 4 Water use pattern of the sample in two clusters

In LC cluster nearly 80% of people claim that increase of water bill from 10% will cause them to use pipe borne water for drinking only. But in HC cluster predicted reduction is slightly lower than 50%. However, 5% increase 10% increase both will change the water use pattern in HC cluster, while, 5% increase has low influence for LC cluster.

The average monthly water bill was 176.67/- ± 108.45/- LKR in LC cluster, while; it was 679.06/- ± 313.89 LKR in HC cluster. Nearly 40% in each group pay more than the average in respective cluster.

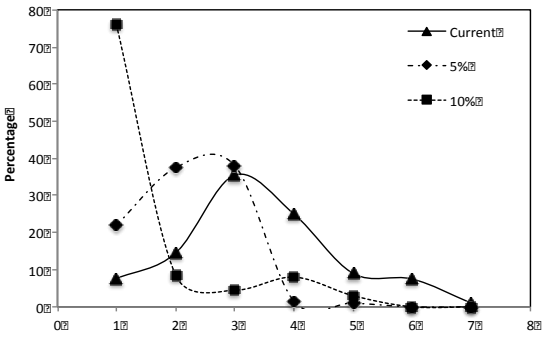

Figure 5 Predicted water use patterns in LC cluster

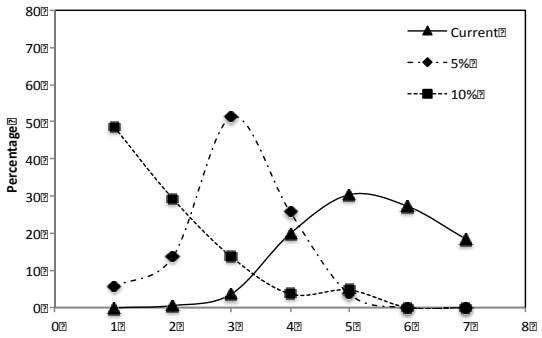

Figure 6 Predicted water use pattern in HC cluster

However, there is no analysis of water quality in those sources. Hence, it is difficult to decide whether it is advisable to use pipe borne water for drinking only. There willingness to adjust for own water resources can be used in a favorable manner in controlling demand for NWS&DB water; if there is a proper water quality assessment is carried out.

4 CONCLUSION

In Batticaloa municipality area about 98% of people have an alternative water supply other than pipe borne water supplied by NWS&DB. The availability of alternative sources enables them to use their own water sources for selected uses. Therefore, in a price hike this kind of a community tries to change their water use patterns to maintain their water bill in the same price range. Use of pipe borne water for drinking only increases drastically in a 10% increase of water bill in both groups. Such flexibilities in demand fro water can be favorably used in demand management by NWS&DB.

5 REFERENCES

Gamini, P.S., 2014, *'Challenges in the water sector and wastewater sector'*, Kandy: Greater Kandy Water Supply Project, National Water Supply & Drainage Board.

Hettiarachi, K., 2012, 'The Gazette of the democratic socialist republic of sri lanka', *General government notification*, 18 september, pp. 2-4.

Ministry of water Supply and Drainage, National water Supply and Drainage Board, 2014, *Handbook for water consumers.* National water Supply and Drainage Board ed. Colombo: Greater Kandy Water Supply Project.

Nauges, C., & van den Berg, C., 2006, Water Markets, Demand and Cost Recovery for Piped Water Supply Services: Evidence from Southwest Sri Lanka.

Singh, M.R., Upadhayay ,V. &. Mittal A.K., 2005, 'Urban water tariff structure and cost recovery oppurtunities in India', *Water Science & Technology,* 52(Indian Institute of Technology), pp. 43-51.

Proceedings of the 7th International Symposium on

Advances in Civil and Environmental Engineering Practices for Sustainable Development

ACEPS - 2019

Column experiment on recycling waste materials to treat dissolved organic matter and nutrients in landfill-leachate.

G.L.P.M. Punyawardhana[1] and W.K.C.N. Dayanthi[1].

[1]Department of Civil and Environmental Engineering, Faculty of Engineering, University of Ruhuna, Hapugala, Galle, SRI LANKA

K E Y W O R D S

Landfill Leachate
Column Experimental
Recycling Waste Materials
Dissolved Organic Matter
Nutrients

A B S T R A C T

The landfill-leachate treatment is mainly achieved in reactors filled with reactive/filter materials. The high-cost of these packing materials has caused most of these methods economically unviable. Hence, low-cost and readily available packing materials can make above treatment systems more cost effective. Therefore, the aim of this study was to determine landfill leachate treatment performances of a composite packing media made of low-cost materials such as 45 % of dewatered alum sludge (DAS) and 45 % of washed sea sand (WSS) mixed with 10 % of granular activated carbon (GAC). The experimental set-up consisted of two laboratory- scale filter columns, namely experimental and control columns. The control column was filled with only GAC, and the experimental column was filled with the composite packing media. BOD_5, COD, Nitrogenous compounds, Phosphorus compound, pH, conductivity, turbidity, ORP and alkalinity were analyzed for influent and effluent samples. The average removal efficiencies of BOD_5 and COD in the experimental column were 49.23 ± 21.1% and 50.78±22.66 respectively. The average removal efficiencies of NH_3-N, TN TP, PO_4^{3-}-P and TP in the experimental column were 33.31±19.53%., 22.06±11.09, 92.06±7.28%, and 92.77±11.08% respectively.

1. INTRODUCTION

Due to urbanization, population growth rate and industrialization, solid waste generation increases. Solid waste can be categorized into three main types: municipal waste, industrial waste and biomedical waste (Liu, 2013). Main pollution problem caused by municipal solid waste landfill is leachate, which is generated as a result of mixing water from precipitation and surface runoff. The leachate consists of large amount of organic matter, nitrogenous compounds, phosphorus compounds and heavy metals. Therefore, proper leachate treatment is essential in landfill handling in order to mitigate environment risk and to protect surface and groundwater. The landfill leachate treatment can be categorized into three methods such as physical, chemical and biological (Nanayakkara, et al., 2013). The main issue associated with the landfill-leachate treatment lies in the fact that the packing materials that most of these systems need are expensive, not readily available and generate unwanted residues into the environment. Hence, investigations on low-cost, environmentally friendly and readily available packing materials is a timely need.

Therefore, the aim of this study was to seek the landfill- leachate treatment potential of a composite waste material packing media using a laboratory- scale column experimental set-up. The objectives of this study were to obtain the removal efficiencies of organic compounds and nutrients found in the landfill – leachate, and find out the changes of several physical and mechanical properties of the composite waste material packing media due to the interaction with the landfill-leachate.

2. METHODOLOGY

2.1. Raw materials collection and influent characterization

Leachate was collected from the Galle municipal council dumpsite (Rathgama). Then initial contaminants concentrations were measured by diluting the leachate by 10%.

Table 1 Influent characteristics

Parameter	Influent concentration
COD	6300mg/l
BOD_5	930 mg/l
Nitrate –N	151mg/l
Ammonia – N	17.36mg/l
TP	0.014mg/l
Orthophosphate	0.012mg/l
Total alkalinity	8300mg/l
pH	7.47
ORP	-83 mv
Turbidity	65.6 NTU
Conductivity	24.5 ms/cm

2.2. Selection of materials in filter columns

Filter materials were selected according to properties of materials. Hence, DAS, GAC and WSS were used as filter materials.

- DAS

  Waste water containing phosphate should be treated before discharging. When considering the phosphate removal methods, most important removal process are chemical removals including phosphorus precipitation with aluminium, calcium and iron salts. (de-Bashan & Bashan, 2004). DAS has aluminium sulphate ($Al_2(SO_4)_3$) which is used as coagulant in water treatment plant. Therefore, this is good filter material to remove phosphate compounds (Yang, et al., 2006).
- GAC

  GAC in combination with biological pre-treatment is the leading technology for the treatment of landfill leachate for the removal of COD and other toxic substances. (Sameer, et al., 2013). In addition, GAC has no enough adsorption capacity of ammonia because of it usually processes a non – polar surface due to manufacturing conditions at high temperatures, which is the disadvantages for some application because of poor interaction with some polar adsorbents (Park & Kim, 2005).
- WSS

  This is a good filter media and remove ammonium and other inorganic pollutants from leachate (Halim, et al., 2010).

Both sea sand and DAS were washed, dried and sieved. The materials were ground to obtain a particle size less than 2.36 mm.

2.3. Experimental set-up and run

Figure 1 depicts the experimental set-up. PVC pipe having an inner diameter of 8.9 cm was used to make filter columns. The height of a column was 50 cm and the thickness of the packed bed was 30 cm. The height was selected in such a way that it would be four times greater than the diameter, which is the minimum value of height to diameter ratio (Relyea, 1982). A gravel layer of 7 cm thick was placed at the bottom of the columns to prevent the blockage of effluent line. Perforated plates were placed at top of the packing media and in between gravel layer and filter media to avoid the suspension of materials and distribute the influent evenly throughout the filter bed. An overhead tank to store influent was placed at a higher elevation. It was allowed to flow under gravity into a constant head tank, from which it was directed to two filter columns through pipe lines under gravity. Each pipe line had valves to control the flow rate of influent. One filter column was used as a controller column and the other was used as the experimental column. The controller column was filled with GAC, and the experimental column was filled with all materials as a composite media (DAS 45%, WSS 45% and GAC 10% on volume basis).

Before starting the experiment, influent leachate characteristics were measured in terms of COD, BOD_5, TN, nitrate – N, TP, orthophosphate, and ammonia –N, total alkalinity and pH. Table 1 shows the influent characteristics. Physical properties such as particle size distribution, specific gravity and void volume ration and mechanical properties such as hydraulic conductivity and shear strength were analyzed. The duration of the experimental run was 55 days, and influent and effluent samples were collected every

5-day time period. Target parameters of leachate were analyzed and removal efficiencies were calculated using mass balance analyses. After the experimental run, physical and mechanical properties of the filter media core were analyzed. Table 2 shows the surface loading rates.

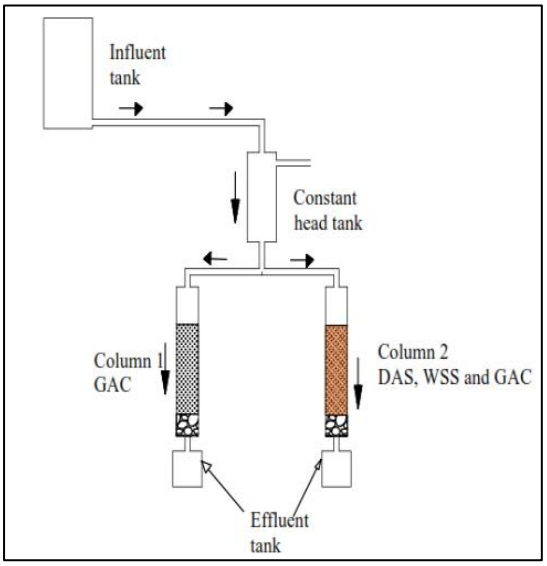

Figure 1 Schematic diagram of the experimental set-up

Table 2 Surface loading rate of leachate parameters

Parameter	Surface loading rates ($g/m^2.d$)
BOD5	157
COD	285
OP	0.001
TP	0.006
N	11.6
TN	263

3. RESULTS AND DISCUSSION

3.1. Removal of Organic Matter

The efficiency of removing organic matter by each packing media was determined in terms of BOD_5 and COD of the influent and effluent. Figure 3(a) and (b) show the variation of removal efficiencies of BOD_5 and COD with respect to time. Removal efficiencies of BOD_5 for controller column and experimental column were 78.85 ± 14.73% and 49.23 ± 21.1%, respectively. The removal efficiencies of COD for the controller column and experimental columns were 48.84 ± 17.07% and 50.78± 22.66%, respectively.

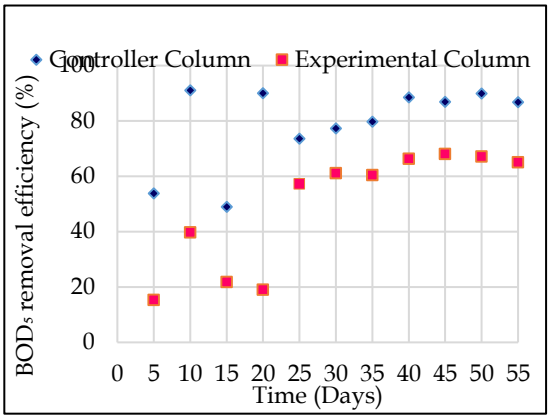

Figure 1 Variation of BOD_5 removal efficiencies with respect to time

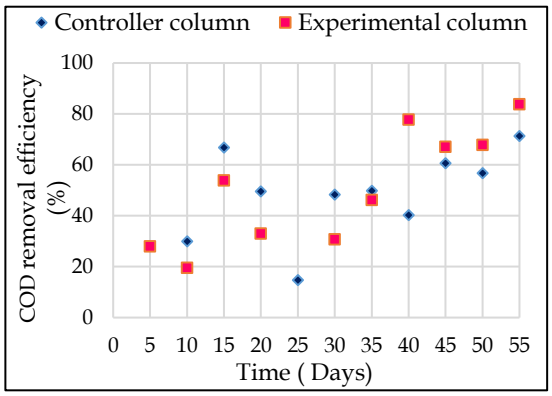

Figure 2 Variation of COD removal efficiencies with respect to time

According to Figure 1, it can be seen that the removal efficiencies of BOD_5 in the experimental column on first 20 days were low compared to the latter stage of the experimental run. The reason for that could be the time requirement for micro-organisms to grow up in the column and initiate decomposition. Adsorption could be the dominant treatment mechanism at the initial stage, and thereafter the biological decomposition could become dominant while adsorption could be dormant due to the gradual decrees of vacant sites.

COD is an indicator for the amount of impurities present in the wastewater. Various pollutants provide COD to the water. Therefore, the removal of COD is the ultimate removal of these impurities from the leachate. COD removal methods are adsorption, coagulation, electrochemical, ultrafiltration and membrane-based technology (Kulkarni, 2013). According to Figure 2, the COD removal efficiency of the controller column was less.

3.2. Removal of nutrients

3.2.1. Removal of phosphorus compounds

Analysis of Phosphorous removal was based on Orthophosphate-Phosphorous (PO_4^{3-} − P) and Total Phosphorous (TP). Figure 3 and 4 show the variation of removal efficiencies of PO_4^{3-} − P and TP with respect to time. Removal efficiencies of PO_4^{3-} −P of the controller column and experimental columns were 90.88±9.95% and 92.06±7.28%, respectively Removal efficiencies of TP of the controller column and experimental column were 89.47±16.51% and 92.77±11.08%, respectively.

Removal efficiencies of PO_4^{3-} − P and TP of the experimental column were higher than those of the controller column. The main reason behind this high treatment performance in the experimental column was the major contribution from its reactive media (DAS), a well-known phosphorus adsorbent in accordance with the past research.

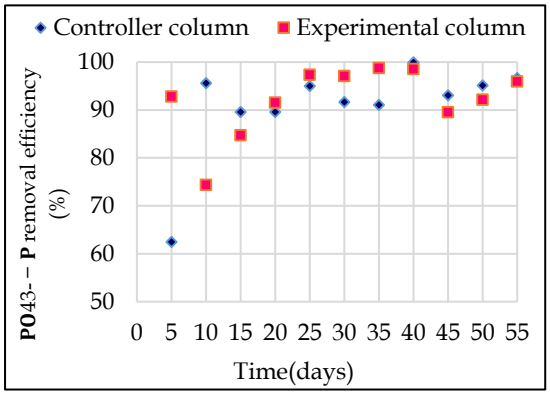

Figure 3 Variation of PO_4^{3-} - P removal efficiencies with respect to time

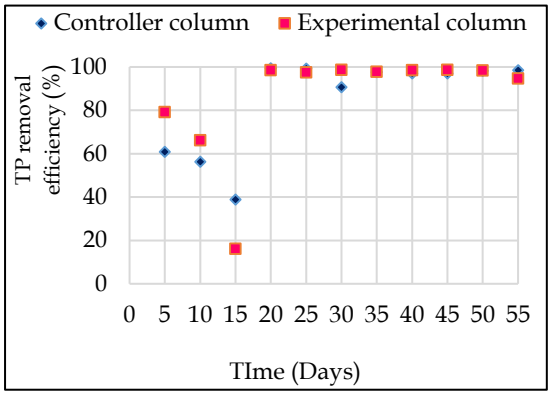

Figure 4 Variation of TP removal efficiencies with respect to time

3.2.2. Removal of nitrogen compounds

Analysis of nitrogen was based on ammonia-nitrogen, nitrate nitrogen and total-nitrogen. The average removal efficiency of ammonia-nitrogen (NH_3-N) of the controller column and experimental are 24.94±14.39%and 33.31±19.53%. Figure 5 shows the variation of removal efficiencies of NH_3-N with time. Denitrification and the adsorption of ammonium, are the possible mechanisms which can treat NH_3-N (Manoj & Wasudevan, 2012). The reason for the low efficiency in treating ammonia could be the limitation of adsorbent zones. The NH_3 removal efficiency of the controller column was lower than that of the experimental column proving that GAC is not an efficient filter material for this contaminant. Generally, granular activated carbon does not have enough adsorption capacity of ammonia because it usually possesses a non-polar surface due to manufacturing conditions at high temperatures. WSS is good for removing ammonia as a natural ion exchanger (Halim, et al., 2010).

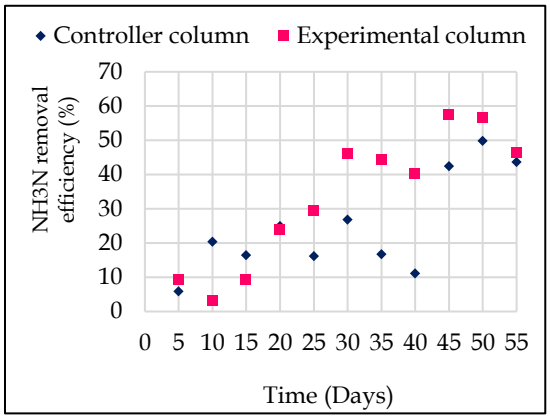

Figure 5 Variation of NH_3-N removal efficiencies with respect to time

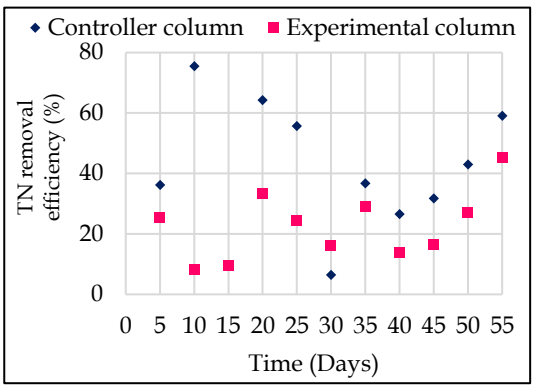

Figure 6 Variation of TN removal Efficiencies with respect to time

Figure 6 shows the TN removal efficiencies. The average removal efficiency of TN in the controller column and experimental column were 48.04 ±24.43% and 22.06±11.09%, respectively. TN removal could occur as a result of ammonia adsorption and nitrification-denitrification process. Ammonium nitrogen is converted to nitrate through the autotrophic nitrification process in addition to that it is assimilated into cells through bio synthesis (Atlas and Bartha 1998, cited in Dayanthi et al 2015). Total Nitrogen is the sum of the Total Kejeldhahl Nitrogen (TKN), nitrate nitrogen and nitrite nitrogen. Analysis of physical and mechanical properties of reactive materials

3.2.3. Physical properties of reactive materials

Sieve analysis test

The sieve analysis test was conducted to find out the particle size distribution because during the experiment run, the grain size distribution of reactive materials can change significantly due to the reactions taking place between the contaminants in the influent and reactive media. Table 3 shows the results of the sieve analysis test.

Table 3 Sieve analysis results

Composite media	Effective size(mm)		Uniformity coefficient (Cu)
	D60	D10	
Before Loading	0.70	0.25	2.80
After Loading	0.85	0.275	3.09

Specific gravity test

Table 4 shows the specific gravity and porosity of the composite packing core before and after loading. Porosity had increased after the experiment run due to clogging of pores by impurities.

Table 4 Specific gravity and porosity

Composite materials	Specific gravity	Void ratio	Porosity
Before Loading	2.43	1.38	0.58
After Loading	2.26	1.13	0.53

3.2.4. Mechanical Properties of the reactive materials

Direct shear test

Table 5 shows cohesion and friction angle of the composite packing core after and before loading. According to cohesion of packing media, the percentage increment of cohesion was 63.51%.

Table 5 Cohesion and friction angle

Composite materials	Cohesion (KN/m^2)	Friction Angle
Before Loading	7.4	44.34
After Loading	12.1	41.69

Permeability test

The values of hydraulic conductivity obtained by permeability test for the experimental column is given in Table 6. The percentage reduction of permeability was 23.08 %. After the experiment run, hydraulic conductivity had decreased due to clogging of pores by impurities.

Table 6 Hydraulic conductivity of composite packing core

Experimental column	Hydraulic conductivity (cm/s)
Before Loading	0.039
After Loading	0.030

4. CONCLUSIONS AND FUTURE DIRECTIONS

The composite packing media described in the present study is satisfactory in treating COD, TP, PO_4^{3-}–P and NH_3-N in landfill-leachate. It can treat nutrients better than GAC alone, owing to its diverse properties. The average treatment efficiencies were COD (50.78 ± 22.66%), PO_4^{3-} − P (92.06±7.28%), TP (92.77±11.08%) and NH_3-N (33.31±19.53%).

Better and alternative arrangements of low- cost and readily available materials as packing materials and alteration of the hydraulic retention time can be highlighted as the recommended further improvements to the present study. Long-term performance of the filter media bed is highly important. To identify the exact treatment failure of the filter bed, more studies should be conducted on this. The possible relationships

between the removal efficiencies and packing material properties, especially the permeability of the packed bed should be investigated for longer period of running time. Waste material combinations should be experimented to figure out the best combination for leachate treatment. When a relationship is built up, the exact treatment failure can be determined and accordingly, limitations of the application of above reactive materials can easily be identified

5. ACKNOWLEDGEMENT

The authors would like to thank all who helped to conduct this research, and especially Ms. D.A.M. Nimal Shanthi for her assistance in laboratory analyses.

6. REFERENCES

Liu, S., 2013., 'Landfill leachate treatment methods and evaluation of Hedeskoga and Måsalycke landfills', Master Thesis, *Sweden: Water and Environmental Engineering*,Department of Chemical Engineering, Lund university.

Yuan, Q., Jia, H. & Poveda, M., 2016, 'Study on the effect of landfill leachate on nutrient removal from municipal wastewater', *Journal of environmental science.*

Abba, A. A. et al., 2009, 'Landfill Leachate Treatments', *American Journal of Applied Sciences,* Volume 6(4), pp. 672-684.

De-Bashan, L. E. & Bashan, Y., 2004, 'Recent advances in removing phosphorus from wastewater and its future use as fertilizer (1997–2003)', *Wat. Res.,*, 38(19), pp. 4222-4246..

Fia, R. et al., 2012, 'Influence of flow direction in the performance of anaerobic filters' *Acta scientiarum,* Volume 34(2), pp. 141-147.

Halim, A. A., Aziz, H. A., Johari, M. A. & Ariffin, K. S., 2010, 'Comparison study of ammonia and COD adsorption on zeolite,activated carbon and composite materials in landfill leachate treatment' *Desalination,* pp. 31-35.

Iqbal, H. B. H. U. A. a. f. M., 2014, 'Lachate of Metal,Organic Carbon and Nutrients from Municipal Waste under SEmi-Arid Condition' 9(1), pp. 187-196.

Kjeldsen, P., Barlaz, M. & Rooker, A., 2002, 'Present and long-term composition of MSW landfill leachate-A review', *Crit. Rev Environ. Sci. Technol.,* Volume 32(4), pp. 297-336.

Kurnaiwan, T., Lo, W. & Chan, G., 2006, 'Physico- chemical treatments for removal of recalcitrant contaminants from landfill leachate', *Journal of Hazardous Materials,* B(129), pp. 80-100.

Madu, J. I., 2003, ,Sweden: Water and Environmental Engineering, Department of Chemical Engineering', Lund University.

Mojiri, A., Aziz1, A. H. & Aziz, . Q. S., 2013, 'Trends in Physical-Chemical Methods for Landfill Leachate Treatment', *Scientific Research in Environmental Sciences,* 1(2), pp. 16-25.

Nanayakkara, Dayanthi, Vidanapathirana & Sriwardana, 2013, 'Up and down flow anaerobic filters using firewood charcoal,dewarted alum sludge and silica sand for landfill - leachate treatment'

Park, S. J. & Kim, ,. B. J., 2005, 'Ammonia removal of activated carbon fibers produced by oxyfluorination' Volume 291, p. 597–599.

Pereira, S. F. et al., 2016. *Nitrogen Removal from Landfill Leachate,* Portugal: s.n.

Renous, s., Givaudan, J., Pouliam, s. & Dirassouyan, F., 2008, 'Landfill leacahte treatment-Review and opportunity', *Journal of Hazardous materials,* Volume 150, pp. 468-493.

Rubio, J., Souza, R. W. & Smith, 2002. Overview of flotation as a wastewater treatment. *Minerals Engineering,* 16(3), pp. 139-155.

Sameer, S., Dhruv, K. & Gaurav, S., 2013, 'Leachate Treatment Technologies', *International Journal of Environmental Engineering and Management.,* 4(5), pp. 439-444.

Wiszniowski, J. et al., 2005, 'Landfill leachate treatment methods-A review', *Environmental Chemistry,* pp. 51-61.

Yang, Y., Tomlinson, . D., Kennedy, S. & Zhao , Y. Q., 2006, 'Dewatered alum sludge : a potential adsorbent for phosphorus removal', 54(5), pp. 207-213.

Proceedings of the 7th International Symposium on

Advances in Civil and Environmental Engineering Practices for Sustainable Development

ACEPS - 2019

Assessment of domestic greywater quality to determine the potential reuse in urban residentials.

H.U.E.Imasha [1], G.G.T.Chaminda [2], M.Otaki [3], Y.Otaki [4] and C.P.Rupasinghe [1]

[1]Department of Agricultural Engineering, Faculty of Agriculture, University of Ruhuna, SRI LANKA.
[2]Department of Civil and Environment Engineering, Faculty of Engineering, University of Ruhuna, SRI LANKA.
[3]Hitotsubashi University, JAPAN.
[4]Ochanomizu University, JAPAN.

K e y w o r d s

Domestic greywater
Filtration
Public acceptance
Reuse
Water quality

A B S T R A C T

The aim of this paper is to evaluate the quality of bathroom and laundry domestic Grey Water (GW) comparing with literature data and reuse standards. By analyzing 30 households composite bathroom and laundry GW samples, the results revealed that bathroom GW in Galle, Sri Lanka contains with very high average concentrations of turbidity, total nitrogen (TN), total phosphorus (TP), chemical oxygen demand (COD) and total suspended solids (TSS) with average values of 135.8 NTU, 78.6 mg/L, 15.9 mg/L, 794.4 mg/L and 195 mg/L, respectively. Laundry GW results of all analyzed parameters complied with the literature data except TN values. COD/ BOD ratio of the bathroom and laundry GW were 11.53 and 12.27, respectively indicating a very low biodegradability potential. Also, bathroom and the laundry GW showed deficient in both N and P. The pollutant loads of all the studied GW indicated that it requires adequate treatment before household reuse such as toilet flushing and irrigation. Therefore, the performance of a batch-fed laboratory-scale simple GW treatment system consisting of a filtration unit and an adsorption unit was also evaluated. It was found that significant reduction of laundry and bathroom GW, turbidity as (59.4%, 57.5%), total coliform as (87.9%, 91.5%), TS as (50%, 50%), TSS as (16.7%, 33.3%), BOD as (61.9%, 65.7%) and COD as (50%, 51.5%), respectively reported during this treatment. However, treated GW was found to be not suitable for toilet flushing according to the WHO standard.

1. INTRODUCTION

Water is a very important and essential resource for humans and all other animals and living organisms. Though the large portion of earth surface is covered by the water, only a small fraction 2.5% of the water in the world is available for human use as most trapped in oceans, tied up in polar ice caps and most of the remainder is beneath the earth's surface (Taikan Oki and Shinjiro Kanae, 2006). The scarcity of water resources, mismanagement, population growth , and climate change have been led to the water shortage and water pollution globally (Ghunmi *et al*., 2011). Population growth, the higher standard of living and climate change has been resulted in constantly increasing water demand in the world. There is a day by day increasing gap between water demand and available water supply (Ghaitidak and Yadav, 2013). Especially in urban areas with very dense populations as well as arid regions (Hourlier *et al*., 2010). Therefore lots of governments facing serious challenges in the water demand management emphasizing the necessity of switching to alternative water resources such as desalinated water, rainwater harvesting and greywater(GW) treatment and reusing (Dolnicar and Hurlimann, 2009).

GW treatment and reuse are emerging as an integral part of water demand management,

promoting the lessen demand from the public water supply and solutions to tackling water shortage (Zhe Li and Reynolds, 2014). Especially as GW is consistently produced and is available onsite for reuse (Winward *et al*., 2008). As per Ghaitidak and Yadav. (2013) GW is a household wastewater (WW) that has not come in to contact with black water. Furthermore, GW did not include WW from kitchen sinks, dishwashers or laundry water from soiled diapers. Treated GW can be used for low-quality water applications such as urinal and toilet flushing, laundry and vehicle washing, fire protection, concrete production, boiler feed water and lawn, garden and crop irrigation (Li et al., 2009). 50%- 80% of domestic WW consist of GW (Kulabako *et al*., 2011).

On the global scene Japan, US, Australia, Canada, UK, and many more countries already involved in GW reuse. In Sri Lankan situation GW is disposal to environment or drainage channels or into sewage pit without any treatment in urban areas. Disposal of untreated GW can be badly affected to the environment, pollution of soil, contaminate freshwater bodies, dispersion of pathogens are some problems create by GW (Li *et al*., 2009). In order to adapt the concept of GW reuse it is essential to have an understanding of GW characteristics. Lots of countries have been conducted studies to find the GW characteristics and based on that they have been developed reuse standards and GW disposal laws also. This research will be conducted as especially Sri Lanka a lack of similar studies.

2. MATERIALS AND METHODS

2.1. Study area and household selection

30 households in Galle District in Southern Sri Lanka were selected using a purposively sampling method for GW characterization considering the convenient for separate bathroom and laundry GW sampling. Also, theses households were selected in a way of representing the urban and rural populations as the GW characteristics highly varying with the life style (Eriksson *et al*., 2002). Laundry GW were collected from both hand washing and washing machine washing operations.

2.2. GW Sample collections

GW produced by bathroom and laundry were separately collected in order to investigate the variability in the GW characteristics in relation to the source. Composite GW samples were collected using sterile bottles and kept in an icebox below 4˚C during transportation to the environmental engineering laboratory of the department of civil engineering, faculty of engineering for influent composition measurement and filter column set up. 1 L of GW from each source was collected 3 times per day (morning, day time and evening) and combined the equal proportion of each grab sample and finally made the composite sample (Dwumfour-Asare *et al*., 2017). The in-situ field parameters including pH, electrical conductivity (EC), total dissolved solids (TDS) and salinity were measured. Laboratory parameters were measured with a maximum delay of 72 hours.

2.3. GW Treatment set up

A laboratory-scale simple GW treatment set up was developed and located in the environmental engineering laboratory of the department of civil engineering of faculty of engineering of the University of Ruhuna. The treatment set up comprised of a sedimentation unit, filtration unit, adsorption unit, and storage unit (Utsev, 2011) (Figure 1). Three batches of each separated bathroom and laundry GW samples taken from the neighboring households were treated and measured the performance of the filter system.

2.4. Analysis of water quality parameters

Physical, chemical and biological parameters measured for each sample. Turbidity, EC, salinity, TDS measured according to the American Public Health Association (APHA) standard, part 100. TN, PH, TP, BOD_5, and COD measured according to the APHA standard, part 4000. Fecal coliforms and T coliform were measured according to the APHA standard, part 9000. One sample t-tests were carried out using Minitab 17 software to analyze the statistical significance in differences between actual GW characteristics

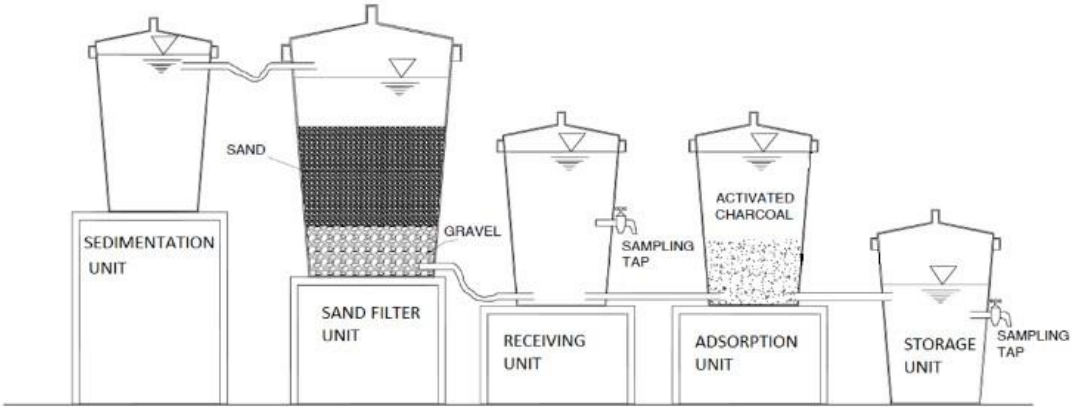

Figure 1 Schematic representation of the laboratory scale GW treatment set up

and reuse standards as well as treated GW characteristics and reuse standards. Paired t-tests were carried out to analyze the statistical significance of the removal efficiencies.

3. RESULTS AND DISCUSSION

3.1. GW Characterization

As can be seen from the data presented in Table 1, there is considerable variability in the concentrations of organic matter fraction expressed as either COD or BOD_5, as well as in suspended material measured by either TSS or turbidity. This variability seems to be an inherent characteristic of GW, in line with previous observations (Halalsheh *et al*., 2008). The laundry GW was moderately alkaline having an average pH value of 8.1, while bathroom GW showed a slightly acidic average PH value of 6.6. The relatively higher pH value of laundry GW water may be due to the alkalinity of the detergents and or soaps that are used. The laundry GW had the higher turbidity most likely due to more soap use compared to that in the bathroom. During sample analysis, the bathroom had a cloudier (milky) appearance which was thought to result from more soap use. Turbidity in these wastewaters could also be related to the presence of high content of suspended solid material. Here, possible high suspended solid material content was found in laundry water followed by bathroom GW. The relatively higher total phosphorus levels in the laundry GW (31.6 mg/L) indicate that phosphorus-containing detergents were used. Although this is the most likely case there is no law inhibiting the use of phosphate-containing detergents in Sri Lanka. However, it can be problematic if these GW enter to the soils and become phosphate saturated resulting in leaching to the groundwater and or to run-off to a surface water source. (Kulabako *et al*., 2011). In compliance with literature data (Table 1), laundry GW shows higher organic loads than bathroom GW. A direct comparison is difficult since various influences would have to be estimated, e. g. the average water demand of the test households for laundry and high dosage recommendations for laundry detergent, etc. It is obvious that laundry GW is more polluted than bathroom GW in terms of all the parameters measured. Bathroom GW in Galle, Sri Lanka is characterized by very high concentrations of turbidity, TN, TP, COD, and TSS with average values of 135.8 NTU, 78.6 mg/L, 15.9 mg/L, 794.4 mg/L and 195 mg/L, respectively compared to the literature values. The high concentration of these parameters is apparently due to the very low per capita water consumption. Nitrogen is from the urine discharges. Higher TP value is possible due to the greater usage of phosphorus-containing soaps.

Table 2 displays the statistical comparison of the average bathroom and laundry GW with the standard of GW for toilet flushing given by the World Health Organization (WHO). A 5% confidence level and $\alpha = 0.05$, the average PH of GW, 6.6 was significantly lower than the proposed WHO standards (6-9) ($p=0.00$).

Table 1 Comparison of GW characteristics of Galle, Sri Lanka with literature data

Parameter	Unit	Galle Sri Lanka				Literature data (Finley, 2008) (Ghaitidak and Yadav, 2013)	
		Bathroom		Laundry		Bathroom	Laundry
		Range	Average	Range	Average	Average	Average
pH		5.3 – 9.2	6.58	5.9-11.2	8.1	7.1-7.6	8.3-9.3
EC	mS/cm	0.1-2.9	0.56	0.1-6.4	1.6	43.7	2.9-703
Turbidity	NTU	25.1 - 598	135.8	36.7-744	273.6	59.8	328-444
TDS	mg/L	69 - 2050	455.8	99.3-4755	1086.7	279-565	2140-2444
Salinity	ppt	0.1- 1.7	0.5	0.1-3.5	0.9		
TS	mg/L	100-4600	630	100-5400	1126.7	778	2021-2700
TSS	mg/L	50 - 600	195	100-610	283.3	58-78	188-315
TN	mg/L	74 – 561.3	78.6	15.2-355	90.9	6.6	14.28
TP	mg/L	3.9-52.6	15.9	4.1-229.1	31.6	1.12	51.58
BOD	mg/L	36-114	68.9	42-105	71.7	19-173	44.3-462
COD	mg/L	88.9 -2504.3	794.4	94.1 -2265.2	879.6	203-367	58-1339
F Coliform	CFU /100mL	1×10^{2} -1.14×10^{4}	2.33×10^{3}	2.20×10^{2} - 1.42×10^{4}	4.02×10^{3}	1.5×10^{5}	13.4×10^{6}
Total Coliform	CFU /100mL	1.22×10^{3} -5.30×10^{4}	2.21×10^{4}	1.12×10^{3} -6.94×10^{4}	2.99×10^{4}	1.05×10^{2}	4.2×10^{6}

3.2. Potential for reuse of bathroom GW and laundry GW for toilet flushing

The average levels of turbidity, BOD_5 and fecal coliform of raw GW was significantly higher than (p=1.0, for each parameter) the proposed WHO standard level for toilet flushing. Average turbidity, BOD_5 and fecal coliform of raw GW, 273.6 NTU, 71.7 mg/L, 4.02×10^{3} cfu /100ml was significantly higher than the WHO standard for toilet flushing. (p=1.00 for each parameter). Therefore, raw laundry GW cannot be reused for toilet flushing.

3.3. Indication on GW composition on biodegradability

Biodegradability of GW is characterized by a COD/ BOD_5 ratio since BOD is the biologically degrade part of COD. Biodegradability of GW is higher than that of the whole domestic wastewater stream with a COD/BOD_5 around 2. Biodegradability is increasing when the ratio of COD/BOD_5 is getting less. That means biological treatment would reduce the majority of pollution. Following Table 3 shows qualitative classification of biodegradability according to the COD/BOD ratio. Determination of biodegradability based on COD/BOD_5 ratio is only of limited information since the actual biodegradability of organic carbon in a treatment system is depending on further features, e. g. on adapted biomass. (Erlangung and Weingärtner, 2013). In this study, both bathroom and laundry data showed higher COD/ BOD_5 ratio values indicating that less potential for biodegradability for aerobic treatment options (Table 4). Biological treatment such as biological aerated filter, membrane bioreactor, sequencing batch reactor, up-flow anaerobic sludge blanket, rotating biological contactor (RBC) and the

The ideal value of COD:N:P ratio for GW treatment as per the treatment of domestic wastewater is 100:20:1. (Eddy, 2003) This value

gives an idea about the main nutrients for the microorganisms' growth; carbon, nitrogen, and phosphorus. This value gives an idea about the nutrient imbalance of GW with regard to biodegradability.(Jefferson et al., 1999) COD:N:P ratio for the bathroom and laundry sources were averaged at 100:9.9:2 100:10.3:3.6 respectively. A comparison with the literature suggests that GW is deficient in both nitrogen and phosphorus in roughly equal proportions. (Edwin and Gopalsamy, 2014) The nitrogen and phosphorus deficiencies are due to the absence of urine in the bathroom and laundry GW. it is suggested to add small amount of kitchen GW to bathroom and laundry GW in order to maintain an optimal COD: N: P ratio. (Jefferson et al., 1999) When looking at these characteristics' filtration appeared as a possible alternative for GW recycling.

3.4. Grey Water treatment set up

3.4.1. Performance of the GW treatment system for laundry GW

PH, turbidity, fecal coliform, total coliform, TS, TSS, BOD and COD were measured before and after treatment of laundry GW. And analyzed results can be shown in Table 5. According to Table 5 turbidity, total coliform, TS, TSS, BOD, and COD of laundry GW were significantly reduced by the GW treatment unit. Turbidity, total coliform, TS, TSS, BOD and COD of GW were removed by 59.4%, 87.9%, 50.0%, 16.7%, 61.9%, 50.0%, respectively.

Table 2 Results of the t -test comparing average laundry GW and bathroom GW values with WHO standards for toilet flushing

Parameter	Unit	Galle Sri Lanka Bathroom Average	Galle Sri Lanka Laundry Average	WHO standards	Comparison α= 0.05 95% confidence level
PH		6.6	8.1	6-9	0.0 (<0.05)
Turbidity	NTU	135.8	273.6	<2	1.0 (>0.05)
BOD_5	mg/L	68.99	71.7	<10	1.0 (>0.05)
F coliform	Cfu /100mL	2.21×10^4	4.02×10^3	<10	1.0 (>0.05)

Table 3 COD/BOD_5 ratio and COD:N:P ratios of bathroom and laundry GW

Biodegradability	Direct	Easy	Very slow
COD/BOD5ratio	< 2	2 - 5	> 5

Table 4 COD/BOD_5 ratio and indicted biodegradability

GW Source	COD/BOD_5Ratio	COD: N:P Ratio
Bathroom	11.53	100:9.9:2
Laundry	12.27	100:10.3:3.6

3.4.2. Performance of the GW treatment system for bathroom GW

According to Table 6 turbidity, total coliform, TS, TSS, BOD and COD of raw laundry GW were significantly reduced by the GW treatment unit. Turbidity, total coliform, TS, TSS, BOD and COD of GW were removed by 57.50%, 98.96%, 91.53%, 50.0%, 33.33%, 65.67%, 51.52%, respectively.

Table 5 Results of the paired t - test comparing raw bathroom GW and treated bathroom GW

Parameters	Raw laundry GW	After filtration		After adsorption	Total effluent Removal (%)	Paired sample t test analysis result	
	Average influent	Filtration Effluent	Efficiency (%)	Adsorption Effluent	Efficiency (%)		
PH	7.29	6.53		7.27			0.431(>0.05)
Turbidity (NTU)	46.8	31.4	32.9	19	39.5	59.4	0.006(<0.05)
Fecal Coliform (CFU/100mL)	2.20×10^2	2.20×10^2	0.0	2.40×10^2	-9.1	-9.1	0.581(>0.05)
Total Coliform (CFU/100mL)	5.30×10^4	4.80×10^4	9.4	6.40×10^3	86.67	87.9	0.0(<0.05)
TS (mg/L)	400	200	50	200	0.0	50.0	0.0(<0.05)
TSS (mg/L)	120	130	10	100	7.4	16.7	0.021(<0.05)
BOD (mg/L)	126	60	52.4	48	20.0	61.9	0.0(<0.05)
COD (mg/L)	188.2	94.12	50	94.1	0.0	50.0	0.0(<0.05)

Table 6 Results of the t- test comparing average treated laundry GW values with WHO standard for toilet flushing

Parameters	Raw bathroom GW	After filtration		After adsorption		Total effluent Removal (%)	Paired sample t test analysis result
	Average influent	Average Effluent	Efficiency (%)	Average Effluent	Efficiency (%)		
PH	7.94	7.9		8		-	
Turbidity (NTU)	40	28	30	17	39.29	57.50	0.0(<0.05)
Fecal Coliform (CFU/100mL)	4.24×10^4	5.40×10^2	98.73	4.40×10^2	18.52	98.96	0.0(<0.05)
TS (mg/L)	200	100	50.00	100	0.00	50.0	0.0(<0.05)
TSS (mg/L)	120	90	25.0	80	11.11	33.33	0.007(<0.05)
BOD (mg/L)	67	36	46.27	23	36.11	65.67	0.0(<0.05)
COD (mg/L)	131.9	89.8	31.92	64.3	28.40	51.52	0.0(<0.05)

1

3.4.3. Potential for reuse of treated laundry GW for toilet flushing

To determine the potential for reuse of treated laundry GW for toilet flushing filtered GW characteristics compared with the WHO standards. As shown in Table 7 average turbidity, BOD_5 and total coliform of treated laundry GW were significantly higher than the WHO standard for toilet flushing. (p=1.00 for each parameter).

3.4.4. Potential for reuse of treated bathroom GW for toilet flushing

As shown in Table 8, average turbidity, BOD_5 and total coliform of raw GW were significantly higher than the WHO standard for toilet flushing (p=1.00 for each parameter). Therefore, treated bathroom GW in this study cannot be reused for toilet flushing.

Table 7 Results of the t- test comparing average treated GW values with WHO standard for toile

Parameters	Unit	After treatment Laundry Average	WHO standards	Comparison α= 0.05 95% confidence level
PH		7.27	6-9	0.0 (<0.05)
Turbidity	NTU	19	<2	1.0 (>0.05)
BOD_5	mg/L	48	<10	1.0 (>0.05)
F coliform	Cfu /100mL	6.40×10^3	<10	1.0 (>0.05)

1

Table 8 Results of the t- test comparing average treated bathroom GW values with WHO standard for toilet flushing

Parameters	Unit	After treatment bathroom Average	WHO standards	Comparison α= 0.05 95% confidence level
PH		8	6-9	0.0 (<0.05)
Turbidity	NTU	17	<2	1.0 (>0.05)
BOD_5	mg/L	23	<5	1.0 (>0.05)
T coliform	Cfu /100mL	1.22×10^3	<10	1.0 (>0.05)

4. CONCLUSION

Bathroom GW in Galle, Sri Lanka is characterized with very high average concentrations of turbidity, TN, TP, COD, and TSS with average values of 135.8 NTU, 78.6 mg/L, 15.9 mg/L, 794.4 mg/L and 195 mg/L, respectively compared to the literature values. Laundry GW results of all analyzed parameters complied with those already published except the TN values. Laundry GW higher in both organics and physical pollutants compared to the bathroom GW. COD/ BOD_5 ratio of the bathroom and laundry GW is found to be very high indicating that less potential for biodegradability for aerobic treatment options. Also, bathroom and the laundry GW are deficient in both nitrogen and phosphors. Therefore, it is suggested to mix kitchen GW to treat through the biological processes. The research showed that the quality of bathroom and laundry GW of Galle, Sri Lanka with respect to physical, chemical and biological characteristics requires adequate treatment prior to household reuse. In order to meet the reuse standards, bathroom and laundry GW filtered through the laboratory scale filtration and adsorption GW treatment system. Overall performance of the treatment system for bathroom GW was 57.5% turbidity removal, 50% COD removal, 33.3% TSS removal, 65.67% BOD removal and 51.5% COD removal. The overall performance of the treatment system for laundry GW treatment was 59.4% turbidity removal, 50% COD removal, 16.7% TSS removal, 61.9% BOD removal and 50% COD removal. However, treated bathroom and laundry GW was found to be not suitable for toilet flushing.

5. ACKNOWLEDGEMENTS

The authors would like to acknowledge Hitosubashi University and the Ochanomizu university of Japan for financial and technical assistance to conduct this research. The authors acknowledge the support of the Faculty of Engineering and Faculty of Agriculture of the University of Ruhuna Sri Lanka. Special thank goes to D. A. M. Nimal Shanthi, W. R. T.

Thathsaranee and A.T.M. Ahsan for their support in this study.

6. REFERENCES

Dolnicar, S. and Hurlimann, A., 2009, 'Drinking water from alternative water sources: differences in beliefs, social norms and factors of perceived behavioural control across eight Australian locations',*Water Science and Technology*, 60(6), pp.1433-1444.

Dwumfour-Asare, B., Adantey, P., Nyarko, K.B. and Appiah-Effah, E., 2017,'Greywater characterization and handling practices among urban households in Ghana: the case of three communities in Kumasi Metropolis',*Water Science and Technology*, p.wst2017229.

Edwin, G.A., Gopalsamy, P. and Muthu, N., 2014,'Characterization of domestic gray water from point source to determine the potential for urban residential reuse: a short review',*Applied Water Science*, 4(1),pp. 39-49.

Eriksson, E., Auffarth, K., Henze, M., Ledin, A., 2002,'Characteristics of grey wastewater', *Urban Water* 4, pp.85–104.

Erlangung, Z., Weingärtner, D.E., 2013,. 'Greywater Characteristics' , Biodegradability and Reuse of some Greywaters.

Ghaitidak, D.M. and Yadav, K.D., 2013, 'Characteristics and treatment of greywater—A review',*Environmental Science and Pollution Research*,20(5), pp.2795-2809.

Ghunmi, L.A., Zeeman, G., Fayyad, M. and van Lier, J.B., 2011,' Grey water treatment systems: A review', *Critical reviews in environmental science and technology*, 41(7), pp.657-698.

H.I, Abdel-Shafy., El-Khateeb, M.A. and Shehata, M., 2014,'Greywater treatment using different designs of sand filters',*Desalination and Water Treatment*, 52(28-30): 5237-5242.

Hourlier, F., Masse, A., Jaouen, P., Lakel, A., Gerente, C., Faur, C. and Le Cloirec, P., 2010, 'Formulation of synthetic greywater as an evaluation tool for wastewater recycling technologies',*Environmental technology,* 31(2)., pp.215-223.

Jefferson, B., Palmer, A., Jeffrey, P., Stuetz, R. and Judd, S., 2004,'Grey water characterization and its impact on the selection and operation of technologies for urban reuse',*Water science and technology,* 50(2): pp.157-164.

Kulabako, R. N., KM Ssonko, N. and Kinobe, J., 2011,'Greywater characteristics and reuse in tower gardens in Peri-Urban Areas-experiences of Kawaala, Kampala, Uganda',*The Open Environmental Engineering Journal,* 4(1).

Li, F., Wichmann, K. and Otterpohl, R., 2009' 'Evaluation of appropriate technologies for grey water treatments and reuses, *Water Science and Technology*,59(2): pp.249-260.

Oki, T. and Kanae, S., 2006,' Global hydrological cycles and world water resources',science,313(5790): 1068-1072.

Utsev, T., Mama, C.N., Ekwueme, A. and Nnaji, C.C., 2014,'Feasibility of a filtration-adsorption grey water treatment system for developing countries',*Hydrology: Current Research*, 1: 1.

Winward, G.P., Avery, L.M., Stephenson, T. and Jefferson, B., 2008,'Chlorine disinfection of grey water for reuse: effect of organics and particles',*Water Research*,42(1-2), pp.483-491.

Li, Z., Boyle, F. and Reynolds, A., 2009,'Rainwater harvesting and greywater treatment systems for domestic application in Ireland',*Science of the Total Environment*,260(1-3),pp.3439–3449.

Proceedings of the 7th International Symposium on

Advances in Civil and Environmental Engineering Practices for Sustainable Development

ACEPS - 2019

Laboratory wastewater treatment using clay bio char composites in horizontal flow bio-geo filters.

S.Niruparan[1], K.Karthika[1] , W.G.D.K.S.Madushika[2] and B.C.L.Athapattu[1]

[1] Department of Civil Engineering, Faculty of Engineering Technology, The Open University of Sri Lanka, Nawala, Nugegoda, SRI LANKA
[2]Department of Civil Engineering, College of Engineering, Institute of Engineering, SRI LANKA

K e y w o r d s

Bio char
Clay bio char composite
Bio-geo filter
Contaminants
Constructed wetland

A B S T R A C T

In Sri Lanka generated laboratory wastewater is onsite stored and then given to licensed collectors by Central Environmental Authority for treatment and disposal. Some are disposing their hazardous waste in unsuitable manner with water streams, cannels, municipal wastes etc. These malpractice lead to create severe environmental and health impacts. This paper proposes an ecofriendly, economical, and efficient method to treat these laboratory wastewaters.
Raw wastewater from laboratory were tested and analyzed. Clays from Murunkan area and cinnamon bio chars were characterized. Based on the results of raw laboratory wastewater pilot type wastewater treatment plant was designed. Bio char and clay-bio char composite was designed as a filter media. Vegetations are planted as bio filter. It has been identified Horizontal flow subsurface flow constructed wetland system using the bio-geo filter is an ecofriendly, cost effective and economical solution to treat laboratory wastewater due to its low flow rate and high contaminants.

1. INTRODUCTION

Wastewater is any water that has been affected by human use. Wastewater is "used water from any combination of domestic, industrial, commercial or agricultural activities, surface runoff or storm water, and any sewer inflow or sewer infiltration" (Tilley *et al*., 2014).

Characteristics of wastewater vary depending on the source. Industrial, commercial and domestic wastewaters and their treatments are preferentially discussed due to their flow rates and their impact on health and environmental system. Wastewater from laboratories are less considered due to their low flow rate (Small scale), even though it gives bad impact on human and environmental system.

Wastewater from the laboratories contains lots of pollutants. Laboratory wastewater contain hazardous chemical wastes, reactive chemicals, corrosive waste, radioactive wastes, infectious wastes, infectious microorganisms and toxic chemicals etc based on the function of laboratory.

Physical and chemical pollutants from laboratory wastewater contain heavy metals such as As, Cd, Hg, Pb, Cr, etc, Soluble Organic materials, Inorganic Particles (sand, grit, metals, ceramics), Soluble inorganic materials (Ammonia, Cyanide, Hydrogen Sulfide), Toxins (Pesticide, Herbicide, Poisons), Pharmaceuticals etc. Biological pollutants from laboratory wastewater contain pathogens (Bacteria, Viruses, Protozoa, and Parasites) (Akpor *et al*., 2014). Laboratory waste generated from various commercial, industrial and other institutional sources causes an immense environmental problem. It affects health and quality of life of people, particularly the residents in urban and sub urban areas. This study focuses on the wastewater from biology and chemistry laboratory of Vavuniya campus, University of Jaffna. Wastewaters from these laboratories

are rich in heavy metal, toxic chemicals and hazardous wastes.

Generation of wastewater from laboratories such as academic and research purposes are considered in this study. There are fifteen UGC authorized state universities, five Ministry of Higher Education authorized university and several colleges and specialist institutes are recognized as degree awarding bodies in Sri Lanka. Meanwhile there are some government laboratories such as SLSI, NBRO, NWSDB, ITI, CEA, CECB, NERD and several private laboratories are extending their service in Sri Lanka. Contaminants from these laboratories have to be treated in a proper manner before discharge in to inland surface water. Central Environmental Authority the implementing body of Democratic Socialist Republic of Sri Lanka has framed regulations for the Management of Hazardous Wastes. CEA has published Hazardous Waste Management in 1996 and initiated Environmental Protection Licensing procedures. "However, these regulations were not fully implemented yet due to a number of practical problems; especially lack of laboratory facility for identification and classification of waste in Sri Lanka and more significantly the absence of an environmentally sound final disposal facility in the country" (Guidelines For The Management Of Scheduled Waste In Sri Lanka-2008). Currently National Environmental (Protection & Quality) regulation No. 01 of 2008 by the gazette notification No 1534/18 is in practice for the Management of Scheduled Waste in Sri Lanka.

Most of the laboratories in Sri Lanka, onsite storing their hazardous wastages for a maximum period of 90 days or a maximum quantity of 10,000 Kgs, permitted by the CEA. Collection and transportation of scheduled waste to off-site storage, treatment and /or disposal facility is done by the registered and licensed person. Ultimately these scheduled wastages can undergo Recovery Co Processing and Recycling, Treatment and Disposal process based on its category. Some laboratories are operating owned treatment and disposal systems. Meanwhile, wastewater from few laboratories is released to the canals, rivers, sewers, municipal wastes, and other water streams without proper treatment. There are lots of hazardous and toxic chemicals in it, which causes diseases to human and pollute our environmental system.

Wastewater generated from laboratory contains heavy metals, flammable, soluble and hazardous and toxic chemicals. Heavy metals have negative effects on the growth of aquatic organisms and depress the number of living organisms in aquatic eco system. Amongst the pollutant's pesticides, heavy metals, and detergents are the major cause of concern for aquatic environment because of their toxicity, persistency and tendency to accumulate in organisms (Rajeswari and Sailaja, 2014). Consumption of heavy metals through vegetables, corn products leads to kidney dysfunction, renal dysfunction, bone defects, etc. Diarrhoea, typhoid, paratyphoid and other *Salmonella* type diseases are caused by bacterial pathogens.

As solicitation it is required to have an eco-friendly, economical small-scale treatment system have to be adopted before discharging the laboratory wastewater in to inland surfaces. Horizontal flow constructed wetlands by using bio-geo filters are well suited for this purpose.

2. LITERATURES REVIEW

Bio-geo filter system is an engineered constructed wetland system to remove pollutants in wastewater by using plants and geo materials. Constructed wetlands are considered a technical, economical, and environmentally sustainable solution for small scale and decentralized wastewater treatment system. The main components of the wetland are wetland vegetation, substrate or media, water and living organisms in the wetland (Bodin, 2013). The high purification efficiency of constructed wetlands can be achieved by choosing suitable growth media. Clay bio char is considered as a filter media. Clay particles are very small and having a high to very high specific surface value. Montmorillonite clay particles having cation exchange capacity, multi cation absorption ability, intercalation/exfoliation chemistry etc. Clay from Murunkan area is rich in Montmorillonite. In Sri Lanka although such deposits are absent, montmorillonite-rich clay occurrences can be found in arid regions. Murunkan is an area which is composed of soil with higher montmorillonite content (Senevirathna, S. M. N. M. S. And Senaratne, A, 2011).

Bio char is a carbon rich material. It is obtained when biomass is heated in a closed

container in absence of air. Generally, bio char is characterised by having a large surface area, low density and high porosity, which makes it an efficient adsorbent and good biofilm carrier. Due to its large surface area, charged surface, and functional groups, Bio char is of great potential to adsorb heavy metal and organic contaminants. Very few studies have been done for the cinnamon bio char in wastewater treatment. But Cinnamon is abundantly available in Sri Lanka and it is a low-cost material. In this study, Murunkan Clay and Cinnamon bio char composites are used as a filter media in horizontal flow constructed wetlands.

Constructed wetlands are more preferred for university laboratory wastewater treatment due to its less flow rate, decentralization and cost effectiveness. This study focuses on treatment of university laboratory wastewater by environment friendly methods.

3. MATERIALS AND METHODS

3.1. Materials

- Clay

  Extracted Montmornolite clay from Murunkan soil was used in this study. The clay was grinded and sieved through 150µm sieve to achieve the particle size smaller than 150 µm.
- Biomass

  Cinnamon bio char was used in these experiments due to its low cost and high availability. It was grinded and sieved to achieve a particle size smaller than 150µm.

3.2. Characterization

3.2.1. Characterisation of clay

Several studies confirm the presence of Montmornolite in Murunkan clay through X-ray fluorometer (XRF), FTIR, UV Visible spectrometry, SEM and XRD tests (2,7). Laser diffraction particle size analysis test was done for Clay Samples collected from Murunka area.

3.2.2. Characterisation of Bio Char

Properties of the bio char bulk density, specific surface area, surface composition, particle density, particle size, macro & micro porosity, and water holding capacity was determined in this test (Jayashree *et al*., 2014).

3.3. Methodology

3.3.1. Sampling of Wastewater

Laboratory wastewater was sampled from on-site storage tank and then diluted with distilled water by 1:10 volume ratio. These laboratory wastewater properties were tested and tabulated.

3.3.2. Bio-Geo Filter

The Bio–Geo Filter (BGF) is based on Horizontal Flow (HF) Constructed Wetlands and it is considered as an ideal treatment system that suits for the treatment of Laboratory Waste water with a combination of bio and geo materials. Constructed wetlands (CWs) are an efficient technology designed for the wastewater treatment by imitating natural principals occurring in natural wetlands, marshes, and lagoons. Wetland technology is simple, inexpensive, efficient, easy to operate and maintain as compared to the traditional methods of wastewater treatment (Kivaisi, 2001).

The pollutant removal in these wetlands is achieved by the intensive action of its biotic and abiotic components such as bacteria, fungi, algae, media type, filtration, adsorption and sedimentation. These organisms contribute to the reduction and removal of organic and inorganic pollutants, and pathogens by various treatment mechanisms such as microbial interactions and uptake by vegetation. Abiotic mechanisms include sedimentation, filtration, chemical precipitation, and adsorption. The main characteristics responsible for the removal efficiency of CWs are hydraulic residence time, temperature, vegetation type, porous media, and microbial activity (Kadlec and Wallace, 2009, Dordio *et al*., 2009

Bio char derived from the agricultural biomass and they are carbon rich material which has the ability to remediate organic and inorganic contaminants (Gupta *et al*., 2014). Bio char is well known for its capability for

carbon storage and reducing or suppressing CO_2, CH_4, and N_2O production in soil and may contribute to the reduction in atmospheric greenhouse gases. Bio char might be used for removing contaminants from water while also being loaded with nutrients for subsequent use as a soil amendment, providing long-term sorption capacity and a fertilizer (Vymazal, 2013, Liang *et al*., 2009, Liu and Zhang, 2009).

In our prototype model first Murunkan clay and cinnamon bio char were grinded and sieved through 150µm sieve and those were mixed in 1:5 mass ratio. This bio char composite again sieved through 150µm and mixed with distilled water to prepare balls. Prepared sample was kept in desiccator to avoid swelling effects. Approximately 2mm diameter balls were prepared for filter media. Pyrolized cinnamon bio char was crushed in to 2mm size particles and filled it in the tank

4. RESULTS AND DISCUSSION

Laboratory wastewater samples were collected form Vavuniya campus in three on site laboratory wastewater storage tanks. This sample shows severely high heavy metal concentration and toxic & harmful concentration. Central Environment Authority has published Wastewater discharge standards (Effluent Standards) in to inland surfaces. Inorganic pollutants are extremely harmful due to their high toxicity and non-biodegradability.

Horizontal flow engineered constructed wetland has been to use to remove laboratory contaminants by physical, chemical and biological methods in environment friendly manner. Though this system design considered the discharge of Industrial Waste Water into Inland Surface Waters, special design considerations are taken for the toxic and heavy metal removal. Under physical treatment method sedimentation and filtration techniques are designed and chemical treatment method adsorption and ion exchange techniques are designed to remove contaminants in laboratory wastewater. Under biological treatment method phytoremediation is used to remove pollutants (Rizwan and Athapattu, 2014).

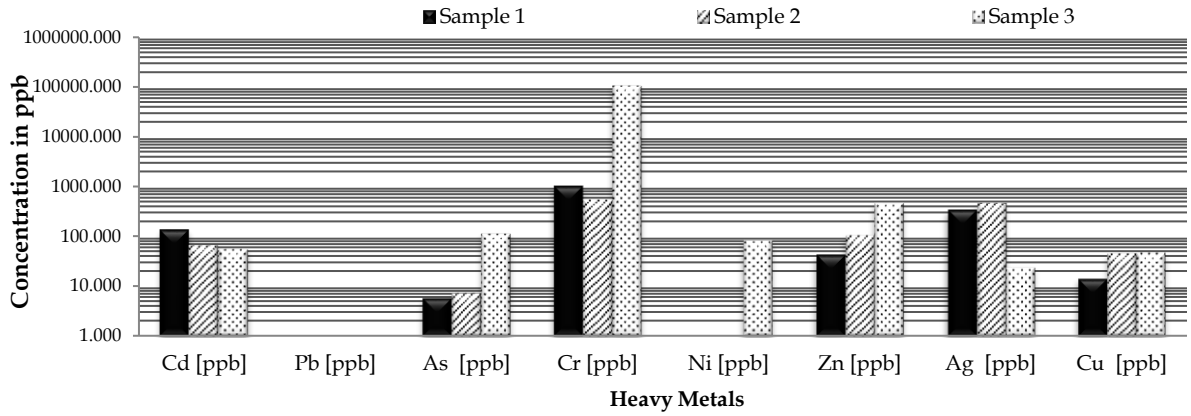

Figure 1 Concentration of heavy metals in laboratory wastewater

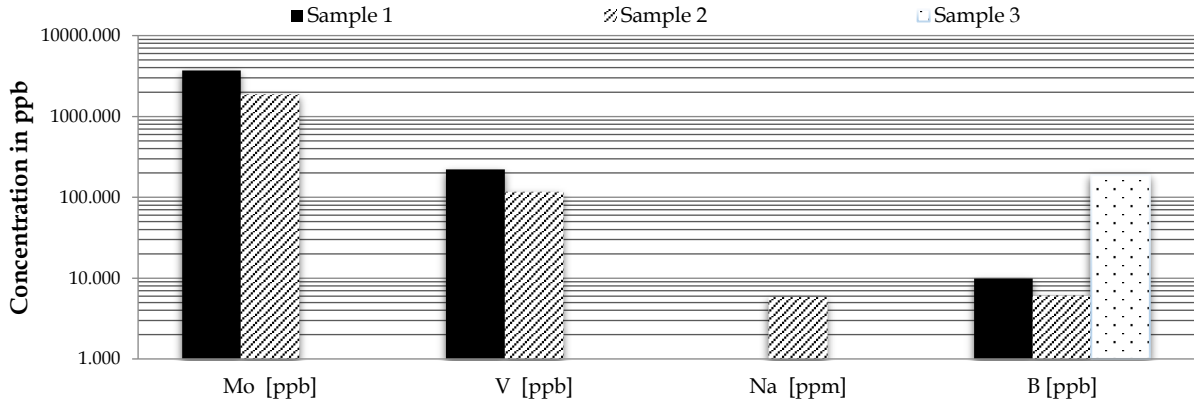

Figure 2 Concentration of toxic and harmful elements in laboratory wastewater

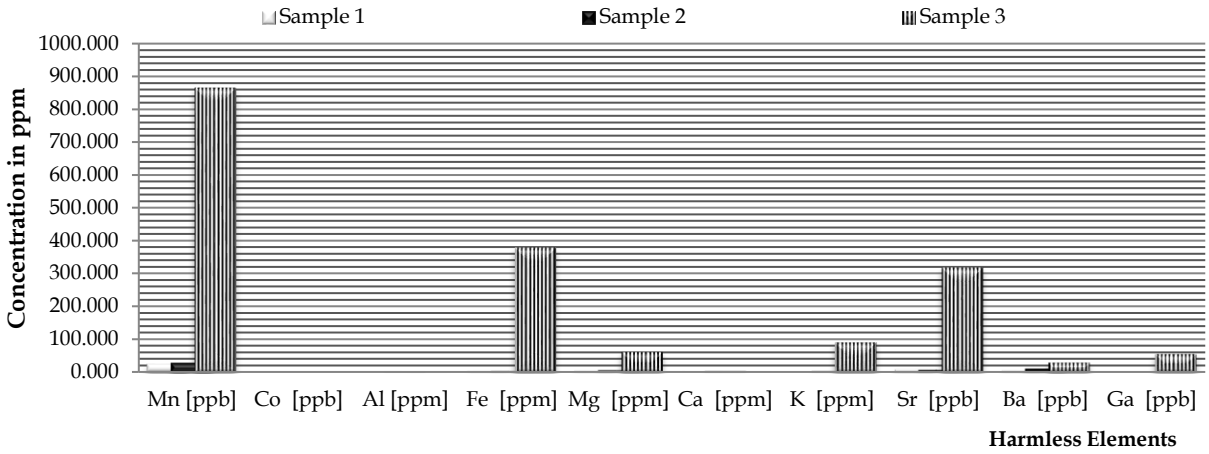

Figure 3 Concentration of harmless elements

Adsorption technology is effective, economical and eco-friendly method, which is used to remove heavy metals in laboratory wastewater. Clay sample collected from Murunkan basin is expected to perform this operation. Several studies conducted in characterisation of montmorillonite in Murunkan area. Clay sample collected from Murunkan basin shows 40% silica content and 5% of Nano particles. In order to increase the efficiency extracted clay can be used for this purpose.

Phytoremediation technology is used to remove heavy metals in wastewater by biological methods. In phytoremediation technique plants breakdown, reduce, degrade, and remove the pollutants from wastewater. This is ecofriendly, simple, and cost-effective method to remove contaminants in laboratory wastewater. Plants like Cattails, reeds, cannas are locally available suitable for this purpose.

Bio char (BC) is the carbon-rich product derived from, when biomass is pyrolized. Cinnamon bio char prepared by low pyrolysis (400°C) is used to remove pollutants. Bio chars have Cation and Anion Exchange ability, Pore volume, aliphatic functional group, etc. which enhance the removal of contaminants from wastewater.

Composite of clay bio char improves the properties of soil such as the water-holding capacity, organic matter content, aeration condition, pH value, cationic exchange capacity (CEC), and the formation of aggregates of soil. Since the heavy metal concentration and toxic and harmful material concentration are high, clay bio char was selected as a filter media in horizontal flow bio-geo filtration. Retention time of wastewater in the constructed wetland is estimated as 3-5 days.

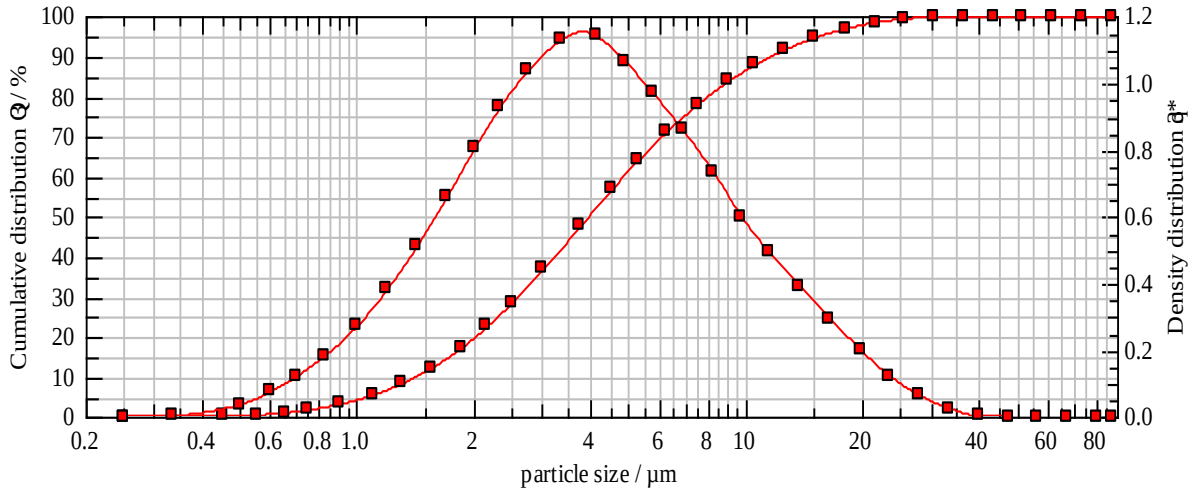

Figure 4 Sample No 01: 8°52'04.0"N 80°00'58.9"E

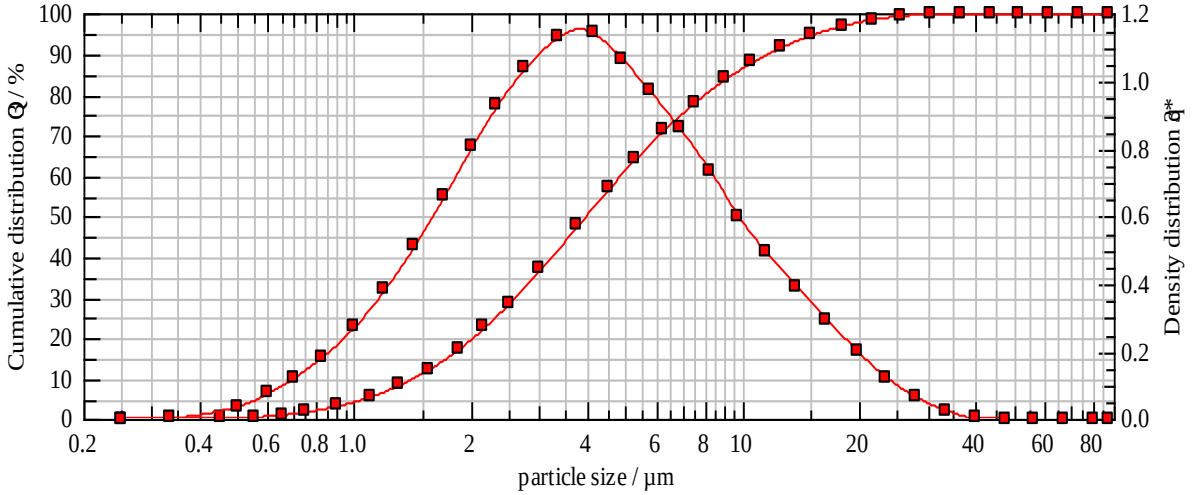

Figure 5 Sample No 02: 8°50'14.1"N 80°01'33.3"E

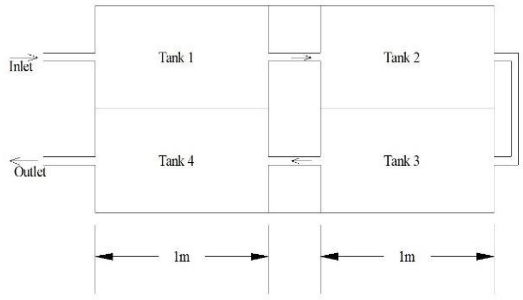

Figure 6 Plan view of pilot plant

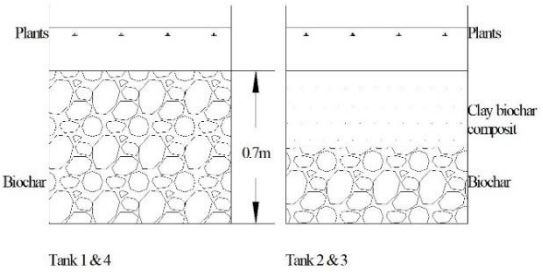

Figure 7 Cross section of tanks

Design of absorption unit is based on the wastewater flow rate and concentration of pollutants in the laboratory waste water. Biochar clay-biochar and plants and designed to remove the pollutants from laboratory wastewater.

5. CONCLUSION

Bio char is having large surface area, charged surface, functional groups, which adsorbs heavy metals and organic contaminants. Further bio char decreases the bioavailability, toxicity, and mobility of organic and inorganic pollutants. Since the Concentration of contaminants in laboratory wastewater is high, Cattails and reeds are selected for high tolerance for many types of wastewater. Treatment of laboratory wastewater by horizontal flow constructed wetland using bio geo filters found to be cost-effective, economical, and simple engineered system to remove contaminants in laboratory wastewater.

6. REFERENCES

Akpor, O. B., Ohiobor, G. O. and Olaolu, T. D., 2014, 'Heavy metal pollutants in wastewater effluents: Sources, effects and remediation', *Advances in Bioscience and Bioengineering*, 2(4), pp.37, Doi: 10.11648/J.Abb.20140204.11.

Aksu, I., Bazilevskaya, E. and Karpyn, Z. T., 2015, 'Swelling of clay minerals in unconsolidated porous media and its impact on permeability', *Georesj*, 7 September 2015, pp.1–13, Doi: 10.1016/J.Grj.2015.02.003.

Ana V. Dordio, A.J. Estêvão Candeias, A.P. Pinto, C. Teixeira Da Costa and Carvalho, A. J. P., 2009, 'Preliminary media screening for application in the removal of clofibric acid, carbamazepine and ibuprofen by ssf-constructed wetlands', Ecological Engineering, 5(35), pp.290–302.

Bodin, H., 2013, 'Wastewater treatment in constructed wetlands: effects of vegetation, hydraulics and data analysis methods', Available at: Https://Pdfs.Semanticscholar.Org/0ee1/8df782c874e8d2447c8d3811755e4204f0bb.Pdf (Accessed: 09 September 2019).

Elvis Fosso-Kankeu, Frans. B. Waanders, F. W. S.,2015, 'The preparation and characterization of clay-biochar composites for the removal of metal pollutants', *In 7th International Conference on Latest Trends in Engineering & Technology (Icltet'2015)*, Irene, Pretoria, South Africa, pp.54–57, Doi: 10.15242/Iie.E1115016.

Gupta, P., Ann, T. W. and Lee, S. M., 2016, 'Use of bio char to enhance constructed wetland performance in wastewater reclamation', *Environmental Engineering Research*, 21(1), pp. 36–44. Doi: 10.4491/Eer.2015.067.

Jayashree, Dhote, C. A. and Sangita, I., 2014, 'Design of laboratory based waste water treatment plant', *International Research Journal of Science & Engineering*, 2(3), pp.104–111.

Kadlec, R. H. and Wallace, S., 2008, *Treatment Wetlands*, Second Edition, CRC Press.

Kivaisi, A. K., 2001, 'The potential for constructed wetlands for wastewater treatment and reuse in developing countries: A Review', *Ecol. Eng*., 16, pp.545–560. Doi: 10.1016/S0925-8574(00)00113-0.

Liang, B., Lehmann, J., Solomon, D., Kinyangi, J., Grossman, J. And O'neill, B., 2006, 'Black carbon increases cation exchange capacity in soils', *Soil Sci Soc Am J*. 70, pp.1719–1730.

Liu, Z., and Zhang, F. S., 2009, 'Removal of lead from water using biochars prepared from hydrothermal liquefaction of biomass', *J. Hazard. Mater*, 167, pp.933–939, Doi:10.1016/ J.Jhazmat.2009.01.085.

Rizwan, M.M. and Athapattu, B C L., 2014, 'Removal of nutrients from urban water by engineered constructed wetland with bio-geo filter and biotope', 2(2), pp.39–55.

Senevirathna, S. M. N. M. S. and Senaratne, A. ,2011, 'Characterization and beneficiation of montmorillonite in clay deposits, murunkan, Sri Lanka', *Proceedings of The Peradeniya University Research Sessions*, Sri Lanka, Vol. 16, 24',In.Doi: Http://Dx.Doi.Org/10.5713/Ajas. 14.0275.

Tilley, E., Lüthi, C., Morel, A., Zurbrügg, C. and Schertenleib, R., 2014, 'Compendium of sanitation systems and technologies', 2nd Rev. Ed. Dübendorf, Switzerland.

Vymazal, J., 2013, 'The use of hybrid constructed wetlands for wastewater treatment with special attention to nitrogen removal: A review of a recent development', *Water Research. Elsevier Ltd*, 47(14), pp. 4795–4811. Doi: 10.1016/J.Watres.2013.05.029.

Raja Rajeswari, T. and Namburu Sailaja (2014) 'Impact of heavy metals on environmental pollution', *National Seminar On Impact Of Toxic Metals, Minerals And Solvents Leading To Environmental Pollution- Journal Of Chemical And Pharmaceutical Sciences,* ISSN: 0974-2115

Proceedings of the 7th International Symposium on

Advances in Civil and Environmental Engineering Practices for Sustainable Development

ACEPS - 2019

Treating heavy metals in the groundwater contaminated by landfill-leachate using Permeable Reactive Barriers (PRBs) packed with building wastes and dewatered alum sludge.

W.R.A.U.Dilrukshi [1] and W.K.C.N.Dayanthi[1]

[1]Department of Civil and Environmental Engineering, Faculty of Engineering, University of Ruhuna, Hapugala, Galle, SRI LANKA

K e y w o r d s

Permeable reactive barriers
Reactive media
Column experiment
Heavy metals
Contaminated ground water

A B S T R A C T

Leachate generation from landfill has become one of the major problems in especially the developing countries. The higher concentration of heavy metals in the leachate may cause severe health problems when it is mixed with groundwater plumes. Permeable reactive barriers (PRBs) can effectively be used to treat the groundwater contaminated by the landfill-leachate as a sustainable in-situ treatment method. The main engineering challenges are to select low-cost and readily available reactive materials to be filled in PRB walls, and effective placement methods so as to increase the heavy metal treatment efficiency. In this study, building wastes, namely concrete waste (CW), brick and mortar waste (BMW), roofing waste (RF), flooring waste (FW); and dewatered alum sludge (DAS) were selected as the reactive materials. The removal efficiencies given by different types of building wastes are as follows: concrete waste -78%, 58% and 56% for Fe^{3+}, Pb^{2+}, and As^{3+}, respectively; brick and mortar waste- 85%, 78% and 68% of Fe^{3+}, Pb^{2+}, and Mn^{2+} respectively; roofing waste-92%, 56% and 58% for Fe^{3+}, Mn^{2+} and Zn^{2+}, respectively; flooring waste-79% and 70% for Fe^{3+} and Pb^{2+} respectively and dewatered alum sludge alone gave 92%, 73% and 64 % for Fe^{3+}, Pb^{2+} and Mn^{2+}, respectively. There were slight changes of physical and mechanical properties of these reactive materials due to the interaction with the landfill leachate during the experimental period.

1. INTRODUCTION

Nowadays, municipal solid waste discarding has become one of the major problems, especially in the developing countries. Although, sanitary landfills have been one of the most economical and widely acceptable methods for solid waste disposal, there is no enough space to discharge all solid waste. On the other hand, landfills give a severe damage to the environment through leachate, odor and etc. Landfill-leachate is generated from water passing through the solid waste or from liquids which already exists in waste (Mahmoudkhani et al. 2011).

Landfill leachate contains many hazardous heavy metals, organic and inorganic compounds and nutrients in large amounts. Although these contaminants are treated to a certain extent by natural processes, a considerable amount of heavy metals remains in the leachate. When this leachate is discharged to a ground water plume, it gets contaminated due to the contaminants contained in the leachate such as heavy metals and organic compounds. Thereafter this groundwater plumes may connect with surface water bodies allowing contaminants to dissolve easily in the fresh water and accumulate. This polluted water resources may cause adverse impacts on the human health and entire environment. Hence this heavily polluted leachate should be treated before it enters the ground water body. There are several types of treatment methods available in the world to treat landfill leachate such as biological, chemical and physical treatment.

Most of research has been conducted to remediate the groundwater using various methods. As well as PRB is an in-situ method, which is a good replacement for 'Pump- and-treat' method. In 'pump- and- treat method', the leachate is pumped onto the ground surface and then treated as required. Due to the drawbacks already found during previous researches, this method cannot be used to treat number of potentially harmful chemicals dissolved in groundwater (Dayanthi et al. 2014). As well as 'pump- and- treat method' is a high cost method, which is not practicable for developing countries.

Landfill-leachate contains high concentration of heavy metals such as Fe, Pb, Zn, Mn, As and Cu. When leachate mixes with a groundwater plume, it gives severe health problems. A permeable reactive barrier (PRB) can be used as a sub-surface emplacement of reactive materials through which the contaminated ground water plume flows typically under natural gradients. Treated water is collected from the other side of the PRB. PRBs are considered as low- cost, effective alternative for remediating contaminated groundwater or sites (Dayanthi et. al. 2014).

PRB is an in-situ method, which is a good replacement for 'Pump- and- treat' method. In 'pump- and- treat method', the leachate is pumped onto the ground surface and then treated as required. Due to the drawbacks already found during previous researches, this method cannot be used to treat number of potentially harmful chemicals (Dayanthi et al. 2014). As well as 'pump- and- treat method' is a high cost method, which is not practicable for developing countries.

In this study, building wastes and DAS were used as reactive media in PRBs targeting heavy metal removal of contaminated groundwater. The application of such waste materials usefully to solve another serious issue of landfill-leachate would be a novel approach. Such application would minimize further the cost associated with PRBs.

2. LITERATURE REVIEW

The past researches have already found that the dewatered alum sludge (DAS) is an effective reactive material in PRBs (Dayanthi et al. 2015). But there are not much past literature about building waste materials as the reactive packing media PRBs. Building wastes such as roof waste, floor tiles, concrete brick and mortar can be potential low-cost and readily available reactive materials, which can effectively be recycled in PRBs as reactive media due to the diverse properties they should have when considered the original materials they are composed of. Heavy metals are a major leachate parameter, which would adversely affect the environment once released. Hence experiments on heavy metal removal in the landfill-leachate using PRBs filled with a mixture of building wastes and DAS would be imperative.

According to the research carried by Gupta (2000) and Quek (2008), were found out that red mud has an ability to remove lead in wastewater up to 88% using column experiments. Demirbas A. (2008) regarding agro-based waste materials to treat heavy metals, Alfalfa was most effective at removing Zn in wastewater. Not only that according to the Ajmal et al. (2005) mustard oil cake removes Zn in wastewater up to 94% and dye loaded groundnut shells and saw dust cleans Zn with 90% removal efficiency.

Tarley C.R.T. (2003) has found that rice milling by products-rice husk can be used for removing Cd (II) from laboratory effluent. Under the optimized conditions, the results obtained were below those required by the EPA with 98% removal efficiency, producing a treated effluent, which could be discarded. Bentonite, compost and anaerobic sludge exhibited the greatest removal capacities of cadmium as 78, 65 and 90% respectively (Ulmanu et al, 2002). Sun H. (2005) has conducted a research to obtain the As removal efficiency of Zero valent ion using batch and column experiments. Panday KK, has found that Fly ash was also utilized for the removal of copper from aqueous solution.

3. METHODOLOGY

3.1. Overall Procedure

Four types of building waste materials and dewatered alum sludge were selected and prepared. For the experimental run, landfill-leachate was collected from Heenpandala dump site. Then the raw leachate was diluted ten times to represent the contaminated groundwater by reducing the contaminant concentrations. The physical properties of the reactive materials such as porosity, particle size distribution and specific gravity were

obtained before filling the reactive materials in columns. The experimental set--up consisted of four columns filled with selected reactive materials. The mechanical properties such as hydraulic conductivity and shear strength parameters (cohesion and friction angle) were also measured before commencing the experimental run. Influent was applied on the columns for a period of 65 days in down flow direction. To measure the heavy metal concentrations, electrical conductivity and ORP during the experimental run, influent and effluent samples were collected every 5-day period. Finally, the columns were unloaded and the reactive media were checked for all physical and mechanical properties mentioned above. A mass balance analysis was conducted for each type of heavy metal to estimate the overall removal efficiency.

3.2. Selection and Preparation of Reactive Materials

The reactive materials were selected under several criteria such as availability, targeted wastewater parameters and outcomes of past research. The selected reactive materials were concrete wastes (CW), brick and mortar wastes (BMW), roofing wastes (RW), flooring waste (FW) and dewatered alum sludge (DAS). Figure 1 shows the reactive materials used for the PRB columns. Concrete is contained with Portland cement, fine and coarse aggregates and admixtures such as fly ash, plasticizers and etc which may have higher heavy metal removal capacity. RW and BMW include clay. According to the past research, quarry dust, which is included in construction and demolition waste, have high efficiencies to remove heavy metals from leachate.

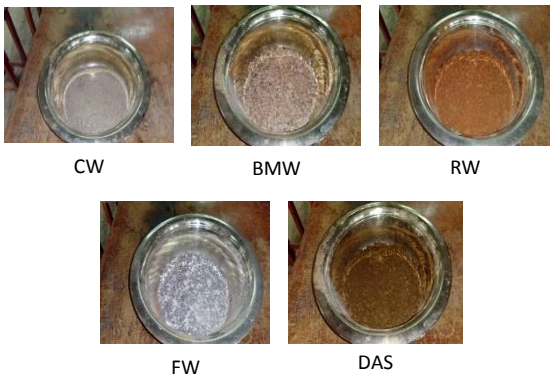

Figure 1 Selected reactive materials

The DAS was collected from the sludge drying bed of the Hapugala water treatment plant. The building wastes were obtained from the construction sites around the Galle area. After collecting reactive materials, all materials were crushed in to small particles to increase the contacts between leachate and reactive media particles.

3.3. Experimental run

The experimental set-up (Figure 2) consisted of an overhead influent storage tank, constant head tank, four PRB columns and an effluent storage tank. The influent flew from the overhead storage tank to PRBs through the constant head tank, which waste maintain the same flow rate in each PRB column

Each of 4 columns was filled with different types of building waste mixed with DAS on a volume ration of 4:1. The remaining column was filled only with DAS. Table 1 depicts the hydraulic loading criteria onto the PRB columns

Table 1 Hydraulic loading criteria on PRB columns

Column	Reactive Media	Hydraulic loading rate ($m^3/m^2.d$)	Pore volume HRT (d)
1	CW and DAS	0.2	0.7
2	BMW and DAS	0.2	0.7
3	RW and DAS	0.2	0.7
4	FW and DAS	0.2	0.6
5	DAS	0.2	0.6

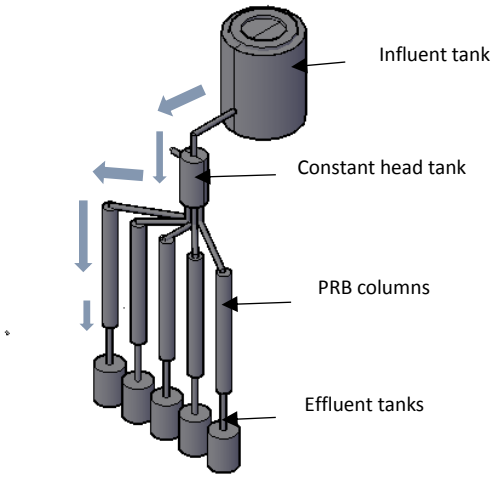

Figure 2 Laboratory- scale Column Experimental Set-up

3.4. Analysis of leachate parameters and reactive media properties

This study mainly focusses on heavy metals in the leachate such as Fe, Pb, Cd, Cu, Mn, Zn and As. The concentrations of these metals were measured using Atomic Adsorption Spectrophometer. Other than heavy metals conductivity, pH, TDS and ORP were measured using respective meters. Table 2 shows the apparatus used for the analyses.

Table 2 Analyses methods of wastewater parameters

Parameter	Unit	Apparatus
Fe, Pb, Cd, Cu, Mn, Zn, As	mg/L	Atomic Adsorption Spectrophotometer
Conductivity	µS/ cm	Multi-meter
Oxygen Reduction Potential (ORP)	mV	ORP meter
pH	-	pH meter

During the experimental run, both the influent and effluent samples were collected every 5-day period.

Figure 3 Collected samples

Figure 4 Atomic Adsorption Spectrophotometer

4. RESULTS AND DISCUSSION

When the ground water plume gets contaminated, there are several natural processes to treat the water plume. However, the treatment efficiency is not up to the desired level. Therefore, another treatment method is used for further treatment. This study has been conducted in order to check the treatment efficiency of building waste and dewatered alum sludge. When considering the results of this study, the treatment efficiency has reduced with time. This kind of efficiency reduction can happen due to the adsorption process. At the initial stage, there may be number of vacant sites for adsorption. During the experimental run, these vacant sites of the reactive media reduce due to the adsorption process. Hence, the adsorption rate decreases with time. Therefore, the treatment capacity of the reactive media could reduce.

4.1. Heavy metal removal

Table 3 shows the overall removal efficiencies for heavy metals. Figure 5 and 6 show the variation of the removal efficiency of Fe and Pb, respectively with time. Each mixture of materials gave a removal efficiency greater than 75% for Fe.

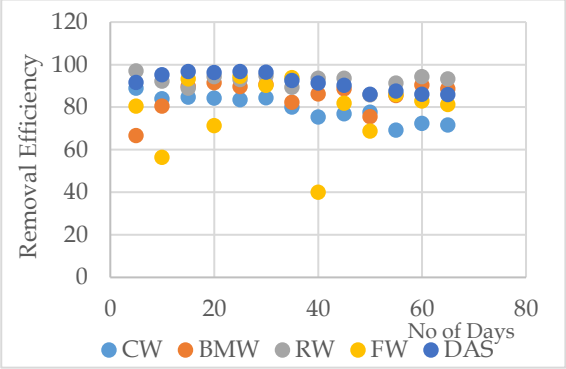

Figure 3 Variation of the removal efficiency of Fe

Except the mixture of roof waste and dewatered alum sludge, other four columns showed greater treatment efficiency for Pb. While BMW and DAS showed better performance on Mn more than 70%, 53%, a great Cu removal was shown by RW and DAS.

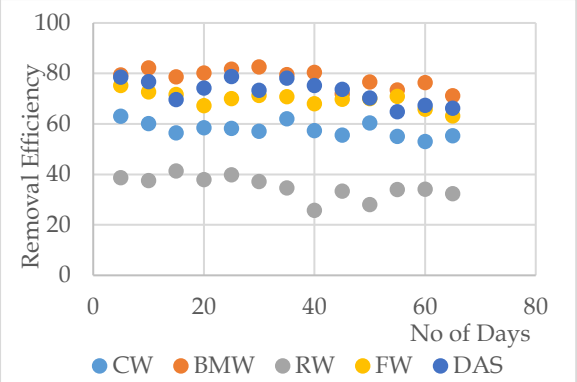

Figure 4 Variation of the removal efficiency of Pb

Table 3 Overall removal efficiencies for heavy metals

Parameter	Overall removal efficiency (%)				
	CW and DAS	BMW and DAS	RW and DAS	FW and DAS	DAS
Fe	79.0	85.0	92.4	79.6	91.4
Pb	57.7	77.5	35.2	69.8	72.6
Mn	42.8	71.5	56.4	60.3	63.8
Zn	48.8	54.6	58.4	51.6	55.2
Cd	48.1	37.5	53.7	57.9	56.2
As	54.9	21.9	45.8	22.6	31.8
Cu	31.0	38.9	53.1	19.3	33.8

Table 4 indicates the drinking water and effluent discharge standards for heavy metals. The effluent concentrations of all the tested heavy metals comply with the effluent discharge standards. The effluent concentrations of Fe, Mn, Zn and Cu satisfy the drinking water standards.

Table 4 Drinking water and discharge standards for heavy metals

Heavy metal	Max Effluent Concentration (µg/l)	Drinking water standards (µg/l)	Discharge Standards (µg/l)
Fe	0.2	300	3000
Pb	58.9	10	100
Mn	43.8	100	
Cd	9.8	3	100
Zn	53.6	3000	2000
As	84.3	10	200
Cu	72.7	1000	3000

4.2. pH, ORP and Conductivity variation

pH, oxidation reduction potential (ORP) and conductivity values were measured from each sample collected every 5-day period. While the mixture of BMW and DAS showed greater values for conductivity, DAS alone possessed the lowest conductivity values among the experimental units.

There is a linear relationship between ORP value and dissolved solid concentration. Nitrification processes happen with ample of DO concentration in aerobic environment. As well as denitrification occurs under anaerobic conditions (less DO concentration) when ORP value is in between -50 to +50 mV.

ORP values in the effluent of all 5 columns were greater than those of the influent. All ORP values were greater than 50 mV. Hence it implies that the PRB columns were in aerobic condition. ORP values increased with time indicating the occurrence of aerobic reactions inside columns.

pH in the influent samples was higher than that of effluent samples. As nitrification utilizes alkalinity, the reduction of alkalinity shown by the decrease of pH, proves the occurrence of nitrification inside columns.

4.3. Variation of reactive media properties

Table 5 depicts the variation of the porosity and hydraulic conductivity of the reactive materials before and after the experimental run.

Table 5 Variation of porosity and hydraulic conductivity

Reactive materials	Porosity		Hydraulic conductivity (cm/s)	
	Before	After	Before	After
CW & DAS	0.43	0.40	8.4×10^{-4}	5.0×10^{-4}
BMW & DAS	0.47	0.46	1.7×10^{-4}	1.3×10^{-4}
RW & DAS	0.51	0.5	1.7×10^{-1}	1.2×10^{-1}
FW & DAS	0.41	0.40	1.7×10^{-1}	1.4×10^{-1}
DAS	0.42	0.40	6.7×10^{-4}	5.1×10^{-4}

In all reactive materials, both of these values have decreased. This could be owing to the entrapment of contaminants inside pores.

5. CONCLUSION

The low-cost reactive media, concrete waste, brick and mortar waste, roof waste, flooring waste and dewatered alum sludge showed quiet different removal efficiencies for different heavy metals. They have the highest potential to treat Fe. Among the tested materials, roof waste, flooring waste and dewatered alum sludge had greater removal efficiencies in treating Fe, Pb, Mn, Zn and Cd. According to the results of past research, material such as granular activated carbon, bio char and sea sand have shown considerable treatment efficiencies in treating heavy metals. The heavy metal removal efficiencies provided by the building waste materials in the present study were on a par with the above materials. The effluent concentrations of Fe, Mn, Zn and Cu satisfy the drinking water standards. Those heavy metals, of which the effluent concentrations do not satisfy the drinking water standards, have to be further treated. Therefore, it can be concluded that reactive materials used for this study have the potential to be applied as reactive media rather than other expensive materials, when considering the both removal efficiency and cost.

The physical and mechanical properties of the reactive materials have only slightly changed due to the interaction with the landfill-leachate.

6. REFERENCES

Abhayawardana, G.,2015, 'Removal of lead in landfill leachate using Permeable Reactive Barriers with Natural Red Earth and Peat', *XLVIII*(04), pp.51-57.

Buluth Yasemin, T. Z.,2007, 'Removal of heavy metals from aqueous solution by sawdust adsorption', *Journal of Environmental Sciences, 5*(ISSN 1001-0742),pp. 160–166.

Emoruwa, I., and Agbozu, F.,2014, 'Batch adsorption of Heavy metals (Cu, Pb, Fe, Cr and Cd) from aqueous solutions using coconut husk', *African Journal of Environmental Science and Technology, 8(4)*(ISSN 1996-0794),pp.239-246.

Etorki, A., El-Rais, M. and Moussa, M. T., 2014, Removal of Some Heavy Metals from Removal of Some Heavy Metals from. *American Journal of Analytical Chemistry, 5*,pp. 225-234.

Snow, and David, H. ,1999, April 5, 'Overview of Permeable Reactive Barriers', pp. 165-182.

Al-Salihy, R., Jabbar, H. and T., A.-B. a. ,2016, 'Removal of heavy metals from aqueous solution by using low cost rice husk in batch and continuous fluidized experiments'; *International Journal of Chemical Engineering and Applications, 7*(10.7763/IJCEA.2016.V7.532).

Council, N. R. ,1994, 'Alternatives for ground water cleanup. National Academy of Sciences'.

Di Nardo, A., Di Natale, M., and Alessandro Erto, D. M. ,2010, 'Permeable Reactive Barrier for ground water PCE remediation: The case study of a solid waste landfill pollution'.

In S. P. Ferraris (Ed.), *Computer aided Chemical Engineering*. Roma 29.

Dayanthi, W., Arthanayaka, A., and Malkanthi, K. A., 2014, Applicability of Waste Matter as Reactive Media in Permeable Reactive Barriers (PRBs) to Treat Landfill Leachate Contaminated Groundwate*r.* iesl/pub.

Gillham, A., Robert, W. and Hannesin, O.S. ,1994, 'Enhanced degradation of halogenated aliphatics by zero-valent iron', *Ground Water, 6*(32).

Higgens, A., and Monica, R. ,2011, 'Environmental Assesment of In Situ Groundwater Remediation with reduced Iron Reactive media', Univeristy of Michigan.

Koffi Akissi, L., Adouby, K., and Boa, B. and. ,2013, 'Batch and column studies for Cadmium (II) removal using sawdust from Triplochiton Scleroxylon' *International Journal of Engineering Science and Technology (IJEST), 5*(ISSN : 0975-5462).

Painter, K., and Brett, D., 2005, 'Optimisation of Permeable Reactive Barrier Systems for the Remediation of Contaminated Groundwater', *Natural Resources Engineering,* Lincoln University,April 2005.

Rowe, and Kerry, R. ,1995, 'Leachate characteristics for MSW Landfills', London: Geotechnical Research Centre, Uniersity of Western Ontario.

Sewwandi, B., 2014, 'Development of Permeable Reactive Barrier to treat Leachate from Municipal Solid Waste Dump sites in Sri Lanka: An effective use of locally available materials for Heavy metals removal. University of Peradeniya.

Shodhganga. ,2009,'Principles of Adsorption. Department of Physical Sciences (Industrial Chemistry Unit)', Landmark University, P.M.B. 1001, Omu-Aran, Kwara, State, Nigeria.

Proceedings of the 7th International Symposium on

Advances in Civil and Environmental Engineering Practices for Sustainable Development

ACEPS - 2019

An analysis of household perception on solid waste separation – special reference to Kesbewa municipal council area.

G.G.R.Wijesingha[1], W.H.A.Shantha[2] and G.M.W.L.Gunawardena[1]

[1]Department of Town and Country Planning, Faculty of Architecture, University of Moratuwa, Katubedda, Moratuwa, SRI LANKA
[2]Hector Kobbekaduwa Agrarian Research and Training Institute, 114, Wijerama Mawatha, Colombo 07, SRI LANKA

K e y w o r d s

Solid waste
Source separation
Household perception
Solid waste management

A B S T R A C T

Solid waste separation is an essential commotion in Municipal Solid Waste Management (MSWM) system. Separation of the waste at the generated location (source separation) is very important to reduce the bulk and the disposal amount. Social communities engage in various levels of source separation. However, mixed waste collection is increasing daily without better solutions to the waste issue. Management of the solid waste at the generated location is very important in solid waste management; therefore household can play a major role in managing solid waste issue in any country. Thus, this research attempts to analyze the household perception on solid waste separation as a initiative to solid waste management.

To achieve this aim, two objectives were set for the research; identifying the household level significant socioeconomic factors affecting solid waste separation and understanding the effect of the awareness, attitudes and behavioral perceptions on waste separation of the household sector. Kesbewa municipal council area was selected for the study. To achieve the first objective, 6 criteria were selected through literature and 16 subcategories of these selected criteria were identified. Using multiple regression analysis, ANOVA and coefficient analysis, the most significant factors were identified. For the second objective, cloud analysis was undertaken for the significant factors identified through regression analysis. The results of the research showed that the age, gender and education level has a high influence on source separation of solid waste. Further the cloud analysis showed that the males have negative perception on solid waste separation than females and the younger generation has more negative perception towards separation. Further the people with poor education have negative perception on solid waste separation. Thus it is essential to make the people aware about the solid waste issue and the importance of managing it at the household level. It is very important to make the younger generation aware about the value of the nature which is destroying by solid waste dumping.

1. INTRODUCTION

Solid waste can be defined as non-liquid and nongaseous products of human activities, regarded as being useless. It could take the forms of refuse, garbage, and sludge Leton and omotosho, (2004). Hagerty,(1973) (as cited in Jinadasa, Munasinghe, Pathirana & Perera, (2015)) mentioned that solid waste can be defined as any discarded or abandoned materials arising from domestic, commercial, industrial, and institutional activities in urban areas. SWM involve with the collection, transfer, resource recovery, recycling and treatment and as well as SWM is associated with control of waste generation, storage, collection, transfer and transport, processing and finally dispose of in a comprehensive way without harming to public health, economics, conservation aesthetics and environment.. Jinadasa, Munasinghe, Pathirana & Perera, (2015).

Moghadam & Ehrampoush, 2005 have reported, "Increasing population levels, booming economy, rapid urbanization and the rise in community living standards have

greatly accelerated the municipal solid waste generation rate in developing countries". Guerrero, Maas & Hogland, (2012) mentioned that solid waste management is a challenge for the cities' authorities in developing countries due to budget limitations to manage the increasing generation of waste.

Sri Lanka mostly discharges Municipal Solid Waste (MSW) as the open dumping, which accounts for more than 85% from collected waste by the local authorities and most are non-engineered sites without any environmental or social protection guards. "In Sri Lanka, the majority of MSWM cost is allocated for waste collection and transportation compared to waste disposal and treatment". Nilanthi, Bandara, Patrick & Hettiarachchi, December (2003).

According to 2016 data of Waste Management Authority of Sri Lanka, municipal solid waste generation in Sri Lanka is around 6500 to 7000 Mt/Day (per capita generation varies around 1- 4 kg /person per day) and the Western province contributes 58.58%, highest national municipal solid waste generation. Further, the lowest solid waste management is also reported in Western province (~6.55%) and the highest waste management is reported in the north-central province (~71.9%) in Sri Lanka. Thus, Western province shows the highest waste generation and lowest solid waste management with an immense gap between waste generation and management rates within western province compared to other provinces in Sri Lanka. National Solid Waste Management Support Center Ministry of Local Government and Provincial Council, Annual Report (2014)

Even local authorities (LAs) practice waste separation service within their boundaries, the growing of waste generation and less waste management is consequently rising in the country as a complicated problem. This is due to less household participation in waste separation. Around 80%- 90% of organic waste is generated at the household level and 55% - 75% out of generated waste is disposed without any composting or recycling, causing burden to local authorities. Bandara & Hettiaratchi, (2010). Therefore household participation is essential to minimize the solid waste issue in Sri Lanka, because they are the smallest nucleus in the society generating mixed waste causing to increase waste separation cost and the fly-tipping fee of local authorities."Source separation efforts will only succeed with positive attitudes and high participation rate of people". Ab, Ghani, Rusli, Biak & Idris, (2012). However, household waste separation is not at a significant level in Sri Lanka due to many deviations of human behavioral patterns and preferences.

Source separation is very crucial to reduce the volume of waste generation and disposal Daniel, Tata & Perinaz, (2012). Most of the developing countries dispose household solid waste as mixed waste. Further waste separation may influence the reduction of financial constraints of local authorities. If household effectively separate solid waste it will cause to reduce, reuse, recycle and compost a significant amount of generated waste.

As discussed above, waste separation in household level is vital to minimize the waste generation in Sri Lanka. The responsible authorities concern about the national and provincial waste management, while the household participation is neglected. The crucial issues and schemes within the waste separation in household level should be identified to encourage waste separation through household participation. Therefore, a detailed analysis of their true behavior is needed to overcome the problems of the entire municipal solid waste management system and expand future suggestions. Therefore, this research tries to analyze the household participation on solid waste separation.

2. OBJECTIVES

With the above background, two objectives were set for this study.

(i) To identify the household level significant socioeconomic factors affecting solid waste separation.
(ii) To understand the effect of the awareness, attitudes and behavioral perceptions on waste separation behavior of the household sector.

3. METHOD

Kesbewa urban council area was selected as the case study area which is located in the Western province of Sri Lanka. The area is characterized by the rapidly increasing population and the rapid conversion of agricultural land to urban uses. Kesbewa UC has 55 GN divisions and 55 sq.km of land

extent. Total population and households are respectively 256,851 and 68,687. Figure 1 displays the study area.

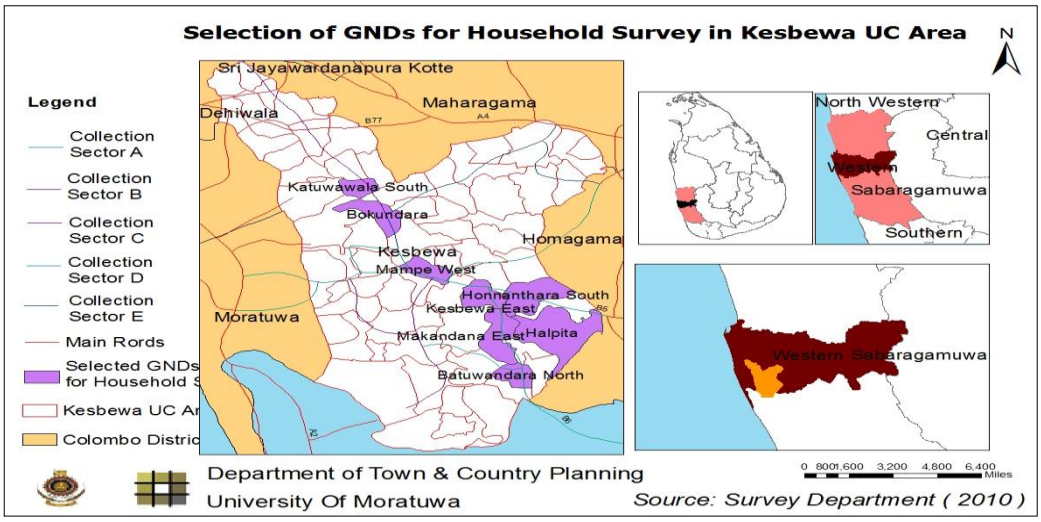

Figure 1 The Study area

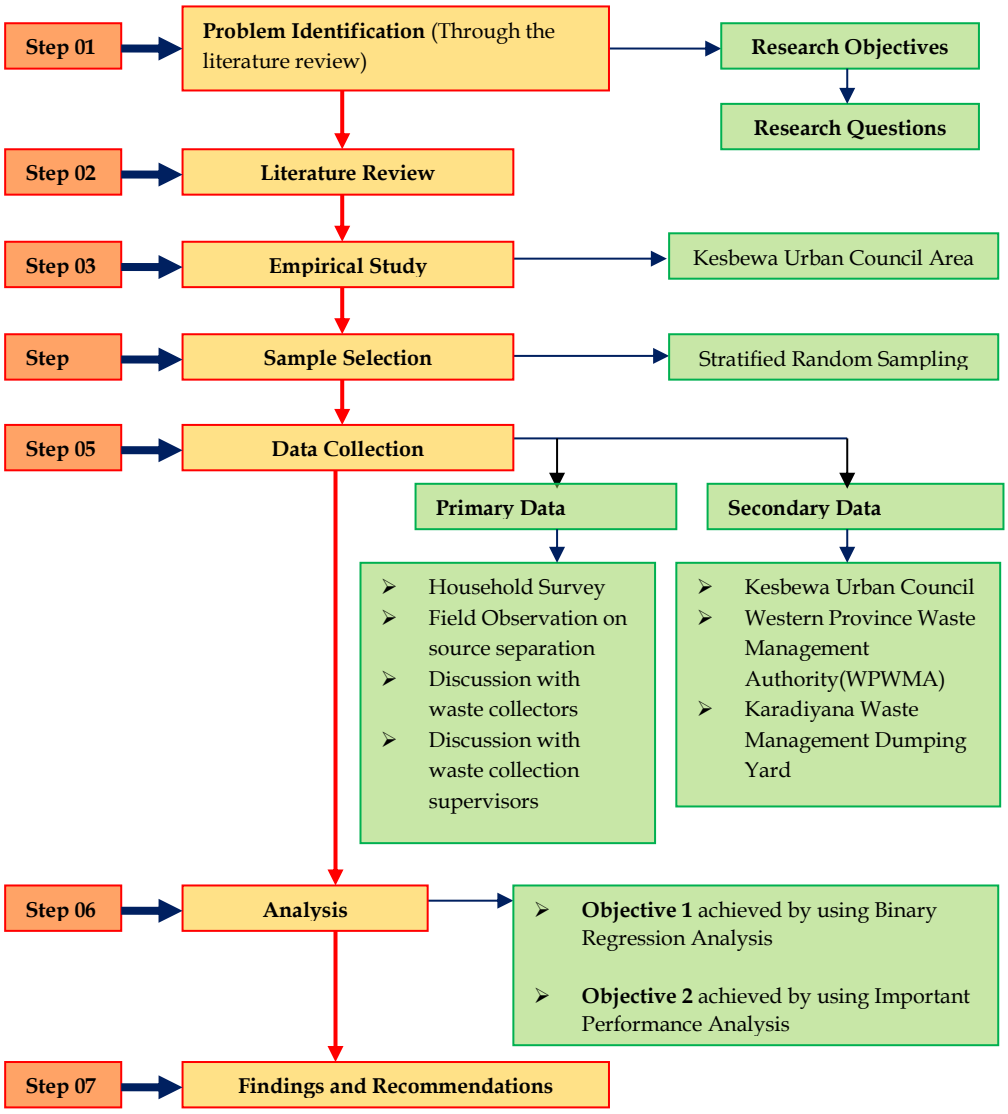

Figure 2 Flowchart of methodology

At present, Kesbewa urban council hasn't any formulated action plan related to municipal solid waste management. Existing policies had been formulated more than 15 years ago and they are not applicable for present condition. (Data Collection Survey on Solid Waste Management, Final Report, February 2016).

As discussed above, western province shows a significant gap between waste generation and management. Moratuwa, Kesbewa and Dehiwala Mt. Lavinia show the highest gap from the local authorities in Western province. Therefore, for this study Kesbewa urban council was selected since it shows the second highest gap. Systematic random sampling technique was applied to select the households for questionnaire survey to analyze the awareness, attitudes, and perceptions on waste separation behavior. The quantitative methods were used to identify significant socio-economic criteria on waste separation. The flowchart of the methodology is given in Figure 2.

4. RESULTS AND DISCUSSION

4.1. Developing the Multiple Linear Regression (MLR) Model

Multiple regression analysis has been done to measure the relationship between solid waste separation amount and six socio-economic criteria such as gender, age, household size, education level, occupation and household income (independent variables). These independent variables were categorized into different levels. The list of variables and their levels were given in Figure 3.

The ultimate focus of this analysis is to develop a model to identify significant household sector socio-economic criteria on waste separation amount. The regression model has used the stepwise method with 95% confident interval. R Square, F and t-test statistics were used to interpret the accuracy of the model. Table 01 displays the results of regression analysis.

Table 1 Regression Analysis results

Model	R	R Square	Adjusted R Square	Std. Error of the Estimate
1	.661[a]	.437	.415	6.66991

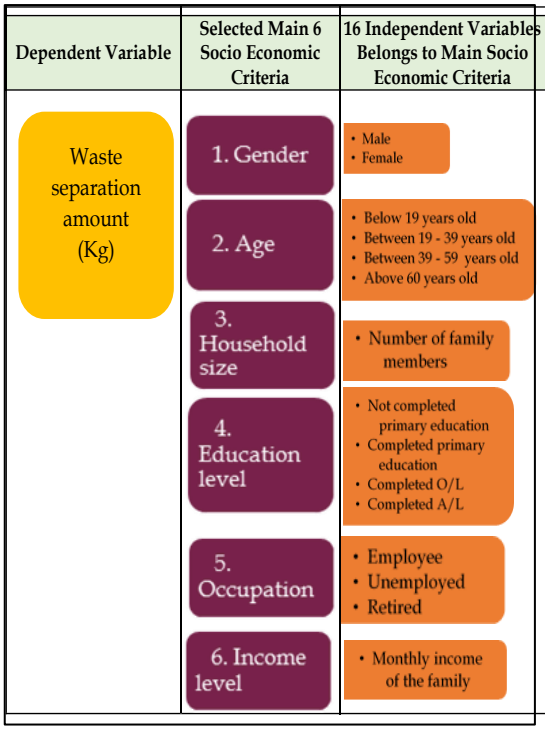

Figure 3 Selected factors and sub factors for Multiple Regression Analysis

R Square can be expressed as a coefficient of multiple determination and use to measure how data are close to the fitted regression line. This model data points were closer to the regression line at 0.437 (approximately 43%) level of data variance. R-value was 0.661 showing a strong relationship between dependent variable and independent variables. Adjusted r square was less than the original R square because it depended on accounted sample size and it was used to identify the percentage of variance of inputs and outputs of the model. Adjusted r square value was 0.415. Table 2 displays the results of ANOVA test.

Table 2 Results of ANOVA est

Model		Sum of Squares	DF	Mean Square	F	Sig.
1	Regression	5152.015	6	858.669	19.301	.000[b]
	Residual	6628.671	149	44.488		
	Total	11780.686	155			

F statistics measure the overall significance of the model. This is basically interpreted whether the independent variables are jointly significant at zero or not. This model showed 0.000 significant value and it interpreted the model has a strong relationship between dependent variable and

independent variables. Coefficients of variables also display significant results. Beta values interpret the contribution of independent variables on their dependent variable. The category; completion of primary education has highly contributed to the regression, it has -0.333, highest beta value. The male percentage and the household size showed medium contribution with beta values of -0.174 and 0.139.

t-statistics show the statistical significance of the individual coefficients. According to regression results, the percentage of completion of primary education has 0 .000 of highest significant value and shows a negative relationship between waste separation amount.

Based on the statistical analysis, a statistical model was developed to show the relationship between independent variables and dependent variable. The developed model is given in equation 01.

$$\textit{Source separation amount} = \beta_0 + \beta_1 + \beta_2 + \beta_3 + \beta_4 + \beta_5 + \beta_6$$

$$Y = 17.339 - 0.090\ (\text{Complete Primary Education}) - 0.068(\text{Employee Percentage}) - 0.0000919\ (\text{Household Income}) - 0.069\ (\text{Male Percentage}) - 0.093(\text{Below 19 Years Age Percentage}) + 0.659\ (\text{Household Size})$$

$$Y = 17.339 - 0.090 - 0.068 - 0.0000919 - 0.069 - 0.093 + 0.659$$

Thus, according to the statistical analysis, there is a significant negative relationship between the percentage of completion of primary education and the waste separation at 0.000 significance. Further, below 19 age population, employment percentage of household, income and male percentage in a household showed negative relationship at 0.01 significant levels. Household size was the only independent variable which showed a positive relationship at 0.05 low level of significant levels.

4.2. Criteria selection for Cloud Analysis

Referring the significant results of the regression model, three socio-economic criteria were selected to conduct the cloud analysis; they are education level, gender and age groups. From education level, Percentage of completion of primary education was selected since it showed a higher negative correlation. From age group, under 19 years old category was selected and from gender male percentage was selected. Cloud analysis has been used to understand the behavioral perceptions of each socio-economic group.

4.3. Cloud Analysis by Gender

According to questionnaire survey results, 59.62% of households discharged their waste as mixed waste and 27% females and 33% males are not engaging in waste separation. Further, 40.38% practiced source separation at household level in Kesbewa UC area. Table 3 displays the cloud analysis results of questionnaire survey.

According to the cloud analysis effect of gender on waste separation is more or less similar with little high positive behavior with females. Local authority enforcement highly pressures on positive male behavior (43%) than female. Further, both male and female positive behavior on waste separation is mainly due to local authority influence. Both males and females claim that the time is a constraint factor for waste separation. 18% male and 25% female negative perceptions are enhanced due to the negligence of mixed waste acceptation by LA.

Similar cloud analysis was undertaken to age and primary education categories as well. When considering the age, below 19 age people have 17% the highest level of positive awareness and attitudes, but they are the people who have highest negative behavior than others. Above 60 age people have the highest positive behavior (42%) on waste separation than others. 61% of age between 39 – 59 people and 70% of above 60 age groups tend to discharge mixed waste due to less inorganic waste collection frequency.

The people with only primary education showed highest awareness and attitudes (19%), but they are the people who practice 23% of highly mixed waste discharge. 42% of people even without primary education discharge mixed waste due to lack of local authority enforcement. 38% of the degree holders tend to give mixed waste to local authority due to poor waste management policies of local authorities themselves. The people with O/L and A/L education background highly attempted to enhance household level organic composting than others.

Table 3 Cloud analysis results

Behavior	Perceptions of the Male	(%)	Perceptions of the female	(%)
Positive behavioural perception	Local authority enforcement	43.32%	LA Enforcement	36%
	Reduction of environmental pollution	23.34%	Interest to make compost from organic waste	25.60%
	My separation may help the others in my home	21.11%	Main responsibility of female	19.20%
	Waste separation is a habit	12.20%	Work in kitchen and garden than other family members	12%
			Think about cleanness of house	7.20%
Negative behavioural perception	No enough time due to jobs	44.26%	No enough time	37.50%
	Waste separation is a duty of female	28.73%	No enough separation facilities	28.14%
	Local authority accepts mixed waste	18.40%	Local authority accepts mixed waste	25%
	Lack of enthusiasm	8.62%	Lack of enthusiasm	9.38%

As a summary of the cloud analysis results, household people had 64% positive awareness and attitudes towards waste separation, but 39% out of them discharge mixed waste due to time limitation and the poor regulations of local authorities. 36% of people had negative awareness and attitudes towards waste separation, but 52% of them showed positive behavioral perceptions due to local authority influence.

5. CONCLUSION

This study was undertaken to find out the household contribution to solid waste separation. To achieve this aim, two tasks were carried out; identify the household level significant socioeconomic factors which affect the solid waste separation and understand the effect of the awareness, attitudes and behavioral perceptions of household on waste separation. The analysis was undertaken using quantitative and qualitative data analysis techniques. Six basic socioeconomic criteria which highly influence on solid waste separation were identified through sound literature review. They are, gender, age, household size, education background, occupation and income level. Each category was divided into subcategories and these subcategories were considered as the independent variables which affect household level solid waste separation. To find out the most influencing factors and to develop a model showing their relationship, multiple regression analysis was applied. According to the analysis educational background, gender and age of household population had a high influence on positive or negative behavior of solid waste separation at household level. To display their relationship a multiple regression analysis model was developed.

Then cloud analysis was carried out to analyze the awareness, attitudes and behavioral perception of household on waste separation. For this task the three factors which showed higher influence on waste separation were selected, they are gender, age and the educational background. Through questionnaire surveys the attributes were evaluated. Accordingly, household people had 64% positive awareness and attitudes towards waste separation, but 39% out of them discharge mixed waste due to time limitation and the poor regulations of local authorities. 36% of people had negative awareness and attitudes towards waste separation, but 52% of them showed positive behavioral perceptions due to local authority influence.

Thus, majority of household people tend to dispose solid waste as mixed waste, they are willing to separate waste, if they are provided with required facilities. Thus, the government or local authorities should have a sound mechanism to induce the waste separation at household level, thus it will be a good

initiative to solve the solid waste problem in Sri Lanka.

The low awareness and attitudes displayed by younger generation towards waste separation is a red light depicting the possibility of aggravating the waste issue in future, therefore, it is essential to take necessary actions to make the younger generation aware about the importance of solid waste management.

Since the education background is also play a major role in waste management, it is essential to improve the weaknesses of education sector, it is very essential to have a good education to the people in the society, not only for waste management, but for all other sectors of the country as well.

6. REFERENCES

Ab,W.A.W., Ghani,K.,Rusli, I.F., Biak,D.R.A. & Idris,A. 2012,'An application of the theory of planned behaviour to study the influencing factors of participation in source separation of food waste',*Waste Management Journal of Malaysia*.

Bandara, N. J. G. J & Hettiaratchi, J. P. A. ,2010, 'Environmental impacts with waste disposal practices in a suburban municipality in Sri Lanka', *Intrnational Journal of Eniornmrnt and Waste Management,Volume 6*.

Daniel,H., Tata, B, & Perinaz.,2012, 'What a Waste : A Global Review of Solid Waste Management. Urban development series', *knowledge papers no. 15 World Bank, Washington*. Retrieved from *https://openknowledge.worldbank.org/handle/10986/17388 License: CC BY 3.0 IG.*

ERM (Environmental Resources Management),1997, Environmental Impact Assessment for a proposed Sanitary Landfill, Alupotaha Division, Salawa Estate.

Guerrero,L.A.,Maas,G & Hogland,W.,2012, Solid waste management challenges for cities in developing countries. *The Review of Waste Management,*23 October 2012.

Jinadasa, A.R.P., Munasinghe, M.A.S.H., Pathirana, P.W.S.K & Perera, W.A.I.D., ' Design an Effective Solid Waste Management Model for Sri Lankan'.

Leton,T.G & Omotosho,O.,2004, 'Landfilling Operations in the Niger Delta Region of Nigeria', *The Journal of Engineering Geology.* 73(1-2), pp.171-177.

Moghadam,B & Ehrampoush. (2005). Survey of Knowledge, Attitude and Practice of Yazd University .

Nilanthi, J.G.J.B., Patrick, J.H., 2003, 'Environmental Impacts Associated with Current Waste Disposal Practices in a Municipality in Sri Lanka – A Case Study'. Workshop on Sustainable Landfill Management 3–5 December, 2003; Chennai, India, pp. 19-26 19

NSWMSC - National Solid Waste Management Support Centre (2012) Data base on faecal sludge management in Sri Lanka: National Solid Waste Management Support Centre, Unpublished, Ministry of Local Government and Provincial Councils.

Proceedings of the 7th International Symposium on

Advances in Civil and Environmental Engineering Practices for Sustainable Development

ACEPS - 2019

Comparison of cyclone performance with theoretical predictions based on inlet velocity and particle loading rate.

G. B. Sakura[1] and Andrew Y. T. Leung[2]

[1] Department of Engineering Technology, University of Sri Jayewardenepura, Gangodavila, Nugegoda, SRI LANKA
[2] Department of Architectural and Civil Engineering, City University of Hong Kong, 83 Tat Chee Avenue, Kowloon, Hong Kong SAR, CHINA

K e y w o r d s

Cyclone Separator
Solid loading rate
Collection efficiency
Grade efficiency

A B S T R A C T

This paper brought a comparison of experimental and theoretical analysis of a cyclone performance, operated under low to moderate solid loading rates (0.0 to 2.5 g/m^3) at two different inlet velocities (5 m/s and 10 m/s). A dramatic increment of overall collection efficiency with the solid loading rate up to a certain value and then levelled off is showed by experimental observations and almost similar turning points of solid loading rates were observed at two different velocities. Moreover, the mass loading effect was seen to be predominant than the classification at high solid loading conditions, especially at low operating velocity. The theoretical applications for predicting cyclone performance showed deviations from experimental results due to inconsideration of particle agglomeration and re-entrainment, particle back- mixing and mass loading effect in theoretical derivations.

1. INTRODUCTION

Cyclone separators are the most widely used particle controlling devices, owing to their simple operational principle, higher collection efficiency together with a simple design, low maintenance cost and easy operation at wide ranges of operational and environmental conditions.

The inlet velocity and the particle solid loading rate are key parameters of the cyclone performance for any type of cyclone design. Conversely, the knowledge based on gas-solid flow inside cyclone separator is still basic and experimental results provided limitations for a general conclusion. Hence, the behaviour of cyclone performance at low to moderate solid loading rates (0 to 2.5 g/m^3) at two different inlet velocities was experimentally studied in this study and results were compared with available theories, to compare the theoretical and experimental results to investigate any deviations between them. However, there are few numbers of theories are available in the literature and thus the objective of this study deviations of the experimental and theoretical was to understand the related reasons for any results.

1.1. Collection efficiency

1.1.1. Effect of particle loading

Based on correlated data in the literature, the increase of solid loading from 2.3 to 228.8 g/m^3 caused an increase in collection efficiency (Ji, et al., 2009; Luís & Jr, 2000; Stern, 1955). Similar behaviour has been investigated by many studies for different particle samples (finer to causer) and different solid loadings (Yoshiro, et al., 1968; Patterson & Munz, 1989; Zenz, 1975; Zenz & F., 1984; Hoffmann, et al., 1991; Hoffmannc, et al., 1992; Ji, et al., 2009).

However, contradiction to increase of collection efficiency with solid loading also resulted by few studies in the literature, only at higher solid loading rate conditions (Chen, 1992; Luís & Jr, 2000), due to the effect of the dramatic reduction of turbulence kinetic energy at high solid loading conditions (Chu, 2011; Wan, 2008).

1.1.2. Effect of inlet velocity

Inlet velocity is important in cyclone separator as it governs the particle separation from the fluid flow. many studies in the literature has proven that the collection efficiency increases at higher inlet velocity conditions for different solid loading rates and cyclone geometries (Yoshiro, et al., 1968; Patterson & Munz, 1989; Kim & Lee, 1990; Zhu & Lee, 1999; Luís & Jr, 2000; Rongbiao, et al., 2001), which can be clarified as due to the increase of centrifugal forces on particles which accelerate particle separation and also increase of the vortex length (Büttner, 1988; Hoffmann, 1995; Hoffmann, et al., 1996).

1.1.3. Theories to calculate efficiency

Theoretical approaches to predict cyclone separator efficiency (e.g., (Barth, 1956; Lapple, 1950) have not deemed about the influence of solid loading rate and are based mainly on geometric and operational conditions. Literature reports four theoretical models to predict cyclone collection efficiency based on the solid loading effect; three empirical models developed by Zenz (Zenz, 1975; Hoffmann & Stein, 2002), by Smolik (Smolik, 1975; Svarovsky, 1981) and by Ganegama B. and Leung (Ganegama B. & Leung, 2016) and a mechanistic method by Muschelknautz (Muschelknautz, 1972; Muschelknautz & Greif, 1997).

Empirical models by Smolik, Zenz and Ganegama B. and Leung completely depend on historical experimental data only on solid loading rate and overall collection efficiency, without considering physical and operational conditions which also significant in particle collection. The graphical relationship proposed by Zenz could not be applied in this study as it can only predict collection efficiencies for solid loading concentrations larger than 2.29g/m^3.

Muschelknautz model is more realistic than formers as consideration of large numbers of unclassified extra parameters in cyclone separator (physical and operational) (Hoffmann & Stein, 2002). Basic equations of Smolik, Muschelknautz and Ganegama B. and Leung theories are listed in Table 1.

Table 1 Theoretical equations of different models for collection efficiency

Model	Equation(s)	
Smolik	$\eta(c_2) = 1 - [1 - \eta(c_1)]\left[\frac{c_1}{c_2}\right]^{1.8}$	*1*
Muschelknautz	$\eta_{tot} = \sum_{i=1}^{N}\left(\frac{1}{1+\left(\frac{d_{50}}{d_i}\right)^{m}}\right) \times \Delta MF_i$ Where, m is the slope of the graph of $\ln\left(\frac{1}{\eta_i} - 1\right)$ versus $\ln d_i$.	*2(a)*
	$c_{0L} = \frac{\left(0.005\left(1+3\sqrt{c_0}\right)\right)\sqrt{DD_e}\,\mu}{2\left(1-\frac{D_e}{D}\right)\rho_p d_{med}^2\sqrt{v_{\theta w}v_{\theta CS}}}$	*2(b)*
	$d_{50} = d_{fact}\sqrt{\frac{18\mu(0.9Q)}{2\pi(\rho_p - \rho)v_{\theta CS}(H-S)}}$	*2(c)*
Ganegama B. and Leung	$\eta(C_2) = 1 - [1 - \eta(C_1)]\left[\frac{C_1}{C_2}\right]^{\left[1-\left(\frac{C_1}{\eta(C_1)}\right)\right]}$	*3*

2. EXPERIMENTAL PROCEDURE

Geometric parameters of studied cyclone separator are shown in Figure 1 and a schematic diagram of the experimental setup is shown in Figure 2. Experiments were performed at two inlet velocities, 5 m/s and 10 m/s. Particle laden air was supplied to cyclone separator through an extended inlet of 800 mm of length to verify a fully developed flow at the

real entrance of cyclone separator. Arizona Test dust (Powder Technology, INC; Size range: 0.742 to 18 µm, Standard deviation: 1.762 µm and Density: 2650 kg/m^3) was used as the solid phase.

The weight of the collected solid mass at the bottom of cyclone separator was measured by using a sensitive balance. Two isokinematic flow volumes were extracted from the inlet and outlet by using sampling probes connected to suction tubes (VRL 50-080108, Nihon Pisco) and the extracted flows were diluted by supplying additional air using air blowers. Fluke particle counter (Fluke 983, FLUKE Inc.) was used to obtain fractional efficiencies of particles. Each experiment was conducted for 3 to 15 min depending on the solid loading rate and the particle blockage of the filter.

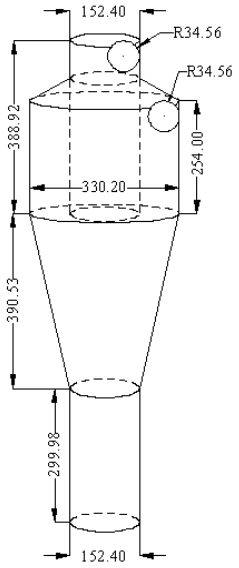

Figure 1 Geometry of the cyclone separator

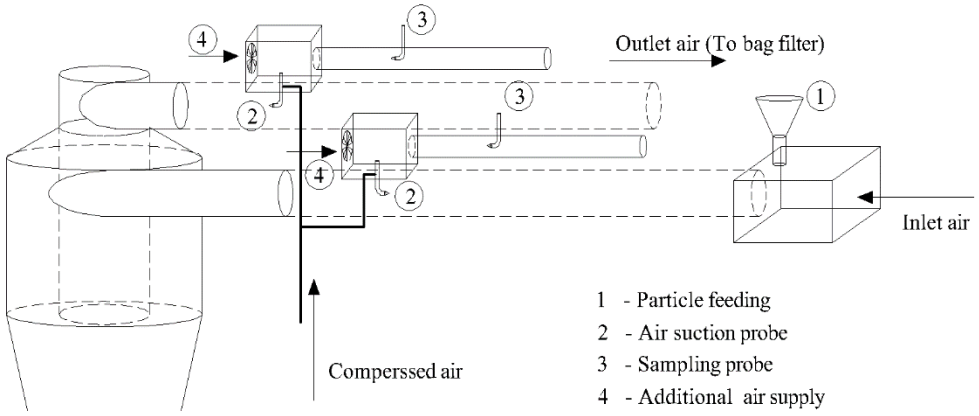

Figure 2 Schematic diagram of the experimental setup

3. RESULTS AND DISCUSSION

3.1. Overall collection efficiency

The experimental observations showed three major particle deposition zones inside the cyclone separator: 1) inside the inlet tube, 2) on the cyclone walls and 3) inside the dust collection section. The particles deposited inside the inlet extended tube were considered to not be supplied (at higher solid loading conditions, the deposition in this zone was considerable) and the deposition inside the cyclone outlet (comparatively negligible) was considered to be lost.

The overall collection efficiency of the cyclone separator was calculated by considering the percentage of solid mass collected as a fraction of total solid mass in (Figure 3). The efficiency of solid collection

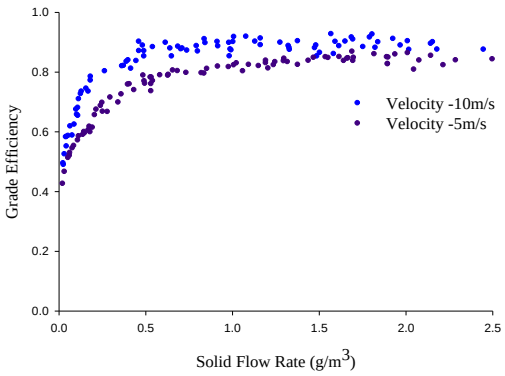

Figure 3 Experimental overall efficiencies at two inlet velocity conditions for different solid loading rates

with solid loading rate increased at both inlet velocities until 0.5 g/m^3; the increment was insignificant thereafter, similar to the report in the literature (Hoffmann, et al., 1991).

Especially after 1.5 g/m^3, the collection efficiency at 5 m/s differed from that at 10 m/s by only 5.7%. This observation contradicts those of earlier studies in the literature, which have reported an increase in the collection efficiency with the inlet velocity (Yoshiro, et al., 1968; Patterson & Munz, 1989; Kim & Lee, 1990), but compatible with only one research in the literature, which was conducted at 10 to 20 m/s velocities for 0 to 25 g/m^3 solid loading rates (Hoffmann, et al., 1991).

Visual observations at 5 m/s were interpreted to discern the reason for the increase in the collection efficiency with solid loading at low velocities. The cyclone separator acts as a two-stage separator (mass loading and classification) (Muschelknautz, 1972; Muschelknautz, 1972; Muschelknautz, 1970) with a limit of the solid carrying capacity of the flow. At high solid loadings, the amount of solids exceeds this limit of loading immediately collected into the cyclone walls and break up with the continuing deposition and fall into the flow field behind the dust hopper (Figure 4). This breakup may cause an increase in back mixing after the classification process.

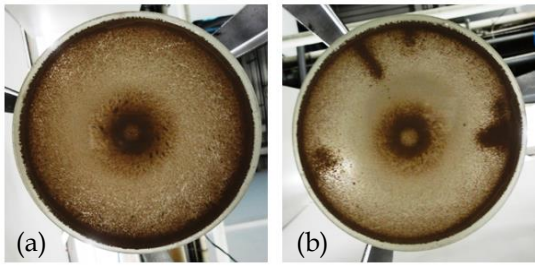

Figure 4 Solid deposition inside Hopper at 5 m/s inlet velocity at solid loading rates of (a) 0.6 g/m^3 and (b) 1.0 g/m^3

The experimental results were compared with theoretical predictions to achieve a better understanding of the relationship between the theories and experiments (Figure 5). For the Smolik method (Eq. (1), Table 1) the results from experimental at 0.5 g/m^3 were used as the known solid concentration, C_1. Figure 5 shows that the Smolik method under-predicts the collection efficiencies at higher solid concentrations than the selected initial values and over-predicted the collection efficiencies at lower solid loading rates.

Well-matched curves for efficiency prediction by Eq. (3) in Table 1 developed by Ganegama B. and Leung by consideration of the turning point of the experimental data is also shown in Figure 5

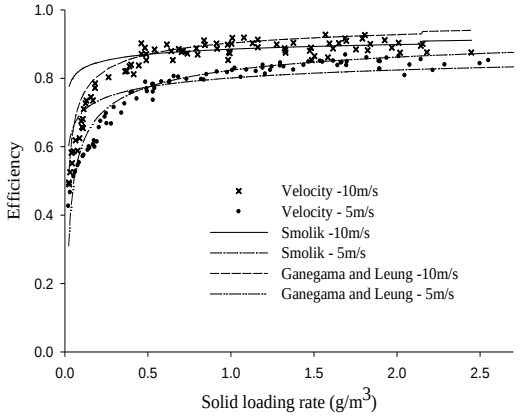

Figure 5 Experimental overall collection efficiencies with the theoretical prediction

A comparison of experimental overall collection efficiencies with the theory of Muschelknautz's (Eqs. 2(a)-2(c) in Table 1) shown in Table 2. At both 5 ms and 10 m/s velocities, the relationships between the experimental data and the theory of Muschelknautz were agreed to low mass loading conditions, but the theoretical data led to over-prediction at high solid loading rates. The deviation between the experimental and theoretical data was lower at 5 m/s of velocity. The over-prediction of the collection efficiencies by the numerical investigation at higher solid loading rates may be due to unaccounted particle re-entrainment and agglomeration.

3.1. Grade efficiency

The grade efficiency curves observed at two velocity conditions at selected solid loading conditions are shown in Figure 6. The differences in fine particle collection were smaller at the two velocity conditions but larger for coarse particle collection. This observation again shows that the back-mixing of fine particles is pronounced at high velocities and higher particle agglomeration due to long residence time at low-velocity conditions.

The experimental grade efficiency curves were compared with the theory of - Muschelknautz (Figure 6). To obtain well matched data from this theory, the modification factor (d_{fact}) was selected in the range of 0.18 to 1.8 for 5 m/s and 0.41 to 3.2 for 10 m/s which differed from the range specified by Muschelknautz (0.9 to 1.4)

Table 2 The theoretical and experimental overall collection efficiencies for considered solid loading rates at two velocities

Solid loading rate (g/m³)	Overall collection efficiency			
	At 10 m/s		At 5 m/s	
	Experiment	Muschelknautz	Experiment	Muschelknautz
0.1	0.6585	0.6061	0.5670	0.5618
0.2	0.7868	0.7727	0.6484	0.6165
0.5	0.8711	0.9474	0.7757	0.7800
1.0	0.8847	0.9534	0.8185	0.8788
1.5	0.8785	0.9320	0.8489	0.8661
2.0	0.8895	0.9315	0.8429	0.8452

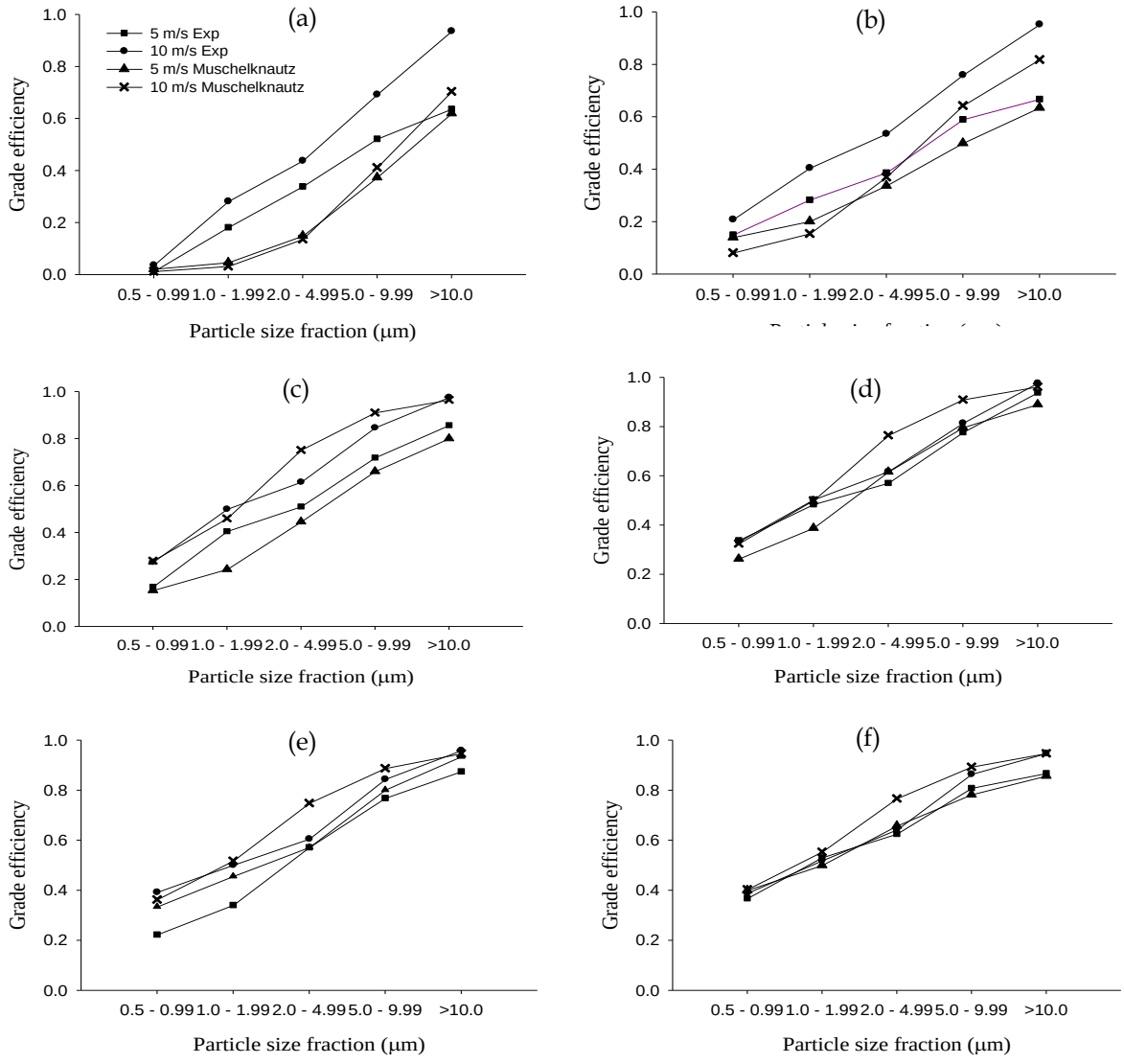

Figure 6 Experimental and theoretical grade efficiency curves for selected solid loading rates at two velocity conditions (a) 0.1 g/m³; (b) 0.2 g/m³; (c) 0.5 g/m³; (d) 1.0 g/m³; (e) 1.5 g/m³ and (f) 2.0 g/ m³

To compute grade efficiencies, Muschelknautz specified *m* values of 2 to 7 but was set to 0.79 to 1.55 for 5 m/s and 1.18 to 1.88 for 10 m/s in this study. The reason for this contradiction may due to assumed overall collection efficiency ranges (90 % to 99 %) by Muschelknautz at low solid loading rates while overall collection efficiencies resulted in this study ranged between 40 % and 95 %.

Results show that the Muschelknautz model underestimates the grade efficiencies at 0.1 g/m³ and 0.2 g/m³ solid loading rates and

agreed at other loading conditions with the experimental investigations while showing an over predicting deviation at particle fractions of 2.0 -9.99 µm.

The cut-size diameter (d_{50}) provides direct information about the particle grade efficiency by means of the smallest particle size with 50 % separation efficiency. Table 3 shows Muschelknautz's theoretical and experimental d_{50} values at the solid flow rates considered and the results show that the d_{50} value decreases with the increase of inlet velocity and particle loading rate. With the limitations of measurements in Fluke 983, only particle fractions were considered in experiments.

Table 3 The theoretical and experimental cut size diameters (d_{50}) at considered solid loading rates

Solid loading rate (g/m³)	d_{50} Value			
	At 10m/s		At 5m/s	
	Experiment	Muschelknautz	Experiment	Muschelknautz
0.1	5.0 - 9.99	8.60	5.0 - 9.99	9.94
0.2	2.0 - 4.99	4.69	5.0 - 9.99	6.67
0.5	1.0 - 1.99	2.74	2.0 - 4.99	3.91
1.0	1.0 - 1.99	1.41	2.0 - 4.99	2.11
1.5	1.0 - 1.99	1.33	2.0 - 4.99	2.50
2.0	1.0 - 1.99	1.17	1.0 - 1.99	1.41

4. CONCLUSION

In this study, the performance of a cyclone separator with a cylindrical inlet type at 0 to 2.5 g/m³ particle loading rates was investigated at two inlet velocities. In general, the common increasing behaviour of the collection efficiency at the considered solid loading range was seen in two cases. Comparison of experimental results with available theories, shown that there are many factors to be considered to derive realistic results from theories, especially, particle agglomeration and re-entrainment, particle back- mixing and mass loading effect. These factors may vary with operating conditions and geometric features of cyclone separators, and yet to be undergone by experimental analysis.

However, experimental and computational analysis of cyclone performance are expensive and time-consuming processes and with the development of accurate theories for cyclone performance, analysis will be beneficial. Thus, the present study draw attention to the significant factors to be considered in improving or developing theoretical applications for cyclone performance.

5. ACKNOWLEDGEMENT

The research is supported by the University Grant Committee of HKSAR grant number GRF 115712.

6. NOMENCLATURE

C	solid loading rate
$C_{(.)}$	solid concentration in the Smolik equation, m^3/s
C_{0L}	critical loading as a mass fraction (in the Muschelknautz theory)
D	diameter of cyclone body, m
D_e	diameter of vortex finder, m
d	diameter, μm
d_{fact}	modification factor in Muschelknautz d_{50} equation
d_{50}	predicted cut size diameter, μm
f'	frictional effect contributes with the effect of air and solid
H	height of cyclone separator, m
MF_i	i^{th} mass fraction
Q	flow rate, m^3/s
S	height of vortex finder, m
v	gas velocity, instantaneous velocity, m/s

Greek Letters:

$\eta_{(.)}$	grade efficiency
Δ	difference in
η	collection efficiency
θ	tangential coordinate
θCS	tangential coordinate at control surface CS
μ	dynamic viscosity of air, m^2/s

ρ density, kg/m^3

Subscripts:

o	initial
CS	cyclone control surface CS
e	vortex finder, cyclone core
i	i^{th} fraction
m	geometric mean
med	median
tot	total/overall
w	cyclone wall

7. REFERENCES

Barth, W., 1956, 'Design and layout of the cyclone separator on the basis of new investigations', *Brenn. Warme Kraft,* Volume 8.

Büttner, H., 1988,'Size Separation of Particles from Aerosol Samples using Impactors and Cyclones', *Particle & Particle Systems Characterization,* Volume 5, pp. 87-93.

Chen, K. T. a. J., 1992,'Performance of a cyclone under high solid loadings', *AIChE Symposium Series,* pp. 130-130.

Chu, K. W. W. B. X. D. L. C. Y. X. &. Y. A. B., 2011, 'CFD–DEM simulation of the gas–solid flow in a cyclone separator', *Chemical Engineering Science,* 66(5), pp. 834-847.

Ganegama B., S. & Leung, A. Y. T., 2016. 'Improvements of the cyclone separator performance by down-comer tubes', *Journal of Hazardous Materials,* Volume 311, pp. 100-114.

Hoffmann, A. C., Arends, H. & Sie, H., 1991, 'An experimental investigation elucidating the nature of the effect of solids loading on cyclone performance', *Filtration & separation,* 28(3), pp. 188-193.

Hoffmann, A. C. D. J. R. A. H. &. H. C., 1995, 'Evidence of the 'natural vortex length'and its effect on the separation efficiency of gas cyclones', *Filtration & Separation,* 32(8), pp. 799-804.

Hoffmann, A. C., Groot, M. D. & Hospers, A., 1996, 'The effect of the dust collection system on the flow pattern and separation efficiency of a gas cyclone', *The Canadian Journal of Chemical Engineering,* 74(4), pp. 464-470.

Hoffmann, A. C. & Stein, L. E., 2002, 'Gas cyclones and swirl tubes', *s.l.:Springer*.

Hoffmannc, A. C., Van Santen, A., Allen, R. W. K. & Clift, R., 1992, 'Effects of geometry and solid loading on the performance of gas cyclones', *Powder Technology,* 70(1), pp. 83-91.

Ji, Z. et al., 2009, 'Experimental investigations on a cyclone separator performance at an extremely low particle concentration', *Powder Technology,* 191(3), pp. 254-259.

Kim, J. & Lee, K., 1990, 'Experimental study of particle collection by small cyclones', *Aerosol Science and Technology,* Volume 12, pp. 1003-1015.

Lapple, C. E., 1950,'Gravity and Centrifugal Separation', *American Industrial Hygiene Association Quarterly,* Volume 11, pp. 40-48.

Luís, F. F. & Jr, L. G., 2000, 'A study of the effect of high inlet solids loading on a cyclone separator pressure drop and collection efficiency', *Powder Technology,* 107(1-2), pp. 60-65.

Muschelknautz, E., 1970, 'Auslegung von Zyklonabscheidern in der technischen Praxis', *Staub-Reinhaltung der Luft,* Volume 30, pp. 187-195.

Muschelknautz, E., 1972, 'Die berechnung von zyklonabscheidern für gase', *Chemie Ingenieur Technik,* Volume 44, pp. 63-71.

Muschelknautz, E., 1972, 'Die berechnung von zyklonabscheidern für gase', *Chemie Ingenieur Technik,* Volume 44, pp. 63-71.

Muschelknautz, E. & Greif, V., 1997, 'Cyclones and other gas—solids separators', In: *Circulating Fluidized Beds.* s.l.:ed: Springer, pp. 181-213.

Patterson, P. A. & Munz, R. J., 1989, 'Cyclone collection efficiencies at very high temperatures', *The Canadian Journal of Chemical Engineering,* Volume 67.2, pp. 321-328.

Rongbiao, X., Park, S. H. & Lee., K. W., 2001, 'Effects of cone dimension on cyclone performance', *Journal of Aerosol Science,* 32(4), pp. 549-561.

Shaw, W. F. a. B., 2006, 'Efficiency and pressure drop of cyclones across a range of inlet velocities', *Applied engineering in agriculture,* Volume 22, p. 155.

Smolik, J., 1975, *Air Pollution Abatement, Part I: Scriptum No. 401-2099,* s.l.: Techn. Univ. of Prague.

Stein, A. C. H. a. L. E., 2002, '*Gas cyclones and swirl tubes*', s.l.:Springer.

Stern, A. C., 1955, '*Cyclone dust collectors*', New York: American Petroleum Institute.

Svarovsky, L., 1981, 'Economics of Gas Cleaning; Equipment Selection', In: E. J. C. Willams and T. Allen, ed. *Handbook of Powder Technology.* Amsterdam: Elsevier scientific publishing company.

Wan, G. S. G. X. X. &. S. M., 2008, 'Solids concentration simulation of different size particles in a cyclone separator', *Powder Technology,* 183(1), pp. 94-104.

Yoshiro, M., Suganuma, A. & Tanaka, S., 1968, 'On collection efficiency of gas cyclone in coarse particle range', *Journal of Chemical Engineering of Japan,* 1(1), pp. 82-86.

Zenz, F., 1975, Chapter11 in Manual on Disposal of Refinery Wastes; Volume on Atmospheric Emissions. In: *Cyclone separators.* s.l.:API Publications.

Zenz, T. & F., T., 1984, 'Evaluating cyclone efficiencies from stream compositions', *Chemical engineering,* Volume 91, pp. 69-73.

Zhu, Y. & Lee, K., 1999, 'Experimental study on small cyclones operating at high flowrates' *Journal of Aerosol science,* Volume 30, pp. 1303-1315.

Infrastructure for Changing Climate and Sustainable Built Environment

Proceedings of the 7th International Symposium on

Advances in Civil and Environmental Engineering Practices for Sustainable Development

ACEPS - 2019

Simulation of pedestrian evacuation in the underground train station: a case study of MRT Huai Khwang station

P. Boonsomparn[1] and M. Piantanakulchai[1]

[1]School of Civil Engineering and Technology, Sirindhorn International Institute of Technology Thammasat University, Pathum Thani, Thailand

K e y w o r d s

Pedestrian simulation
VISSIM/VISWALK
Train station evacuation

A B S T R A C T

Evacuation is the process of emergency response to manage a crowd of people to move out of building safely during the emergency circumstances. Local and international evacuation standards should comply with both facility dimension and evacuation time. The objective of this study is to simulate the evacuation of a pedestrian in MRT Huai Khwang station in Bangkok, Thailand. VISSIM/VISWALK software is applied to simulate the pedestrians' evacuation time where the simulation inputs are collected from site including the facilities dimension, the number of pedestrians and pedestrian speed. The results reveal that the facilities dimension of the MRT Huai Khwang station satisfy the requirements of both international and local standards. On the other hand, the evacuation time in both 2 scenarios (base case scenario and worst case scenario) satisfies both the requirements at the peak 15-min volume in 2019 and 2027. In addition, there should be additional emergency exits at the fare collection gate to overcome the ridership growth.

1. INTRODUCTION

An emergency situation in public space, including man-made incidents (terrorist attacks), technical problems (electricity failure) and natural disasters, is an unplanned and unprecedented sudden event that caused loss of human life or great damage in an area (Mao et al., 2019). One of the most emergency situations that occur in transit station is fire (Kallianiotis et al., 2018). Therefore, plans of evacuation procedure must be made for the safety of people. In this case, there are some influencing factors that can affect evacuation procedure such as pedestrian behavior and location of exits. Normally, preparation of evacuees must be provided in the workplace at least once a year to make sure that crowd can evacuate to safe area in short period of time limited by local or international standards.

Bangkok is one of the most popular cities in Southeast Asia region with more than 10 million people in 2019 (MLA, 2019). Hence, these citizens rely heavily on public transit as commuting mode. MRT (Mass Rapid Transit) is one of the most popular public transportation mode connecting various kind of land use in the Bangkok Metropolitan Region (BMR) including residence, workplace, school, market, etc. MRT blue line is one of the most crowded transit line in Bangkok which has opened for operation since July 2004. In addition, the number of passengers of MRT blue line is gradually increasing from around 170,000 trips/day in 2008 to 290,000 trips/day in 2017 (Figure 1), 6.3% average growth per year (MRTA, 2018). At this growth rate, ridership of MRT blue line will reach about 450,000 trips/day in 2025 and 530,000 trips/day in 2030. The more ridership increases, the longer evacuation time is affected. In which, the evacuation planning should be taken in consideration for safety issue. In 1996 the first subway (MRT blue line) in Bangkok was constructed, even though this mega-infrastructure was designed to meet all necessary requirements including structural standard, flood prevention, fire prevention, etc.

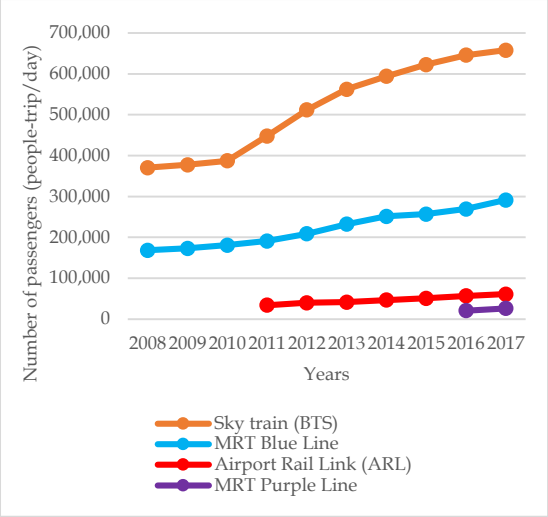

Source: (MRTA, 2018)

Figure 1 The average number of passengers on an urban railway system in Bangkok

In general, the physical characteristic of MRT station is the main factor affecting the evacuation procedure including location of exit, number of stair and obstacles (columns) (Li et al., 2019). There are detail of safety standards to increase safety in transit facilities such as minimum width of stairways, ramps, passageways and proper design platforms including safety equipment in the station about lighting, ventilation, acoustics and fire control (Hoel and Rozner, 1976). Therefore, an international standard of fire evacuation was set by the National Fire Protection Association (NFPA)-130 (NFPA, 2014), which aims to prevent death or injury of people during fire emergencies. In addition, in Thailand there is also local regulation (Ministry of Interior Regulations) to prevent fire disasters in public space and to increase the safety standard for Thailand.

Generally, the evacuation might be designed manually with some conventional methods. Using simulation can provide advantages over conventional design methods. Some complex factors such as emotion and visibility can be modeled in the evacuation process. With the advantages of simulation software and computational modeling, this study adopted VISSIM/VISWALK software (http://vision-traffic.ptvgroup.com/en-us/home/) to evaluate the evacuation time of MRT station (Huai Khwang station) under several scenarios. This study could lead to visualization of actual pedestrian behavior at the MRT station during emergency situation including dynamics of crowds, interaction between pedestrians and the effect of the environment (Johansson et al., 2015).

The results of this showed evacuation time of the pedestrian in MRT Huai Khwang station and the bottleneck issue at the fare gates in order to handle with the future ridership growth. To fulfill the objective of this study, we organized the research work into 5 sections. We described the general idea and objective of this study in the first section, then the previous studies are reviewed in the second section. Methodology and data collection are discussed in the third section. Then, actual facility dimension and evacuation time will be compared with regulations. In the last section, discussion and policy recommendations are presented.

2. LITERATURE REVIEW

2.1. Pedestrian Modeling

Previous studies investigated pedestrian flow characteristics in rail transit system using video recording (Caramuta et al., 2017, Zhao and Liang, 2016) to analyze different pedestrian characteristics and behaviors. The social force model is the most popular model used to describe the movement of the pedestrian with simple mathematical formulation (Ma et al., 2019). A general equation of the social force was written as a sum of different attractive and repulsive effects (Helbing and Johansson, 2009):

$$\vec{f}_i(t) = m_i \frac{v_i^o(t)\vec{e_i^0} - \vec{v_i}(t)}{\tau_j} + \sum_{j(\neq i)} \vec{f}_{ij} + \sum_w \vec{f}_{iw} \quad (1)$$

Where $\vec{f}_i(t)$ is the individual's total motivation to move in a certain direction at a specific time(t). m_i denoted the mass of the individual. $v_i^o(t)\vec{e_i^0}$ is a pedestrian movement with a certain speed and certain direction. $\vec{v_i}(t)$ is a current velocity of a pedestrian. τ_j denotes relaxation time. $\vec{f}_{ij}$ is the repulsive force of pedestrian and $\vec{f}_{iw}$ is the repulsive force of the wall.

Besides the social force model, there are also other models such as agent-based models (Kuligowski et al., 2005), queueing models for studying about the effect of delay in case of queue service (Yanagisawa et al., 2013) and and queue behavior in pedestrian evacuation (Hu et al., 2018).

2.2. Pedestrian Evacuation

Most of the researchers study the parameters that affect pedestrian evacuation with architectural design and evacuation behaviors. Previous studies analyzed and classified the parameters that affect the pedestrian behaviors. Li et al. (2017) studied the behavior of pedestrians in the high temperature during fire which blocks the exit path. Smoke from fire affects the limit of visibility, causing difficulty to evacuate pedestrians from the building (Wang and Cao, 2019, Chen et al., 2019). Evacuation time is longer than normal situation because the density is high due to congestion under emergency situation (Shi et al., 2012). Normally the speed of pedestrians varies due to a person's characteristics example age, sex, apparent, etc and environment condition such as visibility and bottleneck (Kallianiotis et al., 2018).

In Thailand, there are also limited number of previous studies about fire safety. The design of exit door width effects on the evacuation, the results showed that large of exit door size evacuation time will be less and smock curtain not effect on evacuation (Sukkiwanut, 2011). From the study of fire protection system in a hospital using the National Fire Protect Association (NFPA) and Ministry of Interior regulations, it was found that there are some problems in fire protection system occurred due to lack of system monitoring (Saelao, 2001).

2.3. Fire Evacuation Simulation

Simulation technology is key to generate a virtual situation that could be used to forecast and evaluate the safety. Evacuation modeling could provide fire safety and it has been applied in a different of infrastructures such as the underground train (Li et al., 2017). There are many types of software used with different abilities and limitations. Therefore, selecting the appropriate software for specific objectives is very critical, for example, BuildingExodus is suitable to model large-scale urban evacuations by including road network and open space around the building while VISWALK can simulate and calibrate parameters of pedestrian evacuation in smaller scale such as classrooms (Gaddam et al., 2018). The advantages of VISWALK are the ability to simulate real situation with many functions including the detail of results (queueing time, area result and travel time), 3D visualization and various type of file input supported such as BIM and CAD.

2.4. National Fire Protection Association (NFPA) standards

NFPA-130 is an international standard which specifies fire protection and life safety requirements for fixed guideway transit and passenger rail systems. In this study the standard of evacuation time and width requirement were used to analyze infrastructure design in MRT Huai Khwang station (Table 1).

Table 1 Minimum width requirement for facilities in transit station

Facilities	Minimum width requirement (m)
Stairs / Escalator	1.12
Exit corridors	1.73
Exit ramp	1.83
Doors / Gates	0.91
Fare Collection Gates	0.51
Turnstile	0.46

Source: NFPA-130 standard (NFPA, 2014)

NFPA-130 set the maximum time of evacuation from transit station using 2 criteria:

- Evacuation from the platform to the next adjacent floor should be 4 minutes or less and the farthest distance on the platform towards safety not more than 91.4 meters.
- Evacuation from the platform to station's exit should be 6 minutes or less.

2.5. Ministry of Interior Regulations

This is the regulation for the building design in Thailand, providing prevention of fire and fire evacuation. Examples of regulations are:

- The stairs must be shown that it can evacuate all the occupants to the exterior of the building within 1 hour.
- There are fire exit paths that connect to every floor, which contains at least 2 exits per floor with evacuating

occupants to safety area within 5 minutes.

- There must be no obstructions on the fire exit path from building towards the safety area and the width of exit way should be more than 1.70 m.

3. METHODOLOGY

In this study, MRT Huai Khwang station which is one of the most crowded underground station of MRT Blue Line was selected as the case study. The station contains 3 levels: base level concourse level and platform level. The concourse level consists of 4 exits, ticket counters and ticket machines. The platform level enables pedestrians to board the trains in 2 directions. Huai Khwang station has 4 stairways, 2 escalators and 1 elevator connect between concourse level and platform level.

The model of MRT Huai Khwang station was created by VISSIM software using VISWALK module. In this study, we consider two cases (base case scenario and worst case scenario) at a different number of users. In the base case scenario, it supposes that all fare collection gates and swing gates are opened during emergency situation (Figure 2). On the other hand, in the worst case scenario, the electricity might be cut off during the emergency. It is assumed that the fare collection gates do not operate except the swing gate (this gate is normally used for staffs, disable person or person with large luggage, and open manually).

a) Fare collection gates

b) Swing gates

Figure 2 a) Fare collection gates and b) Swing gate

As mentioned above, the growth of ridership is about 6.3% yearly, different number of passengers could lead to better planning to overcome this growth rate. Moreover, we have considered three critical positions such as platform level, fare collection gate, and exit.

3.1. Data Collection

In this study, the data were collected inside the MRT Huai Khwang station using the video camera and manual count described as follows

- Count the pedestrians at concourse level and platform level
- Survey the exit paths and recording the speed of a pedestrian.
- Collect information inside the MRT station such as obstacles (column), facilities width and the number of steps of stairs.

3.2. Evacuation time

This model provides evacuation time to 3 points (Figure 2 and Figure 3); 1) evacuation time from the platform to the next floor (t_1), 2) evacuation time to fare collection gates (t_2), and 3) evacuation to station's exit (t_3). According to NFPA standard and Ministry of Interior regulations, the evacuation time should not be exceeded the minimum required time (see 2.4).

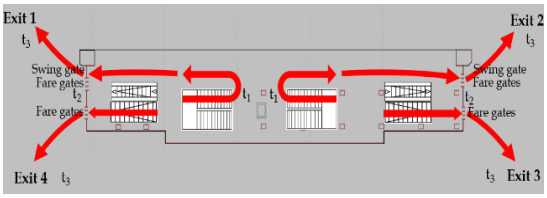

Figure 2 Layout of facilities in the concourse level

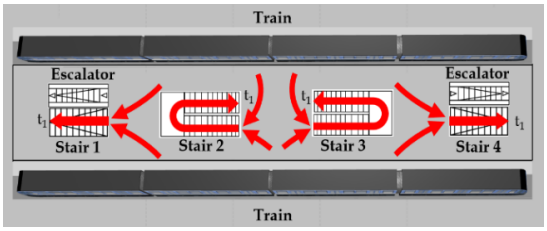

Figure 3 Layout of facilities in the platform level

4. RESULT AND DISCUSSION

4.1. Survey Data

The surveys were conducted on Monday, Wednesday and Friday (22nd, 24th and 26th May 2019) in the morning peak rush hour. (07:30 - 08:30).

4.1.1. Facilities design

The facilities in MRT Huai Khwang station include stairs, escalators, elevation and fare collection gate. The important facilities for evacuation from platform to safety area are 4 main stairs between platform and concourse, 2 fare collection gates, and 4 exits. To evacuate pedestrian on platform, all occupants could use the 4 stairs, then they have to go through one among the 2 fare collection gates (each gate has 3 entrance gates, 3 leave gates and 1 swing gate). After that, they could go the exits to leave the MRT station.

Table 2 Width of facilities in MRT Huai Khwang station

Facilities	Actual width (m)	NFPA-130 Minimum width required (m)
Stairs	2.00	1.12
Escalators	1.15	1.12
Exit corridors	6.00	1.73
Fare collection gate	0.58	0.51

The results shown in Table 2 were obtained by using the laser measuring device. The comparison of the width between actual design and NFPA-130 indicated that facilities inside MRT Huai Khwang station pass all minimum requirement in NFPA-130. In addition, exit corridors width (6.00 m) exceed width required by the Ministry Interior regulation (1.10 m).

4.1.2. The volume of pedestrians

The pedestrian volumes were collected in the underground train station on the concourse level and platform level by using two methods including manual counts and video cameras.

The analysis period was separated into 15 minutes intervals according to NFPA. The result showed that the maximum number of pedestrians is 1300 during 7:46 – 8:00 (Figure 5). At the average annual growth of 6.3%, the number of pedestrians during peak 15-min at this station could reach 2000 in 2027.

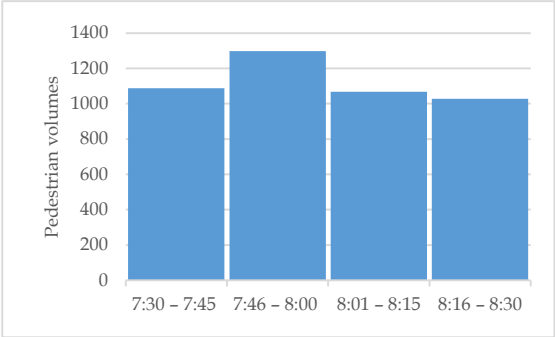

Figure 5 The volume of pedestrians

4.1.3. Pedestrian speed

The pedestrian walking speed during evacuation could not be collected at the train station during normal condition. Therefore, in order to obtain the speed during evacuation, the speed data were collected from the experiment by video cameras at Sirindhorn International Institute of Technology. Students were asked to evacuate from the building through the passageway. The time used in evacuation was recorded in order to calculate the evacuation speed by using the formula.

$$V = {}^{S}/_{t} \qquad (2)$$

Where s is the evacuation distance (m) and t denotes evacuation time (s)

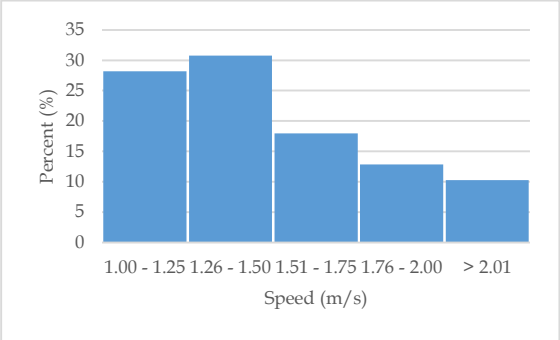

Figure 6 The pedestrian evacuation speed

From Figure 6, the average pedestrian walking speed during evacuation is 1.46 m/s. The average walking speed of pedestrians during the rush hour at MRT Huai Khwang station found from the field survey was 1.31 m/s which is lower than the speed of pedestrians during evacuation.

4.2. Evacuation Time

Table 3 Evacuation time in VISSIM/VISWALK software

Scenarios	Number of pedestrians in peak 15-min	Evacuation time (min)		
		Platform evacuation[a] (t_1)	Fare gate evacuation (t_2)	Station evacuation [b] (t_3)
		Maximum time	Maximum time	Maximum time
Scenario 1: Base case scenario	1300[c]	2.30	2.40	4.39
	1400	2.32	2.47	4.53
	1500	2.38	3.01	4.56
	1600	2.46	3.06	5.12
	2000[d]	3.12	3.37	5.38
Scenario 2: Worst case scenario	1300[c]	2.31	2.58	4.51
	1400	2.33	3.01	5.00
	1500	2.41	3.19	5.06
	1600	2.51	3.24	5.18
	2000[d]	3.16	4.01	5.52

[a] NFPA-130 evacuation from the platform within 4 minutes or less (t_1)
[b] NFPA-130 evacuation to safety area within 6 minutes or less (t_3)
[c] Peak 15-min volume in 2019
[d] Peak 15-min volume in 2027

In VISWALK model, the evacuation started at the platform. So the pedestrians should be evacuated from platform to 4 exit corridors. During the evacuation process, escalators and the elevator are not allowed to use because the electricity would be cut for standard security procedure. Some parameters in the simulation models including grid size, speed, relaxation time (τ_j), repulsive force and desired speed at the stair are calibrated to represent the actual situation at this train station. The evacuees move to exits through the shortest path which is calculated from VISWALK. The average evacuation time from 10 simulation runs was used to validate the model. NFPA evacuation time criteria consist of 2 situations as follows: Platform evacuation time should be within 4 minutes or less and the station should be evacuated within 6 minutes or less.

The platform evacuation time of both scenarios is close (Table 3) due to the fact that all the evacuation conditions are same. However, the fare gates evacuation time and station evacuation time of both scenarios are different due to the assumption of power shut down during emergency. The maximum evacuation time occurred at the stair 1. According to NFPA-130, all of the pedestrians should be evacuated from the platform within 4 minutes or less and the results showed that both scenarios passed the minimum time requirement. The farthest point towards stairs is 40.2 m which is less than the requirement of 91.4 m. In addition, according to the Ministry of Interior regulations, MRT Huai Khawng station meets the requirement that is at least 2 exits in every floor and evacuation should be within 5 minutes.

Table 3 shows that the evacuation time to the fare collection gate of 2 scenarios were different. In the worst case scenario, the simulation showed that there exits the bottlenecks at stairs and swing gates. This made the evacuation time increases around 12.04% from the base case scenario.

The distances from the platform to each exit are different. In which pedestrians prefer to use the shortest path. The farthest distance of exits following exit 3 (138 m), exit 4 (131 m), exit 1 (121 m) and exit 2 (113 m) so, most users select exit 2 (30.20%) following with exit 1

(27.80%), exit 4 (22.13%) and exit 3 (19.88%). According to NFPA-130, the pedestrians should be evacuated out of the station within 6 minutes or less. The results of both 2 scenarios showed that the evacuation time was less than that is required from NFPA-130 standard, and the Ministry of Interior regulations. It is recommended that there should be some additional emergency exits at these points to cope with the ridership growth.

Moreover, the average travel time drops from 2.46 min (normal condition) to 3.21 min (evacuation, base case scenario) and 3.46 min (evacuation, worst case scenario) due to the congestion at the stairs and high density of passageway similar to the result from the previous study (Shi et al., 2012).

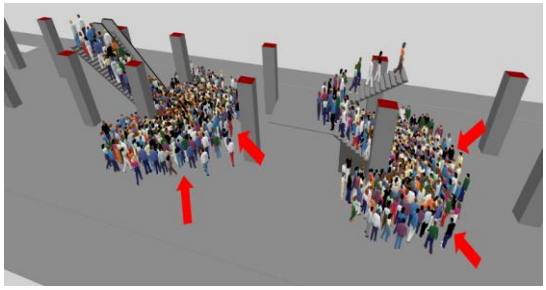

Figure 7 Bottleneck at the stairs during evacuation

5. CONCLUSION

This study applied VISSIM/VISWALK software to create the model to simulate the evacuation from MRT Huai Khwang underground train station under 2 scenarios at the different levels of demand. The evacuation model provided egress time and the path of exits which show the performance of overall evacuation plan. Site data including facilities dimension, number of passengers and pedestrian speed are collected as the input for simulation modeling. It was found that the facilities dimensions (stair width, fare collection gate width, corridor width, etc.) of the MRT Huai Khwang station and maximum time required for evacuation satisfy the requirements of both local and international standards.

Future studies should increase the duration of survey to increase the reliability of data. Evacuation time depends on the characteristics of pedestrians (age, gender, etc). In this study, because the data were collected from an experiment settings at the university, pedestrian speeds were collected from 61.11% male, 38.89% female and age of 17–19 years. Thus, it recommended that the effect of pedestrian characteristics should be considered in the future study. In addition, there also some limitations of this study that could be done in the future work by including other factors such as low visibility, change path planning exit and negative emotions.

6. ACKNOWLEDGMENTS

The authors would like to thank Sirindhon International of Technology (SIIT) for providing facilities and financial support for collecting data. Special thanks of gratitude go to Mass Rapid Transit Authority of Thailand (MRTA) for the permission to collect data in MRT Huai Khwang station.

7. REFERENCES

Caramuta, C., Collodel, G., Giacomini, C., Gruden, C., Longo, G. & Piccolotto, P., 2017, 'Survey of detection techniques, mathematical models and simulation software in pedestrian dynamics', *Transportation research procedia,* 25**,** 551-567.

Chen, Y.-J., Shu, C.-M., Ho, S.-P., Kung, H.-C., Chien, S.-W., Ho, H.-H. & Hsu, W.-S., 2019, 'Analysis of smoke movement in the Hsuehshan tunnel fire', *Tunnelling and underground space technology,* 84**,** 142-150.

Gaddam, H. K., Arya, A., Vanumu, L. D. & Rao, K. R., 2018, 'Calibration and Validation of Pedestrian Simulation Parameters: A Case Study of Classroom Evacuation'.

Helbing, D. & Johansson, A., 2009, *Pedestrian, crowd and evacuation dynamics*, Springer.

Hoel, L. A. & Rozner, E. S., 1976, 'Planning and Design of Intermodal Transit Facilities', *Transportation Research Record*.

Hu, J., You, L., Zhang, H., Wei, J. & Guo, Y., 2018, 'Study on queueing behavior in pedestrian evacuation by extended cellular automata model', *Physica A: Statistical Mechanics and its Applications,* 489**,** 112-127.

Johansson, F., Peterson, A. & Tapani, A., 2015, 'Waiting pedestrians in the social force model', *Physica A: Statistical Mechanics and its Applications,* 419**,** 95-107.

Kallianiotis, A., Papakonstantinou, D., Arvelaki, V. & Benardos, A., 2018, 'Evaluation of evacuation methods in underground metro stations', *International journal of disaster risk reduction,* 31**,** 526-534.

Kuligowski, E. D., Peacock, R. D. & Hoskins, B. L., 2005, *A review of building evacuation models*, US Department of Commerce, National Institute of Standards and Technology.

Li, Q., Gao, Y., Chen, L. & Kang, Z., 2019, 'Emergency evacuation with incomplete information in the presence of obstacles', *Physica A: Statistical Mechanics and its Applications***,** 122068.

Li, Y., Wang, H., Wang, C. & Huang, Y., 2017, 'Personnel evacuation research of subway transfer station based on fire environment', *Procedia Engineering,* 205**,** 431-437.

Ma, L., Chen, B., Wang, X., Zhu, Z., Wang, R. & Qiu, X., 2019, 'The analysis on the desired speed in social force model using a data driven approach', *Physica A: Statistical Mechanics and its Applications,* 525**,** 894-911.

Mao, Y., Du, X., Li, Y. & He, W., 2019, 'An emotion based simulation framework for complex evacuation scenarios', *Graphical Models,* 102**,** 1-9.

MLA., 2019, *World Population Review* [Online]. [Accessed 17 August 2019].

MRTA, 2018, Annul Report 2018. Mass Rapid Transit Authority of Thailand.

NFPA 2014, *NFPA 130: standard for fixed guideway transit and passenger rail systems*, NFPA.

Saelao, T. 2001. *A Study of Fire Evacuation in Student Dormitory at Kasetsart University, Si Racha Campus by Numerical Method.* Master degree, Kasetsart University.

Shi, C., Zhong, M., Nong, X., He, L., Shi, J. & Feng, G. 2012. Modeling and safety strategy of passenger evacuation in a metro station in China. *Safety Science,* 50**,** 1319-1332.

Sukkiwanut, V. 2011. *Study and Analysis for Fire Protection System in Extra Large Building Case Study: Khumklao Building, Bhumibol Adulyadej Hospital.* Kasetsart University.

Wang, P. & Cao, S., 2019, 'Simulation of pedestrian evacuation strategies under limited visibility'. *Physics Letters A,* 383**,** 825-832.

Yanagisawa, D., Suma, Y., Tomoeda, A., Miura, A., Ohtsuka, K. & Nishinari, K., 2013, 'Walking-distance introduced queueing model for pedestrian queueing system: Theoretical analysis and experimental verification', *Transportation research part C: emerging technologies,* 37**,** 238-259.

Zhao, Z. & Liang, D., 2016, 'Pedestrian flow characteristic of Metro Station along with the mall', *Procedia Engineering,* 135**,** 602-606.

Proceedings of the 7th International Symposium on

Advances in Civil and Environmental Engineering Practices for Sustainable Development

ACEPS - 2019

Speed variation of vehicles correspondent to road, driver, and environmental characteristics

N. Amarasingha[1], N.N. Samarasinghe[1]

[1]Department of Civil Engineering, Faculty of Engineering, Sri Lanka Institute of Information Technology, Malabe, SRI LANKA

K e y w o r d s

Speed limit variation
Posted speed limit
Multiple regression analysis

A B S T R A C T

According to the Sri Lankan Police records, the major problem for road crashes can be pointed out as speeding. Speed limit is one of the most important factors for road users, drivers as well as the pedestrians. Variation of speed limit affect the travel time, comfort, economy, and safety. Operating speed models influence the design of traffic flow network models, road design, design consistency, and traffic safety. This research attempts to identify the parameters which affects for the speed variations of vehicles by selecting curved and straight roadway sections in Colombo-Galle road. The research was conducted at a random sample of 1200 vehicles in five roadway sections on road, driver and environmental characteristics. Two multiple regression models for straight and curved roadways sections were developed. The variable which effect on speed variation were found. This study can be used as a baseline for development of more comprehensive speed variation models for Sri Lankan traffic condition.

1. INTRODUCTION

Speed management and traffic controlling are the most complex challenges for every country. To overcome those matters speed models are developed. Speed models influence the design of traffic flow network models, road design, design consistency, and traffic safety. Most urban traffic network models rely on existing traffic flow data as inputs. However, network models are required to make assumptions regarding vehicle operating speeds. Speed models would also improve network performance. The complete road design approach is moving away from a car centric design by setting the design speed as the posted speed limit, allowing narrower lanes, allowing on street parking, reduced pedestrian crossing distances etc. In such an approach knowing how design elements affect operating speeds will serve better design. At the completion of road designing, the major challenge to control the vehicle speed throughout the road sections with different characteristics.

In accordance of economic growth, the number of vehicle population is increasing in Sri Lanka as shown in Table 1. Due to the increasing number of vehicles the huge traffic congestions occur in urban areas. To avoid delays, road users tend to travel faster without paying attention on road safety rules. According to the report published by Ministry of Transport and Aviation of Sri Lanka, around 40,000 crashes were recorded in Sri Lanka during 2017. The Sri Lanka Police mentioned that, over the decade of 2007–2017, six number of people have died daily in Sri Lanka on average of road traffic crashes. Based on the previous research studies, one of the main reasons for road crashes is the uncontrolled speed limit. Setting and enforcing speed limit is important to reduce the speed at road. When deciding speed limits; road engineers consider the vehicle, roadway, and environmental characteristics.

Table 1 Vehicle Population in Sri Lanka from 2012 to 2017 (Source: Department of Motor Traffic, Sri Lanka)

Year	2012	2013	2014	2015	2016	2017
Motor cars	499,714	528,094	566,874	672,502	717,674	756,856
Motor Tricycle	766,784	850,457	929,495	1,059,042	1,116,987	1,139,514
Motor Cycle	2,546,447	2,715,727	2,988,612	3,359,501	3,699,630	4,044,010
Buses	91,623	93,428	97,279	101,419	104,104	107,435
Dual purpose vehicles	280,143	304,746	325,545	365,001	391,888	406,630
Motor Lorries	323,776	329,648	334,769	341,911	349,474	352,275
Land vehicles – Tractors	315,520	326,292	333,362	343,339	353,624	362,275
Land vehicles - Trailers	53,020	55,286	57,298	59,426	63,088	362,446
Total	4,877,027	5,203,678	5,633,234	6,302,141	6,795,469	7,247,122

In Sri Lanka, the national roadways are classified under the class-A, -B, and -E. The maximum speed limit for E-class roadways is 100 km/h and the maximum speed limit of A- and B-class roadways are introduced based on the urban/rural nature and vehicle type. Traditionally, the focus has been made on enforcement to reduce speeding of vehicles. However, on some road sections, enforcement only temporarily reduces operating speeds. Some roads (or road sections) need to be redesigned to more closely match the desired operating speeds. There are many research aimed to study operating speeds, and understanding speed selection. Currently, there is a very little information on setting up the urban speed limits is available in Sri Lanka. Therefore, the objective of this study was to investigate the effect of road, driver, and environmental characteristics on vehicle speed.

2. LITERATURE REVIEW

A research was done to evaluate the applicability of speed limits for Sri Lankan road network and develop a methodology for setting up speed limit for selected road sections (Abeysekara et al. 2012). The scope was limited to straight road sections in flat terrains in sub-urban areas where other characteristics like shoulder conditions, and roadside development were similar. Two A-class roads with similar characteristics and geometry were selected and investigation were done on those road sections. Speed data by vehicle category were collected using radar guns on weekdays ensuring the speed of free flow vehicles with standard headway. The 85 percentile speeds of each vehicle category were estimated comparing them with speed limits. It was found that only three-wheelers and busses exceeded the speed limit and other vehicles managed their speed limits during the selected areas.

Long et al. (2006) evaluated the safety of 1100 km of rural roads in South Australia once speed was reduced from 110 km/h to 100 km/h. Crash data of two years of before and two years of after the speed limit reduction were investigated and found only a 1.9 km/h reduction in the average speed of the vehicles and a 20 percent reduction in casualty crashes. Also, a follow up report on the same roadway segments were analyzed ten years of before and after speed reduction and compared the results with control segments where the speed limit was still 110 km/h. It was revealed that the control segments, which still had the same speed limit, had also experienced a long-term trend of crash counts reduction. However, a pronounced drop in casualty crashes was apparent with speed reduction.

In a similar study, Kockelman (2006) investigated the impact of raising the speed limit on the operating speed as well as the associated variability in the speed on high-speed roadways. It was found that the average speed and the speed variability are more influenced by roadway geometry and cross-sectional characteristics as compared to posted speed limits. These findings were largely reflective of driver opinions on speed limits.

Aljanahi et al. (1999) developed models to investigate trend of crash rates change with regard to various roadway and traffic characteristics including speed. The crash rates were explored on divided highways in two sets of locations, in United Kingdom (UK) and in Bahrain using 200 participants. The data collection was done using automatic speed collectors and vehicle counters. Substantial safety improvement was proposed that could be achieved either by mandating

lower speed limits or reducing the spread of vehicle speeds. Lower crash rates were found in UK sites and there was a strong statistical relationship between crash counts and the variability of traffic speed, while the results for Bahrain were associated with higher crash rates, indicating the mean speed of the traffic is a stronger predictor of crash rates.

Kurlaftis and Golias (2002) investigated road geometric characteristics and crash rates for the straight rural two lane highway. Width of lane, Average Annual Daily Traffic (AADT), Serviceability Index (SI), pavement type, and friction factor of the tire with the contact area of the road were the investigated sub factors. After summarizing the sub factors, speed was identified as the major influenced factor for increment of crashes. When compared the factors with their relative importance, the relative importance was 100% for AADT, 72% for lane width, 59% for serviceability, 32% for tire friction, and 30% for pavement condition.

Classen et al. (2013) done a study on Older Driver's driving behavior using Geographic Position System (GPS) tracking data in Japan. About 108 older drivers were involved in the data collection process over one month period and examined older driver's behavior on road selection, turning, and speed selection. Drivers filled the basic survey and asked them to install data collection devices in their vehicles. Age limit, peak period, and trip mode were considered in the survey. Through previous studies found that older driver's inclined to drive slowly, this research did not prove that. The older drivers drove faster than other drivers in national and ordinary roads. It was recommended to improve the transportation planning by developing driving assistance systems for older drivers.

Calvi and Bella (2014) investigated speed differential parameters in day and night environments using driving simulator. The main objective was to analyze drivers' speed profiles for evaluation of speed in different conditions. Two lane rural road sections with 10 km length were selected and 40 drivers whose age in between 23 and 41 years were investigated in both day and night conditions. Drivers' speed profiles at the midpoint of the tangent, midpoint of circular curve, maximum speed on last 200m of approach tangent and the speed on the tangent at 100m before the beginning of the curve were recorded. After gathering all the data, the models were developed to find out the correlation between parameters. It was revealed that there was a huge difference in visibility between day and night conditions.

3. METHODOLOGY

Five road sectioned on A2 road between Kalutara and Moratuwa were selected; the length of those section were about 250 m to 350 m as shown in Figure 1. The yellow bullets in Figure 1.a show the boundary of the selected area and the numbered locations give approximate location of selected sections. Those locations were further zoomed-in as shown in Figures 1.b, 1.c, and 1.d. Three straight road sections were selected for the research are shown in Figures 1.b and 1.c. Sections 1 is located in Panudura-Pinwatta area and Section 2 is located Waskaduwa – Mahawaskaduwa area while section 3 is located at Moratuwa New Galle road deviation.

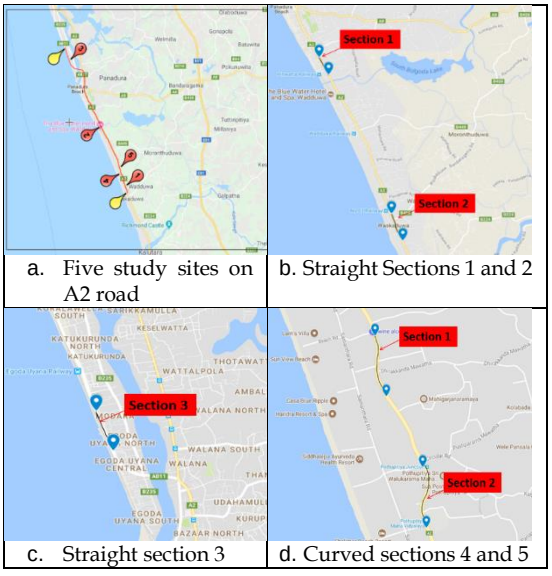

a. Five study sites on A2 road
b. Straight Sections 1 and 2
c. Straight section 3
d. Curved sections 4 and 5

Figure 1 The Study Area

The street views of all three straight road sections are shown in Figure 2. Two curved road sections selected were Pothupitiya Maha Vidyalaya – Pothupitiya Junction area (section 4) and Pohaddaramulla – Molligoda area (section 5). The street views of two curved road sections are shown in Figure 3.

The AADT is these sections approximately 60,000. Every selected section contains a pedestrian crossing, intersection, and a bus stop. The pavement material in all sections was asphalt and pavement performance was similar.

Section 1	Section 2	Section 3
Panadura – Pinwatta area (From Kalutara Side)	Waskaduwa– Mahawaskaduwa (From Kalutara Side)	Moratuwa New Galle Road Deviation (From Panadura Side)

Figure 2 Street Views of Straight Road Sections

Section 4	Section 5
Pohaddaramulla – Molligoda area (From Kalutara Side)	Waskaduwa– Mahawaskaduwa (From Kalutara Side)

Figure 3 Street Views of Curved Road Sections

The characteristics such as length of section, lane width, number of lanes, vegetation density, and posted speed limits of selected sections are given in Table 2. The distances to the pedestrian crossings and intersections have measured from changing the locations at a time.

Table 2 Roadway Features in Study Sites

Road Section	Length of the section	Lane Width (m)	No of Lanes per direction	Total Lanes	Vegetation Density	Posted Speed Limit of light vehicles
1	350 m	3.0	2	4	Medium	50 km/h
2	275 m	2.8	1	2	High	40 km/h
3	300 m	3.7	2	4	Low	50 km/h
4	275 m	2.7	1	2	High	40 km/h
5	300 m	3.5	1	2	Medium	50 km/h

3.1. Effecting Factors for Speed Selection

After reviewing the past research articles, the factors affecting for the speed selection were selected. Also, some other variables which were unique to these sites found by observation and considered for the study. The human factors are the major causes for every incident happens on the road. The possibility of controlling mind of a person and physical fitness are very difficult. Fatigue, inexperience, and inattention of drivers can be identified as the driver behavioral characteristics which may affect the speed of vehicle. The effect of vehicles factors on speed selection were also considered. A set of factors are considered when designing a vehicle which included the braking and deceleration, acceleration, low-speed turning characteristics, high-speed turning characteristics, size, and weight. Defective brakes, worn tires, and other vehicle defects affect the driving, especially at high speeds. It has been observed that the tire at high speeds and lead to loss of control could be undermined. The separation of the tire tread is another factor that leads to loss of control. Vehicles and traffic interaction, such as surface roughness play an important role in the vehicle stop. The above mentioned factors can be identified as the most common factors for variation of speed. The parameters selected for this study are tabulated in Table 3 and the discussed them in following sections.

Vehicle Type: The main categories of vehicles have defined as passenger cars, buses, trucks, and recreational vehicles. As all the five selected sections are located very close to the urban areas there were several types of vehicles. The gathered 1200 participants were divided into 8 classes by visual observation.

Vehicle Condition: Vehicle condition was recorded after observing its number plate which is assigned based on the sequence of registration in Sri Lanka. The category named 'new' was for the numbers which having two or three English letters at the beginning. And for the 'old' category, the number plates which contains only numbers which have been observed. The condition is directly affected for the speed limit selection due to the performance of the engine.

Table 3 Parameter Definition

No	Variables	Abbre.	Description	Type
1	Vehicle Type	VT	0 Motorcycle 1 Three-wheeler 2 Car 3 Van 4 Cab 5 Bus 6 Lorry 7 Multi-axle vehicle	Categorical variable
2	Vehicle condition	VC	0 Old 1 New	Binary variable
3	Gender	GEN	0 Female 1 Male	Binary variable
4	Driver age (approximately)	AGE	0 18-30 years 1 31-40 years 2 41-50 years 3 51-60 years 4 61 70 years	Categorical variable
5	Number of passengers	PAS	The count of the passengers taken as 1,2,3,4 etc.	Nominal variable
6	Speed	SPD	Observed speed entered as nominal value.	Nominal variable
7	Weather condition	WC	0 Sunny 1 Rainy	Binary variable
8	Time of the day	TIM	0 Morning 1 Afternoon 2 Night	Categorical variable
9	Vegetation density	VEG	0 Low 1 Medium 2 High	Categorical variable
10	Lane width	LW	Entered as the measured length meters	Nominal variable
11	Number of lanes	NOL	Entered as a count	Nominal variable
12	Shoulder width	SW	Entered as the measured length in meters	Nominal variable
13	Posted speed limit	PSL	Entered the speed limit in km/h	Nominal variable
14	Distance to the speed limit sign board	DSS	Entered as the measured length in meters	Nominal variable
15	Distance to the nearest pedestrian crossing from location where measuring the speed.	DPC	Entered as the measured length in meters	Nominal variable
16	Distance to the nearest Intersection from location where measuring the speed.	DI	Entered as the measured length in meters	Nominal variable
17	Day of the week	DOW	0 Weekend 1 Weekday	Binary variable
18	Availability of guard rail at the center of road	AGR	0 No 1 Yes	Binary variable
19	Availability of parking bays	APB	0 No 1 Yes	Binary variable
20	Availability of bus stops	ABS	0 No 1 Yes	Binary variable

Gender: The variable gender was identified by visual observation. The selected sections were close to urban areas and considerable number of female drivers were observed in the study.

Driver age: The new license holders and young generation could not have much experience in driving, most of the time they select middle range of speed. But the middle age drivers tend to drive faster and able to take risks while the older drivers need more reaction time than others. Age of driver was determined by visual observation and divided into five groups as shown in Table 3.

Number of passengers: Number of the passengers in a vehicle were counted when it passes the observer. The passenger count in a bus was approximately entered as it is hard to count while it is running.

Vehicle speed: The spot speeds of vehicles were measured using the speed guns and recorded in kilometers per hour by vehicle category.

Weather condition: People tend to drive faster in normal weather conditions and mostly decrease their speed in adverse weather conditions. The survey was conducted in both sunny and rainy conditions to check the speed variance in different conditions.

Time of the day: People tend to drive faster in day time and mostly decrease their speed in night due to reduced visibility.

Vegetation density: Due to the vegetation density of roadside, speed of a vehicle can be varied. The vegetation densities have categorized in three groups as low, medium, and high.

Road width: On urban roads, both lane widths were measured from the curb face. Therefore, most carriageways would be the sum of the lane widths.

Number of lanes: The number of lanes was recorded and taken as a nominal value when analysing.

Posted speed limit: The posted speed limit was recorded in km/h.

Distance to speed limit sign: If the posted speed limits have showed on roads, most of the drivers may pay attention for the signs. In this study, the distance from the observing point to the speed limit sign was measured in meters.

Pedestrian crossings: Pedestrian crossings affect the operating speed of the vehicles. Therefore, the distance form pedestrian crossings was measured in meters.

Impact of Intersections: Mean speeds reduce with the traffic density of an intersection. According to the findings of Wang et al. (2006), T-intersections have a similar impact on operating speeds. The distance for the three-way junctions or four-way junctions was measured in meters.

Day of week: During weekends traffic flow is low and high speed on road can be expected. Therefore, data were collected covering both weekends and weekdays.

Availability of guard rails at the center: Previous studies showed the presence of median barrier as a factor to increase the operating speeds. Having guard rail reduces the unnecessary over-takings of the vehicles, as drivers have to move only in their lanes.

Availability of parking bays: Many researchers demonstrated that on-street parking has a statistically significant impact on reducing operating speeds. A road cross-section with parking bays develop a non-clear zone and vehicles pulling in and out of parking spaces have an impact on through traffic and it affects for the operating speed. In this study, some selected areas contain parking bays.

Availability of Bus stops: Bus stop also effects the operating speed of the vehicles.

3.2. Method

The first step of analysis was to develop correlation matrix to identify strongly correlated variables. After excluding highly correlated variables, the multiple regression techniques were used to develop the relationships. Multiple regression is a statistical technique to understand the relationship between one dependent variable and several independent variables. The purpose of multiple regression is to develop a linear equation that can best determine the value of dependent variable Y for different values of independent variables in X. The basic equation of Multiple Regression is:

$$Y = a + b_1x_1 + b_2x_2 + b_3x_3 + \ldots + b_Nx_N \quad (1)$$

The multiple regression model is based on the following assumptions:

- There is a linear relationship between the dependent variables and the independent variables,
- The independent variables are not too highly correlated with each other,
- Observations are selected independently and randomly from the population, and
- Residuals should be normally distributed with a mean of 0 and variance.

R-squared value: The co-efficient of determination, R-squared (R^2), is a statistical metric that is used to measure how much of the variation in outcome can be explained by the variation in the independent variables.

F value: F-test is used to find out whether the variances between the two populations are significantly different.

p value: A small p-value (typically < 0.05) indicates strong evidence against the null hypothesis. A large p-value (> 0.05) indicates

weak evidence against the null hypothesis. The p-values very close to the cut-off (0.05) are considered to be marginal.

4. RESULTS

A total of 1,200 vehicles were observed in this study. The observed vehicle composition is shown in Figure 4.

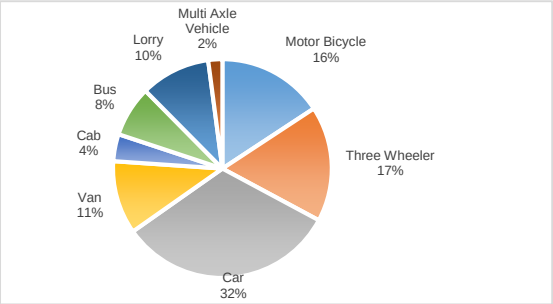

Figure 4 Observed Vehicle Composition

The speeds of observed vehicles were between 18 km/h to 85 km/h. The speed limits of selected sections have shown the common posted speed limits 40 km/h and 50 km/h for every category of vehicles. As shown in Figure 5, the speed versus cumulative percentage curve was drawn considering all the vehicle categories. The estimated 85th percentile speeds for both straight and curved sections were around 65 km/h. Therefore, it can be recommended to increase the posted speed limit up to 65 km/h.

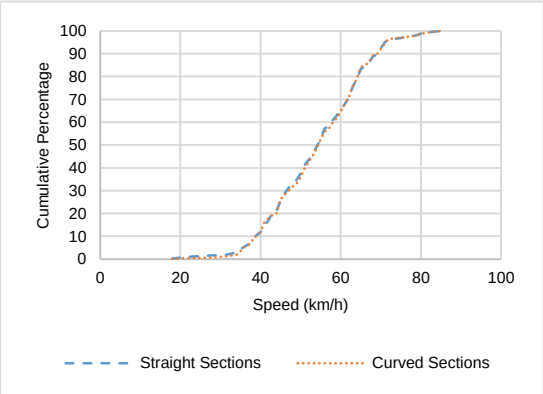

Figure 5 Speed versus Cumulative Percentage Curve

4.1. Multiple Regression Analysis

The correlation coefficient matrixes were developed for both straight sections and curved sections to identify highly correlated variables intending to remove the highly correlated variables in model developments. However, the variables in this study were not highly correlated. Multiple regression analysis models were developed for straight sections and curved sections and given in Table 4. The dependent variable was observed spot speed. The R^2 value which indicates the model fitness is 0.892 for straight sections and 0.914 for curved sections. Therefore, it could be concluded that there is a co-linearity between the results. The independent variables with p-values are lesser than 0.05 ($p < 0.05$) are identified as significant variables with 95% level of accuracy. Vehicle condition, weather condition, lane width, vegetation density, number of lanes, distance the nearest pedestrian crossing, and availability of guard rail affect for the speed variation in straight roadway sections. According to the model developed for curved sections, vehicle type, vehicle condition, weather condition, vegetation density, distance the nearest pedestrian crossing, distance to the nearest intersection, and availability of guard rails, and availability of bus stop affect for the speed variation in curved roadway sections.

5. CONCLUSIONS

The study was conducted by observing 1200 drives in both straight and curved sections. Data collection was done in five sections. From the collected data, it can be identified that most of the vehicles exceeded the posted speed limit. The 85th percentile speed estimated was 65 km/h.

The separate speed models for curved section and straight section were developed. Vehicle type, vehicle condition, weather condition, vegetation density, distance the nearest pedestrian crossing, distance to the nearest intersection, availability of guard rail, and availability of bus stop were considered as the affecting parameters for speed variation on curved roadways. While vehicle condition, weather condition, vegetation density, lane width, number of lanes, distance the nearest pedestrian crossing, and availability of guard rail affect for the speed variation in straight roadway sections.

This study provides the base line to investigate the affecting parameters on speed variations. It is recommended for future research on this topic to be discovered both rural and urban areas covering different classes of roads. The study can be extended for road sections with different geographical features including mountain terrain.

Table 4 Multiple Regression Models

Model	Straight Sections				Curved Sections			
	Unstandardized Coefficients		t	Sig.	Unstandardized Coefficients		t	Sig.
	B	Std. Error			B	Std. Error		
(Constant)	-145.467	170.528	-0.853	0.394	57.574	7.657	7.519	0.000
Vehicle Type	0.291	0.222	1.306	0.192	-0.303*	0.286	-1.060	0.029
Vehicle Condition	-0.024*	1.599	-0.015	0.018	0.528*	1.427	0.370	0.011
Gender	-0.769	1.363	-0.564	0.573	0.604	1.698	0.356	0.722
Age	-0.040	0.044	-0.921	0.358	-0.031	0.056	-0.558	0.577
Number of passengers	-0.386	0.390	-0.990	0.323	0.123	0.488	0.253	0.801
Weather Condition	-7.048*	2.045	-3.447	0.001	-0.036*	0.137	-0.264	0.042
Time of the day	-0.303	0.286	-1.060	0.290	0.28	0.222	1.261	0.168
Vegetation Density	1.207	1.079	1.119	0.024	0.117*	1.594	0.074	0.032
Lane width	0.528*	1.427	0.370	0.011	-0.728	1.363	-0.534	0.593
Number of lanes	2.370	1.565	1.514	0.030	-0.386	0.39	-0.99	0.322
Shoulder width	0.604	1.698	0.356	0.722	-0.046	0.043	-1.066	0.287
Posted speed limit	-0.031	0.056	-0.558	0.577	-10.284	2.404	-4.277	0.139
Distance to nearest ped. crossing	-1.384*	1.131	-1.223	0.022	-6.901*	2.04	-3.382	0.013
Distance to nearest intersection	1.523	1.141	1.335	0.182	3.399*	1.253	2.713	0.007
Distance to the speed limit sign	-0.036	0.137	-0.264	0.092	0.196	0.031	6.338	0.934
Day of the week	0.123	0.488	0.253	0.081	1.165	1.078	1.081	0.428
Availability of guard rail	0.149*	0.286	1.149	0.047	1.546 *	2.191	0.001	0.000
Availability of parking bays	-0.152	0.370	-1.046	0.146	-1.092	4.193	-1.046	0.196
Availability of bus stops	1.467	1.059	-1.051	0.178	4.167 *	1.064	1.493	0.024

*- Significant values at 95% confidence level

Slope and pavement condition were not included this study which could be take into account in future studies.

According to the results, most of the drivers exceed the posted speed limit, hence it is recommended to held workshops and programs to educate the drivers and public about speeding behaviour of drivers. Also, law enforcement could be implemented all over the country.

6. REFERENCES

Abesekara P.T.N., Senanayake M.P.D.S.R.K., Senevirathne S.T.R., Wicramasinghe, & Dissanayake S., 2012, 'Criteria for Setting Speed limits for Sri Lankan Roadways', *Civil Engineering Research Exchange Symposium 2012 Proceedings*, Faculty of Engineering, University of Ruhuna, Galle, March 19, 2012.

Aljanahi, A.A.M., Rhodes, A.H. & Metcalfe, A.V., 1999, 'Speed, speed limits and road traffic accidents under free flow conditions', *Accident Analysis & Prevention*, 31(1-2), 161-168.

Calvi, A. & Bella, F., 2014, 'Modeling speed differential parameters in day and night environments using driving simulator', *Procedia Engineering*, 84, 648-661.

Classen, S., Wang, Y., Crizzle, A.M., Winter, S.M. & Lanford, D.N., 2013, 'Predicting older driver on-road performance by means of the useful field of view and trail making test part B', *American Journal of Occupational Therapy*, 67(5), 574-582.

Long, A. D., Kloeden, C. N., Hutchinson, T. P., & McLean, A. J. 2006, 'Reduction of speed limit from 110km/h to 100km/h on certain roads in South Australia: A preliminary evaluation', *2006 Australasian Road Safety Research, Policing and Education Conference,* Gold Coast, Australia, 25-27 October 2006.

Kockelman, K.M. & Ma J., 2007., 'Freeway speed and speed variations preceding crashes, within and across lanes', *Journal of Transportation Research Forum* 46(1), 43-61.

Wang, J., Dixon, K.K., Li, H. & Hunter, M., 2006, 'Operating-speed model for low-speed urban tangent streets based on in-vehicle global positioning system data', *Transportation research record*, 1961(1), 24-33.

Proceedings of the 7th International Symposium on

Advances in Civil and Environmental Engineering Practices for Sustainable Development

ACEPS - 2019

Carbonized rice husk particles as bitumen modifier in hot mix asphalt

Mohamed Juzaafi[1], T.M.Rengarasu[1], Wasala.M.K.R.T.W.Bandara[1], Nishanthini Jegatheesan[1]

[1]Department of Civil and Environmental Engineering, Faculty of Engineering, University of Ruhuna, Hapugala, Galle, SRI LANKA

K e y w o r d s

Carbonized rice husk particles
Hot mix asphalt
Bitumen modification
Marshall stability
Marshall flow
Optimum binder content

A B S T R A C T

Hot mix asphalt (HMA) is commonly used for flexible pavements for their high service life. Using alternative materials in HMA is one of the favorable way to increase the performance of HMA in field conditions. Aim of this study was to determine the suitability of carbonized rice husk particles (CRHP) as bitumen modifier in HMA. Bitumen was replaced with 5%, 10% and 15% of carbonized rice husk particles by total weight. Conventional properties of CRHP modified bitumen were tested according to ASTM standards and it was found that the replacement of CRHP in to conventional bitumen increased the performance of bitumen against high temperatures. Further Marshall properties of HMA specimens with CRHP modified bitumen were tested and it was found that 10% CRHP replacement by total bitumen weight gave highest Marshall stability. Marshall flow values increased with CRHP replacement. Due to that, flexibility of the pavement was increased. Voids in mineral aggregates (VMA) and voids in compacted mixture (VIM) values satisfied the ICTAD requirements for medium traffic roads. Performance against moisture of specimens prepared with CRHP modified bitumen is less than conventional HMA specimens, however there were no significant deviations in water absorption. Therefore CRHP modified bitumen is suggested to use for road constructions in dry zones for better performance.

1. INTRODUCTION

Increment in population and development of new transportation facilities led to significant demand for road construction (Movilla-Quesada et al. 2018). Hot Mix Asphalt (HMA) is used as common road construction material due to their long service life and high performance in flexible pavements (Tahami et al. 2018). HMA is made of different types of aggregates called Coarse, Fine and filler (Sargin et al. 2013). HMA pavements have become expensive due to the high cost of materials, therefore it is necessary to find the suitability of alternative materials for the economic sustainability of HMA pavements (Huang et al. 2007)

Partial replacement of conventional materials in HMA by waste by-products is one of the practical way to target economic and environmental sustainability in road constructions (Lee et al. 2008) During past years, Plastic or polythene, fly ash, steel slag, glass dust, marble dust, brick waste, roofing shingles and recycled concrete waste were studied through laboratory and field experiments as alternative materials in HMA and the results were favour for partial replacements in HMA (Kalantar et al. 2012, Presti 2013, Shu & Huang 2014).

Bituminous materials are gained during the manufacturing of lubricating oils, bituminous materials are semisolid hydrocarbons with binding properties and viscosity that make them as good bonding agents. Therefore they act as a binder with aggregates in the pavement industry (Garber & Hoel 2014). Bitumen acts as bonding agent between aggregates in HMA mainly. Apart from the bonding agent the bitumen also resists the water penetration in HMA

(Attaelmanan et al. 2001). Temperature susceptibility is one of the most important mechanical property of the bitumen to avoid the softening in the hottest weather situations. One of the best way to increase the performance against temperature of conventional bitumen is modification of bitumen by adding modifiers (Airey et al. 2008, Zhu et al. 2014).

In Sri Lanka, around 2.8 million metric ton of rough rice is produced per annum. During the manufacturing process, around 0.8 million metric ton of rice husk is produced and 44% of them are left to the environment without any use (Perera et al. 2005). Therefore carbonized rice husk particles (CRHP) were selected as bitumen modifier in HMA for this study.

This study aims to find the suitability of CRHP as bitumen modifier in HMA. The objectives of this study are to determine the conventional properties of CRHP modified bitumen, to determine the optimum replacement rate of CRHP as bitumen modifier in terms of Marshall properties and to determine the effect of moisture in Marshall stability of optimum specimens.

2. LITERATURE REVIEW

Cai et al (2013) used rice husk ash (RHA) less than 75 µm in size as bitumen modifier with 60/80 penetration grade bitumen and it was found that, hardness and high temperature performance of modified bitumen were increased while ductility of modified bitumen was decreased with RHA content. Further, they concluded that ageing resistance of modified bitumen was increased with RHA content and the suitable addition is 10%-15% by weight.

Xue et al (2014) conducted a comparative study on RHA and wooden saw dust ash (WSA) as bitumen modifiers in HMA and it was found that, performance against temperature of bitumen was increased with bio mass ash content. Further they found that there was no any chemical reaction between biomass ashes and bitumen but the oxidation process of bitumen was reduced with the addition of bio mass ashes. Further they concluded that RHA was better modifier than WSA in terms of rutting resistance.

Romastarika et al. (2017) used black rice husk ash (BRHA) less than 75 µm in size as bitumen modifier with 60/70 penetration grade bitumen and it was found that, penetration index of modified bitumen was increased with BRHA content. Further it was found that, BRHA modified bitumen has high resistance against thermal cracking and BRHA modified bitumen was more viscous than conventional bitumen.

Han et al. (2017) used RHA less than 75µm in size as bitumen modifier along with bio oil as viscous reducer for 60/70 penetration grade bitumen. From the series of laboratory experiments it was found that addition of RHA into conventional bitumen increased the performance against high temperature and the upper limit of RHA addition is 7% along with bio oil products.

Arabani & Tahami (2017) used RHA less than 75µm in size as bitumen modifier with 60/70 penetration grade bitumen and they found that, addition of RHA into conventional bitumen increased the viscosity and high temperature performance of bitumen significantly. Further it was found that, Marshall stability of specimens prepared with RHA modified bitumen were slightly increased than conventional specimens and preferable RHA addition range was in between 15% to 20% by bitumen weight.

Abdelmagid & Feng (2019) used RHA as bitumen modifier along with crumb rubber. Form the laboratory experiments it was found that, addition of RHA and crumb rubber in to conventional bitumen enhanced the viscosity and performance against temperature significantly. Further they concluded that, combination of crumb rubber and RHA as bitumen modifier increased the resistance against short term ageing of bitumen.

3. MATERIALS AND METHODS

3.1. Materials

3.1.1. Conventional materials

There were three types of aggregates called coarse (20 mm or less in size), Chipped (14 mm or less in size) and fine (less than 4.75 mm in size) used in this study. Physical properties of aggregates were tested according to ASTM C127 (for coarse and chipped aggregates) and ASTM C128 (for fine aggregates). The test results are presented in Table 1. 60/70 penetration grade bitumen was used as asphalt binder in this study. Physical properties of conventional bitumen according

to ASTM standards are shown in Table 3.

Table 1 Physical properties of aggregates

	Coarse	Chipped	Fine
Bulk specific gravity	2.70	2.62	2.57
Bulk specific gravity in SSD	2.72	2.64	2.35
Apparent specific gravity	2.75	2.68	2.44
Absorption (%)	0.67	0.94	3.63

3.1.2. Carbonized rice husk particles

CRHP was prepared by burning rice husk within a sealed container with 600℃ of temperature. CRHP less than 600µm in size were used for experiments. The properties of CRHP are presented in Table 2.

Table 2 Physical properties of CRHP

Bulk specific gravity	1.65
Bulk specific gravity in SSD	1.85
Apparent specific gravity	2.05
Absorption (%)	11.84

3.2. Methodology

According to the methodology presented in Figure 1, initially, sieve analysis test (ASTM C136) was conducted for each type of aggregates to determine the particle size distribution. Suitable proportions of coarse, chipped and fine aggregate were selected based on the sieve analysis test results to ensure that the combined aggregate mixture satisfies the AASHTO specifications.

Bitumen modification was done by replacing CRHP in to conventional bitumen (60/70 penetration grade). Initially the conventional bitumen was heated around to 150℃and the CRHP were mixed at the mixing speed of 150 rpm with the conventional bitumen for 20 minutes. The CRHP modified bitumen was tested for specific gravity (ASTM D70), Softening point (ASTM D36) and Penetration (ASTM D5). Further penetration index (PI) was determined based on the equation 01.

$$PI = \frac{1952 - 500logP - 20SP}{50logP - SP - 120} \quad (1)$$

Where,
SP – Softening point (℃)
P – Penetration at 25℃

During the mixing process, oven dried

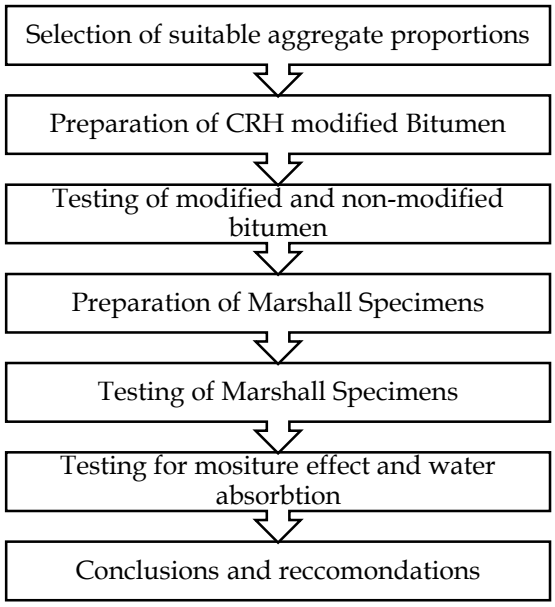

Figure 1 Methodology

(for 24 hours) aggregate sample was taken and mixed thoroughly with heated bitumen with the mixing temperate of 135℃ - 145℃. Thereafter, the mix was placed in to the pre heated mould and compacted by Marshall Compactor with 50 numbers of blows for each side of the specimen.

After 24 hours the Marshall specimens were extracted from the moulds and tested for the physical properties called Voids in Mineral Aggregate (VMA), Voids in Compacted Mixture (VIM), Voids filled with bitumen (VFB), percent volume of bitumen (Vb) and Maximum specific gravity (Gm). Thereafter, the Marshall specimens were kept in to the water bath for 30 minutes with the curing temperature of 60℃. After that Marshall stability and Marshall flow were determined by Marshall testing procedure (ASTM D6927).

Based on the highest Marshall stability values optimum specimens were selected for each CRHP content (0%, 5%, 10% and 15%) with corresponding optimum bitumen content. The selected optimum specimens were subjected to absorb water continuously for 30 days and Marshall stability was checked again after 30 days of water absorption.

Based on five levels of bitumen varied from 4% to 6% with 0.5% and four different CRHP content, namely 0%, 5%, 10% and 15%, 60 specimens (5×4×3 = 60) of CRHP modified HMA were prepared for primary tests. Further 12 CRHP modified specimens were prepared to test the moisture effects. All

together 72 HMA specimens were examined in this study

4. RESULTS AND DISCUSSIONS

4.1. Properties of CRHP modified bitumen

According to the experimental results presented in Table 3, there was around 12% increment in the specific gravity of bitumen for CRHP modified bitumen than conventional bitumen. Further, softening point of CRHP modified bitumen was increased gradually with the CRHP content while penetration values of CRHP modified bitumen were reduced. There were around 20% drop in penetration values for 10% and 15% replacement of CRHP. Penetration indices increased from negative to positive with the replacement of CRHP in to the conventional bitumen.

Table 3 Physical properties of bitumen

CRHP (%)	0	5	10	15
Specific gravity	1.05	1.16	1.18	1.16
Penetration at 25℃	69	64	55	53
Softening point (℃)	49	52	54	57
Penetration index	-0.68	-0.11	-0.02	0.55

Increment of penetration index values shows that, the CRHP replacement in to the conventional bitumen increased the performance of bitumen against high temperatures. For road construction, it is preferred that the penetration index should be in the range of -1 < penetration index < +1(Romastarika et al. 2017).

4.2. Marshall properties of HMA with CRHP modified bitumen

4.2.1. Marshall stability

As shown in Figure 2, Marshall stability values were slightly increased with the increment of CRHP content for 5% and 10% replacement but it was reduced slightly for 15% CRHP modified bitumen. The maximum

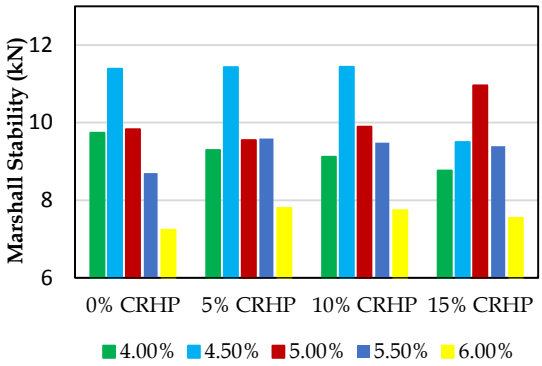

Figure 2 Marshall stability variation with CRHP content

Marshall stability was obtained as 11.44 kN with 10% of CRHP modified bitumen. However 0% and 5% RHA modified bitumen specimens also gave the nearest Maximum stability values as 11.39 kN and 11.43 kN respectively. Further the Marshall stability values satisfied the ICTAD requirement of 5.33kN for medium traffic roads.

4.2.2. Marshall flow

Marshall flow values increased with the increment of the CRHP content in bitumen however the values satisfied the ICTAD requirement of 8 < Marshall flow < 18. The maximum Marshall flow value was obtained for 15% CRHP modified bitumen with 6% binder content as 11.96. The variations of Marshall flow values with CRHP content are shown in figure 3.

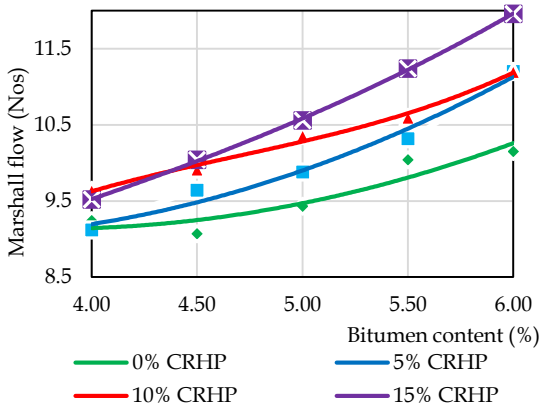

Figure 3 Variation of Marshall flow with bitumen content

Increment of Marshall flow values shows that, replacement of CRHP in to conventional bitumen increased the flexibility of pavement.

4.2.3. Maximum Marshall stability and optimum bitumen content

Maximum Marshall stability and corresponding bitumen content for each CRHP replacement are shown in Table 4. According to the data, it is clearly shown that the bitumen consumption to reach the maximum Marshall stability was reduced for HMA specimens with CRHP modified bitumen. Further there were no any significant changes in maximum Marshall stability for CRHP content 0%, 5% and 10%.

Table 4 Maximum Marshall stability and optimum bitumen content

CRHP (%)	Maximum Marshall Stability (kN)	Optimum bitumen content (%)	Weight of bitumen consumed (g)
0%	11.39	4.50	54.00
5%	11.43	4.60	52.44
10%	11.44	4.60	49.68
15%	10.96	5.10	52.02

4.3. Physical properties of HMA with CRHP modified bitumen

VIM and VMA values of HMA specimens with CRHP modified bitumen are presented in Table 5 and Table 6

Table 5 VIM values

Bitumen content	4.00	4.50	5.00	5.50	6.00
0% CRHP	3.91	4.4	4.25	3.83	4.25
5% CRHP	3.6	3.31	3.82	3.42	3.46
10% CRHP	4.75	4.45	4.39	3.78	3.77
15% CRHP	4.65	4.8	4.06	4.05	4.95

Table 6 VMA values

Bitumen content	4.00	4.50	5.00	5.50	6.00
0% CRHP	12.69	13.36	14.31	15.46	16.74
5% CRHP	11.61	12.6	13.6	14.11	15.01
10% CRHP	12.53	13.15	13.96	14.27	15.11
15% CRHP	12.56	13.52	13.82	14.68	16.31

VIM value should be in the range of 3<VIM<5 according to the ICTAD specifications. In this study, it was observed that, all specimens satisfied the requirement. Further, It was observed that, 10% and 15% CRHP modified HMA specimens achieved higher VIM values than conventional HMA specimens while 5% CRHP modified HMA specimens have lesser VIM values.

VMA values should be greater than 13 according to ICTAD specifications. In this study, it was observed that the requirement was satisfied for the bitumen contents greater than or equal to 4.50. Further it was observed that VMA values of HMA specimens with CRHP modified bitumen are lesser than conventional HMA specimens for corresponding bitumen content.

4.4. Effect of moisture in optimum HMA specimens with CRHP modified bitumen

Water absorption HMA specimens with CRHP modified bitumen were increased with the replacement of CRHP as shown in Table 7. However the water absorption values satisfied the APRG.-18 requirement of 2%-4% maximum water absorption.

According to Figure 4, it can be clearly seen that maximum Marshall stability values were reduced significantly after 30 days of water absorption. Further it was found that, the percentage of reduction in Marshall stability is higher for HMA specimens with CRHP modified bitumen than conventional HMA specimens. However the Marshall stability values after 30 days of water absorption satisfied the ICTAD requirement of 5.33 kN for medium traffic roads construction.

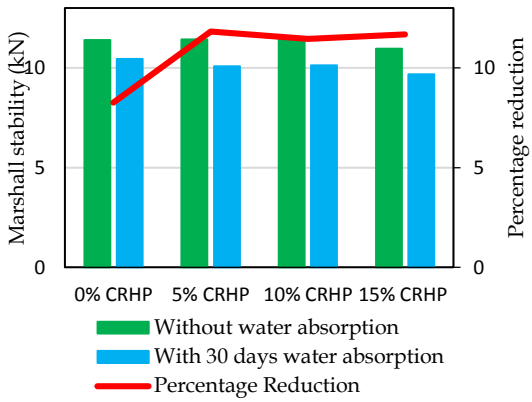

Figure 4 Marshall stability reduction with water absorption

Table 7 Water absorption data

Days	5	10	15	20	25	30
0% CRHP	1.48	1.91	2.15	2.21	2.24	2.25
5% CRHP	1.53	1.96	2.22	2.25	2.28	2.29
10% CRHP	1.61	2.05	2.31	2.35	2.37	2.38
15% CRHP	1.68	2.13	2.35	2.39	2.41	2.43

5. CONCLUSIONS

Replacement of CRHP in to conventional bitumen increased the specific gravity of the bitumen around 10%. Further, the performance of conventional bitumen against high temperature was increased with the replacement of CRHP. Therefore CRHP modified bitumen can be used as alternative bitumen for road construction in dry zones.

According to the Marshall properties of HMA specimens with CRHP modified bitumen, 10% CRHP replacement by total bitumen weight is preferred. Further, the replacement of CRHP increased the flexibility of the HMA. Physical properties HMA with CRHP modified bitumen satisfied the ICTAD requirements for medium traffic roads.

HMA specimens with CRHP modified bitumen have higher water absorption than conventional HMA specimens. Further, percentage reduction in HMA specimens due to moisture is higher for HMA with CRHP modified bitumen than conventional HMA. Therefore it is not suitable for the regions subjected to high moisture continuously.

6. RECOMMENDATIONS

This study mainly focused on the behaviour of HMA specimens with CRHP modified bitumen in terms of Marshall properties and moisture effects. The following recommendations are made for future investigations

- Investigation on durability of HMA specimens with CRHP modified bitumen. (indirect tensile strength test)
- Investigation on cracking resistance of HMA specimens with CRHP modified bitumen (fatigue resistance, rutting resistance)

7. REFERENCES

Abdelmagid, A. & Feng, C., 2019, 'Laboratory evaluation of the effects of short-term aging on high temperature performance of asphalt binder modified with crumb rubber and rice husk ash', *Petroleum Science and Technology*, 37(13), 1557-1565.

Arabani, M. & Tahami, S.A., 2017, 'Assessment of mechanical properties of rice husk ash modified asphalt mixture', *Construction and Building Materials*, 149, 350-358.

Attaelmanan, M., Feng, C. & AI, A., 2011, 'Laboratory evaluation of HMA with high density polyethylene as a modifier', *Construction and Building Materials*, 25(5), 2764-2770.

Cai, J., Xue, Y., Wan, L., Wu, S. & Jenkins, K., 2013, 'Study on Basic Properties and High-Temperature Performance of Rice-Husk-Ash-Modified-Asphalt', *Applied Mechanics and Materials*, 333-335, 1889-1894.

Garber, N.J. & Hoel, L.A., 2014, *Traffic and highway engineering*. Cengage Learning.

Han, Z., Sha, A., Tong, Z., Liu, Z., Gao, J., Zou, X. & Yuan, D., 2017, 'Study on the optimum rice husk ash content added in asphalt binder and its modification with bio-oil', *Construction and Building Materials*, 147, 776-789.

Huang, Y., Bird, R. & Heidrich, O., 2007, 'A review of the use of recycled solid waste materials in asphalt pavements. *Resources, Conservation and Recycling'*, 52(1), 58-73.

Kalantar, Z., Karim, M. & Mahrez, A., 2012, 'A review of using waste and virgin polymer in pavement', *Construction and Building Materials*, 33, 55-62.

Lee, S., Akisetty, C. & Amirkhanian, S., 2008, 'The effect of crumb rubber modifier (CRM) on the performance properties of rubberized binders in HMA pavements', *Construction and Building Materials*, 22(7), 1368-1376.

Movilla-Quesada, D., Muñoz, O., Raposeiras, A. & Castro-Fresno, D., 2018, 'Thermal suspectability analysis of the reuse of fly ash from cellulose industry as contribution filler in

bituminous mixtures', *Construction and Building Materials*, 160, 268-277.

Perera, K.K.C.K., Rathnasiri, P.G., Senarath, S.A.S., Sugathapala, A.G.T, Bhattacharya, S. & Abdul Salam, P., 2005, 'Assessment of sustainable energy potential of non-plantation biomass resources in Sri Lanka', *Biomass and Bioenergy*, 29(3), 199-213.

Lo Presti, D., 2013, 'Recycled Tyre Rubber Modified Bitumens for road asphalt mixtures: A literature review', *Construction and Building Materials*, 49, 863-881.

Romastarika, R., Jaya, R.P., Yaacob, H., Nazri, F.M., Agussabti, Ichwana & Jayanti, D.S., 2017, 'August. Effect of black rice husk ash on the physical and rheological properties of bitumen', In *AIP conference proceedings*, 1875(1), pp. 003-012.

Sargın, Ş., Saltan, M., Morova, N., Serin, S. & Terzi, S., 2013, 'Evaluation of rice husk ash as filler in hot mix asphalt concrete', *Construction and Building Materials*, 48, 390-397.

hu, X. & Huang, B., 2014, 'Recycling of waste tire rubber in asphalt and portland cement concrete: An overview', *Construction and Building Materials*, 67, 217-224.

Tahami, S., Arabani, M. & Foroutan Mirhosseini, A., 2018, 'Usage of two biomass ashes as filler in hot mix asphalt', *Construction and Building Materials*, 170, 547-556.

Xue, Y., Wu, S., Cai, J., Zhou, M. & Zha, J., 2014, 'Effects of two biomass ashes on asphalt binder: Dynamic shear rheological characteristic analysis', *Construction and Building Materials*, 56, 7-15.

Proceedings of the 7th International Symposium on

Advances in Civil and Environmental Engineering Practices for Sustainable Development

ACEPS - 2019

Suitability of recycled concrete aggregates in hot mix asphalt concrete.

T.Pradheep[1], M.K.K.D.Wimalasena[1] and Terrance M. Rengarasu[1]

[1]Department of Civil and Environmental Engineering, Faculty of Engineering, University of Ruhuna, Hapugala, Galle, SRI LANKA
[2]Affiliation, Address, City and Postcode, Country

K e y w o r d s

Concrete waste
Recycling
Hot Mix Asphalt
Marshall method

A B S T R A C T

The amount waste generated in Municipal Solid Waste (MSW) is increasing due to increase in population, urbanization and development activities. Thus disposal of waste becomes a serious problem globally due to their non-biodegradability and unaesthetic view. Hence, this study focused on inspecting whether the properties of Hot Mix Asphalt (HMA), modified by Recycled Concrete Aggregate (RCA), meets the specifications for local roads in Sri Lanka. Here the samples were produced by adding waste materials with natural Crushed Stone Aggregates (CSA). The samples were prepared and tested using the Marshall method. The performance of the samples was investigated in terms of density-void and stability-flow analysis and was compared with the performance criteria. Modified HMA with RCA reduces the Marshall properties, however the values are within the acceptable range of the local specification. The maximum stability obtained for the 50% replacement of recycled coarse aggregate, and it is less than the control sample, but it fulfills the minimum requirement criteria. Hence, it seems that RCA is a feasible option to replace in HMA. Nevertheless, this study should be furthered to evaluate the performance factors of HMA with RCA, such as skid resistance, in order to ensure safety and durability.

1. INTRODUCTION

Flexible pavement constructions are followed the traditional way of using hot mix asphalt as the surface course in most of the countries. Major component of this HMA is aggregate in three varied sizes. HMA contain of approximately more than 90% in volume of mixture is mineral aggregate, which includes fine and coarse particles (Chen, & Liao 2002; Janoo, & Korhonen, 1999; Kandhal, & Parker, 1998). The performance of the pavement design depends on physical properties of aggregates such as gradation, shape of the particle, surface texture, toughness, durability and absorption.

Although cost for this type of pavement is low compared with rigid pavement, the high cost is due to the expense of the aggregates. Necessity of raw materials also increased as the increase of new construction. But the availability of the virgin aggregate is constant. Therefore, the engineers pay more interest to find out a substitution material for the conventional materials

Involvement of new technology in pavement design is very less in Sri Lanka. Using secondary material rather than using conventional material is more suitable and the best way to reduce the unnecessary expense of local road, which has less traffic. Waste materials such as fly ash, saw dust, rice husk, rubber, steel slag, tyres, marble quarry, recycled concrete and reclaimed asphalt pavement can be used as a substitutional material for HMA.

2. LITERATURE REVIEW

In each year due to the rapid development and urbanization many tons of construction and demolition waste are produced due to the

aging of old buildings (Goldstein 1995). Furthermore, in the developing countries like Sri Lanka more efforts have to be taken to reduce the waste disposal problem due to lack of space. About 85% of collecting waste in Sri Lanka is subjected to open or ocean dumping (Hikkaduwa et al. 2016; Visvanathan, 2006). And also most of the countries has an issue in proper disposal system. As disposal of these wastes in landfill is a traditional solution, some of the problems appeared due to lack of proper landfill, cost and the environmental regulations. Therefore, it can be reused to mitigate the impact based on sustainable solid waste management and also it reduces the quarrying of virgin aggregate.

Civil engineers have more responsibility on the impacts caused to environment due the several constructions. Therefore, they have to consider the more suitable place, type of construction, materials, which will not be harmful to environment. They pay more attention to construct eco-friendly construction such as green building and so on to reduce the negative impacts on environment. Based on that waste material and recycled materials are more preferable to use in the construction, which helps to reduce the necessity of the raw materials. This studies are focused on using the waste materials as aggregate for the production of hot mix asphalt. It has some other benefits, more than eco- friendly. One of this is by taking the waste as raw material reduces the cost, compared with conventional material, and it helps to improve the budget of nation. Therefore, the outcome of this research would pave a new path to utilized RCA in road paving as an economical and sustainable alternative to the conventional HMA.

Many researches have been already conducted based on this study (Rafi, Qadir, & Siddiqui, 2011; Aljassar, Al-Fadala, & Ali, 2005; Moghaddam, Soltani, & Karim, 2014; Topal, Ozturk, & Baradan, 2006; Wong, Sun, & Lai, 2007). Recycled concrete aggregate differs from virgin material due to the cement paste retained on the surface of the recycled particles. These increases the water absorption capacity, quality variability and the porosity (Rafi et al., 2011). Increases of the recycled concrete in the mixture reduces the resilient modulus and rutting resistance of the mix was found by Paranavithana et al. But this result contradicts as to Wong et al. In this sense, according to Shen and Du (2004), HMA containing recycled aggregates exhibited satisfactory mechanical behaviour and the stripping impact was also considered satisfactory. Considering all into account, this paper examines the suitability of RCA to produce HMA that meets the minimum requirements for local roads.

3. MATERIALS AND METHOD

3.1. Conventional materials

In this study, crushed rocks were used at required nominal sizes with 20 mm as coarse, 14 mm as chip aggregate and quarry dust as filler. The materials were tested based on American Standards of Testing Materials (ASTM). The mix proportion of three types of aggregates are taken as 20% : 20% : 60% of coarse, chip and filler respectively, and binder were selected according to the CIDA specification. The 60/70 penetration grade binder is used. The aggregates and bitumen were collected from local suppliers to the road construction.

3.2. Waste materials

In terms of waste material, recycled concrete are to be used, which is collected from a local dumping site maintained by Galle municipal council.

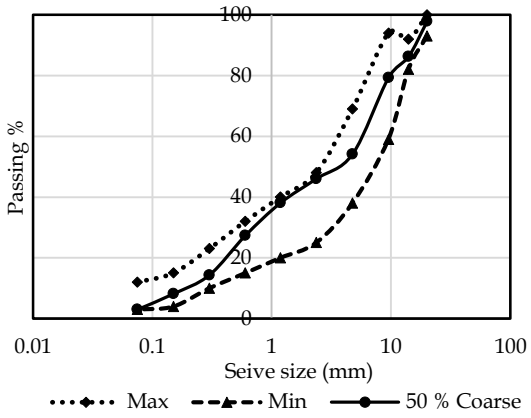

Figure 1 Envelops for combined sample with 50% RCA

In order to determine the suitability of virgin aggregates and recycle aggregates sieve analysis, specific gravity and the water absorption is carried out as per ASTM C 127-88, and the results are tabulated in the following Table 1. Sieve analysis test was carried out, and the envelops for the combined

mix are plotted. Then confirmed that aggregate mix proportion of recycled aggregate are within the specification range. The below envelop as in Figure 1 shows the graphical representation of 50% replacement as coarse. And in terms of bitumen specific gravity, penetration grade tests are carried out as per ASTM D 70 and D 5.

Table 1 Specific gravity and water absorption value for aggregates

Aggregate type	Conventional Aggregate			Recycled Aggregate	
	Coarse	Fine	Filler	Coarse	Fine
Bulk S.G (SSD)	2.72	2.64	2.44	2.44	2.26
Bulk S.G (Dry)	2.70	2.62	2.35	2.32	2.06
Apparent S.G	2.75	2.68	2.57	2.63	2.57
Absorption (%)	0.65	0.94	3.63	5.05	9.65

3.3. Methodology

In this study, Marshall mix design method was used to investigate the properties of modified HMA as per the ASTM D 1559 -89. The major scope of this mix design is to find out the optimum material requirement. The following Figure 2 shows the summary of experimental study. The total weight of three types of aggregate is selected that around 1200 grams and the samples are prepared up to the thick of 63.5 mm. The aggregate mix proportion of coarse, chip and filler was selected as 20%, 20% and 60% respectively. And specific limit for the binder content was chosen as 4 to 6 percent with 0.5% interval of total weight of the aggregate. The recycled concrete is introduced as waste material to the asphalt mix as the replacement for the traditional crushed stone. And also the sieve analysis test is carried out for the replacement material in order to make sure, that the combined grading of the waste material satisfies the requirement.

First of all, the control samples are prepared with virgin aggregate without any intervention of recycled aggregates. All the aggregates were preheated to a temperature around 105 ˚C to 110 ˚C and bitumen should be heated to 155 ˚C for not more than one hour to prevent overheating. The prepared mix is placed into the mould and compacted with pedestal hammer. Fifty blows will be applied each sides of the sample by pedestal hammer. As that three samples are prepared for each combination of bitumen percentage in order to increase the accuracy. The results obtained for each sample is averaged and concluded to one value. Then the samples were kept in the room temperature for overnight and removed from the mould using the sample extractor. Then the weight and submerged weight of the specimens are measured to determine the physical properties. Prior testing, the extruded samples were immersed in water bath for 30 min at the temperature of 60˚C. Marshall stability and flow value was determined by using the Marshall Test apparatus. Finally, optimum material requirement was determined by analysing the result.

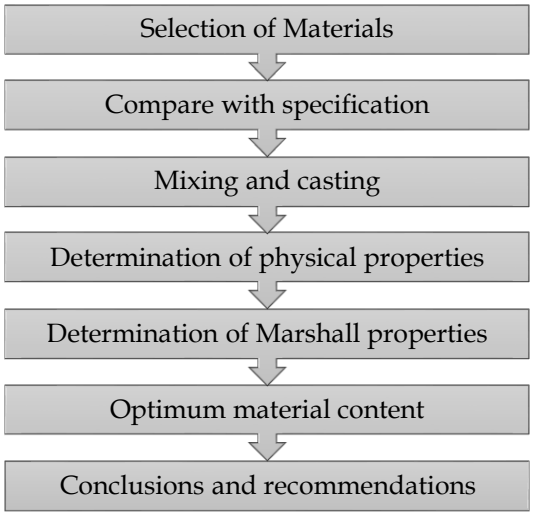

Figure 2 Methodology flowchart

4. RESULT AND DISCUSSION

4.1. HMA with replacement of recycled coarse aggregate

The addition of the RCA as coarse aggregates changes the overall performance of HMA. It was observed that the specific gravity of HMA were reduced with the addition of RCA content, but compared to the control sample the specific gravity was less as shown in Figure 3. But there was not considerable different because of the specific gravity of the recycles coarse aggregate, which was nearly equal to the conventional coarse aggregate. And also specific gravity gradually reduces with bitumen content. In the case of air void in compacted mixture (VIM), the coarse

modified HMA shows lesser value compared to control sample. VIM in the modified HMA increased with addition of RCA as in Figure 4. Even though the VIM was less, the values satisfies the allowable range as 3< VIM <5 according to the CIDA. There was no significant variation in voids in mineral aggregate (VMA) in modified HMA with the increment of RCA, however compared to the control sample modified HMA resulted lesser value, but it lies within allowable range according to the CIDA (VMA >13) as in Figure 5.

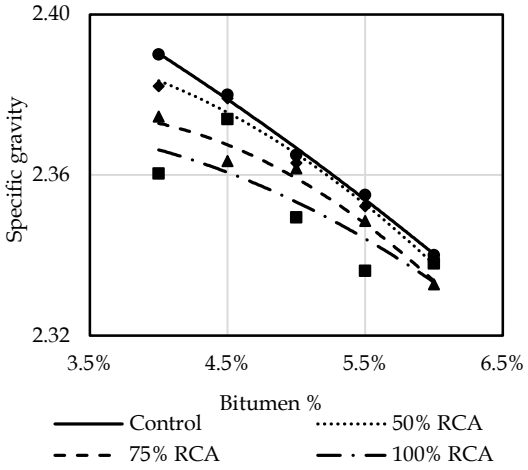

Figure 3 Variation of specific gravity

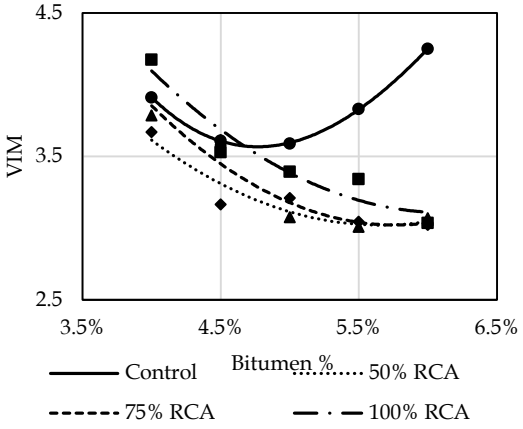

Figure 4 Variation of VIM

According to the CIDA specification the Marshal stability for medium traffic road should be greater than 5.33 kN. Marshall stability of the modified HMA with RCA reduces with the addition of the recycled aggregates as in Figure 6. However, modified HMA satisfies the minimum requirement. Even though optimum binder content of modified HMA was high compared to control sample, it slightly varies with the addition of RCA. High stability was obtained at 4.85% binder content for 50 % replacement as coarse, and the stability was reduced by 6%. Likewise, 75% replacement as coarse showed 9% reduction in stability at 4.9% binder content. But at 4.9% bitumen content, the 100% RCA modified sample resulted 15% lesser value in stability compared to control sample.

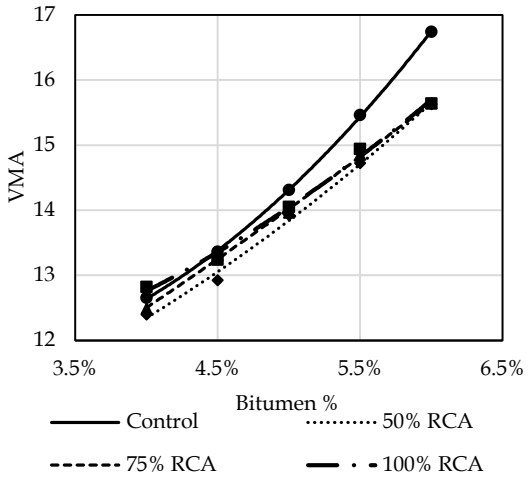

Figure 5 Variation of VMA

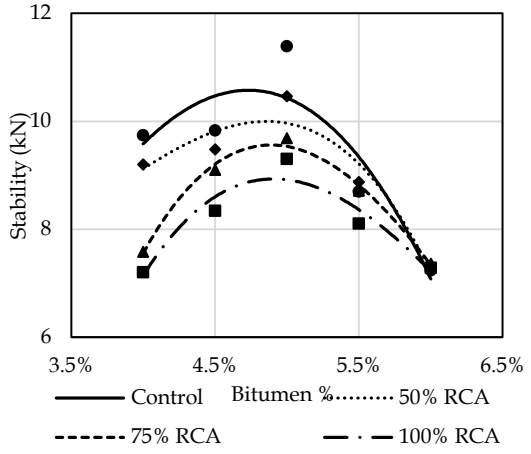

Figure 6 Variation of Marshall Stability

Similarly, Marshall flow reduces with the addition of RCA, but the occurred deformation was within the accepted range (8<Marshall Flow<18) as per the CIDA specification, which is shown in Figure 7. Flow value increased with binder content as control sample.

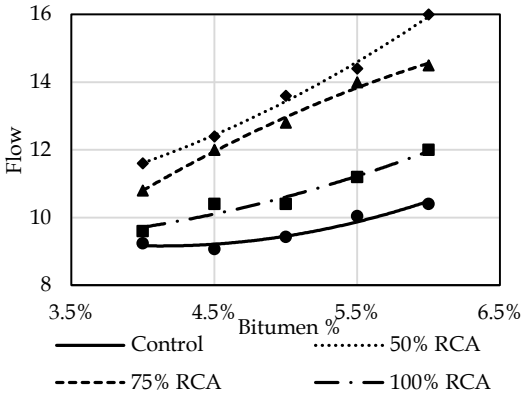

Figure 7 Variation of Marshall Flow

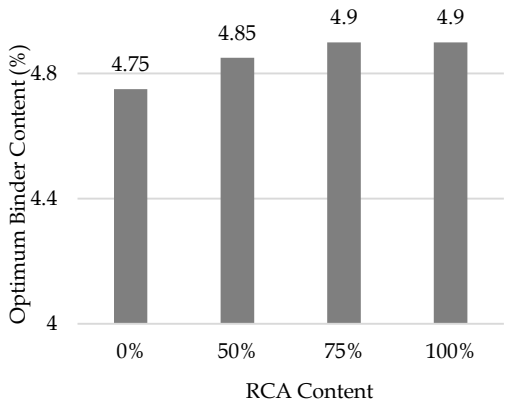

Figure 8 Variation of Optimum Binder Content

4.2. HMA with replacement of recycled fine aggregate

When the amount of RCA as fine aggregates increased in the sample, they became as low quality mix due to lack of binding ability. Therefore, with the increment of binder content, the samples displayed more consistency in the visual inspection due to the increased availability of binder to bind the aggregates together. Due to the absorptive nature of recycled fine particles, the bitumen added to the mix was absorbed. Addition of recycled fine aggregates reduced the specific gravity. Further, the tiny particles of recycled fine particle, filled the small cracks of aggregate. However, VIM was within the allowable range. No significant variation in VMA of modified sample as in Figure 9, however it satisfied the allowable range (VMA > 13) as to the CIDA.

Marshall stability of the asphalt mix with fine replaced was reduces with the addition of the recycled aggregates. Anyhow, it satisfies the minimum requirement as to the CIDA.

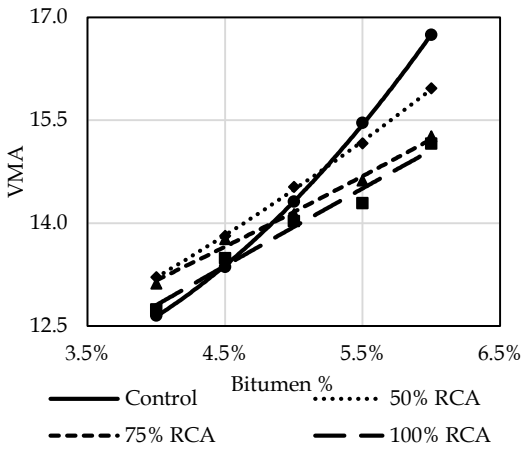

Figure 9 Variation of VMA

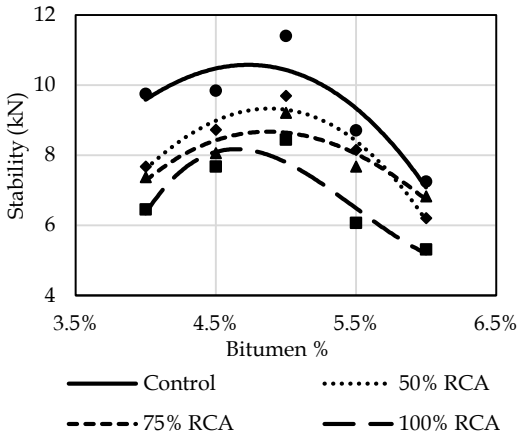

Figure 10 Variation of Marshall Stability

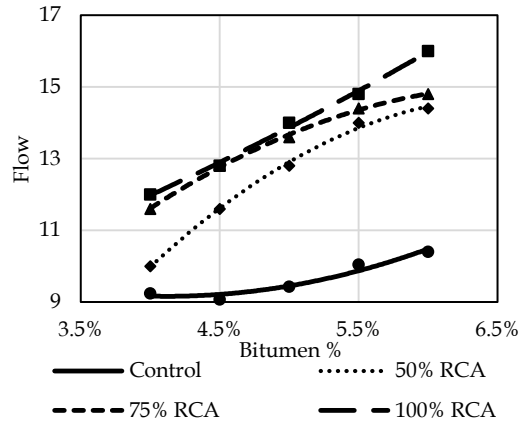

Figure 11 Variation of Marshall Flow

The optimum binder content of the modified sample slightly varies with the addition of RCA. High stability was obtained at 4.9% binder content for 50 % modification of fine aggregates, and the stability was reduced by 10% as in Figure 10. Likewise, 75% of

recycled fine addition showed 17% reduction in stability at 4.85% binder content. But at 4.65% bitumen content, the 100% RCA modified sample resulted 22% lesser value in stability compared to control sample. Similarly, Marshall flow also increased due to the increment of air void, but the occurred deflection was within the accepted range (8<Marshall Flow < 18), which is shown as in Figure 11. Flow value increased with binder content like control sample, but the variation was not like control sample.

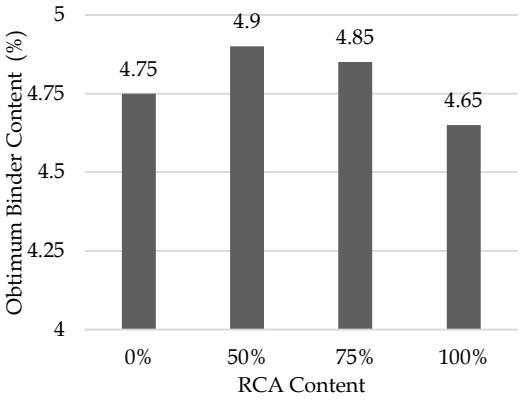

Figure 12 Variation of Optimum Binder Content

4.3. Water absorption

The water absorption is tested for the optimum replaced sample, which is 50% RCA. It is observed until the absorption become relatively constant. Approximately it took 20 days to reach the constant value.

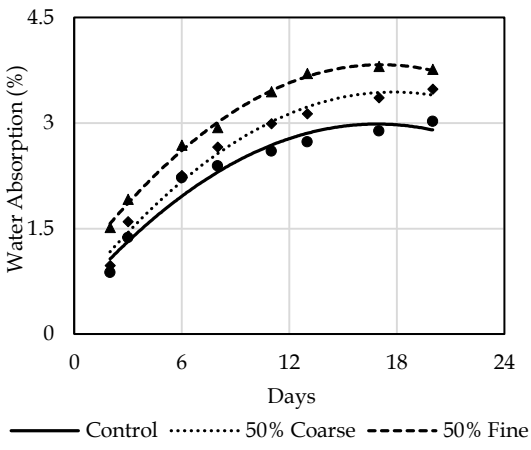

Figure 12 Variation of Water Absorption

According to the report of APRG-18 (1999), the water absorption should be lies between 2% - 4%. However, the water absorption of optimized sample is higher than the control sample, it satisfied as to the above requirement. The following Figure 13 represents the variation of water absorption for control and optimized sample.

5. CONCLUSIONS

The hot mix asphalt modified with recycled concrete aggregate, showed better performance against Marshall properties. Among the replacement percentages, 50% of RCA resulted the maximum stability for coarse, fine and combined samples. Although, 50% replacement achieved reduction in stability compared to control sample, it satisfies the minimum requirement as to CIDA. Marshall flow was increased with RCA, however it was within the specification. In terms of optimum bitumen content, the bitumen requirement is very closer to the modified HMA with conventional mix. However, by considering the overall performance of the modified HMA will results the economic and environmental benefits.

6. FUTURE DIRECTION

In this study maximum 50% of RCA was good enough to modify the hot mix asphalt to the medium traffic load. Even though physical and Marshall properties are in the acceptable range, it is necessary to evaluate the performance in terms of skid resistance, creep resistance and tensile strength, in order to ensure that the modified HMA is safe for durable.

7. ACKNOWLEDGMENTS

Author wish to thank all of the people, who were giving his or her time and resources. Specially, the author would like to offer sincere gratitude to the research supervisors Mr. M.K.K.D. Wimalasena and Dr. T.M. Rengarasu, for providing enough guidance and supervision in correct path. The guidance provided in studying the background, carrying out the literature review and executing all the work is humbly acknowledged. The special gratitude goes to Dr. W.K.C.N. Dayanthi, Head of the Department, Department of Civil and

Environmental Engineering, University of Ruhuna.

8. REFERENCES

Ahmadinia,E.,Zargar,M.,Karim,M.R.,Abdelaziz,M.& Ahmadinia,E., 2012, 'Performance evaluation of utilization of waste polyethylene terephthalate (pet) in stone mastic asphalt', *Construction and Building Materials,* 36, 984–989.

Ali, N., Chan, J. S., Potyondy, A. J., Bushman, R. & Bergan, A., 1995, 'Mechanistic evaluation of asphalt concrete mixtures containing reclaimed roofing materials', *Transportation Research Record*, 1515.

Aljassar, A.H., Al-Fadala, K.B. and Ali, M.A., 2005, 'Recycling building demolition waste in hot-mix asphalt concrete: a case study in Kuwait', *Journal of material cycles and waste management*, 7(2), 112-115.

Arabani, M., Mirabdolazimi, S. & Sasani, A., 2010, 'The effect of waste tire thread mesh on the dynamic behaviour of asphalt mixtures', *Construction and Building Materials*, 24(6), 1060–1068

Bhusal, S. and Wen, H., 2013, 'Evaluating recycled concrete aggregate as hot mix asphalt aggregate', *Advances in Civil Engineering Materials,* 2(1), 252-265.

Cross, S.A. and Parsons, R.L., 2001, 'Evaluation of Expenditures On Rural Interstate Pavements in Kansas: Executive Summary'.

Goldstein, H., 1995, 'Not your father's concrete', *Civil Engineering*, 65(5), p.60.

Hassani, A., Ganjidoust, H. & Maghanaki, A. A., 2005, 'Use of plastic waste (poly-ethylene terephthalate) in asphalt concrete mixture as aggregate replacement', *Waste management & research,* 23(4), 322–327.

Hikkaduwa, I., Gunawardana, K.W., Halwatura, R.U. and Youn, H.H., 2016, 'Sustainable Approaches to the Municipal Solid Waste Management in Sri Lanka'.

Kamil, M., Anggraini, R. and Suryani, F.M., 2011, December, 'The performance of asphalt-concrete wearing-course (AC-WC) mixture by using rice husk ash as filler with the addition of asbuton in asphalt pen 60/70 as binder', *In Proceedings of The Annual International Conference*, Syiah Kuala University-Life Sciences & Engineering Chapter (Vol. 1, No. 2).

Moghaddam, T. B., Soltani, M., & Karim, M. R., 2014, 'Experimental characterization of rutting performance of polyethylene terephthalate modified asphalt mixtures under static and dynamic loads', *Construction and Building Materials*, 65, 487–494.

Paranavithana, S., & Mohajerani, A., 2006, 'Effects of recycled concrete aggregates on properties of asphalt concrete', *Resources, Conservation and Recycling*, 48(1), 1–12.

Rafi, M.M., Qadir, A. and Siddiqui, S.H., 2011, 'Experimental testing of hot mix asphalt mixture made of recycled aggregates', *Waste Management & Research*, 29(12), 1316-1326.

Ramaswamy, S.D. and Aziz, M.A., 1992, 'Some waste materials in road construction', *In Utilization of Waste Materials in Civil Engineering Construction*, 153-165. ASCE.

Tapkin, S., 2008, 'The effect of polypropylene fibers on asphalt performance', *Building and Environment*, 43(6), 1065–1071.

Taylor, M.A. and Khosla, N.P., 1983, 'Stripping of asphalt pavements: State of the art '(discussion, closure) (No. 911).

Topal, A., Ozturk, A. U., & Baradan, B., 2006, 'Use of recycled concrete aggregates in 235

hot-mix asphalt', Special Publication, 235, 291–304

Viswanathan, C., 2006, 'Domestic solid waste management in South Asia', *Environmental Engineering and Management Program Asian Institute of Technology Thailand.*

Warden, W., Hudson, S. & Howell, H., 1959, 'Evaluation of mineral fillers in terms of practical pavement performance', in *Proceedings of the Association of Asphalt Paving Technologists*, 28, 316–352.

Proceedings of the 7th International Symposium on

Advances in Civil and Environmental Engineering Practices for Sustainable Development

ACEPS - 2019

A comparative study of HMA with modified asphalt by polyethylene terephthalate and polypropylene fibers.

Mehalathan .S[1], Jegatheesan .N [1], Juzaafi .M [1], Rengarasu . T.M and Bandara W.M.K.R.T.W [1]

[1]Department of Civil and Environmental Engineering, Faculty of Engineering, University of Ruhuna, Galle, Sri Lanka

K e y w o r d s

Polyethylene terephthalate
Polypropylene
Fibers
Hot mix asphalt
Modifier
Additive

A B S T R A C T

Increasing traffic volume along with the extreme surface temperature fluctuation has increased premature surface deterioration of flexible pavement. Conventional surface course material of flexible pavement, Hot Mix Asphalt (HMA), therefore, has been modified with several virgin and recycled material. This study aimed to compare the properties of modified HMAs with two recycled polymer fibres namely Polyethylene terephthalate (PET) and Polypropylene (PP). PET and PP fibres were utilized binder additive and binder modifier respectively at the rate of 5%, 10% and 15% by total weight of asphalt binder. Effects of both polymers on HMA have investigated in terms of bulk properties, Marshall strength properties, Marshall quotient and indirect tensile strength. Both PET and PP fibres considerably improved the properties of modified HMAs and all modified HMA mixes were met the ASTM specification for medium traffic volume pavement. Addition of PET provided better mix compared to HMA containing binder replaced with PP fibres in terms of higher bulk properties, Marshall properties and tensile strength. This indicated that PET modified HMA has better resistant to rutting failure, shear stress and crack propagation. Overall results show that modifications of asphalt binder with PET and PP have significant positive effects on the properties of HMA, and it can promote the recycle and reuse of waste material in pavement industry in an environmentally friendly and economical way.

1. INTRODUCTION

Increasing traffic volume along with the extreme surface temperature fluctuation has increased premature surface deterioration of flexible pavement, including rutting, cracking, fatigue and stripping. Hot Mix Asphalt (HMA) is used as the primary surface course material of flexible pavement. Conventional HMA, viscoelastic material, consists of asphalt binder refined from crude source and granular aggregates extracted from rock. More attentions have been paid on the asphalt binder to attain durable and functionally stable HMA mix since asphalt is the only deformable and continuous phase changing material (Martinez Boza *et al.* 2001; Akinpelu *et al.* 2013) used in HMA. Though composition of asphalt, which relies on the crude source and the refinery process used to extract the asphalt, strongly depends on performance of asphalt, properties of the base asphalt can be improved with proper selection of crude source (Becker *et al.* 2001; Zhu *et al.* 2014). However, due to limited crude resource and lack of control actions during the refining process, producing good quality asphalt has been difficult which is overcome with asphalt modification.

Modification of conventional asphalt with suitable materials have been identified as an appropriate approach to enhance the properties of asphalt binder and gross mix (Coplantz *et al.* 1993; Huang *et al.* 2007; Akinpelu *et al.* 2013). Modifiers of HMA previously investigated can be categorized as fillers, fibres, extenders, polymers, plastics, anti-strip agents, oxidants and reclaimed

rubber (Coplantz *et al.* 1993; Zhu *et al.* 2014). In the midst of modification investigated, polymer modification has gained importance in the road sector for the last four decades.

Polymers used in the asphalt industry can be categorized into three, which are plastomers, thermoplastic elastomers, and reactive polymers. Plastomers and reactive polymers improve rigidity and rutting resistance. Thermoplastic elastomers are used to improve the elastic properties of modified asphalt. Properties of polymer modified asphalt strongly depends on chemical and physical characteristics of the asphalt as well as dosage, type, manufacturing process and properties of the polymer (Coplantz *et al.* 1993; Zhu *et al.* 2014; Polacco *et al.* 2015). Moreover, mixing speed, performing temperature and period of blending also significantly change the properties of modified asphalt (Yildirim *et al.* 2004; Yildirim 2007; Dominguez & Garcia-Morales 2011; Polacco *et al.* 2015). Polymers included polyethylene, polypropylene, ethylene– vinyl acetate, ethylene–butyl acrylate, styrene–butadiene–styrene, styrene–isoprene–styrene, and butylene–styrene have been studied as asphalt modifier in the pavement construction industry (Coplantz *et al.* 1993; Yildirim 2007; Zhu *et al.* 2014).

Modification of asphalt with polymer, that is arranged as chains of repeated small molecules, has been shown improvements in engineering properties which included rutting resistance cracking, fatigue damage, stripping, stability, moisture susceptibility and temperature susceptibility (Yildirim 2007; Kalantar *et al.* 2012; Zhu *et al.* 2014; Polacco *et al.* 2015) as well as properties of asphalt namely elastic recovery, ductility, storage stability, ageing resistance and stiffness (Coplantz *et al.* 1993; Dominguez & Garcia-Morales 2011).

Polymer fibres, high tensile material, behave as reinforcement in asphalt mix. Polymer fibres used as modifier in asphalt provides additional tensile strength in order to control the formation and propagation of cracks. HMA has higher compression capacity compared to tensile capacity which is nearly same as cement concrete. Utilization of fibres as reinforcement improves the tensile capacity of HMA. Fundamentally, fibre used as asphalt modifier significantly improves dynamic modulus, moisture susceptibility and rutting resistance (Abtahi *et al.* 2010).

Though polymer modification has been shown effective betterment in the performance of pavement, major crisis encountered is high cost of the polymer lead to increase the construction cost. On the other hand, design requirement and performance demands vary among different classes of roads which means it is not always need be achieved higher performance HMA mix. In terms of economic feasibility, using waste polymers as modifier in road surface mix can potentially help to reduce economical issue and material wastage. Utilization of secondary and recycled polymer has also become a more accepted method for addressing economic and environmental issues.

According to the previous studies, waste PET plastic, the thermoplastic polymer has a great potential to be reused as binder modifier in asphalt mixture. Crushed waste PET plastic bottle has been studied as asphalt modifier, and the study showed that addition of PET up to 6% by weight of asphalt, increased the stiffness of HMA. As the result of increases in stiffness, resistance against the permanent deformation and stability of Modified HMA (MHMA) with PET improved compared to unmodified HMA (Ahmadinia *et al.* 2011). Beside, PET improved the fatigue behaviour at low and high temperature (Modarres & Hamedi 2014; Moghaddam *et al.* 2014) and rutting resistance of surface course of the pavement under the heavy loading (Ahmadinia *et al.* 2011).

Polypropylene (PP) commonly used as asphalt modifier, controlled the bleeding of binder at high temperature. Moreover, HMA containing PP have high moisture susceptibility resistance, Marshall stability, compressive strength, temperature susceptibility resistance and shear resistance compared to unmodified HMA (Al-Hadidy & Yi-Qiu 2009). PP MHMA have shown high rutting resistance than HMA containing polythene modified asphalt since PP increased the binder film thickness in the HMA. PP fibres incorporated as asphalt modifier reduced reflection cracking, intensities of crack and rutting. Compared to the other polymers, performance of PP fibres as modifier have functionally and economically proven many improvements (Abtahi *et al.* 2010).

PET cannot be considered as a suitable asphalt modifier in wet process method since PET cannot to be incorporated with asphalt at

normal mixing temperature (less than the melding temperature of PET) (Casey *et al.* 2008; Ahmadinia *et al.* 2011; Earnest 2015). However, incorporation of PET and PP (PP) fibre as binder modifier in wet process can be an advantage since the fibres have a high melting point which means degradation of fibres at high temperature would be deceased and fibres would act as reinforcement agent. Therefore, this study is aimed to compare the effect of recycled PET and PP fibres as binder modifier in HMA.

2. MATERIALS AND METHOD

Three grading levels of gneiss aggregate, a type of metamorphic rocks, namely coarse (20 mm), medium (14 mm) and fine grading, and 60/70 penetration grade petroleum-based asphalt were utilized to produce control and MHMA specimens. Properties of conventional and alternative materials are shown in Table 1. Marshall mix design was followed in this study. Mix proportions of conventional materials used in control and MHMA were determined to meet ASTM D3515 specifications of dense mix designation 'D-4'. Fifteen unmodified specimens were prepared considering five asphalt contents varies from 4% to 6% by total weight of HMA, at 0.5% interval with three replicates. According to Marshall mix design, the optimum asphalt content of unmodified HMA was determined as 5% which has been considered for further modification of HMA.

PP fibres were utilized to modify the conventional asphalt binder by replacing the weight of binder by 5%, 10% and 15%, while PET fibres were incorporated as binder additive at 5%, 10% and 15% by weight of the binder. Physical properties of conventional and alternative material used in this study are shown in Table 01. The overall methodology followed in this study is shown in Figure 01.

In the modification of HMA, the conventional binder was modified in the wet process in which weight of asphalt was replaced with each type fibre at 5%, 10% and 15%. For mixing of fibres, the asphalt was heated to 165°C until it became a liquid. Afterwards, fibres were then slowly incorporated with asphalt. Asphalt binder and fibres were stirred with an asphalt mixer set at 136 rpm beating speed and 165°C for 30 minutes. Approximately, homogeneous binder mix was prepared with minimum change in the form of fibres. Modified asphalt was incorporated with preheated mixtures of aggregates to prepare the MHMA mixes. Fibre modified specimens were investigated in terms of bulk properties, Marshall strength properties and indirect tensile strength.

Table 1 Properties of conventional and alternative material

Materials	Parameter	Value	Remark
Asphalt binder	Specific gravity Penetration grade Melting point	0.94 60/70 49 °C	ASTM D70 ASTM D5 ASTM D36
Chip aggregate (14 mm)	Apparent specific gravity Water absorption	2.61 0.31%	ASTM C127-88
Coarse aggregate (20 mm)	Apparent specific gravity Water absorption Flakiness Index Elongation Index	2.75 0.29% 12.4% 15.7%	ASTM C127-88 BS 812
Fine aggregate	Apparent specific gravity Water absorption	2.71 1.21%	ASTM C128-88
PET fibres	Diameter Length Apparent specific gravity Melting point	0.5 mm 4 mm to 6 mm 1.2 252 °C	Details from manufacturer
PP fibres	Diameter Length Apparent specific gravity Melting point	0.5 mm 4 mm to 6 mm 0.91 171 °C	Details from manufacturer

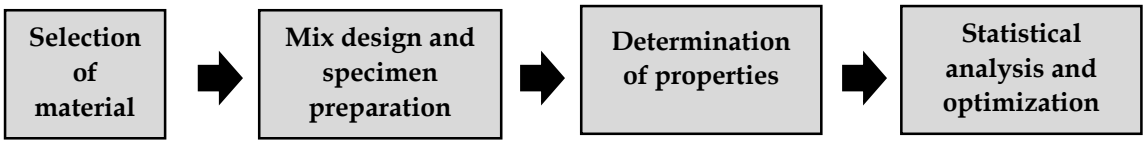

Figure 1 Overall methodology

3. RESULT AND DISCUSSION

3.1. Bulk Specific Gravity

Bulk specific gravity of MHMA gradually declined with increasing PET and PP fibre content. In both modifications, the value of bulk specific gravity was confined a narrow range and varied from 2.23 to 2.22 for PP and from 2.31 to 2.30 for PET. Bulk specific gravity of PET MHMA was higher than that for PP, while it was low compared to control mix having bulk specific gravity of 2.37.

The specific gravity of both polymers are distinct from that of conventional asphalt binder. Asphalt binder and fibres were stirred completely for 30 minutes in order to reduce dispersion effect. Due to the low specific gravity of PP fibres compared to conventional asphalt, bulk specific gravity of PP MHMA decrease as PP content increased. Similarly, addition PET fibres that has greater specific gravity than asphalt binder, also decreased bulk specific gravity of PET MHMA with the increase of PET content. This could be attributed the fact that although addition of PET fibres increased the specific gravity of modified asphalt, orientated PET particles between the aggregates in mix temperature increased the bulk volume of MHMA, which led to decrease bulk specific gravity of PET MHMA. Variation of bulk specific gravity with PET and PP contents is depicted in Figure 2.

3.2. Voids in Mix (VIM)

VIM of modified HMA decreased slightly with increase PP and PET contents; however value of VIM obtained from PET and PP modification was high compared to that for control HMA (3.5%). While PET and PP content varied from 5% to 15%, VIM of modified HMA varied from 4.9% to 4.6% and from 4.4% to 3.8% respectively.

Incorporation of both polymers increased the volume of the mixer and reduce the degree of compaction which led to increase the voids in the mix. Asphalt binder replacement with PP decreased the VIM with increasing PP content which could be attributed the fact that increasing PP content reduce the asphalt absorption. This resulted the decrease in VIM of PP modified HMA. Although, a similar variation was observed in VIM of PET modified HMA, VIM of PET modified HMA was significantly greater than that for PP modified HMA when polymer content changed from 5% to 15%. PET fibres orientated between aggregates in the mixing temperature increased VIM due to the high melting point of PET fibres. Variation of VIM with PET and PP contents is shown in Figure 3. VIM values of PET and PP modified HMA were within the allowable range of ASTM specification (3% < VIM < 5%).

3.3. Marshall Stability

PET and PP modifications increased Marshall stability which was immensely higher than that for control HMA (11.4 kN). Marshall stability of PET modified HMA increased an increasingly rapid rate and varied from 15.5 kN to 23.0 kN as PET content varied from 5% to 15%, while Marshall stability of PP modified HMA slightly increased from 13.5 kN to 15.6 kN as PP content increased (5% - 15%). This increase was resulted due to the higher rigidity of the modified asphalt binder with each polymer.
Melting point of PET fibres (252°C) is considerably higher compared to PP fibres (171°C), and degradation of PET fibres in mixing temperature (165°C) therefore lower than PP fibres. This led to significantly increase Marshall stability of PET modified HMA. Variation of VIM with PET and PP contents is shown in Figure 4. Marshall stability values of PET and PP modified HMA satisfied ASTM specification requirements for

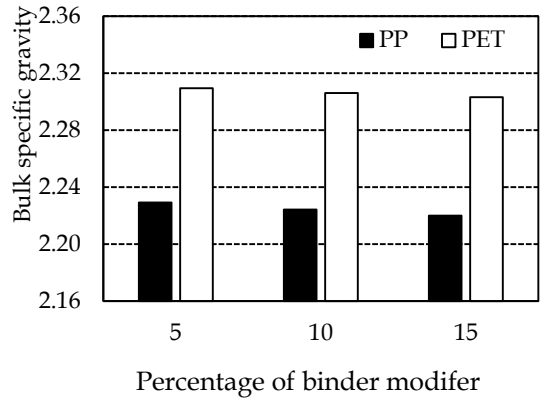

Figure 2 Variation of bulk specific gravity with PET and PP contents

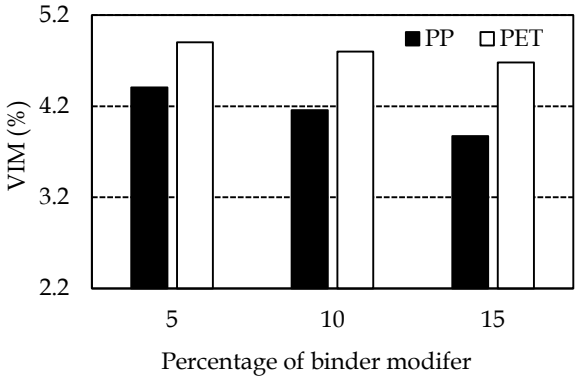

Figure 3 Variation of VIM with PET and PP contents

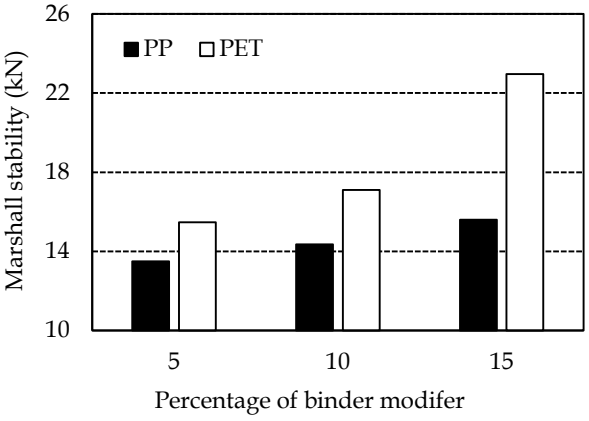

Figure 4 Variation of Marshall stability with PET and PP contents

medium volume traffic pavement (Marshall stability > 5.34 kN)

3.4. Marshall Flow

Marshall flow of both PET and PP modified HMAs increased as polymer content increased and Marshall flow values of polymer modified HMA was sizably greater than that of control HMA having Marshall flow of 9.4. This could be attributed the fact that polymer fibres decreased the absorption of asphalt binder by aggregate in the modified HMA. Availability of free asphalt binder into the voids made the modified HMA as more flexible which tended to increase Marshall flow of polymer modified HMA. Marshall flow values of PET and PP modified HMA satisfied ASTM specification requirements for medium volume traffic pavement (8< Marshall flow < 16). Variation of Marshall flow with PET and PP contents is shown in Figure 5.

3.5. Marshall Quotient

Marshall quotient can be calculated as the ratio of stability (KN) to flow (0.25 mm), which

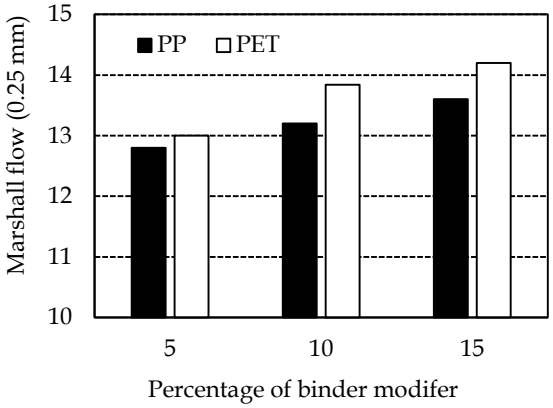

Figure 5 Variation of Marshall flow with PET and PP contents

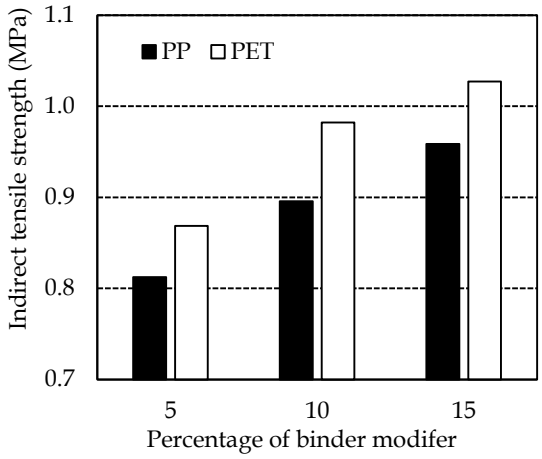

Figure 6 Variation of Indirect tensile strength with PET and PP contents

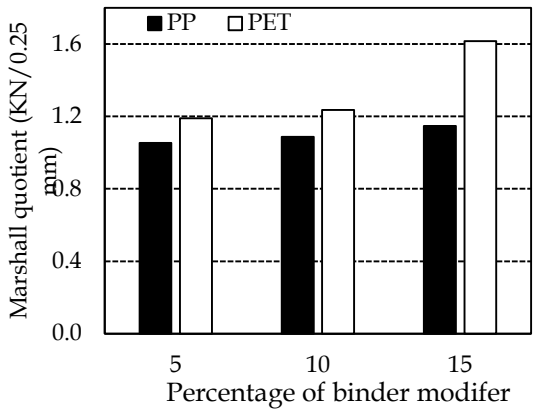

Figure 7 Variation of Marshall quotient with PET and PP contents

increased with increasing both polymer contents conserved in this study. Marshall quotient of PP modified HMA varied in smaller range of 1.05 -1.15 kN/0.25 mm, and these values were lesser than Marshall quotient of control HMA (1.21 kN/0.25 mm). Marshall quotient of PET modified HMA increased an increasingly rapid rate and varied from 1.19 kN/0.25 mm to 1.62 kN/0.25 mm as PET content varied from 5% to 15%.

By this way, a higher value of Marshall quotient indicates a stiffer HMA and hence, indicates that HMA is likely more resistant to permanent deformation, shear stress and rutting in the road service. PET modified HMA show better resistant to rutting failure compared to PP modified HMA. All Marshall quotient of PET and PP modified HMA satisfied ASTM specification for medium volume traffic pavement (> 0.33 kN/0.25 mm). Variation of Marshall quotient with PET and PP contents is shown in Figure 6.

3.6. Indirect tensile strength

Indirect tensile strength of PET and PP modified HMA increased with polymer content considered in this study which variation was as similar as Marshall stability of polymer modified HMA. Indirect tensile strength of PET modified HMA varied from 0.87 MPa to 1.03 MPa, while indirect tensile strength of PP modified HMA varied from 0.81 MPa to 0.96 MPa. However, indirect tensile strength values of polymer modified HMA expect 5% of PP modified HMA, were higher than that for control HMA (0.84 MPa).

PET fibres existed as a semi crystal in modified HMA, made a stiffer mixture which led to increased tensile strength as PET content increased (Ahmadinia *et al.* 2012; Moghaddam *et al.* 2012). Indirect tensile strength of PP modified HMA was lower that PET modified HMA since tensile strength of PET fibre is two times higher compared to PP fibre. This indicated that, incorporation of polymer fibres improved the resistance against the crack propagation. Variation of indirect tensile strength with PET and PP contents is shown in Figure 7.

4. CONCLUSIONS

Both PET and PP fibres utilized as binder additive and binder modifier respectively considerably improved the properties of modified HMAs and all modified HMA mixes were met the ASTM specification for medium traffic volume pavement.

Bulk specific gravity of PET modified HMA as higher than mix containing PP. According to the fact, higher bulk specific gravity results in better mix design. Therefore, the addition of PET provided better mix compared to HMA having binder replaced with PP fibres.

VIM values of PP modified HMA was lower than that of PET modified HMA. This indicated that PP modified HMA is economically effective mix since PP fibre partially replaced the weight of asphalt binder and this mix reduced the binder bleeding during the heavy traffic condition.

Strength properties including Marshall stability, Marshall flow, Marshal quotient and indirect tensile strength showed an increment in each modification. PET modified HMA however resulted in greater improvement in comparison with PP modified HMA. This indicated that PET modified HMA have better resistant to rutting failure, shear stress and crack propagation.

REFERENCES

Abtahi, S.M., Sheikhzadeh, M. & Hejazi, S.M., 2010, 'Fiber-reinforced asphalt-concrete–a review', *Construction and Building Materials* 24(6), 871-877.

Ahmadinia, E., Zargar, M., Karim, M.R., Abdelaziz, M. & Shafigh, P., 2011,' Using

waste plastic bottles as additive for stone mastic asphalt', *Materials & Design* 32(10), 4844-4849.

Airey, G., 1997, *Rheological characteristics of polymer modified and aged bitumens*, Doctoral dissertation, University of Nottingham.

Akinpelu, M., Dahunsi, B.I., Olafusi, O., Awogboro, O. & Quadri, A., 2013, 'Effect of polythene modified bitumen on properties of hot mix asphalt', *ARPN Journal of Engineering and Applied Sciences 8*(4), 290-295.

Al-Hadidy, A.I. & Yi-qiu, T., 2009, 'Effect of polyethylene on life of flexible pavements', *Construction and Building Materials 23*(3), 1456-1464.

Al-Hadidy, A.I. & Yi-Qiu, T., 2009, 'Mechanistic approach for polypropylene-modified flexible pavements', *Materials & Design 30*(4), 1133-1140.

Arabani, M. & Tahami, S.A., 2017, 'Assessment of mechanical properties of rice husk ash modified asphalt mixture', *Construction and Building Materials 149*, 350-358.

Aziz, M.M.A., Rahman, M.T., 1Hainin, M.R. & Bakar, W.A.W.A., 2015, 'An overview on alternative binders for flexible pavement', *Construction and Building Materials 84*, 315-319.

Becker Y, Méndez MP, Rodriguez Y.,2001, 'Polymer modified asphalt', *Vision Technol* 9(1),39–50.

Casey, D., McNally, C., Gibney, A. & Gilchrist, M.D., 2008, 'Development of a recycled polymer modified binder for use in stone mastic asphalt'. *Resources, Conservation and Recycling 52*(10), 1167-1174.

Chen, Z., Wu, S.P., Zhu, Z.H. & Liu, J.S., 2008, 'Experimental evaluation on high temperature rheological properties of various fiber modified asphalt binders', *Journal of Central South University of Technology 15*(1), 135-139.

Coplantz, J.S., Yapp, M.T. & Finn, F.N., 1993. *Review of relationships between modified asphalt properties and pavement performance* (No. SHRP-A-631). Strategic Highway Research Program, National Research Council.

DomíNguez, F.N. & García-Morales, M., 2011, 'The use of waste polymers to modify bitumen', In *Polymer modified bitumen*, pp. 98-135). Woodhead Publishing.

Earnest, M.D., 2015, Performance characteristics of polyethylene terephthalate (PET) modified asphalt.

Epps, A., Harvey, J.T., Kim, Y.R. & Roque, R.E.Y.N.A.L.D.O., 2000, 'Structural requirements of bituminous paving mixtures', *Transportation in the New Millennium*.

Gao, J., Wang, H., You, Z. & Hasan, M.R.M., 2018, 'Research on properties of bio-asphalt binders based on time and frequency sweep test', *Construction and Building Materials*, *160*, 786-793.

Hamzah, M.O., Omranian, S.R. & Golchin, B., 2015, 'A Review on the Effects of Aging on Properties of Asphalt Binders and Mixtures', *Caspian Journal of Applied Sciences Research*, *4*(6).

Hikkaduwa, H.N., Gunawardana, K.W., Halwatura, R.U. & Youn, H.H., 2015, 'Sustainable approaches to the municipal solid waste management in Sri Lanka', *no. December*.

Hinislioglu, S. & Agar, E., 2004, 'Use of waste high density polyethylene as bitumen modifier in asphalt concrete mix', *Materials letters*, *58*(3-4), 267-271.

Huang, Y., Bird, R.N. & Heidrich, O., 2007, 'A review of the use of recycled solid waste materials in asphalt pavements', *Resources conservation and recycling*, *52*(1), 58-73.

Hussein, A.A., Jaya, R.P., Hassan, N.A., Yaacob, H., Huseien, G.F. & Ibrahim, M.H.W., 2017, 'Performance of nanoceramic powder on the chemical and physical properties of bitumen', *Construction and Building Materials*, *156*, 496-505.

Jahromi, S.G. & Khodaii, A., 2008, 'CARBON FIBER REINFORCED ASPHALT CONCRETE', *Arabian Journal for Science & Engineering (Springer Science & Business Media BV)*, *33*.

Jegatheesan,N., Rengarasu,T.M. & Bandara, W.M.K.R.T.W., 2018, 'Effect of Polyethylene Terephthalate (PET) Fibres as Binder Additive in Hot Mix Asphalt Concrete', *Transaction of 112th Annual Sessions of the Institution of*

Engineers, Colombo, Sri Lanka (IESL) , pp.175-182.

Kandhal, P.S., & Parker, F., 1998, *Aggregate tests related to asphalt concrete performance in pavements* (Vol. 405), Transportation Research Board.

Kalantar, Z.N., Karim, M.R. & Mahrez, A., 2012, 'A review of using waste and virgin polymer in pavement', *Construction and Building Materials*, *33*, 55-62.

Martinez-Boza, F., Partal, P., Navarro, F.J. & Gallegos, C., 2001, 'Rheology and microstructure of asphalt binders', *Rheologica acta*, *40*(2), 135-141.

Modarres, A. & Hamedi, H., 2014, 'Effect of waste plastic bottles on the stiffness and fatigue properties of modified asphalt mixes', *Materials & Design*, *61*, 8-15.

Moghaddam, T.B., Karim, M.R. & Soltani, M., 2013, 'Utilization of waste plastic bottles in asphalt mixture', *Journal of Engineering Science and Technology*, *8*(3), 264-271.

Moghaddam, T.B., Soltani, M. & Karim, M.R., 2014, 'Evaluation of permanent deformation characteristics of unmodified and Polyethylene Terephthalate modified asphalt mixtures using dynamic creep test', *Materials & Design*, *53*, 317-324.

Najd, A., Chao, Z. & Ying, G., 2005, 'Experiments of fracture behavior of glass fiber reinforced asphalt concrete', *Journal of Chang'an University (Natural Science Edition)*, *25*(3).

Polacco, G., Filippi, S., Merusi, F. & Stastna, G., 2015, 'A review of the fundamentals of polymer-modified asphalts: Asphalt/polymer interactions and principles of compatibility', *Advances in Colloid and Interface Science*, *224*, 72-112.

Rahman, M.N., Ahmeduzzaman, M., Sobhan, M.A. & Ahmed, T.U., 2013, 'Performance evaluation of waste polyethylene and PVC on hot asphalt mixtures', *American Journal of Civil Engineering and Architecture*, 1(5), 97-102.

Read, J., Whiteoak, D. & Hunter, R.N., 2003, *The shell bitumen handbook*' Thomas Telford.

Sobolev, K., Vivian, I.F., Saha, R., Wasiuddin, N.M. & Saltibus, N.E., 2014, 'The effect of fly ash on the rheological properties of bituminous materials', *Fuel*, *116*, 471-477.

Usman, N. & Masirin, M.I.M., 2019, 'Performance of asphalt concrete with plastic fibres', In *Use of Recycled Plastics in Eco-efficient Concrete* (pp. 427-440). Woodhead Publishing.

Xue, Y., Wu, S., Cai, J., Zhou, M. & Zha, J., 2014, 'Effects of two biomass ashes on asphalt binder: Dynamic shear rheological characteristic analysis', *Construction and Building Materials*, *56*, 7-15.

Yang, X., You, Z., Dai, Q. & Mills-Beale, J., 2014, 'Mechanical performance of asphalt mixtures modified by bio-oils derived from waste wood resources', *Construction and Building Materials*, *51*, 424-431.

Yildirim, Y., Hazlett, D., Davio, R., 2004, 'Toner-modified asphalt demonstration projects', *Resources, conservation and recycling*, *42*(3), 295-308.

Yildirim, Y., 2007, 'Polymer modified asphalt binders', *Construction and Building Materials*, *21*(1), 66-72.

Zhu, J., Birgisson, B. &and Kringos, N., 2014, 'Polymer modification of bitumen: Advances and challenges', *European Polymer Journal*, *54*, 18-38.

Proceedings of the 7th International Symposium on

Advances in Civil and Environmental Engineering Practices for Sustainable Development

ACEPS - 2019

An analysis of frequently observed roadside green boundary wall facades in Western province, Sri Lanka : visual configurations, cost and operational challenges

W.C.M.S.Madushanka[1], M.F.M.Althaf , M.S.M. Sajjad, Tushara Chaminda G.G[2] , G.N. Samarasekara[3]

[1] Faculty of Graduate Studies, University of Sri Jayewardenepura, Gangodawila, SRI LANKA
[2] Department of Civil and Environmental Engineering, Faculty of Engineering, University of Ruhuna, Hapugala, Galle, SRI LANKA
[3] Department Of Civil Engineering, Faculty of Engineering, University of Sri Jayewardenepura, SRI LANKA

K e y w o r d s

Urban green facades
Boundary walls
Green walls
Visual configurations

A B S T R A C T

Greening the roadside boundary walls is a frequent method adopted to introduce greenery to urban areas. Aesthetical appearance is a key motivator for such urban greening. Therefore, it is important to identify the different options available for urban residents to make their boundary wall green. Based on a series of field observations, focus group discussions and cost estimations, this study aimed to identify the different configurations for roadside green boundary walls, species options for each identified type, a unit cost estimation for each type along with operational challenges in adopting such. Based on previous classifications and field observations, 12 distinguishable visual configurations were identified among those. Planting trees within the garden was frequently observed. While those require more installation cost were less preferred. Need for regular pruning, fertilizing and disturbances to utility lines were identified as common operational problems. The identified configurations will be useful for landscape designers in typology designs and for future research on wall types with improved visual appearance.

1. INTRODUCTION

Living in a urban areas is not a preferred option for humans who have a thirst for nature. One of the coping strategies adopted by man is brining nature to his dwelling space. This has resulted in spaces such as urban parks, urban green roads, vegetated gardens, vegetated interior spaces and vegetated urban facades. Many urban dwellers have a boundary wall for security purposes. But the artificial nature of such walls in most cases creates an appearance that is not pleasant. Use of vegetation for covering architecture such as facades is one concept in green architecture Perini and Magliocco (2012). Following such concept urban dwellers attempt to introduce greenery to boundary walls. This research focuses on such boundary walls.

1.1. Literature review

1.1.1. Benefits of urban greenery

Greenery is crucial for human well-being in cities and serves the purpose of shaping local identity, benefits public health, increases resilience to climate change and environmental shocks, promotes biodiversity conservation and improves quality Derkzen *et al.* (2017)

They contribute to noise attenuation Veisten *et al.* (2012), energy savings for air-conditioning, increase of real estate value and durability of façades (Perini and Rosasco, 2013), improvement of environmental conditions of dense urban areas, greenhouse gases output reduction, air quality improvement and improvement of biodiversity Bianchini and Hewage (2012).

1.1.2. Aesthetic appearance as a motivator for urban greenery

Vegetation is one of the three basic landscape elements Appleton (1975). Among many factors aesthetic appearances is an important motivator to have greenery in urban facades Perini and Rosasco (2013) Sutton (2014). green space planning and management for still far too often being based on aesthetic and economic reasons Haaland and van den Bosch (2015). Many studies have proved that people prefer vegetated areas over an above non-vegetated areas Bjerke *et al.* (2006). Trees add visual diversity. Moving beyond traditional landscape elements, urban greenery is now being extended to rooftop gardens, domestic gardens, brownfields, pocket parks and facade greenery. Among these roadside vegetation has not been studied much Weber *et al.* (2014). However as cited by the authors, in a recent nationwide survey in Germany revealed that 92% of the respondents highly value roadside trees and greenery which gives evidence value of roadside facades to residents.

While, trees have been the focus by most of roadside vegetation studies (Fukahori and Kubota (2003), many other variations such as variation of plants, non-planted, spontaneously emerging, plant assemblages that exists along many road verges and in median strips, tree planting sites and paving joints. Trees have the greatest effect on preference, although the space beneath trees, i.e. flowering herbs in combination with trees, can also affect preferences Todorova *et al* (2004). Thus it is important to identify and distinguish different configurations of roadside facades with emphasis on visual configurations which forms the basis for preference.

1.1.3. Configurations of green facades

While configurations of road side vegetation is rare to find, some previous researchers have generally classified green walls on building envelopes. According to classification by Susorova (2015) the green walls are primarily classified as living walls and green facades based where plants are planted Susorova (2015). In living walls the plants either planted on the wall or in soil or similar media embedded to the wall. Such embedding can be done through hanging pots, modular system or a mat. Green facades refer to the plants which mostly grow on ground have been classified as direct green facades which grows without external structural support and indirect green facades which grows with some structural support. Jim (2015) has also classified green walls as climber green walls which are mechanical-dependent plants and herb-shrub green wall which are mechanically independent plants. Place of planting the greenery and mechanical support needed by the plants can be considered as common bases of above classifications. While these provide bases for classification, a classification for visual configuration about boundary walls should incorporate variations of vegetation type, and spatial relationship among road, vegetation and boundary wall. This study initially aims to cover such research gap.

1.1.4. Cost of green walls

Green walls have several associated costs elements. In broad these include, initial cost to set up the green wall and recurrent expenditure and cost of demolishing. When considering all types of green walls design cost, cost for planting material, Cost for pots or digging, cost of potting mixture and fertilizer, transportation and installation cost, irrigation cost , cost for pruning, replacement cost and disposal cost, replacement cost can be identified as main cost components Rosasco (2018). These costs widely vary with the type of green walls, size and material used Perini and Rosasco (2013). Thus it is important to identify different cost components associated with each green wall configuration.

1.1.5. Operational challenges for creating green walls

A house owner will have to face different operational challenges in adopting green boundary wall facades. Specific heat tolerance plants species are required due to surrounding higher temperature, adopting plants the new environmental conditions (Pradhan *et al.*(2019), Pollen allergy Pradhan (2019) and climbing plants may damage to the wall facade and reduce the durability Manso and Castro-Gomes (2015). Thus it is important to identify operational challenges faced by house owners in greening a boundary wall.

2. RESEARCH GAP AND OBJECTIVES

Availability of information on possible green wall configurations to create a better visual appearance would be useful for the house owners as well as designers who intends to have such a green facades. Most of the previous green wall research have focused on their benefits such as thermal comfort, aesthetic appeal, potential species or the economical aspects. Only few studies have attempted to classify the green wall based on their configurations mainly focusing on the way greenery is supported Manso and Castro-Gomes (2015). Even those configurations cannot be directly applied green boundary wall facades where the boundary wall stand out as a major visual element between the property and the road. Spatial relationship among road, vegetation and boundary wall should be considered by such classification.

Thus there is a need to analyse the roadside green boundary wall facades for their visual appearance. Such study should start with an analysis of visual configurations while identifying related cost elements and operational challenges faced in adopting such. This has below research objectives,

I. Identify the different visual configurations for roadside green boundary walls
II. For the aforementioned configurations, identify species options, identify the cost elements and estimate the unit cost and identify operational challenges faced in adopting such.

The study was conducted in urban residential areas of Western Province, Sri Lanka.

3. MATERIALS AND METHODS

3.1. Objective I: Identification of different visual configurations

For the Objective I above, more than 500 roadside urban green boundary wall facades belonging to the Western Province, Sri Lanka were observed by travelling along randomly selected different road stretches covering more than 50 km. This initial observations revealed that configurations differ based on presence of a boundary wall, spatial relationship among road, vegetation and boundary wall, the places of planting the greenery and the nature/ need of mechanical support for plants. After considering above factors two members of the research team who are familiar with roadside visual aesthetics, separately came up with two classifications. After a series of discussion among the two members, a commonly agreed classification of configurations was obtained.

In order to understand the popularity, a frequency distribution of above configurations was obtained by counting the availability of such configurations through site observations using google street view for about 100km.

3.2. Objective II: Optional species, cost elements, operational challenges

A list of frequently used species, was created based on authors' previous research work Samarasekara and Madushanka (2018) and counts based on aforementioned actual and google street view site observations.

Values of different cost elements were established based on published data related to construction and pricing obtained from three plant nurseries in Colombo. The cost estimates were done following standard cost estimation methods and done for a size of 10 feet in length and 5 feet in height.

Operational challenges were obtained by focus group discussions with 25 house owners representing different configurations and 3 landscaping professionals who have experience in similar sites.

4. RESULTS

4.1. Types of visual configurations for urban green wall facades

Table 1 give the description of different wall configurations, their relative popularity, cost associated with walls and operational challenges of the 12 types of visual configurations identified. Among these type A and B are the green facades without any boundary wall. The type C to H are green facades with greenery placed at different with varying mechanical supports and positioning of greenery.

4.2. Optional species, cost elements, operational challenges

For each wall type, the greenery may be trees, bushes, climbers and ornamental plants. Species *Vitex negundo*, *Mahua longifolia* can be

used as trees. Species *Philodendron imbe*, *Syzygium campanulatum, Ixora coccinea, Ficus benjamina, Bauhinia kockiana* can be used for bushes. Climber can be *Asparagus racemosus, Mandevilla sanderi, Uncaria tomentose, Tristellateia australasiae, Thunbergia laurifolia, Thunbergia fragrans, Clitoria ternatea*, *Vernonia elaeagnifolia* A range of ornamental plants such as *Cyrtostachys renda*, *Tradescantia spathacea* can be used.

The initial cost and maintenance costs associated with green walls are given in Table 1. These are associated with below mentioned general and specific operational challenges. The types A,K and H use climbers which generally requires frequent pruning and maintenance. Higher probability of insect growth can be observed in these and care should be exercised in pruning to avoid insect attacks. If the species are edible, there is a risk of theft and damage to the wall. Types C and F use trees which also requires pruning especially when trees grow taller to the level of utility lines. Types A,B,D,E, G and H has greenery growing in the roadside which requires the allocation of spaces for growing. Regular maintenance and pruning is a must for these in order to preserve appearance and prevent disturbance to and from roadside activities. Type G due to lower height faces relatively higher risk of damages due to vehicle parking on the area. In types I and J plants grow in planters while being exposed to severe external environment which requires more care and nurturing.

Type H requires a thin structure on the roadside, and faces the specific risk of structural damages from vehicles or wind. Type J is requires careful constructions, higher effort and cost of maintenance. Poor maintenance leads to patches in the wall creating a negative appearance. Salt accumulation in growing media cause to die the plan. One of the low cost type is Type L in which the plants grow attached to the wall requiring minimal effort for installation and maintenance. However the house owners have the misconception of possible root damages to the wall reducing its life.

5. DISCUSSION

5.1. Types of visual configurations for urban green wall facades

As mentioned in the literature review previous classifications were based on two factors, place of planting the greenery (green facades Vs living walls) and whether / nature mechanical support needed by the plants. The classification presented here, additionally incorporated the presence of a boundary wall, spatial relationship among road, vegetation and boundary wall. Although types A and B do not have boundary walls, these were included as control options in this study related to boundary walls. Further the classification only included the basic configurations. In actual world, other complex configurations resulting from combinations of the above 12 types can be observed.

Accordingly green facades are most common is Type F which is planting trees inside the garden with visibility of tree canopy from the roadside. With a clear foreground created by boundary wall, the trees in background creates a feeling of mystery described by Kaplan (1987) or the viewer from the road. Type B or the Plant walls are the next common type followed by Type E and Type A.

Table 1 Details of wall configurations; description, frequency and cost

No	Image	Name and Description	Frequency (%)	Cost (in Rupees thousands)										
				Initial cost					Maintenance cost (annual)					Demolition cost
				PL	BW	IS	IP	S	I	F	P	T	R	
A		Mesh supported climber walls : Climbers grown on ground and supported by a in a mesh supported on vertical poles and without a boundary wall	9	2	30	0	1	0	2	3	2	0	1	7
B		Plant wall : Trees/ bushes grown as a wall without a boundary wall	14	3	0	0	1	0	2	1	4	0	1	5
C		Partial boundary wall with vegetation and vertical bars : Boundary Wall has significant vertical bars and trees/ bushes visible across metal bars	2	1	84	0	1	0	0	0	1	0	1	15
D		Roadside Fully Planted boundary Wall : Trees/ bushes are grown outside (roadside) of the wall to covering the wall	6	3	84	0	1	0	2	1	4	0	1	15
E		Roadside partially Planted boundary Wall : Trees/ bushes are grown outside (roadside) of the wall to partially covering the bottom part of the wall	9	3	84	0	1	0	2	1	4	0	1	15
F		Garden side Fully Planted boundary Wall : Trees grown in the garden side of the boundary wall and visible above the boundary wall	29	1	84	0	0	0	0	0	2	0	1	15

Table 1 Continued: Details of wall configurations; description, frequency and cost

No	Image	Name and Description	Frequency (%)	Cost (in Rupees thousands)										
				Initial cost					Maintenance cost (annual)					Demolition cost
				PL	BW	IS	IP	S	I	F	P	T	R	
G		Roadside ground covers Infront boundary wall	6	2	84	0	1	0	1	0	0	4	1	15
H		Climbers growing on structure on road side of the boundary wall : Climbers planted on ground and supported by a separate structure	4	2	84	0	1	35	2	3	3	0	1	15
I		Living wall – Hanging Planters: Ornamental plants are grown in planters attached to vertical surface of boundary wall	6	3	84	10	1	20	7	10	3	1	4	15
J		Living wall Mat or modular based : Ornamental plants are grown in a separate structure attached to boundary wall; growing media may a mat or soil filled in to modular unit	2	8	84	15	2	90	9	12	3	1	4	15
K		Living wall - Top Hanging : Vines are grown in soil placed on top of the wall	4	2	84	0	1	0	4	3	1	0	2	15
L		Living wall – Attached climbers : Climbers with roots attached to the boundary wall	5	1	84	0	1	0	0	0	5	0	0	15

PL- Plants, BW- Block wall, IS- Irrigation System, IP- Initial Planting , S- Supportive Structure, I- Irrigation, F- Fertilizer, P- Pruning, T-Thinning out, R- Replanting

In general green facades are more common than living walls in this study area. Green facades require relatively less effort to install. Further those configurations having trees were more frequent than those with climbers which requires a system of mechanical support. In summarising the above trends, it can be observed that those configurations requiring less effort of installation are more frequent than those require more effort for installation.

In assessing the visual configurations of these frequent green walls, an effort to cover the artificial appearance of boundary wall partially or fully can be identified as a common motivation to introduce greenery. Further, desire to have an attractive appearance by utilizing textural effects of vegetation is observed. Types I and L can be quite effective in this manner. Types I and J requires more intervention for design and installation and leaves more room for a landscape designer to create attractive designs in comparison to the other types. In his classifications Jim (2015) has presented more options for green wall configurations such as substrate, options for training systems. However, those complexities may not affect the visual configurations due to which such complications were not included in the classification here.

5.2. Optional species, cost elements, operational challenges

According to author's previous work, *Cyrtostchys renda, Bougainvillea* spp. and *Ixora coccicinea* are the most commonly observed. Among these species *Asparagus racemosus, Mandevilla sanderi, Uncaria tomentose, Tristellateia australasiae, Thunbergia laurifolia, Thunbergia fragrans, Clitoria ternatea* can be used for most of the wall configurations including types A, G and J. However species *Ficus pumila and Campsis radicans* can be used in only for Living wall – Attached climbers.

terms of installation cost types A and B have the lowest cost while I and J requires most cost. When considering maintenance cost, types C and F have the lowest cost while I and J requires most cost.

Need for frequent pruning, maintenance and fertilizing requirements and risk of touching the utility lines are the generic operational challenges faced by almost all walls. However the living wall types I, J and L have some inherent specific challenges.

6. CONCLUSION AND APPLICATIONS

In this baseline study 12 types of green boundary walls were identified to describe the visual configurations associated with green boundary wall configurations in urban residential areas of Colombo, Sri Lanka. According to the frequency data, green facades are more frequent. Further the most frequently occurring types indicate that the decision to select a wall types is dominated by the initial efforts in setting up the wall in comparison to visual appearance. Types which require more installation cost were less preferred. Need for regular pruning, fertilizing and disturbances to utility lines were identified as common operational problems. The identified configurations will be useful for landscape designers in typology designs and for research on wall types with improved visual appearance.

7. ACKNOWLEDGMENTS

This work was funded by the staff research grant ASP/01/RE/ENG/2017/44 of the University of Sri Jayewardenepura.

8. REFERENCES

Appleton, J., 1975, *The experience of landscape*, Wiley, Available at: https://books.google.lk/books?id=7LNPAAAAMAAJ.

Bianchini, F. and Hewage, K., 2012, 'Probabilistic social cost-benefit analysis for green roofs: A lifecycle approach', *Building and Environment*, Elsevier Ltd, 58, 152–162.

Bjerke, T. *et al.*, 2006, 'Vegetation density of urban parks and perceived appropriateness for recreation', *Urban Forestry and Urban Greening*, 5(1), 35–44.

Derkzen, M. L. *et al.*, 2017, 'Shifting roles of urban green space in the context of urban development and global change', *Current Opinion in Environmental Sustainability*, Elsevier B.V., 29, 32–39.

Fukahori, K. & Kubota, Y., 2003, 'The role of design elements on the cost-effectiveness of streetscape improvement', *Landscape and*

Urban Planning, 63(2), 75–91.

Haaland, C. & van den Bosch, C. K., 2015, 'Challenges and strategies for urban green-space planning in cities undergoing densification: A review', *Urban Forestry and Urban Greening*, Elsevier GmbH., 14(4), 760–771.

Jim, C. Y., 2015, 'Greenwall classification and critical design-management assessments', *Ecological Engineering*, Elsevier B.V., 77, 348–362.

Kaplan, S., 1987, 'Aesthetics, affect, and cognition:Environmental Preference from an Evolutionary Perspective', *Environment and Behavior*, 19(1), 3–32.

Manso, M. & Castro-Gomes, J., 2015, 'Green wall systems: A review of their characteristics', *Renewable and Sustainable Energy Reviews*. Elsevier, 41, 863–871.

Perini, K. &nda Magliocco, A., 2012, 'The Integration of Vegetation in Architecture, Vertical and Horizontal Greened Surfaces', *International Journal of Biology*, 4(2), pp. 79–91.

Perini, K. & Rosasco, P., 2013, 'Cost-benefit analysis for green façades and living wall systems', *Building and Environment*, 70, 110–121.

Pradhan, S., Al-Ghamdi, S. G. & Mackey, H. R., 2019, 'Greywater recycling in buildings using living walls and green roofs: A review of the applicability and challenges', *Science of the Total Environment*, Elsevier B.V., 652, 330–344.

Rosasco, P., 2018, *Economic benefits and costs of vertical greening systems*, *Nature Based Strategies for Urban and Building Sustainability*. Elsevier Inc.

Samarasekara, G. . & Madushanka, W. M., . 2018, 'A Baseline Study to Identify Efficient Plant Species Used for Roadside Green Facades in Urban Areas Based on Qualitative Judgment', in *Proceedings of the 23rd International Forestry and Environment Symposium 2018 of the Department of Forestry and Environmental Science, University of Sri Jayewardenepura, Sri Lank*, p. 135. Available at: http://dr.lib.sjp.ac.lk/handle/123456789/8198.

Susorova, I., 2015, *Green facades and living walls: Vertical vegetation as a construction material to reduce building cooling loads*, *Eco-efficient Materials for Mitigating Building Cooling Needs: Design, Properties and Applications*.

Sutton, R. K., 2014, 'Aesthetics for Green roofs and Green walls', *Living Architecture Monitor*, (2), pp. 1–19. Available at: http://digitalcommons.unl.edu/cgi/viewcontent.cgi?article=1018&context=arch_land_facultyschol.

Todorova, A., Asakawa, S. & Aikoh, T., 2004, 'Preferences for and attitudes towards street flowers and trees in Sapporo, Japan', *Landscape and Urban Planning*, 69(4), 403–416.

Veisten, K. *et al.*, 2012, 'Valuation of green walls and green roofs as soundscape measures: Including monetised amenity values together with noise-attenuation values in a cost-benefit analysis of a green wall affecting courtyards', *International Journal of Environmental Research and Public Health*. Elsevier, 9(11), 3770–3778.

Weber, F., Kowarik, I. & Säumel, I. (2014) 'A walk on the wild side: Perceptions of roadside vegetation beyond trees', *Urban Forestry and Urban Greening*. Elsevier GmbH., 13(2), 205–212.

Proceedings of the 7th International Symposium on

Advances in Civil and Environmental Engineering Practices for Sustainable Development

ACEPS - 2019

Factors affecting safety at construction sites of Sri Lanka

R. M. N. D. Rathnayaka, P. I. A. Gomes and A. A. A. Afthal

Department of Civil Engineering, Faculty of Engineering, Sri Lanka Institute of Information Technology, Malabe, SRI LANKA

K e y w o r d s

Accident type
Construction
Factors
Safety

A B S T R A C T

This study conducted in and around the commercial hub, Colombo aimed at studying factors contributing to the safety at construction sites, correlations between factors, and impact of the site size in terms of the labour force on safety. Primary data were obtained through in-person survey questionnaires at fifty sites (in total 300 samples, targeting labour category or similar and Engineer category or similar). The age of a labourer and experience showed a strong correlation, suggesting labour force do not include mid-career entrants. The psychological factor was discovered to be the most impactful variable. Cut wound was observed to be most probable and most accidents happened during welding. Laborer's supplemental experience in workplace can be declared as the most influential factor to reduce accidents in construction sites. In general large sites were safer than medium, whereas small sites seemed to be with the highest risk, an indication that government agencies should look more into small sites.

1. INTRODUCTION

Construction industry is a vital employment sector and it is an important driver of the economy. Construction works include the construction of highways, new buildings and the repair and maintenance of existing infrastructure. Safety is a common factor which should be given importance all types of construction sites. Most of the construction activities in developing countries like Sri Lanka involve substantial labor-intensive tasks compared to developed countries. According to the scale of a construction project involvement of construction workers subjected to vary.

There are many factors contribute to safety at construction sites such as technical, economical, and historical, physiological procedural, and organizational issues. Even though construction sites should provide effective safety plans, unlike the main contractor, many sub-contractors do not have such. Perhaps, this could be the main reason construction sector to have more mortalities than any other sector (Haslam et al, 2005).

Factors affecting safety at construction sites occur also due to the lack of work ethics at sites. Workers' carelessness, defects in machineries and lack of training are some of the factors behind on-site unsafe situations. A safe environment can be obtained by giving first aid training to the staff and the labors in preparation for a tragic incident. Worker experience, job security, education and proper training are some measures that can be taken to minimize the danger to employees through operational management of manageable factors. In addition, motivational and directional program for workers will have a positive impact on making a safe working environment for labors in construction sites (Haadir & Panuwatwanich, 2011).

Main objective of this study was to investigate the factors that affect the safety at construction sites. In order to investigate the factors, minor objectives in particular, determination of safety conditions at

construction sites, assessing the impact of injuries and hazard situations were fulfilled. Also, in certain scenarios the size of the construction site was considered.

2. LITERATURE REVIEW

Construction is the foundation of the world economy. No development exists without any construction (Senouci *et a*l, 2015). Safety is a key construction inherited problem. Safety implies relative freedom from injury, threat and accidents, or minimizing to dangerous condition certain operations (Arslan *et a*l, 2018).

Most of human errors are an important factor in many construction site accidents and most of the fatalities are higher than other industries in the world (Huang & Hinze, 2006). Past studies found negligence of the workers, poor supervision, machinery errors and training conditions as reasons for un-safe conditions. Therefore, the responsible parties in some cases had to spend four times the direct cost of the projects to resolve these issues (Herinch, 1959).

It has indicated that the hazardous conduct of employees is due to a lack of awareness, work stress, financial and psychological factors. Site safety can be accomplished by these factors, the significance of hazard awareness, secure procedures and staff contribution, and the finding of excess expenses for safety programs (Harper and Koehn, 1998). Occupational and operational accidents increase the probability of risk and hazardousness at sites (Hola *et a*l, 2017). Sawacha *et a*l (1999) have examined the influence of factors such as historical, economical, organizational and environmental, psychological, technical and procedural, problems on safety.

3. METHODOLOGY

The primary data were collected from anonymous questionnaire surveys. Questionnaire was designed as close ended questions, with simple terms and multiple answers in printed form. The effective (some samples were incomplete) sample consisted of 300 people in total, in which 250 responses were from labors and 50 were from safety officers, supervisors, and engineers. The questionnaire was designation specific. Labors included machine operators, electricians, bar bender, carpenter, and builder. Questionnaire given to labors were based on experiences, age groups, safety communication, and safety culture. Questionnaires given to safety officers were based on the safety conditions at the site including details about injuries occurred within last three-month period. Selected sites were mainly from the Colombo municipality and its peripheral suburbs. Table 1 shows the categorization of sites based on the labor population and number of sites sampled. Even though more than 300 questionnaire were distributed among the laborers and safety officers only three hundred forms were received with responses that deemed to be complete. Supplementary data were collected from publications such as journals, research papers, and textbooks. In order to discuss the results obtained, a combination of qualitative and quantitative approach was used.

Table 1 Site categorization and number of sampled sites

Types of Construction Site	Number of Labours	Number of visited sites
Small	>50	17
Medium	50 - 500	22
Large	< 300	11

3.1. Survey Questionnaires

Mainly three parts (safety management, safety communication and safety culture/safety attitude) included in the questionnaires given to the labourers. Questions included awareness of the role to play during an emergency situation, knowledge on nearest assembly point during an emergency situation, safe working etc. Safety communication consisted two questions, (1.) recognizing all hazards at construction site (2.) knowing about accidents investigation reports. Safety culture part included accidents that can be prevented and nature of operation etc. Results shows, safety

communication system, safety management system, and safety culture were considered satisfactory by laborers.

4. RESULTS AND DISCUSSION

It was clearly identified that the safety conditions are still having several gaps and loopholes at construction sites in Colombo area. Most of the safety officers described that they had difficulties with working hours, it being considerably higher than they handling of laborers, using personal protective equipment, working space, material wasting and other environment problems such as noise and dust problems and health hazards in particular dengue fever etc. Most of the employees also mentioned that they were facing some problems with hazard pay, external interferences while working and stress that was demanded of their job. Therefore, these gaps should be eliminated to give a better interface to work.

Most of the site management do internal safety audits. However, in general it does not provide satisfactory results to come to conclusions on existing health and safety conditions of the respective construction site. Operation of safety audits should be carried out by a specialized personnel endorsed by an accreditation agency.

4.1. Identification Factors

Responses by labourers on importance on Environmental & organizational, economical, technical & procedural and psychological factors are shown in Figure 1. Psychological factors received the positively highest value (97.7%). Labors said that they did not have any external interferences; no job stress and they were satisfied with their job. Worker's characteristics, worker's attitude are the important facts when considering the ergonomic structure of a construction site. Operation within construction projects completely depends on time. Therefore, workers should work beyond usual working hours. Economical factor obtained highest negative response (12.4%). Laborers stated they were not ensured with the monthly payment money and there were delays in payments which unsatisfied the laborers and seems impacting the safety environment as they tend to work in an ad hoc manner without following their instructors, where certain instructions could be safety related.

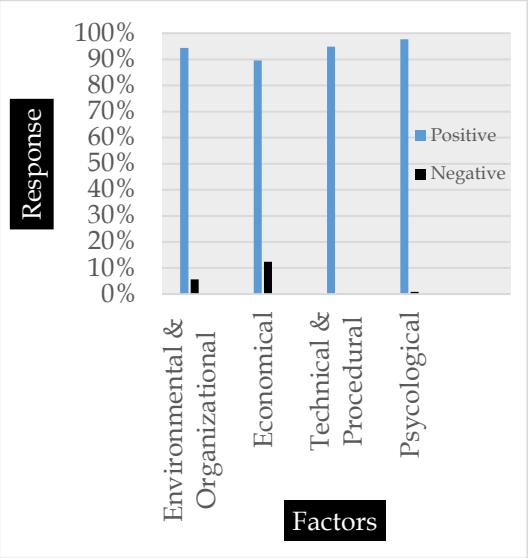

Figure 1 Identification factors

4.2. Identification of Historical Factors

Sawacha *et al* (1999) examined the influencing factors for safety on construction sites and conversed about the impact of historical factor that influence the laborer's experience and the age of his. In line with the above analysis, it is possible to draw a conclusion that the risks of workers' injuries depend on experience of the laborers and number of working years of them. When the age of the laborer increased, the years of experience also increased gradually (should be noted there can be laborers who joined the construction sector at their mid age).

Laborer experience in workplace has an impact on probability of occurring an accident to him. If the laborers' experience is less probability of occurring an accident is high. Laborers in 60-65 age group have obtained high experience level or high skill level and laborers in 18-19 age group have obtained less experience. In Figure 2 the above scenario has been explained. However, the main setback of this categorization of age group is, there were no sufficient number of samples in order to draw a conclusion. Only one laborer per some age categories, therefore percentage cannot be

used to compare with other results. Working efficiency also mainly depend on the working experience and the worker's age. Therefore, this age limit can be neglected as there are not enough results to draw a conclusion.

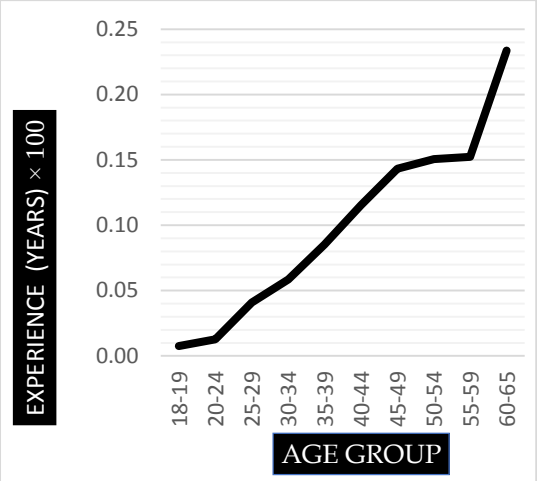

Figure 2 Identification of historical factors

4.3. Number of accidents recorded

Figure 3 shows the conditions that small construction sites were not in compliance with the expected standards. In comparison with medium construction sites and small construction sites, the safety conditions of large construction sites were greater. Overall percentage values in the safety conditions of small sites were shown to be higher than the other two sites (large site data not shown as responses were very low).

Considering this method of assessment, all injuries and hazardous situations have been calculated and classified in site sizes. The percentages were calculated after the total of these values was taken. This difference was shown very well in these complete percentages of injuries and hazardous situations.

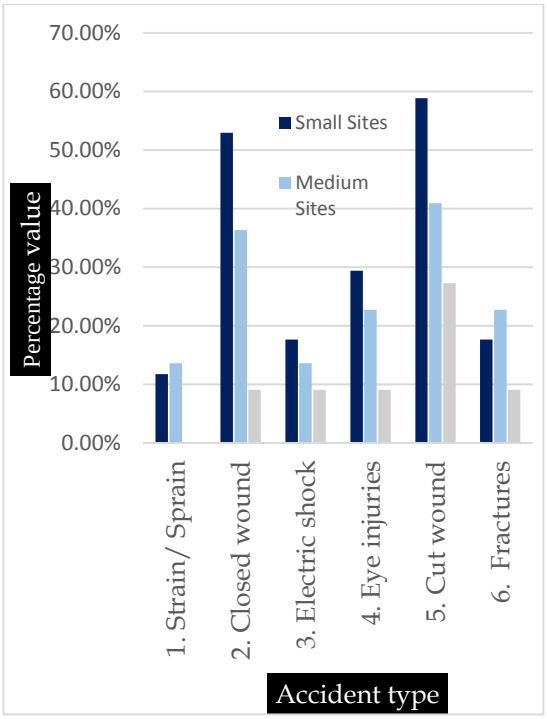

Figure 3 Number of accidents recorded

4.4. Distribution of Hazard Situations

Highest number of hazards were from welding which was 44%. Major cause of this hazard can be identified as unwillingness to use proper protective gears such as welding gloves, head shield and hand shield. Percentage values of hazards from steel grinding, unprotected opening, operating concrete mixture, fire and stack of gravels are 42 percent, 8 percent, 6 percent, 4 percent and 4 percent respectively.

Other than above mentioned aspects hazards during material handling, machine and general area guarding, safety in storage, electrical safeguarding, transportation of hazardous substances, handling of hazardous substances, chemical hazard and fire hazards, etc. should be examined in construction sites.

4.5. Site Categorized from size

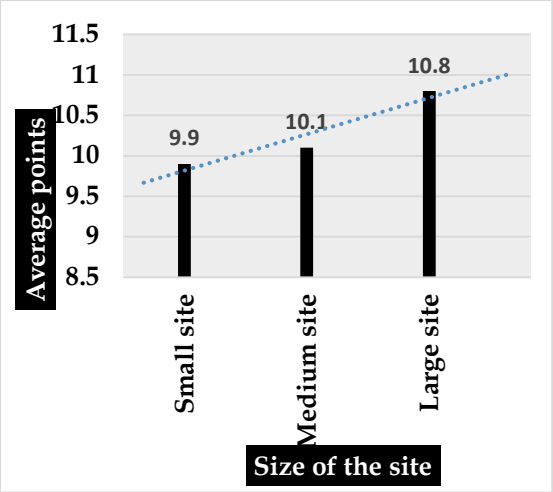

Figure 4 Site categorized from size

Site condition values were obtained by dividing the total points by the number of sites. Afterwards calculated sum of these values was averaged on weighted basis. Largest among the sites had site safety conditions better than the medium sites and small sites. In large construction sites safety plan is well prepared as there are two to three safety officers, safety managers. Furthermore, they are occupied with a good safety precaution system compared to the smaller sites. Consistency in proper operation of safety conditions, frequent safety meetings, priority towards using Personal Protective Equipment and HSE has contributed to higher safety condition standards in larger construction sites.

Considering the analysis method approached, all the injuries and hazardous situations were calculated and categorized in to sizes of the sites. After taking the sum of these values the percentages were calculated. Total percentages of injuries and hazardous situations showed significant variations in results. Below two graphs were presented this difference.

4.6. Distribution of Total Occupational Injuries

Total number of injuries are maximum in small construction sites which is 31.40% and minimum in large sites which is 10.60% as shown in figure 5. This data shows considerable difference. Figure 5 further emphasizes that sites safety of small-scale construction sites is not up to expected standards.

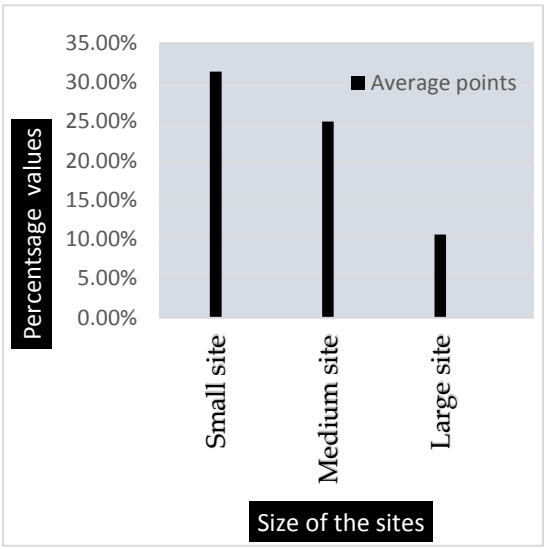

Figure 5 Distribution of total occupational injuries

4.7. Distribution of Total Hazard Situations

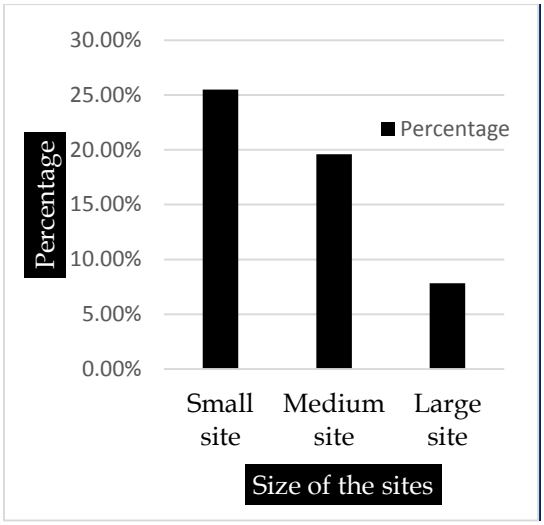

Figure 6 Distribution of total hazard situations

Total number of hazards is higher in small construction sites, 25.50% percentage and minimum in large sites this was 7.84%. Safety of construction site gradually changes when the size of construction site is changed as shown in figure 6. This graph also proves the factor that safety of small-scale construction sites is not up to expected standards.

5. CONCLUSION

It is identified that there is a vital correlation between factors affecting to safety such as safety conditions of the sites, safety management, safety communication and safety culture and attitude, distribution of occupational injuries and distribution of the occupational hazardous situations, which are in line with past studies conducted elsewhere. Five main factors have been identified which impacts site safety. Economical, psychological, technical & procedural and environment & organizational are considered to be directly linked with the level of safety. The psychological factor is identified as the most important factor. This factor assesses the attitude of the safety and behavior of workers on site. Safety attitude is comparatively high and safety attitude toward the main part of the labor's work life cycle. Economic factors also help to dominate safety performance. Significance of the technical and procedural factors shows uplift of workers' skills and informs about hazardous materials and training level of using tools. This information was helpful to obtain awareness of injuries and hazardous situations.

Experience in workplace is one of the main reasons for decrease in accidents. Results indicate that the number of accidents vary with the amount of experience of the laborer. When the experience is less, injuries gradually increase. Furthermore, Injuries and hazard situations depend on the size of a construction site. Larger the construction site, lesser the occurring of accidents and hazard situations. Thus, larger construction sites have good precaution system, and good safety plans. Generally, construction sites have negative impacts towards environment. Dusty environment, noise pollution, health issues such as dengue fever are the most widely available examples in a construction site.

6. ACKNOWLEDGMENTS

Authors would like to thank all the respondents of the survey.

7. REFERENCES

Senouci, A., Al-Abbadi, I. & Eldin, N., 2015, 'Safety Improvement on Building Construction Sites in Qatar,' *Procedia Engineering*, 123, 504-509.

Arslan, M., Cruz, C. & Ginhac, D., 2018, 'Semantic Enrichment of Spatio-temporal Trajectories for worker safety on Construction sites,' *Procedia Computer Science*, 130, 271-278.

Huang, X. & Hinze, J., 2006, 'Owner's Role in Construction Safety: Guidance Model', *Journal of Construction Engineering and Management*, 132(2), 174-181.

Heinrich, H.W., 1959, 'Industrial accidents prevention: A scientific approach', *McGraw-Hill Book Co. Inc. New York*.

Harper, R.S. & Koehn, E., 1998, 'Managing industrial construction safety in southeast Texas', *Construction Engineering and Management*, 124(6), pp.452-457.

Sawacha, E., Naoum, S. & Fong, D., 1999, 'Factors affecting safety performance on construction sites,' *International Journal of Project Management*, 17(5), 309-315.

Haadir, S. & Panuwatwanich, K., 2011, 'Critical success factors for safety program implementation among construction companies in Saudi Arabia', *Procedia engineering*, *14*, 148-155.

Haslam et al, 2005, 'Contributing factors in construction accidents' *Applied ergonomics*, 36(4), 401-415.

Proceedings of the 7th International Symposium on

Advances in Civil and Environmental Engineering Practices for Sustainable Development

ACEPS - 2019

Geocoding for post-disaster compensation projects in Sri Lanka (Special reference to selected disaster prone areas)

R.M.P.S Rathnayake[1], W.H.A. Shantha[2] and G.M.W.L. Gunawardena[3]

[1,3]Department of Town and Country Planning, Faculty of Architecture, University of Moratuwa
Katubedda, Moratuwa, SRI LANKA.
[2]Hector Kobbekaduwa Agrarian Research and Training Institute, 114, Wijerama Mawatha, Colombo 07, SRI LANKA.

K e y w o r d s

Disaster management
Compensation projects
Recovery
Geocoding

A B S T R A C T

Natural disasters such as floods, earthquakes, tsunamis, droughts, landslides and other geologic processes damage the lives and the properties of the people. To overcome these environmental imbalances, countries spend huge amount of money continuously. However due to the drawbacks of damage assessment procedures, the real victims face troubles in receiving compensations for the damages. The purpose of this study is to understand the real drawbacks of the current post-disaster compensation mechanisms and to introduce an evidence-based systematic method to overcome those drawbacks. The geocoding technology is best practiced in many countries for various human related purposes, thus for this research the same geocoding technology was applied to achieve the set objectives. The study has two objectives: understanding the drawbacks of current disaster compensation processes and indicating the use of the systematic method like geocoding for disaster compensation projects. To achieve these objectives a case study was undertaken in Halmillewa area in Sri Lanka, which was severely affected from drought during 2016 to 2018 period. Through intensive questionnaire surveys and focused group discussions, the injustice of disaster compensation mechanisms was identified. A geocoded database was created showing the use of the new technology in overcoming human faults during judgments. The practicability of the application depends on the real-time updating of the location and relevant information database.

1. INTRODUCTION

Natural disasters such as floods, earthquakes, tsunamis, droughts, landslides and other geologic processes damage the lives and the properties of the people. As a result of environmental imbalances, most of the countries spend huge amount of money to restore the prevailed condition. At present, human activities like cut down of trees, land mining, water and air pollution increase natural disasters bringing severe damages.
For last few decades Sri Lanka has been facing floods, droughts and landslides frequently. National disaster Relief services Centre of Sri Lanka mentioned that 24 Districts were affected by flooding and landslides due to torrential rainfall in May 2016. With this event 93 people have died, 33 people injured and 117 people were missing. Majority of the deaths were recorded in Kegalle District. Overall 58925 houses were affected. These figures are a fine evidence to prove the danger of natural disasters Hettiarachchi (2004) and Wickramathilake & Gunawardena (2017).

When natural disasters occur, the affected people usually receive compensations by the government authorities. Recovery is one of the most important parts of disaster management for the welfare of affected people. Through disaster management act, No 13 of 2005, Sri Lanka government constituted the importance of compensation and its operation. Disaster Management Act (2005).

The government implements multiple projects to enhance the welfare of the affected people. It is also the responsibility of government to look into the geographical

factors of the disaster prone areas. The existing methods to identify the affected locations to grant compensations and reliefs are not systematic. The existing methods collect data through manual surveys by Grama Niladhari Division (GND) officers and development officers. Erstwhile these surveys are biased, time consuming and lack of reliance. Affected people often complain the injustice and unfair distribution of compensations.

Hence it is a timely requirement to advocate a systematic method to grant compensations to the people in disaster prone areas of Sri Lanka. Geocoding is one of the best methods to gather correct information about the affected locations in order to make compensations transparent. This method is known to be efficient, reliable and easy to access.

There is an agility of occurring natural disasters in Sri Lanka. Responsible authorities implement disaster compensation projects to recover the livelihoods of victims. However, people have doubts about the mechanisms of distributing compensations. According to the media reports, Daily News (2016), it is evident that affected people are not totally satisfied with what they have received as compensations. People usually complain about the biasness of authorities and the political influences on selecting victims for compensations. As a result, the real victims are neglected.

Ministry of Irrigation, Water Resources and Disaster Management is the main institution for disaster compensation and relief services in Sri Lanka. Natural disaster insurance scheme was implemented through NITF (National Insurance Trust Fund) since 01st of April 2016. It covers lives and properties, specifically all households and small business establishments (any business of which annual turnover does not exceed LKR 10 M) covered up to 2.5 million rupees each in respect of damages (per event) caused to their property and contents, due to cyclones, storm, tempest, flood, landslide, hurricane, earthquake, tsunami and any other similar natural perils, excluding Drought. National Insurance Trust Fund (2016).

When disasters occurred in rural or urban areas, the government executes money for the local authorities. Local authorities distribute received compliers among GND officers. GND officers haven't any systematic method to continue the compensation process and at present, people are struggling and complaining about the irregularities of the compensation processes.

- Example: Pandemonium strikes Aranayaka

"Officials are still unable to give an exact number of houses in Abalankanda". Daily News (2016).

Therefore, there is a high necessity of systematic method for post-disaster compensation projects.

Most of the countries implement more systematic methods using geospatial technologies for damage assessment and disaster compensation projects since disasters are geospatial incidents. Geocoding address is one of such methods.

Geocoding is a technology-based method for increasing the accuracy of location intelligence. It assigns latitude and longitude coordinates to addresses. Geocoding is commonly used for transportation, emergency management, census, housing and urban development activities. Brusentsev, 2017.

Geocoding addresses can be used as a systematic method to provide an evidence for post-disaster compensation projects. Addresses are the only evidence to show the location. When showing the addresses spatially, disaster management agencies and local authorities will be able to identify the real victims and compensate them without any bias or political influence.

Patel Nick (2017) has indicated the geocoding is a fundamental GIS process for plotting data on the map. If a better output is required, the application must be accurately geocoded. The author has clearly mentioned about the importance of accuracy. Accurate and precise geocoding greatly affects the decisions that make with the analysis.

National Geospatial Advisory Committee of US, clearly mentioned the government and businesses of US mostly depend on addresses to provide essential services. They use street addresses every day for emergency response, public and private utility management, taxation, land use planning and many other purposes. The efficiency and effectiveness of the government agencies which currently use address data is higher than traditional institutes. National Geospatial Advisory Committee of US (2017).

Recovery is one of the most important tasks in disaster management cycle. Sri Lanka has institutional framework for disaster recoveries since 1996. National Disaster Relief

Services Center, 2019. However, there are so many issues and challenges in recovery and compensation system in Sri Lanka. At present, more countries are implementing innovative and systematic methods to succeed the recovery system. However, in Sri Lanka there is no well-established systematic method for post-disaster compensation process. Therefore, Sri Lanka needs a deep consideration about the post- disaster compensation mechanisms through new technologies.

2. OBJECTIVES

With the above background two objectives were set for the research;

(i) To understand the drawbacks of current disaster compensation process.

(ii) To indicate the use of a systematic method like geocoding for disaster compensation projects.

1. METHODOLOGY

To achieve the above objectives, Halmillewa Grama Niladhari Division in Wariyapola Pradeshiya Sabha at Kurunegala District in Sri Lanka was selected as the case study area. The area was severely affected from drought from 2016 to 2018. Figure 1 displays the location of the study area. The people of the area are farmers with paddy, chena and coconut cultivations. The drought has affected severely their livelihood and the given compensations were not sufficient to recover the damage caused by the drought.
People perception is very important on the study of drawbacks of post disaster compensation process. Therefore, a detailed questionnaire survey was carried out to identify the people perception on drawbacks of current compensation mechanism and formal interviews were carried out with the respective authorities of the selected case study area to know their perception on compensation mechanism.
Following points were used as interview guides.

- Criteria of the disaster compensation process
- Quantities of compensation received by people
- Co- operation of people for the process
- Challenges of disaster compensation process
- Recommendations

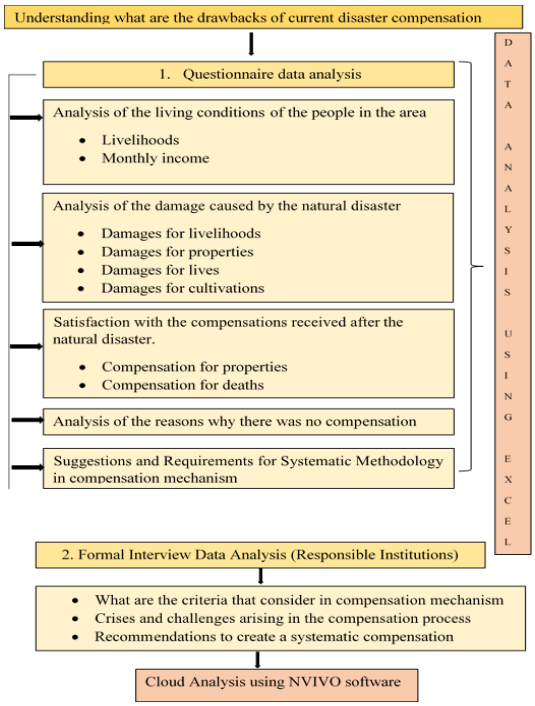

Figure 1 Flowchart in Achieving Objective 1

The data analysis was mainly based on the collected qualitative data. Figure 2 & 3 display the flowcharts of methodology achieving objective 1 and 2.

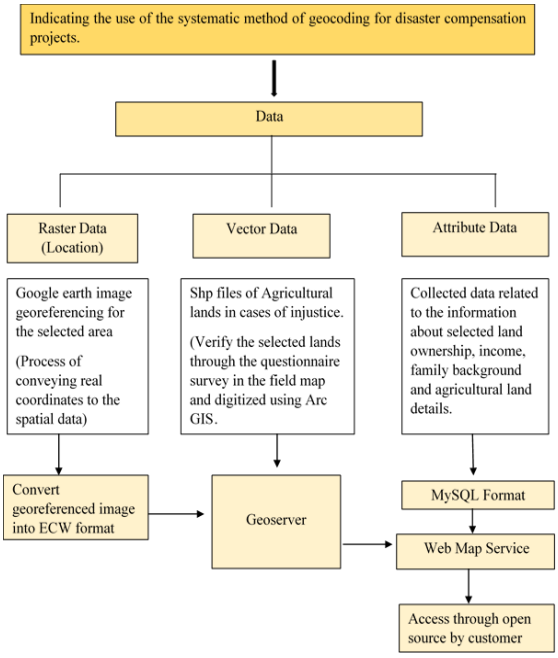

Figure 2 Flowchart in Achieving Objective 2

2. RESULTS AND DISCUSSION

Halmillewa GND is vested in Wariyapola Pradeshiya Sabha area in the Kurunegala District. Total family units of the area are 298 and 175 family units were affected from the continuous drought since 2016. (Sampath pathikada, 2018- Halmillewa GND).

Agriculture is the main livelihood of the area and others are engaging with different employments using specific raw materials and technology available in the area. Figure 3 displays the livelihood of the people in the area.

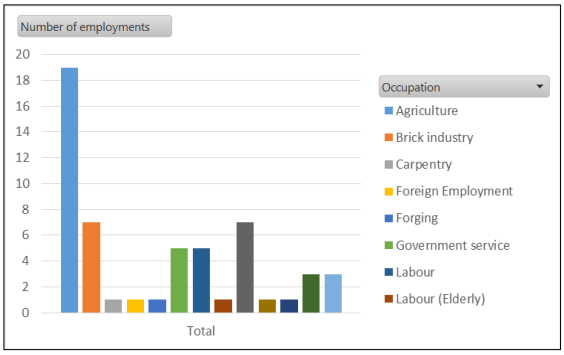

Figure 3 Livelihood of the Halmillewa GND

Figure 4 displays the damages caused by the drought for different livelihood.

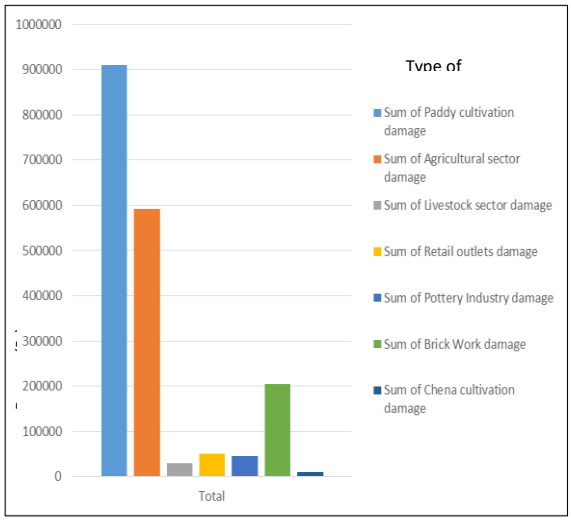

Figure 4 Damages due to Severe Drought in Wariapola Pradeshiya Sabha (2016) in Rupees

During the compensation process, Wariyapola Pradeshiya sabha has decided the people who should receive compensation under the different criteria given by District secretariat office.

According to their criteria, Compensation mechanism is implementing only for the agricultural families who could not cultivate paddy continuously since 2016 (including both Yala, Maha seasons) except those others who work as government workers, private employees, traders, self- employees and people who earn Rs. 20000< monthly income. (Disaster relief services unit, Wariyapola divisional secretariat office).

People have received only dry food worth of Rs. 5000/= for a family consisted with 3 members or more than 3 members, and Rs. 4000/= for a family consisted with less than 3 members. The real damage was immeasurable and the government's estimation on damage is undoubtedly not in a satisfied condition. Therefore, the people in the area were somberly disappointed. Figure 5 displays the satisfaction of the people about the compensation mechanism.

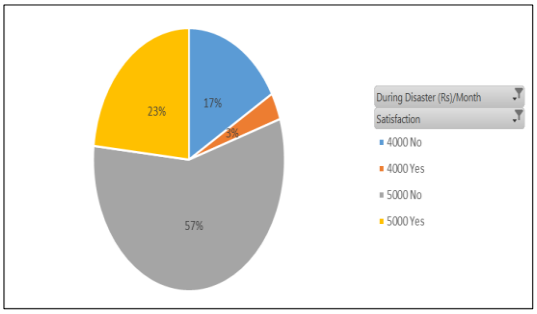

Figure 5 The Satisfaction towards the Compensation Mechanism

According to the assessment, 74% of the people are not satisfied with the compensation mechanism. According to the people's perception, disaster compensation mechanism includes several irregularities such as not assessing the damage, not considering the proper criteria (personal bias of officials) and it is not a good answer for the drought. Further the farmers who harvested half of their cultivations, families with government workers or retired government workers and foreign employees were omitted giving compensations. The drought will not affect only the agriculture and the farmers; it affects all the people in the area. Therefore, the local authorities should have proper damage assessment criteria which will be fairly assess the whole affected area. Figure 6

explains the reasons for not receiving compensations and the percentages of people under each category.

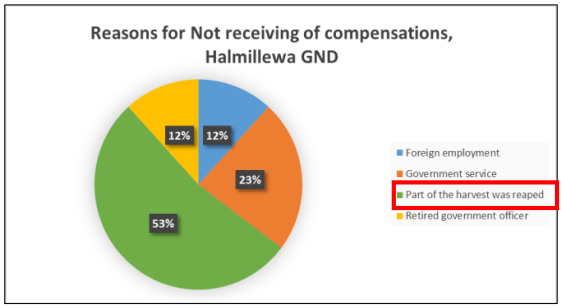

Figure 6 The reasons for not Receiving Compensations and the Percentages of People under Each Category

Drought is a different kind of disaster which affects everyone in the area in different intensities. Although Halmillewa GND is an agricultural area, other government, private and self-employees are also affected due to drought condition. Because of that, they are willing to have following solutions given in figure 7 to enhance their livelihoods than getting just mere dry food compensation.

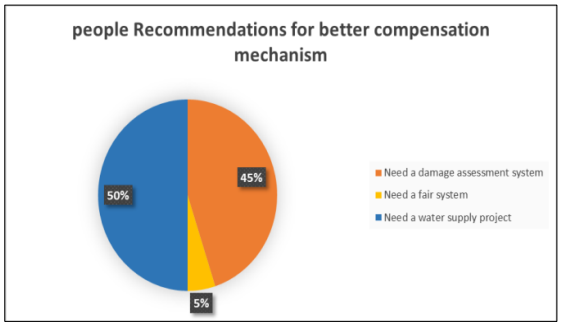

Figure 7 The Recommendations of the People in the Drought affected area

According to the questionnaire survey around 50% of people are asking for a persistent water supply project to the area to overcome the water scarcity problem during drought. Around 45% of people are asking for a proper damage assessment mechanism. Thus all most all the interviewed people are not satisfied with the prevailing condition of post disaster compensation mechanisms.

The same analysis was undertaken for Landslide and flood affected people in Sri Lanka and the results were same with poor satisfaction of affected people on the current disaster compensation mechanisms of Sri Lanka. The present disaster compensation mechanism is not considering the damage and real requirement of the people. Therefore, there is a necessity of a new reform of concessionary disaster compensation mechanism.

3. APPLICATION

The application part is spearheading with the research objective of 'Indicating the use of the systematic method of geocoding for post-disaster compensation projects'. (Objective 2)

Through the questionnaire survey, few important points were highlighted by the affected people and the officers of the responsible authorities. Proper damage assessment, fair and transparent mechanism in compensation and sustainable solutions for such natural disasters were the concerns of the affected people of the area. Enhancing effectiveness and transparency through an effective compensation mechanism was the main concern of the officers. Further they concerned about the annual economic loss due to lack of proper solutions to minimize the damages caused by frequent natural disasters.

The effort of geocoding can be used for damage assessment with a good transparency. Further, authorities can use this geocoding technology to verify the compensation mechanism regularly. Thus geocoding will be a solution for the transparent damage assessment and distribution of compensations.

5.1 Advantages of the application

- It is possible to identify the houses which need compensation with real damages to their cultivations and other affected livelihoods under the below average precipitation.
- Geocoding use real time map images and the database includes the information about the cultivated land extent annually including type of crops and other relevant family background information.
- It is possible to identify the houses which received compensations in an unfair manner.

- Local authorities can distribute compensation with GND officer effectively with high transparency.

5.2 Usage of the application

Any user will be able to access the database and find out any relavant information using a map view of the area. Since the database is freely available as an open sources database application the cost will be zero. Responsible officers will be able to update the geodatabase regularly by connecting the real time image download applications and automated databases applications.

5.3 Procedure of geocoding

- **Step 1: Preparing Raster data**

The satellite images are the base of the geodatabase. It is very accurate to identify the natural disasters through satellite images. High resolution images are preferable for this task. Real time satellite image acquisition is possible with latest technology development. The images will be georefer to get the real location information. Figure 8 and 9 display two image sections showing the effect of drought to Halmillewa area.

Figure 8 An Agricultural Field & its owner's home before Drought

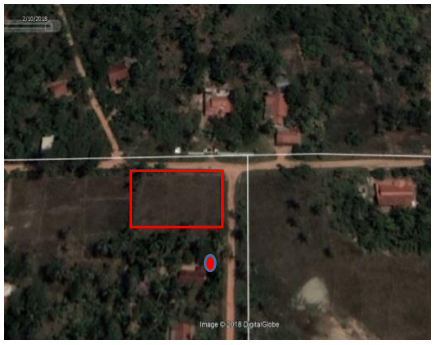

Figure 9 Same agricultural Field during Drought showing the Dryness

- **Step 2: Preparing vector data**

Satellite images will be used as the base maps. The whole area will be digitized and vector layers will be created using base maps. Figure 10 displays an example vector layer.

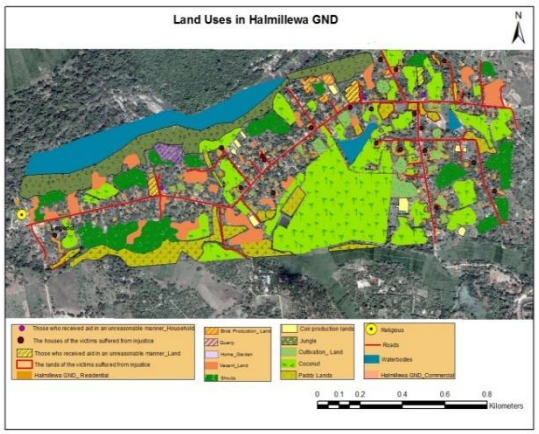

Figure 10 Landuse Layer of Halmillewa GND

- **Step 3: Preparing attribute data**

The database will be filled with all information related to the area which will be useful in compensation process including income, land extent, crops cultivated, family background, etc. the information will be geocoded with the address of each household or any other identifiable key.

- **Step 4:**

The prepared raster images will be converted to ECW file format for higher quality and quick viewing of the data.

- **Step 5:**

The final raster and the vector files will be uploaded to the Geoserver to facilitate sharing, processing and editing geospatial data though open source server.

- **Step 6:**

The geocoded database file will be converted into MySQL (open source relational database management system) for flexible processing, accessing and managing the database.

- **Step 7:**

Finally, the prepared geocoded database will be available in web map service with easy access to any user.

The proposed Geocoding application for drought prone areas is really helpful to minimize the drawbacks of compensation

mechanisms. It helps to assess the damage with least errors. The real time update is crucial in proper analysis of the natural disasters and their aftermath.

4. CONCLUSIONS AND RECOMMENDATIONS

The research study is predominantly carried out on understanding the drawbacks of current post- disaster compensation mechanisms in Sri Lanka and indicating the use of a systematic method like geocoding for disaster compensation projects. Irregularities in post disaster compensation mechanisms are common in Sri Lanka. According to the questionnaire survey and the focused group discussions, few important points were highlighted by the affected people and the officers of the responsible authorities. Proper damage assessment, fair and transparent mechanism in compensation and sustainable solutions for such natural disasters were the concerns of the affected people of the area. Enhancing effectiveness and transparency through an effective compensation mechanism was the main concern of the officers. Further they concerned about the annual economic loss due to lack of proper solutions to minimize the damages caused by frequent natural disasters.

Sri Lanka has many methods, criteria, laws and regulations to regulate the post disaster compensations. However practically, those criteria and methods are not undertaking in proper manner. Therefore, the disaster compensation mechanism should be spearheaded under strong supervision.

Geocoding is one of the best answers for the damage assessment in compensation mechanisms. Since the assessment can be undertaken through real time images, this method is effective and transparent. Further it is a trustworthy mechanism between people and responsible officers since it is evidence-based systematic method.

The prepared geocoded database will be available as an open source database. Thus anyone who is interested will be able to access it freely and use it freely. There will be responsible officers to update the database on time.

The world often invites the latest technologies and innovative ideas. However, the responsible officials in rural areas of Sri Lanka, are having lack of knowledge in modern technology and lack of infrastructure to launch these new technologies. Therefore, the responsible officials should be given a thorough training with infrastructure to regulate these matters.

5. REFERENCES

Brusentsev, V., 2017, 'Disasters in the United State; Frequency', *costs,* compensations.

Daily News Sri Lanka., 2016, 23 May 2016, from http://epaper.dailynews.lk.

Hettiarachchi, N.D., 2004, 'National Disaster Management Policy – Implications for Regional Development', *Proceedings of the Workshop on Regional Development Experience in SL*, 13-14 August at Hotel Galadari, Sri Lanka.

National Geospatial Advisory Committee, 2017,from https://www.fgdc.gov/ngac.

National Insurance Trust Fund, 'Ministry of Finance and Economic Affairs', *Sri Lanka*, from http://www.nitf.lk/ENGLISH/Home.html.

Nick, P., 2017, 'Geocoding delivering high locaion accuracy', *Overview of federal disaster assistence* .

The Disaster Management Act No.13 of 2005 Sri Lanka, from http://www.disastermin.gov.lk/web/images/pdf/DMACTNO13_E.pdf.

Wickramathilake, A.M. & Gunawardena, G.M.W.L., 2017, 'Measuring Landslide Vulnerability, Based on Rainfall Data, Acquired Through Satellite Images', *Proceedings of the International Conference on* Computer Simulation and Modelling, 2017. Colombo, Sri Lanka.

River Engineering and Hydroinformatics

Proceedings of the 7th International Symposium on

Advances in Civil and Environmental Engineering Practices for Sustainable Development

ACEPS - 2019

Assessment of open technologies based measurements as a potential dataset for hydrological modelling in Deduru Oya river basin of Sri Lanka

E.J. Warusavitharana[1], B.H. Sudantha[2], R. Ratnayake[1], P.K.S. Mahanama[1], R.J. Warusavitharana[1], M. Cannata[3] and D. Strigaro[3]

[1]Department of Town and Country Planning, Faculty of Architecture, University of Moratuwa, 10400 Moratuwa, SRI LANKA
[2]Department of Information Technology, Faculty of Information Technology, University of Moratuwa, 10400 Moratuwa, SRI LANKA
[3]IST-DACD, University of Applied Sciences and Arts of Southern Switzerland (SUPSI), 6952 Canobbio, SWITZERLAND

K e y w o r d s

4ONSE
Hydrological modelling
Simulation
Deduru Oya Basin
SWAT

A B S T R A C T

Despite the technological advancements in data collection and processing methods, still for some nations, it is crucial to produce real time valid hydrological estimations owing to the constraints pertaining to hydro-meteorological data. 4ONSE is a joint research project initiated in this background to strengthen developing nations to produce their own hydro-meteorological network using low cost and non-conventional open technologies. Hence, the main objective of this research is to test the potential of such measurements in regional scale hydrological modelling in Sri Lanka. The model was applied to Deduru Oya River Basin to estimate the continuous inflow to the Deduru Oya reservoir, which is the major determinant in controlling floods in the lower basin. Since the parameters like rainfall can vary greatly with small distances, the deployed network at sub-basin level significantly helps to estimate the hourly runoffs with better accuracy, than the daily runoffs. This was well proven for Deduru Oya sub-catchment; the model was able to estimate hourly runoffs for Deduru Oya stream at a NSE value of 0.75, while the NSE value for daily simulation was 0.62. However, the continuity of data is strongly influenced for fitness of the model when performing hourly simulations.

1. INTRODUCTION

Hydro-meteorological network is the key requirement for most hydrological forecasting. However, most developing countries lack weather observing networks that routinely provide real time data of necessary quality, and spatial and temporal density. The common found challenges has been identified as limited (often very limited) budgets, and the lack of technical infrastructure and associated expertise, rapid deterioration, lack of skilled maintenance, high-priced non-locally available spare parts (Snow, 2013).

The 4ONSE project, which is a joint research project between University of Moratuwa (UOM), Sri Lanka and University of Applied Sciences and Arts of Southern Switzerland (SUPSI) was initiated in this context to demonstrate the deployment of open technologies based, high density weather station network in a regional scale for a low cost. 4ONSE is the acronym for 4 times Open and Non-conventional technologies for Sensing the Environment. The established network is 4 times open in terms of hardware, software, data and standards.

Deduru Oya basin was the selected river basin to deploy the stations. The upper part of Deduru Oya basin is divided into four sub-catchments based on the four distinct stream networks that originate from the central high lands. They are Maguru Oya, Deduru Oya, Kimbulwana Oya and Hakwatuna Oya. The water level of the Deduru Oya reservoir,

which locates at the center of the basin, governs by the runoff generated in these four catchments (Figure 1).

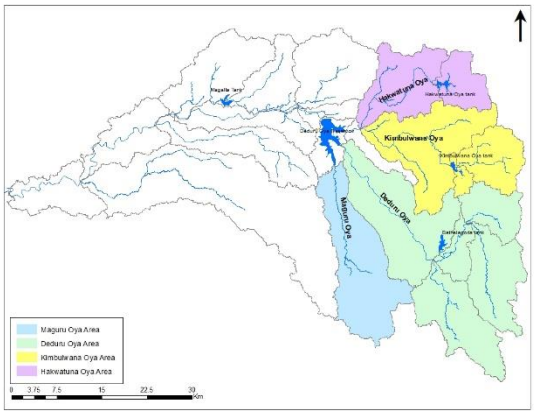

Figure 1 Sub-catchment of Deduru Oya basin

During the rainy periods, reservoir managers face difficulties in taking timely decision on deciding the magnitude of the inflows to the reservoir, for the safe disposal of excess flow. Currently they release water from the reservoir once it comes to a particular level. This creates floods in the downstream areas due to the rapid and massive water flow. Therefore, the flood risk in the downstream areas can be reduced to a considerable level, if the reservoir mangers aware about the runoffs generated in the four catchments during the different rainfall events. Then they can take prior judgment about the water quantity that should be released time to time. Thus, the main objective of this research is to find out whether the 4ONSE system could be used as a viable solution for hydrological modelling at regional scale.

2. LITERATURE REVIEW

Regional scale catchments are characterized typically by natural variability in climatic and land-surface features (Wooldridge, S.A. and Kalma, J.D., 2001). The existing hydro-meteorological network in Sri Lanka is strongly insufficient for adequately accounting for this climatic heterogeneity. Studies done on hydrological models have found the very strong influence of weather station density and their measurements on hydrological model outputs (Andréassian, et. al, 2001; Faurès, et. al, 1995; Duncan, et.al, 1993; Chaplot, et.al, 2005). Especially the rainfall, which is the major input for any hydrological model, can vary greatly with small distances. Hence, inadequate representation of rainfall distribution over a watershed may result in producing unreliable model outputs (Warusavitharana, et.al, 2018)

Most of the weather stations in Sri Lanka are manually operated and data is transmitted vocally over the phone. The Automated Weather Stations (AWSs) have been installed using funds from the international organization and they are restricted to certain locations of the country. Most of the time, the hardware of software of these stations cannot be adjusted to integrate new parameters (Senevirathna, S. and Jayawickrama, V., 2014) and the replacement cost of the sensors is very high. The above drawbacks hinder countries with low economies to increase their network density.

However, thanks to IoT (Internet of Things) enabled technologies, the future of weather station industry has now been made a significant turning point from its high cost sophisticated devices into low cost IoT enabled solutions. Thus, the ultimate destination of deployment of such a system is to create a Global Environmental Sensor web to monitor the environmental changes and to establish a decision support system to safe guard the human race and the entire planet through hazard warning. IBM's "A Smarter Planet" (IBM, 2010) Hewlett Packard's (HP) "Central Nervous System for the Earth (CeNSE)" (HP, 2013), and Geospatial Cyberinfrastructure for Environmental Sensing project (www.geocens.ca) are some of the initiatives which were already begun in this aspect.

Hydrological modelling with lumped conceptual models has now been considered as outdated due to ignorance of heterogeneity of climatic and land surface features. Instead, distributed physically based models which considers the hydrologic process of water movement are modelled either by the finite difference approximation of the partial differential equation representing the mass, momentum and energy balance or by empirical equations (Abbott, et.al., 1986). Physically based distributed models can be further divided into fully distributed models and semi-distributed models. Distributed models model the hydrological processes at pixel level, while the semi-distributed models model them at sub-basin level. Hence, compared to distributed models, semi-

distributed models are less data demanding, require less calibration time and more appropriate for regional scale. Accordingly, in this research, SWAT (Soil and Water Assessment) semi-distributed, open source hydrological modelling tool was used to test the reliability of 4ONSE data in hydrological modelling. Further, SWAT allows to aggregate the parameters at HRU (Hydrological Response Unit) level, which is an even minor unit than sub-basin level.

3. METHODOLOGY

3.1. System development and deployment

The main objective of developing 4ONSE system is to introduce a fully open, low cost and non-conventional system for sensing the environment. The four open technologies utilized in system development are:

(i) Open hardware - Arduino
(ii) Open software – istSOS
(iii) Open standards - OGCSOS
(iv) Open data - CKAN

Accordingly, two types of stations – 4ONSE weather station and 4ONSE river gauge has been developed. The weather station was developed as an Arduino Mega2560 based embedded system and the river gauge was separately developed using Arduino UNO and necessary electronic modules. DS18B20, BME280, Davis Aerocone rain collector-6465, Sl1145 UV IR Visible sensor, YL-69, MB7062 XL-MaxSonar-WR1 are the sensors used to measure the air temperature, relative humidity and atmospheric pressure, rainfall, solar radiation, soil moisture and water level respectively. In addition, the system is also equipped with a wind speed and wind direction sensor. These sensors were selected primarily based on the cost, measuring range, accuracy and resolution. The system was programmed to record the data at 10 minutes interval. The power supply of the system is composed of 30W solar panel, 12V 25Ah rechargeable battery, 100W solar panel voltage controller and power regulators to keep voltage in the recommended range of electronic items. The entire system with the river gauge was built at a cost of 1325 USD.

The weather observations are managed and dispatched by istSOS, which is a free and open source sensor observation service. The system uses OGC-SOS open source standards to manage the weather stations' data in an interoperable way. This allows uniquely addressing each weather station based on standard communication protocols. The data will be published and make available for all the users using CKAN.

Accordingly, 27 weather stations and 6 river gauges have been developed and deployed them in the Deduru Oya basin (Figure 1). The selection of locations for the weather stations was performed through a geostatistical analysis of satellite-based rainfall data and several other factors were also considered in site selection (Warusavitharana, et.al, 2018). Out of the six river gauges, five of them were installed in the upper basin area and the remaining one was installed at the lower basin close to the Deduru Oya reservoir.

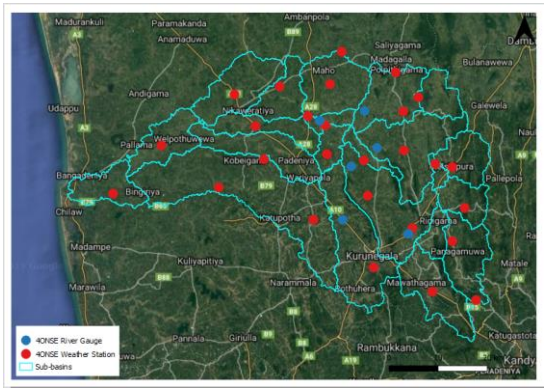

Figure 2 Location of the 4ONSE weather stations and river gauges

3.2. Hydrological model development

Soil Water Assessment Tool (SWAT), which was developed by Dr. Jeff Arnold for the United States Department of Agriculture, was used for hydrological modelling. Its Graphical User Interface (GUI) is embedded in the popular and widely used GIS environments – ArcGIS (ArcSWAT), QGIS (QSWAT) and MapWindow (MWSWAT). In this research, the model was developed using QSWAT plugin embedded in QGIS software (Dile et al. 2016).

The modelling was initiated with delineating the watershed boundary and the sub-basin boundaries. SRTM's (Shuttle Radar Topography Mission) DEM (Digital Elevation

Model) dataset and a digitized stream network was used for boundary delineation. SWAT uses 'Burn-in' function to superimpose the stream network on DEM to define its location. During this process, the elevations of the grids overlapped by the digital channel network are reduced by a little value to increase the slopes with other surrounding grids (Willian and David, 1996). After the 'Burn-in' process, the QSWAT preprocesses the DEM by filling pits, calculating the flow direction, counting the contributing area and finally delineating the watershed. QSWAT uses TauDEM (Terrain Analysis Using Digital Elevation Models) for watershed delineation.

The next step of stream network delineation process takes the output of contributing area as input and delineates the stream network for a user-defined threshold. This defines a stream raster grid as all grid cells with contributing area are greater than a designated threshold. Lesser the threshold value, greater the possibility of visualizing every tiny tributary. Hence, for less threshold values, SWAT develops larger number of sub-basins. This makes the model more complex and consumes more time to run the model. Therefore, for this research, the default value of 1% was selected as the threshold.

The Deduru Oya reservoir is located center of the basin. Considering the convenience of running the model, the reservoir was taken into a single sub-basin. For that, outlets were located at the places where the streams of the upper basin meet the reservoir and the reservoir point was placed at the outlet of the reservoir. The outlet of the river mouth was located at the place, where the stream enters the ocean. SWAT's watershed delineation process generated 28 sub-basins. For the convenience of running the model, sub-basins were further reduced by merging the small sub-basins which have land area less than 25% of the mean area. Accordingly, 22 sub-basins were considered for running the model (Figure 2).

Sub-basins in SWAT further divided into homogeneous areas called Hydrological Response Units (HRUs). HRU is the total area in the sub-basin with a particular land use, soil and slope. Individual fields with a specific land use, soil and slope are lumped together to form one HRU. HRUs simplify the SWAT run by lumping all similar soil, land use and slope areas into a single response unit. Survey Department's 1:50,000 scale land use layer and FAO-UNESCO's 1:5,000,000 soil layer was used for the model. SWAT's default database includes, parameter values for different land use classes and soil types. Therefore, prior to the use of land use and soil layers in the model, they were re-classified to the SWAT land use classes. Slope is automatically created during the watershed delineation process. For the HRU creation, the slope of the study area was classified into four classes in the range of 0-11%, 11-33%, 33-86% and above 86%, considering the natural breaks of slope values.

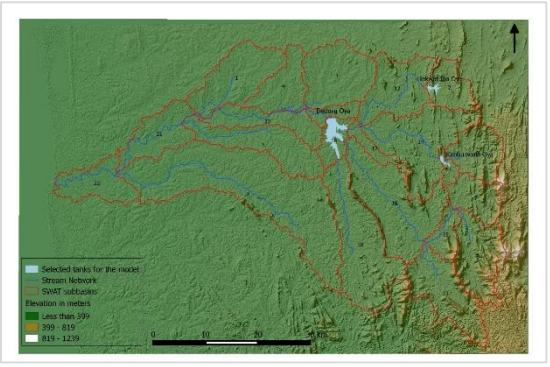

Figure 3 Delineated sub-basins of Deduru Oya Basin

Since SWAT is a continuous model, it is required to consider at least 2 years period as the warm-up period to generate the representative climate for the basin. However, the fully deployment process of the 4ONSE systems was accomplished few months back. Therefore, available 4ONSE data is insufficient for the 2 years warm up period. SWAT overcomes this limitation by generating the missing data using SWAT weather generator. To activate the weather generator, the model requires some statistical data related to precipitation, maximum and minimum air temperature, solar radiation, wind speed and relative humidity, at least about 20 years. Due to the unavailability of adequate historical data at the Meteorological Department, the required data to calculate the statistics have been obtained from the CFSR (Climate Forecast System Reanalysis) database. Table 1 shows all the input data of the model.

Table 1 Input data of the model

	Input data	Source & Link
1	Digital Elevation Model (DEM)	Shuttle Radar Topography Mission (SRTM) Link: https://earthexplorer.usgs.gov/
2	Stream network	Digitized by the author
3	Land use	Survey Department of Sri Lanka
4	Soil	FAO-UNESCO Link: http://www.fao.org/geonetwork/srv/en/metadata.show?id=14116
5	Historical weather data	Climate Forecast System Reanalysis (CFSR) Link: https://globalweather.tamu.edu/
6	Weather data	4ONSE weather stations Link: https://geoservice.ist.supsi.ch/4onse/admin/
7	Stream water level	4ONSE river gauges Link: https://geoservice.ist.supsi.ch/4onse/admin/

In addition to the main model, four separate sub-models have been developed for 4 sub-catchments (Maguru, Deduru, Kimbulwana & Hakwatuna) to calibrate the model with reference to each catchment. As depicted in Figure 2, total inflow to the Deduru Oya reservoir can be calculated as:

$$R_{in} = M_{out} + D_{out} + K_{out} + H_{out} \quad (1)$$

Where, R_{in} represents total inflow to the Deduru Oya reservoir and M_{out}, D_{out}, K_{out} and H_{out} represent total outflow from the Maguru Oya, Deduru Oya, Kimbulwana Oya and Hakwatuna Oya respectively.

Daily outflow / runoff of each sub-catchment is calculated in SWAT as per the below formula:

$$SW_t = SW_0 + \sum_{i-1}^{t}(R_{day} - Q_{surf} - E_a w_{seep} - Q_{gw}) \quad (2)$$

where SW_t is the final soil water content, SW_0 is the initial soil water content on day i, t is the time, R_{day} is the amount of precipitation on day i, Q_{surf} is the amount of surface runoff on day i, E_a is the amount of evapotranspiration on day i, w_{seep} is the amount of water entering the vadose zone from the soil profile on day i, and Q_{gw} is the amount of return flow on day i.

The hydrological processes were tested at both daily and hourly intervals. Table 2 shows the options selected in SWAT model to simulate the hydrological processes at two intervals.

Table 2 Selected option in SWAT model to simulate the hydrological processes

Process	Daily	Hourly
Potential Evapotranspiration	Penman – Monteith	Penman – Monteith
Rainfall/ runoff routing	SCS curve number (CN)	Green & Ampt Mein Larson (GAML)
Daily Curve Number calculation	Soil moisture method	Soil moisture method
Channel flow	Muskingham Cunge	Muskingham Cunge

Except for rainfall / runoff routing, for both daily and hourly processes same methods have been applied. A study conducted by King et al. (1999) suggests that the CN method under-simulates surface runoff while the GAML method has no pattern associated with storm events implying less bias to the model prediction with the GAML method.

The model was run taking the precipitation, maximum temperature, minimum temperature, relative humidity and wind speed data from the 4ONSE weather stations. Prior to use these data in the model the reliability of the data was checked with some reference stations installed in Sri Lanka and Switzerland (Strigaro et al., 2019). For the model calibration, water level data was obtained from the 4ONSE river gauges. The water level data was converted into a flow using Irrigation Department's stage-discharge rating curves.

3.3. Model calibration

The term 'calibration' refers to a procedure where the difference between model simulation and observation are minimized (Abbaspour, et.al, 2017). The

objective function can be optimized as per the equations given below:

$$Min: g(\theta) = \sum_{j=1}^{v}[w_j \sum_{i=1}^{n_j}(x_0 - x_s)_i^2] \quad (3)$$

$$Min: g(\theta) = \sum_{j=1}^{v}[w_j (1 - \frac{\sum_{i=1}^{n_j}(x_0 - x_s)_i^2}{\sum_{i=1}^{n_j}(x_0 - \bar{x}_0)_i^2})] \quad (4)$$

Where g is the objective function, θ is a vector of model parameters, x_0 is the observed variable, x_s is the corresponding simulated variable, v is the number of measured variables to be used to calibrate the model, w_j is the weight of the jth variable.

SWAT-CUP standalone program was used for calibration of model. Prior to calibrate the model in SWAT-CUP, the model was run using some user-defined parameter values. Then the output was uploaded to SWAT-CUP for optimization of parameter values. There are several algorithms available in SWAT-CUP for model calibration. In this research, an Inverse Modeling approach of SUFI-2 algorithm was used. Due to its reverse modelling capability, SUFI-2 can produce outputs closer to measured observations, using different parameter sets. In addition, there are several objective functions available in SWAT-CUP to determine the fitness of the model statistically. In this study, Nash-Sutcliffe Efficiency (NSE) method was used as the objective function. In SUFI-2 algorithm, the fitness between the simulated result and the observed values are expressed as 95PPU – 95% prediction uncertainty. Each simulation produces two statistics: P-factor and R-factor. P-factor is the percentage of observed data simulated in the model. Hence, (1 – P factor) is the percentage of observed data not simulated well in the model, in other words the "model error". R-factor is the thickness of the 95PPU envelop.

Out of the many parameters used in SWAT, the most sensitive parameters were selected performing the One-at-a-time (OAT) local sensitivity analysis. OAT shows sensitivity of a variable to the changes in a parameter if all other parameters are kept constant at some value. Then, using those sensitive parameters 500 simulations were done at each iteration, until a satisfactory result is produced.

4. RESULTS AND DISCUSSION

The model was first tested for daily basis. A shift in the flow was adjusted by increasing the CH_N2 (Manning's "n" value for main channel) parameter value. It was evident that the CANMX (Maximum canopy storage) requires to fix separately based on the maximum land use categories. Compared to other sub-catchments, the CANMX values have shown significant variation in Deduru Oya sub-catchment with respect to the predominant land use categories of Coconut, Rice, Rubber and Low-density residential. Then the ground water parameters which were received as sensitive, GW_REVAP (Groundwater "revap" coefficient) and GWQMN (threshold depth of water in the shallow aquifer required for return flow to occur) were calibrated separately. Different sensitive parameters were received when performing the OAT analysis at daily, hourly and sub-catchment level. As an example, Table 3 shows sensitive parameters received for Deduru Oya sub-catchment at daily and hourly intervals. The definitions of the parameters were elaborated in SWAT Input and Output documentation.

Table 3 Sensitive parameters of Deduru Oya sub-catchment at daily and hourly intervals

Daily	Hourly
CH_N2, ESCO, SOL_AWC, GW_DELAY, CN2, GW_REVAP, GWQMN	SOL_BD, MSK_X, MSK_CO1, MSK_CO2, ALPHA_BF, SOL_K, CN2, SURLAG, GW_REVAP, CH_K2, CH_N1, CH_N2, GWQMN

In every calibration, an acceptable result was produced during the 4th iteration. The figures 3 – 5 shows the observed flow and the simulated flow for two sub-catchments at daily and hourly intervals. Figure 6 shows the validated result for Deduru Oya catchment.

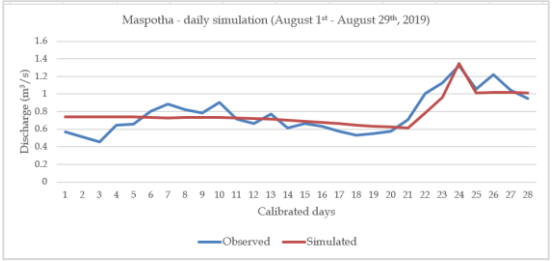

Figure 4 Maguru Oya daily simulation (August 1st – August 29th, 2019)

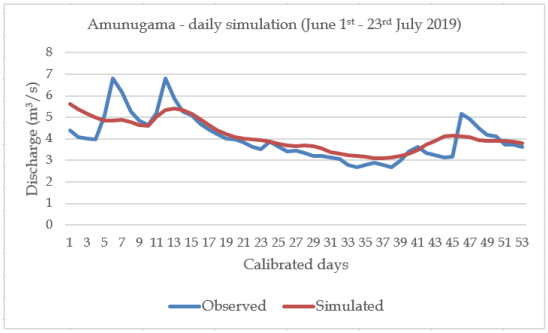

Figure 5 Deduru Oya daily simulation (June 1st – 23rd July, 2019)

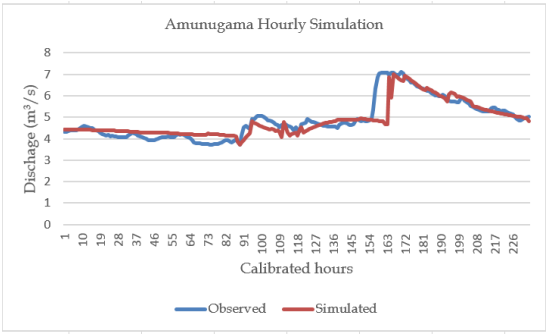

Figure 6 Deduru Oya hourly simulation (June 1st – 15th June, 2019)

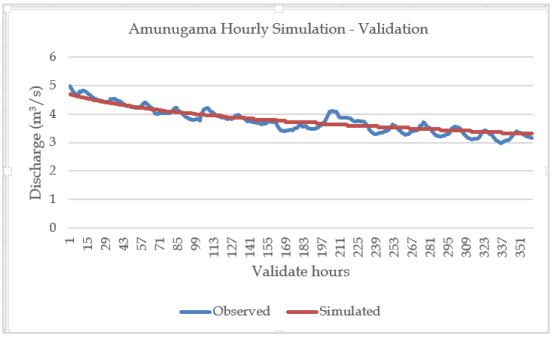

Figure 7 Deduru Oya hourly validation (June 15th – 30th June, 2019)

The P factor, R factor NS value in the above three simulations are given in Table 4. Accordingly, compared to daily simulation, hourly simulation is more capable to simulate the peaks. Using the same parameters and their ranges of the calibrated hourly model for Deduru Oya catchment, the model was validated for the period of 15th June to 30th June 2019. The model was validated in a period where very less rainfall occurred. Hence, the validated model doesn't show any peaks.

Since the recently installed open system is still in an experimental level, in certain time periods, several malfunctioning issues were encountered due to the thunder and lightning and some issues in the solar charges. If such malfunctioning occurs, it significantly affects for continuity of the data and ultimately for the results of model, especially when running the model for hourly basis. Owing to the aforementioned issues, the model could not be validated for the subsequent periods. Since the model parameters vary with the seasonal rainfall pattern of Sri Lanka (Warusavitharana, 2019), further calibration and validation of the model during different rainfall periods are yet to be completed.

Table 4 Statistics of the Amunugama and Maspotha calibration

Simulation	P factor	R factor	NSE value
Maguru Oya-daily	0.82	1.02	0.69
Deduru Oya-daily	0.79	0.62	0.62
Deduru Oya-hourly	0.96	0.76	0.75
Amunugama –hourly-validation	1.0	0.89	0.86

5. CONCLUSION

This research demonstrates the capability of a low cost weather monitoring data and water level data in estimating even runoffs triggered during the rainfall events. The model calibration process has produced an acceptable simulation for both daily and hourly time steps. Hence, this research reveals the possibility of adopting open technologies in filling a big vacuum in the fields of weather monitoring, water resources and disaster management in developing countries.

6. ACKNOWLEDGEMENT

The authors would like to thank Swiss Agency for Development and Cooperation (SDC) and Swiss National Science Foundation (SNSF) for providing necessary funds to carry out this research.

7. REFERENCES

Abbott, M., Bathurst, J., Cunge, J., O'Connell, P., & Rasmussen, J., 1986, 'An introduction to the European Hydrological System - Systeme Hydrologique Europeen, "SHE", 1: History and philosophy of a physically-based distributed modelling system, and 2: Structure of a physically-based distributed modelling system', *Hydrology*, 87, 45-59 and 61-77.

Andréassian, V., Perrin, C., Michel, C., Usart-Sanchez, I. & Lavabre, J., 2001, 'Impact of imperfect rainfall knowledge on the efficiency and the parameters of watershed models', *Journal of Hydrology,* 250, 206–223, doi: https://doi.org/10.1016/S0022-694(01)00437-1

Chaplot, V., A. Saleh, & D. Jaynes, 2005, 'Effect of the accuracy of spatial rainfall information on the modeling of water, sediment, and NO3–N loads at the watershed level', *Journal of Hydrology*, 312, 223–234, doi: https://doi.org/10.1016/j.jhydrol.2005.02.019

Dile, Y., et al., 2016, 'Introducing a new open source GIS user interface for the SWAT model', *Environmental Modelling & Software*, 85, 129–138

Duncan, M., B. Austin, F. Fabry, & G. Austin, 1993, 'The effect of gauge sampling density on the accuracy of streamflow prediction for rural catchments', *Journal of Hydrology*, 142, 445–476, doi:https://doi.org/10.1016/0022-1694(93)90023-3.

Faurès, J.-M., D. Goodrich, D. A. Woolhiser, & S. Sorooshian, 1995, 'Impact of small-scale spatial rainfall variability on runoff modeling', *Journal of Hydrology,* 173, 309–326, doi: https://doi.org/10.1016/0022-1694(95)02704-S

HP, 2013, *Central Nervous System for the Earth (CeNSE)*, viewed June 2017, from http://www8.hp.com/us/en/hp-information/environment/cense.html#.WTLzUmiGM2w

IBM, 2010, *A Smarter Planet*, viewed June 2017, from http://www.ibm.com/smarterplanet/

King, K.W., Arnold, J.G., Bingner, R.L., 1999, 'Comparison of Green-Ampt and curve number methods on Goodwin Creek watershed using SWAT'. *Trans ASABE* 42(4):919–925

Senevirathna, S., & Jayawickrama, A, 2014, 'Developing a National Climate Observatory System for Sri Lanka', *Coordinating Secretariat for Science Technology & Innovation*.

Snow, J., 2013, *Non-traditional approaches to weather observations in developing countries*, viewed March 2017, from http://www.ifc.org/wps/wcm/connect/91c3778042bd94eeb2c6be0dc33b630b/Non-Traditional+Approaches+to+Weather+Observations+in+Developing+Countries+-+John+Snow.pdf?MOD=AJPERES

Strigaro, D., Cannata, M., & Antonovic, M., 2019, 'Boosting a Weather Monitoring System in Low Income Economies Using Open and Non-Conventional Systems: Data Quality Analysis', *Sensors*, 19(5), 1185.

Warusavitharana, E., Ratnayake, R., Mahanama, S. & Cannata, M., 2018, 'An approach to determine the optimum spatial distribution of hydrometeorological stations for hydrological modelling: 4ONSE deployment', *Proceedings of 39th Asian Conference on Remote Sensing (ACRS 2018),*Kuala Lumpur, Malaysia, 15 – 19. October, 018.

Warusavitharana, E. J., 2019, 'Semi-distributed parameter optimization and uncertainty assessment for an ungauged catchment of Deduru Oya Basin in Sri Lanka', *International Journal of River Basin Management*, 1-28.

Willian, K., & David, R., 1996, 'A GIS assessment of non-point source pollution in the San Antonio Nueces Coastal Basin', *Center for Research in Water Resources*, viewed from http://www.ce.utexas.edu/centers/crwr/reports/online.html

Wooldridge, S.A. & Kalma, J.D., 2001, 'Regional-scale hydrological modelling using multiple-parameter landscape zones and a quasi-distributed water balance model', *Hydrology and Earth System Sciences,* 5(1), 59-74.

Proceedings of the 7th International Symposium on

Advances in Civil and Environmental Engineering Practices for Sustainable Development

ACEPS - 2019

Climate change in Sri Lanka - what do the data actually reflect?

P. Hettiarachchi[1] and M.K.J. Madhavie[2]

[1] Irrigation Department, Colombo, SRI LANKA
[2] Swinburne University of Technology, Melbourne, AUSTRALIA

K e y w o r d s

Climatic change
Sri Lanka
Temperature
Rainfall Pattern
Questionable Projections

A B S T R A C T

Since climate change has become a subject of global interest, including certain consultancy firms and financing agencies, some questionable projections have also been disseminated over the media. This paper analyses the behavior of several key indicators of climate change, with respect to Sri Lanka, with the help of historical data and information over last century collected from reliable sources. The data reflect that there was a continuous rise of temperature (0.86 ˚C) in Sri Lanka over the last 115 year. The analysis proves, in general there were no major change in rainfall amount and patterns of Sri Lanka during the period. These findings will be useful for researchers and planners of climate resilience projects to formulate proper mitigation options. Secondly, climate change is not the only issue (or most critical issue) to be addressed by the country. Among many crucial problems to be addressed, the government must prioritize projects based on the severity and urgency of the issues. The outcome of this study will be useful for the experts of various fields to select the most appropriate solutions for climate issues and for policy makers to prioritize the development activities based on the severity of the problems.

1. INTRODUCTION

Global climate change is, more or less, a proven fact. Further, it is obvious that all countries have to face the adverse effects of climate change, however, still there are some important questions to be answered. How large are these threats at the level of individual countries, to what extent we (as Sri Lankans) are exposed to, what areas are being affected and what are the remedial measures to be adopted etc.? Remedial measures which are planned without understanding the local conditions, would lead not only to ineffective solutions but also further damage to the environment. As such, all countries should have correct assessment of impacts of climate change at the local level to identify remedial measures which are most effective and economical. These measures should be country specific and decided by a team of experts covering a variety of fields.

Sri Lanka has been declared as a country highly vulnerable to the effects of climate change (Eckstein et.al 2019, Kurukulasuriya 2007). However, weightage given to this matter is different from one organization to another and person to person.

National Aeronautics and Space Administration (NASA) has accepted that the global climate change has already had observable effects on the environment, in the forms of loss of sea ice, accelerated sea level rise, melting of glaciers, and longer and more intense heat waves (Global Climatic Change 2017). Intergovernmental Panel on Climate Change (IPCC) forecasts a temperature rise of 1.39˚C to 5.56˚C over the next century. According to IPCC, the extent of climate change effects on individual regions will vary over time and with the ability of different societal and environmental systems to mitigate or adapt to change. Further IPCC predicts that an increase in global mean temperature of less than 1˚C to 3˚C above 1990 levels, will produce beneficial impacts in some regions and harmful ones in the others (Global Climatic Change 2017).

IPCC Climatic Change 2014: Synthesis report says that 'Climate Change is a threat to Sri Lanka's hyper diversity, including its marine eco-system and coastal coral reef environment'. Further it says 'Climate variability and sea level rise has the potential to affect the overall abundance of endemic species' (IPCC 2014). However, this is mainly based on the assumption that there will be longer periods of droughts and prolonged intense precipitation over the country because of global climate change.

According to Jayawardana (2015), 'Projections made into the future climate have many uncertainties which include model uncertainties, insufficient data length and their representativeness, calibration and validation issues, and the logic of projecting into 100 years or more into the future with relatively short window of observation'.

Punyawardena (2018), is more critical on the issue and says, 'All the studies we conduct arrive at the conclusion, that it is a real threat, it will affect all the sectors of the economy, especially agriculture, tourism, health, and transport'. Further based on his explanations, there are no sectors with immunity to this complication. All the sectors are vulnerable to climate change.

From some of the key findings of the Climate Risk Index published by Germanwatch at climate summit in Bonn, they have declared a number of developing countries regularly already have to address weather catastrophes; especially poorer countries like Haiti, Sri Lanka and Vietnam are facing great challenges. Finally, in a global climatic risk index in 2019, Sri Lanka has been ranked second among the countries most affected by extreme weather events, in 20 years since 1998. The 2019 Long-Term Climate Risk Index, published by Germanwatch, has listed Puerto Rico, Sri Lanka, and Dominica as the top three affected countries (Eckstein *et al* 2019).

The available studies on climatic change of Sri Lanka are based on the predictions from global models and assumptions (Kurukulasuriya & Ajwad 2007, Pattnayak et.al. 2017, Darshika et.al. 2018). Only very few literatures are available on investigating the existing trends of climate change using available long-term data. Therefore, main objective of this study is to investigate the patterns reflected by the actual data over the last century to identify the local climatic change.

Sri Lanka is a small island located in the Indian Ocean (Figure 1). The land extent is nearly 65000 km^2 surrounded by sea. The central part of the country comprises mountains bounded by coastal plains in all directions. The central hills receive heavy rainfall during North-East and South –West monsoon periods. The river system of the country, has 103 major-medium rivers, originating in the central hills and flows to the sea through the coastal plains where extensive rice (staple food) cultivation is practiced. Generally, paddy (rice) farming consumes large amount of water. The average annual rainfall of the country is varying from 900 mm in the coastal plains to over 5000 mm in the central hills. However, due to the spatial and seasonal variation of rainfall, the major part of the country faces scarcity of water. Due to this, Sri Lanka had acquired a great hydraulic civilization by constructing storage reservoirs and diversion structures throughout its history.

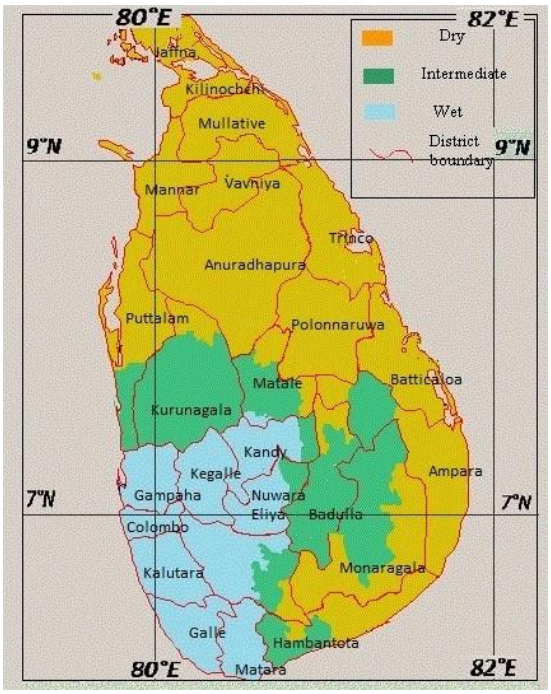

Figure 1 Sri Lanka, Location and Climatic Zones

2. KEY INDICATORS OF CLIMATE CHANGE

The primary indicator of global climate change is the atmospheric temperature which is supposed to have risen due to the burning

of fossil fuels and emission of greenhouse gases (Eckstein et.al. 2019). Secondary indicators are rainfall including its spatial and seasonal variation and intensities, sea level rise, evaporation, evapotranspiration, relative humidity etc. Finally, the increased flooding, prolonged droughts, crop failures, landslides etc. can be considered as the impacts and tertiary indicators of climate change.

However, analyzing all these parameters is a tedious task which requires a large amount of data. Four parameters namely; temperature, rainfall amount, intensity of rainfall and its spatial and temporal distribution were selected for the analysis in this study. Likely impacts associated with the changes of these parameters are also discussed with the help of information available at key government institutions.

3. AVAILABILITY OF DATA AND SOURCES OF INFORMATION

Most of the historical data relevant to weather parameters could be found from the Department of Meteorology, Sri Lanka. The Hydrology Division of the Irrigation Department also possesses the climatic data and information on river flows and flooding. World bank has created the Climatic Change Knowledge Portal (CCKP) to serve as the hub for climatic related data, information and tools. CCKP consist of comprehensive global, regional and country data related to climate and provide a web-based platform to multiple users to use these data in research, decision making, design of projects and policies.

4. ANALYSIS OF DATA

4.1. Temperature

Scientists have high confidence that global temperatures will continue to rise for decades to come, largely due to greenhouse gases produced by human activities (Global Climatic change 2017, Romm 2016). Industrial and transportation developments are main causes for emission of greenhouse gasses. Rapid growth of population, over consumption of natural resources, urbanization and de-forestation are the other factors affecting the global warming (Romm 2016). While industrial development in our country is well below the developed countries, the other factors are common to us also. These activities have increased remarkably during the latter part of the last century and their effects could be expected to be reflected by the historical data collected over the period.

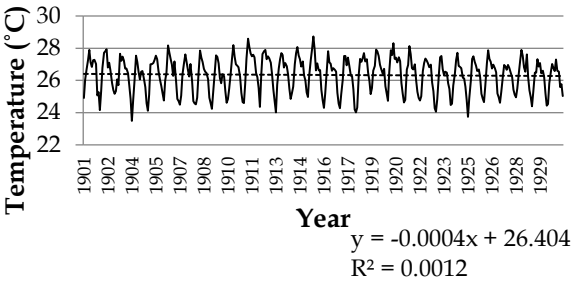

Figure 2 Variation of country average temperature from 1901 to 1930

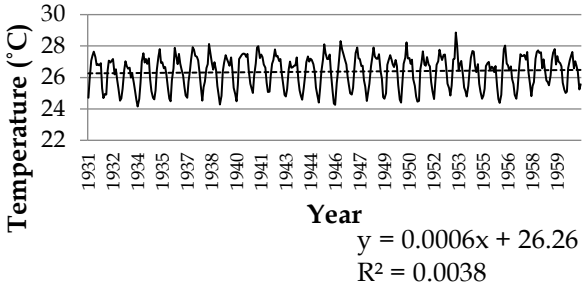

Figure 3 Variation of country average temperature from 1931 to 1960

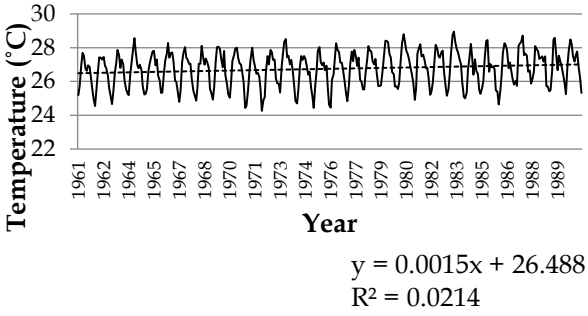

Figure 4 Variation of country average temperature from 1961 to 1990

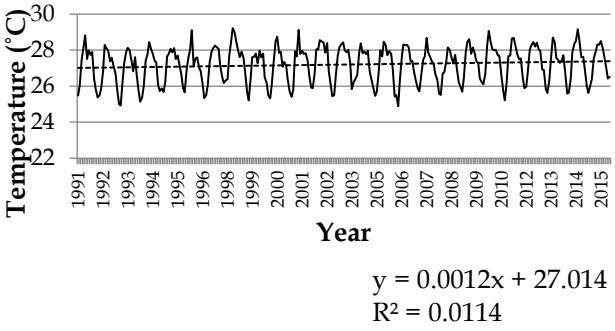

Figure 5 Variation of country average temperature from 1991 to 2015

Table 1 Variation of Average Temperature over the last century; 1901 to 2015

Data Period	Country average temperature	Trend
1901-1930	26.34 ˚C	Insignificant negative trend (-0.0004)
1931-1960	26.37 ˚C	Insignificant positive trend (0.0006)
1961-1990	26.75 ˚C	Significant positive trend (0.0015)
1991-2015	27.20 ˚C	Significant positive trend (0.0012)

Monthly average temperature of the country for 115 years (from 1991 to 2015) was analyzed to examine whether there is an increasing trend in temperature of Sri Lanka. These data were obtained from CCKP of World Bank. First, the data set was split into 30-year periods and averages were computed. Figure 2 to 5 shows the trends of variation of average temperature and Table 1 summarizes the numerical results

The total rise in country average temperature (0.86 ˚C) is little more than the global average. A study by Ratnasiri et.al. 2019 shows a similar temperature increase over the last century (i.e. approximately 1 ◦C). The earth's average temperature has risen by 0.80C during the period from 1880 and two-third of the warming has occurred since 1975 (Jayawardena 2015). This should not be underestimated. A small change in temperature may cause significant changes in the environment.

4.2. Rainfall

In this case the monthly cumulative rainfall over the country (from 1901 to 2015), average annual rainfall (for consecutive 30-year periods), rainfall intensity and the temporal and spatial distribution of rainfall were analyzed.

4.2.1. Monthly Total and Average Annual Rainfall of the Country

The data from 1901 to 2015 from CCKP of World Bank were selected to study the variation of rainfall of the country. First, monthly total rainfall (from January 1901 to December 2015) were plotted as shown in Figure 6. There was no significant variation in monthly rainfall. The highest value (687.5 mm) had been recorded in December 1957 which was evidenced by a devastating flood in the entire country (Hettiarachchi 2014).

Further, the annual rainfall was computed using the same data set. Similar to the analysis of temperature, the total data set was divided into 30-year periods. The 30-year (annual) averages are given in Table 2.

Considering the average annual rainfall from 1901 to 2015 (Table 2), there is no any continuous trend (decreasing or increasing) in average annual rainfall during the past 115 years.

4.2.2. Temporal Distribution of Rainfall

Temporal distribution of rainfall is vital importance since it directly affects agricultural production of the country. The irrigation system of the country has been designed assuming a relatively stable pattern of rainfall over the year. The rainfall distribution pattern of the country is mainly dominated by the two monsoons. The south-western quadrant of the country directly faces the wind direction of the first (i.e. south-west) monsoon.

Table 2 Variation of Average Annual Rainfall over the last century; 1901 to 2015

Data Period	Country average precipitation
1901-1930	1660 mm
1931-1960	1732 mm
1961-1990	1711 mm
1991-2015	1715 mm

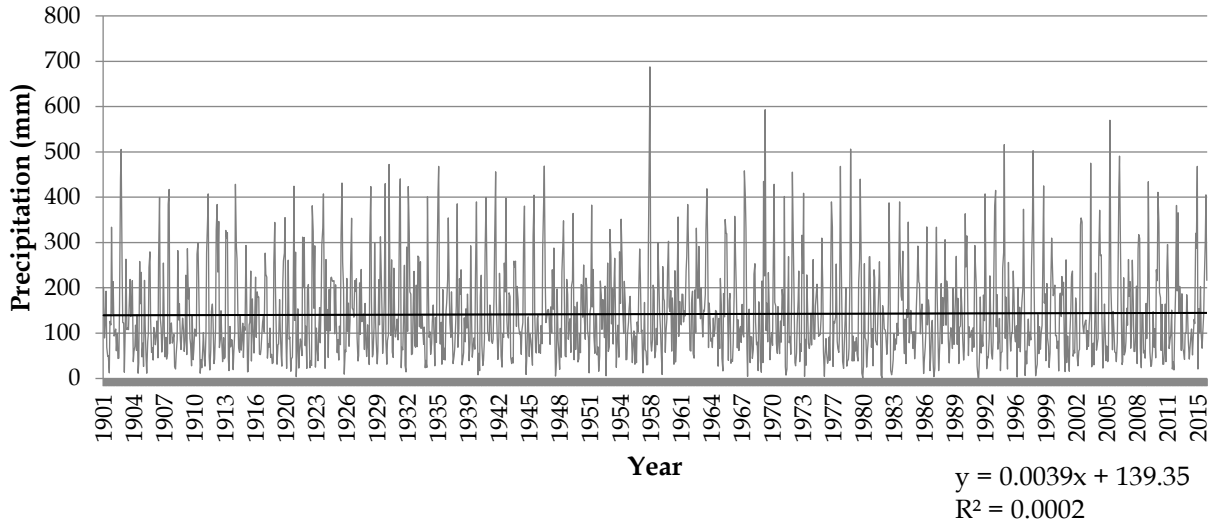

Figure 6 Variation of monthly (total) rainfall of the country from 1901 to 2015

Due to the mountainous barrier (towards the central part), this area receives a substantial amount of rainfall during the period from April to June. This area is designated as the Wet Zone of the country.

The entire country receives high rainfall during the North-East monsoon making the highest rainfall over the country around November. To demonstrate this pattern, the average monthly rainfall was computed using the entire data set and plotted (Figure 7, solid black line). To examine whether there is any deviation from this pattern, the data set was split into 30-year periods and the computed averages were plotted on the same graph. The data used to plot the graphs are summarized in Table 3.

According to predictions the South-West monsoon would strengthen, and the North-East monsoon should weaken due to climate change (Darshika 2018). However, as seen in Figure 7 and Table 3 there is no such change in seasonal distribution of rainfall over the 115 years considered.

4.2.3. Spatial Distribution of Rainfall

Climate researchers are claiming that the wet zone of the country is becoming wetter due to increased rainfall and the dry zone drier due to a decrease of rainfall as per Global Climate Models (Darshika 2018). If there is such a trend that should be apparent in the recorded rainfall at the stations located in the dry and wet zones of the country. Stations with fairly long records of monthly rainfall were selected for this analysis. The data source is the Department of Meteorology, Sri Lanka.

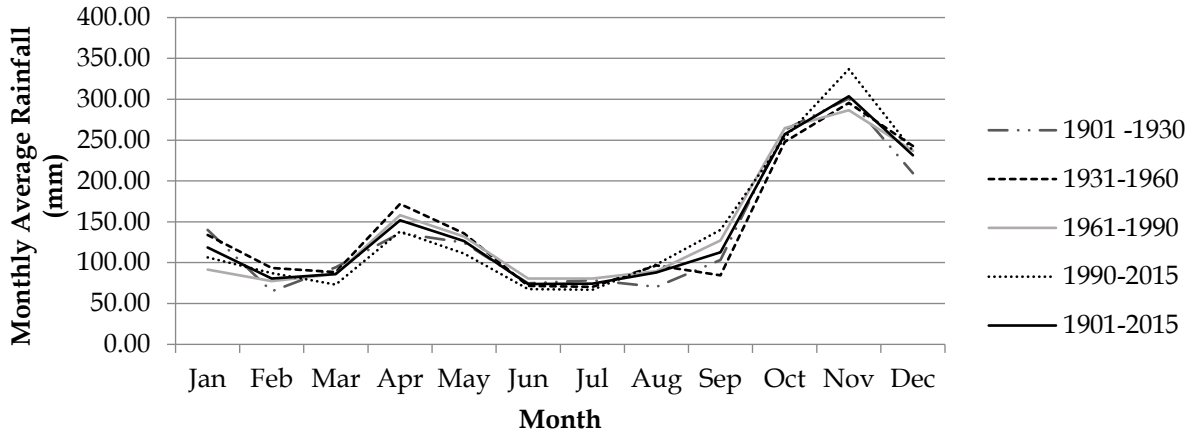

Figure 7 Monthly distribution of average rainfall for the total period and 30- year periods

And the data period is from 1900 to 2015. Station names, locations and other important details are summarized in Table 4.

Similar to previous analysis, the observation period was divided into the segments of 30 years and averages were computed and plotted (dry, intermediate and wet zone stations separately) against time periods to examine the trends (Figure 8, 9 and 10).

As seen in Figure 8, in general, dry zone rainfall do not show a decreasing trend as claimed by the climatic researchers. On the

Table 3 The values of monthly distribution of average rainfall (in mm) for 30 periods from 1901 to 2015

Period	Jan	Feb	Mar	Apr	May	Jun	Jul	Aug	Oct	Nov	Dec	Total
1901-1930	140.0	64.9	94.3	136.3	124.4	74.6	78.6	70.4	262.6	301.0	209.5	1660.2
1931-1960	134.0	93.4	88.4	172.0	135.7	71.4	70.4	96.6	248.0	295.6	242.6	1732.8
1961-1990	91.7	77.4	86.2	158..1	131.7	80.8	80.4	89.7	264.8	286.6	236.8	1711.6
1990-2015	106.5	87.4	73.2	138.2	111.2	67.6	66.8	97.7	253.1	336.9	237.1	1715.7
1901-2015*	118.6	80.5	86.0	151.7	126.4	73.9	74.4	88.2	257.3	303.6	231.3	1704.6

* The average monthly distribution of rainfall in mm for 115 years from 1901 to 2015

Table 4 Rainfall stations selected for the analysis of spatial distribution

Station Name	Location Coordinates	Climatic Zone	Long term (1900 to 2015) Average Annual Rainfall mm
Trincomalee	$8^0$34′48″N, $81^0$15′,60″E	Dry Zone	1646.30
Anuradapura	$8^0$21′00″N, $80^0$22′,48″E	Dry Zone	1372.23
Jaffna	$9^0$40′47″N, $80^0$1′,48″E	Dry Zone	1169.88
Baticaloa	$7^0$42′36″N, $81^0$42′,00″E	Dry Zone	1722.14
Hambantota	$6^0$07′12″N, $81^0$07′,48″E	Dry Zone	1051.37
Mannar	$8^0$58′48″N, $79^0$54′,36″E	Dry Zone	962.07
Putlam	$8^0$01′48″N, $79^0$49′,48″E	Dry Zone	1157.65
Badulla	$6^0$59′48″N, $81^0$03′,00″E	Intermediate Zone	1763.39
Kurunegala	$7^0$10′12″N, $79^0$52′,48″E	Intermediate Zone	2068.06
Diyatalawa		Intermediate Zone	1617.42
Galle	$6^0$01′48″N, $80^0$13′,12″E	Wet Zone	2400.07
Colombo	$8^0$54′00″N, $79^0$51′,36″E	Wet Zone	2355.86
Kandy		Wet Zone	2002.37
Nuwaraeliya	$6^0$57′36″N, $80^0$45′,36″E	Wet Zone	2072.57
Ratnapura	$6^0$48′36″N, $79^0$52′,48″E	Wet Zone	3796.00

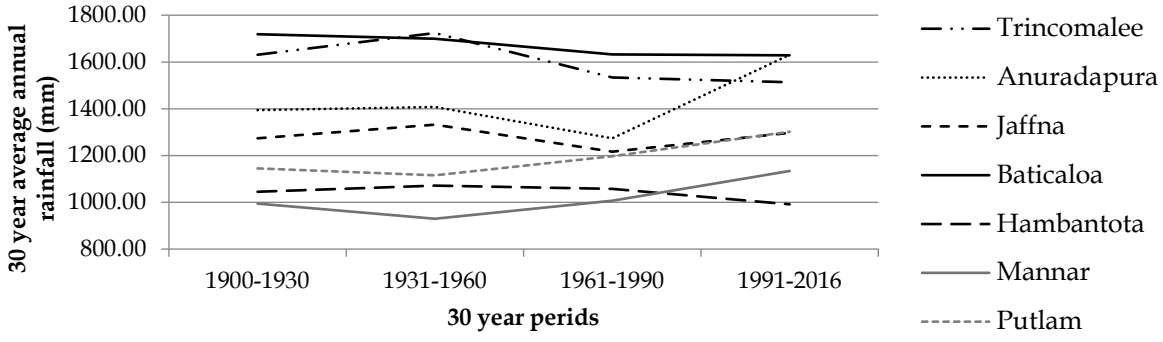

Figure 8 Variation of 30-year average rainfall with time in Dry Zone, Sri Lanka

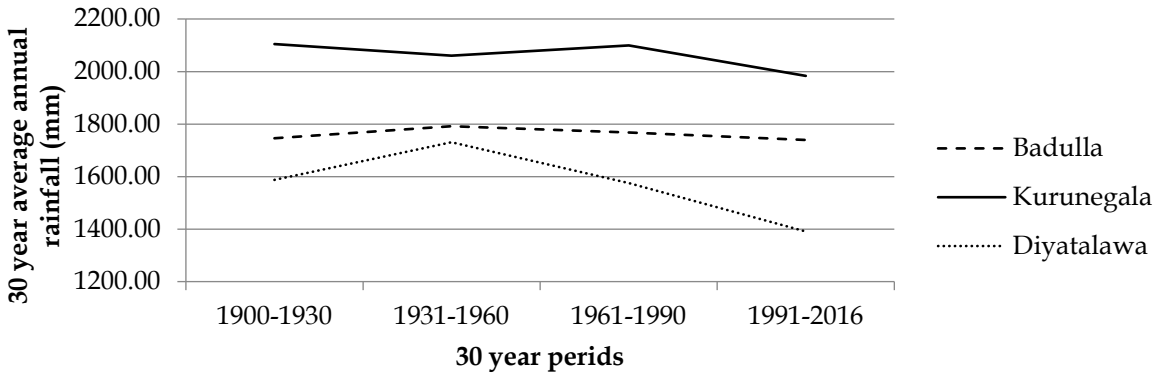

Figure 9 Variation of 30 year average rainfall with time in Intermediate Zone, Sri Lanka

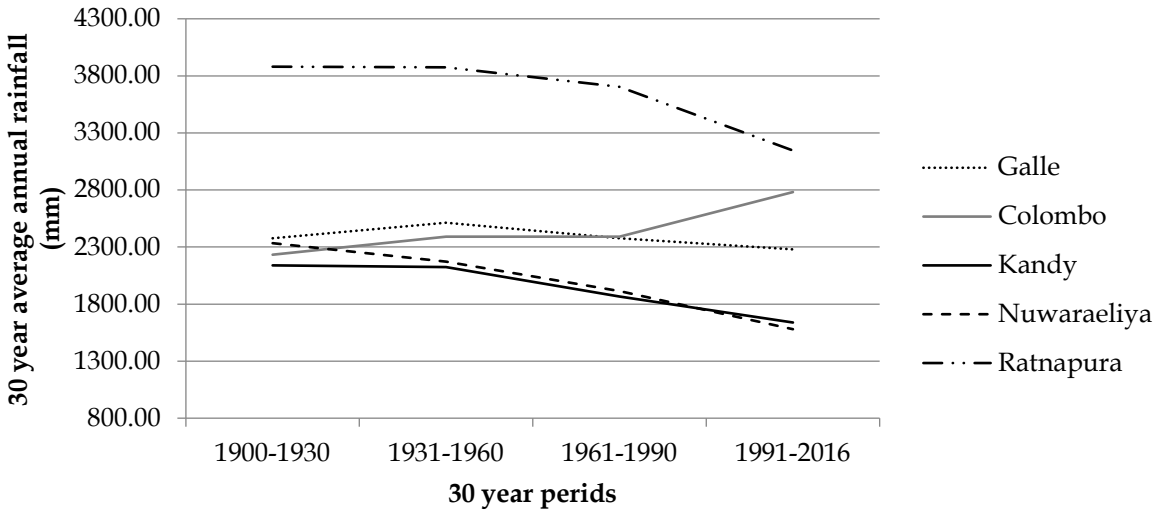

Figure 10 Variation of 30-year average rainfall with time in Wet Zone, Sri Lanka

contrary, Anuradapura Puttalam and Mannar rainfall have increased significantly during the last 30 years.

Intermediate Zone rainfall do not show common pattern of increasing or decreasing. However, Diyatalawa station shows significant decrease of rainfall during latter part. Climate researchers have not considered these areas as a separate zone but may be considered as a part of Wet Zone.

Wet zone rainfall also does not show any common pattern of continuous increase as suggested by the researchers. In contrast, Nuwara Eliya and Ratnapura show a continuous decrease of rainfall. This should be investigated by the researchers. There may be local reasons (e.g. urbanization and de-forestation) for this pattern rather than the global warming or emission of greenhouse gases. However, Colombo rainfall have been increased during the recent period. This must be observed for a further period to examine whether this is a continuous trend or not.

4.2.4. Rainfall Intensity Studies

Long-term observations of daily rainfall are abundant in Sri Lanka. However, rainfall intensity studies require data with respect to shorter durations. Department of Meteorology and the Irrigation Department have maintained several stations of recording rain gauges representing different climatic zones. However, only few stations are available with continuous records of data for the required length of period.

First the annual maximum rainfall from several stations were analyzed to examine

whether there is an increasing trend in 24 hours rainfall with respect to extreme events. Four stations Trincomalee, Batticaloa, Anuradhapura and Hambantota were selected from the Dry Zone for this purpose. The record length was from 1954 to 2013. The results are presented graphically in Figure 11. Batticaloa show an increasing trend (Figure 11) while Trincomalee station show decreasing trend. Other two stations' (i.e. Hambantota and Anuradhapura) extreme rainfall show nearly stationary values throughout the period.

Three stations from the Intermediate Zone, Badulla, Diyatalawa and Kurunegala were selected to study the variation of extreme rainfall in the zone. Kurunegala station shows an increasing trend (Figure 12). However, it is mainly dominated by a single event in the year 2012. Badulla station shows an insignificant positive trend while the data from Diyatalawa show slightly negative trend. These results are

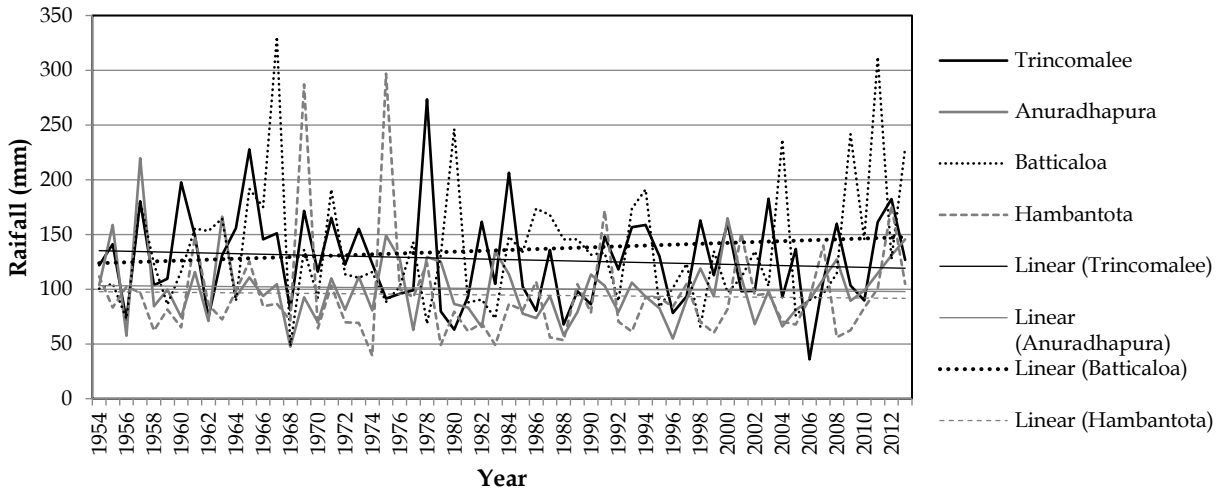

y = -0.2721x + 135.45 (Trincomalee)

y = -0.0922x + 103.36 (Anuradhapura)

y = 0.4032x + 123.34 (Batticaloa)

y = -0.1026x + 97.789 (Hambantota)

Figure 11 Annual maximum rainfall from the dry zone meteorological stations

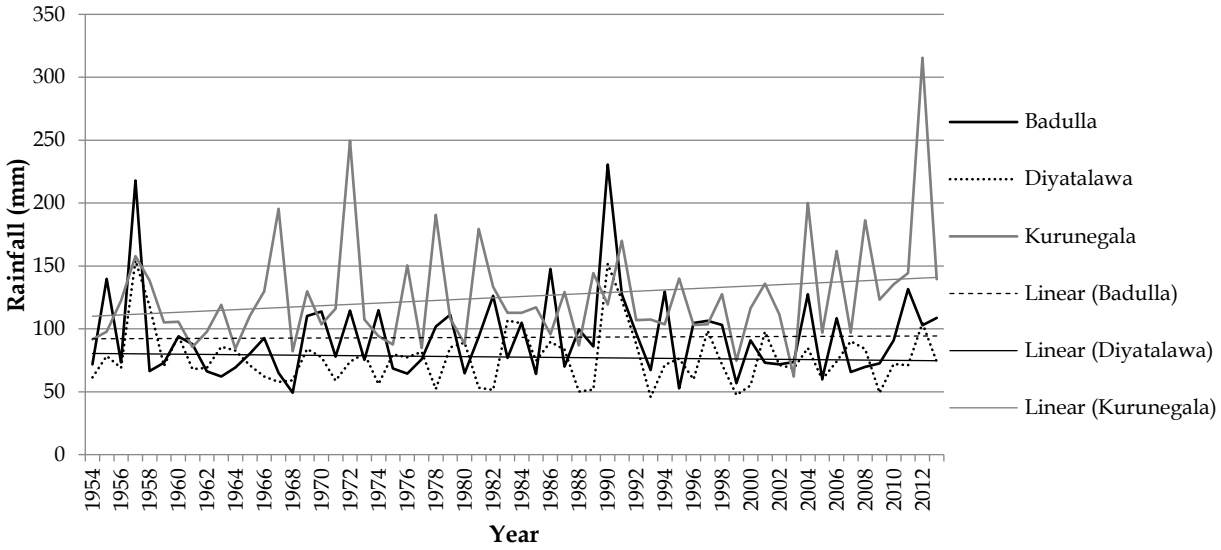

y = 0.0378x + 92.072 (Badulla) y = -0.0975x + 80.527 (Diyathalawa) y = 0.5229x + 109.5 (Kurunegala)

Figure 12 Annual maximum rainfall from the intermediate zone meteorological stations

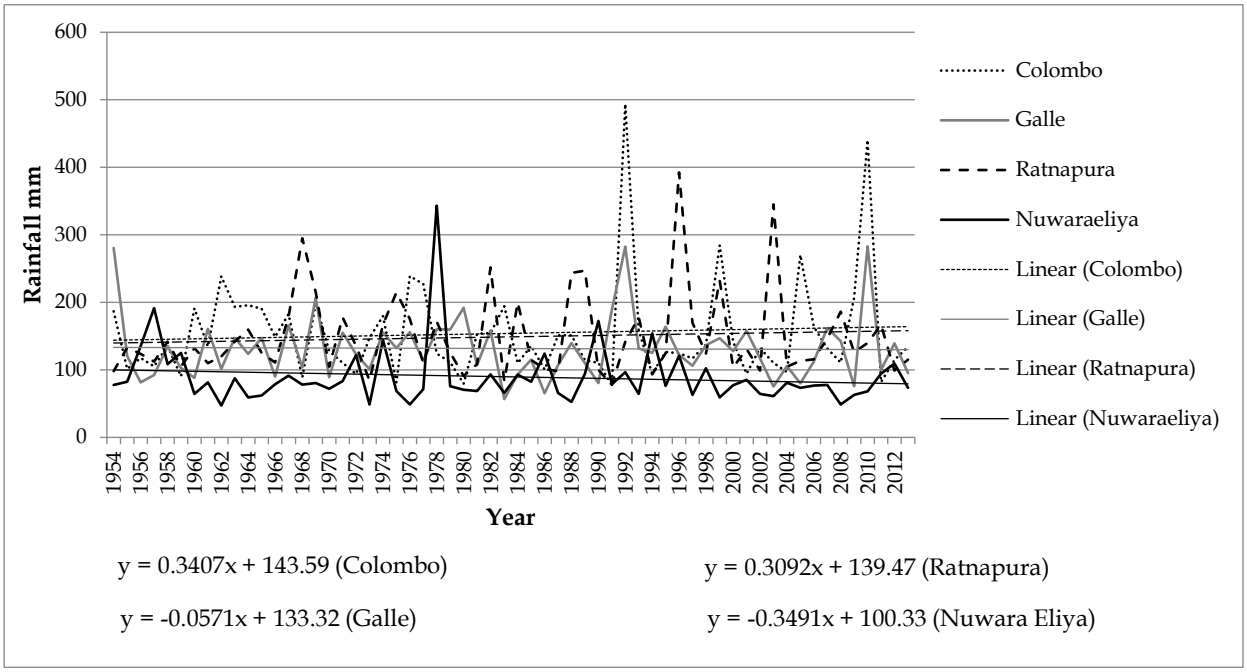

Figure 13 Annual maximum rainfall from the wet zone meteorological stations

not enough to make any common conclusion.

Finally, four stations from the Wet Zone, Colombo, Galle, Ratnapura and Nuwara Eliya were selected for extreme value analysis and the results are presented in Figure 13. Colombo and Ratnapura stations show increasing trend of extreme rainfall (Figure 13). In contrast Nuwaraeliya shows a decreasing trend while the data from Galle are nearly stationary. Hence it is not possible to find any regular pattern of increasing (or decreasing) trend of extreme events over the Wet Zone.

Spearman's rank correlation method was used to check the statistical significance of the rainfall intensities. As summarized in Table 5, test indicated that there is no any significant increasing or decreasing trend in rainfall.

Finally, to check whether there is any change (increasing trend) in short duration rainfall the annual maximum rainfall of shorter durations at Ratnapura station from 1955 to 2011 were analyzed. There is no significant trend in 3 hour duration rainfall (Figure.14) at Ratnapura. The trend in 6-hour duration rainfall was also not that significant (Figure 15). Several other stations were analysed following the same procedure and there was no common trend showing increasing intensities of rainfall over the country.

Table 5 Summary: Spearman's rank correlation analysis for rainfall intensity data, considering annual maximum rainfall from 1954 to 2013

Station	Station Name	Climatic Zone	R_{sp}	t	t_{cr}	Trend
1	Anuradapura	Dry Zone	0.03	0.23	+,-2.00	No trend
2	Trinkomalee	Dry Zone	-0.07	-0.53	+,-2.01	No trend
3	Baticalloe	Dry Zone	0.08	0.59	+,-2.02	No trend
4	Hambantota	Dry Zone	-0.01	-0.11	+,-2.03	No trend
5	Collombo	Wet Zone	-0.05	-0.36	+,-2.04	No trend
6	Galle	Wet Zone	-0.03	-0.21	+,-2.05	No trend
7	Ratnapura	Wet Zone	0.02	0.15	+,-2.06	No trend
8	Nuwaraeliya	Wet Zone	-0.14	-1.1	+,-2.07	No trend
9	Badulla	Intermediate Zone	0.08	0.64	+,-2.08	No trend
10	Diyatalawa	Intermediate Zone	-0.02	-0.16	+,-2.09	No trend
11	Kurunegala	Intermediate Zone	0.22	1.71	+,-2.10	No trend

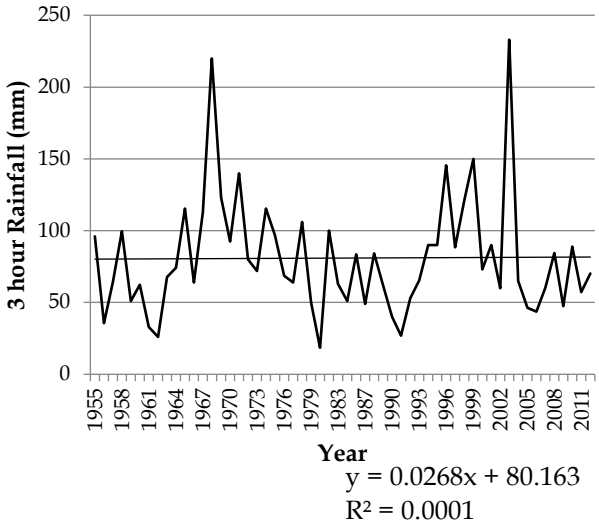

Figure 14 Annual maximum rainfall of 3-hour duration at Ratnapura

5. CONCLUSION

As per above, there was no major change in rainfall pattern of Sri Lanka during the last century.

There is no any continuous trend (i.e. decreasing or increasing) identified in average annual rainfall in Sri Lanka during past 115 years. Similarly, there is no any change visible in the seasonal distribution of rainfall over the island.

Considering the spatial distribution of rainfall, in general dry zone rainfall does not show a decreasing trend and wet zone rainfall does not show an increasing trend as claimed by the climatic researchers. Similarly, intermediate zone does not show any continuous trend (i.e. decreasing or increasing) in average annual rainfall.

However, Nuwara Eliya and Kandy (stations in the wet zone) showed significant decrease of rainfall throughout the period. Rather than the global warming and greenhouse gas emissions, local reasons such as urbanization and deforestation may be caused for such changes.

Any of the stations doesn't show statistically significant trend in rainfall intensities. Hambantota and Anuradhapura (in dry zone), Galle (in wet zone) showed nearly stationary based on the intensity of rainfall (i.e. annual maximum rainfall) from 1954 to 2012.

However, there was a continuous rise (0.86^0C for last 115 years) in temperature. This may not have much influence on agricultural production. Nevertheless, it should not be underestimated since a small increase in temperature may cause significant changes in the environment. Being a small island surrounded by the sea, influences of sea level rise might have adverse effects on coastal environment which has not been covered by this study.

6. RECOMMENDATIONS

Influence of climate change with respect to Sri Lanka seems exaggerated by some of the agencies (as per the literature available) and individuals. This study covers the behavior of temperature and rainfall over the last century with the help of historical records. According to that there is a significant rise in average temperature (0.86^{0C} for last 115 years) over the country. But there are no major changes in rainfall amounts and pattern. Therefore, the development works (in water sector) should be planned for the existing conditions but not for the predicted conditions, under different climate scenarios, which are highly uncertain. That will save the economy of the country.

However, it is important to be vigilant on climate change including global predictions and projections. Environmental degradation at the local level, which happens continuously due to urbanization and overutilization of natural resources, may have a greater impact on the climate of Sri Lanka than global warming. Sri Lanka hasn't paid enough attention to improve or preserve the natural environment.

The country must make a continuous effort to safeguard the land and water which are the most important natural resources for the economy of the country. Since existing rainfall pattern of the country is seasonal, it is essential to store water for different purposes throughout the year. This truth had been realized by the ancient rulers of the country and it was the secret behind the great hydraulic civilization by which had reservoirs throughout the Island. The same principles and technologies can be adapted to address the issues of climate change. Protecting the environment including natural forests, river systems and existing reservoirs is of vital importance. Increasing storage capacities by construction of new reservoirs will also be useful to meet the additional demands of an increasing population, regardless of having

good or bad impacts of climate change.

7. REFERENCES

Darshika, D.W.T.T., Jayawardana, I.M.S.P. & Disanayaka, D.M.S.C., 2018, 'Multi Model Ensemble climate change projections for annual and seasonal rainfall in Sri Lanka', *Sri Lanka Journal of Meteorology* 3, 19-27.

Eckstein, D., Hutfils, M.L. & Winges, M., 2019, *Who Suffers Most From Extreme Weather Events? Weather-related Loss Events in 2017 and 1998 to 2017*, Global Climate Risk Index, Germanwatch, Berlin

Global climate change, 2017, The effect of climate change, viewed 22 December 2018, from https://climate.nasa.gov/effects/

Hettiarachchi, P., 2014, 'Comparison of 2014 Flood with the Devastating Flood in 1957 in the Dry Zone of Sri Lanka', *Hydrological Annual 2013/2014*, Hydrological Division, Irrigation Department, Sri Lanka

Jayawardena, A.W., 2015, ' Climate Change - Is it the Cause or the Effect?', *KSCE Journal of Civil Engineering*, 19(2), 359-365.

K.C. Pattnayak, K.C., Kar, S.C., Dalal, M. & Pattnayak R.K., 2017, *Projections of annual rainfall and surface temperature from CMIP5 models over the BIMSTEC countries'*, Global and Planetary Change 152, 152-166.

Kurukulasuriya, P. & Ajwad, M.I., 2007,'Application of the ricardian technique to estimate the impact of climate change on smallholder farming in Sri Lanka', *Climatic Change* 81, 39-65.

Pachauri, R.K. & Meyer, L.A. (eds.), 2014, *Climatic change 2014:Synthesis report*, Contribution of working groups I, II and III to fifth assessment report of Intergovernmental Panel on Climatic Change (IPCC), Geneva, Switzerland, 151pp

Punyawardena, R., 2018, 'Tackling the threat of climate change', Daily FT, 13 August 2018, viewed 5 December 2018, http://www.ft.lk/opinion/Tackling-the-threat-of-climate-change/14-660741

Ratnasiri, S., Walisinghe, R., Rohde, N. & Guest, R., 2019, ' The effects of climatic variation on rice production in Sri Lanka', *Applied Economics* 51, 4700-4710.

Romm, J., 2015, *Climatic change, What Eeveryone needs to know*, Oxford University Press, New York

World Bank Group, 2018, Climatic change knowledge portal, viewed 7 August 2018, from https://climateknowledgeportal.worldbank.org/country/sri-lanka

Structures and Building Materials

Proceedings of the 7th International Symposium on

Advances in Civil and Environmental Engineering Practices for Sustainable Development

ACEPS - 2019

Behaviour of cold-formed stainless steel beams with elliptical web opening under web crippling.

Ishqy Fareed*, [1,2], K.S. Wanniarachchi [1], P. Keerthan[2], S. Gunalan[3], P. Gatheeshgar[2], R. Heshachanaa[4]

[1]Department of Civil and Environmental Engineering, University of Ruhuna, SRI LANKA
[2]Faculty of Engineering & Environment, Northumbria University, Newcastle upon Tyne, UK
[3]School of Engineering and Built Environment, Griffith University, Gold Coast, QLD, 4222, AUSTRALIA
[4]Department of Civil Engineering, Sri Lanka Institute of Information Technology, Malabe, SRI LANKA

K e y w o r d s

Finite element modelling
Cold-formed stainless steel beams
Web crippling
Interior Two Flange
Unlipped channel sections
Elliptical web openings

A B S T R A C T

Over the past decades, Cold-formed stainless steel sections are increasingly been used in the construction industry, for both architectural and structural applications. The excellent combination of mechanical properties and corrosion resistance makes stainless steel a very good material for structural applications. However, web crippling behavior of unlipped channel sections with web openings has not been investigated sufficiently. Hence, a numerical analysis was undertaken to capture the exact web crippling behavior of unlipped channel beams. Finite element models of cold-formed ferritic stainless steel unlipped channel beam with offset circular web openings were developed under the Internal-Two-Flanges (ITF) loading conditions. They were validated with currently available web crippling test results and a detailed parametric study was undertaken. Numerical results showed that the currently available reduction factor equations for web opening are either conservative or unsafe. Hence, numerical results were used to develop a new reduction factor equation to the web crippling capacities of cold-formed stainless steel beams with web opening.

1. INTRODUCTION

Stainless steel has many desirable characteristics which can be exploited in a wide range of construction applications. It is corrosion resistant, long lasting, thinner and lightweight, and more durable structures possible. It is popular because it possesses an appealing combination of properties, such as durability and tremendous resistance to corrosion. Since then, Cold-formed steel has become inevitable construction material in the steel industry due to its beneficial identities such as lightweight, high durability, ease of fabrication, ease of transportation and higher strength to weight ratio. Conventional carbon cold-formed steel channel beams have been used on a large scale in the building industry. But nowadays, stainless steel cold-formed channel beams are gaining popularity because of their promising physical and mechanical properties. Figure 1 shows one of the applications of cold-formed stainless steel sections. Due to the lack of existing design rules for stainless steel, the rules for carbon steel have been generally adopted in the stainless steel design. However, the prominent non-linear behavior of stainless steel, which is the main difference with carbon steel, makes the standards for carbon steel not always acceptable in the stainless steel design.

Figure 1 Pedestrian bridge at Cheung Kong Center, Hong Kong, stainless steel

Cold-formed unlipped channel sections are mostly used as the supports for walls and railings in building construction, floor joist and many other load bearing. However, these sections are susceptible to various failure modes such as shear, bending and web crippling. Web crippling is one of the most critical failure modes of cold-formed stainless steel members. Various shapes of web openings are commonly made in the channel section beams used in buildings to facilitate various services systems as shown in figure 2. But opening in the web leads to the section being susceptible to web crippling failure and it causes to reduce the web crippling capacity considerably. Many parameters affect the web crippling capacity of cold-formed stainless steel beams with web openings. Past researches (Keerthan *et al*. 2014), (Yousefi & Lim 2017 and Ishqy et. al. 2019) have reported that the most influential parameters for the web crippling capacity of unlipped and unlipped channel beam with web opening are shape, size, location of the web openings, slenderness of the web element and loading plate size.

Figure 2 Structural stainless steel with web opening used as load bearing element

Many researches have been studied the web crippling behaviour cold-formed stainless steel lipped channel beams with circular web opening under interior and exterior load conditions (Yousefi *et al*. 2017) and Ishqy *et al* 2019). In conventional carbon cold-formed steel beams, Keerthan and Mahendran (2012 and 2014) have investigated the web crippling strength of hollow flange channel beams without web openings. Yousefi *et al* (2017) focused on the stainless steel unlipped channel beam with circular web opening but not on the beam with non-circular web openings such as elliptical shapes. Again, Ishqy *et al* (2019) focused on the cold-formed stainless steel unlipped channel beam with non-circular web openings but rectangular and square shape of web opening.

Numerical results showed that the currently available design equations to predict the web crippling capacity of lipped channel beams with circular web openings and non-circular web opening are inadequate to determine the web crippling capacity of the unlipped channel beam with elliptical web opening. Hence, detailed finite element analyses were undertaken and proposed unified strength reduction factor equation for the web crippling strength of cold-formed stainless steel unlipped channel sections with elliptical web opening under ITF load case.

2. FINITE ELEMENT MODELLING

2.1 FE model development

Finite element modelling is becoming increasingly popular. This is due in part to the increased freedom one has in terms of reinforcement geometry and distribution, interface, and mechanical properties, and in part due to advances in computational power and user-friendly codes. With modern computers elastic models containing many thousands of elements can be constructed and solved quickly. ABAQUS software was used to develop the finite element model with suitable geometric and material properties and loading and boundary conditions to simulate the web crippling test conditions (Yousefi *et al*. 2017). In FEA, a bifurcation buckling analysis was initially performed to obtain the eigenvectors for the inclusion of geometric imperfections in the non-linear analysis. Then, non-linear dynamic explicit analyses were employed to study the web crippling behaviour of cold-formed stainless steel unlipped channel beam with unreinforced elliptical web opening.

In this analysis, adequate numbers of elements were chosen for both flanges and web based on detailed convergence studies in order to obtain sufficient accuracy of results without excessive use of computing time. Available Quad-structured S4R shell element type was assigned to the FEA beam to simulate the thin section behaviour. 5 mm × 5 mm sized mesh (Figure 3a) was able to reach convergence with reasonably good accuracy. Simply supported boundary conditions were

simulated in the finite element models of channels with elliptical web openings.

Elastic-linear hardening material model was used to incorporate the strain hardening behaviour of stainless steel. Elastic modulus and Poisson's ratio of all the stainless steel grades were taken as 194,000 MPa and 0.3 respectively (3). The "hard" contact model (Figure 3b), which is the default contact formulation in ABAQUS (2017), was used in this study to simulate the simply supported boundary conditions and roller supports were assigned at the two flanges. Details of boundary conditions used are elaborated below. The u_x, u_y and u_z are translational degree of freedom (d.o.f) while θ_x, θ_y and θ_z are rotational d.o.f in the x, y and z directions, respectively.

Bottom support condition:

u_x = restrained θ_x = free
u_y = restrained θ_y = free
u_z = free θ_z = retrained

Top loading point condition:

u_x = restrained θ_x = free
u_y = Displacement θ_y = free
u_z = restrained θ_z = retrained

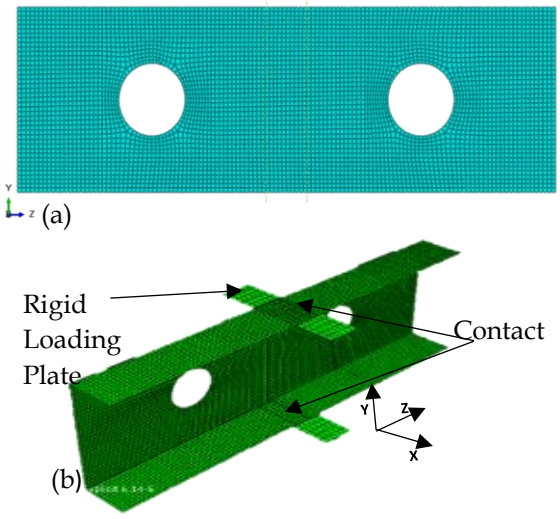

Figure 3 Geometry and finite element mesh (a) Mesh (b) Boundary condition and contact

The effect of geometric imperfections to the model was introduced through the *IMPERFECTION option which is available in ABAQUS. Initially, Buckle analysis was performed on the same model and appropriate Eigenvalue of the model was selected based on experimental simulation. The imperfection coefficient was taken as the 0.006d1 (where d1 is the clear web height) for all the models. The manufacturing process of unlipped channel beams may induce some residual stresses in thin stainless steel sections. However, the effect of these residual stresses was not taken into account, as previous research (Keerthan & Mahendran 2012) has found that the effect of residual stress on the shear capacity of unlipped channel sections is about 1%, thus it is negligible.

2.2 FE model validation and parametric study

It is essential to validate the developed FE models for non-linear analyses of unlipped channel beams with web openings under web crippling failure. So, developed models were fully validated against the experimental test results by using failure mode, load versus displacement graph and ultimate web crippling capacity. Web crippling experimental test results of cold-formed stainless steel unlipped channel beam with circular web opening under ITF loading condition from Yousefi *et al* (2017) are used for modelling and validation. Validated cold-formed stainless steel unlipped channel beams with circular web openings were further used for the parametric study.

In this study, three sections with different parameters were used to develop the database and selection was chosen based on industrially available material specifications. Normal dimensions of web thickness (t_w) around 1 mm - 2 mm, web heights (d1) from 175 mm to 250 mm, and web yield stress (f_{yw}) = 300 MPa were used in the analyses. For this purpose, FE models were developed to simulate 11 web crippling test on cold-formed stainless steel unlipped channel beam specimens of 175x60x15x1.2, 200x75x1.2 and 200x100x1.2 unlipped channel beams with circular web openings published by Yousefi *et al* (2017). Models were analysed first, and their results

Table 1 Comparison of web crippling strength predicted from finite element analysis with experiment results for flanges unfastened case (ITF Load Case)

Specimen	Web Slenderness (d_1/t_w)	(d_{wh}/d_1)	P_{EXP} (N)	P_{FEA} (N)	P_{EXP} / P_{FEA}
175×60-t1.2-N50-A0	156.08	0.00	4160	4008	1.03
175×60-t1.2-N50-MA0.4	154.25	0.39	3730	3375	1.10
175×60-t1.2-N75-A0	157.43	0.00	4280	4156	1.02
200×75-t1.2-N50-A0	185.03	0.00	3400	3514	0.96
200×75-t1.2-N50-MA0.4	186.53	0.39	3030	3088	0.98
200×75-t1.2-N50-OA0.4	189.91	0.39	2850	2991	0.95
250×75-t1.2-N50-A0	246.58	0.00	2440	2383	1.02
250×100-t1.2-N50-A0.4	241.78	0.39	2200	2276	0.96
250×100-t1.2-N50-OA0.4	251.75	0.39	1910	1933	0.98

were compared with those from the test, with particular attention given to the ultimate loads, load-deflection curves and failure mechanisms (Figure 4).

Table 1 shows the validation results for cold-formed stainless steel beams with circular web openings where d_1, d_{wh} and t_w are the clear web height, depth of web opening and web thickness of the section, respectively. Hence it shows that the FE models were able to predict the ultimate web crippling capacities of tests with good accuracy. The mean and coefficient of variance (COV) of the results are 1.01 and 0.046, respectively.

2.2 Parametric study

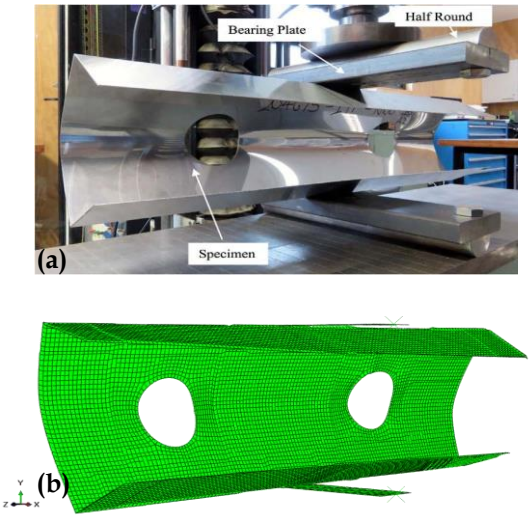

Figure 4 web crippling failure mode of stainless steel section 200x75x1.2
a) Experiment (Yousefi *et al*); b) FEA

Following the validation of the developed FE models, a detailed parametric study was undertaken to develop an extensive web crippling strength database for unlipped channel sections with elliptical web opening. In the parametric study, web openings were located at different locations, different sizes, opening depths, web opening widths and loading plate width were considered for ITF load case (Figure 5) to predict the web crippling strength.

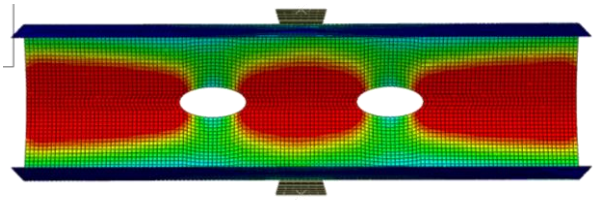

Figure 5 Web crippling failure mode of 80x40 elliptical web opening 175x60x1.2 ULCB

The ultimate web crippling capacities of channel sections with web openings and the corresponding web crippling capacity reduction factors (R_c) were obtained for varying ratios of d_{wh}/d_1, N/h and d_w/b_w. The ultimate web crippling capacities of the selected sections without web openings (P_n) were also obtained from FEA. Web opening depth to beam height ratio (d_{wh}/d_1) of 0, 0.2, 0.4, 0.6, 0.8and 0.95, bearing plate width (N) of 50, 100 and 150 and web opening depth to width ratio (d_w/b_w) of 0.6, 0.5 and 0.3 were studied. Web crippling capacity reduction factor (R_c) was calculated as the ratio of web crippling capacity of stainless unlipped channel beam with elliptical web opening to web crippling capacity of stainless unlipped channel beam with solid web (P_n).

3. COMPARISON OF WEB CRIPPLING CAPACITIES WITH CURRENT DESIGN PREDICTIONS

The ultimate web crippling capacities of channel sections with elliptical web openings obtained from FEA were compared with the predictions from the currently available design equations based on suitable web crippling capacity reduction factors. Yousefi *et al* (2017) design equations are very conservative for channel sections with elliptical web openings. Since the stainless steel material shows a complex behaviour and having enhanced strength due to the material strain hardening, conventional cold-formed design equations give over-conservative results. Other than that, North American Specification (NAS) provided design equation to predict web crippling capacity reduction factor only based on one flange loading case. Due to the lack of existing design rules for stainless steel, the rules for carbon steel have been generally adopted in the stainless steel design. However, the prominent non-linear behaviour of stainless steel, which is the main difference with carbon steel, makes the standards for carbon steel not always acceptable in the stainless steel design. Hence the predictions provide unconservative results for channel sections with elliptical web opening. Therefore, new web crippling design equations are necessary to predict the web crippling capacities of channel sections with elliptical web openings.

4. PROPOSED EQUATIONS FOR WEB CRIPPLING STRENGTH OF ULCB WITH ELLIPTICAL WEB OPENINGS

EN 1993-1-4 (2006) gives supplementary provisions for the design with stainless steels. Even so, for the ultimate resistance design of cold-formed stainless steel members, the specifications given in EN 1993-1-3 (2006) which are conceived for carbon steel, are applied. Over the lasts decades, numerous studies have conducted in this field in order to achieve a better understanding of the stainless steel behaviour, as well as to check the applicability of the existing specifications, and to obtain new designing rules to provide the designers with more efficient ways of designing.

In this study, by comparing the ultimate web crippling strength of channel sections with web openings and without web openings it clearly seems that failure strength is reduced. Other than that it can be observed the failure load decreases largely as the size of the web opening increases. The experimental and the numerical results showed that the ratios d_{wh}/d_1, d_{wh}/b_{wh} and x/d_1 are the basic parameters which impact the web crippling strength of the sections with non-circular web openings.

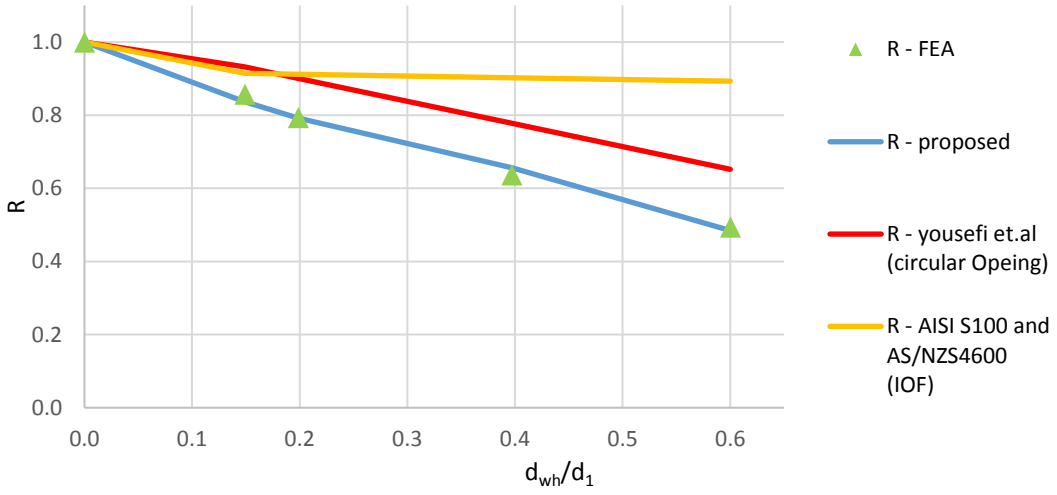

Figure 6 Comparison of web crippling capacity of stainless steel 200x75x1.2 ULCBs with elliptical offset(x/d_1 = 0.4) web opening from FEA with current design equations

Therefore, based on both existing experimental and the numerical results obtained from this study, strength reduction factor equation (R_c) is proposed as a function of the ratio of depth of web opening to clear web height (d_{wh}/d_1), shape factor (d_{wh}/b_{wh}) and ratio of offset distance of opening to clear web height (x/d_1). Eq. (2). is the proposed design equations for cold-formed stainless steel unlipped channel beam with elliptical web openings for ITF load case. The mean value of the numerical results over the results from the proposed both equations are equal to 1.03, having the coefficient of variation (COV) of 0.04 for ITF load case.

$$P_{nl} = R_c P_n \quad (1)$$

Where *Pn* is the Nominal web crippling strength of cold-formed stainless steel, refer SEI/ASCE 8-02: 2002.

$$R_p = 0.685 + 0.096\frac{x}{d_1} + 0.326\frac{d_{wh}}{b_{wh}} - 0.731\frac{d_{wh}}{d_1} \quad (2)$$

Where *Rc* is the for rectangular and square offset web opening under ITF load case:

5. CONCLUSIONS

This paper has presented a detailed investigation into the web crippling behaviour and strength of cold-formed stainless steel unlipped channel beam with elliptical web openings using finite element analyses. Comparison with these web crippling capacities showed that the unified web crippling design equations (Figure. 6) shows that NAS for the design of cold-formed steel structural members; AISI S100 (AISI, 2012), AS/NZS 4600 (Standard Australia/New Zealand 2005) and other existing design equations are either too conservative or unsafe for stainless steel unlipped channel beam with elliptical offset web opening under ITF load case. In this study, existing design equations were modified according to the aforementioned web opening shapes and included the shape factor d_{wh}/b_{wh}. The obtained FEA results were perfectly matched with the proposed design rules. Proposed design equations are able to predict the web crippling capacity of cold-formed stainless steel unlipped channel beam with elliptical web openings accurately.

6. REFERENCES

Bock, M., Mirada, F. and Real, E., 2015, 'Statistical evaluation of a new resistance model for cold-formed stainless-steel cross-sections subjected to web crippling', *International Journal of Steel Structures*, 15(1), 227-244.

Keerthan, P., Mahendran, M. and Steau, E., 2014, 'Experimental study of web crippling behaviour of hollow flange channel beams under two flange load cases', Thin-*Walled Structures*, *85*, 207-219.

Fareed, I., Somadasa, W., Poologanathan, K., Gunalan, S., Beatini, V. and Sivabalan, S., 2019, 'Web Crippling Behaviour of Cold-formed Stainless Steel Beams with Non-Circular Web Opening', *ce/papers*, *3*(3-4), 937-942.

Keerthan, Poologanathan, and Mahen Mahendran, 2012, 'New design rules for the shear strength of LiteSteel beams with web openings', *Journal of Structural Engineering, 139*, 640-656.

Yousefi, A. M., Lim, B.P., 2017, 'Web bearing capacity of unlipped cold formed stainless steel channels with perforated web subject to end two flange loading', *Engineering Structures, 152,* 804-818.

Sundararajah, L., Mahendran, M. and Keerthan, P., 2016, 'Experimental studies of lipped channel beams subject to web crippling under two-flange load cases', *Journal of Structural Engineering*, *142*(9), 04016058.

Eurocode 3, 2006, 'Design of Steel Structures-Part 1–4: General Rules - Supplementary Rules for Stainless Steels', British Standards Institution, Brussels.

American Iron and Steel Institute (AISI), 2012, *North American Specification for the Design of Cold-formed Steel Structural Members*, AISI, Washington, DC, USA.

Standards Australia/Standards New Zealand., 2005, 'Cold-Formed Steel Structures', Australia/New Zealand Standard AS/NZS4600, Sydney, Australia.

Abaqus/CAE Standard, 2017, 'Abaqus/CAE, User's Guide', Dessault Systems Simulia Corp, Providence, RI, USA

Proceedings of the 7th International Symposium on

Advances in Civil and Environmental Engineering Practices for Sustainable Development

ACEPS - 2019

Condition assessment and rating of building structures in Sri Lanka against tsunami.

B.H.J. Pushpakumara[1], H.D.K.A. Wijerathne[2] and W.S.W. Mendis[3]

[1]Senior lecturer, Department of Civil Engineering, General Sir John Kotelawala Defence University, Ratmalana, Sri Lanka.
[2]Instructor, Department of Civil Engineering, General Sir John Kotelawala Defence University, Ratmalana, Sri Lanka.
[3]Reaserch student, Department of Civil and Environmental Engineering, Faculty of Engineering, University of Ruhuna, Sri Lanka.

K e y w o r d s

Tsunami countermeasures
Buildings
Rating method
Condition assessment

A B S T R A C T

Tsunami was the most grievous disaster experienced by Sri Lanka in 2004 due to an earthquake generated in Sumatra, Andaman Islands of 9.1 in magnitude. Due to this Sri Lanka is becoming an earthquake prone zone and there is a huge possibility to occur similar Tsunami events in the near future. So, preparedness for a sudden disaster is very crucial to reduce the impacts on humans as well as properties. To minimize damages on structures, the current condition of the structures in coastal area should be evaluated. This study aims to propose a condition assessment and rating method to investigate the adequacy of building structures in coastal belt in Southern Province to withstand Tsunami and to propose remedial measures that can be applied to buildings. Condition of 50 structures was assessed in the research area. Standard eigenvectors were obtained from comparison matrices which were developed by using Analytical Hierarchy Process (AHP) to determine the priority weight of each data. Visual Inspection Factor (VIF) and Casual Factor (CF) of each building were separately calculated and Building Performance Factor (BPF) was determined by adding both factors together. Finally, Overall Building Condition (OBC) was determined and was used to conclude building remediation plan. The proposed method has the ability to rate the overall building condition and decide suitable remediation.

1. INTRODUCTION

The Tsunami devastation occurred on 26th December 2004 due to an earthquake generated near Sumatra, Andaman Islands which recorded 9.1 magnitude in Richter scale was the biggest natural disaster recorded in the Sri Lankan history. Due to this earthquake, a new fracture is being formed 500 km away from the Hambantota district, Sri Lanka (Wasunara et al. 2019). Sri Lanka had previously been free from major natural disasters except monsoonal flooding, droughts, landslides and occasional cyclones. But, the Tsunami in 2004 was by far the largest natural disaster experienced by the country. Unlike in several other countries which were affected by this Tsunami, the destruction in Sri Lanka was so extensive and that about two thirds of the 1400 km long shoreline was affected (Wasunara et al. 2019).

The coastal belt in Southern Province between Hikkaduwa to Bentara was the most inundated extent and one of the most tragic events due to the Tsunami occurred at Pereliya on the Southern coast, where a train that was stopped between stations was swept off the rail tracks when the Tsunami waves struck, and around 1,000 people were estimated to have lost their lives due to this incident. This type of Tsunami effect would be caused to accelerate the corrosion of RC structures (Pushpakumara, et al. 2013).

Sri Lanka, as a country, was totally unprepared for this kind of natural disasters. Since no warning was given, no mitigation measures were in place, no any previous experience, the Tsunami caused huge loss of human lives and extensive damages to coastal infrastructure and the environment as well

(Mendis et al. 2014).

In the present, people are well educated on how to react in a Tsunami disaster due to the experience gained from the previous disaster in 2004. Thus, the damage caused for the infrastructure facilities should be mainly focused.

2. METHODOLOGY

A condition assessment and rating method was proposed to evaluate the current condition of existing buildings in coastal belt between Hikkaduwa to Bentara. The rating method was developed by using Analytical Hierarchy Process (AHP) which can be used to evaluate the priority values among data set. Conditions of 50 building masonry structures were assessed in the research area and the data were collected by using a questionnaire.

2.1. Condition Assessment Procedure

The current conditions of the building structures were evaluated by deriving a Building Performance Factor (BPF) which is a combination of Visual Inspection Factor (VIF) and Casual Factor (CF). For each and every building, both Visual Inspection Factor and Casual Factor were initiated individually and then the Building Performance Factor was defined for each of the building in the sample.

Finally, an equation was obtained for the Overall State of the Buildings in the aid of the Building Performance Factor.

2.1.1. Visual Inspection Factor (VIF)

Ratings values and priority weights of visual inspection data were used to determine Visual Inspection Factor (VIF). Type of the walls facing sea (WT), Distance to the nearby building (DB), Walls facing sea (WS), Foundation type of the building (FT), Foundation depth (FD), Maximum length of walls facing sea (LW), Total area of openings in walls facing sea (OA) and Type of the material used to build walls (TM) were the main facts considered in buildings under Visual Inspection Factor (VIF). Rating values were assigned to quantify building conditions based on visual inspection data as shown in Table 1. Rating value "1" represents the best case while rating value "4" represents the worst case.

$$\begin{array}{c} \\ WT \\ DB \\ WS \\ FT \\ FD \\ LW \\ OA \\ TM \end{array} \begin{array}{c} \begin{array}{cccccccc} WT & DB & WS & FT & FD & LW & OA & TM \end{array} \\ \begin{bmatrix} 1 & 3 & 3 & 1 & 1 & 1/3 & 1 & 3 \\ 1/3 & 1 & 1 & 3 & 3 & 1/3 & 1/3 & 1/3 \\ 1/3 & 1 & 1 & 1/3 & 1/3 & 1 & 1/3 & 1/3 \\ 1 & 1/3 & 3 & 1 & 1 & 1 & 1 & 1 \\ 1 & 1/3 & 3 & 1 & 1 & 1/3 & 1 & 1 \\ 3 & 3 & 1 & 1 & 3 & 1 & 3 & 3 \\ 1 & 3 & 3 & 1 & 1 & 1/3 & 1 & 3 \\ 1/3 & 3 & 3 & 1 & 1 & 1/3 & 1/3 & 1 \end{bmatrix} \end{array} \quad (1)$$

AHP, which was developed by Saaty (1980), was used to determine the priority vector of the visual inspection data. Pushpakumara et al. (2017) has used AHP method to develop a comprehensive bridge rating method. Table 2 shows the scales for relative importance values for different criteria proposed by Saaty (1980). The importance intensity values were assigned to the matrix by comparing visual inspection

Table 1 Rating Values for Visual Inspection Data

[RV]	WT	DB (m)	WS (%)	FT	FD (m)	LW (m)	OA (m^2)	TM
1	RM - LB	10 <	0	Raft foundation	2 <	< 5	10 <	Burned clay bricks
2	RM - NLB	5 – 10	0 – 20	Strip foundation	1.5 – 2.0	5 – 8	5 – 10	Cement blocks - Solid
3	URM - LB	0 – 5	20 – 40	Pad foundation	1.0 – 1.5	8 – 10	2 – 5	Cement blocks- Hollow
4	URM - NLB	0	40 <	Random rubble foundation	0 – 1.0	10 <	< 2	Natural masonry/Adobe

factors with reference to the scales for relative importance in Table 1 and categorized in a reciprocal comparison matrix (Equation 1). For an example, both wall type (WT) and distance between buildings (DB) influence on the adequacy of buildings and wall type is more important than the distance between buildings. So, the value 3 was assigned in the matrix. Also, wall type (WT) is more important than percentage of walls facing sea (WS). So, the value 3 was assigned in the matrix.

Table 2 Scales for Relative Importance (Saaty, 1990)

Importance Intensity Explanation	Explanation
1	Equal importance
3	Moderate importance of one over another
5	Strong importance of one over another
7	Very strong importance of one over another
9	Absolute importance of one over another
2, 4, 6, 8	Intermediate values between the two judgments
Reciprocals	Reciprocals for inverse comparison

After assigning the importance intensity values for the matrix, the final weights of visual inspection data (Table 3) were assessed as a normalized eigenvector by dividing each element by the sum of that column and then computing the average of each row that shows the priority weight of the corresponding visual inspection data. Considering an element (i.e., Xij) of a matrix having n rows and columns, the priority weight (i.e., ui) of each category (i.e., ith row) with respect to other elements can be obtained by using the Equation 2.

$$U_i = \frac{\sum_{i=1}^{n} \frac{x_{ij}}{\sum_{j=1}^{n} x_{ij}}}{n} \quad (2)$$

Then the Visual Inspection Factor was derived by using the priority weights of visual inspection data Table 3 as the coefficients. Visual Inspection Factor ranges from 1 to 4.

$$VIF = 0.14\,RV_{WT} + 0.11\,RV_{DB} + 0.06\,RV_{WS} + 0.12\,RV_{FT} + 0.10\,RV_{FD} + 0.23\,RV_{LW} + 0.14\,RV_{OA} + 0.10\,RV_{TM} \quad (3)$$

Where, RV_{WT}, RV_{DB}, RV_{WS}, RV_{FT}, RV_{FD}, RV_{LW}, RV_{OA}, RV_{TM}, RV_{OA}, RV_{TM} are rating values of wall type (WT), distance between adjacent buildings (DB), percentage of walls facing sea (WS), foundation type (FT), Foundation depth (FD), length of walls facing sea (LW), opening area of walls facing sea (OA) and type of the material used to construct walls (TM) respectively. For an example, if RV_{WT} was found to be reinforced masonry-load bearing, then RV_{WT}= 1 and if RV_{FT} was found to be pad foundation, then RV_{FT} = 3.

2.1.2. Casual Factor (CF)

Ratings values and priority weights of casual data were used to determine Casual Factor (CF). Age of the Building (AB), Number of Floors in the building (NF), Density of the Green Belt (GB), Distance between the sea shore and the building (DS), Type/ purpose of the building (TB) and Soil Condition (SC) were the main factors (Suppasri et al. 2012) considered under casual Factor (CF). Rating values were assigned to quantify building conditions based on casual data as shown in Table 4.

Table 3 Priority weights of visual inspection data

Category of Visual Inspection	Priority Weight
Type of the walls facing sea (WT)	0.14
Distance to the nearby building (DB)	0.11
Walls facing sea (WS)	0.06
Foundation type of the building (FT)	0.12
Foundation depth (FD)	0.10
Maximum length of walls facing sea (LW)	0.23
Total area of openings in walls facing sea (OA)	0.14
Type of the material used (TM)	0.10

Table 4 Rating Values for Casual Data

RV	AB	NF	GB	DS (m)	TB	SC
1	Newly built, after Tsunami	1	High	100 <	Residential	Loamy
2	Built before Tsunami, not affected	2	Medium	50-100	Commercial	Sandy
3	Built before Tsunami, slightly affected	3	Low	25– 0	Educational	Clayey
4	Built before Tsunami, severely affected	4 ≤	No	0– 25	Medical	Silty

Rating value "1" represents the best case while rating value "4" represents the worst case. Each and every casual parameter was divided into 4 sub categories and the rating values were defined for each factor considering their qualities. Casual Factor was derived as similar to the derivation of Visual Inspection Factor.

Pair wise comparison of casual details was performed by using AHP and is presented in the reciprocal comparison matrix (Equation 4). Both age of the building (AB) and number

$$\begin{array}{c} \\ AB \\ NF \\ GB \\ DS \\ TB \\ SC \end{array} \begin{array}{c} \begin{array}{cccccc} AB & NF & GB & DS & TB & SC \end{array} \\ \begin{bmatrix} 1 & 3 & 3 & 1/3 & 3 & 1/3 \\ 1/3 & 1 & 3 & 1/3 & 1 & 1/3 \\ 1/3 & 1/3 & 1 & 1/3 & 3 & 1/3 \\ 3 & 3 & 3 & 1 & 3 & 1 \\ 1/3 & 1 & 1/3 & 1/3 & 1 & 1/3 \\ 3 & 3 & 3 & 1 & 3 & 1 \end{bmatrix} \end{array} \quad (4)$$

of floors (NF) are influence on the adequacy of structures against Tsunami. But, age of the building is more important than number of floors in the building and the value 3 was assigned in the matrix. Age of the building (AB) and the density of the green belt (GB) (Kathiresan & Rajendran, 2005) are another two factors influence on the adequacy of buildings. But, age of the building is more important than the density of the green belt. So, value 3 was assigned in the matrix. Likewise, reciprocal comparison matrix was developed. Then the priority weights of casual data were obtained by using equation 2 and listed in the table 5. Then the equation for Casual Factor was derived by using the priority weights of casual data (Table 5) as the coefficients. Casual Factor ranges from 1 to 4.

$$CF = 0.18\ RV_{AB} + 0.10\ RV_{NF} + 0.09\ RV_{GB} + 0.28\ RV_{DS} + 0.07\ RV_{TB} + 0.28\ RV_{SC} \quad (5)$$

Where, $RV_{AB}, RV_{NF}, RV_{GB}, RV_{DS}, RV_{TB}, RV_{SC}$ are rating values of the age of the building (AB), number of floors in the building (NF), density of the green belt (GB), distance between the sea and the building (DS), type/purpose of the building (TB) and soil condition under the building (SC) respectively. For an example, if the age of the building RV_{AB} was found as newly built building after Tsunami, $RV_{AB} = 1$ and if the number of the floors RV_{NF} of the building found to be 3, $RV_{NF} = 3$.

Table 5 Priority weights of casual data

Category of Casual Data	Priority Weight
Age of the building (AB)	0.18
No of floors (NF)	0.10
Density of the Green Belt (GB)	0.09
Distance between the sea and the building (DS)	0.28
Type/purpose of the building (TB)	0.07
Soil condition around the building (SC)	0.28

2.1.3. Building Performance Factor (BPF)

Building Performance Factor (BPF) gives the overall rating value of the building and it was derived by combining Visual Inspection Factor (VIF) and the Casual factor (CF). Since, Visual Inspection Factor adversely affect the adequacy of buildings against Tsunami than the Casual Factor, Visual Inspection Factor has a greater priority value than the Casual Factor. Hence, priority values 0.7 and 0.3 were assigned for VIF and CF respectively.

$$BPF = 0.7\ RV_{VIF} + 0.3\ RV_{CF} \quad (6)$$

Where, RV_{VIF} and RV_{CF} are rating values of Visual Inspection Factor and Casual Factor respectively.

2.1.4. Determination of overall state of the building

Overall Building Condition of the building (OBC) was calculated as a percentage using the Equation 7.

$$OBC = \frac{(HBPF - BPF)}{HBPF} \times 100 \quad (7)$$

Where, OBC is Overall Building Condition, HBPF is Highest value of Building Performance Factor and BPF is Building Performance Factor respectively. In this equation, Highest value of Building Performance Factor (HBPF) acquire when both Casual Factor (CF) and Visual Inspection Factor (VIF) equals to 4, which is the highest value both factors can achieve. Therefore, the highest value which the HBPF can obtain is 4. Table 6 provides the overall states of buildings according to the percentage of Overall Building Condition (OBC).

Table 6 Overall state of the buildings

OBC (%)	Building condition description	Overall state of the building
75 – 100	Condition of the building is very high and the building is adequate for a Tsunami hazard	Good condition
50 – 75	Condition of the building is high and the adequacy of the building is high	Satisfactory condition
25 – 50	Condition of the building is low and some remedial measures can be applied to uplift the level	Poor condition
0 – 25	Condition of the building is very low and remedial measures should be applied to uplift the level	Failure condition

3. RESULT AND DISCUSSION

The obtained results of Visual Inspection Factor (VIF), Casual Factor (CF), Building Performance Factor (BPF) and the Overall Building Condition (OBC) for each building were analysed under this section.

3.1. Evaluation of current condition of existing buildings

Case study - Current condition of building number 49. This building is located in Madampe. In this building, type of the walls facing sea (WT) is reinforced masonry – load bearing (i.e. rating value is 1). The distance between the adjacent buildings (DB) is 11.5 m which is more than 10 m (i.e. rating value is 1). Percentage of walls facing sea (WS) is 15%, which ranges between 0% - 20% (i.e. rating value is 2). Foundation type (FT) is raft foundation (i.e. rating value is 1). Foundation depth (FD) is 2.5 m, which is more than 2 m (i.e. rating value is 1). Maximum length of the walls facing sea (LW) is 6.5 m which ranges between 5 - 8 m (i.e. rating value is 2). Approximate total area of openings facing sea (OA) is 14 m^2 which is more than 10 m^2 (i.e. rating value is 1). Type of the material used to erect walls (TM) is burned clay bricks (i.e. rating value is 1).

According to the casual data (Table 7), Age of the building (AB) is built after Tsunami and slightly affected (i.e. rating value is 3). Number of floors (NF) is 1 (i.e. rating value 1). Density of the green belt is high; where many of the coastal plants were present in 1 m^2 of area (i.e. rating value is 1). The building is situated more than 100 m from the coastal shore line (DS) (i.e. rating value is 1). Type/purpose of the building (TB) is residential (i.e. rating value is 1). Soil Condition (SC) is Loamy (i.e. rating value is 1). Hence, the obtained rating

Figure 1 Building No. 49 (Location - Madampe)

value for the Visual Inspection Factor was 1.29 and the rating value for the Casual Factor was 1.36 and the Building Performance Factor was 1.311. Thus, the Overall Building Condition was 67.23% which ranges between 50% - 75%. So, the overall state of the building no. 49 is "Satisfactory".

Table 8 Summary of the buildings in the Research area

Overall state of the building	No of buildings	Percentage of buildings
Good Condition	0	0
Satisfactory Condition	21	42%
Poor Condition	25	50%
Failure Condition	4	8%

3.2. Implementing a remediation plan for buildings

According to the results obtained, 42% of structures are in the satisfactory condition, 50% structures are in the poor condition and 8% structures are in the failure condition. Therefore, nearly half of the structures should be subjected to immediate retrofitting to improve the current condition of those buildings. For that purpose, a remediation plan which can improve the current condition of buildings should be implemented (Figure 2).

4. CONCLUSIONS

This study aimed to propose a condition assessment and rating method to investigate the adequacy of building structures in the coastal line in Southern Province to withstand Tsunami and to propose remedial measures that can be applied to buildings to reduce the impacts on Tsunami. According to the results obtained, none of the structures were in "Good Condition", 42% of the structures were in "Satisfactory Condition", 50% of structures were in "Poor Condition" and 8% of structures were in "Failure Condition". The building which had the highest overall building condition was building no. 49, which accounted 67.23% and the building which had the lowest overall building condition was building number 10, which accounted 19.03%. Reasons can be identified as inadequate opening areas in walls facing sea, usage of low strength materials to build walls, erection of lengthy walls which are facing sea, inadequate foundation depths, usage of inappropriate foundation types without considering the soil type, erection of buildings with walls facing sea, erecting of buildings with low distance between adjacent buildings, erection of buildings which are so close to the sea, inadequate thickness of green belt, inappropriate number of floors in the buildings, unsuitable soil condition in the area etc. In general, many of the above-mentioned reasons have been caused for the reduction of overall building conditions of most of the coastal buildings in the research area. Therefore, when erecting new buildings in the coastal region, above mentioned facts should be taken into account to build a structurally safe building against Tsunami disaster

Finally, remedial measures were proposed for buildings which are in satisfactory, poor, and failure conditions to improve their overall building conditions (Figure 2). In order to improve the overall building conditions of the buildings in poor and failure conditions, building elements or buildings should be partially or fully replaced.

Table 7 Evaluation of current condition of building no. 49

Structure	Visual Inspection Data								Casual Data						VIF	CF	BPF	OBC (%)
	WT	DB	WS	FT	FD	LW	OA	TM	AB	NF	GB	DS	TB	SC				
49	1	1	2	1	1	2	1	1	3	1	1	1	1	1	1.29	1.36	1.311	**67.23**

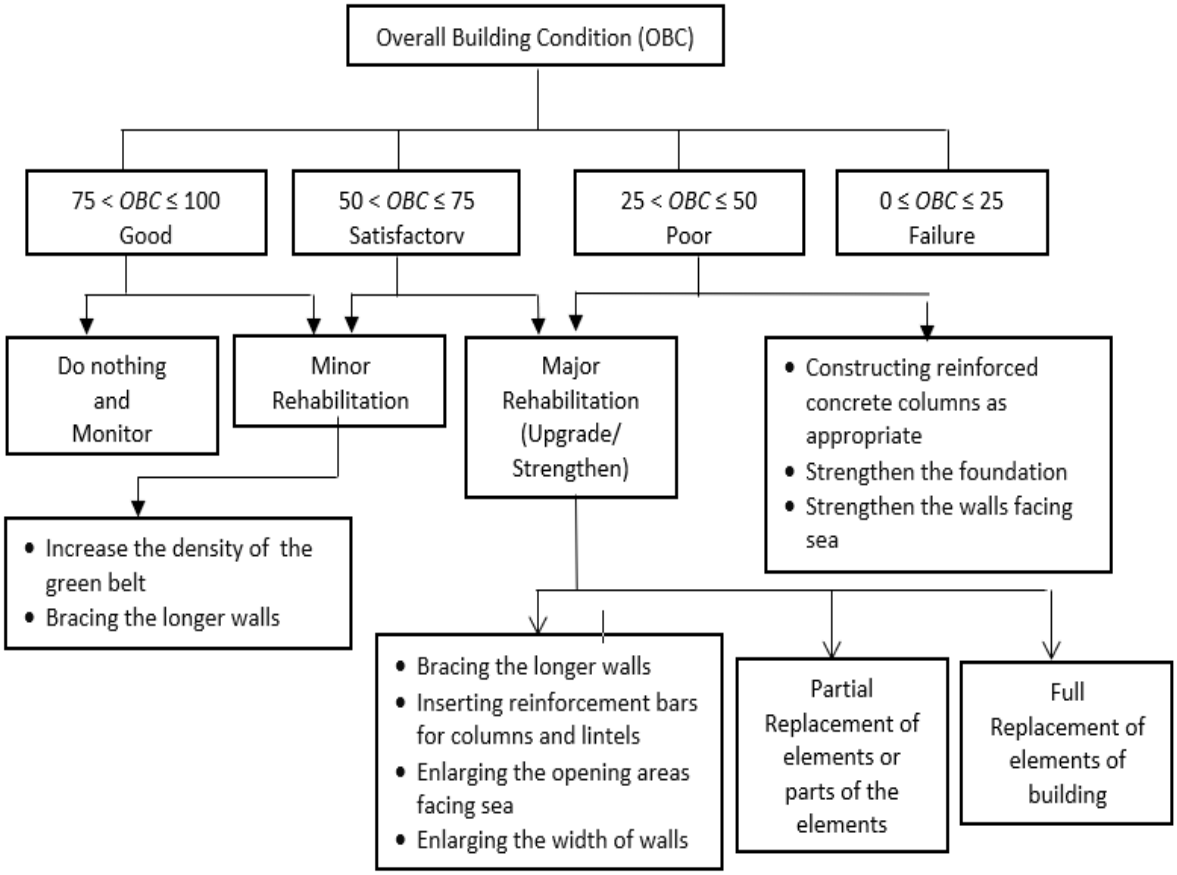

Figure 2: Proposed Remediation Plan

5. ACKNOWLEDGEMENT

Authors would like to express their gratitude to Department of Civil Engineering, Faculty of Engineering, General Sir John Kotelawala Defence University for providing support throughout the period of research.

6. REFERENCES

Kathiresan, K. & Rajendran, N., 2005, 'Coastal mangrove forests mitigated tsunami, Estuarine', *Coastal and Shelf Science*, 601-606.

Mendis, W.S.W., Sudhira De Silva & Subashi De Silva G.H.M.J., 2014, 'Performance and Retrofitting of Unreinforced Masonry Building against Natural Disasters – A Review Study', "ENGINEER", *Journal of the Institution of Engineers, Sri Lanka (IESL)*, Vol. XLVII (3), 71-82.

Pushpakumara, B.H.J., Sudhira De Silva & Subashi De Silva, G.H.M.J., 2013, ,Investigation on Efficiency of Repairing and Retrofitting Methods for Chloride induced Corrosion of Reinforced Concrete Structures,, "*ENGINEER", Journal of the Institution of Engineers, Sri Lanka (IESL)*, Vol. XXXXVI, No. 04, 19-30.

Pushpakumara, B.H.J., Sudhira De Silva & Subashi De Silva, G.H.M.J., 2017, 'Visual Inspection and Non-Destructive Tests-based Rating Method for Concrete Bridges', *International Journal of Structural Engineering*, 8(1), 74-91.

Saaty, T., 1990, 'How to make a decision: The Analytic Hierarchy Process', *European Journal of Operational Research.*

Suppasri, A., Shuto, N., Imamura, F., Koshimura, S., Mas, E., & Yalciner A.C., 2012, 'Lessons Learned from the 2011 Great East Japan Tsunami: Performance of Tsunami Countermeasures, Coastal Buildings, and Tsunami Evacuation in Japan', *Journal of Pure and Applied Geophysics*, 170, (6–8), 993–1018

Wasundara Mendis, W.S., De Silva, G.S.Y. a& Subashi De Silva, G.H.M.J., 2019, 'Performance of Un-Reinforced Burned Clay Brick Masonry Walls Retrofitted with Locally Available Materials', *Journal of the National Science Foundation Sri Lanka*, 47(1), 29-38.

Proceedings of the 7th International Symposium on

Advances in Civil and Environmental Engineering Practices for Sustainable Development

ACEPS - 2019

Investigation on flexural performance of heavily cracked concrete beams strengthened with CFRP

H.A. Dissanayake[1], P.D. Dharmaratne [1], M.A.L. Silva[1], J.C.P.H. Gamage[1]

[1]Department of Civil and Environmental Engineering, Faculty of Engineering, University of Moratuwa, SRI LANKA

K e y w o r d s

CFRP sheets
End anchors
Flexural capacity
Intermediate anchors
Pre-cracked concrete beams

A B S T R A C T

The flexural behavior of pre-cracked reinforced concrete beams strengthened with Carbon Fiber Reinforcement Polymer (CFRP) arrangements was investigated. A total of eight reinforced concrete beams with dimensions of 125 mm × 200 mm × 1900 mm were tested. Three different arrangements of CFRP; non- end anchored CFRP sheet, end anchored CFRP sheet and CFRP sheet with end and intermediate anchors at cracked locations were considered. Beams were tested in accordance with ASTM C78 guidelines. Four-point bending test was carried out. The observed flexural strength gain was in the range between 15 % to 68 % in CFRP strengthened arrangements with respect to non-strengthened specimens.

1. INTRODUCTION

Structures are designed to have longer life span. It may not have the desired design life due to vary demand, errors in the design process and the construction stage, environmental deterioration; corrosion, cracks, loss of section and structural damage. Therefore, retrofitting of the structures is a timely need. In early stages, steel plates had been popular as external strengthening material. MacDonald and Calder (1982) identified that this will improve stiffness, ultimate load and also will control the cracks. However, there were many drawbacks with the use of steel plates. One of them is the requirement of special equipment to install heavy steel plates. The corrosion of steel plates along the adhesive material result in reduced bondage between steel plates and concrete. Therefore, necessity of new alternative materials has arisen. Nowadays Fiber Reinforced Polymer (FRP) materials are widely used in civil engineering constructions. These materials can be used to strength the structures made out of reinforced concrete, pre-stress concrete, steel, timber and also masonry. Among these materials Carbon Fiber Reinforced Polymer (CFRP) has become more popular due to its high strength to weight ratio, resistance to corrosion, low thermal expansion, good fatigue performance and ease of application (Ding 2014).

The most common types of failures of concrete beams occur due to exceedance of flexural capacity or shear capacity. Many experiments have been carried out to identify various aspects of failure modes of non-cracked CFRP strengthened concrete beams.

Researchers have also proved that the application of CFRP will increase flexural capacity in large scale (Norris *et al* 1997). Then the attention was paid on factors affecting the strength in order to find most economical solutions. One of the parameters was length of the CFRP used at the tension face of the member (Balamuralikrishnan & Jeyasehar 2009). Investigations showed experimentally and numerically about the thickness and length of CFRP on re-paired reinforced concrete beams and identified that there is a limit and beyond that CFRP will not increase the strength and stiffness of the member (Li *et al* 2006)

Majority of the research studies were carried out regarding strengthening of un-cracked concrete beams in flexure (Ashour *et al* 2004) But, a few have addressed about

strengthening of pre-cracked concrete beams with CFRP. In general, heavily cracked or deflected beams replaced with new beams rather than strengthening. However, strengthening is a sustainable and economical solution. Proper investigation should be carried out to determine the performance of pre-cracked concrete beams strengthened with CFRP for flexure. This research study is focused on the behavior of pre-cracked concrete beams retrofitted with CFRP materials.

2. MATERIALS AND SPECIMEN PREPARATION

2.1. Material properties

A total of eight, medium scale reinforced concrete beams were prepared using grade 30 concrete. Measured average 28th day compressive strength of concrete was 30 MPa. Deformed steel bars with the yield strength of 500 MPa were used for reinforcements.

The cracked areas of beams were repaired using an industrially used epoxy grout and it was injected through the cracks to provide the required bond between two concrete faces. The properties of grout are listed below in Table 1.

Normal modulus CFRP sheets were used to strength cracked concrete beams (Table 2). Carbon content of the CFEP was 300 g/m^2. The bond between CFRP sheet and sand blasted concrete surface was created using two-part epoxy adhesive to transfer the stresses between CFRP reinforcement and concrete. The strengthened beams were kept more than 7 days before testing.

Table 1 Epoxy grout properties

Property	Typical results		
Compressive strength	24 hours 60MPa	3 days 65MPa	7 days 85MPa
Tensile strength	-	-	50Mpa
Flexural strength	-	-	60MPa

Table 2 Material properties of CFRP sheets

CFRP Sheet		Adhesive	
Technical data	value	Technical data	value
Elastic modulus (GPa)	240	Density (kg/Liter)	1.1
Tensile strength (MPa)	4300	Mix ratio by weight (resin to hardener)	2:1
Elongation at rupture (%)	1.7	Tensile strength after 14 days (MPa)	38.5
Design thickness	0.168	Elongation at break after 14 days 2.3%	
Weight per unit area of sheet (g/m^2)	330		

2.2. Specimen Preparation

Eight reinforced concrete beams with dimensions of 125 mm × 200 mm × 1900 mm were cast. Reinforcement details are shown in Figure 1. All steel reinforcement including shear links and longitudinal reinforcement were provided with mild steel.

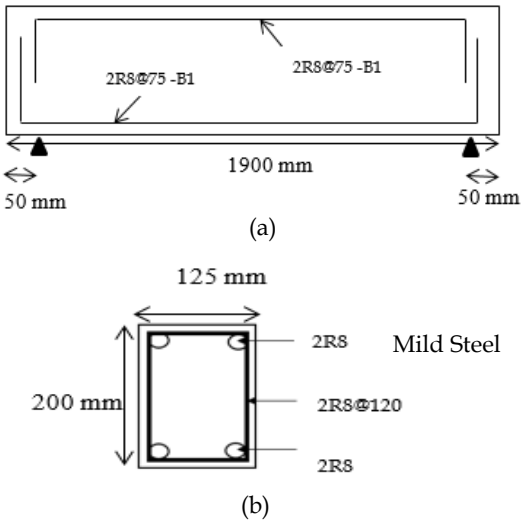

Figure 1 Steel reintorcement details (a) Longitudinal section (b) Cross section

Out of eight reinforced concrete beams six beams were loaded using Amsler loading machine according to ASTM C78 2018 in order

to achieve the pre-cracked condition. Load was applied at the mid span of each beam and the beams were supported at two ends 50 mm away from each discontinuous edge as shown in Figure 2. Beams were loaded until 0.3 mm wide cracks appeared at the bottom of the mid span. Deflection at the mid span was recorded using two dial gauges. Then the beams were unloaded.

Crack repairing was done using the epoxy grout. Cracks were drilled using a drilling machine. Three sides of each beam on crack surface and injection packers were fixed in to drilled holes as shown Figure 3. Then the cracks were sealed the surface of the crack with the epoxy (Figure 4) and allowed to cure for 12 hours. Injected the resin using injector and allowed to cure for 24 hours before strengthening.

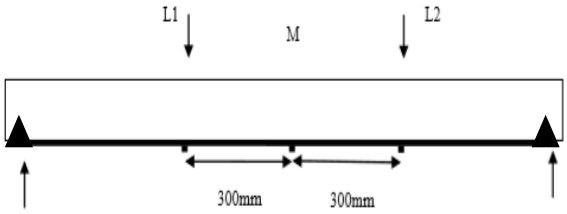

(a)

(b)

Figure 2 Test Set-up (a) Schematic diagram (b) Instrumentation

Before applying CFRP strengthening scheme on the concrete directly, concrete substrate should be prepared to enhance the bond between adhesive and concrete to ensure the maximum strength enhancements by delaying the de-bonding or delamination of CFRP system which leads to premature failure of the system. Sand blasting technique was used to prepare the substrate to be strengthened (Figure 5).

Figure 3 Fixing of injection packers

Figure 4 Crack filled beams

Figure 5 Sand blasting of beams

In sand blasting technique, Silica particles were injected under high pressure on to the beam surface to remove the outer cement grout surface of concrete beams to get a rough surface as necessary for the application of CFRP strengthening scheme. Sand blasting was done on three sides of each beam. Table 3 shows different bonding arrangements used in this test program. All end anchor wraps were of 500 mm in width. The schematic diagrams for the listed configurations in Table 3 are shown in Figure 6.

Table 3 Specification details

Design	Arrangement	Descriptions	Number of samples
S1	Fig 2- 6(a)	Non-cracked beams, CFRP at tension face	2
S2	Fig 2- 6(b)	Cracked beams, CFRP at tension face	2
S3	Fig 2- 6(c)	Cracked beams, CFRP at tension face with end anchors	2
S4	Fig 2- 6(d)	Cracked beams, CFRP at tension face with end and intermediate anchors at cracked places	2

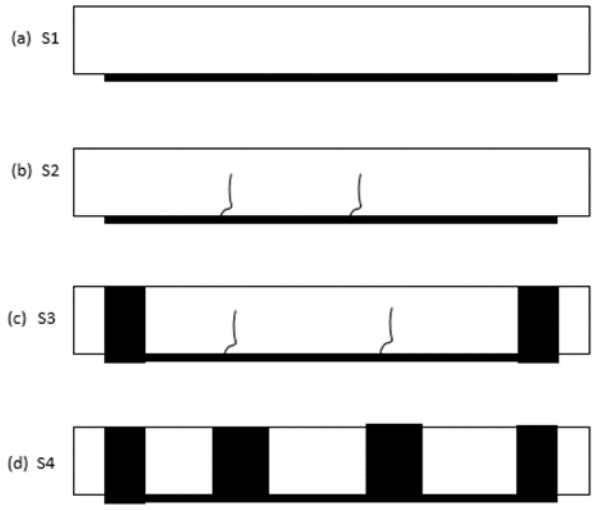

Figure 6 Strengthening arrangements

3. RESULTS AND DISCUSSION

3.1. Flexural Capacity

Six reinforced concrete beams were tested as non-CFRP strengthened control specimens. Load at 0.3 mm crack initiation was measured and listed in Table 4. The crack propagation from the tension surface of a beam is indicated in the Figure 7. The average load carrying capacity when the 0.3 mm wide crack occurrence of a control beam was 12.6 kN and that is nearly 87% of the average ultimate failure load. The load versus deflection curve for each non-strengthened control beams are shown in Figure 8.

Figure 7 Control beams with 0.3 mm cracks

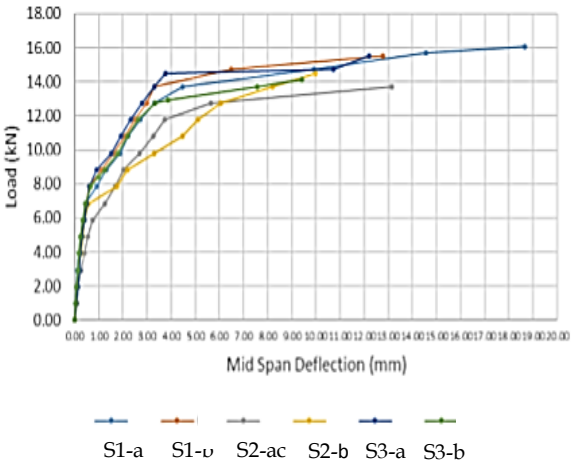

Figure 8 Load versus Deflection of non-strengthened non-cracked beams

After testing all six control beams, they were strengthened with CFRP as indicated in Figure 6 and tested along with non-cracked CFRP strengthened specimen. The failure loads were measured during the testing program. The results are listed in Table 5 and the test series conducted had shown that the application of CFRP on the tension face can increase flexural capacity of both un-cracked and pre-cracked beams drastically. When compared to none CFRP strengthened beam, a non-cracked CFRP strengthened beam showed an average flexural capacity increment of 23%.

Table 4 Failure loads of control beams

Specimen	Load at 0.3 mm cracks (kN)		Average Load at crack 0.3 mm (kN)	Ultimate Load at Failure (kN)		Average ultimate Load at Failure (kN)
S2	12.95	14.72	13.84	15.5	14.7	15.10
S3	14.72	14.72	14.72	16.09	14.5	15.30
S4	10.79	7.85	9.32	13.73	14.5	14.12

Table 5 Failure loads of CFRP strengthened beams

Specimen	Load at 0.3mm Cracks (KN)		Average Load at 0.3 mm Crack (kN)	Failure Load (kN)		Average Failure Load (kN)	Percentage Increment in Load w.r.t. its Non-Strengthened Control Beam		Mid span Deflection at Failure (mm)
S1	16.7	19.6	18.15	17	20	18.5	-	-	5
S2	18.63	27.47	23.05	23	23	23	48.39%	56.46%	5.2
S3	18.63	27.47	23.05	18.5	23	20.7	14.98%	58.62%	6
S4	25.5	13.73	19.61	23	14	18.5	67.52%	-3.45%	5

Further, it has to be noticed that the cracked specimens strengthened with CFRP showed a flexural capacity increment around 24% compared to non-cracked CFRP strengthened specimens. This may be because of the additional strength provided to the damaged beam in the process of crack repairing. Altogether, cracked specimens strengthened with CFRP had shown a maximum flexural capacity increment of 56%.

The cracked specimens retrofitted with both CFRP attached on tension face and end anchors (S3) indicated a flexural capacity increment of 59%. The specimens with additional CFRP wraps at heavily cracked locations (S4) showed an increase of flexural capacity up to 67%. Therefore, it is clear that the provision of CFRP end anchor wraps to support for flexural CFRP reinforcement has contributed by avoiding end debonding (Table 6). Further, the provision of additional CFRP wraps at heavily cracked locations improves the flexural capacity due to the provision of additional strength to resist flexure by delaying the reopening of cracks.

3.2. Load versus Deflection

Deflection at loaded points and mid-span were measured. The location of dial gauges is shown in Figure 9 mentioning D1, D2 and D3. When beams were strengthened with CFRP sheets it has shown increase of deflection over 50%. Results further emphasize that under the same load strengthened beams have lower deflection compare to un-strengthened beams even though they were heavily cracked.

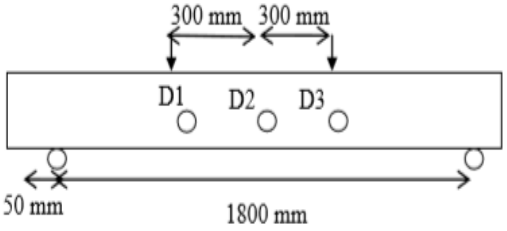

(a)

(b)

Figure 9 Location of dial gauges (a) schematic diagram (b) practical installation

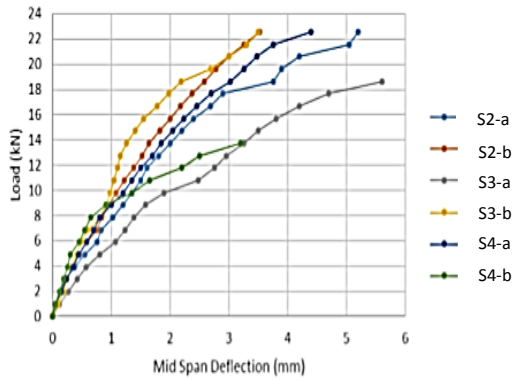

Figure 10: Load versus Deflection behavior of pre-crakced CFRP strengthened beams

According to the results maximum deflection in pre-cracked strengthened beams are higher than that of un-cracked strengthened beams. Under the same load, un-cracked beams have shown lower deflec-tion than cracked ones when strengthened with CFRP (Figure 10).

3.3. Failure mode and crack propagation

All beams were strengthened using externally bonded method. Observed failure mechanism was de-bonding of CFRP sheet. This type occurs due to the initiation of cracks which spread through the boundaries result in loss of composite action between the bonded CFRP and the reinforced concrete member. At the failure of each strengthened specimen, debonding of CFRP was observed as listed in the Table 6. In specimen type S1 and S2, the end anchor debonding was observed (Figure 12). This indicates that the provision of end anchorages at suitable locations may enhance performance.

Flexural cracks were observed before the failure of all CFRP strengthened and non-strengthened specimens. The typical propagation of cracks at the failure is shown in Figure 11.

Table 6 Failure modes

Beam	Failure mode
S1 (1)	End CFRP de-bonding
S1 (2)	End CFRP de-bonding
S2 (1)	End CFRP de-bonding
S2 (2)	End CFRP de-bonding
S3 (1)	CFRP de-bonding (initially u wraps)
S3 (2)	CFRP de-bonding (initially u wraps)
S4 (1)	CFRP de-bonding

Figure 11 Cracks of strengthened pre-cracked beams (a) S2 (b) S3 (c) S4

The most dominant failure mode observed was end delamination, that caused for premature failure. Initiation of shear cracks at the end of bondline due to concentration of shear stress may cause for end delamination. The same phenomenon had been observed from non-cracked beams strengthened with CFRP.

Figure 12 De-bonding of CFRP

4. CONCLUSION

This study was carried out to monitor the behavior of heavily cracked reinforced concrete beams retrofitted with externally applied CFRP strips. Three alternative CFRP bonding arrangements of CFRP were used to strengthen heavily cracked beams. Following conclusions were drawn.

- Heavily cracked reinforced concrete beams strengthened with CFRP indicated improved performance of

beams in terms of load carrying capacity, stiffness and ductility.

- The beam specimens with external CFRP attached at the tension face with additional CFRP wraps provided at crack opened locations increase their load carrying capacity up to a maximum of 68% with respect to non-strengthened non-cracked control beams. Therefore, the pro-vision of CFRP wraps at repaired locations is more effective in increasing flexural capacity.
- Pre-cracked reinforced concrete beams strengthened with CFRP indicated evenly distributed cracks along the span.
- If flexural damaged area of a pre-cracked beam is repaired accurately, a higher flexural capacity could be achieved compared to its non-cracked stage with strengthening using CFRP technology.

5. ACKNOWLEDGMENTS

Authors would like to extend their gratitude to the technical officers, Mr. D.M.N.L. Dissanayake and Mr. Roshan at Structural Testing Laboratory and Building Material Laboratory; and staff at Structural Testing Laboratory, Department of Civil Engineering, University of Moratuwa.

6. REFERENCES

Ali, N., Samad, A., Mohamad, N. and Jayaprakash, J., 2013, 'Shear Behaviour of Pre-cracked Continuous Beam Repaired using Externally Bonded CFRP Strips', *Procedia Engineering*, 53, 129-144.

Li, L., Guo, Y., Liu, F. and Bungey, J., 2006, 'An Experimental and Numerical Study of the Effect of Thickness and Length of CFRP on Performance of Repaired Reinforced Concrete Beams', *Construction and Building Materials*, 20(10), 901-909.

Macdonald, M. & Calder, A., 1982, 'Bonded Steel Plating for Strengthening Concrete Structures', *International Journal of Adhesion and Adhesives*, 2(2), 119-127.

Ashour AF, El-Refaie S.A. and Garrity, S.W., 2004, 'Flexural strengthening of RC continuous beams using CFRP laminates', *Cement & Concrete Composites*. 26, 765-775.

Balamuralikrishnan, R. & Jeyasehar, C.A., 2009, 'Flexural Behavior of RC Beams Strengthened with Carbon Fiber Reinforced Polymer (CFRP) Fabrics', *TOCIEJ*, 3.1, 102-109.

Ding, J., 2014, 'The Effect of CFRP Length on The Failure Mode of Strengthened Concrete Beams', *Polymers*, 6.6, 1705-1726.

Proceedings of the 7th International Symposium on

Advances in Civil and Environmental Engineering Practices for Sustainable Development

ACEPS - 2019

Lime stabilization for compressed stabilized earth blocks with reduced clay and silt

S.N. Malkanthi[1], N. Balthazaar[1] and A.A.D.A.J. Perera[2]

[1]Department of Civil and Environmental Engineering, Faculty of Engineering, University of Ruhuna, Hapugala, Galle, SRI LANKA
[2]Department of Civil Engineering, University of Moratuwa, SRI LANKA

K e y w o r d s

Compressed Stabilized Earth blocks
Lime Stabilization
Lime : Cement Combined Stabilization

A B S T R A C T

Compressed Stabilized Earth Blocks (CSEB) are comparatively new earth-based material among others like rammed earth, adobe, bricks. The most common stabilizers used for CSEB production are cement and lime. Lime is environmentally friendly than cement. This study aims to find the suitability of lime and lime: cement combination as the stabilizer for CSEB production with reduced clay & silt. The soil selected for this study is modified to get the clay & silt content as 5%, 10%, and 15%. River sand was used to change the clay & silt content of the soil. 5%, 10% and 15% lime were used as the stabilizer. Stabilized blocks were tested for dry density, water absorption, 28 days wet and dry compressive strength and compared with SLS 1382 standards. Cement stabilized blocks with 10% and 8% cement were prepared for comparing purposes. The study showed that lime alone did not give sufficient properties as in SLS 1382. Out of the lime percentage used, 10% shows the maximum performance; hence this optimum percentage of lime replaced by the cement of 3%, 5%, and 7%. Lime stabilized blocks can be used for single-story buildings while the combined stabilizer helped to get higher compressive strength compared to others. Other properties of CSEB are also satisfied with all the specification value. Grade 2 blocks strength was achieved by 15% and 10% clay & silt content soil blocks with 5% lime: 5% cement combined stabilizer and 5% clay & silt contented soil blocks with 3% lime: 7% cement combined stabilizer.

1. INTRODUCTION

The masonry constructions were introduced in the Mesopotamians civilization period (c.5000-3500 BCE). At that time bricks and alluvial deposits were used for their construction purposes (Deboucha and Hashim 2011). Nowadays also bricks are the most common building material used for masonry construction. The Department of Census & Statistics says, in Sri Lanka, approximately 6.09 billion bricks were used in 2015 for construction works (Department of Census & Statistics 2016). Compressed Stabilized Earth Blocks (CSEB) are newly introduced blocks due to the problems identified in the fired clay bricks. The major issue regarding the bricks is CO_2 emission during the manufacturing process of bricks and it leads so many environmental problems such as acid rain, global warming, etc.

Unfired bricks need lesser energy than the fired bricks and the CO_2 emission to the atmosphere is 80% less than the fired bricks (Nagaraj *et al*. 2014). When CSEB are used, CO_2 emission can be controlled and the adverse effects on the environment can be reduced. Also, the manufacturing cost of the unfired brick is comparatively low with fired brick (Nagaraj *et al*. 2014). CO_2 and energy emission comparison between different types of bricks is shown below Table 1.

Table 1 Energy emission comparison between different types of bricks

Type	Initial Embodied Energy per m^3 of Wall	Pollution Emission (Kg of CO2) per m^3 of Wall
CSEB wall	631 MJ / m3	56.79 Kg / m3
Kiln Fired Brick	2,356 MJ / m3	230.06 Kg / m3
Country Fired Brick	6,358 MJ / m3	547.30 Kg / m3

(Source: www.earth-auroville.com)

Normally most of the soil types have lack of strength, durability, and stability in natural; the properties are improving by using both mechanical and chemical stabilization in compressed stabilized earth blocks (Walker 1995). Commonly used chemical stabilizers are cement, lime, waterproof agents, chemical binders, bitumen, asphalt and natural and industrial by-products (Walker 1995).

Lime and cement are the most common stabilizers used for the stabilization of the compressed stabilized earth blocks manufacturing (Deboucha and Hashim 2011). Lime is used from ancient times as an earth stabilizer (Bell 1996) and also used for CSEB manufacturing nowadays (Raheem *et al*. 2010). Cement is the most popular stabilizer for the earth blocks stabilization, but in the manufacturing process of cement, CO_2 emission is high, which is globally 5% (Alavez-Ramirez *et al*. 2012). Compared to cement with lime, energy and pollution (CO_2 emission) is high for cement that is given in Table 2 for $1m^3$ material (Alavez-Ramirez *et al*. 2012). Therefore lime was selected as the stabilizer for this study.

Table 2 Energy emission in production of cement and lime blocks (Alavez-Ramirez *et al*.2012)

Material	CO_2 emission (kg)	Energy emission (MJ)
Cement	73	772
Lime	54	583

1.1. Role of Lime Stabilization

Stabilization is used to improve the properties of CSEB blocks (Bell 1993).

Lime is the very oldest material used in soil stabilization. When lime is added to the clayey soil, soil properties are changing. According to Bell's explanation, when the calcium ion in lime reacts with clay soil, metallic ion and cation exchange between them is occurring. Because of that clay particle is surrounded by a diffuse hydrous double layer. Due to this layer, electrical density will change around the particle and it makes the particle closer and makes flocks that called flocculation. This is the primary influence for the change of engineering property of the lime-treated clay soils.

In past researches a different range of lime percentages was used as a stabilizer, Alavez-Ramirez *et al* (2012) used lime alone, the lime combination with sugarcane bagasse ash (SBA) and cement alone for the stabilization of the CSEB. Sandy soil was used for CSEB production. The plasticity index and the liquid limit for the soil were 12% and 25.28% respectively and clay percentage and silt percentage of the soil were 23.1 and 4.3. Alavez-Ramirez *et al* (2012) used 10% lime without SBA and got 28days dry compressive strength as 16.5 Mpa, for cement 10% 23.5 Mpa compressive strength was achieved. Raheem *et al* (2010) used laterite soil sample for lime stabilization with 5-25% lime, the highest 28 days compressive strength was achieved as 1.25 Mpa for 10% lime. Guettala *et al* (2002) used 8% lime as the stabilizer and changed the sand percentage between 0- 40. For 40% sand (clay 21.6%) 15 Mpa dry compressive strength and 5 Mpa wet compressive strength was obtained. Bell (1996) used 0-10% lime as the stabilizer and the result was obtained as the optimum percentage of lime in the range between 4 - 6. Ngowi (1997) used 0-15% lime as a stabilizer and got the optimum percentage as 15. Akpokodje (1985) used the different types of soil with different clay and silt percentages and used lime as the stabilizer. Lime percentage was selected as 0-12 and optimum percentage of the lime for 41%, 85%, 64%, 30%, 29% clay and silt are 10%, 12%, 6%, 12%, 12% respectively. Bogas *et al* (2018) indicated from the past research review 6-12% lime is the advantage average percentage.

1.2. Role of Lime Combined with Cement as Stabilizers in CSEB

Nagaraj *et al* (2014) used cement and lime combination for stabilized CSEB. The lime is replaced in the cement percentage to improve the long-term strength compared with using cement alone. The combination used as 6% cement: 2% lime and 4% cement: 4% lime. A high strength was obtained at the proportion of 4% cement: 4% lime combination in the long term. When using the combination of cement and lime, it was very useful because cement will be stabilized the sand portion and lime will be stabilized clay portion due to this strength and durability will be increased (Nagaraj *et al*. 2014). Rahman *et al* (2016) used two types of soil with 70% clay, 25% silt, 5% sand and 75% sand, 15% silt 10% clay. Two blocks were prepared for 6 and 8 percentage of lime for clay soils, three blocks were prepared for 4, 6 and 8 percentage of cement for sandy soil, four blocks were prepared for 4, 6, 8 and 10 percentage of cement. Also 6% cement:3% lime and 6% cement:5% lime blocks were prepared for modified soil samples with 70:30 clay and sand ratio. 6% cement:3% lime combination and 6% cement:5% lime combination produced optimum compressive strength as 5.2 N/mm^2.

1.3. Objectives of the Study

There are many types of researches, conducted with different stabilizers for CSEB. The suitability of those stabilizers for soil with low clay & silt (less than 15%) is still a researching area. The aim of this research is to find the feasibility of using lime as a stabilizer for CSEB production with low clay & silt content soil as a sustainable construction material. The objectives of this research are to determine the optimum percentage of lime as a stabilizer in CSEB, and replace the optimum lime percentage with cement as a part of the stabilizer to enhance the properties of CSEB.

2. METHODOLOGY

2.1. Materials

In this study, soil, sand, lime, and cement were used to make CSEB. The soil was obtained from nearby draw pit in Happugala, Galle, Sri Lanka. The geotechnical analyses were done for the soil to determine the characteristics of the soil. According to ASTM C136-06 Sieve analysis test and according to the ASTM D4318 Atterberg limit test were conducted to identify the particle size distribution and plasticity index. Wet sieve analysis as per ASTM 117 was conducted to identify the clay & silt (finer) content accurately. Clay & silt content was obtained as 17.7%. Specific gravity test also was performed to identify the physical property of soil. The physical properties of the soil and sand are shown in Table 3. River sand was used to modify the finer percentage of the soil. Sieve analysis for three modified soil samples with finer 5%, 10% & 15% and the original soil sample are shown in Figure 1. Combinations of the sand and soil by weight are shown in Table 4.

Table 3 Physical properties of soil and sand

Properties	Soil	Sand
Plastic limit (%)	26.3	-
Liquid limit (%)	37	-
Plasticity index (%)	10.7	-
Specific gravity (%)	2.49	2.58
Clay and silt (%)	17.75	0.04

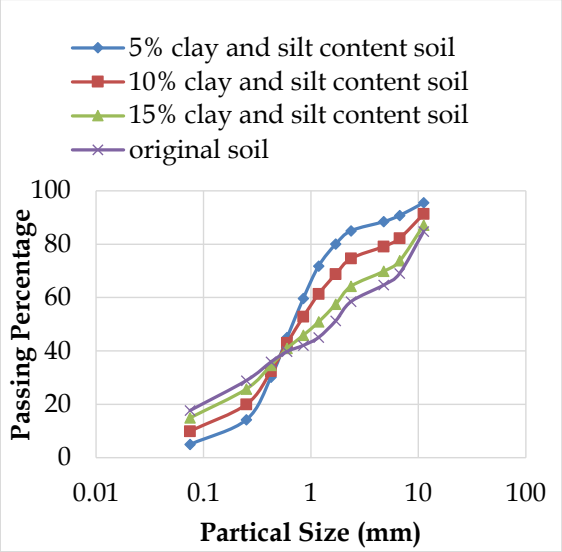

Figure 1 Sieve analysis for Modified soil and Original soil sample

Table 4 Combination of soil and sand percentage for modified soil

Percentage of silt & clay in modified soil	Soil percentage	Sand percentage
15	84.1	15.9
10	55.3	44.7
5	26.5	73.5

Both lime and combination of lime and cement were used to stabilize the blocks. Cement stabilized blocks were used to compare the results. Ordinary Portland cement was used with the percentage of 10 and 8 by weight. Lime was added to each modified soil samples with 5%, 10% and 15% by weight and also optimum lime percentage (10%) replaced by cement with 3%, 5% and 7% to each modify soil samples to make CSEB specimens.

2.2. Manufacturing of the Test Blocks

First, the modified soil sample was prepared by mixing dry soil and river sand. Then the stabilizer was added into the modified soil sample at dry state. The concrete mixture was used to mix the components. Then gradually water was added to the mix up to the optimum level. The optimum level of the water was ensured by the drop test according to SLS 1382 part 2. In each proportion, 9 blocks were cast. Moulds were used for the block casting with the dimension of (150 ×150 ×150) mm. The mix was put into the mould by 3 layers and every layer was compacted by the steel rod with 35 blows. The prepared blocks were cured for 7 days on the damp proof floor by gunny bag. Figure 2 shows the soil mixture and cast blocks.

Figure 2 Soil mixture and cast bocks.

2.3. Testing of blocks

All the blocks were tested according to the SLS 1382 part 2. Blocks for the testing were randomly selected from the block series. Dry density, water absorption and compressive strength at dry and wet state were determined to identify the property of the blocks. Tests were conducted at 7days and 28days period. For the dry compressive strength test and dry density test oven dried (24 hours 105^{o}C) blocks were used and for the wet compressive strength test and water absorption test 24 hours immersed samples were used.

3. RESULTS AND DISCUSSION

3.1. Compressive Strength

When considering the lime stabilization, 10% lime achieved the optimum strength among the lime percentages (5%,10%, and 15%). 28 days dry compressive strength achieved as 1.7 N/mm^2 for 15% finer contained soil blocks. 1.6 N/mm^2 was reported for both 10% and 5% finer contained soil blocks. Figure 3 shows the 28 days dry compressive strength variations for lime and cement stabilization. But for the combined stabilization, for 15% and 10% finer contained soil blocks 5% lime: 5% cement combined stabilizer achieved greater compressive strength as 4.0 N/mm^2 and 5.5 N/mm^2 respectively. For 5% finer soil blocks, 7% cement: 3% lime combined stabilizer achieved greater strength as 4.1 N/mm^2. Figure 4 shows the 28 days dry compressive strength variation for combined stabilizers, 10% lime stabilizer and 10% cement stabilizer.

For the lime stabilization, when the finer percentage increased, 28 days compressive strength also increased. Considering the cement stabilization when the finer content got to increase, 28 days dry compressive strength got to decrease. 28 days dry compressive strength for the lime stabilization is less than cement stabilization. But combined stabilizer stabilization achieved the 28 days dry compressive strength greater than the cement stabilization and lime stabilization. Also, lime stabilization and cement stabilization didn't achieve the 28 days dry

compressive strength greater than the minimum specification value in SLS 1382 (2.8 N/mm²).

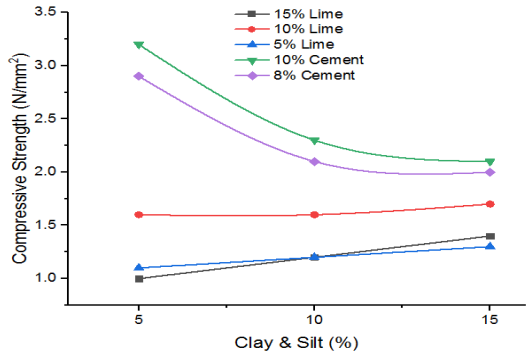

Figure 3 28 days Dry compressive strength variation for lime and cement stabilization

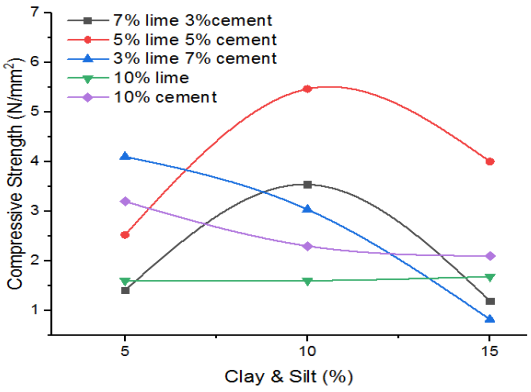

Figure 4 28 days Dry compressive strength variation for combined stabilizer, 10% lime stabilizer and 10% cement stabilizer

The combined stabilizer achieved the compressive strength greater than the specification value. For 15% and 10% finer soil blocks, when the cement percentage got to increase in combined stabilizer 28 days dry compressive also got to increase up to 5% cement: 5% lime combined stabilizer then got decrease to 7% cement: 3% lime combined stabilizer. For 5% finer soil blocks when cement percentage got to increase in combined stabilizer compressive strength also got increase. For the 10% finer content soil blocks, all the combined stabilization achieved the compressive strength greater than the specification value.

For the lime stabilization, 28 days wet compressive strength values for every finer percentage soil blocks are less than or equal to 0.5 N/mm². But the cement stabilization achieved the wet compressive strength greater than the lime stabilization and 10% cement stabilization achieved the 28 days wet compressive strength greater than the specification value (1.2 N/mm²). Combined stabilizers achieved the 28 days wet compressive strength variation same as 28 days dry compressive strength. The optimum 28 days wet compressive strength achieved at the optimum percentage as per the 28 days dry compressive strength. Also, these values are greater than the specification value. Same as 28 days dry compressive strength, 10% finer contained soil blocks achieved the wet compressive strength greater than the specification value for all combined stabilization. Figure 5 shows the 28 days wet compressive strength variation for lime and cement stabilization and Figure 6 shows the 28 days wet compressive strength variation for combined stabilizer, 10% lime stabilizer and 10% cement stabilizer.

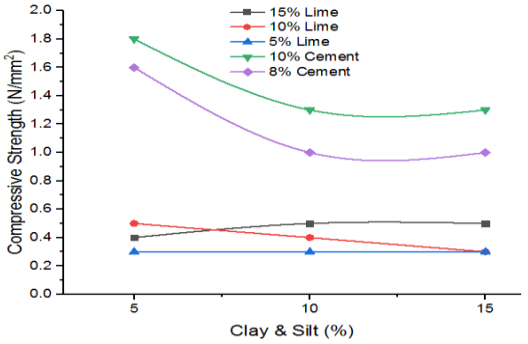

Figure 5 28 days wet compressive strength variation for lime and cement stabilization

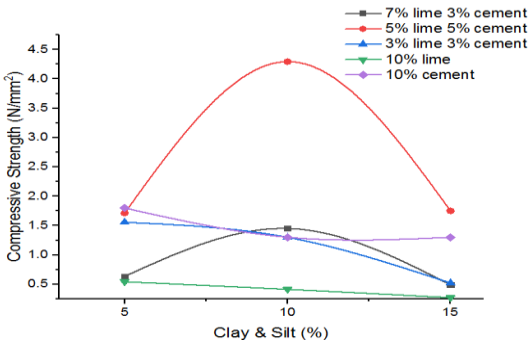

Figure 6 28 days wet compressive strength variation for combined stabilizer, 10% lime stabilizer and 10% cement stabilizer

3.2. Water Absorption

Water absorption is increased with the finer content for all stabilization. For the 15% finer soil, 10%, 5% lime stabilizer and 5% lime:

5% cement combined stabilizer achieved the water absorption less than the specification value (15%). For the 10% finer contented soil only 15% lime stabilizer did not achieve the water absorption less than the specification value. For 5% finer contented soil, all the stabilizers achieved the water absorption less than the specification value. 5% of lime stabilization achieved the minimum water absorption compared with other stabilizers. Table 5 shows the water absorption of CSEB with various clay percentage and different percentage of stabilizers.

Table 5 Water absorption (%) of CSEB

Stabilizer	5% finer	10% finer	15% finer
15% lime	10.8	15.7	18.6
10% lime	8.9	12.8	13.0
5% lime	6.2	10.2	12.4
10% cement	5.9	12.5	18.5
8% cement	7.2	14.3	19.1
7% lime 3% cement	11.7	12.0	17.3
5% lime 5% cement	9.1	10.1	14.2
3% lime 7% cement	9.1	10.2	15.9

3.3. Dry Density

SLS 1382 specified for the compressed stabilized earth blocks should have a dry density greater than 1750 kg/m^3. For all stabilization when the clay percentage got to decrease the dry density of the soil blocks got to increase except 8% cement stabilization. The specification value was not achieved by the 15% lime stabilized blocks for the dry density of all clay and silt content soil blocks. For the 15% finer contained soil blocks, only 10%, 5% lime stabilizer, 8% cement stabilizer and 5% lime: 5% cement combined stabilizer achieved the dry density greater than the specification value. For 10% finer contained soil blocks, 15% lime stabilization and 8% cement stabilization didn't achieve the dry density greater than the specification value. Other than 15% lime stabilization 5% finer contained soil blocks achieved the dry density greater than the specification value. Table 6 shows the dry density of CSEB with various clay percentages and different percentages of stabilizers.

Table 6 Dry density (kg/m^3) of CSEB

Stabilizer	5% finer	10% finer	15% finer
15% lime	1737.3	1676.1	1610.7
10% lime	1954.0	1841.6	1763.5
5% lime	1817.6	1805.1	1798.8
10% cement	1889.3	1771.1	1547.2
8% cement	1822.3	1642.4	1763.9
7% lime 3% cement	1889.1	1882.7	1678.4
5% lime 5% cement	1877.2	1890.7	1815.5
3% lime 7% cement	1922.1	1808.6	1603.5

4. CONCLUSIONS

This study focused on manufacturing of compressed stabilized earth blocks with lime stabilization for low clay & silt contained soil. The study was able to reveal the following findings.

- The optimum level of compressive strength was achieved for 10% lime stabilized blocks which are below the values specified in SLS 1382.
- 10% Lime stabilized blocks can be used for the single-story building units (According to SLS 855, part 1 specification, limiting value is 1.2 N/mm^2).
- For 15% and 10%, clay & silt contained soil, all the lime stabilization got the strength same or greater than 1.2 N/mm^2
- For low clay & silt contained soil blocks, combination of cement and lime is suitable than the lime or cement stabilization.
- Maximum strength was achieved with 5% lime: 5% cement for 15% and 10% clay & silt contained soil and 7% cement: 3% lime for 5% clay & silt contained soil. These strengths satisfied the SLS 1382 specification of Grade 2 blocks.
- For 5% and 10% clay & silt contained soil blocks, water absorption is less than 15% which is the specified level in SLS 1382.
- Dry density of the blocks made with 5% and 10% clay & silt are above the specification value (1750 kg/m^3) given in SLS 1382.

When clay & silt percentage got decrease, cement percentage increment in stabilizer is useful. When a small amount of clay & silt is in the soil, a small percentage of lime wanted to be added to get good strength. That was shown in 5% clay & silt percentage soil results. Because only with cement stabilizer compressive strength was achieved as 3.2 N/mm^2 but 7% cement and 3% lime combine stabilizer compressive strength was achieved as 4.1 N/mm^2.

5. REFERENCES

Akpokodje, E.G., 1985, 'The stabilization of some arid zone soils with cement and lime', *Quarterly Journal of Engineering Geology and Hydrogeology*, 18(2), 173-180.

ASTM Standards C136-06, 2006, 'Standard test method for sieve analysis of fine and coarse aggregates', ASTM International.

ASTM Standards D4318., 2010, 'Standard Test Methods for Liquid Limit', *Plastic Limit, and Plasticity Index of Soils*.

ASTM Standards C117-13, 2013, 'Standard test method for materials finer than 75-µm (No. 200) sieve in mineral aggregates by washing', ASTM International.

Alavez-Ramirez, R., Montes-Garcia, P., Martínez-Reyes, J., Altamirano-Juárez, D.C. and Gochi-Ponce, Y., 2012, 'The use of sugarcane bagasse ash and lime to improve the durability and mechanical properties of compacted soil blocks', *Construction and Building Materials*, *34*,296-305.

Bell, F.G., 1996, 'Lime stabilization of clay minerals and soils', *Engineering Geology*, *42*(4), 223-237.

Bogas, J.A., Silva, M. and Gomes, M.D.G., 2018, 'Unstabilized and stabilized compressed earth blocks with partial incorporation of recycled aggregates', International *Journal of Architectural Heritage*, 1-16.

Colley, E., 2014, 'Effects of Polyethylene Terephthalate Fibers in the Water Resistance of Compressed Stabilized Earth Blocks'.

Deboucha, S. and Hashim, R., 2011, 'A review on bricks and stabilized compressed earth blocks', Scientific *Research and Essays*, *6*(3), 499-506.

Department of Census & Statistics, Survey of Construction Industries, 2016.

Guettala, A., Houari, H., Mezghiche, B. and Chebili, R., 2002, 'Durability of lime stabilized earth blocks', *Courrier du Savoir*, *2*(1), 61-66.

Nagaraj, H.B., Sravan, M.V., Arun, T.G. and Jagadish, K.S., 2014, 'Role of lime with cement in long-term strength of Compressed Stabilized Earth Blocks', *International Journal of Sustainable Built Environment*, *3*(1), 54-61.

Ngowi, A.B., 1997, 'Improving the traditional earth construction: a case study of Botswana', *Construction and Building Materials*, *11*(1), 1-7.

Raheem, A.A., Bello, O.A. and Makinde, O.A., 2010, 'A comparative study of cement and lime stabilized lateritic interlocking blocks', *The pacific Journal of science and Technology*, *11*(2), 27-34.

Rahman, M.M., Rashiduzzaman, M.M., Akhand, F.Z. and Kabir, K.B., 2016, 'Compressed Stabilized Earth Block: A Green Alternative for Non-load Bearing Building Block in Developing Countries like Bangladesh', *American Chemical Science Journal*.

SLS 855, 1989, *Sri Lanka Standard Specification for Cement Blocks*, Part 1.

SLS 1382, 2009, Sri *Lanka Standard Specification for Compressed Stabilized Earth Blocks*, Part 1.

SLS 1382, 2009, *Sri Lanka Standard Specification for Compressed Stabilized Earth Blocks,* Part 2.

Walker, P.J., 1995, 'Strength, durability and shrinkage characteristics of cement stabilized soil blocks', *Cement and concrete composites*, *17*(4), 301-310.

Proceedings of the 7th International Symposium on

Advances in Civil and Environmental Engineering Practices for Sustainable Development

ACEPS - 2019

Investigating the behavior of Clay Roof Tile (CRT) physical properties by introducing lime as an additive.

B. D. K. K. Thilakarathna[(1)*], K.M.A.K. Kulatunga[(2)], C. P. Jayalath[(1)]

[1]Department of Physics, University of Peradeniya, SRI LANKA.
[2]Department of Manufacturing and Industrial Engineering, University of Peradeniya, SRI LANKA.

K e y w o r d s

Additives
Clay Roof Tile
Flexural strength
Linear shrinkage
Porosity
Water permeability

A B S T R A C T

Clay Roof Tile (CRT) demand is significant in the construction field, due to its positive effect on health and social lifestyle. The main barrier in supplying to the demand is the cost of production associated, and many researchers have experimented to overcome this barrier using organic and inorganic additives to raw clay. The porosity level increment by organic additives is still questionable. However, using inorganic industrial waste and cheap dopants to enhance mechanical properties are among the leading research prospects of production engineers. The raw material, 205B (mixture code) clay type was used in this experiment and 1.2 %wt. commercially available lime was used as an additive, which mainly consisted of CaO and MgO. These two minerals are mainly used as a fluxing agent and hardening material in the ceramic industry. At the production flow, tested samples were prepaid according to factory standards. Particle size analysis and XRF test were conducted for raw materials. Linear shrinkage, water absorptivity, water permeability, percentage porosity, bulk density, flexural strength and microstructure (using SEM) were analyzed for both raw and additive CRT samples. The results showed that lime added CRTs had high flexural strength, low linear shrinkage and low bulk density than reference (raw) CRTs. Decreasing the sintering temperature and formation of Anorthite phase, which was identified using XRD, directly caused the increase of the flexural strength in lime added CRTs. The complete firing of lime added CRT and its higher water favorability appearance suggests the possibility of further research with higher thickness samples or with emulation coating for lime added CRTs.

1. INTRODUCTION

1.1 Demand of clay roof tile

The demand of Clay Roof Tile (CRT) is unparalleled and has been ever increasing in the construction field from the beginning of the human civilization. Though the technology and materials used are traditional in the production chain, CRT has lot of advantages over its counterparts. Attractive appearance, lightweight roofing options and ability to maintain cooler temperatures inside the building are some of them. The negative effects on health caused by asbestos sheets are another factor that increases the demand for CRT. Asbestos sheets are known to cause lung carcinoma due to inhaling the small structural fibres

1.2 Properties of clay minerals and deposits

Clay and clay related industry has a long legacy in Sri Lanka, which is also proven by the discovery of red and black clay vessel in Anuradhapura area dating to 900 BC (Amarasinghe 2010). Clay is a mixture of several kinds of primary minerals and basically consists of hydrated aluminosilicates (Guwahati 2009). Based on deposit appearance of clay deposits, they are divided into two kinds: primary (in situ) deposits and secondary (sedimentary) deposits. Clay consists of kaolin, montmorillonite and micaceous clay as the major minerals. Alluvial clay forms by the sedimentation of primary clay minerals deposited on lakes and river

banks. This clay type is widely spread around Sri Lanka. Mainly, in the dry zone, clay is found with a higher percentage of montmorillonite. Alluvial clay contaminates with a considerable amount of organic matter and is used as the major raw material for clay bricks, tiles and potteries (Jayatileke *et al.* 2013).

Clay minerals are water sorbents and their properties are based on their structure. Due to this, different clay minerals show different swelling (with water) and shrinking capacities when it is dried (Gaskova 2009). Therefore, for industrial applications, clay sources are chosen based on its clay mineral composition. All Clay minerals are also negatively charged and can attract positively charged particles around the clay and repel negatively charged particles (Murdock & Wells, 1978). Because of that, for CRT, it is expected that additive cations can be held without leaching by these clay minerals until those cations are involved in further reactions at firing stage.

Wanasinghe & Adikary (2014) have experimented on characterization clay deposits in Nachaduwa area (the same area where the clay bulk was gathered for this study) and tested four major lakes in there; Dematawewa Tank Clay, Galkulama Tank, Illanthagaha-wewa Tank and Pallankulama Tank. The results showed 50% of particle sizes of clay were less than 2 microns, and consisted of the higher percentage of kaolinite, montmorillonite and quartz minerals.

1.3. Organic and Inorganic additives.

Demir (2008) have used sawdust, tobacco residue and grass as additives, up to 10 wt.%. X-ray powder diffraction (XRD) characterization was used to identify clay minerals in used clay bulk. They observed pore formation (which caused low bulk density), due to the emission of CO2 at the burning stage. These were at an acceptable level but caused lowering of the compressive strength of the final fired product. Volume shrinkage of burned samples was also much higher than the products which were prepared using inorganic additives. They had not observed any black core, which means residues underwent complete burning.

To overcome these organic additives usage drawbacks, many researchers tend to utilize inorganic additives (Rajasooriya *et al* (2017) such as the dimensional stone waste, coal fly ash, aluminum sludge, rock quarry dust and glass (abandoned monitor and TV screens).

Reis *et al* (2015) have experimented on a Brazilian clay type CRTs with stone waste as an additive. 60wt.% stone waste sample showed the most optimized mechanical properties, that had the lowest apparent porosity and lowest water absorption. This is due to the almost same order particle size of raw materials and wastage, products achieving their maximum packing density and intrinsic gaps not being able to be filled further (after 60 wt.% additive level).

Hojamberdiev *et al* (2011) have researched the effect of adding granite wastage to ceramic tiles and express a great explanation for the effect of calcium oxide on the sintering process. Muscovite in granite waste contains 6.04% Calcium oxide percentage, which is considerably high. It is suggested that alkali earth oxides behave as a fluxing agent and slow down the crystal formation rate. This oxide reduces the formation of the mullite crystalline and encourages the formation of an anorthite phase, which is more thermodynamically stable, which in turn leads to the better mechanical properties of particular samples.

Dolomite is one of the major resources that lime (which could be possible to test as additive) industry depends on, which consists of 20 - 46% MgCO3, 54 - 80% CaCO3 (department of Minerals and Energy 2003). Although dolomite is much cheaper, release of CO2 from dolomite upon thermal treatment may cause pores in the CRT. The increased porosity may cause higher water absorption, water permeability and weaker structural strength in tiles.

Clay industry is not the only field of research with fly ash as an additive. Jayasinghe *et al* (2005) used fly ash, paper and mine clay to form synthetic lightweight soil aggregator with starch as the organic binder. Samples showed more than 40% aggregation stability relative to normal samples, and this property of fly ash is also utilized in clay industry. Dana *et al* (2004) have tested the capability of replacing felspar of triaxial porcelain (consisting of quartz clay and feldspar) with fly ash. At 1250^0C, 15 wt.% fly ash substituted samples showed higher Bulk density and flexural strength, compared other samples. They have suggested that it is due to

the presence of low viscous glass phase, which flows easily and contributes to good liquid phase sintering. SEM images of the samples fired up to 13000C have shown better interlock of mullite needle structure, and equal distribution into the glass matrix. This was explained as the reason for the higher strength.

Another experiment was conducted by Dana et *al* (2005) to improve mechanical strength using fly ash and blast furnace (B.F) slag as additives for ceramic tiles. They have found that, with particular potions (kaolin clay 45 wt.% feldspar 24 wt.% Quartz 22 wt.% Fly ash 3 wt.% B.F 6 wt.%) and at particular temperatures(11750C), microcrystalline structures of quartz and mullite in fly ash and alkaline earth oxides in blast furnace slag have caused to form anorthite phase and mullite phases, which lead to higher mechanical strength.

Since some industrial waste may contain heavy metals, radioactive elements and nano-scale particles, and some of these may easily contact with human body, causing health issues, products need to pass a leaching test, a radioactivity dose test, standardizing handling precautions and other appropriate tests before these materials are used in the industrial field.

1.4. Utilization of alkali earth oxides

CaO is the main component of lime used as a common fluxing agent (lowering the melting temperature and promoting liquefaction) in glass industry. It is also a hardening material, which makes glass stretch and acid resistant. Thought it does not behave as a fluxing agent below the con-4 temperature (10600C), it resists leaching of some metals. In absence of lead, CaO support the reduction of crazing in crystallization at high temperatures, and when a larger amount of Fe2O3 is present, it tends to form yellowish crystals. Furthermore, CaO dolomite mineral (or lime produce by dolomite) supplies MgO to the system, which also create a flux (action start about 11700C) and other desirable properties. Frueh (2017) have studied about the powder chemistry of MgO doped alumina, and using TEM, they observed grain boundary thickness reduced during the densification. They have also demonstrated MgO and SiO_2 both dissolving together is more thermodynamically favourable in alumina than dissolving separately.

This study was conducted to utilize materials science technology to reduce the opportunity cost of CRT production, in order to satisfy both customer and supplier. The opportunity cost is the benefits, forgone due to particular use of resources.

2. MATERILS AND METHODS

2.1. Sample preparation.

Initially, Alluvial clay was mined from Maminiyawa land Dematawawa lakes, and allowed to decompose organic matters for six months. Then, it was separately gathered to the primary bins and tested for sand (lower sand content than 34 wt.% and particle size in between 710 and 63 microns) and moisture content. Such that, moisture content was maintained at 19 wt.% and allowed to age for 36 hours. Next, bulk (205B clay type consists Maminiyawa -50 wt.% Dematawawa-15 wt.% drier reject-30 wt.% grog (fired reject)-5 wt.%) was prepared by mixing a proper composition of each material, and was screened and taken for research approach.

First, 25.0 kg of screened 205B bulk sample was taken and tested for moisture content, and maintained at 19 wt.% according to the factory standards. Then, 12.5 kg of the clay sample was roll milled using a lab scale roll miller and extruded using lab extruder with vacuum pump action. Next, the extruded "bat" sample was cut into slices with 2-inch width, and these were kept separately on a fixed pre-prepared mould (with the cross-section area, 81.32 mm X 142.48 mm; thickness 12 mm) in the mould machine, and CRT green body was punched. For lubrication purposes, mould surface was well oiled, and clay slice upper surface was covered with polyethene paper. Resulted green bodies were removed from the mould and were indexed. Then, the procedure was repeated for other 12.5 kg of sample, with added 0.1230 kg (1.2 wt.% for dry clay weight) of lime before roll milling process, and indexed lime added green body CRTs were prepared. Those CRT green bodies were kept for 24 hours to air dry, and 5 days in a lab scale drier. Next, those CRTs were placed in a tunnel kiln and burned with maximum temperature 900^0C for 3 hours.

2.2. Moisture test

30.0 g of 205B clay sample was measured and tested under lab IR light drier for 1hour and the resulting mass reduction was measured.

The relevant moisture amount of initial bulk corresponding to the resulted mass reduction was taken from a standard data table.

2.3. Mechanical and characterization analysis

For particle size analysis, 0.5 g of lime was dissolved in 10.0 ml of ethanol solution, and stirred for 1h using a magnetic stirrer and sonicated for 10 minutes. Then, the solution was tested by CILAS Nano DS Particle size analyzer machine. Next, 10 g of 205B clay sample was kept in a furnace at 300^0C for 10 minutes to remove organic matters, dissolved in ethanol solution and tested for particle size using same machine.

XRF analysis was followed using FISCHERSCOPE. ®. X-RAY XAN machine. Here, both lime and organic matters were removed, and crushed clay powdered sample were used for XRF test (in-between the accuracy range of atomic mass number 15(P) to 86 (Rn)). For calculation of liner shrinkage measurement, length of each of fired CRTs and the mould were measured and recorded. For each mechanical/physical tests and measurements, (linear shrinkage, water absorptivity, water permeability, porosity, tile weight, bulk density and flexural strength) six tiles were used from each CRT samples (Lime incorporated and raw). For calculation of Percentage water absorptivity,(ASTM International, 2002) percentage porosity and bulk density (Demir, 2008), first, each CRT's weights were measured. Then, the samples were dipped in a water container for 24 hours. Next, CRTs were taken out of the container and wiped to remove the water on CRTs surface. After that, the final weights of the CRTs were measured. Pre-prepared frames were placed on CRTs and were filled with water to test for permeability, and observation were taken after 24 hours(ASTM C778-13 2014).

For each sample, the loaded forces at fracture points were measured using – Hounsfield HK-50 universal testing (UTM) and flexural strengths were calculated. Finally, the resulting CRT samples and 205B raw clay sample were analysed for XRD (by Rigako Ultima iv machine) and SEM (by ZISS EVO®LS 15 machine) (ASTM International, 2002).

2.3.1. Linear Shrinkage

Liner shrinkage percentage (Percentage length reduction after the fire) is given by the Eq.(1).

$$L.S.\% = \frac{(M.L.-F.L.)}{M.L.} \times 100\% \quad (1)$$

Where L. S is the linear shrinkage, M. L is the mould length, F. L is the fired CRT length.

2.3.2. Water absorption test

Percentage water absorption (measured after 24 hours since sample dipped in water) is given by the Eq. (2).

$$W.A.(wt.\%) = \frac{(M.-I.M.)}{I.M.} \times 100\% \quad (2)$$

Where W. A is the water absorptivity, M is the mass after 24h and I. M is the initial mass.

2.3.3. Porosity

Volume of the sample is utilized for porosity and bulk density calculation, and it is given by the Eq. (3).

$$V = L. \times W. \times T \quad (3)$$

Where V is the volume, L is the length, W is the width and T is the thickness.

Sample porosity percentage (pore volume percentage) is given by the Eq. (4).

$$P.\% = \frac{(M.-I.M.)}{W.D. \times V.} \times 100\% \quad (4)$$

Where, P. % is the percentage porosity, M is the mass after 24h, I. M is the initial mass; W. D is the density of water, V is the volume.

2.3.4 Bulk Density

Bulk Density of the sample is calculated by the Eq. (5).

$$B.D. = \frac{W.}{V.} \quad (5)$$

Where B. D is the bulk density, W is the weight of the fired CRT and V is the volume of the CRT.

2.3.5. Flexural strength (Three-point Loading)

Flexural strength is given by the Eq. (6),

$$F.S. = \frac{3FL}{2WT^2} \quad (6)$$

Where F.S is the flexural strength, F is the loaded force on rectangular sample at fracture point, L is the distance between two supportive edges, W is the width of the sample and T is the thickness of the samples.

2. RESULTS AND DISCUSSION

Presence of compounds consisting of iron (Figure 1 A; by red peaks and Figure 1 B; by blue peaks) caused the red colour of the fired CRTs (Reis *et al*. 2015).

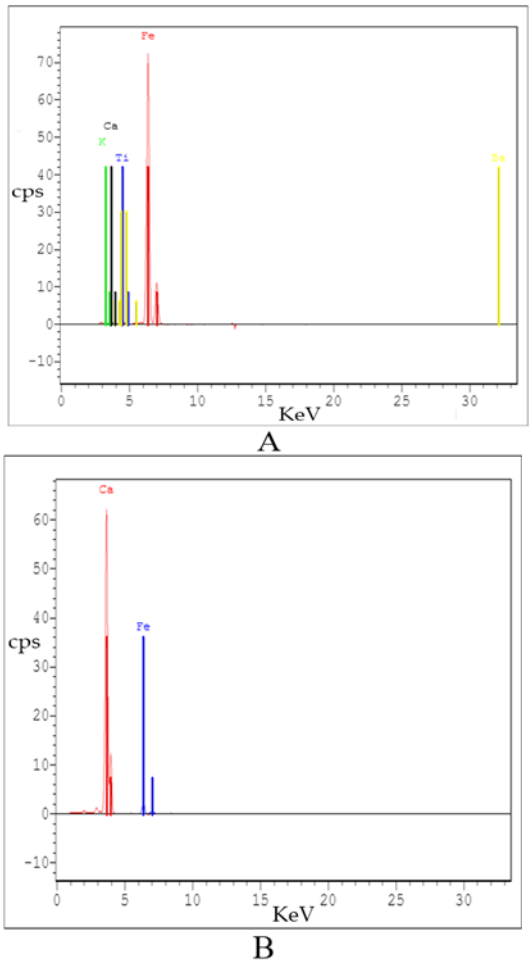

Figure 1 XRF pattern for (A) 205B clay. (B) lime

Initial average particle sizes were recorded at 4068.8nm for clay and 279.6nm for lime (Figure 2). Generally, inequality of particle sizes leads to a non-uniform packing (fine particles not packing as tightly as large particles), followed by a non-uniform sintering (lightly packed regions shrink more than densely packed regions, leading to internal voids) (Koutný *et al*. 2016).However, this argument was not valid within the discussed context (lime added CRT), since the system was added with only a trace amount of lime. Strong fluxing capability of alkali earth oxides (like CaO) caused to reduce the sintering temperature of the ceramic tile and aided a complete firing (Cengiz & Kara 2018).

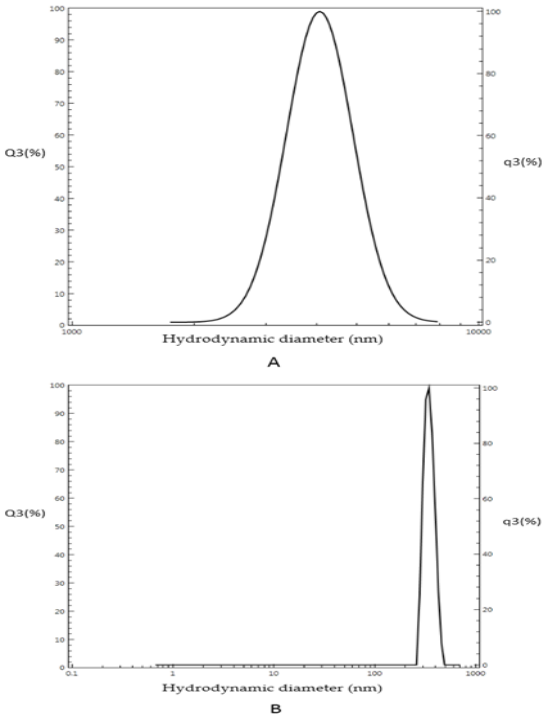

Figure 2 Particle size distribution of (A) 205B Clay body mixture and (B) lime

This has been clearly illustrated through the cross-section images of both lime added and raw CRTs in figure 3. Maroon colour area in the core of the raw CRT (Figure 3 A) is due to a partial burning while fully burnt structure have been observed in Lime added CRT.

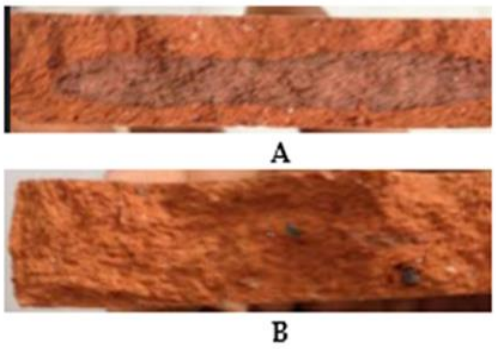

Figure 3 Cross-section images of the (A) Raw CRT and (B) Lime added CRT

Physical and mechanical test results (except permeability) are tabulated in table 1 with their percentage increment/decrement of lime added CRTs compared to raw CRTs.

Table 1 Analysis of numerical value results of tests

Test	Raw CRTs Values (Reference)	Lime added CRTs value	Percentage increment/ decreme
Pct. Liner shrinkage (%)	7.5788	6.7031	-11.556
Pct. water absorptivity (%)	8.447	9.354	10.738
Percentage porosity (%)	16.4	17.6	7.32
Tile weight (x 10^{-3}kg)	260.7	268.3	2.915
Bulk density (x 10^{-3}kgm^{-3})	1.930	1.878	-2.694
Flexural strength (MPa)	7.40	7.84	5.95

Relative high void percentage caused resulted low bulk density (Table 1) in Lime added CRTs (2.694% lower value compared to reference). This phenomenon leads to relatively 10.738% high-water absorptivity (Table 1), and negatively affects water permeability in Lime added CRTs (Table 2).

Table 2 Water permeability results for raw and lime added CRTs

Sample No	Raw CRT	Lime added CRT
1	Fail	Fail
2	Pass	Fail
3	Pass	Fail
4	Pass	Fail
5	Fail	Fail
6	Fail	Fail

Void formation positively affects the cooling process of the interior of a building. When the inside of the building is getting warmer, the heat absorbed by water molecules could pass through the void paths in the CRT, leading to cooling of inside the building.

Formed voids could be clearly visualized through Figure 4, SEM images of lime added CRT (Figure 4 A and C) comparing with raw CRT figure 4 image B and D. Complete firing in the presence of strong fluxing oxides resulted in the growth of pores within the entire volume. This phenomenon was also proved by percentage porosity increment (by 7.32%), and bulk density decrement of lime added CRTs relative to raw CRT samples. Relative 11.556% lower linear shrinkage (Table 1) and higher permeability (Table 2) of Lime added CRT were directly caused by the increment of porosity.

Marghussian & Yekta (1994) also observed the comparative low linear shrinkage with the presence of alkali earth oxide. The relative higher liner shrinkage was sufficient for increase the formation of micro cracks. Raw CRT sample also exhibited micro cracks on the structure (Figure 4B), and this led to a comparatively lower flexural strength (Table 1), 5.95% relative flexural strength increment in Lime added CRT.

In addition to the low-temperature sintering process, the formation of anorthite crystal phase (Dana *et al*. 2005) at 900^0C, strengthens the structure of CRT. This phase abundancy was identified by XRD analysis (PDF2 card No 00-070-0287; Figure 6).

Anorthite crystal phase is more thermally stable, thus accelerates the reaction (Equation 7) between the calcium oxide and metakaolin (Zaiou *et al*. 2016). Figure 5 XRD analysis shows the abundance of kaolinite (PDF2 card No 00-012-0447, XRD) in the bulk. Metakaolin is formed by decomposition of kaolinite at 6500C.The reaction between the Metakaolin and calcium oxide is given by Eq. (7).

$$Al_2O_3.SiO_2 + CaO \rightarrow CaO.Al_2O.2SiO_2 \quad (7)$$

(Zaiou *et al*. 2016).

Though Mullite crystallization (which also causes a higher mechanical strength phase) is another possibility of metakaolin transformation, it is not common under this maximum temperature of 900^0C (generally happens at 962^0C) (Hojamberdiev *et al*. 2011).

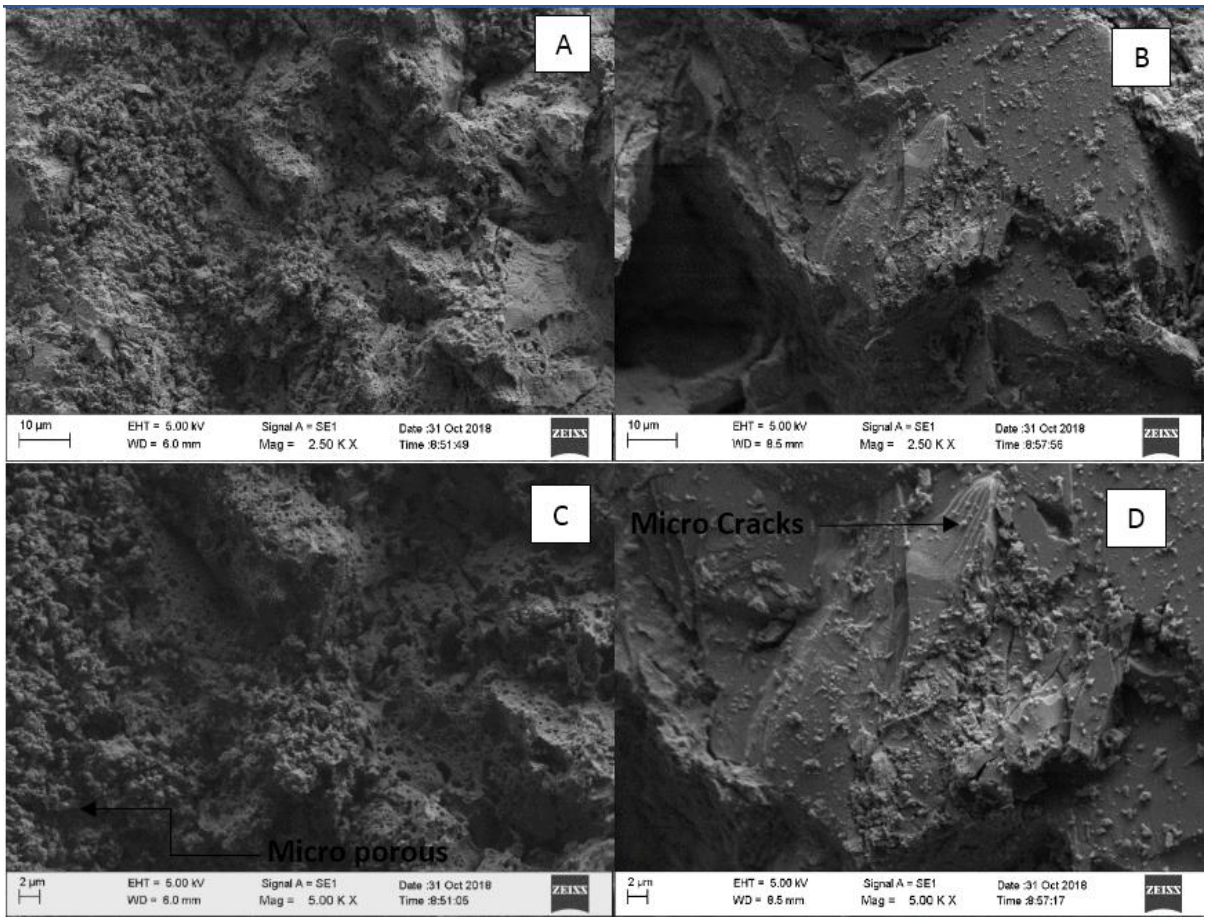

Figure 4 SEM image of the mid area cross section of the (A) lime added CRT (bar =10 µm) (B) raw CRT (bar = 10 µm) (C) lime added CRT (bar = 2 µm) (D) raw CRT (bar =2 µm)

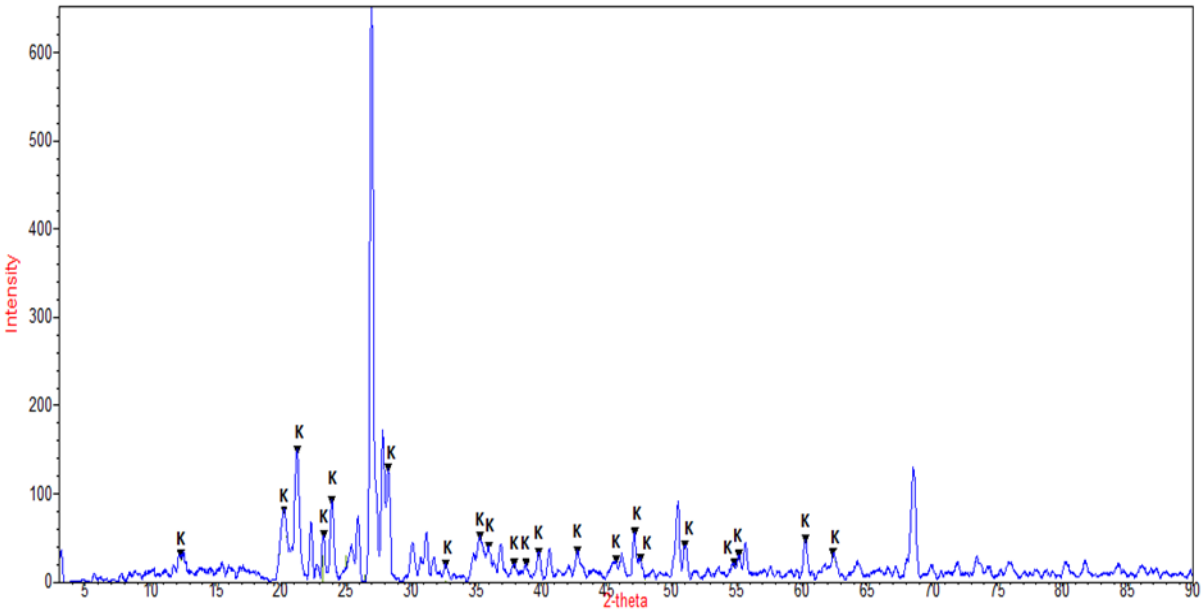

Figure 5 XRD pattern for 205B clay body mix with the identification of Kaolinite(K) mineral abundance

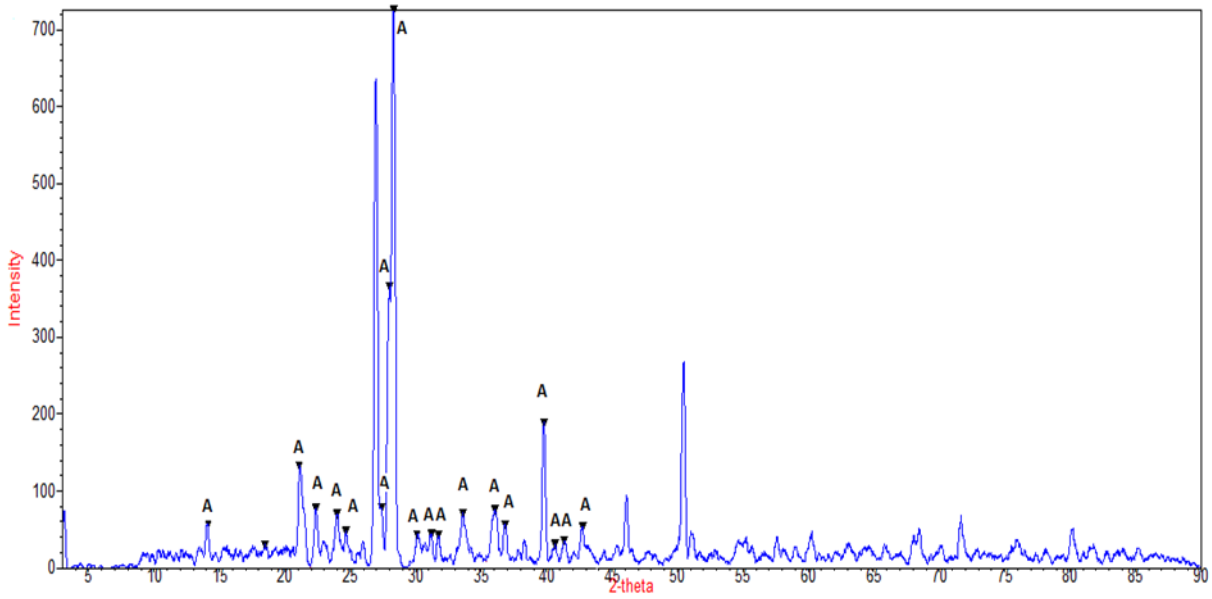

Figure 6 XRD pattern for Lime in cooperated CRT with the indication of the abundance of Anorthite (A) phase.

3. CONCLUSION

Commercial lime added CRTs show higher flexural strength than normal 205B CRT products. These findings can be utilized to reduce the amount of crack rejected CRT in the production flow of CRT, and to reduce the kiln firing temperature. However, because of the water favorability of lime added CRT, implementation is still questionable. Lime industry causes an increase in the carbon footprint, while reducing crack rejected CRT could independently lead to decrease of the same. Therefore, the net carbon footprint of the process should be calculated before utilizing into the production level.

4. ACKNOWLEDGMENTS

Authors sincerely acknowledge Mr. A. Kirsnaragavan, Mr. T. Ajanthan and Mr. M. N. Jayasinghe for the invaluable help extended in using the resources, facilities and the support provided throughout the sample preparation process. Further, authors extend their sincere gratitude to Dr H.M.J.C Pitawala, Senior Lecturer, and Mr. H. J. K. S. S. Wijerama, Technical Officer, Uva Wellassa University of Sri Lanka for the support provided instrumentation of XRD analysis.

5. REFERENCES

Amarasinghe, U., 2010, *Sri Lankan Pottery: A Continuing Tradition*, Serendib, viewed May 13 2018, from http://www.serendib.btoptions.lk/article.php?issue=8&id=159#

ASTM Standards C778-13, 2014, 'Standard Specification for Sand 65.198.187.10', 14, 1–3.

ASTM Standards C67-02, 2002, 'Standard Test Methods for Sampling and Testing Brick and Structural Clay', 0–10.

Cengiz, O., & Kara, A., 2018, 'Effect of alkaline-earth oxides on firing behaviour of monoporosa wall tile bodies', Journal *of Ceramic Processing Research* ,19.

Dana, K., Das, S., & Das, S. K., 2004, 'Effect of substitution of fly ash for quartz in triaxial kaolin-quartz-feldspar system', *Journal of the European Ceramic Society*, 24(10–11), 3169–3175.

Dana, K., Dey, J., & Das, S. K., 2005,' Synergistic effect of fly ash and blast furnace slag on the mechanical strength of traditional porcelain tiles', *Ceramics International*, 31(1), 147–152.

Demir, I., 2008, 'Effect of organic residues addition on the technological properties of clay bricks', *Waste Management*, 28(3), 622–627.

Department of Minerals and Energy Republic of South Africa, 2003, *A Review of the Dolomite and Limestone Industry in South Africa*, viewed May 27 2018, from http://www.dmr.gov.za/LinkClick.aspx?fileticket=gpszd6p3bqQ%3D&portalid=0.

Frueh, T., 2017, 'Powder Chemistry Effects on the Sintering of MgO-doped Specialty Al2O3 T', *ARPN Journal of Engineering and Applied Sciences*, 12(10), 3218–3221.

Gaskova, O. L., 2009, ' Semiempirical model for the description of sorption equilibria on clay mineral surfaces', *Geochemistry International*, 47(6), 611–622.

Guwahati, I., 2009, *Structure of Clay Mineral Npte*l, viewed 2 May 2018, from https://nptel.ac.in/courses/105103097/16.

Hojamberdiev, M., Eminov, A., & Xu., Y., 2011, 'Utilization of muscovite granite waste in the manufacture of ceramic tiles', *Ceramics International*, 37(3), 871–876.

Jayasinghe, G. Y., Tokashiki, Y. and Kitou M., 2005, 'Development of Synthetic Lightweight Soil Aggregates Utilizing Coal Fly Ash and Mine Clay as Waste Materials', *Tropical Agricultural Research Extension*, 8, 1-12

Jayatileke, S., 2013, 'Geology Mineral Resourcesof Sri Lanka', *Vidurava*, 30(1), 7-14

Koutný, O., Kratochvíl, J., Svec, J. and Bednárek, J., 2016, 'Modelling of Packing Density for Particle Composites Design', *Procedia Engineering*, 151, 198-205.

Marghussian, V. and Yekta, B., 1994, 'Single Fast Fired Wall Tiles Containing Iranian Iron Slag', *British Ceramic Transactions*, 93, 141-145.

Murdock, L. and Wells, K., 1978, '*Potassium in Kentucky Soils, University of Kentucky College of Agriculture*', viewed 25 May 2018, from http://www2.ca.uky.edu/agcomm/pubs/agr/agr11/agr11.html.

Rajasooriya, T. R., Peiris, R. L., Kulatunga, A. K. and Jayalath, C. P., 2017, 'Enhancement of strength by incorporating Rock Quarry Dust and optimize the thickness of plain type Clay Roof Tile', *ICSEM, 116*, 48-51.

Reis, A., Della-Sagrillo, V.and Valenzuela-Diaz, F., 2015, ' Analysis of Dimension Stone Waste Addition to the Clayey Mass Used in Roof Tile Production', *Materials Research*, 18 (suppl 2), 63–69.

Wanasinghe, D. D., & Adikary, S. U., 2014, 'Characterization of clay deposits in Nachchaduwa area for ceramic fabrication', *National Engineering Conference, 18th ERU Symposium*, 116–121.

Zaiou, S., Harabi, A., Harabi E., Guechi, A., Karboua, N., Zouai, S. andGuerfa, F., 2016, 'Sintering of Anorthite Based Ceramics Prepared from Kaolin DD2 and Calcite Sinterização de CerâMicas à Base de Anortita Preparadas', *CerâMica,* 62,317–22.

Proceedings of the 7th International Symposium on

Advances in Civil and Environmental Engineering Practices for Sustainable Development

ACEPS - 2019

Finite Element Modelling of Reinforced Concrete Horizontally Curved Beams strengthened for shear using Carbon Fiber Reinforced Polymer

M.W.C.Himasha [1] and J.C.P.H.Gamage [1]

1Dept. of Civil Engineering, Faculty of Engineering, University of Moratuwa, Katubedda, Moraduwa, SRI LANKA.

K e y w o r d s

Horizontally curved concrete beams
CFRP
Shear strengthening
Finite Element Modelling (FEM)

A B S T R A C T

In the current world with the trend of constructing architecturally complex structures, use of horizontally curved beams has been popular. Strengthening of shear deficient such curved beams to improve performance is an important aspect. Since Carbon Fiber Reinforced Polymer (CFRP) materials have been used for strengthening straight beams for shear successfully, assessing the application of this technology on curved beams is an innovative approach. A numerical model was developed using an advance finite element analysis technique. The predicted results are in good agreement with test results. More than 23% strength gain in shear was noted from strengthened beams.

1. INTRODUCTION

Reinforced concrete (RC) curved beams can currently be seen in many applications such as highway intersections, bridges, curved buildings and ring shaft conveying vaults. Apart from bending and shear, curved beams subject to torsion. With the increasing applications of RC curved beams in structural work, the importance of strengthening methods on such elements are getting highlighted.

Concrete beams fail in different mechanisms. Shear failure is a one such mechanism. Shear failure has a tendency to occur prior to flexural failure when the shear strength of beam is inadequate to develop its flexural capacity. Such beams are known to be shear critical beams (Balakrishnan *et al*.1988).

RC beams are usually strengthened by CFRP laminates fixed to the bottom of the beam. But often they fail due to the debonding of the CFRP laminate from the concrete substrate (Rvendran *et al.* 2016). Most of the researches have conducted focusing on the suggestion of a better bonding technique to avoid the debonding of CFRP from the concrete substrate in the enhancement of flexural performance of strengthened RC beams (Ariyachandra *et al*. 2017, Premarathne & Gamage 2013, Amarasinghe & Gamage 2015).

Chaallal *et al* (1998) have investigated external shear strengthening of RC beams using CFRP. They suggest the use of diagonal CFRP side strips over vertical CFRP side strips as they perform well in terms of shear strength, crack propagation and stiffness. But all those studies are done on straight RC beams, whereas this particular research accounts for horizontally curved RC beams. Abating of strength due to debonding issue can be avoided by wrapping CFRP fabrics around the RC beam. Therefore, this study is focused on shear strengthening of curved RC beams using CFRP wraps in shear region.

2. NUMERICAL MODELLING

A three dimensional (3D) model was developed. A computer with an Intel(R) Core(TM) i5-4200U processor and an 8 GB RAM was used to run the model. Two configurations; non strengthened (1-1/2-2-CO) and strengthened with CFRP (2-1/2-2-FA and 3-1/2-4-FA) were developed as shown in

Figure 1(a) and 1(b). All the beams were with 1.8 m curve length and 0.2 m x 0.2 m cross sectional dimensions. Developed models of CFRP strengthened and non-strengthened beams are shown in Figure 2(a) and 2(b).

Figure 1(a) Non-strengthened control beam

Figure 1(b) CFRP strengthened beam

Figure 2(a) Numerical model of control beam

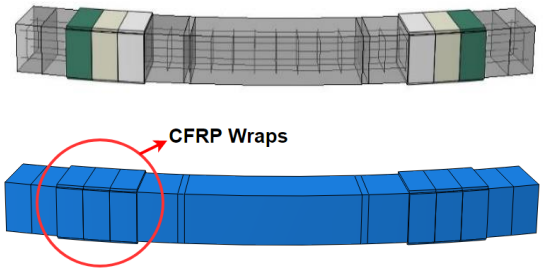

Figure 2(b) Numerical model of CFRP strengthened beam

2.1. Material properties

Grade 30 concrete was used. Mechanical properties were assigned based on the previous research studies (Tamura & Murata, 2010; Muralidharan *et al.* 2017). The concrete damaged plasticity model is used in modelling the nonlinear behaviour of concrete (Wahalathantri *et al.* 2011). Table 1 presents the properties of concrete used for modelling the substrate behaviour.

Table 1 Properties of concrete

Properties	Units	Value
Density	kg/m^3	2400
Young's modulus, E_{cm}	MPa	31000
Compressive yield stress, f_{ck}	N/mm^2	34
Poisson's ratio		0.2
Dilation angle		5
Eccentricity		0.1
fbo/fco		1.16
K		0.667
Viscosity parameter		0.0001

CFRP fabric was modelled as an orthotropic elastic material of thickness 1.2 mm. For such material, stress- strain relationship is defined as follows (Sharcnet.ca, n.d.).

$$\begin{bmatrix}\sigma_{11}\\ \sigma_{22}\\ \sigma_{33}\\ \sigma_{12}\\ \sigma_{13}\\ \sigma_{23}\end{bmatrix} = \begin{bmatrix} D_{1111} & D_{1122} & D_{1133} & 0 & 0 & 0 \\ & D_{2222} & D_{1212} & 0 & 0 & 0 \\ & & D_{3333} & 0 & 0 & 0 \\ & & & D_{1212} & 0 & 0 \\ & Sym. & & & D_{1313} & 0 \\ & & & & & D_{2323} \end{bmatrix} \begin{bmatrix}\varepsilon_{11}\\ \varepsilon_{22}\\ \varepsilon_{33}\\ \gamma_{12}\\ \gamma_{13}\\ \gamma_{23}\end{bmatrix} \quad (1)$$

Where σ_{11}, σ_{22} and σ_{33} are direct stresses in x, y and z directions, respectively while σ_{12}, σ_{13} and σ_{23} are shear stresses. $\varepsilon_{11}, \varepsilon_{22}, \varepsilon_{33}$, γ_{12}, γ_{13} and γ_{23} are strains in corresponding directions.

Each stiffness parameter in the matrix is defined as equations shown below (Sharcnet.ca, n.d.)

$$D_{1111} = E_1(1 - v_{23}v_{32})\Upsilon \quad (2)$$

$$D_{2222} = E_2(1 - v_{13}v_{31})\Upsilon \quad (3)$$

$$D_{3333} = E_3(1 - v_{12}v_{21})\Upsilon \quad (4)$$

$$D_{1133} = E_1(v_{31} - v_{21}v_{32})\Upsilon \quad (5)$$

$$D_{2233} = E_2(v_{32} - v_{12}v_{31})\Upsilon \quad (6)$$

$$D_{1122} = E_1(v_{21} - v_{31}v_{23})\Upsilon \quad (7)$$

$$D_{1212} = G_{12}, D_{1313} = G_{13}, D_{1212} = G_{12} \quad (8)$$

$$\Upsilon = 1/(1 - v_{12}v_{21} - v_{23}v_{32} - v_{13}v_{31} - 2v_{21}v_{32}v_{13}) \quad (9)$$

$$v_{ij} = \frac{E_i}{E_j} v_{ji} \qquad (10)$$

The material properties found in the literature to calculate stiffness parameters for modelling CFRP fabric is listed in Table 2 (Daud *et al.* 2015).

Table 3 shows the stiffness parameters calculated using Eq. (2) to (10), to define the material properties of the CFRP fabric in FE model.

Table 2 Properties of CFRP (Daud *et al.* 2015)

Property	Values found from literature	
	Value	Unit
E_1	230	GPa
E_2	23	GPa
E_3	23	GPa
G_{12}	6.894	GPa
G_{23}	4.136	GPa
G_{13}	6.894	GPa
v_{12}	0.3	
v_{23}	0.25	
v_{13}	0.25	
Tensile strength	3400	MPa

Manufacturer provided material properties are listed in Table 4. These ranges satisfy the Tensile strength and Modulus of Elasticity found in literature (Table 2).

Deformed steel bars were used to reinforce the concrete beams. Properties are given in Table 5.

Table 3 Calculated stiffness parameters (Sharcnet.ca, n.d.)

Data	Value
D1111	2.88E+11
D2222	3.06E+10
D3333	3.05E+10
D1122	7.31E+09
D1133	5.38E+09
D2233	7.46E+09
D1212	6.89E+09
D1313	6.89E+09
D2323	4.14E+09
γ	1.337793

Table 4 Properties of CFRP provided by manufacturer (X-Calibur Construction Chemistry Inc., n.d)

Properties	Unit	Value
Density	g/cm³	1.6
Tensile Strength	MPa	4000
Modulus of Elasticity	GPa	240

Table 5 Properties of steel rebars (British Standards Institution, 2005; British Standards Institution, 2004)

Properties	Units	Value
Density	kg/m³	7850
Young's modulus	MPa	210000
Shear modulus	MPa	81000
Poisson's ratio		0.3
Coefficient of linear thermal expansion	/K	12×10^{-6}
Yield strength (f_y)	MPa	460
Ultimate strength (f_u)	MPa	540

2.2. Finite element mesh, Boundary conditions and loading

In meshing of RC beam, Hex element shape- C3D8R elements were used (Daud et al. 2015). This element has 8 nodes with 3 degrees of freedom at each node and capable of predicting cracking in three orthogonal directions, plastic deformation and crushing (Tejaswini & Raju, 2015).

Reinforcing bars were modelled using B31 beam elements (Tejaswini & Raju, 2015). CFRP fabric was modelled as a skin reinforcement for the concrete beam. This tool defines a skin that perfectly bonds to the surface of an existing part (Pereira, 2005). Figure 3 presents the Finite element mesh of the beam.

Figure 3 Finite Element Mesh of the Horizontally Curved RC beam (Curvature Radius = 4 m)

So as to select the optimum mesh size, a mesh sensitivity analysis was carried out with mesh sizes of 40 mm, 35 mm, 30 mm, 25 mm, 20 mm and 15 mm. Results started converging at 25 mm mesh size. Hence, the typical mesh size selected in this analysis is 25 mm. Clamp

used in the experimental setup, the torsion along the beam was restrained with the vertical and horizontal translations. So the same support conditions were assigned in the model as shown in Fig. 4.

Beam was loaded at two points. Loading was done at 650 mm from the beam edge. In FE model simulation, load was modelled as a displacement with an amplitude of uniformly increasing displacement (0.001 m/s).

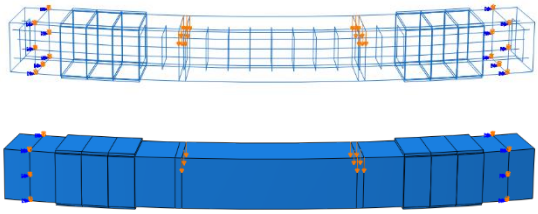

Figure 4 Boundary conditions and loading applied on the beam

Bond between RC beam and the reinforcing bars is defined using embedded constraint. With this constraint reinforcement is hosted inside RC beam. Aspect ratio of 1 was selected for the FE model to increase the accuracy of the results.

3. MODEL RESULTS

FEM of the beams were developed using ABAQUS software (Sharcnet.ca, n.d.). The concept behind Finite Element (FE) modelling is the subdivision of the mathematical model into disjoint components of simple geometry called finite elements (Friswell, 1995). An initial model was developed to validate experimental results found in literature. Then this model was further developed to validate the obtained experimental results accordingly. This validated model was used in predicting the behavioural patterns of CFRP strengthened curved beams under varying parameters.

3.1. Model validation

As an initial attempt, the experimental setup in Tamura & Murata (2010) was used to evaluate the behaviour of horizontal curved RC beams. Table 6 gives the details of the corresponding beam. All attributes, geometry and material properties assigned were the same as in the test programme. Figure 5 shows the comparison between predicted and tested load - deflection relationship.

Table 6 Details of the beam (Tamura & Murata, 2010)

Beam	Shear span/ Depth	Curvature Radius	Curved Length	Cross Sectional Dimensions
		mm	mm	mm²
B2-3.2	3.2	4000	1800	200 x 200

Following are the results obtained.

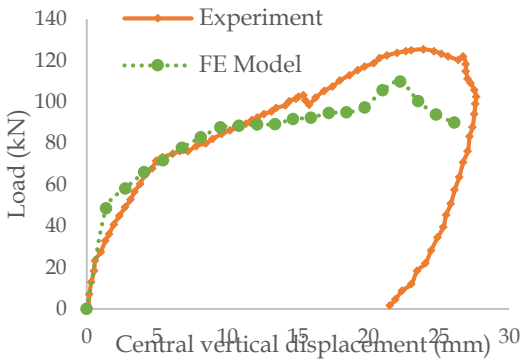

Figure 5 Predicted and tested (Tamura & Murata, 2010) Load vs. Displacement curves

Initially both tested and predicted behaviours indicated a similar behaviour up to 89 kN load. Then a slight deviation from the experimental results were noted in the predicted results. Average discrepancy between predicted and experimented values within this region is 12%.

Table 7 Comparison of failure loads and deflection tested (Tamura & Murata 2010)

Parameter	Experiment	FE Model	Deviation
Failure Load	125.42 kN	109.8 kN	12%
Corresponding Deflection	23.9 mm	22.3 mm	7%

The predicted failure load shows a 12% deviation from the tested load. A 7% deviation was noted from the corresponding mid span displacement (Table 7). These figures clearly indicate the accuracy of the model

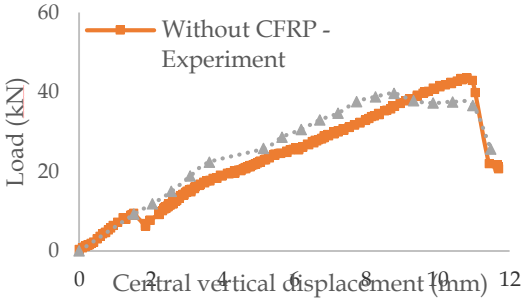

Figure 6 Load vs. Displacement graph with 2 m out of plane curvature

Further, this model was used to predict the performance of tested beams in the current ongoing research. Figure 6 shows the comparison of the experimental results in the current study with the model predicted results.

Table 8 Comparison of failure loads and deflection of control beam

Parameter	Experimental Data	FEM Results	Deviation
Failure Load	43.52 kN	39.65 kN	8%
Corresponding Deflection	10.81 mm	8.77 mm	18%

In this case, the FE model gives an ultimate load capacity of 39.65 kN while in experimental results show 43.52 kN capacity. This is about an 8% difference. In FE model, displacement at ultimate load is 8.77 mm while it is 10.81 in tested sample which indicate 18% difference. Even though this indicates a large discrepancy, the average deviation observed from both cases was 13%. These results also indicate the evidence for the accuracy of the model.

3.2. CFRP strengthened curved beam with 2 m curvature

The load vs. deflection relationships are shown in Figure 7. It is clearly observed that the predicted results follow a path similar to the experimental curve of specimen 2-1-2-FA.

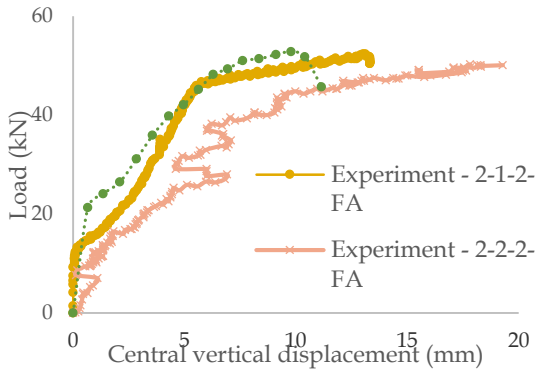

Figure 7 Load vs. Displacement – CFRP retrofitted out of plane curved beam with 2 m curvature

As indicated in Table 9, FE model gives an ultimate load capacity of 52.82 kN. This is about 1% difference from the average failure load of experimental data. In FE model, the displacement at ultimate load is 9.79 mm which indicates 39% difference from the average displacements observed during testing.

Table 9 Comparison of failure loads and deflection CFRP strengthened curved beam with 2 m curvature

Parameter	Experiment (2-1-2-FA)	Experiment (2-2-2-FA)	FEM Results	Deviation
Failure Load	54.40 kN	52.32 kN	52.82 kN	1%
Corresponding Deflection	19.29 mm	13.02 mm	9.79 mm	39%

3.3. Behavior of CFRP retrofitted curved beam with 4 m curvature

The load vs. deflection curves are shown in Figure 8.

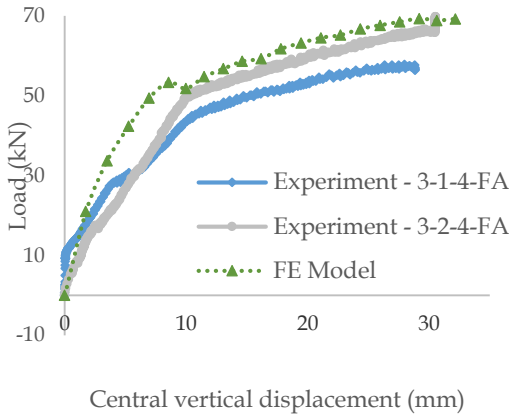

Figure 8 Load vs. Displacement – CFRP retrofitted beam with 4 m curvature

Graphs follow a similar path till the load increment up to 30 kN. From 30 kN to 50 kN, predicted results show slightly higher values than experimental results. Beyond 50 kN, both predicted and experimental (3-1-4-FA) results follows a similar behaviour till failure.

Table 10 Comparison of failure loads and deflection CFRP strengthened curved beam with 4 m curvature

Parameter	Experiment (3-1-4-FA)	Experiment (3-2-4-FA)	FEM Results	Deviation
Failure Load	57.76 kN	69.76 kN	69.27 kN	8.6%
Corresponding Deflection	28.86 mm	30.53 mm	29.21 mm	1.6%

As indicated in Table 10, FE model predictions give an ultimate load capacity of 69.27 kN. This is about 8.6% difference from the average failure load of tested samples. In FE model, displacement noted at ultimate load is 29.21 mm which indicate 1.6% difference from the average displacements observed during testing.

All these results indicate the accuracy of the developed numerical model. Hence this model can be used to predict the effects of bond parameters.

4. PARAMETRIC ANALYSIS

The parametric analysis was carried out to evaluate the behaviour of CFRP wrapped horizontally curved beams with varying parameters.

4.1. Effects of beam curvature

Figure 9 shows the comparison of load vs deflection behaviour of CFRP wrapped beams to enhance the shear performance. Failure loads of beams with curvature radius for 1 m, 2 m, 3 m and 4 m are 31.16 kN, 52.82 kN, 54.32 kN and 69.27 kN, respectively

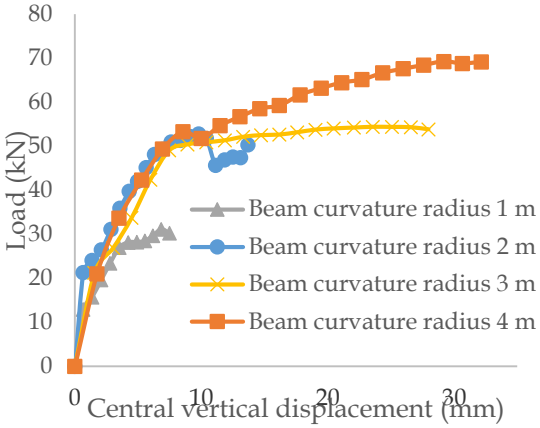

Figure 9 Effects of beam curvature of CFRP retrofitted beam for shear

Graphs clearly depict an enhancement in the failure load under the increased curvature. From shear strengthened beam with curvature radius 1 m to 2 m, a 69.51% of strength enhancement is noted. This lowers to 2% from beam with curvature radius 2 m to 3 m. Again the strength enhancement increases up to 27.5% from the beam with curvature radius 3 m to curvature radius 4 m. Therefore, the increment is uneven. Further, a clear increment in beam displacement at failure is shown. This provides evidence of on improved ductility with increasing curvature of shear strengthened out of plane curved beams.

4.2. Effects of support condition

When the support condition changes from partially fixed to totally fixed condition, the failure load increases from 69.27 kN to 75.88 kN. At simply supported condition, the failure load is 53.97 kN while it is 93.93 kN under pinned support condition. When one side of the beam is pinned while other is simply supported, analysis shows a failure load of 76.28 kN (Figure 10). This failure load is closer to the failure load of fixed support condition. Even the load paths follow slightly similar routes. Hence it can be concluded that under these two conditions, beams behave in a similar manner. Moreover, both fixed and pinned condition and pinned support condition follows a similar loading path.

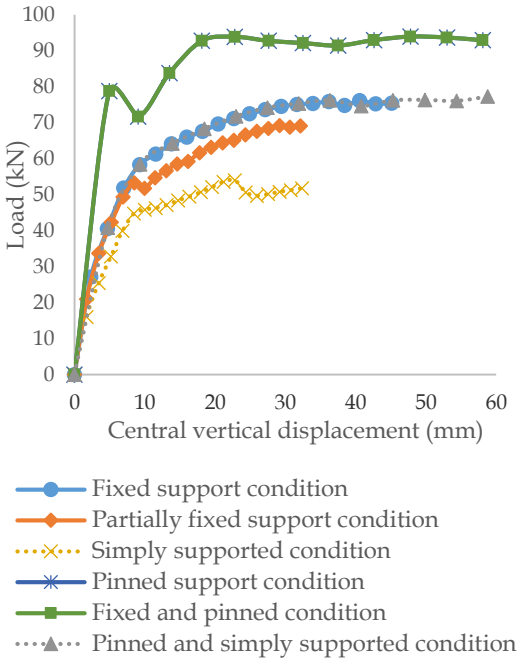

Figure 10 Effects of support condition

All these instances provide clear evidences to prove that if at least one support condition is a pinned support, it highly affects the enhancement of failure load of the CFRP strengthened curved RC beams.

4.3. Effects of number of CFRP layers

Referring Figure 11, it can be clearly concluded that the enhancement of failure load of horizontally curved RC beams depends on the number of CFRP wraps.

Here the failure loads in the ascending order of number of CFRP wraps are 69.27 kN, 85.29 kN and 88.02 kN. Further these results depict that the percentage of the increment of failure load, decreases with the number of CFRP wraps.This highlights the fact that the strengthening effect caused by the number of CFRP layers wrapped reaching an optimum limit. So further increment of number of wraps beyond this optimum limit might not create a greater influence on strength enhancement.

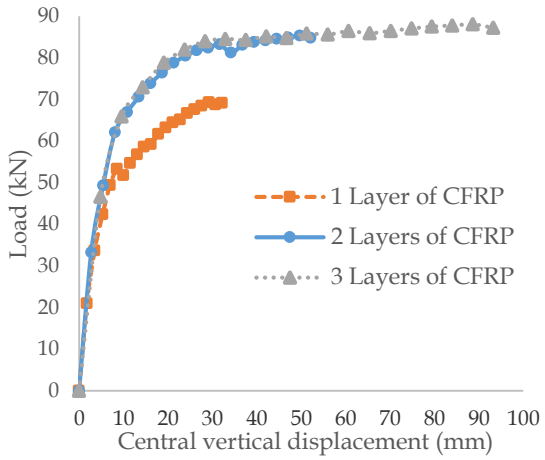

Figure 11 Effects of number of CFRP layers

5. CONCLUSIONS

As predicted, wrapping CFRP fabrics closer to the support, enhanced the shear capacity of RC horizontally curved beams until the shear capacity exceeds the flexural capacity. Strength gain in shear due to CFRP wrapping is around 23%. It seems that the CFRP wraps increase the stiffness of the beam since the deflection of the CFRP wrapped 2 m radius curved beam is lower than that of the 2 m radius curved control beam.

Further the experimental results show that the increase of curvature radius of CFRP wrapped beams enhance the failure load of the beam. This fact can be clearly seen when focusing on the parametric study done on the effects of beam curvature. Moreover, an enhancement in the ductility of the beam was noticed with the increase of curvature of strengthened beams.

Through the parametric analysis it was concluded that the shear performance of a CFRP wrapped RC curved beam enhances when at least a single support is provided with a pinned restraint. Further, the predicted results depicted that when the number of CFRP wraps increase, strength gain reaches a limit. Beyond 3 wraps strength gain will be very low.

6. ACKNOWLEDGMENTS

A special acknowledgment goes to the computer laboratory staff of Department of Civil Engineering, University of Moratuwa for their invaluable guidance. The financial support given to the undergraduate project from University of Moratuwa is greatly appreciated.

7. REFERENCES

Balakrishnan, S., Elwi, A. and Murray, D., 1988, 'Effect of Modeling on NLFE Analysis of Concrete Structures', *Journal of Structural Engineering*, 114(7), 1467-1487.

Rvendran, A., Perera, D. and Gamage, J., 2016, 'Finite Element Analysis of CFRP Strengthened Concrete Beams', *4th International Symposium on Advances in Civil and Environmental Engineering Practices for Sustainable Development (ACEPS)*.

Ariyachandra, M., Gamage, J., Al-Mahaidi, R. and Kalfat, R., 2017, 'Effects of surface roughness and bond enhancing techniques on flexural performance of CFRP/concrete composites', *Composite Structures*, 178, 476-482.

Premarathne, H. and Gamage, J., 2013, 'Alternative bonding techniques to delay end debonding of CFRP strengthened reinforced concrete beam', *4th International Conference on Structural Engineering and Construction Management*, Kandy, pp.154-160.

Amarasinghe, N. and Gamage, J., 2015, 'Experimental study on integrated method of NSM and EBR techniques for flexural strengthening of Concrete Beams using CFRP', *6th International Conference on Structural Engineering and Construction Management*, Kandy, pp.170-177.

Chaallal, O., Nollet, M. and Perraton, D., 1998, 'Shear Strengthening of RC Beams by Externally Bonded Side CFRP Strips', *Journal of Composites for Construction*, 2(2), 111-113.

Tamura, T. and Murata, H., 2010, 'Experimental study on the ultimate strength of R/C curved beam', *Fracture Mechanics of Concrete and Concrete Structures*, Korea Concrete Institute, 1783-1788.

Muralidharan, R., Jeyashree, T. and Krishnaveni, C., 2017, Analytical Investigation of RC Curved Beams, *Journal of Industrial Pollution Control.*

Wahalathantri, B.L., Thambiratnam, D.P., Chan, T.H.T. and Fawzia, S., 2011, 'A material model for flexural crack simulation in reinforced concrete elements using ABAQUS', *Proceedings of the first international conference on engineering, designing and developing the built environment for sustainable wellbeing*, Queensland University of Technology, pp. 260-264

Sharcnet.ca. n.d., *Abaqus Analysis User's Manual 6.10*, viewed 10 October 2018, from https://www.sharcnet.ca/Software/Abaqus610/Documentation/docs/v6.10/books/usb/default.htm?startat=pt05ch19s02abm02.html#usb-mat-clinearelastic-orthoterms.

Daud, R., Cunningham, L. and Wang, Y., 2015 'Non-linear FE Modelling of CFRP-strengthened RC slabs under cyclic loading', *Athens Journal of Technology and Engineering*, 2(3), 161-180.

X-Calibur Construction Chemistry Inc., n.d., *X-Wrap C300-High strength carbon fiber fabric for structural strengthening*, viewed 15 Novmber 2018, from <https://www.x-calibur.us/files/X-Wrap%20C300.pdf >.

Eurocode 3: Design of steel structures - Part 1-1, 2005, 'General rules and rules for buildings', British Standards Institution, London.

BS EN 10025-3:2004. Hot rolled products of structural steels - Part 3, 2004, 'Technical delivery conditions for normalized/normalized rolled weldable fine grain structural steels', British Standards Institution, London.

Tejaswini, T. and Raju, M., 2015, 'Analysis of RCC Beams using ABAQUS', *International Journal of Innovations in Engineering and Technology (IJIET)*, 5(3), 248-255

Pereira, J., 2005, '*FE Modeling of FRP Strengthening Systems on the White Bayou Bridge'*, M.Sc. Chalmers University of Technology.

Friswell, M., 1995, *Introduction to Finite Element Modeling.*

Proceedings of the 7th International Symposium on

Advances in Civil and Environmental Engineering Practices for Sustainable Development

ACEPS - 2019

Use of superabsorbent polymers to improve the properties of fresh concrete.

G.H.P.N. Pushpakumara [1] and J.M.R.S. Appuhamy [2]

[1]Dept. of Civil Engineering, Faculty of Engineering, University of Ruhuna, Hapugala, Galle, SRI LANKA.

K e y w o r d s

Super absorbent polymers
Concrete
Compressive strength
Shrinkage

A B S T R A C T

Providing a satisfactory amount of moisture in concrete at its early stage is essential in order to achieve the desired properties such as strength and low autogenous shrinkage. Since it is not always possible to provide sufficient amount of curing, attempts are being made to develop self-curing concrete by using Super Absorbent Polymers (SAP). SAP acts as a water-retaining agent can absorb intense amount of water and release it when the external conditions are dry. Though adding SAP may increase the strength by enhancing the degree of hydration there by controlling the autogenous shrinkage; voids left by releasing stored water will weaken the microstructure ultimately causing a strength reduction. Therefore, aim of this research was to evaluate the properties of concrete when mixed with SAP Therefore SAP was added to three different concrete mixes (G40, G45, G50) as a percentage of the cement weight (0.1%,0.15%,0.2%,0.25% and 0.3%). Mixing was carried out without adding extra water and samples were casted to evaluate the compressive strength under both cured and uncured conditions flexural strength under cured conditions and shrinkage under uncured condition. It was found that the 0.2% of SAP gives higher values in terms of compressive and flexural strength-wise compared to control samples under both conditions and shows a higher strength gain with the time also. It was also found that the uncured samples did not reach the target compressive strength therefore action of SAP without curing isn't as effective as samples under curing conditions. Ultimate compressive strength of concrete was increased only by 4-5 % for the 0.2% SAP mix therefore has a negligible effect in strength-wise. In terms of shrinkage 0.3% SAP mix has shown favorable results compared to all the other samples.

1. INTRODUCTION

Water in concrete has a significant influence throughout the lifetime of concrete. It is an imperative compound in mixing curing and hardening stages of concrete. Water can even cause matured concrete to shrink, swell and crack. Furtherly, it can influence the strength of concrete also.

Apparently controlling the water content of concrete is essential. This can be achieved by applying additives to the concrete mixture such as superabsorbent polymers (SAP) which has the capability of dominating the behavior of water in concrete. Super absorbent polymers are white granules which can take in and contain an intense amount of water relative to its weight (300 times of its own weight). Mixed with concrete (SAP) ensures internal water curing as the curing agent act as an internal reservoir of water, releasing water gradually as the concrete begins to dry out. While the internal curing provided by SAP agent enhances the degree of hydration thereby increase the strength, voids generated by the SAP causes reduction of strength. Dominant of these two effects depends upon water-cement ratio(w/c), amount of SAP added and concrete maturity. In particular, at a high w/c (>0.45), SAP addition has very little effect on hydration and therefore generally reduces compressive strength. At a low w/c (<0.45), SAP addition may increase the compressive strength (Jensen 2013). Yet the past studies suggest that the compressive strength gets reduced at a linear rate up to

0.4% SAP content (i.e. strength loss<25%) but 40% loss at 0.6% SAP content (Olawuyi & Boshoff 2013) even under cured conditions. Similar to the compressive strength, tensile strength can be improved by using SAP. Studies show that the 0.4% of SAP may produce better strength results in terms of tensile strength wise when mixed with extra water for sealed and normal curing methods. SAP percentages above or lesser than 0.4% would not reach the tensile strength of control sample. Rate of improving the tensile strength is slightly higher compared to compressive strength (Abbas & Jasmin 2015).

1.1. Background

Superabsorbent polymers are normally used in high performance concrete (HPC). HPC is a generic term for certain types of concrete having properties and constructability which exceeds that of normal concrete. HPC is specially designed to meet certain levels in terms of high workability, high strength, high early strength and durability. Though it has been a trend in the industry to utilize HPC, due to susceptibility of these types of concrete to develop autogenous shrinkage, researches for developing materials to use as internal curing agents (IC agents) is continuously growing. The real site situation hardly can offer effective curing by complete immersion in water. It is defined that IC agents should be of appropriate type and optimum proportion while its addition should not result in any detrimental effect on the requisite properties of concrete. Though the SAP is primarily introduced to HPC concrete it still can be beneficial in normal concrete also. Provided with proper mix proportions SAP may act as an effective IC agent providing enough curing to enhance the degree of hydration thereby control autogenous shrinkage ultimately causing an increment of strength. Previous studies show that the increasing SAP content can actually reduce the shrinkage and can be used to achieve almost zero shrinkage despite the effect on strength. In such a study 0.4% of SAP mix has shown almost zero shrinkage (Jensen & Hansen 2001). Thus, the purpose of adding SAP into concrete which is to control the degree of hydration thereby to control the shrinkage can be achieved effectively.

1.2. Objectives

Objectives of this research are to,

- Evaluate compressive strength performance
- Evaluate autogenous shrinkage
- Find out an optimum percentage of SAP can be added,

When the concrete is provided with low w/c ratio (< 0.45) and mixed with SAP at different percentages without adding extra water.

2. METHODOLOGY

Conventional materials used in this study included river sand, ordinary Portland Cement and coarse aggregate(20mm). Sodium polyacrylate was used as the superabsorbent polymer with chemical formula $[-CH_2-CH(COONa)-]_n$ having a white fine powder appearance with 230-100µm particle size distribution and absorbance capacity of 350-500g/g of water.

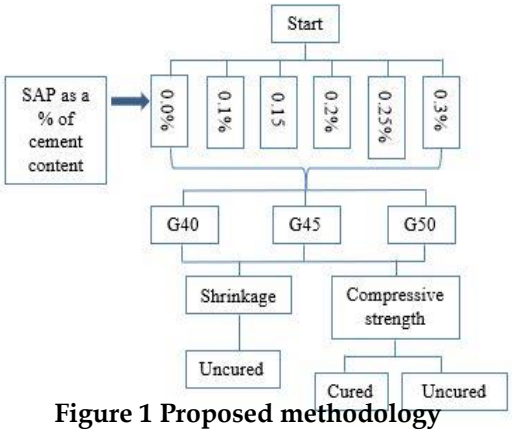

Figure 1 Proposed methodology

Three concrete grades of G40, G45, G50 was selected for testing. Five SAP percentages were selected as shown in the Figure 1. SAP was added to the mix before adding water and kept mixing for about 1 minute. Set of samples were left under normal curing conditions and Another set was left uncured. Compressive strength test was done for the samples as per the BS 1881 part 116 & flexural strength was carried out as per the BS 1881 part 117. For shrinkage test; from each mix mortar samples were taken.

2.1. Experimental approach

As suggested by the literature review SAP may affect to properties of concrete compared

to High Performance Concrete when the water cement ratio is less than 0.45(Alnasra 2013). Therefore G40, G45, G50 concrete grades were selected. In a range of 0.1% to 0.3% test results have shown better results in the past studies therefore 0.1%,0.15%,0.2%,0.25%,0.3% of SAP as a weight of cement added in each mix was selected (Table 1). Sodium polyacrylate was ordered from India. For the concrete mix river sand and ordinary Portland cement was used. In total 324 cubes for 24 different combinations were casted and 54 number of beams were casted for the flexural strength test. For autogenous shrinkage measurement three different SAP percentages 0%, 0.2% and 0.3% was selected.

Table 1 Specimen detail summary

Con. Grade	SAP %	Spec. code	SAP weight(kg)
G -40	0	40 S1	0.000
	0.1	40 S2	0.009
	0.15	40 S3	0.013
	0.2	40 S4	0.018
	0.25	40 S5	0.022
	0.3	40 S6	0.027
G -45	0	45 S1	0.000
	0.1	45 S2	0.024
	0.15	45 S3	0.037
	0.2	45 S4	0.049
	0.25	45 S5	0.061
	0.3	45 S6	0.073
G -50	0	50 S1	0.000
	0.1	50 S2	0.019
	0.15	50 S3	0.029
	0.2	50 S4	0.039
	0.25	50 S5	0.048
	0.3	50 S6	0.058

3. RESULTS AND DISCUSSION

3.1. Effect on compressive strength

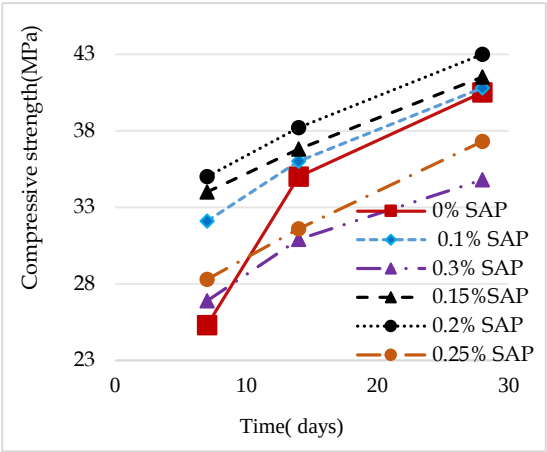

Figure 2 Compressive strength results for G 40 cured concrete

Compressive test results of the cured samples show that the Strength gain of SAP mixed concrete has a higher value compared to control samples (Figure 2). But with the time, rate of increasing the strength drops and at the end of 14 days 0nly 0.1%., 0.15% and 0.2% SAP mixed concrete shows higher strength gain over the control sample and other two mixes show a considerable drop in strength. At the end of 28 days where concrete is expected to reach its maximum strength; from Figure 3 it is quite clear that the control samples have reached the target strength while 0.25% and 0.3% SAP mixed concrete was unable to. But for the other mix types; all the samples have shown higher strength gain and among them, 0.2% SAP mix shows the highest strength gain. All three grades test results follow this similar pattern. Yet the improvement of 28-day strength is not so significant even for the 0.2% SAP mix compared to the control sample.

Uncured samples still follow similar compressive strength gain pattern similar to cured samples where 0.2% of SAP mix shows the highest strength (Figure 3). But the issue with the uncured samples is that none of the samples have been able to reach the target strength. Strength reduction was very high; percentage wise in between 15-20% of strength has been lost compared to control samples (Figure 4).

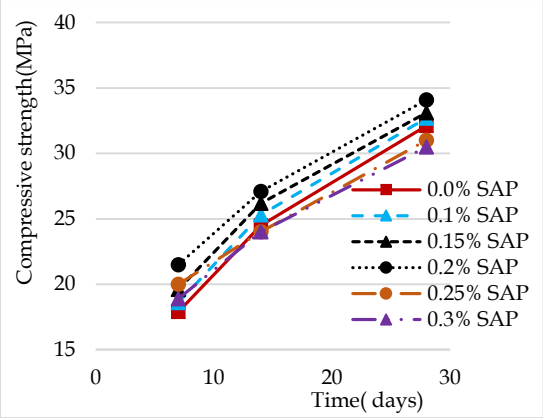

Figure 3 Compressive strength results for G 40 uncured samples

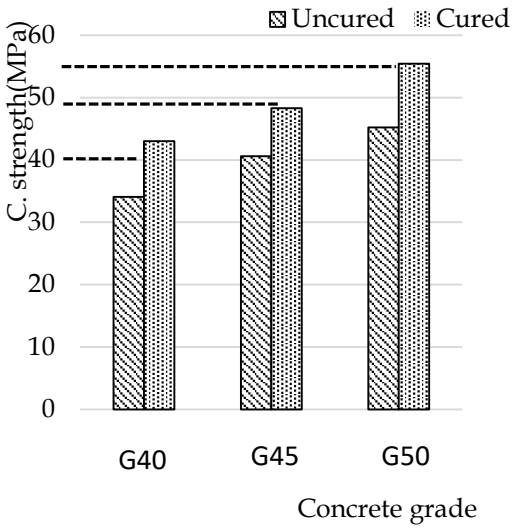

Figure 4 Compressive strength comparison

Therefore, it is obvious that the SAP under uncured conditions isn't as effective as under cured conditions. Possible caution would be that the voids become dominant over the strength gain caused by controlled hydration by SAP and the unsatisfactory amount of degree of hydration under uncured conditions. Percentage-wise at the end of 7 days, both cured and uncured samples show 37%and 20% strength gain respectively over the control samples for 0.2% SAP mixes. But at the end of 14 and 28 days, this increment gets reduced and at the end of 28 days, nearly 5-6% strength increment can be noticed. Significant strength reduction can be notified at the end of 28 days, for 0.25% and 0.3% SAP mixes where nearly15% of strength reduction for cured samples and 5% strength reduction for uncured samples. No significant difference can be notified for the samples of 0.1%, 0.15%, and 0.2% SAP mixes under both cured and uncured conditions at the end of 28 days. Strength increment by enhancing the degree of hydration becoming dominant over the strength loss due to voids causes increment in strength gain or vice versa.

3.2. Effect on Flexural strength

Prisms casted and kept under cured conditions shows similar strength gain pattern to the compressive strength gain pattern where 0.2% SAP mix shows higher flexural strength compared to other samples (Figure 6). Percentage wise the increment of flexural strength is nearly 30-40% that of the control samples.

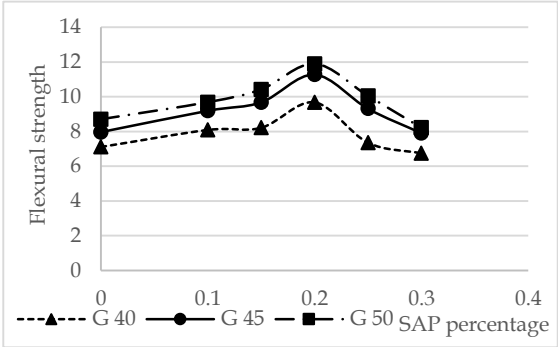

Figure 5 Flexural strength variation

3.3. Effect on autogenous shrinkage

Primary idea of introducing SAP in concrete is to provide internal curing thereby increase the degree of hydration. This process will cause concrete to minimize the autogenous shrinkage thereby to increase the strength (Arbili 2014).

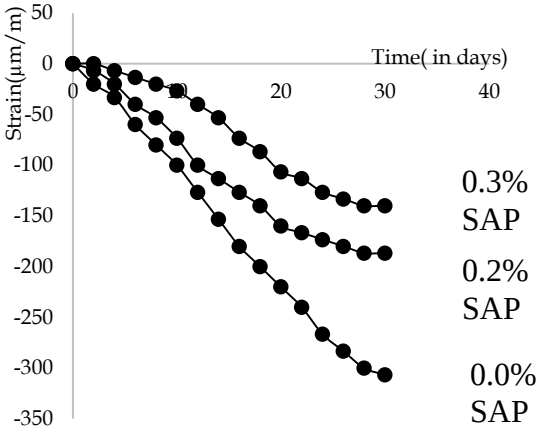

Figure 6 Strain Vs. time for different SAP mixed concrete

Most of the research studies have been carried out under cured condition to identify the effect on shrinkage and test results revile that the 0.4% of SAP mix under cured

condition can almost remove the shrinkage (Jenson 2013).

In this research study, the samples were kept under uncured conditions and it was found out that the 0.3% SAP mix mortar shows lesser shrinkage compared to control sample (Figure 7). It is obvious that the SAP is still effective under uncured conditions in achieving lesser autogenous shrinkage.

4. CONCLUSION

Considering compressive strength wise adding 0.2% of SAP can increase the strength of concrete up to 5-6% that of Control sample if the curing is provided. Beyond that level, concrete tempts to lose its strength due to voids left by SAP. Though adding SAP will cause lesser shrinkage it will cause concrete to lose the homogeneity by leaving voids as the drought happens and concrete becomes mature. These voids will weaken the microstructure of concrete hence cause concrete to lose its strength. Though the uncured samples follow similar strength gain pattern with the increment of SAP none of the samples reached the target strength which suggests that the voids have become dominant and the purpose of adding SAP to control the hydration process has not been fully accomplished. Adding more SAP will enhance the degree of hydration but again the voids left behind will cause a reduction in strength. The Primary objective of adding SAP which is to control the shrinkage has been a success as the test results shows 0.3% SAP mix show lesser strain values compared to control sample. Therefore, SAP is quite capable of controlling the shrinkage even under uncured conditions, yet more effective results could be gained if the satisfactory amount of curing is provided. By reacting with water super absorbent polymers releases hydroxides such as sodium hydroxide or potassium hydroxide. Therefore, introducing PH responsive SAP in control, the hydration process will be beneficial in several ways. On the other hand, certain researches can be done to identify the effect of adding extra water into concrete for the grades used in this research study to find out the effectiveness of SAP. Since the particle size do matter in absorbance capacity of SAP, SAP with different particle sizes can be introduce to concrete.

5. REFERENCES

Al-Nasra, M. & Daoud, M., 2013, 'Investigating the Use of Super Absorbent Polymer in Plain Concrete', *International Journal of Emerging Technology and Advanced Engineering*, 3(8), 599-603.

Jensen, O.M., 2013, 'Use of superabsorbent polymers in concrete', *Concrete international.*

Olawuyi, B. & Boshoff, W., 2013, 'Compressive strength of high-performance concrete with absorption capacity of Super-Absorbing-Polymers (SAP)', *Research and Applications in Structural Engineering, Mechanics and Computation*.

Abbas, A.W. & Jasim, M.A., 2017, 'Fresh and Hardened properties of Concrete', *International Journal of Science and Research*, 6

Jensen, O.M. & Hansen, P.F., 2002, 'Water-Entrained Cement-Based Materials: II. Experimental Observations', *Cement and Concrete Research*, 32(6), 973-978.

Nasra, A., 2013, 'Optimizing the Use of Sodium Polyacrylate in Plain Concrete', *International Journal of Engineering Research and Applications*, 03(3), 1058-1062.

BS1881-116: Testing concrete, 1983, '*Method for determination of compressive strength of concrete cubes*', British Standards Institution, London:

BS1881-118: Testing concrete, 1983, 'Method for determination of flexural strength', British Standards Institution, London.

Proceedings of the 7th International Symposium on

Advances in Civil and Environmental Engineering Practices for Sustainable Development

ACEPS - 2019

Possibility of production of bricks using waste materials and natural binding materials in Sri Lanka

D.M. Shanuka Jayathunge[1],Rohantha Rukshan Jayasinghe[1] and Madujith Sagara[2]

[1]University of West of England, Bristol, UK
[2]Department of Civil Engineering, University of Moratuwa, Katubedda, SRI LANKA

K e y w o r d s

Cashew tree latex
Eco-bricks
Sludge waste
Waste materials

A B S T R A C T

This paper discusses about the possible waste materials for brick production and natural binding materials that have been used for ancient constructions also. Main waste materials were taken as sludge waste from drains and waste putty dust. Naturally occurring cashew tree latex was selected to be binding agent. Cashew tree latex was crushed into small pieces added to 150-200 ml distilled water and heated until it melted. The molten glue of that was used as the binding agent. 215 x 102.5 x 65 mm bricks were cast by changing mix ratio. It was identified that brick manufacturing is possible using above mentioned materials.

1. INTRODUCTION

Conventional burnt bricks are the most commonly used building material for residential buildings in tropical countries. Clay is the main material that used for the brick manufacturing process. The most common method of obtaining clay is an open pit method. Commonly, these harvesting areas are abandoned without any reclaiming process causing resource depletion and environmental degradation resulting contamination, emission of greenhouse gases, loss of bio-diversity, etc. Furthermore, energy consumption and carbon footprint of the brick production (427.985 kg.CO_2/1000 bricks) is comparatively high when compared with other building materials such as concrete (Maheshwari and Jain, 2017). Many researchers have investigated to enhance the properties of brick materials by proportionally replacing with other materials such as bamboo (Chandra et al., 2019), soil, fly ash, waste materials, plastic waste (Raut, Ralegaonkar and Mandavgane, 2011). Some researches have invented eco-friendly bricks from entirely waste materials. When considering about binding materials, cement, lime and gypsum are the most common binding material that has been used for centuries (Al-Ajmi et al., 2016). But according to the Mahavamsa book, ancient Sri Lankan constructions have used natural glues as binding agent such as cashew tree latex, wood apple latex etc.

Eco-bricks that are produced from waste materials need to have acceptable physical and mechanical properties to be met with relevant standards (Antico et al., 2017). However, there are no proper records of any methods or mix proportions regarding natural glues. Thus, this paper discusses the possibility of producing eco-bricks using waste materials based on natural binders.

2. LITREURE REVIEW

2.1. Major types of waste materials

Several types of waste products are get produced with development and population growth (Brunner and Rechberger, 2015). Because of the large amount of solid materials consists of long-living construction materials, the amount of waste that generation must be treated much bigger than today's waste flowers. In general, the developed countries generate much higher quantities of waste

compared to the developing countries (Vergara and Tchobanoglous, 2012). However, many of these countries are practicing the solid waste management system to control the amount of waste generated and to prevent environmental pollution. The principal sources of solid waste can be categories by its type (Dixon and Jones, 2005; Demirbas, 2011). The major types of waste can be categorized as municipal solid, industrial, agricultural, and hazardous waste (Singh, Gupta and Chaudhary, 2014).

2.1.1.Municipal solid waste

Municipal solid waste is mostly generated from the activities of household, offices, hotels, school and other institutions. The major components of this category are food waste, paper, plastic, rags, metal and glass. Also the demolition and construction debris are often get included under municipal waste. However, if municipal waste is considered as raw material for produce bricks, material sorting should be carried out. There, it could be small quantities of hazardous waste such as electric light bulbs, batteries, automotive parts etc. (Dehghanifard and Dehghani, 2018). The rate of generation of Municipal solid waste gets varied from city to city and season to season and also, it has a strong relationship with economic development.

2.1.2. Industrial solid waste

The industrial solid waste gets produced as a result of processing of raw materials for the production of new materials (Ngoc and Schnitzer, 2009). The industries are generating different kinds of waste and some wastes are toxic while others being non-toxic. Typically this industrial waste consists of paper, packaging materials, waste from food processing, oils, solvents, resins, paints, sludge, glass, ceramics, stones, metals, plastics, rubber, leather, wood, cloth, straw, abrasives etc.

Construction and demolished waste, also fall under industrial solid waste. Solid waste from the construction industry is one of the main components that affect waste generate in many countries. The major types of waste that generated from construction activities are concrete leftover, demolished debris, steel scrap (Wang, Kang and Wing- Yan Tam, 2008). According to some researches (Poon, Yu and Ng, 2001), there are two main kinds of construction waste. Those are structural waste and finishing waste. Concrete fragments, steel reinforcement, abandoned timber plates, and pieces are generated as structural waste. Other waste, including surplus cement mortar, Paint, plastering materials (waste putty dust), broken tiles and ceramics are categorized as finishing works. Those are the most common waste materials that have been generated during the finishing and structural stage.

2.1.3. Agricultural waste and residues

Development of the agricultural production has naturally resulted for increment of the quantities of livestock waste, agricultural crop residues and agro-industrial by-products (Nagendran, 2011).

2.1.4. Hazardous waste

With the rapid development in agriculture, industry, hospital and health care facilities, consumption of significant quantities of toxic chemicals and other hazardous waste materials has been increased widely (Mmereki et al., 2016). In Sri Lanka, most of the hazardous wastes are byproducts of the production and consumption of industrial products, such as chemicals, petroleum, metals, wood treatments, pulp and paper, leather, textiles, agricultural and hospital waste etc.

2.2. Types of waste materials used for manufacturing bricks

There are several materials that have been used for manufacturing and eco-friendly lightweight bricks. Those are paper mill sludge and soil (Goel and Kalamdhad, 2017), residual coal waste rocks (Taha et al., 2017), natural waste materials such as orange peels, coconut waste (Arshad, 2014), construction waste such as brick debris, quarry dust and cement (Ramkumar and Rubini, 2017). Apart from that, mud-concrete technology is also known as an innovative method that reduces the use of raw materials to minimize the environmental impacts (Arooz and Halwatura, 2018).

3. METHODS AND MATERIALS

In the contemporary manufacturing process of eco-bricks, base material were selected as urban drain sludge waste and cashew tree latex was selected as binding agent. Brick sample size was selected to be 215 x 102.5 x 65 mm accordance with BS 3921 of 1995 and Sri Lanka Standard (SLS) 39 of 1981.

3.1. Materials

3.1.1. Drain sludge waste

Due to the poor surface drainage and water stagnation in the town and country areas in Sri Lanka, drain blockages and sedimentation taken place. Therefore, drain sludge waste was taken from a main city, "Negambo" as the brick construction material aiming the reduction of environmental impact. Samples were collected from the main drainage system that covers the Negambo area. Collected waste sample from drains is as shown in Figure 1.

Figure 1 Collected sludge waste sample from drains

Collected sludge was air dried for 2 days for removing odor. Then it was oven dried for 24 hours to conduct the particle size distribution test accordance with the British Soil Classification System (BSCS). It was identified that sample is a poorly graded soil contained more than 90% of sand particles. Figure 2, shows sieved sludge waste. Thus, sludge waste soil is considered as not suitable for brick production due to poor particle distribution. As an initial trial, an improvement media, waste putty dust was decided to be tried with sludge waste.

3.1.2. Waste putty dust

Wall putty is basically a white cement-based powder that is created into a smooth mixture

Figure 2 Sieved sludge waste

and applied on wall before painting. However, during the surface smoothing, large quantity of putty dust gets formed. Collected putty dust is being dumped as construction waste. Samples were collected from construction sites to be tried as an improvement to the aforesaid mix.

3.1.3. Cashew tree latex

Cashew tree latex is naturally occurring glue that hardens with time. Solid state latex was collected to be used as a binding agent to replace cement and/or lime. Natural state of cashew tree latex is as shown in Figure 3.

Figure 3 Natural state of the cashew tree latex

500 g of cashew tree latex was collected and added to 150-200 ml distilled water to be heated. After becoming molten glue, it was used as the binding agent. Figure 4 shows the molten cashew tree latex.

Figure 4 Molten cashew tree latex

3.2. Manufacturing of brick samples

Several brick samples were casted by changing mix ratio. After 7 days of curing process samples were decided to be tested for soundness, hardness and weight. Figure 5 shows the prepared brick samples.

Figure 5 Prepared brick samples

4. DISCUSSION

This paper presents the first part of an ongoing investigation. Therefore, the conclusions derived from the experiments are partial conclusions. It was identified that bricks can be effectively produced using sludge waste, waste putty dust and cashew tree latex. Further research should need to be carried out to find the optimum mix design for eco-bricks and test to identify the physical and mechanical properties. Also, proper research needs to be conducted to find other possible natural bindings that have been used in ancient constructions. With these improvements and with the knowledge of properties of binding materials, innovative designs can introduce using modern technology, minimizing the use of cement based binders.

5. CONCLUSIONS

Many researches are having attempts to develop eco-bricks using various types of waste materials. Hence, successful attempts were made to incorporate waste materials in the manufacturing of bricks in Sri Lanka context. According to this paper, it was identified that it is possible to use cashew tree latex with waste materials to manufacture eco-bricks. The initial mix-design was identified and the optimum method to be proposed based on future experiments.

6. REFERENCE

Al-Ajmi, F., Abdalla, H., Abdelghaffar, M. & Almatawah, J., 2016, 'Strength Behavior of Mud Brick in Building Construction', *Open Journal of Civil Engineering*, 06(03), 482-494.

Antico, F., Wiener, M., Araya-Letelier, G. & Gonzalez Retamal, R., 2017, 'Eco-bricks: a sustainable substitute for construction materials', *Revista de la construcción*, 16(3), 518-526.

Arooz, F. R., & Halwatura, R. U., 2017, 'Mud-concrete block (MCB): mix design & durability characteristics', *Case Studies in Construction Materials,* 39-50.

Brunner, P.H. & Rechberger, H., 2015, 'Waste to energy – key element for sustainable waste management', *Waste Management*. 37, 3–12.

Dehghanifard, E. & Dehghani, M.H., 2018, 'Evaluation and analysis of municipal solid wastes in Tehran', Iran. *MethodsX*. 5 pp. 312–321.

Demirbas, A., 2011, 'Waste management, waste resource facilities and waste conversion processes', *Energy Conversion and Management*, 52 (2), 1280–1287.

Dixon, N. & Jones, D.R.V., 2005, 'Engineering properties of municipal solid waste, *Geotextiles and Geomembranes*, 23 (3), 205–233.

Goel, G. & Kalamdhad, A.S., 2017, 'An investigation on use of paper mill sludge in brick manufacturing, *Construction and Building Materials*, 148, 334–343..

Chandra, M.S., Nandapala, K., Priyadarshana, G. & Halwatura, R.U., 2019, 'Developing a durable thermally insulated roof slab system using bamboo insulation panels', *International Journal of Energy and Environmental Engineering* [online]. Available from: http://link.springer.com/10.1007/s40095-019-0308-xdoi:10.1007/s40095-019-0308-x

Mahānāma, Geiger, W., Bode, M. & Mendis, G., 2001, *The Mahāvaṁsa, or, The great chronicle of Ceylon*. London: Pali Text Society.

Maheshwari, H. & Jain, K., 2017, 'Carbon Footprint of Bricks Production in Fixed Chimney Bull's Trench Kilns in India', *Indian Journal of Science and Technology*, 10(16), 1-11.

Mmereki, D., Baldwin, A., Hong, L. & Li, B., 2016, 'The Management of Hazardous Waste in Developing Countries. In: Hosam El-Din M. Saleh and Rehab O. Abdel Rahman (eds.)', *Management of Hazardous Wastes* [online]. (no place) InTech. Available from: http://www.intechopen.com/books/management-of-hazardous-wastes/the-management-of-hazardous-waste-in-developing-countries [Accessed 11 August 2019].

Nagendran, R., 2011, 'Agricultural Waste and Pollution', In: *Waste* [online]. (no place) Elsevier. pp. 341–355. Available from: https://linkinghub.elsevier.com/retrieve/pii/B9780123814753100245doi:10.1016/B978-0-12-381475-3.10024-5 [Accessed 11 August 2019].

Ngoc, U.N. & Schnitzer, H., 2009, 'Sustainable solutions for solid waste management in Southeast Asian countries', *Waste Management*. 29 (6), 1982–1995.

Poon, C.S., Yu, A.T.W. & Ng, L.H., 2001, 'On-site sorting of construction and demolition waste in Hong Kong', *Resources, Conservation and Recycling*. 32 (2), 157–172.

Raut, S., Ralegaonkar, R. & Mandavgane, S., 2011, 'Development of sustainable construction material using industrial and agricultural solid waste: A review of waste-create bricks', *Construction and Building Materials*, 25(10), 4037-4042.

Singh, G., Gupta, K. & Chaudhary, S., 2014, 'Solid Waste Management: Its Sources, Collection, Transportation and Recycling', *International Journal of Environmental Science and Development*, 5(4), 347-351.

Taha, Y., Benzaazoua, M., Hakkou, R. & Mansori, M., 2017, 'Coal mine wastes recycling for coal recovery and eco-friendly bricks production' *Minerals Engineering*. 107, 123–138.

Vergara, S.E. & Tchobanoglous, G., 2012, 'Municipal Solid Waste and the Environment: A Global Perspective', *Annual Review of Environment and Resources*. 37 (1), 277–309.

Wang, J., Kang, X. & Wing- Yan Tam, V., 2008, 'An investigation of construction wastes: an empirical study in Shenzhen', *Journal of Engineering, Design and Technology*. 6 (3), 227–236.

Proceedings of the 7th International Symposium on

Advances in Civil and Environmental Engineering Practices for Sustainable Development

ACEPS - 2019

Study on suitable wall thermal insulation methods for dwellings under tropical climatic conditions: a review.

E.M.J.C.Silva[1], Madujith Sagara Chandra[2]

[1]University of the West of England, Bristol, UK
[2]Department of Civil Engineering, University of Moratuwa, Katubedda, SRI LANKA

K e y w o r d s

Wall thermal insulation
Passive cooling
Energy efficiency
Sustainable walls
Natural thermal insulation

A B S T R A C T

Utilization of thermal insulation methods is the most effective and energy efficient way to achieve indoor thermal comfort of dwellings. Thermal insulation will improve the energy efficiency of the building envelope by minimizing heat gain/loss through the building envelope. Key aspects of building thermal insulation are; insulation of external walls and roofs. Walls occupy the largest area of a dwelling and about 30% of total heat gain occurs through walls. Thermal insulation of walls with appropriate materials will result in a significant reduction of heat transmission into dwellings. Since there are previous studies done for insulation of roofs by other researchers for tropical climatic conditions, this study is conducted for thermal insulation of walls. In this study, the most suitable and effective thermal insulation methods in terms of energy efficiency and financial feasibility for tropical climate conditions were discussed. Even though there are many thermal insulation materials available only few materials are suitable for tropical climatic conditions. They are mineral wool, EPS, XPS, PUR, cellulose, cork, fibreglass, EPS wall panels etc. But the most suitable eco-friendly wall thermal insulant method is, producing insulated walls using natural insulation materials mixed with wall construction materials.

1. INTRODUCTION

The development of the world with the growth of world population, a drastic increment of urbanization has taken place. Due to the lack of greenery, the temperature within the city has increased. The energy demand of buildings contributes to more than 40% of the total global energy consumption and major half of greenhouse gas (GHG) emissions (Ozel, 2014; Rahman *et al.*, 2019). High emission of GHG has caused global warming and it is one of the burning issues that the world is facing. Active cooling methods can be used to reduce the inside temperature of buildings, but those aspects require higher demand of energy which relies on carbon fossil fuel, which causes the increment in CO_2 emission which contributes to the greenhouse effect (Chandra *et al.*, 2019). Therefore, enhancing the energy efficiency of dwellings will reduce the overall energy usage and greenhouse gas emission. Due to the higher interior temperatures, occupants tend to use air conditioning and other active cooling methods which directly augment the daily energy demand. According to predictions, global energy consumption will increase by 53% and will lead to an energy crisis in near future (International Energy Agency, 2019). In recent years, sustainable and green concepts were developed to mitigate higher global warmth. The energy performance of a dwelling depends on the thermal properties of building envelope. One of the most common energy efficacy methods is the thermal insulation of the external walls and roofs (Chandra *et al.*, 2019; Nandapala *et al.*, 2018). Thermal insulation will reduce the cooling energy demand which is used in active cooling systems. This study is focused on the methods of thermal insulation of the walls suitable for tropical countries.

1.1. Passive cooling

Passive cooling methods are used to minimize heat gain/loss of buildings in order to enhance the indoor thermal comfort without any mechanical method (Chandra *et al.*, 2019). It is the most effective way to improve the indoor thermal comfort of dwellings with less energy consumption and null environmental pollution. Even though there are many passive cooling techniques, thermal insulation is one of the most fruitful solutions.

2. OBJECTIVE

The main objective of this study is to propose a suitable wall thermal insulation method for dwellings, under tropical climatic conditions.

3. METHODOLOGY

3.1. Investigating existing wall thermal insulation methods

Existing wall thermal insulation methods/materials were investigated through a detailed literature review and available records.

3.2. Selecting the most suitable wall thermal insulation method for dwellings under tropical climatic conditions

Most suitable thermal insulation method for dwellings under tropical climatic conditions was proposed comparing the thermal properties and financial aspects of prevailing insulation systems.

4. LITERATURE REVIEW

4.1. Thermal insulation

In tropical climatic conditions, the maximum outdoor daytime air temperature reaches about 30-32 ℃ in most of the days in a year and night time air temperature could drop to 22-25 ℃ (Halwatura and Jayasinghe, 2008). High temperature and low airflow significantly affect the thermal comfort of an indoor environment. The inside temperature of dwellings increases mainly due to solar heat gain through the building envelope. Thermal insulation plays an important role in the enhancement of energy efficacy of dwellings controlling the fibreglass. Building thermal insulation is capable of keeping the indoor environment comfortable by controlling penetration of heat flux through the envelope. Other benefits of utilizing thermal insulation are acoustic insulation, sustainability and fire resistance (Aditya *et al.*, 2017). The main objective of installing wall thermal insulation material in a dwelling is to reduce energy consumption for cooling/heating by enclosing the building envelope (Chandra *et al.*, 2019).

Wall is one of the most substantial components in a dwelling where the majority of the heat transfer occurs through (Udawattha and Halwatura, 2017). Walls which occupy the biggest area of a dwelling is responsible for about 30% of total heat gain into dwellings (Nandapala *et al.*, 2018). Thermal insulation of walls directly affects the overall heat gain of the dwelling. Walls can be insulated with different thermal insulating materials and the thermal performance of the insulation layer can be affected by the placement of insulation material. The insulation layer can be installed in mainly four ways such as; on the outside, inside, both inside and outside of the wall or at the middle of two walls (sandwich wall) (Al-Homoud, 2005).

4.2. Thermal insulation materials

Although all thermal insulation materials provide the same function to minimize the rate of heat gain/loss, some particular materials have better properties (Aditya *et al.*, 2017). The thermal insulation materials must fulfil certain standard requirements and they should be able to maintain their thermal characteristics throughout the life span of the structure. There are many types of thermal insulation materials available and they can be classified in many ways such as (Jelle, 2011),

- Traditional thermal insulation materials
- State-of-the-art thermal insulation materials
- Possible future thermal insulation materials

4.2.1. Existing wall thermal insulation materials/methods

(i) Mineral wool

Rock wool and glass wool which are the main types of mineral wool are as shown in **Figure 1**, these can be produced as boards, mats and loose filling material as well. Glass wool is produced at a temperature around 1400 ℃ using borosilicate glass and rock wool is produced at a temperature around 1500 ℃ by melting stones such as diabase and dolerite where final product creates fibres. To improve the product properties and to bind the fibres together dust abatement oil and phenolic resin are added to both glass wool and rock wool. The thermal conductivity value for glass wool lies between 31 to 37 mW/mK and that of rock wool lies between 33 to 40 mW/mK. Temperature, moisture content and mass density directly affect the thermal conductivity of mineral wool. When the moisture content increased from 0 vol% to 10 vol%, the thermal conductivity of mineral wool may increase from 37 mW/mK to 55 mW/mK (Jelle, 2011; Schiavoni *et al.*, 2016).

Figure 1 (a) glass wool and (b) rock wool (Nuclear Power, 2019)

(ii) Expanded polystyrene (EPS)

Expanded polystyrene is produced from small spheres of polystyrene with an expansion agent. Due to its superior properties, it can be used as a thermal insulation material. This material is manufactured as either boards or continuous on a production line. EPS has a partially open pore structure. Thermal conductivity of EPS lies between 30 to 40 mW/mK may rise from 36-54 mW/mK with an increment of moisture content from 0-10 vol%. Temperature, moisture content and mass density directly affect the thermal conductivity properties of EPS. This material can be easily cut and handled without losing its thermal conductivity properties (Jelle, 2011; Schiavoni *et al.*, 2016).

(iii) Extruded polystyrene (XPS)

Extruded polystyrene is made from melted polystyrene by adding an expansion gas. This material is produced in continuous lengths which are cut into pieces after cooling. XPS has a closed pore structure and thermal conductivity values of XPS lies between 30 to 40 mW/mK may rise from 34-44 mW/mK with an increment of moisture content from 0-10 vol%. Hence also temperature, moisture content and mass density directly affect the thermal conductivity properties of XPS. But it absorbs less moisture compared to EPS. This material can be easily cut and handled without losing its thermal properties (Jelle, 2011; Schiavoni *et al.*, 2016). EPS and XPS are shown in Figure 2.

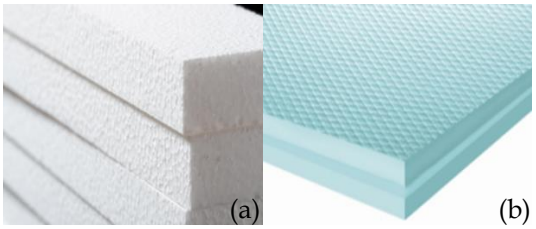

Figure 2 (a) EPS and (b) XPS (Nuclear Power, 2019)

(iv) Cork insulation

Cork thermal insulation is produced from cork oak which is a natural raw material. It can be manufactured as both a filler material and boards. It is good in acoustic insulation performance as well. The thermal conductivity of cork lies between 40 to 50 mW/mK. Cork products can be used as excellent thermal insulation material under compressive loads due to high compressive strength. This material can be recycled easily and generally used to insulate walls. Products made from cork are lightweight, impermeable to both liquid and gases, rich in both elastic and compressive properties, completely biodegradable, having high thermal resistance, acoustic, fire and abrasion resistance. Cork insulation products can be easily cut and handled without losing its thermal conductivity properties in the site and products may also be perforated (Abu-Jdayil *et al.*, 2019; Jelle, 2011; Schiavoni *et al.*, 2016).

(v) Cellulose

Cellulose is made from grounding recycled papers or wood fibre mass with some chemicals to improve the product properties. Cellulose insulation materials are produced in two forms such as; batts (loose-fill) insulation and as a filler material. The thermal conductivity values of cellulose lie between 40 to 50 mW/mK and may rise from 40 to 66 mW/mK with an increment of moisture content from 0 vol% to 5 vol%, respectively. Temperature, high moisture content and mass density directly affect the thermal conductivity properties of cellulose. Loose-fill insulations can be easily cut and handled without losing its thermal conductivity properties and filler cellulose material insulation must be done with in-situ scenarios (Jelle, 2011; Schiavoni *et al.*, 2016). Loose-fill and blown-in filler cellulose are as shown in Figure 3.

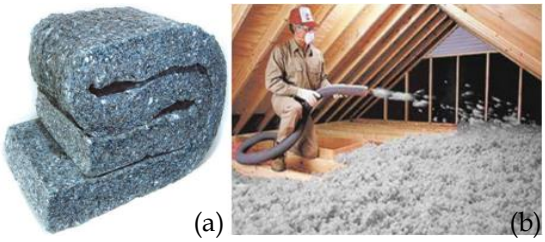

Figure 3 (a) cellulose loose-fill and (b) blown-in filler (Nuclear Power, 2019)

(vi) Polyurethane (PUR)

Polyurethane is produced through an exothermic reaction between isocyanates and polyols. This insulation material can be produced as boards or as an expanding form at the site as shown in Figure 4. Polyurethane has considerably lower thermal conductivity values between 20 to 30 mW/mK and may rise from 25 to 46 mW/mK with an increment of moisture content from 0 vol% to 10 vol%, respectively. Temperature, moisture content and mass density directly affect the thermal conductivity properties of cellulose. This material can be cut and handled without losing its thermal conductivity properties. PUR has some serious health concerns and hazards in case of a fire releasing hydrogen cyanide (HCN) which is a toxic gas (Abu-Jdayil *et al.*, 2019; Jelle, 2011; Schiavoni *et al.*, 2016).

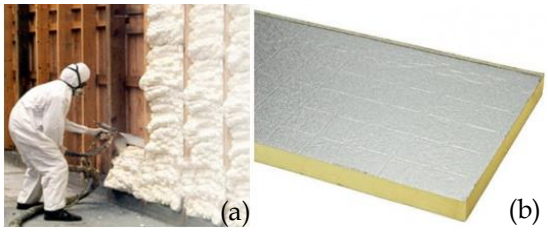

Figure 4 (a) PUR form and (b) rigid board (Nuclear Power, 2019)

(vii) Vacuum insulation panels (VIP)

Vacuum insulation panels consist of open porous core filled with fumed silica covered by multilayer metallized polymer. View of VIP is as shown in Figure 5. A vacuum is created inside the panel by allowing all the air to evacuate hence it will increase the thermal resistance of the panel. The thermal conductivity values of fresh VIP lies between 3 to 4 mW/mK and after about 25 years ageing due to diffusion of air and moisture, the thermal conductivity will become 8 mW/mK. VIPs are generally used in wall thermal insulation. VIPs have one of the lowest thermal conductivity as a thermal insulator and thermal insulation capacity is about 10 times higher than traditional thermal insulation materials. One of the main disadvantages is lack of flexibility and the risk of perforation of the material as well as their high costs. These insulation materials cannot be cut and adjusted at the site without losing the thermal performance (Abu-Jdayil *et al.*, 2019; Jelle, 2011; Schiavoni *et al.*, 2016).

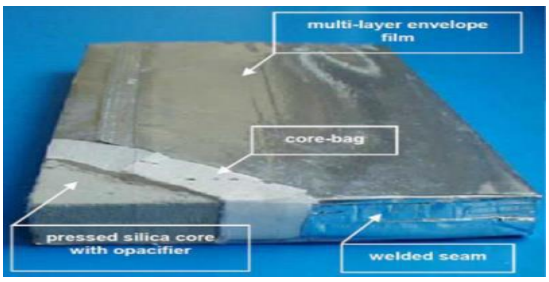

Figure 5 VIP (Jelle, 2011)

(viii) Gas filled panels (GFP)

Gas filled panels are made of reflective layer (baffle) envelope with gas filled inside. View of GFP is as shown in Figure 6. Gas can be air or other gas with low thermal conductivity such as Argon (Ar), Krypton (Kr) or Xenon (Xe). The thermal performance of GFP depends on the gas concentration inside

the panel. Penetration of air and moisture into the panels will affect the thermal performance negatively. The thermal conductivity of GFP is about 40 mW/mK which is quite high and still in developing stages but doubtful. The radiative heat transfer is controlled by the low emissivity surfaces inside the GFPs. These materials cannot be cut and adjust at the site since it will increase the thermal conductivity. GFPs are quite similar to VIPs in many ways (Abu-Jdayil *et al.*, 2019; Jelle, 2011).

Figure 6 GFPs (Jelle, 2011)

(ix) Aerogels

Aerogel is a transparent, ultra-light material with high open porosity and very low density. View of aerogel is as shown in Figure 7. Aerogels are made from drying a gel, where the liquid phase of the gel is replaced with gas. This is one of the most outstanding thermal insulation materials with high thermal resistance. The thermal conductivity of aerogels lies between 13 to 14 mW/mK. Even though aerogels have a relatively high compression strength, they are very fragile because of low tensile strength but tensile strength may be increased using carbon fibre matrix. Production of aerogels are very expensive (Jelle, 2011; Schiavoni *et al.*, 2016).

Figure 7 Aerogel (Schiavoni *et al.*, 2016)

(x) Coconut fibre

These fibres are obtained from coconut husk which is a waste material of dry coconut. Coconut husks are available in large quantities locally. These can be produced as mats as shown in Figure 8. The thermal conductivity values of coconut fibre are between 40 to 45 mW/mK. Coir fibre products are good in thermal resistance, acoustic resistance and dynamic stiffness. These materials can be easily recycled and reused. Since no special equipment is needed it can be easily manufactured (Abu-Jdayil *et al.*, 2019; Schiavoni *et al.*, 2016).

Figure 8 coconut fibre mats

(xi) EPS concrete wall panels

These EPS concrete wall panels are produced using waste regiform as the main raw material. Since it contains a mixture of regiform and cement compressive strength, fire resistance, acoustic insulation and thermal insulation properties are at a significant level. EPS light-weight concrete wall panels are produced locally in Sri Lanka. The views of wall panels are shown in Figure 9. Key benefits of these panels are waterproof, good chemical resistance, good mechanical resistance and rigidity, resistant to seismic movement and low cost. They are available in different panel sizes. Hence, it is easy to transport and install (EPCI Homes, 2019).

Figure 9 EPS concrete wall panels at the site

(xii) Fibreglass

The fibreglass is produced using sand and recycled glass. It can be produced in forms of rolls, mats or as loose-fill material. The thermal conductivity of fibreglass lies between 33 to 40 mW/mK. Fibreglass thermal insulation products are good in acoustic resistance and it

does not absorb moisture. fibreglass insulation products can be easily cut and handled without losing its thermal conductivity properties in the site and products may be perforated (Aditya *et al.*, 2017).

5. RESULTS AND DISCUSSION

5.1. Most suitable wall thermal insulation method for dwellings under tropical climatic conditions

Even though methods such as VIPs, GFPs and aerogels have considerably low thermal conductivity, most of these methods have more disadvantages over advantages. Their inability to be cut and adjusted at the site without losing its thermal properties, not being locally available and being very expensive compared to other materials are the main drawbacks. These methods require specialised persons to install them which makes these methods more expensive.

By analysing all the above-mentioned methods/materials, it was clear that all the materials are not available locally and importing them makes the attempt much expensive. By considering all the aspects including thermal conductivity and giving priority to local availability as well as financial feasibility, the materials and methods which are suitable for wall thermal insulation under tropical climatic conditions were filtered. They are listed in Table 1.

Table 1 Suitable insulation materials

Material/methods	Thermal conductivity (mW/mK)	Remarks	Reference
Glass wool	31-37	• Have high thermal insulation properties due to the presence of small air pockets among glass fibres but compaction will reduce thermal insulation properties	(Schiavoni *et al.*, 2016)
Rock wool	33-40	• Harder than glass wool having a higher melting point, and suitable for higher temperature scenarios	(Schiavoni *et al.*, 2016)
EPS	30-40	• Key benefits are lightweight, high thermal resistivity, vibration resistance, durability and low thermal conductivity • Low in cost compared to other materials	(Jelle, 2011)
XPS	30-40	• Possess the same benefits as EPS and both are easy to handle • Absorbs less moisture compared to EPS but expensive than EPS	(Jelle, 2011)
PUR	20-30	• Absorption of less moisture, lightweight, durable and strong • PUR has some serious health concerns and hazards in case of a fire • Cost is higher than both EPS and XPS	(Jelle, 2011)
Cork	40-50	• Products are lightweight, impermeable to both liquid and gases, rich in both elastic and compressive properties, completely biodegradable • Easy victim of moisture and insects	(Abu-Jdayil *et al.*, 2019),(Jelle, 2011)

Cellulose	40-50	• Greenhouse gases are not emitted during the production and completely biodegradable • Expensive compared to other materials • Higher vulnerability to moisture and insect attacks	(Jelle, 2011)
Fibreglass	33-40	• Does not absorb moisture • Does not seal walls and air-exchange may take place	(Al-Homoud, 2005)
Coconut fibre	40-45	• Can be easily manufactured recycled and reused	(Schiavoni *et al.*, 2016)
EPS concrete wall panels	24-26	• Waterproof, having good chemical and mechanical resistance, rigid, resistant to seismic movement and economical • Not decaying easily	(EPCI Homes, 2019)
Green walls	Depends on the applicant	• Higher maintenance cost and high instalment cost	-

From the above selected suitable materials, EPS is the most common thermal insulation material in tropical countries due to its thermal properties and low cost. It is also used for roofs insulation (Chandra *et al.*, 2019)

As mentioned in section 4.1 insulation layer can be installed in four ways. When the walls are insulated on the external side, it will address solar heating and reduce the heat gain into the dwelling, but durability is less due to the exposure to the outside environment. When the internal side of the wall is insulated it will be more durable since there will not be any damage from the outside environment, but only the inside temperature can be effectively controlled. When both sides of the walls are insulated, all the aforementioned benefits can be achieved but it will be more expensive. The best way is to place the insulation layer at the middle of two walls (sandwich wall) but building two walls will be expensive too.

Sandwich wall insulation is the best method, but it not economical due to the construction of two walls. And since EPS is the most common and best insulation material due to its properties, EPS concrete wall panels will be good because it is a mixture of EPS and cement, but these wall panels will not decay since EPS is not an easily decaying material.

Using the same technology used in EPS concrete wall panels, separate wall panels can be manufactured by mixing natural insulation materials such as coconut fibre, coir dust or sawdust with walling materials. Further, properties of these natural insulation material wall panels such as; thermal resistance, crowd loading, compressive strength, nailing resistance, fire resistance, impact resistance, flexural resistance, lateral resistance and other properties can be significantly enhanced.

6. CONCLUSION AND FUTURE WORKS

This paper reflects the first part of ongoing research. Therefore, the conclusions have been achieved basically based on a literature review. Following the necessity of selecting the most suitable wall thermal insulation method for dwellings under tropical climatic conditions, a detailed literature review was done to study existing methods. It can be concluded that the most suitable method for dwellings under tropical climatic conditions is wall panels constructed using natural insulation materials mixed with wall construction materials.

As for future works, a questionnaire survey will be conducted to collect data about wall insulation and energy demand of local dwellings. Then, the simulation will be done using a calibrated virtual model based on collected data. The selected thermal insulation materials will be applied to the developed

model separately and simulations will be done for the wall based on heat gain reduction and cooling load reduction. Energy conservation analysis of the dwelling followed by a life cycle assessment will be done to select the most suitable and effective wall thermal insulation method for tropical climatic conditions.

7. REFERENCES

Abu-Jdayil, B., Mourad, A.-H., Hittini, W., Hassan, M. & Hameedi, S., 2019, 'Traditional, state-of-the-art and renewable thermal building insulation materials: An overview', *Construction and Building Materials*, 214, 709–735.

Aditya, L., Mahlia, T.M.I., Rismanchi, B., Ng, H.M., Hasan, M.H., Metselaar, H.S.C., Muraza, O. & Aditiya, H.B., 2017, 'A review on insulation materials for energy conservation in buildings', *Renewable and Sustainable Energy Reviews*. 73, 1352–1365.

Al-Homoud, Dr.M.S., 2005, 'Performance characteristics and practical applications of common building thermal insulation materials', *Building and Environment*, 40 (3), 353–366.

Chandra, M.S., Nandapala, K., Priyadarshana, G. & Halwatura, R.U., 2019, 'Developing a durable thermally insulated roof slab system using bamboo insulation panels', *International Journal of Energy and Environmental Engineering* [online]. Available from: http://link.springer.com/10.1007/s40095-019-0308-xdoi:10.1007/s40095-019-0308-x [Accessed 20 June 2019].

EPCI Homes, 2019, *EPCI Homes (Pvt) Ltd*. Available from: https://epci-homes-pvt-ltd.business.site [Accessed 30 August 2019].

Halwatura, R.U. & Jayasinghe, M.T.R., 2008, 'Thermal performance of insulated roof slabs in tropical climates', *Energy and Buildings*, 40 (7), 1153–1160.

International Energy Agency, 2019, *International Energy Agency*. Available from: https://www.iea.org/ [Accessed 8 September 2019].

Jelle, B.P., 2011, 'Traditional, state-of-the-art and future thermal building insulation materials and solutions – Properties, requirements and possibilities', *Energy and Buildings*, 43 (10), 2549–2563.

Nandapala, K., Chandra, M. & Halwatura, R., 2018a, *Roof Slab Insulation Syatem for Tropical Climatic Conditions*.

Nandapala, K., Chandra, M.S. & Halwatura, R.U., 2018b, '*EFFECTIVENESS OF A DISCRETELY SUPPORTED SLAB INSULATION SYSTEM IN TERMS OF THERMAL PERFORMANCE*', In: 2018 pp. 11.

Nuclear Power, 2019, *Insulation Materials - Types of Insulation*. Available from: https://www.nuclear-power.net/nuclear-engineering/heat-transfer/heat-losses/insulation-materials/ [Accessed 31 August 2019].

Ozel, M., 2014, 'Effect of insulation location on dynamic heat-transfer characteristics of building external walls and optimization of insulation thickness', *Energy and Buildings*, 72 288–295.

Rahman, M.M., Mahlia, T.M.I. & Uddin, M.N., 2019, 'Energy Efficiency Analysis in Building Walls in Tropical Climate Using Thermal Insulation System', In: *Reference Module in Materials Science and Materials Engineering* [online]. (no place) Elsevier. Available from: https://linkinghub.elsevier.com/retrieve/pii/B9780128035818111142doi:10.1016/B978-0-12-803581-8.11114-2 [Accessed 13 April 2019].

Schiavoni, S., D'Alessandro, F., Bianchi, F. &and Asdrubali, F., 2016, 'Insulation materials for the building sector: A review and comparative analysis', *Renewable and Sustainable Energy Reviews*, 62, 988–1011.

Udawattha, C. & Halwatura, R., 2017, 'Life cycle cost of different Walling material used for affordable housing in tropics', *Case Studies in Construction Materials*, 7, 15–29.

Udawattha, C. & Halwatura, R., 2017, 'Life cycle cost of different Walling material used for affordable housing in tropics', *Case Studies in Construction Materials*, 7, 15–29.

Proceedings of the 7th International Symposium on

Advances in Civil and Environmental Engineering Practices for Sustainable Development

ACEPS - 2019

Investigation of properties of reusable interlocking cement blocks

R. Heshachanaa[1] and S.V.T.J. Perera[1]

[1]Department of Civil Engineering, Faculty of Engineering, Sri Lanka Institute of Information Technology, Malabe, SRI LANKA

K e y w o r d s

Cement blocks
Interlocking blocks
Sustainable construction

A B S T R A C T

This study was conducted in order to explore a new interlocking and reusable block design which will help in promoting sustainable building construction to aid the rural community to obtain affordable, reusable and easily installable cement blocks made of sustainable materials. As an efficient and cost-effective design approach, interlocking block designs which can be a competitive replacement for existing conventional block masonry were proposed, analyzed and the most suitable design was identified. In addition to that, considering the scarcity of river sand, manufactured sand was used as fine aggregate for this study. According to the results obtained from the tests performed, the compressive strength of individual blocks, tri-stack prisms and wall panels were identified as 6.14 MPa, 4.90 MPa and 2.07 MPa respectively. All results were satisfactory with the minimum required compressive strength of 1.20 MPa. Similarly, flexural strength tests and water absorption tests were also exhibiting acceptable results as expected. It was ensured that the proposed interlocking block satisfies the required strength, durability and applicability under different testing conditions. Therefore, these blocks can be recommended for housing construction as an alternative to the existing conventional masonry blocks.

1. INTRODUCTION

Construction industry is a sector in which most developing communities highly depends on. Nowadays due to the raise in number of buildings especially dwelling units, the demand for construction materials have reached an unprecedented level. This rise in demand is mainly due to lack of resources and raw materials. The price of construction materials such as sand, cement and aggregates have increased drastically over the past few decades influencing the cost of construction.

The issue of increase in construction cost has the potential to affect the wealth of country. This can be mainly observed in rural housing schemes, rehabilitation projects carried out by governments which includes individual temporary housing for displaced people by war and natural disasters. These houses are not permanent. These will be temporary accommodation for affected people which are likely to be demolished during future developments. Here, the raw materials which were used for the construction of these houses will be wasted once these houses get demolished and sent to landfills.

Current situation in Sri Lanka addresses some key challenges in the low cost and affordable housing shortages. This is mainly due to lack of resources, insufficient funds, shortage of skilled workers and time constraints. When considering this current situation of local construction industry, it is crucial to identify a suitable methodology to mitigate the high rise in construction cost due to increase in material cost. Several research studies have been done, however, a solution for this particular identified issue of cost increase in construction is a work in progress.

These days the construction industry has developed in a way that they have incorporated construction materials from waste and recycling the construction waste etc. However, the knowledge regarding upcycling is not much focused due to lack of interest and

researches in such respective application. The main advantage of upcycling over recycling is that the energy required for recycling can be avoided in upcycling where the material is reused as it is without any further modification. In that sense, interlocking blocks are one of the construction elements which can be reused if dry stacked without motor. This can be considerably cost effective as it requires no skilled labourers for construction and no new raw materials required for the manufacturing of blocks repeatedly. It should be noted that in addition to economic benefits, an introduction of interlocking, reusable cement block will also be advantageous in environmental aspects. Introduction of this type of brick into real life application will add value to the existing houses as they can be rebuilt. Also, this can help in the reduction of natural resource depletion as reusing or upcycling of blocks will not require new materials or resources for its modification.

The main advantages of interlocking blocks over the conventional masonry are that they can be dry-stacked without any mortar joints increasing the speed of construction, that is interlocking blocks saves construction time and a large amount of mortar, (Gupta and Deshmukh 2015) which would otherwise be required for the horizontal and vertical joints for a standard conventional masonry block. Without the need for high-waged skilled masons, the labour costs (Anand and Ramamurthy 2000) can be reduced compared to the standard masonry construction.

Against this background, considering the issues faced by current housing industry, this study aims to carry out a research to identify the most suitable solution for an economical housing strategy by means of an accelerated dry stack-interlocking block design.

Accordingly, for this research it has been considered that, as cement blocks contributes the most in the total cost of a building construction compared to other structural elements (mainly in single story houses), an economical design approach of either replacing or remodelling the existing conventional cement block masonry will help in reduction of total construction cost. An Interlocking- Reusable Cement (IRC) Block was designed with projections and depressions where the projections will perfectly set in to the depressions of the blocks placed above, such that the blocks will get aligned automatically both in horizontal and vertical direction which makes these blocks to be laid without special masonry skills. The block also was designed to be cast so as to obtain best surface finishing, thereby reducing the need and cost for plastering.

2. MATERIALS AND METHODS

2.1. Design Concepts

2.1.1. Identification of Most Suitable Design

Initially designs for interlocking blocks as with overall standard dimension of 390 mm x 150 mm x 190 mm (length x breath x height) were developed and analysed. Out of the proposed block designs, the most suitable and effective design as shown in Figure 1 was chosen considering horizontal movement restraints, proper interlock horizontally and vertically by the tongue and groove system (while dry stacked) and most importantly ease of casting (mould design).

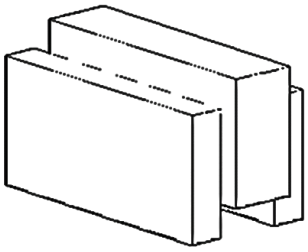

Figure 1 Proposed block design

The geometry of the block was designed to achieve the bond between each block by just dry stacking or interlocking without the use of cement motor.

2.2. Materials

2.2.1. Cement

In this study Ordinary Portland Cement (OPC) was used as the binder to produce the interlocking blocks. The OPC used was under strength class 42.5 N and with specific gravity of 2.965.

2.2.2. Fine Aggregate

Considering the cost reduction in manufacturing, the blocks were cast with Manufacture sand (M-Sand) of density 1695 kg/m^3.

2.2.3. Coarse Aggregate

Aggregate with maximum nominal size of 14 mm and density of 1475 kg/m^3 was used as the coarse aggregate for the mix. For all trial mixes the percentage of course aggregate was kept constant, such that 30% of total aggregate content as coarse aggregate and the rest 70 % as fine aggregate.

2.2.4. Water

Water used for the concrete mixing and curing was free from acids, alkaline, salts, oil and organic matters. It was crucial in deciding the amount of water to be added as Water: Cement (W/C) ratio highly influence the strength of the block. The decision upon the W/C also highly based on the workability of the concrete. Specially in case of interlocking block production the workability will be a huge constrain. Accordingly, in this study based on experience and trials the W/C ratio was determined as 0.5.

2.3. Interlocking Block Production

2.3.1. Mould Design

The mould design for the proposed interlocking block was developed by using 3 mm thick steel plates. As interlocking blocks are complicated in design compared to the conventional masonry blocks, it was necessary to come up with a mould design which can hold the concrete as wet mix for 24 hours.

2.3.2. Mix Design

Determining the best mix ratio for Cement: Aggregate was vital to obtain a smooth surface finish in block; a trial and error method was adopted to select the best suitable and workable mix. The selected mix proportion is given in Table 1 below.

Table 1 Mix design for the blocks

Material	Cement	M-sand	Agg.	W/C
Ratio	1.0	3.5	1.5	0.5

Agg: 14mm coarse aggregate

2.3.3. Curing Procedure

As the mix used was wet, the formwork (mould) was kept supporting the block for at least 24 hours until the block gets set.

2.4. Experimental Procedure

2.4.1. Identification of Suitable Mix Design

Suitable mix design for the interlocking block was chosen based on its strength, surface finishing and workability. The best-chosen mix based on workability and surface finishing was 1:5 cement: aggregate ratio. Similarly, the best suitable mix ratio for the mix with M-sand was identified based on strength by performance of compression strength test for individual blocks.

2.4.2. Compressive Strength Test for Individual Block

Compressive strength of a masonry unit is the first and foremost concern to define its physical properties such as durability and strength. To ensure a block is safe and stable to be used in construction with intended service load, it is vital to specify that the block being used has met or exceeded the specified required compressive strength of masonry, which in case of SLS 855: Part 1 (1989) has been specified as minimum of 1.2 N/mm^2.

In this study, The Digital Compression Testing Machine (CTM-2000) was used for testing compressive strength of individual block in accordance with SLS 855: Part 2 (1989).

2.4.3. Compressive Strength Test for Prism

Tests were conducted for tri-stacked prisms for compressive strength by subjecting them to axial compression using Universal Testing Machine (UTM).

Two 30 mm thick mild steel plates were used in the top and bottom of the prism to ensure uniform distribution of compression and in addition to that, 5 mm thick softwood capping were provided on top and bottom of the prism block between the steel plates and the blocks. The provision of the soft wood is to account for the unevenness surface of the specimen. The prisms consisted of 7 days aged blocks. Care was taken while stacking and aligning the tri-stacked prism in the UTM for testing to avoid accidental eccentricity. After positioning the specimen, the block specimens were loaded under uniform axial compression until the failure. The load was applied with a uniform increment of 90 KN/min. From the test conducted the maximum load for the

crack and failure of each blocks were recorded. Test setup detail of the Tri-stack prism is provided in Table 2 below.

Table 2 Tri-Stack Prism Detail

Tri-stack Prism Dimension	
No. of Blocks	3 Full
Prism Height	450 mm
Prism Width	150 mm
Prism Length	387 mm

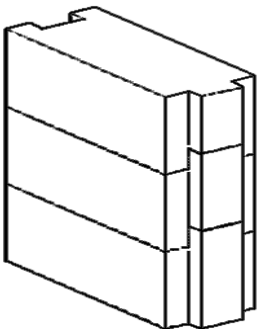

Figure 2 Tri-stacked prism setup model

As shown in Figure 2 the top and the bottom blocks were cast without top tongue part and the bottom groove part filled. This is to avoid the uneven load distribution due to the tongue and groove. This tri-stacked prism tests were performed in accordance with ASTM C1314-07 (2007) test methods and specifications.

2.4.4. Compressive Strength Test on Panels

Similar to the test conducted in tri-stacked prisms for compressive strength, compression test was performed on block panels by subjecting the dry stacked block panels to axial compression using UTM-1000E. The block panels consisted of six 7 days aged blocks, where one block was cast in two parts as shown in Figure 3. The blocks were arranged as panels resembling an actual wall construction pattern. Further detail about the block panel is as provided in Table 3.

Table 3 Block panel detail

Block Panel Dimension	
No. of Blocks	5 Full + 2 Half
Panel Height	450 mm
Panel Width	150 mm
Panel Length	720 mm

Figure 3 Panel testing setup

2.4.5. Flexural Strength Test

Flexural strength of individual masonry block and wall unit is an important parameter just as compressive strength of block in grading a masonry unit. Ultimate flexural strength and modulus of rupture are two parameters which can be identified by a flexural strength test.

In this study interlocking block units were tested in flatwise (in bed direction) and in inverted direction in accordance with ASTM C67-14 (2014) Blocks were tested both sides because of its difference in shape on top as tongue projection and bottom as grove depressions. The blocks were loaded at the mid span by a steel rod of 30 mm diameter and length equal to the width of the block. The block specimens tested were supported with another two similar 30 mm diameter steel rods from the both ends of the bottom which were not restrained both longitudinally and in transverse directions during the test. This testing procedure was mainly focused to induce the failure plane to propagate in the middle span. Weights and dimensions of all the blocks tested were measured and recorded before the test. As accordance with ASTM C293-07 (2007) the modulus of rupture of the block units were calculated as follows,

$$\textit{Modulus of Rupture } (R) = 3PL / 2bd^2 \qquad (1)$$

Where P is maximum applied load, b is width of specimen, L is span length and d is depth of the specimen. The tests were performed using UTM - 1000E and the tested specimens were loaded continuously without shock at a constant rate so that the maximum stress on the tension face increases at a rate of 0.95 MPa/min.

2.4.6. Water Absorption Test

According to BS EN 772 (2000), Bricks should not absorb water more than 12% by its weight. (Manish and Lokesh 2017) The samples to be tested were dried till they attain constant weight then were cooled to room temperature and weighed (W1). Then the brick pieces were immersed in clean water for 24 hours. Later the brick pieces were removed and wiped out for any traces of water and were weighed immediately (W2). And by using the measured weights the percentage of water absorbed (WA) by weight was calculated as follows.

$$WA\ (\%) = [\ (W2 - W1)\ /\ W1]\ x\ 100 \qquad (2)$$

3. RESULTS AND DISCUSSION

Results obtained from all compressive test on individual, prism and panel blocks are provided in Figure 4 below.

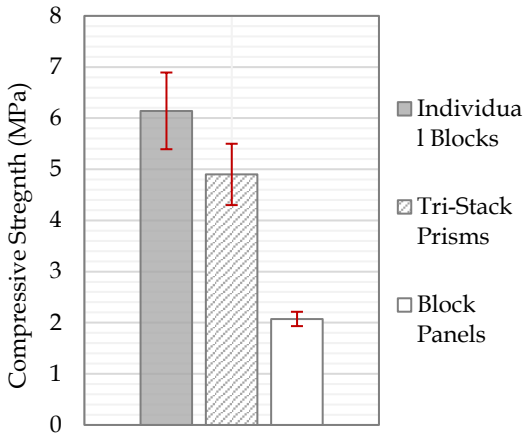

Figure 4 Results obtained from compressive tests on Individual, Prism and Panel

3.1. Compressive Strength of Individual Block

As of the results obtained from testing blocks with the mix of 1:5, all the test results were within the allowed variation of 15%. During the experiment it was noted that the block started cracking well before the failure of the block. The load at which the block started cracking was recorded and an average value of 286.65 KN was obtained. From that results the compressive strength of the crack load was acknowledged as 5.03 MPa. And the ultimate average compressive strength was determined as 6.14 MPa. When considering the mode of failure, it was concluded that the failure of individual blocks were mainly due to the beam action of web causing the shear failure between the shells or splitting of walls inducing collapse. The failure was initially observed at the header face as vertical cracks followed by the minor cracks at the stretcher face near the bottom and top of the blocks.

Here it can be noted that the compressive strength value obtained were greater than the minimum allowable compressive strength of 1.2 MPa according to SLS 855: Part 1 (1989) which assures the employability of blocks for wall construction.

3.2. Compressive Strength of Prism

It was noted that the failure encountered in three stages. Initially the top block failed following that the middle block and then finally the bottom block. These three stages of failures were also observed visually during the testing procedure as in Figure 7.

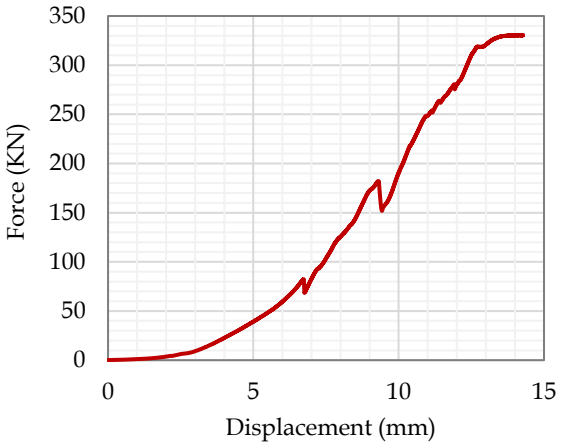

Figure 5 Force displacement curve of prism test

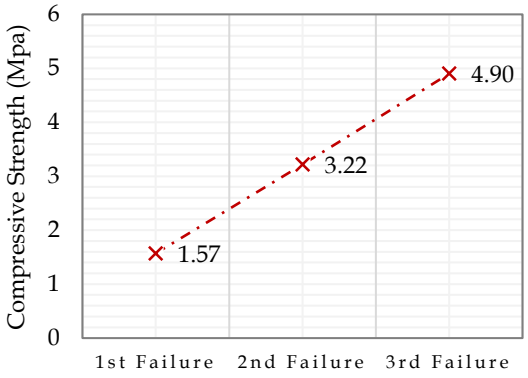

Figure 6 Three stage failure stresses of prism

Figure 7 Crack propagation in prism

The Figure 5 and 6 indicates the three stage failure loads of the tri-stacked prisms and the corresponding compressive strength. From the mode of failure, it was detected that the dry stacked prism has failed mainly due to beam action of web shell (middle part) inducing collapse of each blocks in stages. Initially the cracks were observed to be developed vertically in the header face followed by the minor cracks in the stretcher face and eventually the failure of the block. Due to the clearance along the web shell (middle part) of the block, the loaded face shells were appeared to have acted as beam spanning along the stretcher faces and as a result of this, the bending action has created shear stress concentration between the shells developing cracks at the interface between the middle and the face shells. This failure can be defined accordance with ASTM C 1314-07 (2007) as Type 7- face shell separation. Due to this detailed behaviour of blocks similar to actual wall construction application, the tri-stack prism compressive strength is regarded as the better representation of actual strength of the blocks compared to the individual block compressive strength test.

The average minimum and maximum compressive strength of the prism was obtained as 1.57 MPa and 4.90 MPa respectively. When considering the correlation for strength of prism with individual block, the compressive strength of prism is 0.79 times the compressive strength of individual block. This strength variations (higher individual block strength and lower prism compression strength) was mainly due to uneven contact area for compression and clearance between the blocks causing the compressive strength to decrease in the prisms.

In addition, according to ASTM C-1314-07 (2007) the height to thickness correction factors for masonry prism compressive strength must be applied based on the ratio of prism height to least lateral dimension of prism which in the case here is 3.0. Therefore, the correction factor for the prism compressive strength is 1.07. Accordingly, the finalized compressive strength of prism accommodating the above-mentioned correction will be of minimum of 4.59 MPa and of maximum of 6.02 MPa. Where both the values including the average of 5.24 MPa satisfies the standard minimum individual block compressive strength requirement of 1.20 MPa according to SLS 855: Part 1 (1989).

3.3. Compressive Strength of Block Panels

The Figure 8 below shows the graph obtained from UTM-1000E which indicates the failure pattern of the dry stacked block panels.

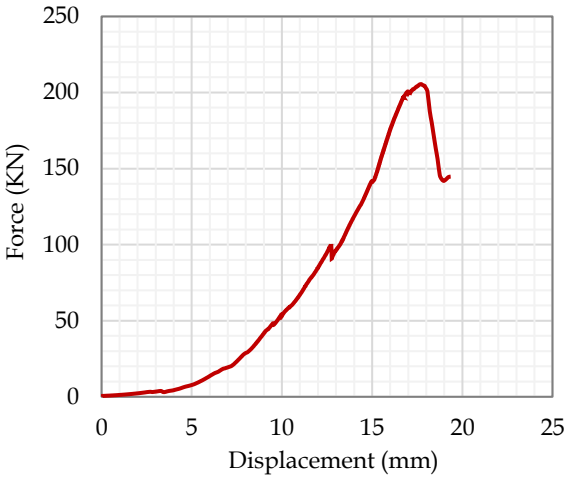

Figure 8 Force displacement curve of panel test

Figure 9 Crack propagation in Panel

The reason behind variations in failure patterns and failure loads of block panels were

justified based on the summary of average compressive strength obtained for the failure at each stage. Similar to test results obtained from Tri-stack prism test mode of failure, it was observed that the dry stacked prism has failed mainly due to beam action of web shell (middle part) inducing collapse of each blocks in stages. But unlike prisms, here the cracks were initially observed to be developed vertically in the stretcher face followed by the minor cracks in the header and eventually the failure of the block. Figure 9 shows the crack propagation in the wall panel tested.

Even if the worst case out of all parameters are considered the finalized compressive strength of an individual block accommodating all possible safety factors will be of minimum of 1.91 MPa. Where this lowest strength value satisfies SLS requirement of 1.20 MPa. (SLS 855: Part 1, 1989)

When considering the results obtained from individual blocks, prisms and panels; The correlation of strength variation illustrates that the geometric imperfections of the interlocking block significantly affect the behaviour of the dry bed joint between the brick layers. This influence of dry joints in reduction of strength can be justified by Table 4 below which demonstrates the comparison of compressive strength with respect to individual block.

Table 4 Correlation of compressive strength

Compressive Strength Comparison		With respect to Individual unit
Individual Block	6.14 MPa	100 %
Tri-Stack Prism	4.90 MPa	80 %
Block Wall Panel	2.07 MPa	34 %

3.4. Flexural Strength Test

Figure 10 shows the results obtained from the flexural strength test performed in inverted and flatwise direction of interlocking block. Accordingly, the average flexural strength of blocks in inverted and flatwise direction was identified as 3.70 MPa and 1.80 MPa respectively.

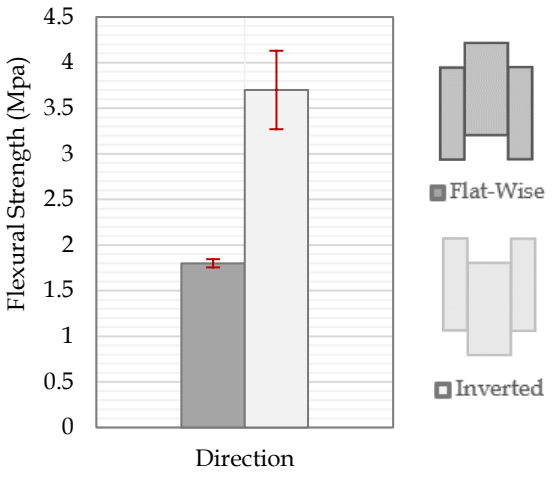

Figure 10 Results obtained from flexural test

The failure of block specimen for the flexural strength test in flat wise direction was mainly due to propagation of tension crack from the bottom towards top of the block specimen right at the mid span of the block. It can be noted that the flexural strength in the invented direction is more than twice greater than the flexural strength in the flat wise direction. This may be because in flatwise direction, it possesses deeper groove at the bottom makes it have less surface in contact for supports and more void under the block unlike in the inverted direction where tongue part is at the bottom providing higher contact with supports (Silva *et al.* 2014).

Considering the flatwise and inverted flexural strength results obtained, it was acknowledged that all results obtained were greater than the minimum allowable flexural strength of 0.25 MPa accordance with ASTM C 140 (2018).

3.5. Water Absorption Test

According to the results obtained from water absorption test performed on the block specimens, the average water absorption by weight of block was acknowledged as 5.40 %.

It was identified that the water absorption capacities of the block samples were within the acceptable range of 12 % according to BS EN 772 (2000) and lower than the allowable maximum value of 240 kg/m^3 as specified under SLS: 855: Part 1 (1989). Therefore, it can be stated that the proposed interlocking blocks will exhibit higher durability to moisture and resistance to moisture movements.

4. CONCLUSION

This research study demonstrates the benefits to be derived from the use of proposed reusable blocks over traditional wall blocks. The tests performed on blocks were used successful in assessing the structural behaviour of proposed mortar less joints and to understand the ranges of strength variation due to different types of geometric imperfection of block beds for single and multiple joints (prism and panel tests). It should be noted that according to the minimum required compressive strength of 1.20 MPa, which represents 20% of the individual block strength obtained; 24 % of prism block strength; 58 % of panel strength. This results variation clearly shows that the compressive behaviour of the mortar less system is strongly influenced by dry joint behaviour and number of dry joints. Still there is a very large reserve in terms of compressive strength in all testing conditions.

In addition, considering the flatwise and inverted flexural strength results obtained with respect to the minimum allowable flexural strength of 0.25 N/mm^2, all results obtained exhibits comparatively even higher reserve in terms of strength compared to compression.

In conclusion the proposed dry stack, interlocking masonry is satisfying specific strength and durability parameters and therefore is highly recommended to be used in housing construction as an alternative to conventional block masonry.

Further improvements in this approach can be made by developing the awareness among users, professionals and financial supporters for incorporating waste materials such as plastic to reduce the density of blocks in addition to balance the economy and to achieve energy conservation.

Moreover, the durability issues and depreciation of stacking capability in long run can be addressed by investigating the geometric imperfection of block beds especially the imperfection caused by differences in the size of clearance within the projections and depressions.

5. REFERENCES

Anand, K. B., and Ramamurthy, K., 2000, 'Development and performance evaluation of interlocking-block masonry', *Journal of Architectural Engineering*, 6(2), 45-50.

ASTM C1314-07, 2007, *Standard Test Method for Compressive Strength of Masonry Prisms,* ASTM International, West Conshohocken, Pennsylvania.

ASTM C140, 2018, *Standard Test Methods for Sampling and Testing Concrete Masonry Units and Related Units,* ASTM International, West Conshohocken, Pennsylvania.

ASTM C293-07, 2007, *Standard Test Method for Flexural Strength of Concrete (using simple beam with center-point loading)*, ASTM International, West Conshohocken, Pennsylvania.

ASTM C67-14, 2014, *Standard Test Methods for Sampling and Testing Brick and Structural Clay Tile*, ASTM International, West Conshohocken, Pennsylvania.

BS EN 772, 2000, *Methods of test for masonry units.,* British Standards Institution, London, England.

Gupta, A. and Deshmukh, S., 2015, 'Interlocking Brick Design-Paradigm for Sustainable'. *International Journal for Research in Applied Science & Engineering Technology (IJRASET)* 3(I), 257-264.

Manish, k., and Lokesh, S., 2017, 'Critical Review on Types of Bricks Type 14: Plastic Sand Bricks'. *International Journal of Mechanical and Production Engineering* 5 (III), 84-88.

Silva, R., Soares, E., Oliveira, V., Miranda, T., Cristelo, M., and Leitão, D., 2015, 'Mechanical characterization of dry-stack masonry made of CEBs stabilized with alkaline activation', *Construction & Building Materials*, 349-358.

SLS 855: Part 1, 1989, *Specification for cement blocks, Part 1 – Requirements,* Sri Lanka Standards Institution, Sri Lanka.

SLS 855: Part 2, 1989, *Specification for cement blocks, Part 2 – Test Methods,* Sri Lanka Standards Institution, Sri Lanka.

Proceedings of the 7th International Symposium on

Advances in Civil and Environmental Engineering Practices for Sustainable Development

ACEPS - 2019

Effect of waste rice husk ash and ceramic sludge on structural properties of fired clay roof tiles.

T.H.F. Aagani[1] and G.H.M.J. Subashi De Silva[1]

[1]Department of Civil and Environmental Engineering, Faculty of Engineering, University of Ruhuna, Hapugala, Galle, Sri Lanka

K e y w o r d s

Rice husk ash
Ceramic sludge
Clay roof tiles
Transvers breaking load
Dry mass
Apparent porosity

A B S T R A C T

The effect of waste rice husk ash and ceramic sludge on the structural properties of the clay roof tiles was studied in this research study. The clay, RHA and ceramic sludge were collected from Waikkala (Puttalam district), Mirissa (Matara district) and Dankotuwa Porcelain LTD (Puttalam district) respectively. The fired clay roof tiles were manufactured in industrial scale by replacing the RHA percentage (i.e.5%, 10% and 15%) and ceramic sludge percentages (i.e.10%, 15%, 20% and 25%). The manufactured tile specimens were tested according to ASTM standards and compared with the conventional tile. Sieve analysis, hydrometer analysis, specific gravity, bulk density and amorphous silica determination were done to determine the characterization of the raw materials. The structural properties such as transverse breaking strength, dry mass and apparent porosity of clay roof tiles were analyzed after the addition of Rice husk ash (RHA) and ceramic sludge. The fineness modulus of clay, RHA and ceramic sludge are 0.41, 1.72 and 1.05 respectively. While the specific gravity of clay, RHA and ceramic sludge are 2.50, 2.08 and 2.24 respectively. The bulk density of clay, RHA and ceramic sludge are 1294.5 kg/m^3, 336.9 kg/m^3 and 1276.8 kg/m^3 respectively. Transverse breaking load was optimum at the 10% RHA and 10% sludge level, showing 30.5% strength increment as compared to the conventional tile.. Dry density of the tiles reduces with the incorporation of RHA and ceramic sludge producing light weight tiles compared to the conventional tile. However, the apparent porosity of the tile got increased. The study has concluded that the RHA and ceramic sludge affected in improving strength properties while light weight tiles can be produced. This will is a sustainable solution for accumulating of industrial waste.

1. INTRODUCTION

Asbestos roofing sheets are very popular among the people as they are high strength, easy to handle, easy to assemble, and cost effective. However, the world health organization has stated that the usage of asbestos sheets would cause larynx and ovary, mesothelioma, and asbestosis (World Health Organization 2014). Therefore, many countries are banning the usage of asbestos sheets.

Clay roof tiles can be used as an alternative for the asbestos sheets. However, the properties of the existing clay roof tiles must be enhanced to be used as a substitute for asbestos. Therefore, utilization of industrial waste for enhancing the structural properties of the clay roof tiles is a sustainable solution. Because this would enhance the structural properties of the clay roof tiles while being a solution for the accumulating industrial waste. Furthermore, the substituting industrial waste materials as secondary raw material in the clay roof tile production decreases the production cost of the clay roof tile.

Rice husk ash (RHA) and ceramic sludge are abandoned industrial waste in Sri Lanka. Industries, which produces RHA and ceramic sludge as waste materials have no proper way to dispose these waste materials. These waste materials are just left in the environment without further utilization.

Researches have shown that the addition of RHA and ceramic sludge as secondary raw materials to clay roof tiles has improved the strength, durability, thermal properties while satisfying runoff standards. For example, the transverse breaking load of clay roof tile has been improved by 47.24% with the addition of 10% waste RHA (De Silva and Surangi, 2017) and by 22.9% with the incorporation of 20% of ceramic sludge (De Silva and Malwatta, 2018).

The purpose of this research is to incorporate different combination of RHA and ceramic sludge in the production of clay roof tile and to investigate the structural properties:transverse breaking strength, dry mass and apparent porosity.

While being a sustainable solution for the accumulating industrial waste, in the current study, an attempt was used to utilize Rice husk ash and ceramic sludge. RHA is produced either in controlled environment or uncontrolled environment by the combustion of rice husk. Twenty percent (20%) of rice husk become ash during burning (Agus 2002). RHA produced in controlled environment has more pozzolanic nature and can be used to enhance the properties of the roof tile. The usage of rice husk as fuel in brick kilns produces RHA, which shows similar characteristics as burnt in controlled environment (Uduweriya and De Silva 2010). Around 10,000 brick kilns are functioning in Sri Lanka and 20% of them uses rice husk as the fuel and produces waste RHA (Asian Institute of Technology 2003).

Ceramic sludge is silico – aluminious waste from pozzolanic factories. There are more than 100 types of top-rated ceramic factories which produces 60,000 tons of ceramic sludge annually (De Silva and Malwatta 2018).

Researches have shown that the addition of ceramic sludge increases the strength of the fired clay roof tiles (De Silva and Mallwattha 2018). In addition, the ceramic sludge has less amount of ferrous which can improve the durability of the clay roof tile. The clay used for the production of roof tile is consisted of kaolinite, quartz and feldspars (Ingunza 2015). The clay used in the production of ceramic products also comprises of those compounds. Therefore, effect of rice husk ash and ceramic sludge on structural properties of fired clay roof tiles was investigated.

2. METHODOLOGY

2.1 Tests for the raw materials

Laterite clay was collected from Waikkala in Puttalam district. RHA was collected from brick kiln in Mirissa in Matara district and ceramic sludge was collected from Dankotuwa porcelain company in Puttalam district.

2.1.1. Sieve analysis test for RHA

The RHA were cleaned and the weight of them was measured. Each sieve was weighed. The stack of sieves was arranged in a descending order of the mesh opening size from the top to bottom and a pan was attached to the bottom of the sieve stack. The measured sample of the material was placed in the top most sieve and a cover plate was used to cover the topmost sieve to prevent the loss of materials while shaking. The stack of sieves with the material was placed on the mechanical shaker for 10 minutes for a horizontal shacking. The weight of each sieve with the material was measured to determine the percentage of material which passes through each sieve.

2.1.2. Wet sieve analysis for ceramic sludge and the clay

Wet sieve analysis was carried out to study the particle size distribution of the ceramic sludge and the clay. The materials were oven dried at 100°C to 110°C for at least five hours before testing. The samples were poured into one litre measuring cylinder. Then water and sodium hexa-sulphate was poured to the sample and mixed thoroughly. The cylinder with sample was kept for 24 hours. Then the samples were stirred and sieved by 0.075mm sieve. The particle remaining on the sieve was washed to make all fine particles pass through the sieve. Then the samples remaining in the pan and the sieve were oven dried.

2.1.3. Specific gravity of the raw materials

The pycnometer was completely filled with distilled water up to its full capacity with the screw in position. Then the weight of pycnometer with water was measured (P). Then a known weight (B) of dried sample

was placed into the pycnometer. Then the remaining portion of the pycnometer was filled with water. Then the pycnometer was wiped outside and weighed (Ps). The specific gravity (Gs) was calculated using Eq. (1).

$$G_s = B/(P + B + P_s) \quad (1)$$

2.1.4. Determination of amorphous silica content

The amorphous silica in clay, RHA and ceramic sludge was determined according to the procedure mentioned in Deshmuksh *et al* (2012). The sample were weighed and boiled in 100 ml of 2.5N NaOH. Then a filter paper was used to filter the boiled solution. Then the filtrate was poured into an evaporating dish and dried in the oven at 400° C until constant mass was gained. And then the evaporating dish was kept in the desiccator and weighed.

2.2. Manufacturing of clay roof tiles

Twelve mixtures (Table 1) were prepared by replacing the clay with varying content of RHA (5%, 10%,15%) and ceramic sludge (10%, 15%. 20%, 25%). The mixtures were determined based on the previous studies.

The manufacturing of clay roof tiles was done in an industrial scale plant. Initially the raw materials were mixed manually by trampling and then the mixture was subjected to machine mixing. A homogeneous mixture was prepared by mixing and grinding the mixture.

The cuboidal clay plates with larger dimensions than the roof tiles were produced from the clay mixture using a machine. Then the clay plates were pressed with pressing machine to get the standard shape. The excessive clay was removed by a cutting tool and the prepared wet tile was shaped. The prepared tiles were dried naturally by storing them in wooden frames 5 days before firing.

The moulded roof tiles were arranged one over the other in longitudinal way in the kiln. Initially the smoke was passed through the flues for 12hours at the beginning of the firing until the white steam disappears. Then the amount of fire was increased for 72hours from the bottom to the top. And then the kiln was maintained at 850°C for 24hours after interior flues got red.

Ultimately, the doorways of the kiln were opened to reduce the temperature of the kiln to room temperature. Then the tiles were taken out.

Table 1 Mix proportion (by weight)

Mixture	RHA (%)	Ceramic Sludge (%)	Laterite clay (%)
Mixture 1	0	0	100
Mixture 2	5	10	85
Mixture 3	5	15	80
Mixture 4	5	20	75
Mixture 5	5	25	70
Mixture 6	10	10	80
Mixture 7	10	15	75
Mixture 8	10	20	70
Mixture 9	10	25	65
Mixture 10	15	10	75
Mixture 11	15	15	70
Mixture 12	15	20	65
Mixture 13	15	25	60

2.3. Tests for the fired clay roof tile

2.3.1 Transverse breaking strength (TBS)

Transverse breaking load was performed in accordance with ASTM C 1167. Six tile specimens were tested from each mixture. Tiles were kept in an oven a 110°C for 24 hours before testing. Universal testing machine (INSTRON 600DX) shown in Figure 1 was used to test the tiles in a horizontal plane in three-point bending mode. Tile was supported in the bottom by 40mm wide faced self-aligning members with the span of 305 mm. Third member, which is at mid span of the lower supports, applied the load to the upper (exposed) surface of the tile by moving perpendicular to plane of the tile. Loads were applied uniformly and continuously until fracture at a rate of 0.45 kN/min without a shock.

Figure 1 Testing the TBS

2.3.2 Dry mass

Five specimens from each mixture were used to determine dry mass of the tiles. The tile specimen was kept in an oven at 110°C for minimum 24 hours until two consecutive weights in 2-hour interval become identical or the difference is not greater than 0.2%. And then the dry mass was weighed(Figure 2) after keeping the tile specimens in room temperature for 4 hours without exposing it to dust and dirt.

Figure 2 Testing dry mass of the tile

2.3.3 Apparent porosity

The tile specimens were placed in oven for 24 hours at the temperature of 100°C and weighed (D). Then the specimens were boiled in distilled water for 2 hours and cooled to room temperature while keeping in water and then suspended weight (S) was measured by immersing the tile in water and the saturated weight (W) was measured after wiping the tile with a cloth. The porosity was determined using Eq. (2).

$$P = \frac{(W - D)}{(W - S)} X\ 100 \qquad (2)$$

3. RESULTS AND DISCUSSION

3.1 Characterization of raw materials

3.1.1 Particle size distribution

The fineness modulus of RHA, ceramic sludge and clay was found to be 1.72, 1.05 and 0.41 respectively. Figures 3 and 4 show particle size distribution of raw materials. it was observed that major part of the raw materials is fine.

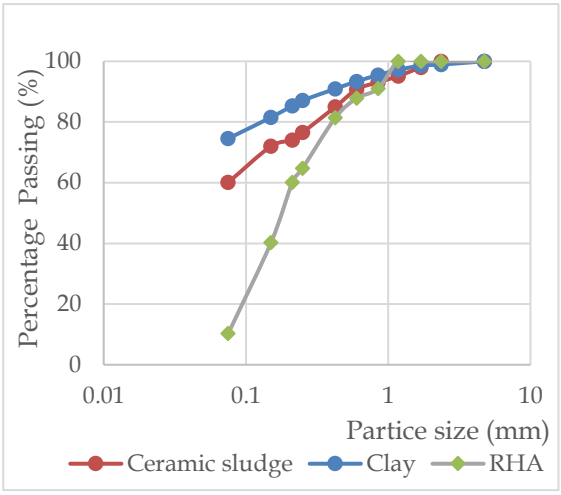

Figure 3 Sieve analysis of raw materials

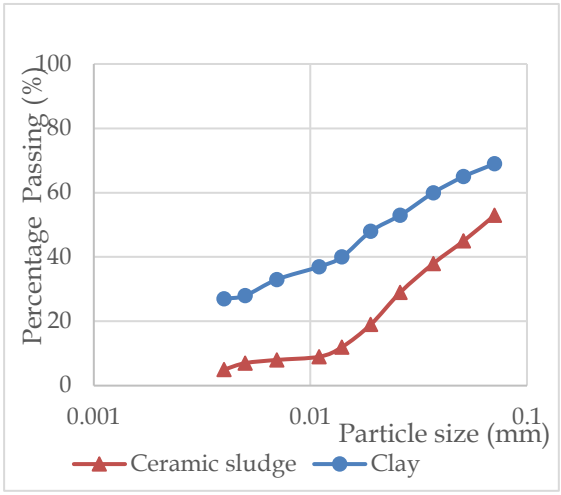

Figure 4 Hydrometer analysis of raw materials

Therefore, waste materails can get mixed with clay properly as they can easily move through the clay particles. The fineness modulus of clay shows that the clay consists of large number of micro particles which would help for the effective mixing of the raw materials. USDA soil classification mention that the soil passing through 75 mm, soil passing between 75mm size and 2mm size, soil passing between 2mm and 0.05mm size, soil passing between 0.05mm and 0.002mm size was classified as gravel, sand, silt and clay, respectively.

3.1.1 Specific gravity and Bulk density

Specific gravity of RHA and ceramic sludge are less than the clay (Table 2), promising a reduction in the weight of the waste added tile as compared to the conventional tile. Similar valuefor the bulk

density of RHA was obtained by Venkatanarayanan *et al* (2013) as 351 kg/m3. Amorphous silica determination shows the presence of more amorphous silica (Table 2), which would reduce the firing shrinkage (Kumara *et al*. 1999).

Table 2 Properties of raw materials

Property	RHA (%)	Ceramic Sludge (%)	Laterite clay (%)
Amorphous silica (%)	82.47	67.53	62.25
Finess modulus	1.72	1.05	0.41
Specific gravity	2.08	2.24	2.50
Bulk density (kg/m^3)	336.9	1276.8	1294.5

3.2 Characterization of clay roof tiles

3.2.2 Transverse breaking strength (TBS)

Transverse breaking strength of tile specimens is shown in Figure 5.

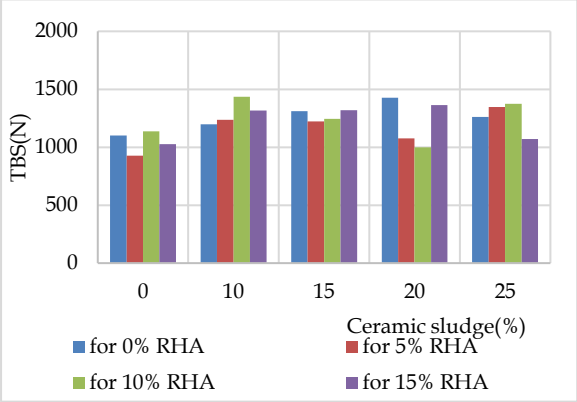

Figure 5 Comparison transverse breaking load of different mixtures

The replacement of clay with RHA and ceramic sludge had a significant effect on the transverse breaking strength of the tile. Maximum transverse breaking strength was obtained for Mixture 6 (10% RHA and 10% ceramic sludge) showing 30.5% increase of strength as compared with conventional roof tile.

Because the strength become optimum when the SiO_2/Al_2O_3 ratio lies between 2.87-4.79. Therefore, high amount of SiO_2 present in RHA and sludge contributes to the strength gain. Nevertheless, large amount of RHA and ceramic sludge addition to clay is not desired.

Strength increment of the tiles with individual addition of RHA, ceramic sludge and the combination of RHA and ceramic sludge is shown in Table 3.

Table 3 Comparison of optimum percentage and strength increment of tiles

Waste incorporated	Optimum percentage	Strength improvement
Only RHA	10% RHA	47.24%
Only ceramic sludge	20% Ceramic sludge	22.9%
Combination of RHA and ceramic sludge	10% RHA & 10% ceramic sludge	30.5%

3.2.2 Dry mass

The replacement of clay with RHA and sludge reduced the dry mass of the tile (Figure 6). This was attributed by the less specific gravity of RHA and sludge as compared to the clay. The maximum reduction in dry mass was observed for Mixture 2 (5% RHA and 10% sludge) which is 6.4% compared to conventional tile. Dry mass of Mixture 6 was reduced by 4.8%.

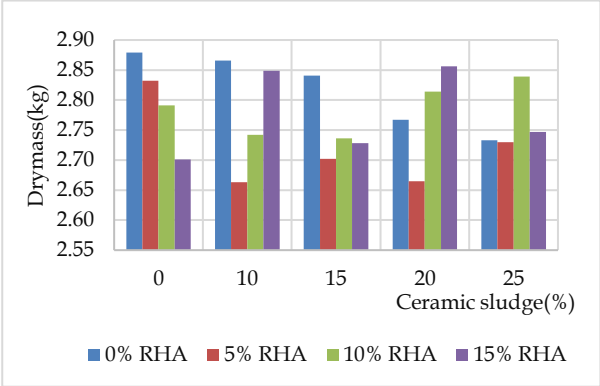

Figure 6 Variation of dry mass for different specimens

3.2.3 Apparent Porosity

Addition of RHA and ceramic sludge to the clay roof tile has increased the apparent porosity (Figure 7).

The apparent porosity of conventional tile is 22% while the apparent porosity of the tile specimen with 10% RHA and 10% ceramic sludge is 24.7%.

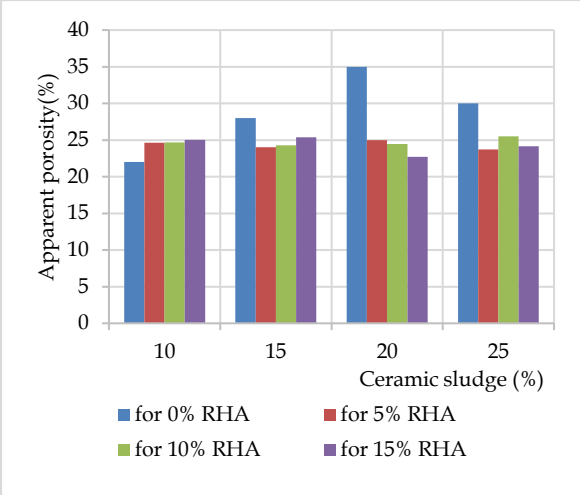

Figure 7 Comparison in apparent porosity of different mixtures

4. CONCLUSIONS

The study concludes that the addition of 10% RHA and 10% ceramic sludge, as clay replacement, affected to improve transverse breaking strength. It was found that, at this level,30.5% increment in the transverse breaking strength, showing an enhancement in the strength with ceramic sludge and rice husk ash.

The specific gravity of RHA, ceramic sludge and clay found to be 2.08, 2.24 and 2.50, respectively, indicating that ceramic sludge and RHA are lighter in weight compared to clay. Dry mass got reduced by 4.8% for 10 % RHA and 10% ceramic sludge, promising a light weight roof tile, when the clay was blended with RHA and ceramic sludge.

In addition, the apparent porosity of the clay roof tiles with sludge and RHA has increased than the conventional tile.

The current study has shown the enhancement of the structural properties of the tile with corporation of ceramic sludge and RHA, which are abandoned industrial waste in Sri Lanka.

5. ACKNOWLEDGEMENTS

Financial support from the research grant "UGC special allocation for strengthening research" (grant no RU/PG-Com/18/01) is greatly appreciated.

6. REFERENCES

Agus, S. M., 2002, 'Utilization of Uncontrolled Burnt Rice Husk Ash in Soil Improvement', *Dimensi Teknik Sipil*, 4(2), 100-05.

Asian Institute of Technology, 2003, *Brick and Ceramic Sectors*, Regional Energy Resources Information Center (RERIC), Thailand.

De Silva, G. H. M. J. S. and Surangi, M. L. C. 2017, 'Effect of waste rice husk ash on structural, thermal and run-off properties of clay roof tiles', *Construction and Building Materials*, 154, 251–257.

Deshmukh, P., Bhatt. J., Peshwe, D. and Pathak, S., 2010, 'Determination of silica activity index and XRD, SEM and EDS studies of amorphous SiO_2 extracted from rice Husk Ash', *Transactions of the Indian Institute of Metals*, 65(1), 63–70

Ingunza, D., Pilar, D. M. and Dantas, L. A., 2015, 'Use of Sewage Sludge as a Raw Material in the Manufacture of Roofs', *International Conference on Civil, Material and Environmental Sciences (CMES)*, Brazil.

Kumar, S., Das, U. S. and Sing, K. K., 1999, 'Sintering studies on fly ash and clay mixes', in Chatrerjee, B., Simla, K. K. & N. G. Goswarni, N. G.(eds), *Fly Ash Utilization for Value Added Productspp*, NML, Jamshedpur 99-105.

De Silva, G. H. M. J. S and Mallwattha, M. P. D. P., 2018, 'Strength, durability, thermal and run-off properties of fired clay roof tiles incorporated with ceramic sludge', *Construction and Building Materials. Elsevier Ltd*, 179, 390–399.

Uduweriya, R. B.Y. B. and De Silva, S., 2010, 'Effect of mechanical properties of concrete containing rice husk ash', *Proceedings of the 8th Academic Sessions*, University of Ruhuna 2010, Vol.8, 87-94.

Venkatanarayanan, Kizhakkumodom H. Rangaraju, Rao R., 2013, 'Material Characterization Studies on Low- and High-Carbon Rice Husk Ash and Their

Performance in Portland Cement Mixtures, *Advances in Civil Engineering Materials*, Vol. 2, 266–287

World Health Organization, 2014, Chrysotile Asbestos, WHO publications, Switzerland.

Proceedings of the 7th International Symposium on

Advances in Civil and Environmental Engineering Practices for Sustainable Development

ACEPS - 2019

Effects of cassava peel powder as an admixture on properties of concrete.

H.M.I.D. Dissanayake[1] and S.V.T.J. Perera[1]

[1]Department of Civil Engineering, Faculty of Engineering, Sri Lanka Institute of Information Technology, Malabe, SRI LANKA

K e y w o r d s

Admixtures
Cassava Peel
Concrete properties
Sustainable materials

A B S T R A C T

Admixtures are artificial or natural materials which are added to the concrete during mixing besides cement, water, and aggregate to improve certain property of concrete. Admixtures can change the setting time, enhance the durability, strength characteristics of a given concrete mixer, improve freeze, reduce water and for better workability of the concrete mix. However, the high demand for admixtures causes a huge problem for the economy. Therefore, this study was aiming to examine the use of sustainable materials such as Cassava Peel Powder as an admixture to enhance the properties of concrete. By varying the proportions of Cassava Peel (CP) (1.0%, 1.5%, 2.0% and 3.0%) results were investigated. Finally, it was found out that CP acts as a retarding admixture and a 1.5% dosage level is the optimal percentage that gives higher compressive strength, splitting tensile strength and it increases the workability of the concrete. By replacing CP instead of chemical admixtures in concrete is an eco-friendly concept.

1. INTRODUCTION

Concrete is the most common material used in building construction nowadays. To change or improve some properties of concrete according to the task, admixtures or additives can be used when mixing. Admixtures are mainly categorized into main two parts which are known as mineral and chemical admixtures. The mineral admixtures are Calcined clay and shales, volcanic rock (Volcanic glass), Granulated blast furnance, opaliniccherts, Fly ash, Lignin, etc. The examples of chemical admixtures are superplasticiers, plasticiers, retarders, and accelerators, etc. According to the functions of chemical admixtures, they can be categorized into various classes. The five main classes of chemical admixtures are air-entraining water-reducing, retarding, accelerating and plasticizers (superplasticizers), etc. It is important to understand the specific effects of admixtures before they are used. The specific effects produced may vary with the properties and the proportions of the materials that will be used for the concrete mix. The most important admixtures presently used in preparing concrete are superplasticizers and plasticizers.

However, the high demand for admixture causes to increase the price. Therefore, in this research work, it was examined the properties of concrete by using waste materials.

Cassava peel was selected as a sustainable admixture to inspect the behavior of the properties of concrete. Cassava is eco-friendly material and the use of cassava peel can reduce the additional cost of using chemical admixtures. Cassava is an agricultural product that can be used as a replacement for chemicals. The decomposition period of cassava peel is more than 3 years. In this experiment, cassava peel was used with different dosages to find the best value that can mostly affect the properties.

2. LITERATURE REVIEW

The tapioca (Cassava) and maize can be identified as agricultural products that can be used as admixtures replacing chemical admixtures. The use of these kinds of natural material is eco-friendly and it reduces the cost of using chemical admixtures. The effect of these two admixtures on properties of concrete was examined by Joseph and Xavier (2014). In this study, it was found that the setting time and workability of concrete has increased by using tapioca and maize. This experiment found out the optimum dosages of 1.5% maize and tapioca 2% can increase compressive strength, split tensile strength, and flexural strength of concrete. (Joseph 2014)

The performance of the cassava flour as an admixture was investigated by Okafor (2008). In this study, it has been observed that the cassava flour has appreciable fluidifying action in the fresh concrete. By using cassava flour as an admixture in concrete it was proved that is possible to achieve a water reduction of at least 8% relative to concrete without admixture for nominally equal workability. Obtained compressive strength values for 28 days were higher than those to be expected from water reduction alone. Finally, this study suggested that cassava flour performs satisfactorily as a water-reducing admixture. (Okafor 2008)

The effect of quality sugar and cassava starch on grade 35 concrete was examined by Abalaka (2011). In this experiment, the compressive strength was examined by using various concentrations of white sugar and cassava starch separately. Experiment was found out that the maximum short-term strength gain for cassava starch was 22.60% at 3 days at 0.1% starch concentration and the case of sugar, short term strength gain was not sustained at 28 days. The use of Cassava starch proved to be beneficial as well as significantly affected concrete slump and the addition of white sugar was able to increase the initial setting time. (Abalaka 2011)

Flexural and compressive strength characteristics of cement-cassava peel ash (CPA) blended concrete, was studied by Salau (2012). Cement was replaced partially by cassava peel ash within the margin of 5%-25% and obtained results show that the replacement of CPA increases the amount of water was required to make the concrete workable. It was found that the water bind ratios to produce optimum workable blended concrete. A maximum of 15% CPA with a water binder ratio of 0.7 was suggested to produce cement-CPA blended concrete of appropriate concrete. (Salau 2012)

Olekwu *et al* (2014) examined the use of cassava starch as admixture in burnt earth bricks. Production of burnt earth bricks by using cassava admixture was able to enhance the physical properties such as compressive strength, water absorption, and abrasion resistance. For the experiment different dosages of cassava starch was used (0%, 4%, 6%, 10% and 12%). The obtained results denoted the water absorption of burnt earth bricks was reduced with the addition of cassava starch. Finally, the optimum percentage of cassava starch was found (6%) and was able to achieve satisfactory performance as an additive in producing burnt earth bricks. (Olekwu 2014)

George (2014) presented how to eliminate or minimize the fresh and hardened concrete problems by implementing hot weather concrete practices using cassava powder admixture. It was found that hot weather increases the temperature of fresh concrete and demanding more water. The results concluded that the cassava powder has retarding setting time, increasing workability an increasing the long and early term strength of concrete. (George 2014)

3. METHODOLGY/ MATERIALS AND METHODS

3.1. Material Selection

The main types of materials used in this research work are cement, water, coarse aggregates, fine aggregates and natural admixtures (Cassava Peel). These materials are further described below.

- Coarse aggregate – Metal

Crushed granite with 20mm particle size was used.

- Fine aggregate -Sand

As fine aggregate, river sand was used. The sand used was clean, sharp and that was free from clay, dirt and organic or chemical matter of any description. The sand passing through a 4.75 mm British Standard test sieve (BS812, 1990) and containing no coarser material was used.

- Cement

Ordinary Portland Cement (OPC) with the strength class of 42.5 N.

- Water

Portable water which was fresh, colorless, odorless and tasteless water that is free from organic matter of any type was used producing the concrete mixture.

- Admixtures

In this research work, Cassava Peel was used as an admixture. The Cassava Peel was collected from different sources such as dumped areas. After collecting, peels were washed by using clean water. Then the peels were dried under the sunlight a minimum of 5-10 days. After complete drying, the peels were powdered. The Cassava Peel Powder production process is shown in Figure 1.

a). Cassava Peel

b). Dried Cassava Peel

c). Dried Cassava Peel Powder

Figure 1 Process of Preparing CP Powder

3.2. Material Testing

First, a Sieve analysis test was carried out to determine the particle size distribution of aggregates (Coarse and fine aggregate). The Water Absorption test and Aggregate Impact Value test for the coarse aggregates were done. Observed results are indicated in Table 1 and Table 2.

Table 1 Water Absorption Test Results

Material	Water Absorption
20mm Granite Coarse Aggregate	0.49%
River Sand	0.56%

Table 2 Aggregate Impact Value Test Results

Test	Aggregate Impact Value (AIV) %
Test 1	20.11
Test 2	21.12
Test 3	20.14
Average Value	20.45

3.3. Concrete Testing

Concrete cubes of 150mm x 150mm x 150mm in size were subjected to destructive compressive strength test using the cube crushing machine. Moreover, cylinders of 150mm x 300mm were used to obtain the tensile strength of concrete using the splitting tensile strength.

3.4. Experimental Procedure

The experimental procedure commenced after the production of the required amount of Cassava Peel for casting work.

Subsequently, material properties were identified. Then using various proportions of CP (which shows in Table 3), the effects of the properties of concrete (such as slump variation, compressive strength, splitting tensile strength and temperature variation) were examined. The effectivity of the process increased with the identification of optimum admixture dosage level.

Table 3 Design Variables for Each Concrete Mix Design

Mix Identification	Materials	Concrete Grade	Addition of Admixtures as a Percentage (Cassava Peel)
Mix– Design 1	Cement, Coarse Aggregates, Fine Aggregate, Water	Grade 30	0%
Mix- Design 2	Cement, Coarse Aggregates, Fine Aggregate, Water, Cassava Peel	Grade 30	1.0% 1.5% 2.0% 3.0%

4. RESULTS AND DISCUSSION

This research project was mainly focused on improving the strength of concrete with the use of natural sustainable materials. Behavior of concrete mixture with Cassava peel convinced that the Cassava Peel act as a retarding admixture. The variation of slump, compressive strength and splitting tensile strength with the addition of CP will be discussed in this section.

4.1. Workability of Concrete

The effect of Cassava Peel as a retarding admixture on the workability of concrete with different dosage levels was examined at 15-minute intervals.

The observed results in Figure 2 convinced that the workability of a concrete mixture increases with the presence of CP in it. The increment was high when the percentage of CP is between 1.5%-2% dosage levels. (The experiment was conducted twice with 1.5% dosage level to ensure the results)

The improvement in workability was due to the surface-active agents in Cassava Peel which were immersed in the cement particles by giving them a negative charge and leading to repulsion between the particles with a resultant dispersion and

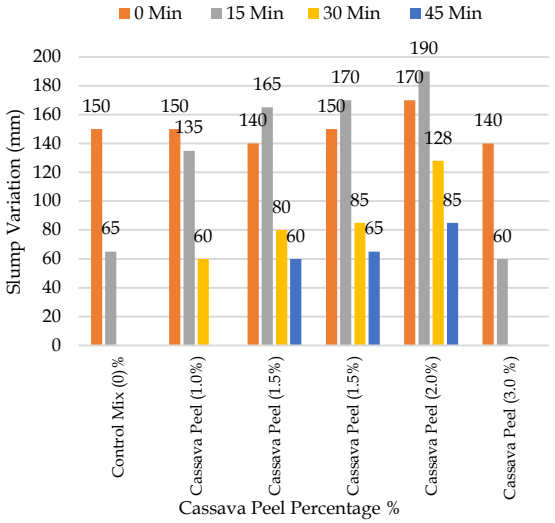

Figure 2 Slump Variation (Concrete with CP)

greater particle mobility. When the percentage of CP in the concrete was increased up to 2%, an increment in workability was observed.

With the addition of a 1% dosage level of CP, the slump limit became 60mm or less within 10-15 minutes. The slump variation of the normal concrete also had a more effective working manner during the first 10-15 minutes. But when CP percentage was increased up to 1.5% to 2%, it gained a more workable quality condition of the concrete compared to the normal concrete.

It was clear that concrete within CP shows more workability than the normal concrete. Furthermore, these results showed that the effective usage was during the first 30-45 minutes with a dosage level of 1.5% and 2%.

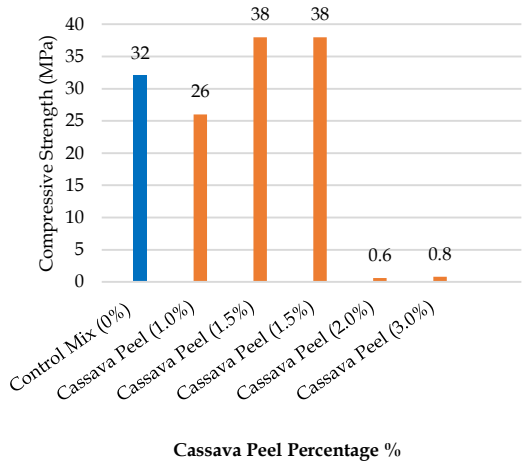

Figure 3 The 7 -Day Compressive Strength (MPa)

4.2. Compressive strength of concrete

Concrete with the admixture dosage level of 2% and 3%, have shown a sudden decrement of 7-day compressive strength compared to the normal concrete strength and concrete with different dosages of CP. Therefore, the strength of concrete with those dosage levels remained much lower at the age of 7-day. The lower compressive strength attributed to the prolonged retarding action of Cassava Peel due to the high percentage of the admixture.

When comparing the 7- day and 28-day compressive strength (refer Figure 4) between 2% and 3% dosage levels of CP, it represented the contrast point since the dosage level 3% illustrated a higher compressive strength than the dosage level 2%.

However, it determined the retarding process of Cassava Peel as an admixture and when the percentage of Cassava Peel was increased, the compressive strength of early stages (7-day compressive strength) was decreased. According to the above-observed results the optimum percentage of Cassava peel that gave a better compressive strength at all stages was 1.5% dosage level.

4.3. Splitting tensile strength of concrete

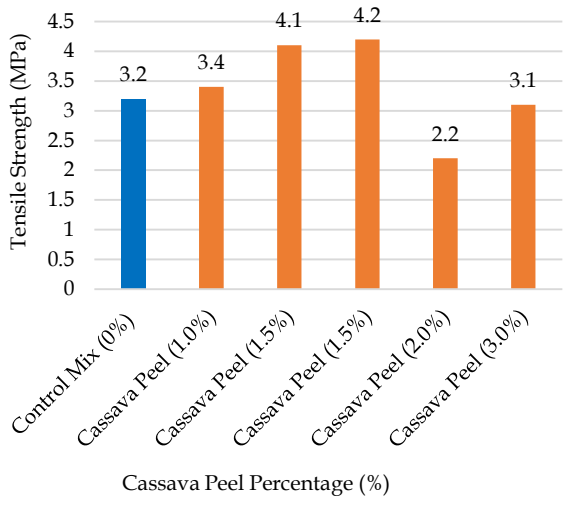

Figure 4 Tensile Strength Variation (MPa)

Figure 5 indicates that the splitting tensile strength increased while the CP percentage increased up to 1.5% and the strength increased relative to the control mix samples.

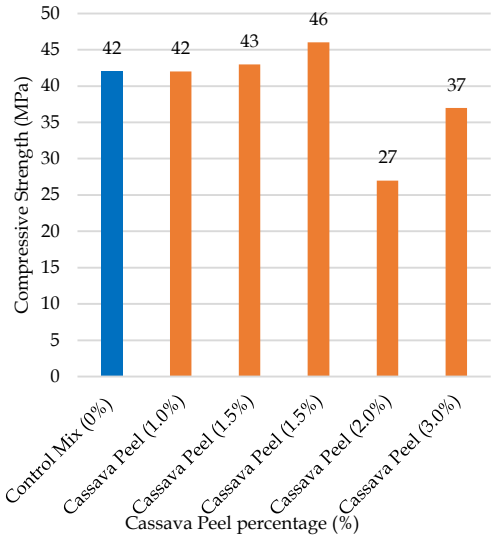

Figure 5 The 28 -Day Compressive Strength (MPa)

The optimum increment was observed when the CP percentage became 1.5% and the splitting tensile strength with 2% and 3% dosage levels indicated slightly low values compared to the normal mix samples. Anyhow the split tensile strength of 3% had a bit higher value than the 2.0% of CP dosage. According to the obtained results, the splitting strength increased with the addition of CP as an admixture to the concrete, but it was not a gradual increment.

5. CONCLUSION

The effects of Cassava Peel as an admixture on the properties of concrete were examined in this research. This study was conducted using various proportions of Cassava Peel. It was observed that the compressive strength, workability and tensile strength of the tested concrete mixture is high when the Cassava Peel percentage was 1.5%. Anyhow it was able to enhance the practical working scenarios which were co-related with the construction industry. Especially finding a sustainable solution for the construction industry which led to an eco-friendly concept instead of using chemical admixtures was the main advantage gained from the research. Further, as a future recommendation, this research work can be continued by using other natural chemical admixtures which can be used in a practical environment.

6. ACKNOWLEDGMENTS

The authors gratefully acknowledge the Department of Civil Engineering, Sri Lanka Institute of Information Technology for the valuable guidance and supervision throughout the research project.

7. REFERENCES

Abalaka, A. E., 2011, 'Comparative effects of Cassava Starch and Simple Sugar in Cement Mortar and Concrete', *ATBU Journal of Environmental Technology,* 4(1), pp. 13-22.

British Standards Institution, 185. Testing aggregates. Method for determination of particle size distribution. Sieve tests, s.l:s.n.

Elah, O. B., 2014, 'The use of Cassava Starch in Earth Burn Bricks', *International Journal of Engineering and Technology,* 27(1), pp. 5-11.

Joseph S. K., 2014, Effect of Starch Admixtures on Fresh and Hardened Properties of Concrete, '*International Journal of Scientific Engineering and Research',* 4(3), pp. 27 - 30.

Okafor F.O, 2010, 'The Performance of Cassava Flour as a Water-reducing admixture of concrete', *Nigerian Journal of Technology,* 29(2), pp. 106-110.

Otoko, G. R., 2014, 'Minimizing Hot Weather Effects on Fresh and Hardened Concrete by Use of Cassava Powder as Admixture', *European International Journal of Science and Technology,* 3(2), pp. 1-8.

Industry Research and Case Studies

Proceedings of the 7th International Symposium on

Advances in Civil and Environmental Engineering Practices for Sustainable Development

ACEPS - 2019

Structural performance of novel technique to repair corroded reinforced concrete elements

H.P Sooriyaarahchi

Department of Civil and Environmental Engineering, Faculty of Engineering, University of Ruhuna, Hapugala, Galle, SRI LANKA.

K e y w o r d s

Corrosion of reinforcement
Mechanical repair
Addition of reinforcement
Structural performance
Novel technique of repair

A B S T R A C T

Corrosion of steel reinforcement in concrete structure elements is a common durability concern in aggressive environments. Due to high concentrations of chloride presence in the environments and the less concerns about the concrete durability, structural intervention at a very early age of design life has become the norm and not the exception in most of the coastal environments. The first line of intervention of corroded structures in the event of corrosion is mechanical repair. This study investigates the structural performance of mechanically repaired beams based on both conventional repair technique and novel technique. This paper also makes comparison of conventional mechanical repair with novel technique of repair methods and shows that employing the novel technique provides better overall structural performance. The paper also provides industrial application of this novel repair technique detailing how this technique can be practically employed in actual industrial applications. Use of repair beams that have been firstly subjected to extensive corrosion damage using laboratory based accelerated corrosion conditions for the performance evaluation is a unique feature of this experimental investigation. Beams subjected to corrosion damage were then repaired with and without addition of reinforcement to study the influence of additional reinforcement in restoring the structural performance. It was found that the mechanical repair on its own cannot address the loss of capacity of corroded RC elements and that reduction in structural capacity due to sustained corrosion is more than the actual loss of reinforcement area due to corrosion. Research conducted with additional reinforcement on corroded flexural elements have found that addition of new reinforcement and mechanical repair is capable of recovering and improving the load carrying capacity of the repaired beam elements subjected to corrosion damage.

1. INTRODUCTION

Reinforced corrosion is one of the main durability concerns in reinforced concrete structures in aggressive environments like in the costal environment. Mechanical repair is first line of intervention for corroded structures. Figure 1 shows the usual practice of repair and retrofitting of corroded structure which involved removing a corroded damage concrete around reinforcement, surface preparation of the parent concrete and application of repair system to the cavities created with or without addition of new reinforcement (ICRI 2008; and Kothandaraman 2010; Sooriyaarachchi 2012). Usually repair systems are shot created to the cavity during preparation. For the performance of repair the bond between repair material and parent concrete plays a significant role (Eduardo *et al*. 2004; Stanish *et al*. 1999; Santos *et al*. 2012). As the shot created concrete is hanging against the gravity it tends to develop weak bond between parent concrete and repair material affecting the overall performance of the systems and the repair systems developed with properties to counter these disadvantages have been found costly. It is also the case that repairs carried out through shotcrete application is also technically more demanding that it is not accessible to construction practitioners without a significant investment.

Figure 1 Conventional method of repair

2. METHODOLOGY

Due to limitation of conventional repair and difficulties associated with application novel technique of repair is developed. This method involved pouring self-compacting concrete (Lacombe *et al.* 2012) through holes drilled on the slab. This way it is possible to repair both slab and beam systems that sustained corrosion damage. As the method involved supporting structure underneath the slab beam system it has the ability to provide better bond between repair material and parent concrete. Drill holes through the slab act as dowels and provide resistance against possible delamination of repair mortar from parent concrete. Figure 2 shows the repair process using the novel technique. One of the other important features of this study is evaluation of repair based on structures that have already been subjected to accelerated corrosion and evaluation of the performance of repair with and without additional reinforcement. Figure 3 shows testing set up used for experimental investigation. Figure 4 shows the bond between repair mortar and concrete under the two methods of repair.

Figure 2 Novel technique repair

Figure 3 Testing set up

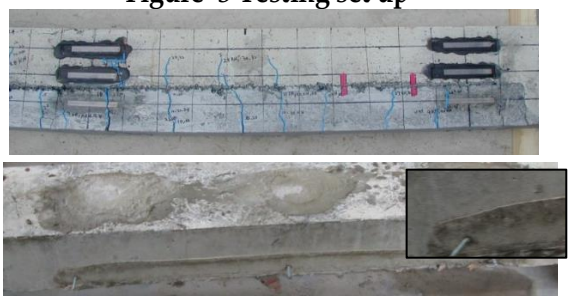

Figure 4 Bond resulted by the two method

3. RESULTS

Figure 5 (a) and (b) show the comparison of structural performance of tension side repaired beams using the conventional repair and the novel method of repair introduced in this investigation respectively Sooriyaarachchi (2012).

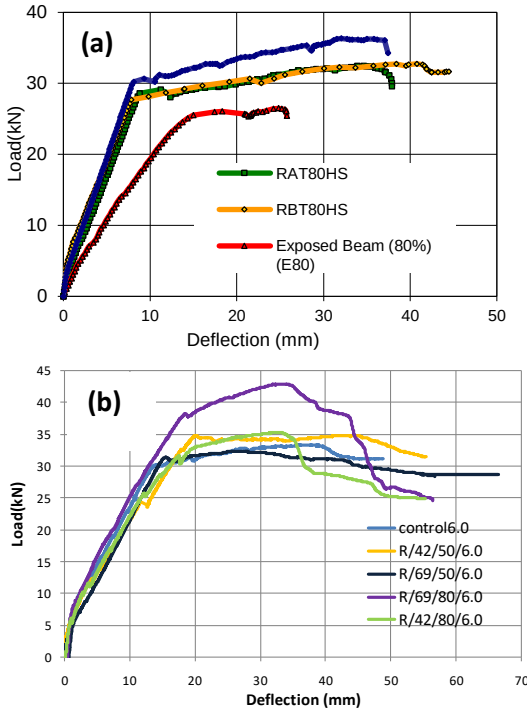

Figure 5 Comparison of test results under two method of repair

Figure 6 shows a comparison of the performance of repaired beam with and without reinforcement. Results indicate that additional reinforcement can restore the structural performance of corroded reinforcement.

4. DISCUSSION

This study introduces a novel technique of repair and compares the structural performance of the novel technique against the conventional method of repair. In addition study includes evaluation the performance of repair beams that have already been subjected to corrosion damage. As this research study considers the repair of corroded members, results obtained are more realistic to the actual behaviour. From the test results it is found that,

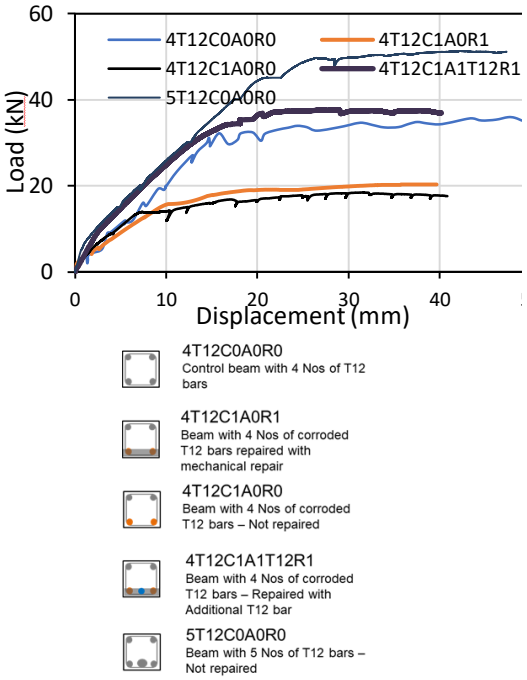

Figure 6 Structural performance of repaired beams with additional reinforcement.

- Ultimate load carrying capacities of concrete beams are significantly affected by corrosion of reinforcement.
- Mechanical repairing of concrete beams with addition of reinforcement is capable in restoring and strengthening the corroded beams.
- Loss of capacity in corroded beams is not proportional to the loss of reinforcement and compensating only the lost area due to corrosion is not sufficient to restore the structural behaviour of repaired beams.
- Delamination of repair system from the parent concrete has become a failure mode of most of the beams especially with the increase of additional reinforcement.
- It is possible that the loss of capacity more than the area reduction of reinforcement due to corrosion may have been caused by the delamination of the repair layer from the parent concrete.
- It is difficult to establish whether the yielding of reinforcement followed by delamination or vice versa as the response of the two on the overall performance of the beam is similar.

The most import feature of this study is extension of it to industrial application. Figure 7 shows the application of this novel repair technique in real construction.

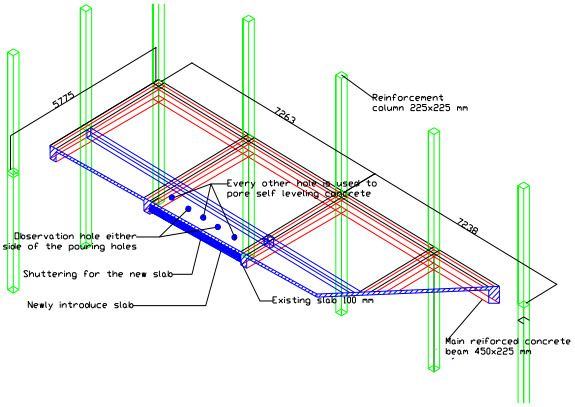

Figure 7 Industrial application of the new repair technique.

REFERENCES

Sooriyarachchi, H.P., 2012, 'Static and fatigueperformance of repaired reinforced ,concrete beams', *Engineer,* Vol. XXXXV, No. 04, pp. 1-22.

Eduardo, N.B.S.J., Fernando, A.B.B. and Silva, V.D., June 2004, 'Concrete to concrete bond strength – Influence of the roughness of the substrate surface', *Construction and building materials,* 18, pp. 675-681.

Lacombe, P., Beaupre, D. and Pouliot, N., October 1999 'Rheology and bonding characteristics of self-levelling concrete as a repair material', *Materials and Structures,* Vol.32, , pp. 593-600.

Stanish, K., Hooton and R.D., Pantazopoulou, S.J., 1999, 'Corrosion effect of bond strength in reinforced concrete', *ACI Structural journal,* Title no. 96-S100, pp. 915-922.

International Concrete Repair Institute (ICRI)., 2008, 'Guide for surface preparation for the repair of deteriorated concrete resulting from reinforcing steel corrosion', 310.1R-2008.

Santos, D.S., Santos, P.M.D and Da Costa, D.D., 2012, "Effect of surface preparation and bonding agent on the concrete to concrete interface strength", *Construction and building materials,* pp. 102-110.

Kothandaraman, S. and Vasudevan, G, "Flexural retrofitting of RC beams using external bars at soffit level – An experimental study", 2010, *Construction and Building materials,* 24, pp. 2208 – 2216.

Proceedings of the 7th International Symposium on

Advances in Civil and Environmental Engineering Practices for Sustainable Development

ACEPS - 2019

Failure of gravel compaction pile supported embankment: Case study

N. H. Priyankara

Department of Civil and Environmental Engineering, Faculty of Engineering, University of Ruhuna, Hapugala, Galle, SRI LANKA.

K e y w o r d s

Expressway embankment
Gravel Compaction Pile
Peaty clay
Site investigation

A B S T R A C T

Gravel Compaction Pile was suggested by the contractor as a ground improvement technique in one of the expressway construction projects in Sri Lanka. In order to show the performance of the Gravel Compaction Pile improved ground, a trial embankment has been constructed on the Gravel Compaction Pile improved soft peaty clay. According to the initial site investigations, thickness of the soft peaty clay layer was about 6 – 13 m. Finished road level is 9.8 m above the existing ground level and it was expected to raise the embankment up to 11.6 m above the existing ground level in order to compensate the consolidation settlement and surcharge load. However, during Gravel Compaction Pile installation, it was realized that soft soil layer thickness is more than 13 m in right hand side of the embankment; some locations it is about 18 m. Soon after the Gravel Compaction Pile installation, embankment construction was started and, during soil filling it was noted that embankment is sliding towards right hand side leading to reduce the slope stability of the embankment. Further, according to field observations, it was realized that excess pore water has not been dissipated during the stage construction. Hence, as a precaution, berm has been constructed in order to control the lateral movement. However, it was observed that lateral movement is continuing during the further filling of the embankment. As such, by considering all these facts, construction has been abandoned due to uncertainties of the stability of the embankment losing about 250 million rupees to the contractor. This clearly indicates the importance of proper site investigation prior to construction.

Proceedings of the 7th International Symposium on

Advances in Civil and Environmental Engineering Practices for Sustainable Development

ACEPS - 2019

Case study on efficiency of domestic wastewater treatment plants in western province of Sri Lanka

T. Prasanthan[1], D.K. Pathirana[2] and W.K.C.N. Dayanthi[3]

[1]Engineering Services and Construction Division, National Housing Development Authority, Colombo-02, SRI LANKA
[2]Sewerage Section, National Water Supply and Drainage Board, Ratmalana, SRI LANKA
[3]Department of Civil and Environmental Engineering, Faculty of Engineering, University of Ruhuna, Galle, SRI LANKA

K e y w o r d s

Wastewater
Institutions
Performance
Health hazards
Wastewater treatment plants

A B S T R A C T

Western province is the most densely populated province in Sri Lanka and faces various issues related to domestic wastewater management. By considering these issues, wastewater treatment plants (WWTP) constructed in most of the housing projects implemented by government and private sectors in order to reduce the degradation of water quality and to safeguard the natural environment. However, the effectiveness of wastewater treatment in these plants is still questionable. Therefore, this case study focuses on the efficiency of selected six domestic wastewater treatment plants representing different locations of the western province which comes under public and private institutions. The methodology consists of field survey under four categories such as general, technical, physical and operational & maintenance, contributed by group discussion, formal and informal discussion with professionals and stakeholder interviews. The results summarized that only 3 out of 6 WWTPs studied performed well. In general, the physical and technical aspects were found to be satisfactory in selected 6 WWTPs whereas operational and maintenance aspects were deplorable in few plants. The result shows that constructing technically strong STPs does not necessarily guarantee its success. Necessary training to households and recruitment of trained personnel to operate plants required for better performance of WWTPs. However, government institutions necessitate public support to manage the operation and maintenance of WWTPs.

Proceedings of the 7th International Symposium on

Advances in Civil and Environmental Engineering Practices for Sustainable Development

ACEPS - 2019

Durability of mass concretes in hot weather

Kalinda Dasanayaka

INSEE Cement, Colombo, SRI LANKA.

K e y w o r d s

Mass concretes
Hot weather
Durability
Ettringite formation

A B S T R A C T

According to ACI 116R, mass concrete is defined as "any volume of concrete with dimensions large enough to require that measures be taken to cope with generation of heat from hydration of the cement and attendant volume change, to minimize cracking." since this definition doesn't provide a specific limit, many standards have developed their own definitions for mass concrete. For example, mass concrete is defined by some agencies as "any concrete element having a least dimension greater than 3 ft. (0.9 m)." and other agencies use different minimum dimensions, ranging from 1.5 to 6.5 ft. (0.46 to 2.0 m), depending on experience. Therefore, general guides of line parameters considered as the definition of a mass concrete are Walls > 500 mm and Slabs, pile caps, raft foundations > 800– 1000 mm. Older specifications generally limit temperatures for mass concrete specifying values as 70^0 C for the maximum allowable core temperature and 20^0C for the maximum allowable temperature gradient between the core and surface of the mass concrete section which is having lowest temperature at the considered period. Those limitations were defined to prevent any detrimental Effects of excessive temperature rise at early age of a concrete such as, Early age cracking due to thermal stresses, Changes in composition / micro structure of hydrated cement paste which may leads to later stage cracks called delayed Ettringite formation

But recent studies have shown that there are several parameters which leads the said early & delayed cracks. With that new specifications were risen the given temperature limits based about the concrete applications. Usually, well-established temperature controlling measures are sufficient to meet project specifications. However, if these are underestimated or poorly understood, they could lead for higher concrete temperatures and temperature differences that greatly exceed specified limits, causing deterioration of the durability expectations of the concrete. The limiting temperature differential depends on many factors such as type of aggregate, early age tensile strain capacity of concrete and degree of restraint. According to the recent experimental investigations carried out for major construction projects, it was found that the limiting temperature differential could be increased to 25 °C for the context of Sri Lanka. Furthermore, per CIRIA report C760, the limiting temperature differential under internal restraint for concrete with aggregate granite is 28 °C.

The other important limit with respect to temperature rise in a concrete element is the peak temperature at the core. Based on the findings of the research project done by Center for Transportation Research, The University of Texas At Austin (Report 0-4085-S:2006) the maximum temperature has been limited to 170 °F (76.7 °C) for concrete containing SCM such as fly ash to prevent DEF.

Furthermore, "IFSTTAR France – 2018 Recommendations for preventing disorders due to Delayed Ettringite Formation" has described a more performance-based approach to select the possible maximum temperature with the exposure condition of the concrete.
Additionally, recent trends in construction industry, such as increasing the size of concrete sections and demanding high early strength concretes with high minimum cement contents or low water-cementitious materials ratios, make temperature control even more difficult. Therefore, understanding the mass concrete specially in hot weather is the key to controlling temperatures and ultimately saving time, effort, and money.

Proceedings of the 7th International Symposium on

Advances in Civil and Environmental Engineering Practices for Sustainable Development

ACEPS - 2019

Cost-effective structural system for retrofitting existing houses in flood prone areas

T. R. S. T Wijewardana[1], Dhanushka Jayathilaka[1], Gihan Ranasinghe[2], C. Jayasinghe[2], M. T. R Jayasinghe[2], Shawn L. Platt[3] and Pete Walker[3]

[1]National Building Research Organisation, 99/1, Jawatta Road, Colombo 5. SRI LANKA.
[2]University of Moratuwa, Bandaranayake Mawatha, Moratuwa, SRI LANKA.
[3]BRE Centre for Innovative Construction Materials, Department of Architecture and Civil Engineering University of Bath, UK.

K e y w o r d s

Disaster
Hazards
Retrofitting
Geo grid
Livelihoods
Refuge space

A B S T R A C T

Intensity of the occurrence of natural disasters such as landslides, floods and high winds in Sri Lanka have been increased during the last decade due to several natural and manmade reasons. Disaster statistics shows that in 2017, flood hazard was triggered by heavy rain at the onset of the southwest monsoon on 25th and 26th May affecting 879,778 people with 219 deaths and 74 missing. The disaster caused destruction and damaged nearly 80,000 houses and affected livelihood of over 342,000 people. This was a long-term issue for the government due to the loss of lives, loss of livelihoods and economic activities. Other than that, after each disaster event, government spent huge amount of money for response and recovery. There are different approaches to design new buildings in flood prone areas in a way that minimize the damage to buildings. However, there are very few methods which can be used to retrofit existing buildings. With that background this research study focuses on developing retrofitting methodology for flood affected houses. According to the outcome of the research, plaster reinforced by geogrid could be used for strengthening the existing walls of the house. Reinforced plaster has the capacity to withstand the lateral loads created by water during a flood hazard. Geo grid was selected based on the laboratory test results conducted at University of Moratuwa with the collaboration of University of Bath (UK), using different test samples for masonry elements. Additionally, one bed room of the house will be converted in to two stories and it can be used as an evacuation place during a disaster situation. In order to apply the outcomes of the research, a flood affecting house was selected in Bulathsinhala Divisional secretariat area and construction of refuge space and strengthening of walls completed by the time. With the successful outcomes of the research it will be able to introduce a new cost-effective methodology to retrofit existing houses in flood prone areas.

Proceedings of the 7th International Symposium on

Advances in Civil and Environmental Engineering Practices for Sustainable Development

ACEPS - 2019

Design a transitional shelter for post disaster recovery

S.M.M.Infas[1],T. R. S. T Wijewardana[1], Dhanushka Jayathilake[1], Udeni P Nawagamuwa[2]

[1]National Building Research Organisation, 99/1, Jawatta Road, Colombo 5, SRI LANKA.
[2]University of Moratuwa, Bandaranayake Mawatha, Moratuwa, SRI LANKA.

K e y w o r d s

Transitional shelters
disaster recovery
Alternative construction methods

A B S T R A C T

During the recent past it was observed the increasing trend of natural disasters in Sri Lanka. Frequent occurrence of natural disasters has become a huge burden on the National Economy of the country. After each disaster event different government agencies spent money on disaster recovery and reconstruction activities. Providing temporary shelters & related services for disaster affected communities is one of the key activities in post disaster recovery period. Public buildings such as schools, temples, community centers, etc. are currently use as the temporary shelters. According to the past experiences it was identified that it is very difficult to use those public buildings as temporary shelters for long time. Accordingly, a study was carried out to design a transitional shelter for disaster affected communities. A review of the literature, case studies, guidelines and reports relating to the design of transitional shelters indicate that their provision and performance are not currently as effective as they could be. A lack of adequate consideration with climatic conditions, locally available materials and skills, cultural and social issues, delays and poor location selection for transitional shelters have each been identified as sources of poor performance contributing to an unacceptable standard of living. Moreover, there seems to be a lack of sufficient consideration with regard to the design of shelters for future storage and re-use.

Objective of the research study is to introduce a reusable transitional shelter which is livable, stable against natural disasters, minimum impact to existing environment and at a lowest possible cost and minimize carbon footprint on the surrounding environment. A questionnaire survey was conducted to gather the opinions and ideas of the stakeholders in order to determine the most feasible design for transitional shelter. The structure was designed to withstand for the possible bad weather conditions expected in disaster periods and adjustable to different terrain conditions in hilly areas. The research is focused on design & provision of disaster relief shelters.